

# **Taxonomic Studies of Dicot flora Using Microscopy in Thal Desert, Punjab-Pakistan**



**By**

**Salman Majeed**

**Department of Plant Sciences  
Quaid-i-Azam University Islamabad, Pakistan  
2023**

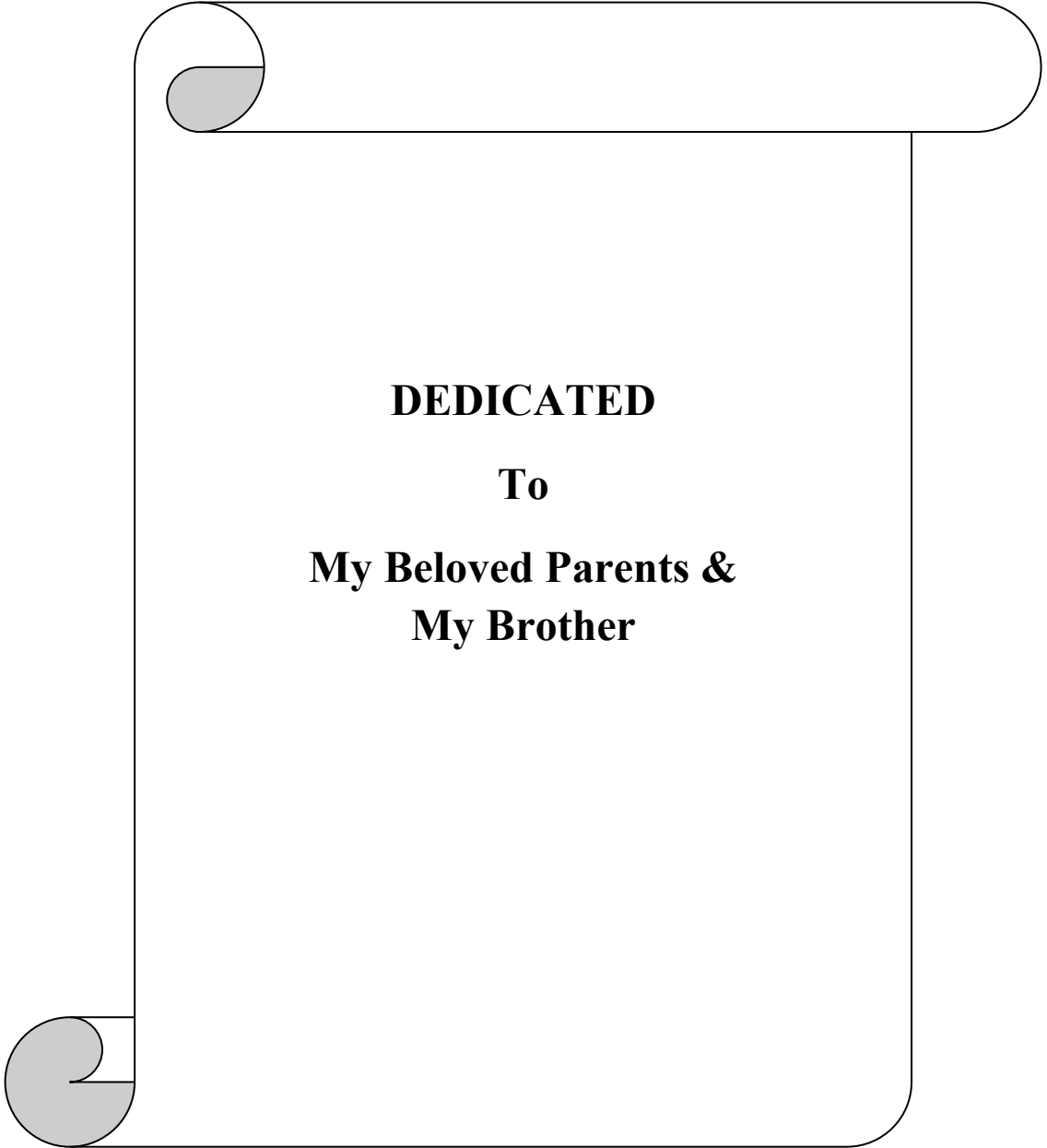
# **Taxonomic Studies of Dicot flora Using Microscopy in Thal Desert, Punjab-Pakistan**



**A Thesis Submitted to the Quaid-i-Azam University in Partial  
Fulfillment of the Requirements for the Degree of Doctor of  
Philosophy (Ph.D.)**

**In  
Botany/Plant Sciences (Plant Systematics and Biodiversity)**

**Department of Plant Sciences  
Quaid-i-Azam University Islamabad, Pakistan  
2023**



**DEDICATED**

**To**

**My Beloved Parents &  
My Brother**



قائد اعظم يونيورسٹی  
**QUAID-I-AZAM UNIVERSITY**

---

*Department of Plant Sciences  
Islamabad, Pakistan 45320*

---

**Subject: Author Declaration**

I Mr. Salman Majeed hereby state that my Ph.D. thesis entitled "**Taxonomic Studies of Dicot flora Using Microscopy in Thal Desert, Punjab-Pakistan**" is my work and has not been submitted previously by me for taking any degree from the Department of Plant Sciences, Quaid-i-Azam University or anywhere in the country/world.

At any time if my statement is found to be incorrect even after my Graduate, the university has the right to withdraw my Ph.D. degree.

**Salman Majeed**



قائد اعظم یونیورسٹی  
**QUAID-I-AZAM UNIVERSITY**

*Department of Plant Sciences  
Islamabad, Pakistan 45320*

**Subject: Plagiarism Undertaking**

I solemnly declare that the research work presented in the thesis titled "**Taxonomic Studies of Dicot flora Using Microscopy in Thal Desert, Punjab-Pakistan**" is solely my research work with no significant contribution from any other person. Small contribution/help wherever taken has been duly acknowledged and that complete thesis has been written by me.

I understand the zero-tolerance policy of the HEC and Quaid-i-Azam University towards plagiarism. Therefore, I as an author of the above-titled thesis declare that no portion of my thesis has been plagiarized and any material used as reference is property referred/cited.

I undertake that if I am found faulty of any formal plagiarism in the above-titled thesis even after awarding of Ph.D. degree, the University reserves the right to withdraw/revoke my Ph.D. degree and that HEC and the University has the right to publish my mime on the HEC/University website on which name of students are placed who submitted plagiarized thesis

**Student/Author Signature** \_\_\_\_\_

**Salman Majeed**



قائد اعظم يونيورسٹی  
**QUAID-I-AZAM UNIVERSITY**

---

*Department of Plant Sciences*  
*Islamabad, Pakistan 45320*

---

**SIMILARITY INDEX CERTIFICATE**

It is certified that Mr. Salman Majeed has completed his Ph.D. research work and compilation of the thesis. The title of his thesis is "Taxonomic Studies of Dicot flora Using Microscopy in Thal Desert, Punjab-Pakistan". His thesis has been checked on Turnitin for similarity index and found 7% that lies in the limits provided by HEC (20%).

**Dr. Muhammad Zafar**  
**Supervisor**

Turnitin Originality Report

Taxonomic Studies of Dicot flora Using Microscopy in Thal Desert, Punjab-Pakistan  
Salman Majeed .



From PhD (PhD DRSMML)

- Processed on 31-Jan-2023 10:20 PKT
- ID: 2003126835
- Word Count: 34461

Similarity Index

7%

Similarity by Source

Internet Sources:

3%

Publications:

5%

Student Papers:

0%

**sources:**

1 < 1% match (Internet from 28-Jan-2023)

[https://www.researchgate.net/publication/329395647\\_Role\\_of\\_trees\\_in\\_climate\\_change\\_and\\_their\\_auther](https://www.researchgate.net/publication/329395647_Role_of_trees_in_climate_change_and_their_auther)

2 < 1% match (Internet from 27-Jan-2023)

[https://www.researchgate.net/publication/271948484\\_Fruits\\_seeds\\_and\\_pollen\\_morphology\\_of\\_Turkish\\_F](https://www.researchgate.net/publication/271948484_Fruits_seeds_and_pollen_morphology_of_Turkish_F)

3 < 1% match (Internet from 26-Jan-2023)

[https://www.researchgate.net/publication/333304597\\_Stem\\_anatomy\\_diversity\\_in\\_Iresine\\_Amaranthaceae](https://www.researchgate.net/publication/333304597_Stem_anatomy_diversity_in_Iresine_Amaranthaceae)

4 < 1% match (Internet from 28-Jan-2023)

[https://www.researchgate.net/publication/233716487\\_Seed\\_Morphology\\_of\\_the\\_Tribe\\_Hyoscyameae\\_Sol](https://www.researchgate.net/publication/233716487_Seed_Morphology_of_the_Tribe_Hyoscyameae_Sol)

5 < 1% match (Internet from 12-Dec-2022)

[https://link.springer.com/chapter/10.1007/978-3-030-78444-7\\_3?code=5987de78-d09a-414a-b5b3-f921347c32ab&error=cookies\\_not\\_supported](https://link.springer.com/chapter/10.1007/978-3-030-78444-7_3?code=5987de78-d09a-414a-b5b3-f921347c32ab&error=cookies_not_supported)

6 < 1% match (Internet from 01-Oct-2020)

[https://link.springer.com/referenceworkentry/10.1007%2F978-1-4614-7501-9\\_3](https://link.springer.com/referenceworkentry/10.1007%2F978-1-4614-7501-9_3)

7 < 1% match (Internet from 14-Dec-2022)

<http://pr.hec.gov.pk/jspui/bitstream/123456789/2547/1/2591S.pdf>

8 < 1% match (Mouldi Gamoun, Azaiez Ouled Belgacem, Mounir Louhaichi. "Diversity of desert rangelands of Tunisia", Plant Diversity, 2018)

## **FOREIGN EXAMINERS**

**1) Professor Elizabeth M Williamson**

School of Pharmacy  
University of Reading  
Reading, UK

**2) Professor Geoffrey Michael Gadd**

Department of Biological Sciences  
University of Dundee Dundee DD1 5EH  
Scotland UK



## CERTIFICATE OF APPROVAL

This is to certify that research work presented in this thesis, entitled is "Taxonomic Studies of Dicot flora Using Microscopy in Thal Desert, Punjab-Pakistan" was conducted by Mr. Salman Majeed under the supervision of Dr. Muhammad Zafar. No part of this thesis has been submitted anywhere else for any other degree. This thesis is submitted to the Department of Plant Sciences, Quaid-i-Azam University, Islamabad, Pakistan in partial fulfillment of the requirements for the degree of Doctor of Philosophy in the field of Plant Sciences (Plant Systematics and Biodiversity), Department of Plant Sciences, Quaid-i-Azam University, Islamabad, Pakistan.

Student name: Mr. Salman Majeed

Signature:



Examination committee

External Examiner 1

**Prof. Dr. Abida Akram**  
Department of Botany  
Pir Mehr Ali Shah Arid Agriculture University,  
Rawalpindi

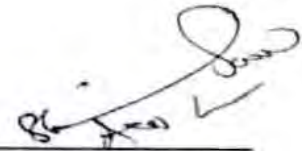
Signature



External Examiner 2

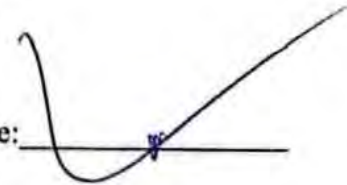
**Prof. Dr. Shaikh Saeed**  
Environmental Sciences Program  
Fatima Jinnah Women University  
The Mall  
Rawalpindi

Signature



Supervisor  
**Dr. Muhammad Zafar**  
Associate Professor  
Department of Plant Sciences  
Quaid-i-Azam University, Islamabad

Signature:



Chairman  
**Prof. Dr. Mushtaq Ahmad**  
Department of Plant Sciences  
Quaid-i-Azam University,  
Islamabad

Signature:



Dated: 17-07-2023

## Table of Contents

S. No	Title of Content	Page#
I	List of Plates	VI
II	List of Figures	XX
III	List of Tables	XXIII
IV	Acknowledgment	XXV
V	Abstract	XXVI
<b>1.</b>	<b>CHAPTER 01: INTRODUCTION</b>	<b>01-10</b>
1.1	Desert Rangelands	01
1.2	Species Diversity in Deserts	02
1.3	Plant Taxonomy	02
1.4	Dicot Angiosperms	03
1.5	Taxonomic Identification	03
1.6	Plant Taxonomy in Relation to Pollen Micromorphology	04
1.7	Plant Taxonomy in Relation to Seed Micromorphology	05
1.8	Plant Taxonomy in Relation to Microscopic Anatomy	06
1.9	Justification of the Project	07
1.10	Aims of the Study	10
<b>2.</b>	<b>CHAPTER 02: MATERIAL AND METHODS</b>	<b>11-28</b>
2.1	Research Work Outline	11
2.2	Study area: Thal Desert	12
2.3	Sampling of Dicot flora	16
2.4	Identification of Dicot flora	16
2.5	Preservation and Mounting of Dicot Specimens	16
2.6	Taxonomic Characterization via Microscopic Techniques	23
2.6.1	Pollen Micromorphology	23
a)	Light Microscopy (LM)	23
b)	Scanning Electron Microscopy (SEM)	23
2.6.2	Seed Micromorphology	24
2.6.3	Foliar Epidermal Anatomy	24
a)	Lactic acid and Nitric acid Method	24
b)	Nail Polish Method	24
c)	Bleach Method	25
d)	Scanning Electron Microscopy (SEM)	25
2.6.7	Petiole Anatomy	25
2.7	Statistical Analysis	26
2.7.1	P/E Index	26
2.7.2	Pollen Fertility and Sterility (%)	26
2.7.3	Stomatal and Trichome Index	27
2.7.8	Exploratory Multivariate Analysis	27
2.8	Data Compilation Using Optical Microscopy	27
2.9	Microphotography	27
<b>3.</b>	<b>CHAPTER 03: RESULTS AND DISCUSSION</b>	<b>29-351</b>
3.	Summary	29

<b>Section-I</b>		
3.1	Floristic Checklist of Desert Dicot Angiosperms and Field Pictorial Guide	56
<b>Section-II</b>		
3.2	Pollen Micromorphological Studies of Dicot flora	68
3.2.1	Micromorphological Pollen Structure of Amaranthaceous taxa	69
a)	Pollen Size	69
b)	Pollen Shape	69
c)	Pore Number	69
d)	Operculum	70
e)	Sculpturing Elements	70
f)	Tectum	70
g)	Ektexinious Bodies	70
h)	Aperture Group	70
i)	Mesoporia	71
j)	Quantitative Attributes	71
3.2.11	UPGMA Dendrogram and PCA Clustering	71
3.2.2	Taxonomic Key for Amaranthaceous Pollen Identification	73
3.2.3	Discussion	85
3.2.4	Micromorphology of Asteraceous Pollen	91
a)	Shape and Size	91
b)	Apertures Characteristics	92
c)	Pollen wall and Lacunate Grains	92
d)	Taxonomy of Echini Features	93
e)	Numerical Statistics via UPGMA Dendrogram and PCA Analysis	93
3.2.5	Taxonomic Keys Based on Asteraceous Pollen Characters	95
3.2.6	Discussion	109
3.2.7	Micromorphological Description of Fabaceous Pollen	115
a)	Palynomorph description of <i>Acacia jacquemontii</i> Benth.	115
b)	Palynomorph description of <i>Acacia modesta</i> Wall.	116
c)	Palynomorph description of <i>Acacia nilotica</i> (L.) Delile	116
d)	Palynomorph description of <i>Astragalus homosus</i> L.	116
e)	Palynomorph description of <i>Crotalaria burhia</i> Benth.	116
f)	Palynomorph description of <i>Dalbergia sissoo</i> DC.	117
g)	Palynomorph description of <i>Parkinsonia aculeata</i> L.	117
h)	Palynomorph description of <i>Prosopis cineraria</i> (L.) Druce	117
i)	Palynomorph description of <i>Prosopis juliflora</i> (Sw.) DC.	117
j)	Hierarchical UPGMA Clustering and PCA Analysis	118
3.2.8	Taxonomic Keys based on Fabaceous Pollen Characters	119
3.2.9	Discussion	127
3.2.10	Micromorphological Details of Solanaceous Pollen	129
a)	Polarity, Dispersal Unit, and Shape	129
b)	Polar Area	129
c)	Size and Polar Area Index (PAI)	129
d)	Apertures and Mesocolpium	130
e)	Sculpturing Elements	130

3.2.11	Taxonomic Keys Based Pollen Features of Solanaceous Species	131
3.2.12	Discussion	139
3.2.13	Pollen Micromorphology of Boraginaceous Species	142
a)	Palynomorph description of <i>Arnebia hispidissima</i> (Lehm.) A. DC.	142
b)	Palynomorph description of <i>Heliotropium bacciferum</i> Forssk.	142
c)	Palynomorph description of <i>Heliotropium europaeum</i> L.	143
d)	Palynomorph description of <i>Heliotropium strigosum</i> Willd.	143
e)	Palynomorph description of <i>Nonea micrantha</i> Boiss. & Reut.	143
3.2.14	Pollen Micromorphology of Brassicaceous Species	147
a)	Palynomorph description of <i>Brassica nigra</i> (L.) K.Koch	147
b)	Palynomorph description of <i>Eruca vesicaria</i> (L.) Cav.	147
c)	Palynomorph description of <i>Lepidium didymum</i> L.	148
d)	Palynomorph description of <i>Sisymbrium irio</i> L.	148
3.2.15	Pollen Micromorphology of Cactaceae Species	150
a)	Palynomorph description of <i>Opuntia dillenii</i> (Ker-Gawl) Haw	150
b)	Palynomorph description of <i>Opuntia monacantha</i> (Willd.) Haw	151
3.2.16	Pollen Micromorphology of Capparaceae Species	153
a)	Palynomorph description of <i>Capparis decidua</i> (Forssk.) Edgew	153
b)	Palynomorph description of <i>Cleome brachycarpa</i> (Forssk.) Vahl ex DC.	153
3.2.17	Pollen Micromorphology of Aizoaceae Species	155
a)	Palynomorph description of <i>Trianthema portulacastrum</i> L.	155
b)	Palynomorph description of <i>Zaleya pentandra</i> (L.) C. Jeffrey	155
3.2.18	Pollen Micromorphology of Cucurbitaceous Species	157
a)	Palynomorph description of <i>Citrullus colocynthis</i> (L.) Schrad.	157
b)	Palynomorph description of <i>Cucumis melo</i> L.	157
3.2.19	Pollen Micromorphology of Euphorbiaceous Species	159
a)	Palynomorph description of <i>Chrozophora plicata</i> (Vahl) A.Juss. ex Spreng.	159
b)	Palynomorph description of <i>Euphorbia dracunculoides</i> Lam.	159
3.2.20	Pollen Micromorphology of Rhamnaceous Species	161
a)	Palynomorph description of <i>Ziziphus nummularia</i> (Burm.f.) Wight	161
b)	Palynomorph description of <i>Ziziphus spina-christi</i> (L.) Desf.	161
3.2.21	Pollen Micromorphology of Tamaricaceae Species	163
a)	Palynomorph description of <i>Tamarix aphylla</i> (L.) H.Karst.	163
b)	Palynomorph description of <i>Tamarix dioica</i> Roxb. ex Roth	163
3.2.22	Pollen Micromorphology of Zygophyllaceous Species	165
a)	Palynomorph description of <i>Fagonia bruguieri</i> DC.	165
b)	Palynomorph description of <i>Tribulus terrestris</i> L.	165
3.2.23	Pollen Micromorphology of Apiaceous Species	167
a)	Palynomorph description of <i>Psammogeton biternatum</i> Edgew.	167
3.2.24	Pollen micromorphology of Apocynaceous Species	167
a)	Palynomorph description of <i>Rhazya stricta</i> Decne	167
3.2.25	Pollen Micromorphology of Bignoniaceous Species	169
a)	Palynomorph description of <i>Tecomella undulata</i> (Sm.) Seem.	169
3.2.26	Pollen Micromorphology of Malvaceous Species	169
a)	Palynomorph description of <i>Malva parviflora</i> L.	169

3.2.27	Pollen Micromorphology of Myrtaceae Species	171
a)	Palynomorph description of <i>Eucalyptus globulus</i> Labill.	171
3.2.28	Pollen Micromorphology of Nitrariaceae Species	171
a)	Palynomorph description of <i>Peganum harmala</i> L.	171
3.3.29	Pollen Micromorphology of Nyctaginaceae Species	173
a)	Palynomorph description of <i>Boerhavia procumbens</i> Banks ex Roxb.	173
3.2.30	Pollen Micromorphology of Papaveraceous Species	173
a)	Palynomorph description of <i>Argemone mexicana</i> L.	173
<b>Section III</b>		
<b>3.3</b>	Seed Micromorphology of Dicot Angiosperms	175
3.3.1	Seed Shape and Color Variations	175
3.3.2	Seed Surface Pattern	176
3.3.3	Seed Surface Ultrastructure	176
3.3.4	Variations in Quantitative Parameters	177
3.3.5	Dendrogram and PCA Clustering	177
3.3.6	Discussion	218
<b>Section IV</b>		
3.4	Anatomical Characterization of Dicot flora	224
3.4.1	Foliar Epidermal Micromorphology of Amaranthaceous taxa	225
a)	Epidermal Morphology	225
b)	Morphological Parameters of Stomatal Complex	226
c)	Trichome Diversity	226
3.4.2	UPGMA Dendrogram Statistics	227
3.4.3	Taxonomic Keys Based on Amaranthaceous Foliar Anatomy	228
3.4.4	Discussion	250
3.4.5	Foliar Epidermal Micromorphology of Fabaceous taxa	254
a)	Foliar Epidermis	254
b)	Stomatal Complex	254
c)	Trichomes	255
3.4.6	Identification Keys based on Foliar Anatomy of Fabaceous taxa	255
3.4.7	Discussion	267
3.4.8	Foliar Epidermal Micromorphology of Cucurbitaceous Species	270
a)	Foliar anatomical description of <i>Citrullus colocynthis</i> (L.) Schrad.	270
b)	Foliar anatomical description of <i>Cucumis melo</i> L.	271
c)	Foliar anatomical description of <i>Cucurbita maxima</i> Duchesne	271
d)	Foliar anatomical description of <i>Luffa cylindrica</i> (L.) M.Roem.	272
e)	Foliar anatomical description of <i>Momordica charantia</i> L.	273
f)	Foliar anatomical description of <i>Mukia maderaspatana</i> (L.) M.Roem.	273
3.4.9	Discussion	283
3.4.10	Foliar Epidermal Micromorphology of Capparaceae Species	285
a)	Foliar anatomical description of <i>Capparis decidua</i> (Forssk.) Edgew.	285
b)	Foliar anatomical description of <i>Capparis spinosa</i> L.	286
c)	Foliar anatomical description of <i>Cleome brachycarpa</i> (Forssk.) Vahl ex DC.	286
d)	Foliar anatomical description of <i>Cleome viscosa</i> L.	287
e)	Foliar anatomical description of <i>Dipterygium glaucum</i> Decne.	288
3.4.11	Identification Keys Based on Foliar Anatomy of Capparaceae taxa	289
3.4.12	Discussion	300

3.4.13	Stem Epidermal Micromorphology of Cactaceae Species	302
a)	Foliar anatomical description of <i>Opuntia dillenii</i> (Ker-Gawl) Haw	302
b)	Foliar anatomical description of <i>Opuntia monacantha</i> (Willd.) Haw	302
3.4.14	Discussion	303
3.4.15	Petiole Micromorphology of Amaranthaceous Species	305
a)	Petiole Description of <i>Aerva lanata</i> (L.) Juss.	305
b)	Petiole Description of <i>Achyranthes aspera</i> L.	305
c)	Petiole Description of <i>Alternanthera ficoidea</i> (L.) Sm.	305
d)	Petiole Description of <i>Alternanthera sessilis</i> (L.) R.Br. ex DC.	306
e)	Petiole Description of <i>Amaranthus graecizans</i> L.	306
f)	Petiole Description of <i>Amaranthus retroflexus</i> L.	306
g)	Petiole Description of <i>Amaranthus viridis</i> L.	306
h)	Petiole Description of <i>Atriplex stocksii</i> Boiss.	307
i)	Petiole Description of <i>Bassia indica</i> (Wight) A.J.Scott	307
j)	Petiole Description of <i>Chenopodium album</i> L.	307
k)	Petiole Description of <i>Chenopodium ficifolium</i> Sm.	308
l)	Petiole Description of <i>Chenopodium murale</i> L.	308
m)	Petiole Description of <i>Digera muricata</i> (L.) Mart.	308
n)	Petiole Description of <i>Gomphrena celosioides</i> Mart	308
3.4.16	Hierarchical Cluster Analysis (UPGMA) Dendrogram	309
3.4.17	Identification Keys Based on Amaranthaceous Petiole Features	310
3.4.18	Discussion	330
3.4.19	Petiole Micromorphology of Euphorbiaceous Species	333
a)	Petiole Outline	333
b)	Vascular Bundle	333
c)	Epidermal Cells	334
d)	Parenchyma Cells	334
e)	Collenchyma Cells	334
f)	Trichomes	335
3.4.20	Identification Keys Based on Euphorbiaceous Petiole Features	336
3.4.21	Discussion	350
<b>4.</b>	<b>Conclusion</b>	352
<b>5.</b>	<b>Future Perspectives</b>	354
	<b>References</b>	355-414

## List of Plates

S. No	Title of Plate	Page#
Plate 01	Panoramic view of Thal desert areas; (a) Noorpur Thal (District Khushab), (b) Hyderabad Thal (District Bhakkar)	14
Plate 02	Panoramic view of Thal desert areas; (a) Mankera Fort (District Bhakkar), (b) Chubara Chak 69/ML (District Layyah).	15
Plate 03	Field plant collection from Thal area; (a) <i>Carthamus oxyacantha</i> M.Bieb. (b) <i>Haloxylon stocksii</i> (Boiss.) Benth. & Hook. f.	18
Plate 04	Field plants collection from Thal areas; (a) <i>Opuntia dillenii</i> (Ker Gawl.) Haw. (b) <i>Prosopis cineraria</i> (L.) Druce.	19
Plate 05	Dicot floral Herbarium specimens (a) Preservation (b) Mounting of on herbarium sheets.	20
Plate 06	Mounted Herbarium Specimens: (a) <i>Acacia jacquemontii</i> Benth. (b) <i>Chrozophora plicata</i> (Vahl) A.Juss. ex Spreng. (c) <i>Dipterygium glaucum</i> Decne. (d) <i>Euphorbia granulata</i> Forssk.	21
Plate 07	Mounted Herbarium Specimens: (a) <i>Haloxylon stocksii</i> (Boiss.) Benth. & Hook. f. (b) <i>Peganum harmala</i> L. (c) <i>Pulicaria boissieri</i> Hook.f. (d) <i>Tamarix dioica</i> Roxb.	22
Plate 08	Microscopic measurement and visualization and (a) Optical microscopic slide data measurement (b) Scanning electron microscopic observation and microphotography	28
Plate 09	Field pictorial view of (a) <i>Acacia jacquemontii</i> ; floral parts with spiny branch, (b) <i>Acacia modesta</i> ; pedunculate spike with paired leaflets, (c) <i>Acacia nilotica</i> ; bright yellow flower, (d) <i>Achyranthes aspera</i> ; elongating inflorescence	41
Plate 10	Field pictorial view of (a) <i>Aerva javanica</i> ; dense and stout floral parts, (b) <i>Aerva lanata</i> ; leaves with floral branches, (c) <i>Albizia lebbeck</i> ; inflorescence pedunculate heads, (d) <i>Alternanthera ficoidea</i> ; evergreen leaves with floral buds	42
Plate 11	Field pictorial view of (a) <i>Alternanthera sessilis</i> ; oblong leaves, (b) <i>Amaranthus graecizans</i> ; glabrous leafy branches, (c) <i>Amaranthus retroflexus</i> ; flower terminal spikes, (d) <i>Amaranthus viridis</i> ; brown paniculate spikes	43
Plate 12	Field pictorial view of (a) <i>Argemone mexicana</i> ; showy bright yellow flower, (b) <i>Arnebia hispidissima</i> ; annual sub-erect stem, (c) <i>Astragalus hamosus</i> ; imparipinnate compound leaves, (d) <i>Atriplex stocksii</i> ; rhombic leafy and floral parts	44
Plate 13	Field pictorial view of (a) <i>Azadirachta indica</i> ; white floral branches, (b) <i>Bassia indica</i> ; sub-glabrous leafy branches, (c) <i>Boerhavia procumbens</i> ; axillary panicle flowers, (d) <i>Brassica nigra</i> ; bright yellow flower with leafy branches	45
Plate 14	Field pictorial view of (a) <i>Capparis decidua</i> ; brick red flowers, (b)	46

	<i>Capparis spinosa</i> ; flowers solitary, (c) <i>Carthamus oxyacantha</i> ; spiny branches with head, (d) <i>Centaurea iberica</i> ; simple broad leaves with light pinkish capitulum	
Plate 15	Field pictorial view of (a) <i>Chenopodium album</i> ; cymosely branched panicle, (b) <i>Chenopodium ficifolium</i> ; terminal panicles, (c) <i>Chenopodium murale</i> ; olive green leafy branch, (d) <i>Chrozophora plicata</i> ; triangular ovate leaf	47
Plate 16	Field pictorial view of (a) <i>Chrozophora tinctoria</i> ; leaf-blades broadly ovate-rhombic, (b) <i>Citrullus colocynthis</i> ; elongate leaf and yellowish flower, (c) <i>Cleome brachycarpa</i> ; sub-erect herb, (d) <i>Cleome viscosa</i> ; foliolate leaf and yellow	48
Plate 17	Field pictorial view of (a) <i>Convolvulus arvensis</i> ; campanulate whitish flower, (b) <i>Conyza candensis</i> ; flower head with tiny phyllaries, (c) <i>Corchorus depressus</i> ; floral branches, (d) <i>Corchorus olitorius</i> ; lanceolate leaf	49
Plate 18	Field pictorial view of (a) <i>Cousinia prolifera</i> ; dense floral heads, (b) <i>Crotalaria burhia</i> ; floral branches with yellow corolla, (c) <i>Croton bonplandianus</i> ; pedicels with male flower, (d) <i>Cucumis melo</i> ; trailing angular stem with fruit	50
Plate 19	Field pictorial view of (a) <i>Cucurbita maxima</i> ; 5-lobed leaves, (b) <i>Dalbergia sissoo</i> ; imparipinnate leaves, (c) <i>Datura innoxia</i> ; broadly ovate leaves with showy flower, (d) <i>Datura stramonium</i> ; purplish suffused flower	51
Plate 20	Field pictorial view of (a) <i>Digera muricata</i> ; leafy branches with immature inflorescence, (b) <i>Dipterygium glaucum</i> ; branched undershrub, (c) <i>Eclipta prostrata</i> ; lanceolate leaves, (d) <i>Eruca vesicaria</i> ; dull yellow large flower	52
Plate 21	Field pictorial view of (a) <i>Eucalyptus globulus</i> ; umbel inflorescence, (b) <i>Euphorbia dracunculoides</i> ; subglobose fruit, (c) <i>Euphorbia granulata</i> ; ephemeral herbaceous habitat, (d) <i>Euphorbia helioscopia</i> ; pseudo-umbel inflorescence	53
Plate 22	Field pictorial view of (a) <i>Euphorbia hirta</i> ; opposite leaves with cyathia, (b) <i>Euphorbia serpens</i> ; prostrate growth habitat, (c) <i>Fagonia bruguieri</i> ; pale pink flower, (d) <i>Farsetia stylosa</i> ; whitish flower with vegetative branches	54
Plate 23	Field pictorial view of (a) <i>Gisekia pharnaceoides</i> ; lanceolate leaves, (b) <i>Haloxylon stocksii</i> ; divaricate shrub, (c) <i>Heliotropium bacciferum</i> ; white corolla flower, (d) <i>Heliotropium europaeum</i> ; obovate leaves with terminal inflorescence	55
Plate 24	Field pictorial view of (a) <i>Heliotropium strigosum</i> ; bracteates inflorescence, (b) <i>Iphiona grantioides</i> ; yellowish flower head, (c) <i>Launaea nudicaulis</i> ; habit growth with floral parts, (d) <i>Launaea procumbens</i> ; yellow flower-head	56



Plate 25	Field pictorial view of (a) <i>Lepidium didymum</i> ; glabrous decumbent stem, (b) <i>Leptadenia pyrotechnica</i> ; branched leafless shrub, (c) <i>Luffa cylindrica</i> ; palmately leaf with bright yellow flower, (d) <i>Malva parviflora</i> ; orbicular leaves	57
Plate 26	Field pictorial view of (a) <i>Mollugo cerviana</i> ; whorled leaves, (b) <i>Mollugo nudicaulis</i> ; basal leafy branches habit growth, (c) <i>Momordica charantia</i> ; orbicular leaves with yellow flower, (d) <i>Mukia maderaspatana</i> ; sagittate leaves with berry	58
Plate 27	Field pictorial view of (a) <i>Nonea micrantha</i> ; hispid leaf with flowers, (b) <i>Opuntia dillenii</i> ; showy yellow flower, (c) <i>Opuntia monacantha</i> ; flattened cladodes with yellow reddish flower, (d) <i>Parkinsonia aculeata</i> ; floral branches with stamens	59
Plate 28	Field pictorial view of (a) <i>Peganum harmala</i> ; scabrous leaf with whitish flower, (b) <i>Physalis divaricata</i> ; vegetative branches, (c) <i>Physalis minima</i> ; sinuate leaves with globose berry, (d) <i>Prosopis cineraria</i> ; creamy white pedunculate spike	60
Plate 29	Field pictorial view of (a) <i>Prosopis juliflora</i> ; pinnate leaves with axillary spike, (b) <i>Psammogeton biternatum</i> ; vegetative branches, (c) <i>Pulicaria boissieri</i> ; floral branches with capitulum, (d) <i>Rhazya stricta</i> ; white foliaceous flowers	61
Plate 30	Field pictorial view of (a) <i>Ricinus communis</i> ; inflorescence with calyx lobes, (b) <i>Salsola tragus</i> ; solitary floral branch, (c) <i>Salvadora oleoides</i> ; Leaves coriaceous, (d) <i>Salvadora persica</i> ; sub-fleshy elliptic ovate leaves	62
Plate 31	Field pictorial view of (a) <i>Senna italica</i> ; obovate leaves with yellow flowers, (b) <i>Sisymbrium irio</i> ; floral branch with yellow pedicel, (c) <i>Solanum incanum</i> ; sinuate leaves, (d) <i>Solanum surattense</i> ; purple flower with elongated anther.	63
Plate 32	Field pictorial view of (a) <i>Sonchus asper</i> ; lanceolate leaves with capitulum, (b) <i>Suaeda fruticosa</i> ; shrubby bush, (c) <i>Tamarix aphylla</i> ; subsessile pinkish white flower, (d) <i>Tamarix dioica</i> ; purplish pink subsessile flower	64
Plate 33	Field pictorial view of (a) <i>Tecomella undulata</i> ; filaments of longer stamens, (b) <i>Tephrosia purpurea</i> ; leaf imparipinnate with seed pod, (c) <i>Tragopogon gracilis</i> ; flower-heads phyllaries, (d) <i>Trianthema portulacastrum</i> ; sub-orbiculate leaves	65
Plate 34	Field pictorial view of (a) <i>Tribulus terrestris</i> ; paripinnate leaves with yellow flower, (b) <i>Trichodesma indicum</i> ; densely hairy branches, (c) <i>Verbesina encelioides</i> ; yellow flower-heads, (d) <i>Withania coagulans</i> ; elliptic-ovate leaves	66
Plate 35	Field pictorial view of (a) <i>Withania somnifera</i> ; axillary cluster flower, (b) <i>Zaleya pentandra</i> ; oblong leaves, (c) <i>Ziziphus nummularia</i> ; orbicular leaves, (d) <i>Ziziphus spina-christi</i> ; ovate-elliptic leaves with	67

	axillary tomentose inflorescence	
Plate 36	Scanning electron photomicrographs of pollen grains of Amaranthaceae. (a-c) <i>Achyranthes aspera</i> ; sparsely granulate non punctate (Scale bar = 5 $\mu$ m, 2 $\mu$ m), (d-f) <i>Aerva javanicia</i> ; Scabrate spiniulose and ektexiniuos bodies (Scale bar = 5 $\mu$ m, 1 $\mu$ m), (g-i) <i>Aerva lanata</i> ; micro-echinate perforate, non-punctate (Scale bar = 5 $\mu$ m, 1 $\mu$ m), (j-l) <i>Amaranthus graecizans</i> ; Granulate-spinulose exine (Scale bar = 5 $\mu$ m, 2 $\mu$ m, 1 $\mu$ m)	77
Plate 37	Scanning electron photomicrographs of pollen grains of Amaranthaceae. (a-b) <i>Achyranthes retroflexus</i> ; micro-echinate perforate exine (Scale bar = 5 $\mu$ m), (c-d) <i>Amaranthus viridis</i> ; granulate perforate exine (Scale bar = 5 $\mu$ m), (e-f) <i>Bassia indica</i> ; micro-echinate perforate, mesoporia narrow (Scale bar = 2 $\mu$ m), (g-h) <i>Chenopodium album</i> ; Scabrate micro-spinulose exine (Scale bar = 2 $\mu$ m), (i-j) <i>Chenopodium ficifolium</i> ; Non-punctate, broad flat mesoporia (Scale bar = 5 $\mu$ m), (j-l) <i>Chenopodium murale</i> ; micro-echinate perforate sculpturing (Scale bar = 5 $\mu$ m)	78
Plate 38	Scanning electron photomicrographs of pollen grains of Amaranthaceae. (a-c) <i>Digera muricata</i> ; meta-reticulate exine (Scale bar = 5 $\mu$ m, 2 $\mu$ m, 1 $\mu$ m), (d-e) <i>Haloxylon stocksii</i> ; dense micro-echinate exine (Scale bar = 5 $\mu$ m), (f-g) <i>Salsola tragus</i> ; granulate nano spiniules, mesoporia narrow (Scale bar = 5 $\mu$ m, 1 $\mu$ m), (h-i) <i>Suaeda fruticosa</i> ; granulate-spinulose perforate exine (Scale bar = 5 $\mu$ m)	79
Plate 39	Scanning electron microscope photographs of Asteraceous taxa. (a-c) <i>Carthamus oxyacantha</i> ; short spines and micro-perforate exine (Scale bar = 10 $\mu$ m, 1 $\mu$ m), (d-f) <i>Centaurea iberica</i> ; scabrate exine and regular flat based echini (Scale bar = 10 $\mu$ m, 2 $\mu$ m), (g-i) <i>Conyza candensis</i> ; echinate sculpture and mucronate pointed echini shape (Scale bar = 10 $\mu$ m, 5 $\mu$ m)	100
Plate 40	Scanning electron microscope photographs of Asteraceous taxa. (a-c) <i>Cousinia prolifera</i> ; echino-perforate sculpture and micro spiniules (Scale bar = 10 $\mu$ m, 5 $\mu$ m), (d-f) <i>Eclipta prostrata</i> ; micro-perforate echinate exine and broad based echini (Scale bar = 5 $\mu$ m, 2 $\mu$ m), (g-i) <i>Iphiona grantioides</i> ; echino-perforate tectate exine and brad base perforate echini (Scale bar = 5 $\mu$ m, 1 $\mu$ m)	101
Plate 41	Scanning electron microscope photographs of Asteraceous taxa. (a-c) <i>Launaea procumbens</i> ; fenestrate lophate sculpture and lacunate (Scale bar = 10 $\mu$ m, 5 $\mu$ m, 2 $\mu$ m), (d-f) <i>Launaea nudicaulis</i> ; Echino-perforate lophate exine and lacunate (Scale bar = 5 $\mu$ m, 2 $\mu$ m), (g-i) <i>Pulicaria boissieri</i> ; echino-perforate exine and sharp regular echini (Scale bar = 10 $\mu$ m, 5 $\mu$ m, 2 $\mu$ m)	102
Plate 42	Scanning electron microscope photographs of Asteraceous taxa. (a-c) <i>Sonchus asper</i> ; fenestrate lacunate (Scale bar = 5 $\mu$ m), (d-f)	103

	<i>Tragopogon gracilis</i> ; Echino-perforate scabrate and bulged echini (Scale bar = 10 $\mu$ m, 5 $\mu$ m, 2 $\mu$ m), (g-i) <i>Verbesina encelioides</i> ; echino-perforate exine and pointe tips spines (Scale bar = 10 $\mu$ m, 2 $\mu$ m), (j-l) <i>Xanthium strumarium</i> ; micro-echinate verrucate exine (Scale bar = 10 $\mu$ m, 5 $\mu$ m).	
Plate 43	SEM micrographs of pollen grains, pollen surface pattern and exine peculiarities. (a-b) <i>Acacia jacquemontii</i> scale bar 5 $\mu$ m, (c-d) <i>Acacia modesta</i> scale bar 50 $\mu$ m & 2 $\mu$ m, (e-f) <i>Acacia nilotica</i> scale bar 5 $\mu$ m	120
Plate 44	SEM micrographs of pollen grains, pollen surface pattern and exine peculiarities. (a-b) <i>Astragalus hamosus</i> scale bar 5 $\mu$ m & 1 $\mu$ m, (c-d) <i>Crotalaria burhia</i> scale bar 5 $\mu$ m, (e-f) <i>Dalbergia sissoo</i> scale bar 5 $\mu$ m	121
Plate 45	SEM micrographs of pollen grains, pollen surface pattern and exine peculiarities. (a-b) <i>Parkinsonia aculeata</i> scale bar 5 $\mu$ m & 2 $\mu$ m. (c-d) <i>Prosopis cineraria</i> scale bar 5 $\mu$ m & 2 $\mu$ m. (e-f) <i>Prosopis juliflora</i> scale bar 5 $\mu$ m	122
Plate 46	Scanning electron microphotographs of pollen and exine ornamentation types of Solanaceous grains. (a-c) <i>Datura innoxia</i> ; striate psilate exine (scale bar = 10 $\mu$ m, 2 $\mu$ m), (d-f) <i>Datura stramonium</i> ; muri reticulate (scale bar = 10 $\mu$ m, 5 $\mu$ m), (g-i) <i>Physalis divaricata</i> ; verrucate colpus membrane (scale bar = 5 $\mu$ m, 1 $\mu$ m), (j-l) <i>Physalis minima</i> ; granulate sculptured (scale bar = 5 $\mu$ m, 2 $\mu$ m)	134
Plate 47	Scanning electron microphotographs of pollen and exine ornamentation types of Solanaceous grains. (a-c) <i>Solanum incanum</i> ; homobrochate exine (scale bar = 10 $\mu$ m, 2 $\mu$ m), (d-f) <i>Solanum surattense</i> ; granulate scabrate (scale bar = 10 $\mu$ m, 5 $\mu$ m, 2 $\mu$ m), (g-i) <i>Withania coagulans</i> ; regulate striate exine (scale bar = 5 $\mu$ m), (j-l) <i>Withania somnifera</i> ; verrucate sculptured colpi (scale bar = 5 $\mu$ m, 2 $\mu$ m)	135
Plate 48	Scanning electron microscope photographs of Boraginaceous taxa. (a-b) <i>Arnebia hispidissima</i> ; micro-echinate exine sculpture (Scale bar 2 $\mu$ m), (c-d) <i>Heliotropium bacciferum</i> ; rugulate pollen wall (Scale bar = 10 $\mu$ m, 2 $\mu$ m), (e-f) <i>Heliotropium europaeum</i> ; verrucate exine peculiarities (Scale bar = 5 $\mu$ m)	145
Plate 49	Scanning electron microscope photographs of Boraginaceous taxa. (a-b) <i>Heliotropium strigosum</i> ; psilate verrucate exine (Scale bar = 5 $\mu$ m, 2 $\mu$ m), (c-d) <i>Heliotropium bacciferum</i> ; rugulate pollen wall (Scale bar = 10 $\mu$ m, 2 $\mu$ m), (e-f) <i>Nonea micrantha</i> ; verrucate gemmate exine wall (Scale bar = 5 $\mu$ m, 2 $\mu$ m)	146
Plate 50	Scanning electron microscope photographs of Brassicaceous taxa. (a-b) <i>Brassica nigra</i> ; compact reticulate exine (Scale bar = 5 $\mu$ m, 1 $\mu$ m), (c-d) <i>Eruca vesicaria</i> ; semi tectate pollen wall (Scale bar = 5 $\mu$ m, 1 $\mu$ m), (e-f) <i>Lepidium didymum</i> ; reticulate sculpturing (Scale bar = 5	149

	$\mu\text{m}$ , 1 $\mu\text{m}$ ), (g-h) <i>Sisymbrium irio</i> ; reticulated pollen stratification (Scale bar = 5 $\mu\text{m}$ )	
Plate 51	Scanning electron microscopic photographs of Cactus species (a) <i>Opuntia dillenii</i> polar view (20 $\mu\text{m}$ ), (b) <i>Opuntia dillenii</i> exine sculpturing (10 $\mu\text{m}$ ), (c) <i>Opuntia monacantha</i> polar view (20 $\mu\text{m}$ ), and (d) <i>Opuntia monacantha</i> exine surface (5 $\mu\text{m}$ )	152
Plate 52	Scanning electron microscope photographs of Capparaceae species. (a-b) <i>Capparis decidua</i> ; reticulate striate exine (Scale bar = 5 $\mu\text{m}$ , 1 $\mu\text{m}$ ), (c-d) <i>Cleome brachycarpa</i> ; spinulose verrucate pollen wall (Scale bar = 5 $\mu\text{m}$ , 1 $\mu\text{m}$ )	154
Plate 53	Scanning electron microscope photographs of Aizoaceae species (a-b) <i>Trianthema portulacastrum</i> ; foveolate punctate sculpturing (Scale bar = 2 $\mu\text{m}$ , 1 $\mu\text{m}$ ), (c-d) <i>Zaleya pentandra</i> ; scabrate granulate pollen tectum (Scale bar = 10 $\mu\text{m}$ , 5 $\mu\text{m}$ )	156
Plate 54	Scanning electron microscope photographs of Cucurbitaceae species (a-b) <i>Citrullus colocynthis</i> ; coarsely reticulate exine wall (Scale bar = 10 $\mu\text{m}$ , 5 $\mu\text{m}$ ), (c-d) <i>Cucumis melo</i> ; reticulate-regulate pollen ornamentation (Scale bar = 10 $\mu\text{m}$ , 2 $\mu\text{m}$ )	158
Plate 55	Scanning electron microscope photographs of Euphorbiaceous species (a-b) <i>Chrozophora plicata</i> ; reticulate heterobrochate wall tectum (Scale bar = 10 $\mu\text{m}$ , 5 $\mu\text{m}$ ), (c-d) <i>Euphorbia dracunculoides</i> ; perforate gemmate exine stratification (Scale bar = 10 $\mu\text{m}$ )	160
Plate 56	Scanning electron microscope photographs of Rhamnaceae species (a-b) <i>Ziziphus nummularia</i> ; bulged colpus orientation (Scale bar = 5 $\mu\text{m}$ , 1 $\mu\text{m}$ ), (c-d) <i>Ziziphus spina-christi</i> ; rugulate exine stratification (Scale bar = 5 $\mu\text{m}$ )	162
Plate 57	Scanning electron microscope photographs of Tamaricaceae species (a-b) <i>Tamarix aphylla</i> ; micro-reticulate ornamentation (Scale bar = 5 $\mu\text{m}$ , 2 $\mu\text{m}$ ), (c-d) <i>Tamarix dioica</i> ; reticulate perforate pollen wall stratification (Scale bar = 2 $\mu\text{m}$ , 1 $\mu\text{m}$ )	164
Plate 58	Scanning electron microscope photographs of Zygophyllaceous species (a-b) <i>Fagonia bruguieri</i> ; acute end apertures and reticulate ornamentation (Scale bar = 5 $\mu\text{m}$ , 1 $\mu\text{m}$ ), (c-d) <i>Tribulus terrestris</i> ; micro-reticulate exine wall (Scale bar = 5 $\mu\text{m}$ , 10 $\mu\text{m}$ )	166
Plate 59	Scanning electron microscope photographs of Apiaceous and Apocynaceous taxa (a-b) <i>Psammogeton biternatum</i> ; verrucate gemmate peculiarities (Scale bar = 5 $\mu\text{m}$ , 1 $\mu\text{m}$ ), (c-d) <i>Rhazya stricta</i> ; psilate scabrate exine sculpturing (Scale bar = 10 $\mu\text{m}$ )	168
Plate 60	Scanning electron microscope photographs of Bignoniaceous and Malvaceous taxa (a-b) <i>Tecomella undulata</i> ; rugulate reticulate pollen stratification (Scale bar = 10 $\mu\text{m}$ , 2 $\mu\text{m}$ ), (c-d) <i>Malva parviflora</i> ; echinate sculpturing (Scale bar = 20 $\mu\text{m}$ )	170
Plate 61	Scanning electron microscope photographs of Myrtaceous and	172

	Nitrariaceous taxa (a-b) <i>Eucalyptus globulus</i> ; scabrate verrucate exine tectum (Scale bar = 5 µm), (c-d) <i>Peganum harmala</i> ; rugulate perforate wall stratification (Scale bar = 5 µm, 1 µm)	
Plate 62	Scanning electron microscope photographs of Nyctaginaceous and Papaveraceous taxa (a-b) <i>Boerhavia procumbens</i> ; spinulose tectum (Scale bar = 10 µm), (c-d) <i>Argemone mexicana</i> ; reticulate-verrucate gemmate exine stratification (Scale bar = 10 µm, 2 µm)	174
Plate 63	Scanning electron micrographs of seed micromorphology; (a-c) <i>Acacia jacquemontii</i> (a) shape (b) texture (c) striate foveolate sculpture. (d-f) <i>Acacia modesta</i> (d) terminal hilum (e) very fine texture (f) striate-regulate sculpture (g-i) <i>Acacia nilotica</i> (g) shape (h) fracture line (i) striate sculpture	204
Plate 64	Scanning electron micrographs of seed micromorphology; (a-c) <i>Albizia lebbeck</i> (a) terminal hilum (b) coarse texture (c) rugose sculpture. (d-f) <i>Astragalus homosus</i> (d) sub-terminal hilum (e) coarse texture (f) foveolate rugose sculpture (g-i) <i>Azadirachta indica</i> (g) shape (h) coarse texture (i) foveolate sculpture	205
Plate 65	Scanning electron micrographs of seed micromorphology; (a-c) <i>Brassica nigra</i> (a) central hilum (b) very fine texture (c) rugulate sculpture. (d-f) <i>Capparis decidua</i> (d) depressed hilum (e) very fine texture (f) foveolate striate sculpture (g-i) <i>Chenopodium album</i> (g) raised hilum (h) coarse texture (i) papillate sculpture	206
Plate 66	Scanning electron micrographs of seed micromorphology; (a-c) <i>Citrullus colocynthis</i> (a) raised hilum (b) medium texture (c) striate psilate sculpture. (d-f) <i>Crotalaria burhia</i> (d) terminal hilum (e) coarse texture (f) papillate rugose sculpture (g-i) <i>Dalbergia sissoo</i> (g) sub-terminal hilum (h) medium texture (i) rugose sculpture	207
Plate 67	Scanning electron micrographs of seed micromorphology; (a-c) <i>Fagonia bruguieri</i> (a) raised hilum (b) coarse texture (c) striate sculpture. (d-f) <i>Farsetia stylosa</i> (d) central hilum (e) coarse texture (f) reticulate sculpture (g-i) <i>Heliotropium europaeum</i> (g) general view (h) sub-terminal depressed hilum (i) foveolate sculpture	208
Plate 68	Scanning electron micrographs of seed micromorphology; (a-c) <i>Leptadenia pyrotechnica</i> (a) terminal hilum (b) coarse texture (c) papillate scabrate sculpture. (d-f) <i>Mullago cerviana</i> (d) raised hilum (e) coarse texture (f) reticulate sculpture (g-i) <i>Mullago naudicaulis</i> (g) general shape (h) raised hilum (i) papillate foveolate sculpture	209
Plate 69	Scanning electron micrographs of seed micromorphology; (a-c) <i>Parkinsonia aculeata</i> (a) shape (b) irregular fracture line (c) rugose sculpture (d-f) <i>Peganum harmala</i> (d) shape (e) deeply convex periclinal wall (f) striate reticulate sculpture (g-i) <i>Prosopis cineraria</i> (g) oblong shape (h) depressed hilum (i) Rugose papillate sculpture	210
Plate 70	Scanning electron micrographs of seed micromorphology; (a-c)	211

	<i>Prosopis juliflora</i> (a) shape (b) U shape pleurogram (c) rugose sculpture (d-f) <i>Psammogeton biternatum</i> (d) shape (e) spiny projections (f) rugulate (g-i) <i>Senna italica</i> (g) obovate shape (h) coarse texture (i) Rugose scabrate sculpture	
Plate 71	Scanning electron micrographs of seed micromorphology; (a-c) <i>Tephrosia purpurea</i> (a) shape (b) visible depressed hilum (c) smooth papillae sculpture (d-f) <i>Tribulus tressteris</i> (d) spiny scabrous shape outline (e) coarse spiny texture (f) wrinkled spiny sculpture (g-i) <i>Withania coagulans</i> (j) shape (k) coarsely rough texture (l) undulate granulate sculpture	212
Plate 72	Light Micrographs (LM) illustrated stomata, shape of cells and wall pattern and trichomes of Amaranthaceous species; <i>Achyranthes aspera</i> (a) Abaxial surface showing trichome (b) Abaxial surface showing stomata (c) Adaxial surface showing trichome; <i>Aerva lanata</i> (d) Abaxial surface showing stomata (e) Abaxial surface showing trichome (f & g) Adaxial surface showing trichomes; <i>Alternanthera ficoidea</i> (h) Abaxial surface showing stomata (i) Adaxial surface showing trichome (j) Adaxial surface showing stomata; <i>Alternanthera philoxeroides</i> (k) Abaxial surface showing stomatal (l) Adaxial surface showing stomata.	239
Plate 73	Light Micrographs (LM) illustrated stomata, shape of cells and wall pattern and trichomes of Amaranthaceous species; <i>Alternanthera sessilis</i> (a) Abaxial surface showing stomata (b) Abaxial surface showing trichome (c) Adaxial surface showing stomata (d) Adaxial surface showing trichome; <i>Amaranthus graecizans</i> (e) Abaxial surface showing trichome (f) Abaxial surface showing stomata (g) Adaxial surface showing trichome (h) Adaxial surface showing stomata; <i>Amaranthus viridis</i> (i) Abaxial surface showing stomata (j) Adaxial surface showing stomata.	240
Plate 74	Light Micrographs (LM) illustrated stomata, shape of cells and wall pattern and trichomes of Amaranthaceous species; <i>Atriplex stocksii</i> (a) Abaxial surface showing stomata (b) Abaxial surface showing trichome (c) Adaxial surface showing stomata; <i>Bassia indica</i> (d) Abaxial surface showing stomata (e) Abaxial surface showing trichome (f) Adaxial surface showing trichome; <i>Chenopodium album</i> (h) Abaxial surface showing stomata & trichome (i) Adaxial surface showing epidermis cells	241
Plate 75	Light Micrographs (LM) illustrated stomata, shape of cells and wall pattern and trichomes of Amaranthaceous species; <i>Chenopodium ficifolium</i> (a) Abaxial surface showing stomata (b) Adaxial surface showing stomata <i>Digera muricata</i> (d) Abaxial surface showing stomata (e) Abaxial surface showing trichome (f) Adaxial surface showing trichome (g) Adaxial surface showing stomata; <i>Amaranthus</i>	242

	<i>retroflexus</i> (h) Abaxial surface showing stomata (i) Abaxial surface showing trichome (j) Adaxial surface showing trichome and epidermal cells	
Plate 76	SEM micrograph of Amaranthaceous taxa showing shape of cell, pattern of anticlinal wall, trichomes and stomata type; <i>Achyranthes aspera</i> (a-b) Abaxial surface (scale bar = 100 $\mu$ m, 5 $\mu$ m), (c-d) Abaxial surface (scale bar = 100 $\mu$ m, 50 $\mu$ m); <i>Atriplex stocksii</i> (e-f) Abaxial surface (scale bar = 10 $\mu$ m, 5 $\mu$ m), (g-h) Adaxial surface (scale bar = 50 $\mu$ m, 5 $\mu$ m); <i>Alternanthera ficoidea</i> (i-j) Abaxial surface (scale bar = 50 $\mu$ m, 5 $\mu$ m), (k-l) Adaxial surface (scale bar = 50 $\mu$ m, 5 $\mu$ m).	243
Plate 77	SEM micrograph of Amaranthaceous taxa showing shape of cell, pattern of anticlinal wall, trichomes and stomata type; <i>Amaranthus graecizans</i> (a-b) Abaxial surface (scale bar = 50 $\mu$ m, 10 $\mu$ m), (c-d) Abaxial surface (scale bar = 100 $\mu$ m, 10 $\mu$ m); <i>Aerva lanata</i> (e-f) Abaxial surface (scale bar = 50 $\mu$ m, 5 $\mu$ m), (g-h) Adaxial surface (scale bar = 10 $\mu$ m, 5 $\mu$ m), <i>Alternanthera sessilis</i> (i-j) Abaxial surface (scale bar = 100 $\mu$ m, 5 $\mu$ m), (k-l) Adaxial surface (scale bar = 120 $\mu$ m, 5 $\mu$ m)	244
Plate 78	SEM micrograph of Amaranthaceous taxa showing shape of cell, pattern of anticlinal wall, trichomes and stomata type; <i>Alternanthera philoxeroides</i> (a-b) Abaxial surface (scale bar = 100 $\mu$ m, 5 $\mu$ m) (c-d) Abaxial surface (scale bar = 100 $\mu$ m, 5 $\mu$ m), <i>Amaranthus viridis</i> (e-f) Abaxial surface (scale bar = 100 $\mu$ m, 5 $\mu$ m). (g-h) Adaxial surface (scale bar = 100 $\mu$ m, 5 $\mu$ m), <i>Bassia indica</i> (i-j) Abaxial surface (scale bar = 50 $\mu$ m, 5 $\mu$ m), (k-l) Adaxial surface (scale bar = 5 $\mu$ m, 50 $\mu$ m)	245
Plate 79	SEM micrograph of Amaranthaceous taxa showing shape of cell, pattern of anticlinal wall, trichomes and stomata type; <i>Chenopodium album</i> (a-b) Abaxial surface (scale bar = 10 $\mu$ m, 2 $\mu$ m), (c-d) Abaxial surface (scale bar = 50 $\mu$ m, 1 $\mu$ m), <i>Chenopodium ficifolium</i> (e-f) Abaxial surface (scale bar = 10 $\mu$ m, 5 $\mu$ m), (g-h) Adaxial surface (scale bar = 5 $\mu$ m), <i>Digera muricata</i> (i-j) Abaxial surface (scale bar = 50 $\mu$ m, 10 $\mu$ m), (k-l) Adaxial surface (scale bar = 10 $\mu$ m, 5 $\mu$ m), <i>Amaranthus retroflexus</i> (m & n) Abaxial and adaxial surfaces (scale bar = 20 $\mu$ m, 100 $\mu$ m); <i>Salsola tragus</i> (o & p) Abaxial and adaxial surface (scale bar = 50 $\mu$ m, 5 $\mu$ m)	246
Plate 80	Light microscopic anatomical photographs, scale bar 10 $\mu$ m: <i>Acacia jacquemontii</i> Benth. (a) Adaxial surface 40x, (b) Abaxial surface 40x; <i>Acacia modesta</i> Wall. (c) Adaxial surface 40x, (d) Abaxial surface 40x; <i>Acacia nilotica</i> (L.) Delile (e) Adaxial surface 40x, (f) Abaxial surface 40x; <i>Astragalus hamosus</i> L. (g) Adaxial surface 40x, (h) Abaxial surface 40x	261
Plate 81	Light microscopic anatomical photographs, scale bar 10 $\mu$ m:	262

	<i>Crotalaria burhia</i> Benth. (a) Adaxial surface 40x, (b) Abaxial surface 40x; <i>Dalbergia sissoo</i> DC. (c) Adaxial surface 40x, (d) Abaxial surface 40x; <i>Parkinsonia aculeata</i> L. (e) Adaxial surface 40x, (f) Abaxial surface 40x	
Plate 82	Light microscopic anatomical photographs, scale bar 10 µm: <i>Prosopis cineraria</i> (L.) Druce (a) Adaxial surface 40x, (b) Abaxial surface 40x; <i>Prosopis juliflora</i> (Sw.) DC. (c) Adaxial surface 40x, (d) Abaxial surface 40x; <i>Tephrosia purpurea</i> (L.) Pers. (e) Adaxial surface 40x, (f) Abaxial surface 40x	263
Plate 83	Scanning microscopic anatomical micrographs: (a) <i>Acacia jacquemontii</i> , SEM epidermis surface scale bar 100 µm; (b) <i>Acacia modesta</i> , epidermis and stomata scale bar 5 µm; (c) <i>Acacia nilotica</i> , SEM stomatal view scale bar 10 µm; (d) <i>Astragalus hamosus</i> , SEM stomatal view scale bar 5 µm; (e) <i>Crotalaria burhia</i> , epidermis surface scale bar 20 µm; (f) <i>Dalbergia sissoo</i> , stomatal view scale bar 100 µm; (g) <i>Parkinsonia aculeata</i> , epidermis and stomata scale bar 5 µm; (h) <i>Prosopis cineraria</i> , epidermis surface scale bar 20 µm; (i) <i>Prosopis juliflora</i> , stomatal view scale bar 5 µm; (j) <i>Tephrosia purpurea</i> , epidermis and stomata scale bar 10 µm	264
Plate 84	Light Micrographs (LM) illustrated stomata, epidermal cells and trichomes of Cucurbitaceous species; <i>Citrullus colocynthis</i> (a) Adaxial surface showing epidermis (b) Abaxial surface showing trichomes, <i>Cucumis melo</i> (c) Adaxial surface showing trichome (d) Abaxial surface showing epidermal cells, <i>Cucurbita maxima</i> (e) Adaxial surface showing epidermal cells (f) Abaxial surface showing trichomes, <i>Luffa cylindrica</i> (g) Adaxial surface showing stomata (h) Abaxial surface showing cells and glandular trichome, <i>Momordica charantia</i> (i) Adaxial surface showing stomata (j) Abaxial surface showing epidermis, <i>Mukia maderaspatana</i> (k) Adaxial surface showing epidermal cells (l) Abaxial surface showing multicellular trichomes	279
Plate 85	Light Micrographs (LM) illustrated stomata, epidermal cells and trichomes of Capparaceae species; <i>Capparis decidua</i> (a) Adaxial surface showing stomata (b) Abaxial surface showing epidermis cells, <i>Capparis spinosa</i> (c) Adaxial surface showing epidermal cells (d) Abaxial surface showing stomata, <i>Cleome brachycarpa</i> (h) Adaxial surface showing trichome (i) Abaxial surface showing trichome and epidermis cells.	293
Plate 86	Light Micrographs (LM) illustrated stomata, epidermal cells and trichomes of Capparaceae species; <i>Cleome viscosa</i> (a) Adaxial surface showing glandular trichome (b) Abaxial surface showing stomata and trichomes, <i>Dipterygium glaucum</i> (c) Adaxial surface showing stomata (d) Abaxial surface showing straight anticlinal walls and	294



	paracytic stomata	
Plate 87	Stem anatomical micrographs taken at 10X showing (EC) epidermal cells and (st) stomata of (a) <i>Opuntia dillenii</i> , (b) <i>Opuntia monacantha</i>	303
Plate 88	Photomicrographs of Petiole Section of <i>Aerva lanata</i> (L.) Juss. (A): Transverse Section (100 µm), (B): Section of median vascular bundle (20 µm), (C): Adaxial epidermis Section (50 µm), (D): Section of vascular bundle showing xylem and phloem (20 µm), (E): Sectioning of collenchyma cell (10 µm), (F) Abaxial epidermal surface (50 µm)	314
Plate 89	Photomicrographs of Petiole Section of <i>Achyranthes aspera</i> L. (A) Transverse Section showing cuticle layer (100 µm), (B) Section of median vascular bundle (20 µm), (C) Section of lateral vascular bundle (20 µm), (D) Lateral side view of transverse section (50 µm), (E) Abaxial epidermal surface (50 µm), (F) Sectioning of collenchymatous cell (10 µm), (G) Sectioning of VB (20 µm), (H) Parenchymatous cell layering (50 µm) (I) VB (20 µm), (J) Adaxial epidermis section (50 µm), (K) polygonal epidermal cell (10 µm), (L) collenchyma and parenchyma cell surface (20 µm)	315
Plate 90	Photomicrographs of Petiole Section of <i>Alternanthera ficoidea</i> (L.) Sm. (A) Transverse Section (100 µm), (B) Section of median vascular bundle (20 µm), (C) Abaxial epidermal surface (50 µm), (D) Petiole cell layering (20 µm), (E) Parenchyma cell layering (50 µm), (F) Adaxial epidermis cell (50 µm), (G) VB partition into xylem and phloem (20 µm), (H) Dorsolateral epidermal layer (50 µm), (I) Collenchyma cells (10 µm)	316
Plate 91	Photomicrographs of Petiole Section of <i>Alternanthera sessilis</i> (L.) R.Br. ex DC. (A). Transverse Section (100 µm), (B and C) Section of median vascular bundle (20 µm), (D) Adaxial epidermis section (50 µm), (E) Abaxial epidermal layer (50 µm), (F) Dorsolateral epidermis (50 µm), (G) VB section (20 µm), (H) VB partition into xylem and phloem (20 µm), (I) Collenchyma and Parenchyma cells (10 µm)	317
Plate 92	Photomicrographs of Petiole Section of <i>Amaranthus graecizans</i> L. (A) Transverse Section (100 µm), (B) Adaxial epidermis and cuticle layer (50 µm), (C) Trichome (20 µm), (D) Parenchymatous cell layers (50 µm), (E) Collenchyma cell layering (50 µm), (F) Section of median vascular bundle (20 µm)	318
Plate 93	Photomicrographs of Petiole Section of <i>Amaranthus retroflexus</i> L. (A) Transverse Section (100 µm), (B) Lateral ventral side epidermis and bundle (50 µm), (C) Adaxial epidermis and trichome (20 µm), (D) Adaxial epidermis and median vascular bundle section (50 µm), (E) Lateral side view of TS (50 µm), (F) Trichomes (20µm), (G) Parenchymatous cell (20 µm), (H) Collenchyma cells, xylem and phloem (10 µm), (I) Lateral VB (20 µm)	319
Plate 94	Photomicrographs of Petiole Section of <i>Amaranthus viridis</i> L. (A and	320

	B) Transverse Section (100 $\mu\text{m}$ ), (C) Adaxial epidermal surface along with trichome (50 $\mu\text{m}$ ), (D) Abaxial epidermal surface (50 $\mu\text{m}$ ), (E) Lateral VB (50 $\mu\text{m}$ ), (F) Parenchyma cell layering (20 $\mu\text{m}$ ), (G) Collenchyma cell layering (10 $\mu\text{m}$ ), (H) Xylem and phloem partition in VB (20 $\mu\text{m}$ ), (I) Parenchyma cells (10 $\mu\text{m}$ )	
Plate 95	Photomicrographs of Petiole Section of <i>Atriplex stocksii</i> Boiss. (A) Transverse Section showing lateral vascular bundle (100 $\mu\text{m}$ ), (B) Adaxial epidermal surface (50 $\mu\text{m}$ ), (C) Abaxial epidermis (50 $\mu\text{m}$ ), (D) Trichomes (50 $\mu\text{m}$ ), (E) Collenchyma cells (20 $\mu\text{m}$ ), (F) Parenchyma cell (20 $\mu\text{m}$ ), (G) Lateral VB (10 $\mu\text{m}$ ), (H) Parenchymatous and collenchyma cell (10 $\mu\text{m}$ ), (I) Xylem and Phloem cells (10 $\mu\text{m}$ )	321
Plate 96	Photomicrographs of Petiole Section of <i>Bassia indica</i> (Wight) A.J.Scott. (A) Transverse Section (100 $\mu\text{m}$ ), (B) Lateral vascular bundle (20 $\mu\text{m}$ ), (C) Abaxial epidermis and collenchymatous layering (50 $\mu\text{m}$ ), (D) Adaxial epidermis (50 $\mu\text{m}$ ), (E) Cuticle cell layer (20 $\mu\text{m}$ ), (F) VB sectioning (20 $\mu\text{m}$ ), (G) Trichomes and parenchyma cells (50 $\mu\text{m}$ ), (H) Collenchyma cells along abaxial side (50 $\mu\text{m}$ ), (I) Annular Collenchyma cells (10 $\mu\text{m}$ )	322
Plate 97	Photomicrographs of Petiole Section of <i>Chenopodium album</i> L. (A, B and C) Different view of transverse section (100 $\mu\text{m}$ ), (D) Median vascular bundle (50 $\mu\text{m}$ ), (E and F) Lateral epidermis and collenchyma cell layers (50 $\mu\text{m}$ ), (G) Parenchyma cells (20 $\mu\text{m}$ ), (H) Abaxial epidermis (10 $\mu\text{m}$ ), (I) Adaxial epidermis (10 $\mu\text{m}$ )	323
Plate 98	Photomicrographs of Petiole Section of <i>Chenopodium ficifolium</i> Sm. (A and B) Different view of transverse section (100 $\mu\text{m}$ ), (C) Adaxial epidermis (50 $\mu\text{m}$ ), (D) Collenchyma cells layer (20 $\mu\text{m}$ ), (E) Parenchyma cell sectioning (20 $\mu\text{m}$ ), (F) Abaxial epidermal surface (50 $\mu\text{m}$ ), (G and H) Median VB section of xylem and phloem (10 $\mu\text{m}$ ), (I) Annular Collenchyma cells (10 $\mu\text{m}$ )	324
Plate 99	Photomicrographs of Petiole Section of <i>Chenopodium murale</i> L. (A and B) Transverse Section (100 $\mu\text{m}$ ), (C) Adaxial epidermis layer (20 $\mu\text{m}$ ), (D) Trichomes (20 $\mu\text{m}$ ), (E) Lateral VB and parenchymatous cell (20 $\mu\text{m}$ ), (F) Abaxial layering of epidermis (20 $\mu\text{m}$ ), (G and H) Lamellar collenchyma cells (10 $\mu\text{m}$ ), (I) VB showing xylem and phloem cells (10 $\mu\text{m}$ )	325
Plate 100	Photomicrographs of Petiole Section of <i>Digera muricata</i> (L.) Mart. (A) Mid view of Transverse section (100 $\mu\text{m}$ ), (B) Lower side of TS (100 $\mu\text{m}$ ), (C) Upper side view of TS (100 $\mu\text{m}$ ), (D, E and F) Median VB sectioning (20 $\mu\text{m}$ ) (G) Adaxial epidermal layer with collenchymatous cell (50 $\mu\text{m}$ ), (H) Abaxial epidermis and parenchyma cells (50 $\mu\text{m}$ ), (I) Xylem and phloem cells in VB (10 $\mu\text{m}$ )	326
Plate 101	Photomicrographs of Petiole Section of <i>Gomphrena celosioides</i> Mart.	327

	(A and B) TS and lateral vascular bundle (100 $\mu\text{m}$ ), (C) Collenchyma layering of cell (20 $\mu\text{m}$ ), (D and E) Lateral side views of TS (20 $\mu\text{m}$ ), (F) Abaxial epidermis with trichomes (20 $\mu\text{m}$ ), (G) Cuticle layer and collenchymatous cells (20 $\mu\text{m}$ ), (H) Adaxial epidermal side (20 $\mu\text{m}$ ), (I) VB portioned into xylem and phloem	
Plate 102	Photomicrographs of Petiole Section of <i>Chrozophora plicata</i> (Vahl) A.Juss. ex Spreng. (L.) Juss. (a): Transverse Section (100 $\mu\text{m}$ ), (b): Section of abaxial epidermis, palisade cells and parenchyma cells (20 $\mu\text{m}$ ), (c): Median vascular bundle (10 $\mu\text{m}$ ), (d): Section of adaxial epidermis and cuticle (20 $\mu\text{m}$ ), (e): Sectioning of lateral side epidermis and collenchyma cell (10 $\mu\text{m}$ ), (f) Abaxial isodiametric polygonal epidermal cell (10 $\mu\text{m}$ ).	340
Plate 103	Photomicrographs of Petiole Section of <i>Chrozophora tinctoria</i> (L.) A.Juss. (a): Transverse Section (100 $\mu\text{m}$ ), (b): Section of abaxial epidermis, and parenchyma cells (50 $\mu\text{m}$ ), (c): Lateral ventral side isodiametric polygonal cells (20 $\mu\text{m}$ ), (d): Section of adaxial epidermis (20 $\mu\text{m}$ ), (e): Sectioning of lateral vascular bundle (10 $\mu\text{m}$ ), (f) Abaxial isodiametric polygonal epidermal cell and lateral epidermis (10 $\mu\text{m}$ )	341
Plate 104	Photomicrographs of Petiole Section of <i>Croton bonplandianus</i> Baill. (a): Transverse Section (100 $\mu\text{m}$ ), (b): Section of adaxial epidermis cells and parenchyma cells (50 $\mu\text{m}$ ), (c): Lateral vascular bundle (20 $\mu\text{m}$ ), (d): Section of collenchyma cells (10 $\mu\text{m}$ ), (e): Sectioning of lateral side epidermis (10 $\mu\text{m}$ ), (f) Abaxial isodiametric polygonal epidermal cell (10 $\mu\text{m}$ )	342
Plate 105	Photomicrographs of Petiole Section of <i>Euphorbia granulata</i> Forssk. (a): Transverse Section (100 $\mu\text{m}$ ), (b): Section of lateral vascular bundle showing xylem and phloem vessels (10 $\mu\text{m}$ ), (c): Collenchyma and isodiametric polygonal epidermis cells (10 $\mu\text{m}$ ), (d): Section of abaxial epidermis (20 $\mu\text{m}$ ), (e): Sectioning of lateral side epidermis (10 $\mu\text{m}$ ), (f) Adaxial isodiametric polygonal epidermal cell (20 $\mu\text{m}$ )	343
Plate 106	Photomicrographs of Petiole Section of <i>Euphorbia helioscopia</i> L. (a): Transverse Section (100 $\mu\text{m}$ ), (b): Section of adaxial epidermis cells and collenchyma cells (20 $\mu\text{m}$ ), (c): Median vascular bundle (10 $\mu\text{m}$ ), (d): Section of lateral epidermal cells (20 $\mu\text{m}$ ), (e): Sectioning of palisade layer (5 $\mu\text{m}$ ), (f) Abaxial epidermis and collenchyma cells (20 $\mu\text{m}$ ). TS=Transverse section, MVB= Median Vascular Bundle, ad epi= adaxial epidermis, ab epi= abaxial epidermis, co = collenchyma cells; LEC = Lateral epidermal cells.	344
Plate 107	Photomicrographs of Petiole Section of <i>Euphorbia hirta</i> L. (a): Transverse Section (100 $\mu\text{m}$ ), (b): Section of adaxial epidermis cells and trichome (50 $\mu\text{m}$ ), (c): Lateral vascular bundle (10 $\mu\text{m}$ ), (d): Section of collenchyma cells (5 $\mu\text{m}$ ), (e): Sectioning of abaxial	345

	epidermis (20 $\mu\text{m}$ ), (f) Lateral epidermis side and trichome (10 $\mu\text{m}$ ). TS=Transverse section, LVB= Median Vascular Bundle, ad epi= adaxial epidermis, ab epi= abaxial epidermis, co = collenchyma cells; LES = Lateral epidermal surface, tri=Trichome	
Plate 108	Photomicrographs of Petiole Section of <i>Euphorbia serpens</i> Kunth (a): Transverse Section (100 $\mu\text{m}$ ), (b): Section of adaxial epidermis (50 $\mu\text{m}$ ), (c): Lateral epidermal side (10 $\mu\text{m}$ ), (d): Section of median vascular bundle showing xylem and phloem (5 $\mu\text{m}$ ), (e): Sectioning of trichome (10 $\mu\text{m}$ ), (f) Polygonal epidermis cells parenchyma and collenchyma cells(10 $\mu\text{m}$ ).	346
Plate 109	Photomicrographs of Petiole Section of <i>Ricinus communis</i> L. (a): Transverse Section (100 $\mu\text{m}$ ), (b): Section of median vascular bundle (20 $\mu\text{m}$ ), (c): Lateral epidermis side and parenchyma cells (10 $\mu\text{m}$ ), (d): Section of abaxial epidermis (10 $\mu\text{m}$ ), (e): Collenchyma cells (5 $\mu\text{m}$ ), (f) Ventral epidermis side and cuticle (10 $\mu\text{m}$ ). TS=Transverse section, MVB= Median Vascular Bundle, ad epi= adaxial epidermis, ab epi= abaxial epidermis, co = collenchyma cells; pc = parenchyma cells; VES= Ventral epidermal surface, ct= Cuticle	347

## List of Figures

<b>Figures</b>	<b>Title of Figure</b>	<b>Page#</b>
Figure 1	Flow sheet showing research outline	11
Figure 2	Map of the study area: Thal Desert	13
Figure 3	Graphical illustration of plant families of dicot flora	39
Figure 4	Life Form Classification of Dicot flora	40
Figure 5	Average pollen size variability among Amaranthaceous taxa	80
Figure 6	Polar to equatorial distance (P/E ratio) among Amaranthaceous taxa	80
Figure 7	Mean exine thickness measurements among Amaranthaceous taxa	81
Figure 8	Average variations in pore diameter among Amaranthaceous taxa	81
Figure 9	Mean pore density variations among Amaranthaceous taxa	82
Figure 10	Average interpore distance variability among Amaranthaceous taxa	82
Figure 11	Dendrogram clustering showing relationship among different Amaranthaceous species	83
Figure 12	Principal component analysis (PCA) performed with the pollen quantitative data from Amaranthaceous species	84
Figure 13	Mean pollen size variations among Asteraceous taxa	104
Figure 14	Polar to equatorial diameter index ratio among Asteraceous taxa	104
Figure 15	Average colpi length and width variations among Asteraceous taxa	105
Figure 16	Mean exine thickness variations among Asteraceous taxa	105
Figure 17	Spine measurement variations among Asteraceous taxa	106
Figure 18	Mean distance variations of mesocolpium among Asteraceous taxa	106
Figure 19	Cluster groupings through UPGMA dendrogram clustering among Asteraceous taxa based on quantitative pollen morphometrics	107
Figure 20	Principal component analysis (PCA) biplot of matrix variables of Asteraceous pollen	108
Figure 21	Mean pollen size variations among Fabaceous taxa	123
Figure 22	Polar to equatorial diameter ratio (P/E) among Fabaceous taxa.	123
Figure 23	Average variations in exine thickness among Fabaceous taxa	124
Figure 24	Pollen fertility and sterility percentage count among Fabaceous taxa	124
Figure 25	UPGMA tree of Fabaceous taxa based on pollen quantitative characters	125
Figure 26	Principal component analysis (PCA) case scores of the palynological characters based on Fabaceous pollen traits	126
Figure 27	Average pollen size variations among Solanaceous taxa	136
Figure 28	Polar to equatorial diameter index ratio (P/E) among Solanaceous taxa	136
Figure 29	Mean colpi length and width variations among Solanaceous taxa	137
Figure 30	Average exine thickness measurements among Solanaceous taxa	137
Figure 31	Mesocolpium distance mean variations among Solanaceous taxa	138
Figure 32	Average variations among polar area index in Solanaceous taxa	138
Figure 33	Pie chart showing percentages of overviewed dicot and monocot.	213
Figure 34	Graphical representation of number of taxa within different angiosperm families whose seed morphology has been published.	213
Figure 35	Comparison of mean seed length and width in dicot angiosperm species	214

Figure 36	Graph showing seed length-to-width (L/W) ratios in studied dicot species	214
Figure 37	Cluster groupings through dendrogram of dicot angiosperm desert species based on qualitative seed morphological traits	215
Figure 38	Principal component analysis (PCA) biplot of matrix variables of seeds of dicot taxa	216
Figure 39	Mean size variation of epidermal cells along adaxial and abaxial surfaces	247
Figure 40	Stomatal length and width comparison along adaxial and abaxial sides	247
Figure 41	Average variation in stomatal Index on adaxial and abaxial surface	248
Figure 42	Mean variations of trichome size along epidermis surface	248
Figure 43	Variation in trichome index on adaxial and abaxial surface	249
Figure 44	Dendrogram based hierarchical clustering of foliar anatomical features	249
Figure 45	Epidermal cell size variations among Fabaceous taxa	265
Figure 46	Subsidiary cell size variations along among Fabaceous taxa	265
Figure 47	Stomatal size variations along epidermal surface among Fabaceous taxa	266
Figure 48	Stomatal index variations along epidermis among Fabaceous taxa	266
Figure 49	Mean size variation of epidermal cells among Cucurbitaceous species	280
Figure 50	Average stomatal size variations among Cucurbitaceous species	280
Figure 51	Stomatal pore mean size variations among Cucurbitaceous species	281
Figure 52	Average guard cell size variations among Cucurbitaceous species	281
Figure 53	Subsidiary cell size variations among Cucurbitaceous species	282
Figure 54	Mean trichome size variations among Cucurbitaceous species	282
Figure 55	Mean epidermal cell size along adaxial surface in Capparaceae species	295
Figure 56	Average stomatal size along adaxial surface in Capparaceae species	295
Figure 57	Average subsidiary cell size along adaxial surface in Capparaceae species	296
Figure 58	Average guard cells size along adaxial surface in Capparaceae species	296
Figure 59	Mean stomatal pore size along adaxial surface in Capparaceae species	297
Figure 60	Mean epidermal cell size along abaxial surface in Capparaceae species	297
Figure 61	Stomata length and width along abaxial surface in Capparaceae species	298
Figure 62	Mean subsidiary cell size along abaxial surface in Capparaceae species	298
Figure 63	Mean guard cell size along abaxial surface in Capparaceae species	299
Figure 64	Mean stomatal pore size along abaxial surface in Capparaceae species	299
Figure 65	Cluster groupings via UPGMA dendrogram of Amaranthaceous species based on petiole morphometric features.	309
Figure 66	Mean epidermal cells size on Abaxial surface in Amaranthaceous taxa	328

Figure 67	Mean epidermal cells size on Adaxial surface in Amaranthaceous taxa	328
Figure 68	Variations of parenchyma cell size in Amaranthaceous taxa	329
Figure 69	Mean collenchyma cell size variations in Amaranthaceous taxa	329
Figure 70	Mean epidermal cells size on abaxial surface in Euphorbiaceous taxa	348
Figure 71	Mean epidermal cells size on adaxial surface in Euphorbiaceous taxa	348
Figure 72	Mean collenchyma cell size variations in Euphorbiaceous taxa	349
Figure 73	Variations of parenchyma cell size in Euphorbiaceous taxa	349

## List of Tables

<b>Tables</b>	<b>Title of Table</b>	<b>Page#</b>
Table 1	Checklist of Dicot flora of Thal Desert with life form, vouchering data, localities and geographical coordinates	31
Table 2	Cumulative variance and eigenvectors of principal component analysis (PCA) using quantitative palynological characters	72
Table 3	Pollen morphological characters among desert inhabited Amaranthaceous species	74
Table 4	Qualitative pollen micromorphological features of desert inhabited Amaranthaceous taxa	75
Table 5	Pollen morphometric characters measurements among Amaranthaceous pollen	76
Table 6	Eigenvalues, percentage of total variance explained by each axis among Asteraceous pollen	94
Table 7	Qualitative palynological attributes among desert inhabited Asteraceous species	96
Table 8	Qualitative pollen morphological features of desert inhabited Asteraceous species	97
Table 9	Quantitative measurements of Asteraceous pollen data among desert inhabited Asteraceous species	98
Table 10	Quantitative pollen measurements data of desert inhabited Asteraceous species	99
Table 11	Principal component analysis (PCA) % variance loadings for the Fabaceous pollen	118
Table 12	Micromorphological characters of Solanaceous pollen	132
Table 13	Measurements of the pollen diameter, colpus, exine layer, mesocolpium and polar area index (PAI), of pollen grains of Solanaceae	133
Table 14	Comprehensive review literature on seed micro-morphological features of angiosperms	179
Table 15	Qualitative and quantitative seed micro-morphological attributes among Desert Dicot Angiosperms	196
Table 16	SEM ultrastructural seed coat micro-morphological features of selected Desert Dicot Angiosperms	198
Table 17	Matrix of qualitative morphological features coding used for the statistics	200
Table 18	Matrix with qualitative seed morphological ultrastructure features coding used for the UPGMA dendrogram and PCA analysis	201
Table 19	Variance for seed morphological metric variables of the first and the second axis of PCA component analysis	203
Table 20	Qualitative analysis of Adaxial and Abaxial surface of Leaves among Amaranthaceous taxa	230
Table 21	Qualitative observation of leaf adaxial and abaxial surface among Amaranthaceous taxa	232
Table 22	Quantitative measurements of leaf epidermal cells, stomata and trichomes of Amaranthaceous taxa	235
Table 23	Quantitative measures of stomatal pore, guard and subsidiary cells of	237



	Amaranthaceous taxa	
Table 24	Foliar qualitative characters of epidermis among Fabaceous species	257
Table 25	Quantitative data analysis for stomatal index among Fabaceous species	258
Table 26	Quantitative measurements of foliar epidermal anatomical characters among Fabaceous taxa	259
Table 27	Qualitative foliar anatomical characters of Cucurbitaceous species	275
Table 28	Quantitative foliar anatomical features of adaxial side epidermis and trichomes among Cucurbitaceous species	276
Table 29	Quantitative foliar anatomical features of adaxial side stomata among Cucurbitaceous species	276
Table 30	Quantitative foliar anatomical features of abaxial side epidermis and trichomes among Cucurbitaceous species	277
Table 31	Quantitative foliar anatomical features of abaxial side stomata among Cucurbitaceous species	278
Table 32	Qualitative foliar anatomical features of Capparaceae species	290
Table 33	Quantitative measurement of epidermal cells and stomata for Stomatal Index determination	291
Table 34	Quantitative characters of foliar epidermal anatomy of Capparaceae species.	292
Table 35	Petiole micro-morphological qualitative attributes of Amaranthaceous species	311
Table 36	Quantitative Characters of Petiole anatomical studies of selected Amaranthaceous species	312
Table 37	Petiole micro-morphological qualitative attributes of Euphorbiaceous species	337
Table 38	Quantitative measurements of petiole anatomical traits of selected Euphorbiaceous species	338
Table 39	Quantitative measurements of petiole anatomical traits of selected Euphorbiaceous species	339

## ACKNOWLEDGEMENT

Up and above anything else, all praises to The Allah Almighty alone, the Omnipotent, the Merciful and Compassionate. Knowledge is limited and time is short to express the dignity, the Propitious, the Benevolent and Sovereignty of ALLAH, Whose blessings and glories have flourished my thoughts and thrived my ambitions. Peace and blessings of Allah be upon last Prophet Hazrat Muhammad (PBUH). Trembling lips and wet eyes pray for the Holy Prophet Hazrat Muhammad (PBUH) for enlightening our conscience with an essence of faith in Allah, converging all His kindness and mercy upon him.

I gratefully acknowledge the support of Chairman, Department of Plant Sciences, Professor Dr. Mushtaq Ahmad for providing excellent spectral facilities during the entire course of my research work.

I take pride in acknowledging the insightful guidance of my Supervisor Dr. Muhammad Zafar (Associate Professor), Department of Plant Sciences, Quaid-i-Azam University, Islamabad, Pakistan. His reliable comments, dynamic supervision, vast experience, sincere help, and erudition throughout the course of my research work, guided me in faltering steps. No words can adequately express my deep gratitude to my supervisor for all his guidance and kindness. I sincerely thank for all his trust and support to pursue my research work under his guidance.

In my journey towards this degree, I have found a teacher, a mentor, an inspiration, a role model and a pillar of support in my research work; Prof. Dr. Mushtaq Ahmad (Chairman), Department of Plant Sciences, Quaid I Azam University, Islamabad, Pakistan. He has been there providing his heartfelt support and guidance at all times and has given me invaluable guidance, inspiration and suggestions in my quest for knowledge. Without his able guidance, this thesis would not have been possible and I shall eternally be grateful to him for his assistance.

I wish to express my gratitude to my teachers for their active help and support. I would also like to acknowledge Professor Dr. Mir Ajab Khan and Dr. Shazia Sultana (Post Doc.) for their able guidance and continuous support throughout my Ph.D. I gratefully acknowledge the funding received for my Ph.D. from the Higher Education Commission (HEC), Pakistan for the financial support under project no. 7837/Federal/NRPU/R&D/HEC/ 2017.

I have great pleasure in acknowledging my gratitude to my colleagues and fellow research scholars of Plant Systematics & Biodiversity lab, for their endless support and good wishes. I wish to express my deep sense of appreciation and gratitude to my lab fellows; Dr. Ghulam Yaseen, Nabila, Dr. Nabila, Rozina, Maria Ameen, Shaista Jabeen, Shabir Ahmad and Naveed Abbas for their help and cooperation during various steps of my research. I also owe my special thanks to Mr. Sufyan and Mr. Farooq for their kind help during my research work.

**Salman Majeed**

## ABSTRACT

This project is confined to presenting taxonomic information on angiosperms plant species from the Thal Desert Punjab-Pakistan. This study elucidates the micromorphological characterization of Dicot flora adapted to arid environment. We hypothesized that comparative micromorphological attributes of pollen, seed, and the leaf of Dicot floral species were analyzed using light (LM) and scanning electron microscope (SEM). A total of 111 Dicot floral species were categorized into 80 genera and 26 dicot families. Pollen grains of dicot species were acetolyzed, observed and measured through statistical software. Dicot species showed variation in shape, type, aperture, and exine sculpturing. Amaranthaceae was the dominant family revealed smooth sparsely granulate, scabrate-spinulose, micro-spinulose perforate, micro-echinate scabrate to meta-reticulate, granulate, nano-spinulate, and micro-echinate perforate exine stratification. Exine thickness was noted highest in *Salsola tragus* 2.15  $\mu\text{m}$  and lowest in *maranthus. graecizens* 0.78  $\mu\text{m}$ . The maximum number of pores was examined 32-36 in *Digera muricata*. Taxonomic utility of seed microstructural features has been explored using scanning microscopy. Seeds varied in shape from elliptical to obovate, D-shaped, reniform, rhomboid, and ellipsoidal. The periclinal boundaries, and sculpture pattern of the anticlinal wall were generally rugulate, reticulate, and striate, papillate and rugose, and undulate granulate. The phenetics of 109 character-states using principal component and dendrogram statistics supported the affinities among desert species. Foliar micromorphology of leaf and petiole vasculature of dicot species were analyzed. Both surfaces of the leaves exhibited differences in the microanatomy of stomata, epidermis, anticlinal wall, and diversity of trichomes. Stellate trichomes were observed on both surfaces of *Aerva lanata* while capitate trichomes in the inter-coastal zone in *Alternanthera sessilis*. The largest trichome length was measured for *Alternanthera sessilis* (127  $\mu\text{m}$ ) along adaxial side, while along abaxial surface was calculated for *Amaranthus graecizens* (117.5  $\mu\text{m}$ ). Petiole transverse sectioning of Amaranthaceous and Euphorbiaceous taxa showed petiole and vascular bundle shape, petiole length, trichomes, layers of collenchyma, and shape of parenchyma cells. Petiole shapes observed are cordate, slender, spherical, and ovoid. The annular shape was dominant in collenchymatous cells. The taxonomic keys were also developed to reveal micromorphological markers for the correct identification. The identified micromorphological traits provide base for correct identification of dicot angiosperms and their systematics relationships.



**CHAPTER: 1**

**Introduction**

## 1.1 Desert Rangelands

Rangelands constitute approximately 40% of the world's geographical area and are as significant ecologically as rain forests. Arid ecosystems cover one-third of the total land surface, contain 14% of the world's population, and contribute significantly to global agriculture (Nicholson, 2011). Desert is classified as a biome for climatically arid terrestrial parts of Earth with little vegetation cover. Desert ecosystems are vulnerable ecosystems and, sites of overexploitation and resource depletion, which have an indirect impact on human habitation and lifestyles. Desert rangelands, like other arid zones, face significant natural disruptions such as high soil deterioration and relatively low annual rainfall, which may be induced in part by climate change due to their geographical site. Anthropogenic factors like overgrazing and wood harvesting exacerbate these problems. When these factors are considered combined, they contribute to decreasing biological variety and rangeland productivity, as well as high rates of erosion, both of which are widespread issues (Gamoun et al., 2018; Tarhouni et al., 2014). Desert rangeland degradation is an unfavorable trend toward decreased sustainability. Despite decreased biological production in desert environments, these resources' particular usage values play critical roles in their long-term survival. Thus, rehabilitation and environmental sustainability in drylands are the primary approaches utilized to ensure their long-term usage and to prevent desertification, and long-term maximum production is a key management factor (Gamoun 2014).

Deserts cover roughly one-third of the earth's land surface, with low and variable rainfall, nutrient-poor soils, and little vegetation cover. Deserts provide numerous benefits that can suit the needs of both local inhabitants of the communities. These assets include water, food, medicine, and raw resources (Bidak et al., 2015). Desert rangeland briefly explains the areal extent and provincially based distribution of this ecosystem type; and it explains in precise detail the flora, fauna, and microflora that make up the distinct ecosystems (Tarhouni et al., 2014). Pakistan's deserts cover 11 million hectares (13.82% of the country's total land area) and are located in the central and southern regions. Sand dunes can grow up to 150 meters above the ground. These dunes are widely scattered and range in elevation from 100 to 1000 meters above sea level. These are monsoon-type deserts, which are characterized by a

wind system that fluctuates seasonally in response to climate changes across continents and oceans.

## 1.2 Species Diversity in Deserts

The species diversity and ecosystem productivity typically correspond on a global scale, deserts should be predicted to have very low biodiversity due to limited resources and harsh climate conditions. Deserts have a high degree of geographical variation in their physical environments, which generally supports increasing species diversity and endemism. Plant diversity and endemism in the world's deserts are surprisingly high, in contrast to hyper-arid regions. Alpha-diversity, the measure of species diversity on a regional level, can be remarkably high, as seen in the Negev Desert, where some areas have over 100 species per 0.1 ha. Annual plant species make a significant contribution to desert biodiversity and are the basis for ecological adaptations and their conservation. Desert environments often have little biomass and little to no vegetation. Small xeric, halophilic shrubs and resilient perennial herbaceous plants make up the majority of the desert's topography. Researchers neglect deserts because they are difficult to access and have hostile climates while exploring flora and their usage in the economy. Arshad and Rao (1994) conducted preliminary research on the flora of Cholistan and the Nara Desert. The vegetation growth in deserts is significantly influenced by the harsh climate, arid soils, and extreme temperature changes. The majority of natural plants have developed xeric adaptations. The density of flora in the Thal desert rises from west to east as rainfall increases. The Thal desert is mostly covered with arid open grassland, shrubland, forestland, and ephemerals (Majeed et al., 2023).

## 1.3 Plant Taxonomy

Taxonomy is a biological science concerned with the identification, description, categorization, and naming of organisms at species level. Plant taxonomy comprises the tasks of identifying and classifying species. Taxonomy is a dynamic field that evolves in response to taxonomists' data collection. Plant data collections of rich biodiversity are required to determine the ancestry of species based on their taxonomic traits. Morphological traits were the primary evidence for the broad taxonomy, which was frequently employed by beginners for identification. Plant taxonomy became more

precise in higher education regarding the basis of classification based on morphological, anatomical, histologic, and genetic traits. The development of taxonomy serves as a foundation for all fields of biology, is essential for society, and is also a stand-alone, challenging, and robust hypothesis-driven scientific discipline. (Maskour et al., 2016). Historically, a taxonomic study was carried out and motivated by a sense of interest in biodiversity and a desire to explore a particular species. Taxonomic research is important because it serves as a guideline for essential research and fills the demand for research strategies. It communicates the taxonomic research values to users in related fields and encourages the dissemination of taxonomic knowledge (Kusumawardani et al., 2019).

## 1.4 Dicot Angiosperms

Flowering plants, commonly known as angiosperms, are the most abundant and prominent class of modern plants. Angiosperms (angio = covered, sperm = seed) are flowering plants with seeds enclosed in a fruit that originates from an ovary. There are two classes: Liliopsida, which includes monocots (embryos with one seed), and Magnoliopsida known as dicotyledonous (embryos with two seed leaves). Magnoliopsids are the most primitive flowering plants. Their flowers typically have an enormous part, including multiple petals, stamens, and free carpels (Glimn-Lacy and Kaufman, 2006). Embryos have two cotyledons, occasionally one, and rarely three or four. Cotyledons typically have three vascular bundles. Petiolate leaves with reticulate venation, either pinnate or palmate compound (Takhtajan, 2009).

The characteristic features of the dicot angiosperms are: (1) Ovules are enveloped in a more or less fully closed cavity produced by one or several to many fused carpels; (2) pollen grains are deposited on the stigma surface rather than the ovule's micropyle.; (3) both male and female cotyledons lack gametangia (antheridia and archegonia) and are highly simple and specialized.; (4) triple fusion: one male gamete fuses with the egg cell the other with two free polar nuclei of the female gametophyte and (5) sieve tube perforation with companion cells (Takhtajan, 2009).

## 1.5 Taxonomic Identification

Taxonomic characterization of any plant species identification is the most important step. It depends on taxonomists' fundamental instincts, abilities, and

knowledge. Historically, morphological methods were more commonly used for species identification. However, as research advances, modern taxonomy integrates numerous disciplines like as palyno-anatomy, phytochemistry, molecular genetics, embryology, ecology, and so on. Micromorphology was described by Blair and Turner (1972) as one of the major tools for identifying plants and resolving their taxonomic issues. The development of scanning electron microscopy (SEM) changed the application of micromorphological traits in plant taxonomy. Floristic and taxonomic inventory is helpful for identifying local plants and finding out the particular species of the area, their distribution, growing conditions, species hardness, unique species, and the discovery of new life forms. It helps in recognizing the impact of climate such as drought and desertification on species (Wariss et al., 2014). Plant morphologists and taxonomists tackle problems in different plants group utilizing descriptive and quantitative data on macro and micro characters (Majeed et al., 2022).

## 1.6 Plant Taxonomy in Relation to Pollen Micromorphology

Pollen morphology (aperture type and number, symmetry, polarity, shape, and size) has been considered to be rather stable within a plant species. The mature pollen grains are considered to have defined morphology, and their variation within a species is usually small enough that they have been used as a taxonomic trait. However various studies have shown that pollen parameters, especially pollen size, may change based on environmental factors (Aguilar García et al., 2021). The numbers, orientation, and structure of pollen apertures, exine stratification, and, in some cases, size and sculpting are the most important trends in angiosperms at higher taxonomic levels (Bose et al., 2012). Researchers identify plants based on the comparison between pollen microscopic characters of examined specimens in order to determine differences between them. Scanning electron microscopy (SEM) is the advanced form of microscopy that is used for the characterization of pollen morphological features of plants (Hameed et al., 2020).

Pollen morphology in the Sinai Peninsula has been a subject of study in the context of the endemic species (El-Ghamery et al., 2018). The pollen morphological features variability in the eastern ACA desert was characterized by Lu et al. (2018). While recently Wan et al., (2020) investigated the morpho-palynology of *Caragana* species from the Alashan desert Mongolia. Researchers identifies plants based on a



comparison between microscopic characters of examined specimens in order to determine differences between them. Scanning microscopy visualization using advanced tools of microscopic imaging for the characterization of morphometric traits of plants. SEM can be utilized to distinguish between taxonomic features of closely related genera (Raza et al., 2022).

## 1.7 Plant Taxonomy in Relation to Seed Micromorphology

Seeds are critical to a plant's ability to regenerate. Many plant species rely on viable and dormant seeds in the soil (seed bank) for regeneration, and they are an important reflection and resilience of unpredictable and severe environments like deserts (Commander et al., 2017). Many useful aspects of seed morphology have been discovered for studying systematic relationships in a wide range of plant groups. In addition to the morphological features of seeds, the texture and sculpting aspects of the outer seed coat vary greatly between species and can be systematically proved to be significant (Varela et al., 2021). Microscopic imaging with a scanning electron microscope is another method for determining the boundaries between species. Scanning microscopy is an effective technique for determining the identity of seeds. SEM combines extreme magnification and deep ultrastructure aspects to uncover variations that optical microscopy is not able to identify (Ahmad et al., 2021; Rashid et al., 2021; Rewicz et al., 2020).

Because of its high intraspecific uniformity, seed shape has been considered as a major source of important evolutionary information. A number of angiosperm taxa have already undergone extensive seed morphological studies in conjunction with phenetic or phylogenetic analysis at the genus level (Ghimire et al., 2018). Seed surface properties provides detailed information for taxonomic classification. Cell size, shape, periclinal and anticlinal wall sculpturing, and microrelief are all important taxonomic and biological attributes of the seed testa cell (Lin and Tan 2017). Micromorphological and ultrastructural data have been valuable in phylogenetic analyses and seed plant classification. It is also important in modern angiosperm systematics (Rashid et al., 2018). Because ornamentation and sculpturing on seed coats are recognized as non-specific for revealing taxonomic relationships at the inter-specific level, comparative information about seed micromorphology in connection to their climate preferences is needed (Chaudhary et al., 2014). Seed morphological qualities are recognized to be

useful for species delimitation, and taxonomic investigations reveal that many seed morphological traits are evolutionarily stable traits with a degree of inertia in their evolution (Tomlinson, 2012).

## **1.8 Plant Taxonomy in Relation to Microscopic Anatomy**

Comparative anatomical studies of angiosperms have a remarkable track record, with anatomical features being used to solve challenging taxonomic difficulties with considerable success. Characters' worth is determined by their consistency. The greater the reliance that can be placed on a character, the more consistent it is (Ingole and Kaikade, 2015). In plant taxonomy, anatomical features are very essential. Anatomical features have proven to be more beneficial in defining higher taxonomic ranks like genera and families (Sheikh and Kumar, 2017). The botanical control of species especially anatomical is necessary for the pharmaceutical and spices industries (Aoyama et al., 2019).

Anatomical features of angiosperms have been frequently used to identify species at various taxonomic levels and to determine their taxonomic affinities. The higher taxonomic ranks, such as genera and families, can be recognized more accurately by anatomical traits. Anatomical traits are highly effective in determining relations between orders and genera, and their features have become increasingly essential in evolutionary relationships. Comparative anatomy of leaves with attributes of the transverse section of leaves has shown useful for angiosperms species identification and understanding of existing taxonomy linkages (Dias et al., 2013). The introduction of the SEM has provided a new dimension to the morph-structural traits that are available for the detailed evaluation of the leaf surface. The trichome morphology was studied, and the taxonomic problem was resolved using the scanning visualization approach. The SEM technique revealed that the leaf surface was covered in different kinds of trichomes, and that the stomatal complex features had a significant systematic relevance (Beilstein et al., 2006).

Foliar microanatomical characters provide sufficient structured variations about specific plant families with evidence of their ecological adaptations. Diverse epidermal features such as length and types of epidermal cells, stomatal complex, and trichome morphotypes proved to be significant device in the delimitation of dicot angiosperms

(Stenglein et al., 2003). Comparative petiole anatomical sectioning has proven to be morphologically significant in the taxonomy of dicot angiosperms (Okwuchukwu et al., 2017; Song and Hong, 2018). Petiole vascular structures are often complex, with a variety of features that may be of taxonomic significance. It has been reported that the central area of the petiole is the most reliable area from which a single segment can be taken for comparisons (Talip et al., 2017). Several studies on petiole anatomy were proven to be taxonomically valuable in various angiosperms groups (Abeysinghe et al., 2019; Faghir et al., 2017; Jahanzeb et al., 2020; Priya et al., 2018). Petiole vascularization is of great systematic relevance in angiosperms because it is less influenced by environmental fluctuations (Sheikh and Kumar, 2017). The existence and absence of trichomes in the epidermal layer of the petioles is invaluable taxonomically. Hence Anatomical traits of the petiole have taxonomic value, can be used in categorization, and can help identify species (Talip et al., 2017).

## 1.9 Justification of the Project

The majority of the world's biodiversity hotspots are located in tropical regions with only 1.82% of hotspots in dry zones, indicating the deserts are under-prioritized in international biodiversity conservation plans (Myers et al., 2013). Hot deserts are locations of high endemism where species are unique, geographically restricted, and vulnerable. Furthermore, plant species in desert places are suited to arid climates, which is important in their evolutionary, ecological, and taxonomic potential in the context of global change (Malyshkina and Ward, 2016).

The subtropical desert in arid zones served as a corridor for the Silk Road and One Belt and One Road, linking East and West economic and cultural exchanges. Governments and the research community are concerned about the link between human sustainable growth and the dynamic change in the Thal desert ecosystem. However, a barrier to a greater insight into the development and management of this desert ecosystem is the lack of a taxonomic spectrum of the dominant species. This temperate desert ecology provides a relationship between taxonomic assemblages of unique desert floral inventory (Lu et al., 2018). In this project, we utilize morphological and palyno-anatomical tools for dicot angiosperms to link taxonomic assemblages to specific Thal desert vegetation, providing a solid base to trace the evolution in the desert ecosystem. In recent years field explorations, regional floras, and taxonomic reviews about Dicot

angiosperms have been increasingly published, although the taxonomic data about the Dicot flora from the Thal desert is lacking and show significant research gaps.

Systematics exploration is of great importance to record the occurrence of plant species. Their taxonomic characterization enables one to describe the economic utilization of wild botanicals. To undertake such an investigation it is important that the flora of the region should be well known. It would be possible to evaluate the vegetable wealth of the region only when all the plants are properly collected and preserved, accurately identified, and described for a system of classification. In Pakistan, systematics is now a well-recognized field, and explored various eminent angiosperm species to characterize their taxonomic traits to identify them correctly but still many regions such as deserts lands are still unexplored systematically. Many taxonomic studies on higher land plants have been conducted in various regions of Northern Pakistan (KPK and GB), Azad and Jammu Kashmir, Plain areas of Punjab, Baluchistan, and Sindh but the majority of the studies are conducted in Northern mountainous regions of Pakistan while, southern plain regions of Pakistan reported few studies or still completely unexplored. Among such regions, Thal deserts rangeland of South Punjab are not explored yet. With respect to spectrum of taxonomic elaboration dicot angiosperm species in the Thal deserts has been ignored for many reasons. The major reasons are unavailability of research and academic institutes in the desert area.

The study of systematic features representing Dicot flora has proved very helpful in taxonomy at different hierarchical levels. Therefore, this study is in the continuity of previous work conducted on the Thal desert (Ahmed et al., 2014; Chaudhari et al., 2013; Khan, 2009; Malik et al., 2015; Shaheen et al., 2014), however, the majority of above-reported studies from Thal desert presents only checklist of plant species along with ethnomedicinal documentation without any focus on pollen, seed and anatomical micromorphological traits of dicot flora. Thal desert presents a distinct geographical location in the Deserts of Pakistan and presents particular habitats for endemic and most important medicinal plants.

Biodiversity serves as a chief character for the appropriate functioning of an ecosystem. The deserts of Pakistan is enriched with xeric flora and their growth is favoured by various habitats. In order to find out the association among closely linked taxa systematic enquiries are very useful. Intricate taxa can be identified by taxonomic

tools (Rodríguez-Estrella et al., 2019). In taxonomic studies of different plant families a key role is played by the scanning and light microscopy of pollen surface, seed morphotypes and microanatomical characters (Hussain et al., 2018). The notion of characterization is essential for taxonomic research in which basic information is provided by the identification and classification. The description and classification of plants is the major route for evolutionary pattern recognition (Dickison, 2000).

Life form diversity in desert rangeland is intrinsically linked to topography and land cover. The distribution of life forms in Thal reflects a typical desert flora, with therophytes and chamaephytes comprising the majority of species. Thal vegetation is not consistent; it varies from year to year depending on moisture content. Many factors influence the growth, reproduction, and distribution of plant communities in Thal deserts, including geography, climatic conditions, and human impacts (Fakhireh et al., 2012). The surveys of the Thal desert dicot flora, as well as identification, vegetative cover, life forms, and floristic inventory of the dicot angiosperms were taken into account. Voucher herbarium specimens of dicot angiosperms were pressed and deposited in the Herbarium of Pakistan (ISL) for future reference.

This project explore the diversity of dicot angiosperms, the most important groups of land plants and summarize available taxonomic data at the family level. The work is a helpful source of reference not only for taxonomists but for all who are interested in the different aspects of plant diversity. It contains evidence from practically all disciplines linked to modern systematics. An updated floral inventory of Dicot flora was provided, along with diagnostic traits, keys for identification, and literature references. The current project was designed to revise and describe, micromorphological taxonomic variations of vegetative and reproductive structures of Dicot flora from the Thal desert with a set of identification characters that could be provided for dicot angiosperms. This project provided information on the taxonomic characterization of Dicot flora by incorporating a multidisciplinary approach using morpho-anatomical, palynological, and seed sculpturing data using light and scanning electron microscopy (LM and SEM). The study also examines the taxonomic relationships within the Dicot angiosperms by particular stress on medicinally important species of the Thal desert. The systematics of dicot flora has not been studied specifically from the Deserts of Pakistan, thus this work provides baseline information

that can aid in the identification and classification of dicot angiosperms. The systematic classification of the dicot angiosperms is still problematic from the perspective of its taxonomical relevance. Therefore, the current project evaluates the taxonomic characterization of dicot angiosperm flora, based on multiple parameters including morpho-anatomy, palynology, and seed morphometry to aid in their correct identification.

### **1.10 Aims of the Study**

- Enlist comprehensive floristic checklist of Dicot flora along distribution localities and their geographical coordinates.
- Identification and preservation of Dicot flora using flora of Pakistan and herbarium techniques.
- Micromorphological studies based on taxonomic tools using palynological (SEM), seed ornamentation (SEM) and anatomical characterization of leaf and petiole (LM and SEM) for accurate Dicot flora identification.
- Interpretation of taxonomic micromorphological differences based on palynomorphs, seed morphotypes and microanatomical structure at species, genus and family level.



**CHAPTER: 2**

**Materials and  
Methods**

## 2.1 Research Work Outline

The research project's approach is outlined in this section. The choice of the research area, the sampling method, and the experimentation protocols are described briefly. It also details the source of the sample data, as well as the process of data collection and analysis. The Thal desert located in the Punjab province was selected to collect dicot flora throughout the desert rangelands of Thal, various field trips were carried out from March 2021 to August 2022. Field trips were carried out in different seasons across various places of the Thal desert. The study's main objective is to find out the taxonomic markers of dicot angiosperms. The laboratory analysis of the selected plants was performed in Plant Systematics and Biodiversity Laboratory of Quaid-i-Azam University Islamabad. Geographic distribution of plants was mainly taken into account in the current study. The study mainly focuses on the palynological, seed morphological and anatomical perspectives of dicot flora.



**Figure 1.** Flow sheet showing research outline



## 2.2 Study area: Thal Desert

The Thal desert is located in Pakistan's Punjab region, between 31° 10' N and 71° 30' E. The region is a subtropical sandy desert with a maximum width of 112 km and a length of 350 km. Bhakkar, Khushab, Mianwali, Jhang, Layyah, and Muzaffargarh are the districts that constitute this area. Geographically, the Thal Desert is similar to the Cholistan and Thar Deserts. It is a subtropical sandy desert between the Indus and the eastern plains of the Jhelum and Chenab rivers. Thal is defined by arid to hyper-arid climatic conditions; a mean annual rainfall is less than 200 mm, and semiarid climate conditions and a mean annual rainfall of 200-500 mm. June and August are the months with the highest precipitation. The territory is divided into several districts, including Khushab, Mianwali, Layyah, Jhang, Bhakkar, and Muzaffargarh. The major towns of the Thal area are Hyderabad Thal, Mankera, Piplan, Koat Adu, Chowk Azam, Kot Sultan, Gohar wala, Dullewala, Harnoli, Sarai Muhajir, Nawan Jandan Wala, Rangpur, and Noorpur Thal (Shaheen et al., 2014). Ephemerals annual herbs, perennial grasses, and sparse shrubs scattered among small trees cover the majority of the habitat. The common trees of this region include farash (*Tamarix aphylla*), jand (*Prosopis cineraria*), karen (*Capparis decidua*), kikar (*Acacia nilotica*), wan (*Salvadora oleoides*) and *Zizyphus nummularia* (Abd El-Ghani et al., 2017).

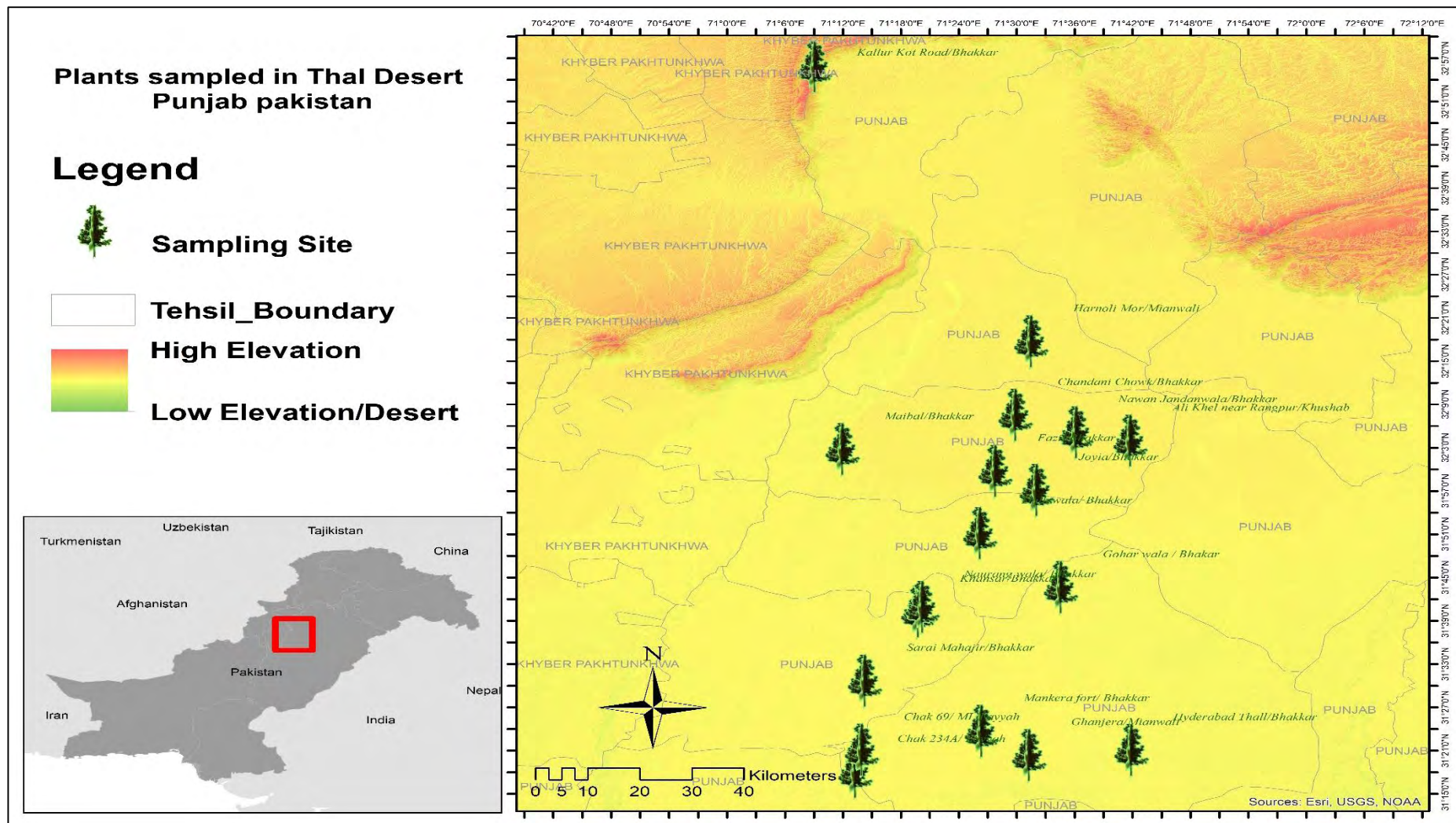


Figure 2. Map of the study area: Thal Desert



**Plate 1.** Panoramic view of Thal desert areas; (a) Noorpur Thal (District Khushab), (b) Hyderabad Thal (District Bhakkar).



**Plate 2.** Panoramic view of Thal desert areas; (a) Mankera Fort (District Bhakkar),  
(b) Chubara Chak 69/ML (District Layyah).

### 2.3 Sampling of Dicot flora

Plants collection, pressing and preservation is one of the most important and basic step in research. Frequent field trips and taxonomic experience is required to achieve the objectives. Dicot floral species were collected by doing various field trips to various localities of the Thal desert including Chubara, Hyderabad Thal, Mankera Fort, Norrrpur Thal, Gohar wala, and Janjoon. The collection was mainly done in the month of March-August, 2021 because almost dicot flora become vigor in spring and monsoon season. A specific area was selected for each trip. Before leaving the field, weather updates were observed, and reference later was placed in the pocket to avoid any trouble during the field. Plants were collected by cutting with a cutter and then placed in the newspaper. Ten samples of each plant were collected. The samples were collected from fresh plants. Voucher number was given to each plant. Unidentified dicot species were tagged. The plants were brought to the Herbarium of Pakistan QAU Islamabad, cleared it of dust particles. They were kept in newspapers and placed under presser. Care was done by regularly changing the newspaper till the plants become completely dry.

### 2.4 Identification of Dicot flora

Identification of plants is the most important and primary step in plant taxonomy. For identification of dicot flora, various sources were used including eflora of Pakistan Tropicos (<https://www.tropicos.org/Project/Pakistan>), compared plants with the already deposited herbarium specimens, and images of plants were searched through Google, various websites, articles, and literature. The identified plants were placed on a herbarium sheets and were stored in the Herbarium of Pakistan, QAU Islamabad (Ali, 1983).

### 2.5 Preservation and Mounting of Dicot Specimens

Completely dried specimens were prepared for poisoning to save it permanently from fungus and other insects. The standard method was applied. Ethanol (absolute 99.8%) was taken in jar and then mercuric chloride (fine crystals) was mixed with it. When the solution was prepared, each plant was dipped in it. Caution was done during poisoning by wearing gloves, glasses, a lab coat and a mask as chemicals are volatile and can harm the body. The preserved samples were placed in the shade for some time

to dry. After drying, plants were mounted on herbarium sheets of standard size i.e. 12×16 inch. Afterwards, specimens were mounted on sheets using glue, and tags were pasted on them on which required information such as specimen name, voucher number, locality, collector name, and date of collection, and collector names were mentioned. For better preservation herbarium sheets were placed into zipper plastic bags so that spores and parts of plants remain to save and these plants can easily be used for different purposes of research. Three voucher specimens of each dicot angiosperm were deposited in the ISL Herbarium (De Vogel, 1987).



**Plate 3.** Field plant collection from Thal area; (a) *Carthamus oxyacantha* M.Bieb.  
(b) *Haloxylon stocksii* (Boiss.) Benth. & Hook. f.



**Plate 4.** Field plants collection from Thal areas; (a) *Opuntia dillenii* (Ker Gawl.) Haw. (b) *Prosopis cineraria* (L.) Druce.





**Plate 5.** Dicot floral Herbarium specimens (a) Preservation (b) Mounting of on herbarium sheets.

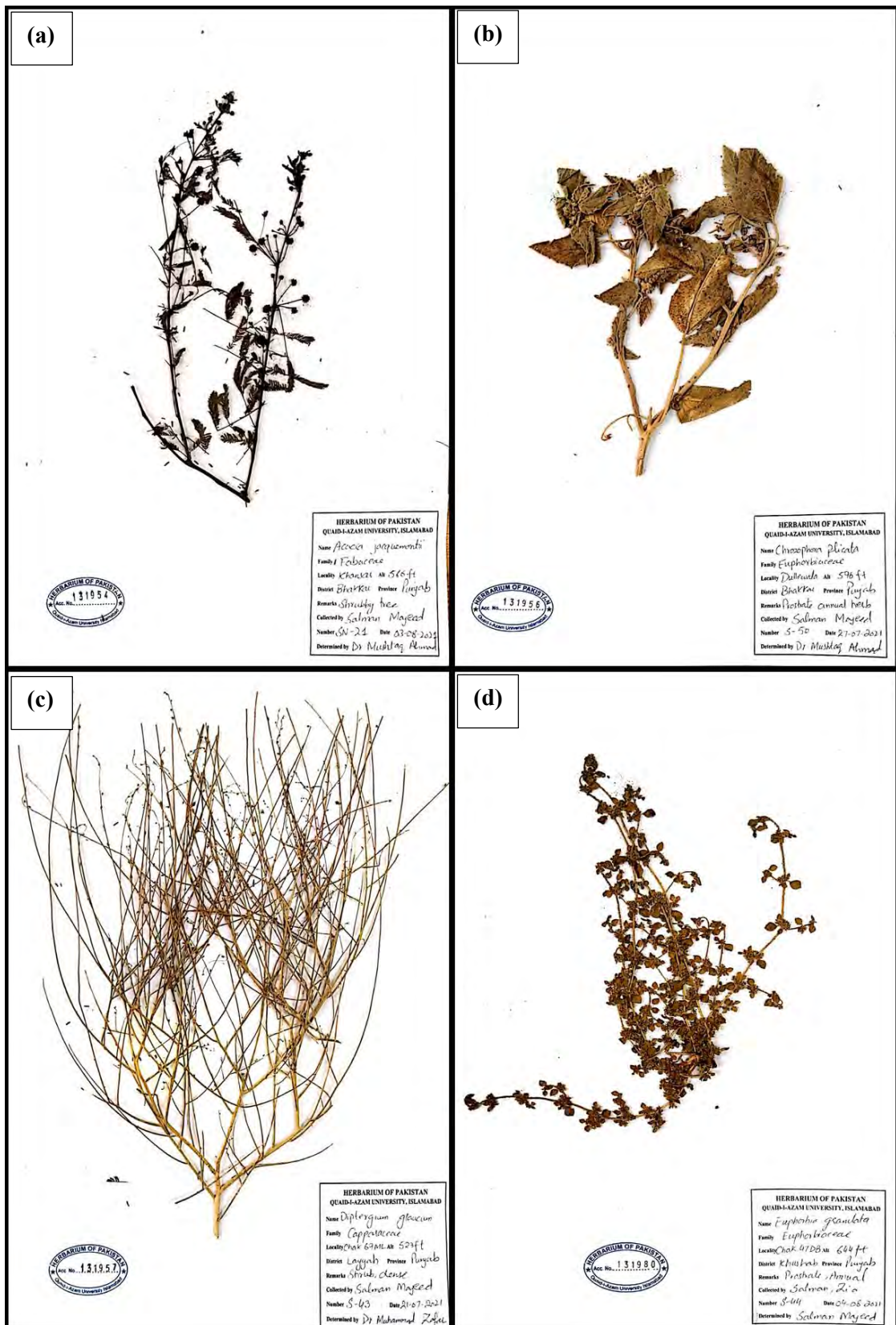


**Plate 6.** Mounted Herbarium Specimens: (a) *Acacia jacquemontii* Benth. (b) *Chrozophora plicata* (Vahl) A.Juss. ex Spreng. (c) *Dipterygium glaucum* Decne. (d) *Euphorbia granulata* Forssk.

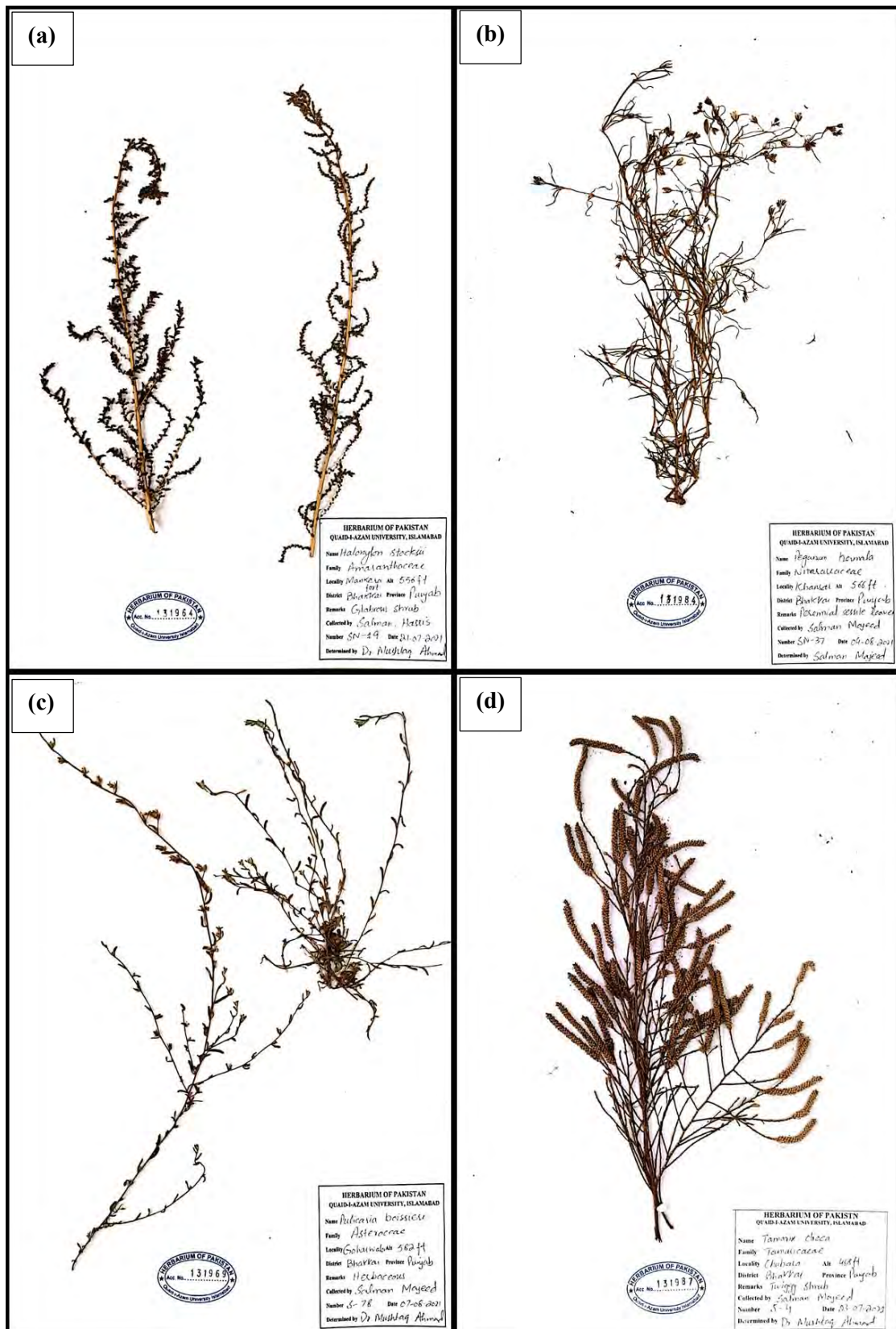


**Plate 7.** Mounted Herbarium Specimens: (a) *Haloxylon stocksii* (Boiss.) Benth. & Hook. f. (b) *Peganum harmala* L. (c) *Pulicaria boissieri* Hook.f. (d) *Tamarix dioica* Roxb.

## 2.6 Taxonomic Characterization via Microscopic Techniques

### 2.6.1 Pollen Micromorphology

#### a) Light Microscopy (LM)

The acetolysis process introduced by (Erdtman 1986) was followed by a few modifications. Anthers from dried specimens were transferred to microscopic slides with forceps. Because some species of flowers are so small that an anther cannot be separated as a whole, the entire flower was photographed on a slide. 1-2 drops of acetic acid were poured into the slide and then plant material was crushed by using a glass rod for about 1 minute. The debris was removed from the slide by using a needle. A drop of glycerin jelly was poured on the slide and then covered with a coverslip. Permanent nail varnish was used to make the slide permanent. A total of 4–5 slides were prepared for each specimen. A well-prepared slide was used for calculations of morpho-palynological features under the microscope Nikon (Japan) eyepiece WF40X-18MM) and readings were taken on 40X magnification. For each quantitative trait, 15 readings were measured to calculate the mean value. The eyepiece (ocular; 10X) scale was used to measure the pollen grains, and the measurement data were then converted into  $\mu\text{m}$  in diameter after multiplying them by 2.5. From each prepared slide 20 pollen was measured to calculate the mean value and standard deviation.

#### b) Scanning Electron Microscopy (SEM)

Pollen grains from dicot angiosperms were prepared for SEM using the method as described by Butt et al., (2018). Pollen were suspended in acetolyzed solution (90% ethanol), after some time pollen were mounted onto the metallic stubs and coated with the particles of gold palladium. Pollen characters were described using the terminologies of Punt et al., (2007) was followed for light microscopic observations and Halbritter et al., (2018) for scanning microscopic descriptions of pollen characters. The definitions of (Nilsson and Pragowski, 1992) were used for pollen shape classes (P/E index). According to Erdtman (1971), the pollen sizes were measured; very small  $< 10 \mu\text{m}$ , small 10-25  $\mu\text{m}$ , medium 25–50  $\mu\text{m}$ , large 50-100  $\mu\text{m}$ , very large 100-200  $\mu\text{m}$  and huge  $> 200 \mu\text{m}$ .

## 2.6.2 Seed Micromorphology

Seed micromorphological aspects such as hilum, pattern anticlinal wall, periclinal thickness, structure of epidermal cells, and cell boundaries were analyzed and measured. A scanning electron microscope (SEM) (Model JEOL JSM-5910) installed at the Central Resource Laboratory Physics Department, University of Peshawar, was used to study the detailed characteristics of seed morphology and ornamentation. Seeds from the collected species were dehydrated in a series of 60–80% ethanol for 4 minutes. The treated seeds were placed directly on stubs and attached with adhesive tape. SEM was used to examine seed specimens that had been sputter coated with gold palladium. Using Polaroid P/N 665 film, the samples were examined and photographed (Ahmad et al., 2022).

## 2.6.3 Foliar Epidermal Anatomy

### a) Lactic acid and Nitric acid Method

Preserved plant specimens were utilized to study foliar anatomy. 2-3 leaves were cut with razor blades and placed in test tubes and boiled for 1-3 minutes in a solution of 30% lactic acid, 70% of nitric acid and 2.0g of potassium chloride. Then leaves were discharged in petri dishes and sweep away the acid solution with water. The adaxial and abaxial epidermis was peeled by using camel hair brushes. The peeled epidermis was then placed on a clean microscope slide with a drop of lactic acid and covered with a cover slip (Nazir et al., 2013). Glass slides were made permanent by using nail paint. 2-3 slides of both surfaces were made to obtain accurate data. The clear slides were then visualized under Nikon (Japan) microscope fitted with an eyepiece (WF10X-18MM).

### b) Nail Polish Method

During this process, leaf epidermis is used to treat with transparent nail polish. Nail polish applied on leaf epidermis and let for few mints to be dry. Nail polish dried and grasp epidermis tightly that it can easily peeled off with the help of forceps. The segment was then peeled and put on a glass slide with a drop of lactic acid and a cover slip. Glass slides were made permanent by using nail paint.

### c) Bleach Method

In this method, preserved plant specimens were utilized to study foliar anatomical characters. 2-3 leaves were cut with razor blades and placed in test tubes. Boil for 1-3 minutes in a solution of 30% lactic acid and 70% nitric acid. After that, the leaves were placed in petri dishes and rinsed to eliminate the chemicals. The leaf epidermis was peeled by using camel hair brushes and a pointed needle. In another petri dish bleach were taken along with peeled section of leaf. Around 2-4 drops of lactic acid were added to peeled section (epidermis) and let it merge for 2-4 minutes. After few minutes the peeled section was taken in glass slide again with a drop of lactic acid and cover slip. Nail paint was used to make glass slides permanent. After then, the clear slides were examined under a microscope.

### d) Scanning Electron Microscopy (SEM)

Dried leaf samples were used for scanning microscopic studies. From each leaf sample, two pieces from both upper and lower sides were taken for mounting on stubs with a two-fold coating of scotch tape. Leaf samples were sputtered with gold palladium and examined with a JEOL JSM-5910 scanning electron microscope in the Physics Department, Peshawar University, Pakistan. Polaroid P/N 665 film was used to take pictorial visualized microphotographs (Shah et al. 2018).

## 2.6.4 Petiole Anatomy

For each species, one individual was examined, with five fully grown leaves growing from the stem node. Petioles were separated from the leaves and grouped as basal, middle, and apical zones. The petiole was preserved using FAA solution, a mixture of formaldehyde, glacial acetic acid, and ethyl alcohol in the following proportions (5:5:95) (Akhtar et al., 2021). Petioles were dipped in the solution for a week. Then, with a few slight modifications, the Okwuchukwu and Uwabukeonye (2017) method was used to dissect the petioles. For about 1 minute, sections were soaked in distilled water before being treated with a series of alcohol concentrations of 70, 80, 90, and 100 %, respectively. Afterwards the dehydrated tissues were processed through xylol for 1 hour. The tissues were immersed in paraffin wax at 58-60° C, as modified by Srivastava et al., (2018).

Tissues were maintained at 60°C in molten wax. Mold was utilized for this purpose, and needle bits were transferred using forceps. Shandon Microtome was used

to trim a piece of about 15–20  $\mu\text{m}$ . The wax ribbon fragment was created by covering slides with egg albumen. The waxy ribbons were spread when the slides were shifted to hot plate and subsequently in an oven at 60° C. The sections are then dewaxed for 5 minutes in pure xylol, before being rehydrated in a series of alcohols; 100%, 90%, 80%, and 70% before being placed in distilled water for 1 minute. The sections were then stained with safranin for about 15 minutes. After that surface was cleaned with xylol for 1 minute before being mounted in Canada balsam. The slides were dried on a hot plate set to 30 ° C (Vovides et al., 2018).

## 2.7 Statistical Analysis

The statistical software (SPSS 16.0) used data to statistically measured the mean, maximum, minimum, and standard error values. About 15 to 20 readings were calculated for each parameter to statistically analyze the mean (minimum-maximum) SE (Zafar et al. 2019).

### 2.7.1 P/E Index

P/E ratio is determined based on equatorial diameter of same pollen as given by Butt et al. (2018).

$$P/E \text{ ratio} = P/E \times 100$$

Where P is the polar diameter and E is the equatorial diameter.

### 2.7.2 Pollen Fertility and Sterility (%)

Using the following formula the fertility and sterility percentage were calculated (Umber et al., 2022).

$$Fertility = F/F + S \times 100$$

F represents the number of fertile whereas S is the number of sterile pollen on ocular.

$$Sterility = S/S + F \times 100$$

S is the number of sterile pollen and F representing number of fertile pollen on ocular.

### 2.7.3 Stomatal and Trichome Index

Stomata measurement was calculated under optical microscope in unit area for stomatal index. Stomatal index was measured using given formula.

$$S.I = S/E + S \times 100$$

(S.I = Stomatal index; E= Epidermal cells per unit area; S= Stomata per unit area).

The Trichome index was also quantified using the equation given below.

$$T.I = T/E + T \times 100$$

(T.I= Trichome index, T= Trichome per unit area, E= Epidermal cells in unit area).

### 2.7.4 Exploratory Multivariate Analysis

The correlation among anatomical, pollen, and seed morphological characteristics of the dicot angiosperms was determined based on Euclidean distance, and the species were grouped using a hierarchical clustering analysis method (Unweighted pair group method with arithmetic mean) UPGMA was carried out with the PAST statistical tool version 3.0 software (Kovach 2013).

Principal component analysis (PCA) was performed to determine the most significant characters accounting for the greatest proportion of the variability. Thus, the pollen and seed morphological characters investigated were first separately subjected to PCA analysis via PAST software. The eigenvalues were plotted in a two-dimensional scatter plot to show variance percentage along the two principal component axis (Metz et al., 2021).

## 2.8 Data Compilation Using Light Microscopy

Permanent slides were placed under light microscope for recording of anatomical studies. Data of petiole anatomical features was observed under 10X and 40X. Readings were taken at 40X resolution of light microscope.

## 2.9 Microphotography

Microphotographs were taken from the light microscope Leica Dialux 20 at different resolutions 4X (25  $\mu$ m) and 10X (10  $\mu$ m) of objective lenses.





**Plate 8.** Microscopic measurement and visualization and (a) Optical microscopic slide data measurement (b) Scanning electron microscopic observation and microphotography



**CHAPTER: 3**

**Results &  
Discussion**

### 3.1 Summary

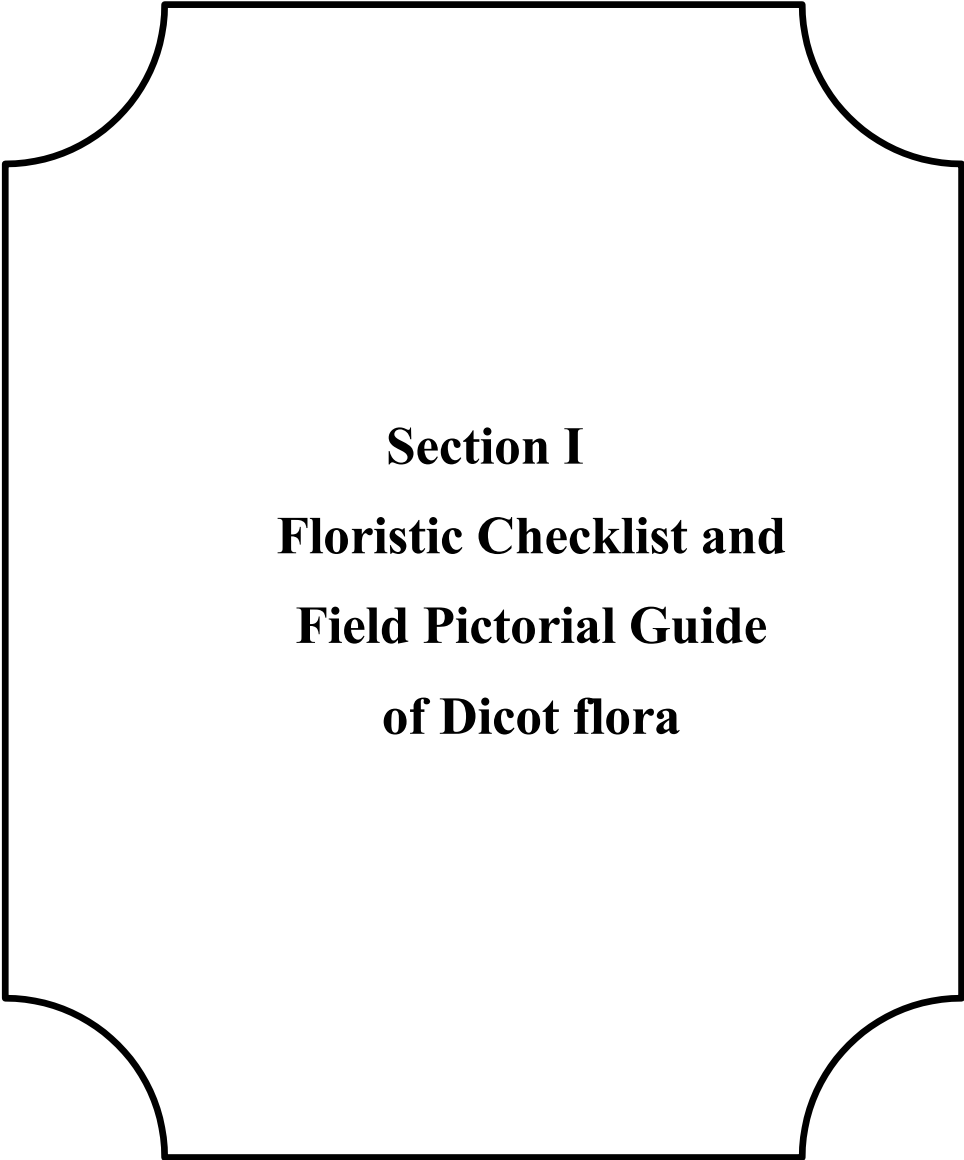
The Thal desert Punjab, Pakistan has been bestowed with rich floristic diversity. Some endemic and medicinal plants of the country are restricted to these desert areas. The current research project was conducted in the selected Districts i.e. Bhakkar, Khushab, Layyah and Mianwali. These areas were explored first time systematically. Previous work was fragmented but the present research project is comprehensive and includes the taxonomic study of 111 desert-inhabited dicot plants classified into 26 families and 80 genera. The results are compiled and presented separately in four sections.

**Section 1:** Floristic checklist of desert dicot plants and field pictorial guide

**Section 2:** Micromorphological qualitative and quantitative attributes. Qualitative features such as pollen shape, types and exine peculiarities. Quantitative traits including polar and equatorial diameter, P/E index ratio, pore size, pore number, exine thickness, colpi size, mesocolpium distance, spine size, and pollen fertility and sterility.

**Section 3:** Micromorphological seed features such as shape, color, size, surface texture, apex, hilum position, sculpturing, anticlinal wall, cell outline, epicuticular projections, texture crudeness, and periclinal wall pattern.

**Section 4:** Qualitative and quantitative leaf epidermal and petiole anatomical characteristic include length width and shape of epidermal cells, subsidiary cells shape and size, morpho-structure of guard cells, anticlinal wall pattern, stomatal complex morphology, size of stomata, trichomes types and diameter. Distinguished taxonomic petiole microanatomical traits include petiole shape, vascularization with the varied number and shapes of vascular bundles, petiole diameter, collenchyma layers, parenchyma shape and epidermal trichomes.



**Section I**  
**Floristic Checklist and**  
**Field Pictorial Guide**  
**of Dicot flora**

### 3.1 Floristic Checklist of Desert Dicot Plants and Field Pictorial Guide

These results are comprised of 111 desert-inhabited dicot plant species belonging to 26 diverse families, organized into a checklist. The floristic checklist in the form of Table 1 includes botanical name, family, life form, voucher specimen, accession number, localities, and geographical coordinates.

The present research examined taxonomic attributes of dicot desert species belonging to various plant families, of which Amaranthaceae was dominant 19 species, followed by 13 species of Asteraceae, Fabaceae (12 species), Euphorbiaceae (nine species), Solanaceae (eight species), Boraginaceae and Cucurbitaceae (six species each), Brassicaceae and Capparaceae (five species each), Azioaceae and Malvaceae (three species each), Apocynaceae, Cactaceae, Molluginaceae, Rhamnaceae, Salvadoraceae, Tamaricaceae and Zygophyllaceae (two species each) and Apiaceae, Bignoniaceae, Convolvulaceae, Meliaceae, Myrtaceae, Nitrariaceae, Nyctaginaceae and Papaveraceae with single species each (Figure 3). Among dicot desert species, the herb was the dominant life form (72 species), followed by 24 shrubby species, trees (10 species), and five climbers species (Figure 4).

During the field surveys, field photography including different photographs of desert inhabited dicot species was captured using Samsung Digital Camera. The floral pictorial guide aids the taxonomist to visualize the dicot floral morphology of live plants in the field for correct identification (Plate 9 to 35).

**Table 1.** Checklist of Dicot flora of Thal Desert with life form, vouchering data, localities and geographical coordinates.

S. No	Dicot species	Family	Voucher Specimen no.	Accession No.	Life form	Locality/District	GPS Coordinates
1.	<i>Acacia jacquemontii</i> Benth.	Fabaceae	SN-21	131954	Shrub	Khansar/Bhakkar	31° 39'42.16"N 71°19'44.38"E
2.	<i>Acacia modesta</i> Wall.	Fabaceae	SN-98	131893	Tree	Dullewala/ Bhakkar	31° 50'33.75"N 71°20'09.76"E
3.	<i>Acacia nilotica</i> (L.) Delile	Fabaceae	SN-14	131896	Tree	Naurang wala Khansar/Bhakkar	31° 40'16.93"N 71°26'09.14"E
4.	<i>Achyranthes aspera</i> L.	Amaranthaceae	SN-40	131967	Herb	Rangpur to Noorpur thal road/Khushab	32° 01'23.31"N 71°49'22.34"E
5.	<i>Aerva javanica</i> (Burm.f.) Juss. ex Schult.	Amaranthaceae	SN-58	131916	Herb	Chak 47DB Rangpur/Khushab	32° 03'17.33"N 71°43'30.63"E
6.	<i>Aerva lanata</i> (L.) Juss.	Amaranthaceae	SN-29	131953	Herb	Gohar wala/Bhakkar	31° 43'04.49"N 71°34'31.31"E
7.	<i>Albizzia lebbeck</i> (L.) Bth.	Fabaceae	SN-2	131951	Tree	Barranga/Bhakkar	31° 54'43.86"N 71°26'45.55"E
8.	<i>Alternanthera ficoidea</i> (L.) Sm.	Amaranthaceae	SN-111	131959	Herb	Ghanjera/Mianwali	32° 19'48.55"N 71°31'14.28"E
9.	<i>Alternanthera philoxeroides</i> (Mart.) Griseb.	Amaranthaceae	SN-83	131952	Herb	Gohar wala/Bhakkar	31° 43'04.49"N 71°34'31.31"E
10.	<i>Alternanthera sessilis</i> (L.) R.Br. ex DC.	Amaranthaceae	SN-91	131915	Herb	Nawan Jandanwala/Bhakkar	32° 04'34.45"N 71°36'07.44"E
11.	<i>Amaranthus graecizans</i> L.	Amaranthaceae	SN-47	131982	Herb	Joyia/Bhakkar	31° 56'33.15"N 71°32'01.75"E
12.	<i>Amaranthus retroflexus</i> L.	Amaranthaceae	SN-94	131985	Herb	Chak 234A/ Layyah	31° 17'29.54"N 71°13'14.15"E
13.	<i>Amaranthus viridis</i> L.	Amaranthaceae	SN-34	131950	Herb	Dullewala/ Bhakkar	31° 50'33.75"N 71°26'09.14"E
14.	<i>Argemone mexicana</i> L.	Papaveraceae	SN-54	132082	Herb	Rangpur/Khushab	32° 01'23.31"N 71°49'22.34"E

15.	<i>Arnebia hispidissima</i> (Lehm.) A. DC.	Boraginaceae	SN-36	131961	Herb	Chak 113 ML/Layyah	31° 10'30.05"N 71°09'13.27"E
16.	<i>Astragalus hamosus</i> L.	Fabaceae	SN-41	131913	Herb	Ali khel/ Khushab	32° 03'30.78"N 71°41'25.17"E
17.	<i>Atriplex stocksii</i> (Wight) Boiss.	Amaranthaceae	SN-110	131949	Shrub	Harnoli Mor/Mianwali	32° 17'09.66"N 71°31'27.43"E
18.	<i>Azadirachta indica</i> A.Juss.	Meliaceae	SN-18	131914	Tree	Gohar wala/Bhakkar	31° 43'04.49"N 71°34'31.31"E
19.	<i>Bassia indica</i> (Wight) A.J.Scot	Amaranthaceae	SN-5	131917	Herb	Sarai Mahajir/Bhakkar	31° 30'07.17"N 71°14'12.96"E
20.	<i>Boerhavia procumbens</i> L.	Nyctaginaceae	SN-39	131912	Herb	Retri/Bhakkar	31° 39'42.16"N 71°19'44.38"E
21.	<i>Brassica nigra</i> (L.) K.Koch	Brassicaceae	SN-51	131962	Herb	Ali Khel near Rangpur/Khushab	32° 03'24.91"N 71°41'43.90"E
22.	<i>Capparis decidua</i> (Forssk.) Edgew.	Capparaceae	SN-13	131918	Shrub	Near Khansar/Bhakkar	31° 39'42.16"N 71°19'44.38"E
23.	<i>Capparis spinosa</i> L.	Capparaceae	SN-73	132083	Shrub	Ghanjera/Mianwali	32° 19'48.55"N 71°31'14.28"E
24.	<i>Carthamus oxyacantha</i> M.Bieb.	Asteraceae	SN-6	131948	Herb	Janjoon/Bhakkar	31° 46'32.06"N 71°35'35.40"E
25.	<i>Centaurea iberica</i> Trev.	Asteraceae	SN-7	131986	Herb	Retri/Bhakkar	31° 39'42.16"N 71°19'44.38"E
26.	<i>Chenopodium album</i> L.	Amaranthaceae	SN-26	131911	Herb	Chak 69/ ML/Layyah	31° 20'31.74"N 71°13'54.25"E
27.	<i>Chenopodium ficifolium</i> Sm.	Amaranthaceae	SN-109	131947	Herb	Chandani Chwok/Bhakkar	32° 06'59.17"N 71°29'49.90"E
28.	<i>Chenopodium murale</i> L.	Amaranthaceae	SN-95	131989	Herb	Maibal/Bhakkar	32° 02'13.36"N 71°11'53.96"E
29.	<i>Chrozophora plicata</i> (Vahl) A.Juss. ex Spreng.	Euphorbiaceae	SN-50	131956	Herb	Dullewala/ Bhakkar	31° 50'33.75"N 71°20'09.76"E
30.	<i>Chrozophora tinctoria</i> (L.) A.Juss.	Euphorbiaceae	SN-77	131910	Herb	Kallur Kot/Bhakkar	32° 09'26.89"N 71°16'10.57"E

31.	<i>Citrullus colocynthis</i> (L.) Schrad.	Cucurbitaceae	SN-3	131919	Herb	Gohar wala/Bhakkar	31° 43'04.49"N 71°34'31.31"E
32.	<i>Cleome brachycarpa</i> (Forssk.) Vahl ex DC.	Capparaceae	SN-86	131946	Herb	Gohar wala/Bhakkar	31° 43'04.49"N 71°34'31.31"E
33.	<i>Cleome viscosa</i> L.	Capparaceae	SN-76	131963	Herb	Janjoo/Bhakkar	31° 46'32.06"N 71°35'35.40"E
34.	<i>Convolvulus arvensis</i> L.	Convolvulaceae	SN-59	131944	Herb	Nawan Jandan wala/Khushab	32° 04'34.45"N 71°36'07.44"E
35.	<i>Conyza candensis</i> (L.) Cronquist	Asteraceae	SN-108	132084	Herb	Maibal/Bhakkar	32° 02'13.36"N 71°11'53.96"E
36.	<i>Corchorus depressus</i> (L.) Stocks	Malvaceae	SN-96	132096	Herb	Darya Khan/Bhakkar	32° 47'22.36"N 71°06'27.84"E
37.	<i>Corchorus olitorius</i> L.	Malvaceae	SN-82	131945	Herb	Chak 234A/Layyah	31° 17'29.54"N 71°13'14.15"E
38.	<i>Cousinia prolifera</i> Jaub. & Spach	Asteraceae	SN-23	131943	Herb	Janjoo/Bhakkar	31° 46'32.06"N 71°35'35.40"E
39.	<i>Crotalaria burhia</i> Buch.-Ham. ex Benth.	Fabaceae	SN-45	131958	Shrub	Chubara/Layyah	30° 54'25.06"N 71°30'14.91"E
40.	<i>Croton bonplandianus</i> Baill.	Euphorbiaceae	SN-52	131909	Herb	Rangpur/Khushab	32° 01'23.31"N 71°49'22.34"E
41.	<i>Cucumis melo</i> L.	Cucurbitaceae	SN-48	131920	Climber	Maibal/Bhakkar	32° 02'13.36"N 71°11'53.96"E
42.	<i>Cucurbita maxima</i> Duchesne	Cucurbitaceae	SN-107	131983	Climber	Near Chak 13 ML/Mianwali	32° 15'18.17"N 71°31'30.62"E
43.	<i>Dalbergia sissoo</i> Roxb.	Fabaceae	SN-78	131942	Tree	Chandani Chwok/Bhakkar	32° 06'59.17"N 71°29'49.90"E
44.	<i>Datura innoxia</i> Mill	Solanaceae	SN-33	131973	Herb	Ali Khel Rangpur/Khushab	32° 03'24.91"N 71°41'43.90"E
45.	<i>Datura stramonium</i> L.	Solanaceae	SN-97	131981	Shrub	Retri/Bhakkar	31° 39'42.16"N 71°19'44.38"E
46.	<i>Digera muricata</i> (L.) Mart.	Amaranthaceae	SN-53	131921	Herb	Chak 234A/Layyah	31° 17'29.54"N



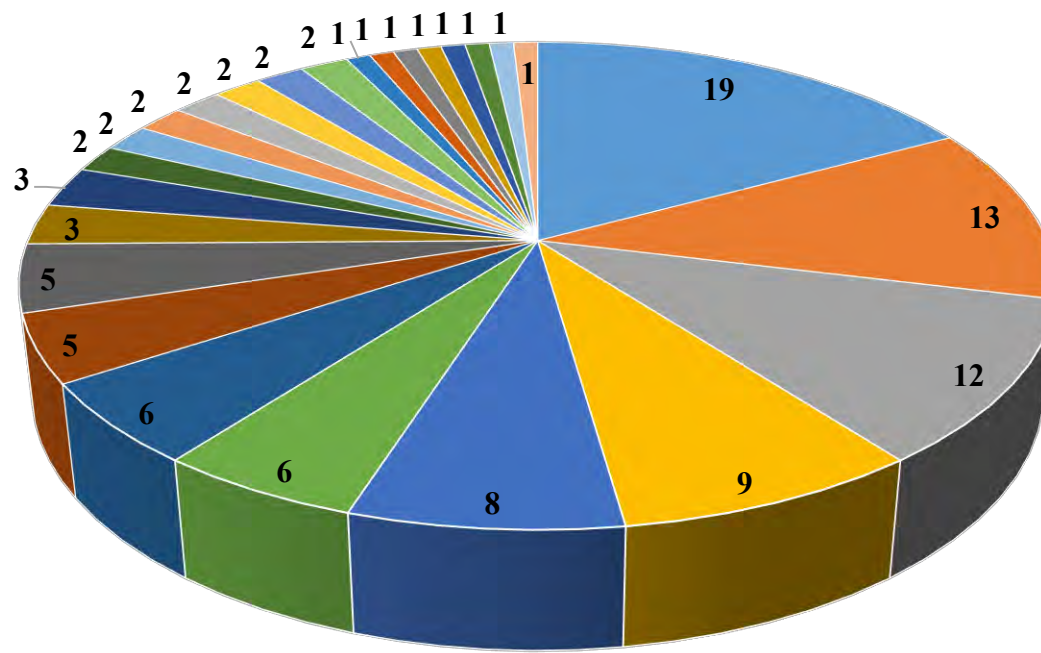
							71°13'14.15"E
47.	<i>Dipterygium glaucum</i> Decne.	Capparaceae	SN-55	131957	Shrub	Maibal/Bhakkar	32° 02'13.36"N 71°11'53.96"E
48.	<i>Eclipta prostrata</i> (L.) L.	Asteraceae	SN-106	132085	Herb	Kallur Kot/Bhakkar	32° 09'26.89"N 71°16'10.57"E
49.	<i>Eruca vesicaria</i> (L.) Cav.	Brassicaceae	SN-46	131908	Herb	Chak 47DB Rangpur/Khushab	32° 03'17.33"N 71°43'30.63"E
50.	<i>Eucalyptus globulus</i> Labill.	Myrtaceae	SN-56	131941	Tree	Near Chandani Chowk/Bhakkar	32° 06'59.17"N 71°29'49.90"E
51.	<i>Euphorbia dracunculoides</i> Lam.	Euphorbiaceae	SN-28	132095	Herb	Noorpur thal road/Bhakkar	31° 53'50.30"N 71°53'22.57"E
52.	<i>Euphorbia granulata</i> Forssk.	Euphorbiaceae	SN-44	131980	Herb	Kallur Kot/Bhakkar	32° 09'26.89"N 71°16'10.57"E
53.	<i>Euphorbia helioscopia</i> L.	Euphorbiaceae	SN-92	131972	Herb	Dullewala/Bhakkar	31° 50'33.75"N 71°20'09.76"E
54.	<i>Euphorbia hirta</i> L.	Euphorbiaceae	SN-57	131940	Herb	Chak 69/ ML/Layyah	31° 20'31.74"N 71°13'54.25"E
55.	<i>Euphorbia serpens</i> Kunth	Euphorbiaceae	SN-105	131988	Herb	Maibal/Bhakkar	32° 02'13.36"N 71°11'53.96"E
56.	<i>Fagonia bruguieri</i> DC.	Zygophyllaceae	SN-62	131906	Shrub	Sarki/Bhakkar	31° 25'21.77"N 71°22'40.74"E
57.	<i>Farsetia stylosa</i> R.Br.	Brassicaceae	SN-25	131979	Herb	Janjoon/Bhakkar	31° 46'32.06"N 71°35'35.40"E
58.	<i>Gisekia pharnaceoides</i> L.	Aizoaceae	SN-61	131922	Herb	Darya Khan/Bhakkar	32° 47'22.36"N 71°06'27.84"E
59.	<i>Gomphrena celosioides</i> Mart.	Amaranthaceae	SN-104	131907	Herb	Ghanjera/Mianwali	32° 19'48.55"N 71°31'14.28"E
60.	<i>Haloxylon stocksii</i> (Boiss.) Benth. & Hook. f.	Amaranthaceae	SN-19	131964	Shrub	Near Mankera Fort/Bhakkar	31° 23'08.65"N 71°26'19.11"E
61.	<i>Heliotropium bacciferum</i> Forssk.	Boraginaceae	SN-64	131960	Herb	Kot Afzal/Bhakkar	31° 24'40.81"N 71°24'11.59"E
62.	<i>Heliotropium europaeum</i> L.	Boraginaceae	SN-1	131905	Herb	Sarai Mahajar/Bhakkar	31° 30'07.17"N

							71°14'12.96"E
63.	<i>Heliotropium strigosum</i> Willd.	Boraginaceae	SN-65	131970	Herb	Dullewala/Bhakkar	31° 50'33.75"N 71°20'09.76"E
64.	<i>Iphiona grantioides</i> (Boiss.) Anderb.	Asteraceae	SN-103	131895	Herb	Darya Khan/Bhakkar	32° 47'22.36"N 71°06'27.84"E
65.	<i>Launaea nudicaulis</i> (L.) Hook.f.	Asteraceae	SN-68	131902	Herb	Rangpur/Khushab	32° 03'24.91"N 71°41'43.90"E
66.	<i>Launaea procumbens</i> (Roxb.) Ramayya & Rajagopal	Asteraceae	SN-60	131923	Herb	Sarai Mahajar/Bhakkar	31° 30'07.17"N 71°14'12.96"E
67.	<i>Lepidium didymum</i> L.	Brassicaceae	SN-93	131939	Herb	Harnoli Mor/Mianwali	32° 17'09.66"N 71°31'27.43"E
68.	<i>Leptadenia pyrotechnica</i> (Forssk.) Decne.	Apocynaceae	SN-66	131974	Shrub	Naurangwala/Bhakkar	31° 40'16.93"N 71°20'09.76"E
69.	<i>Luffa cylindrica</i> (L.) M.Roem.	Cucurbitaceae	SN-75	132086	Climber	Kallur Kot/Bhakkar	32° 09'26.89"N 71°16'10.57"E
70.	<i>Malva parviflora</i> L.	Malvaceae	SN-67	131924	Herb	Retri/Bhakkar	31° 39'42.16"N 71°19'44.38"E
71.	<i>Mollugo cerviana</i> (L.) Ser.	Molluginaceae	SN-49	131938	Herb	Ali Khel Rangpur/Khushab	32° 03'24.91"N 71°41'43.90"E
72.	<i>Mollugo nudicaulis</i> Lamk.,	Molluginaceae	SN-38	131903	Herb	Dullewala/Bhakkar	31° 50'33.75"N 71°20'09.76"E
73.	<i>Momordica charantia</i> L.	Cucurbitaceae	SN-93	131977	Climber	Sarai Mahajar/Bhakkar	31° 30'07.17"N 71°14'12.96"E
74.	<i>Mukia maderaspatana</i> (L.) M.Roem.	Cucurbitaceae	SN-102	131925	Climber	Kallur Kot/Bhakkar	32° 09'26.89"N 71°16'10.57"E
75.	<i>Nonea micrantha</i> Boiss. & Reut.	Boraginaceae	SN-27	131971	Herb	Janjoon/Bhakkar	31° 46'32.06"N 71°35'35.40"E
76.	<i>Opuntia dillenii</i> (Ker Gawl.) Haw.	Cactaceae	SN-90	131937	Shrub	Near Chak 13 ML/Mianwali	32° 15'18.17"N 71°31'30.62"E
77.	<i>Opuntia monacantha</i> Haw.	Cactaceae	SN-100	131926	Shrub	Harnoli Mor/Mianwali	32° 17'09.66"N 71°31'27.43"E
78.	<i>Parkinsonia aculeata</i> L.	Fabaceae	SN-12	131928	Tree	Sarai Mahajar/Bhakkar	31° 30'07.17"N

							71°14'12.96"E
79.	<i>Peganum harmala</i> L.	Nitrariaceae	SN-37	131984	Herb	Khansar/Bhakkar	31° 39'42.16"N 71°19'44.38"E
80.	<i>Physalis divaricata</i> D.Don	Solanaceae	SN-101	131900	Herb	Darya Khan/Bhakkar	32° 47'22.36"N 71°06'27.84"E
81.	<i>Physalis minima</i> L.	Solanaceae	SN-85	131904	Herb	Shah Wal South/Khushab	31° 52'05.52"N 71°44'08.00"E
82.	<i>Prosopis cineraria</i> (L.) Druce.	Fabaceae	SN-22	131968	Shrub	Chak 234A/Layyah	31° 17'29.54"N 71°13'14.15"E
83.	<i>Prosopis juliflora</i> (Sw.) DC.	Fabaceae	SN-20	131936	Shrub	Mankera fort/Bhakkar	31° 23'08.65"N 71°26'19.11"E
84.	<i>Psammogeton biternatum</i> Edgew.	Apiaceae	SN-31	131927	Herb	Janjoo/Bhakkar	31° 46'32.06"N 71°35'35.40"E
85.	<i>Pulicaria boissieri</i> Hook.f.	Asteraceae	SN-81	131969	Herb	Near Gohar wala/Bhakkar	31° 43'04.49"N 71°34'31.31"E
86.	<i>Rhazya stricta</i> Decne.	Apocynaceae	SN-69	131955	Shrub	Harnoli Mor/Mianwali	32° 17'09.66"N 71°31'27.43"E
87.	<i>Ricinus communis</i> L.	Euphorbiaceae	SN-11	131898	Shrub	Near Gohar wala/Bhakkar	31° 43'04.49"N 71°34'31.31"E
88.	<i>Salsola tragus</i> L.	Amaranthaceae	SN-89	131966	Herb	Maibal/Bhakkar	32° 02'13.36"N 71°11'53.96"E
89.	<i>Salvadora oleoides</i> Decne.	Salvadoraceae	SN-70	131929	Shrub	Barranga/Bhakkar	32° 55'02.23"N 71°26'19.83"E
90.	<i>Salvadora persica</i> Wall.	Salvadoraceae	SN-88	132088	Shrub	Barranga/Bhakkar	32° 55'02.23"N 71°26'19.83"E
91.	<i>Senna italica</i> (Mill.) F.W.Andr	Fabaceae	SN-71	131930	Herb	Darya Khan/Bhakkar	32° 47'22.36"N 71°06'27.84"E
92.	<i>Sisymbrium irio</i> L.	Brassicaceae	SN-63	131975	Herb	Rangpur/Khushab	32° 01'23.31"N 71°49'22.34"E
93.	<i>Solanum incanum</i> L.	Solanaceae	SN-74	132087	Shrub	Janjoo/Bhakkar	31° 46'32.06"N 71°35'35.40"E

94.	<i>Solanum surattense</i> Burm. f.	Solanaceae	SN-43	131978	Herb	Rangpur to Noorpur thal road/Khushab	32° 01'23.31"N 71°49'22.34"E
95.	<i>Sonchus asper</i> (L.) Hill	Asteraceae	SN-72	132094	Herb	Darya Khan/Bhakkar	32° 47'22.36"N 71°06'27.84"E
96.	<i>Suaeda fruticosa</i> Forssk. ex J.F.Gmel.	Amaranthaceae	SN-15	131976	Shrub	Chak 234A/Layyah	31° 17'29.54"N 71°13'14.15"E
97.	<i>Tamarix aphylla</i> (L.) H.Karst.	Tamaricaceae	SN-24	131897	Tree	Gohar wala/Bhakkar	31° 43'04.49"N 71°34'31.31"E
98.	<i>Tamarix dioica</i> Roxb.	Tamaricaceae	SN-4	131987	Shrub	Chubara/Layyah	30° 54'25.06"N 71°30'14.91"E
99.	<i>Tecomella undulata</i> (Sm.) Seem.	Bignoniaceae	SN-8	131931	Tree	Near Chandani Chowk/Bhakkar	32° 06'59.17"N 71°29'49.90"E
100.	<i>Tephrosia purpurea</i> (L.) Pers.	Fabaceae	SN-9	131935	Herb	Chandani Chowk/Bhakkar	32° 06'59.17"N 71°29'49.90"E
101.	<i>Tragopogon gracilis</i> D.Don	Asteraceae	SN-42	132089	Herb	Ali Khel Rangpur/Khushab	32° 03'24.91"N 71°41'43.90"E
102.	<i>Trianthema portulacastrum</i> L.	Aizoaceae	SN-10	131965	Herb	Darya Khan/Bhakkar	32° 47'22.36"N 71°06'27.84"E
103.	<i>Tribulus terrestris</i> L.	Zygophyllaceae	SN-32	131901	Herb	Mankera to Hyderabad Thal road/Bhakkar	31° 23'08.65"N 71°26'19.11"E
104.	<i>Trichodesma indicum</i> (L.) R. Br.	Boraginaceae	SN-87	131932	Herb	Shah Wal South/Khushab	31° 52'05.52"N 71°44'08.00"E
105.	<i>Verbesina encelioides</i> (Cav.) Benth. & Hook.f. ex A.Gray	Asteraceae	SN-79	132090	Herb	Harnoli Mor/Mianwali	32° 17'09.66"N 71°31'27.43"E
106.	<i>Withania coagulans</i> (Stocks) Dunal	Solanaceae	SN-16	132093	Shrub	Gohar wala/Bhakkar	31° 43'04.49"N 71°34'31.31"E
107.	<i>Withania somnifera</i> (L.) Dunal	Solanaceae	SN-35	131933	Shrub	Chandani Chowk/Bhakkar	32° 06'59.17"N 71°29'49.90"E
108.	<i>Xanthium strumarium</i> L.	Asteraceae	SN-80	132091	Herb	Gohar wala/Bhakkar	31° 43'04.49"N 71°34'31.31"E
109.	<i>Zaleya pentandra</i> (L.) C.Jeffrey	Aizoaceae	SN-99	131934	Herb	Maibal/Bhakkar	32° 02'13.36"N 71°11'53.96"E

110.	<i>Ziziphus nummularia</i> (Burm.f.) Wight & Arn.	Rhamnaceae	SN-17	131894	Shrub	Gohar wala/Bhakkar	31° 43'04.49"N 71°34'31.31"E
111.	<i>Ziziphus spina-christi</i> (L.) Desf.	Rhamnaceae	SN-84	131899	Tree	Near Chak 13 ML/Mianwali	32° 15'18.17"N 71°31'30.62"E



- Amaranthaceae ■ Asteraceae ■ Fabaceae ■ Euphorbiaceae ■ Solanaceae ■ Boraginaceae
- Cucurbitaceae ■ Brassicaceae ■ Capparaceae ■ Aizoaceae ■ Malvaceae ■ Cactaceae
- Zygophyllaceae ■ Molluginaceae ■ Apocynaceae ■ Salvadoraceae ■ Tamaricaceae ■ Rhamnaceae
- Bignoniaceae ■ Apiaceae ■ Nitrariaceae ■ Myrtaceae ■ Nyctaginaceae ■ Meliaceae
- Papaveraceae ■ Convolvulaceae

**Figure 3.** Graphical illustration of plant families of dicot flora

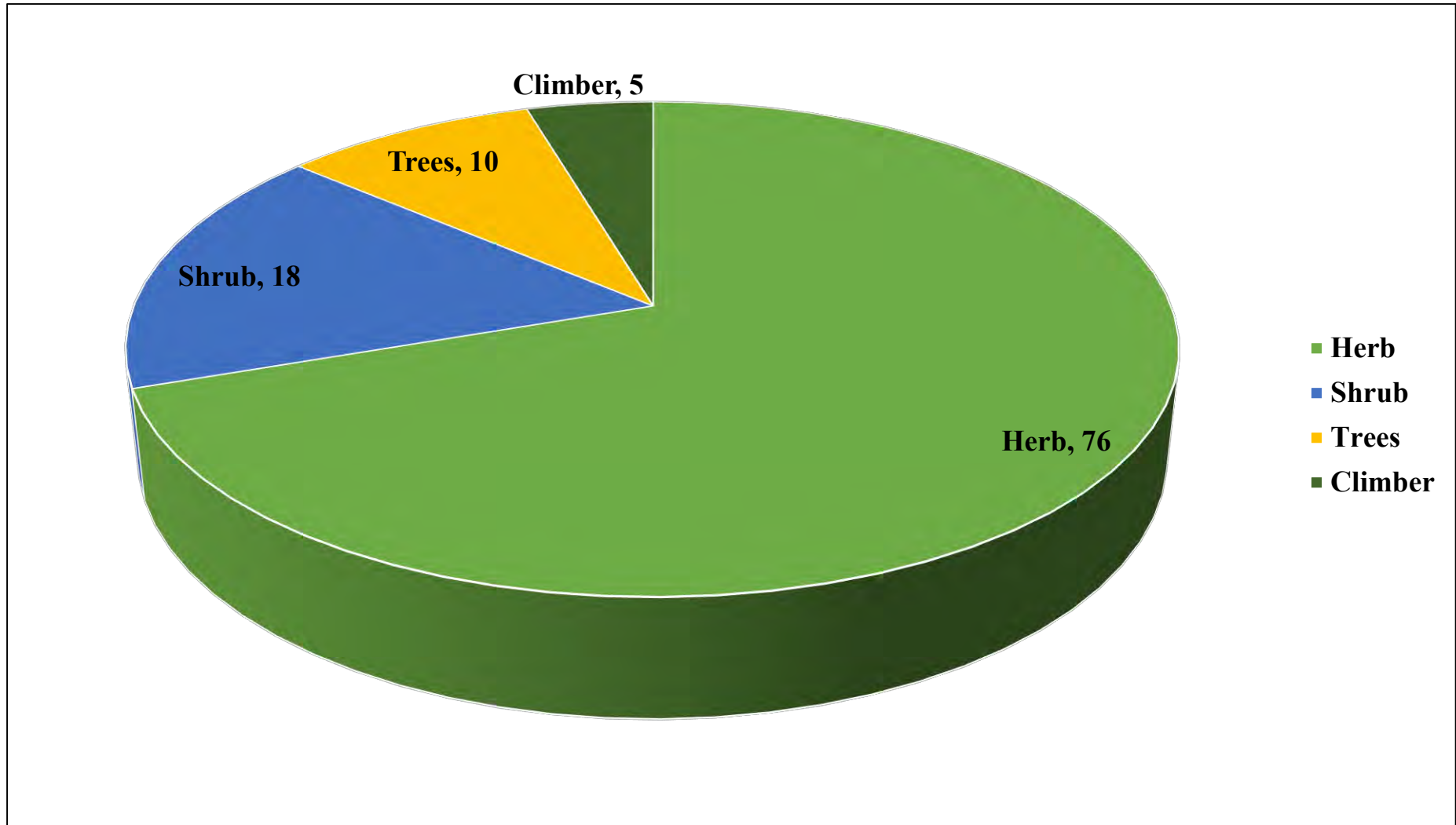


**Figure 4.** Life Form Classification of Dicot flora

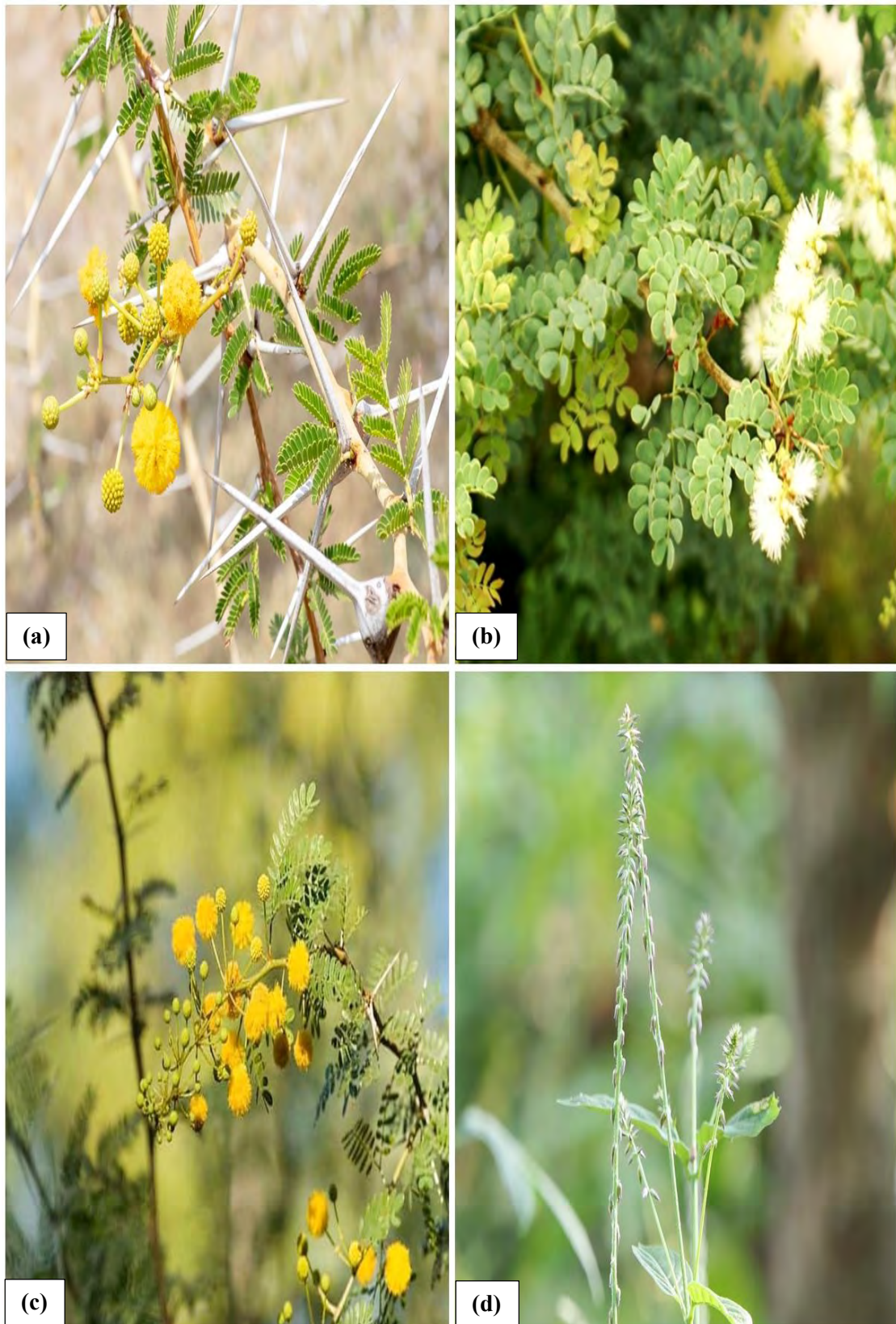


**Plate 9.** Field pictorial view of (a) *Acacia jacquemontii*; floral parts with spiny branch, (b) *Acacia modesta*; pedunculate spike with paired leaflets, (c) *Acacia nilotica*; bright yellow flower, (d) *Achyranthes aspera*; elongating inflorescence



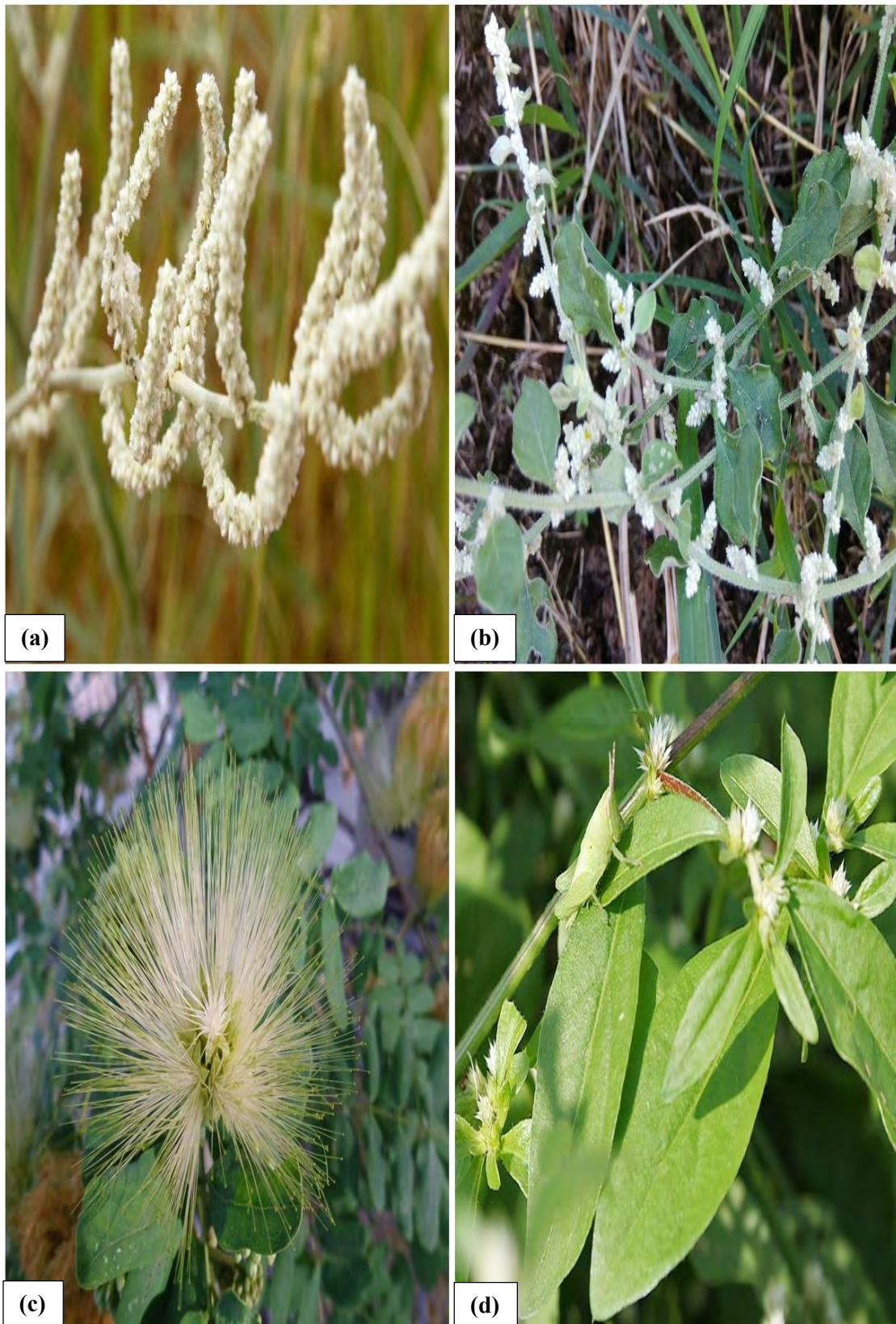


**Plate 10.** Field pictorial view of (a) *Aerva javanica*; dense and stout floral parts, (b) *Aerva lanata*; leaves with floral branches, (c) *Albizzia lebbeck*; inflorescence pedunculate heads, (d) *Alternanthera ficoidea*; evergreen leaves with floral buds

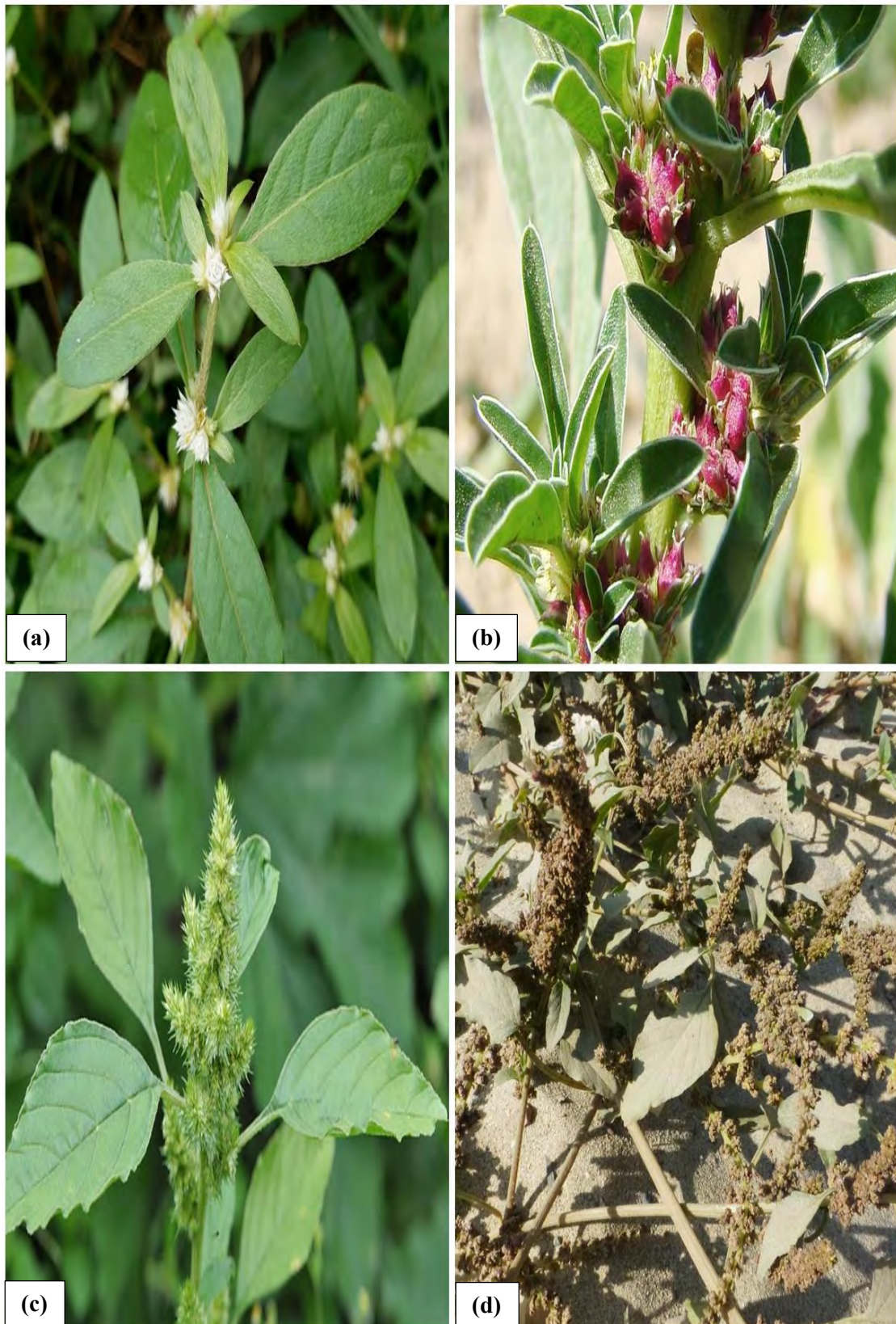


**Plate 11.** Field pictorial view of (a) *Alternanthera sessilis*; oblong leaves, (b) *Amaranthus graecizans*; glabrous leafy branches, (c) *Amaranthus retroflexus*; flower terminal spikes, (d) *Amaranthus viridis*; brown panicle spikes

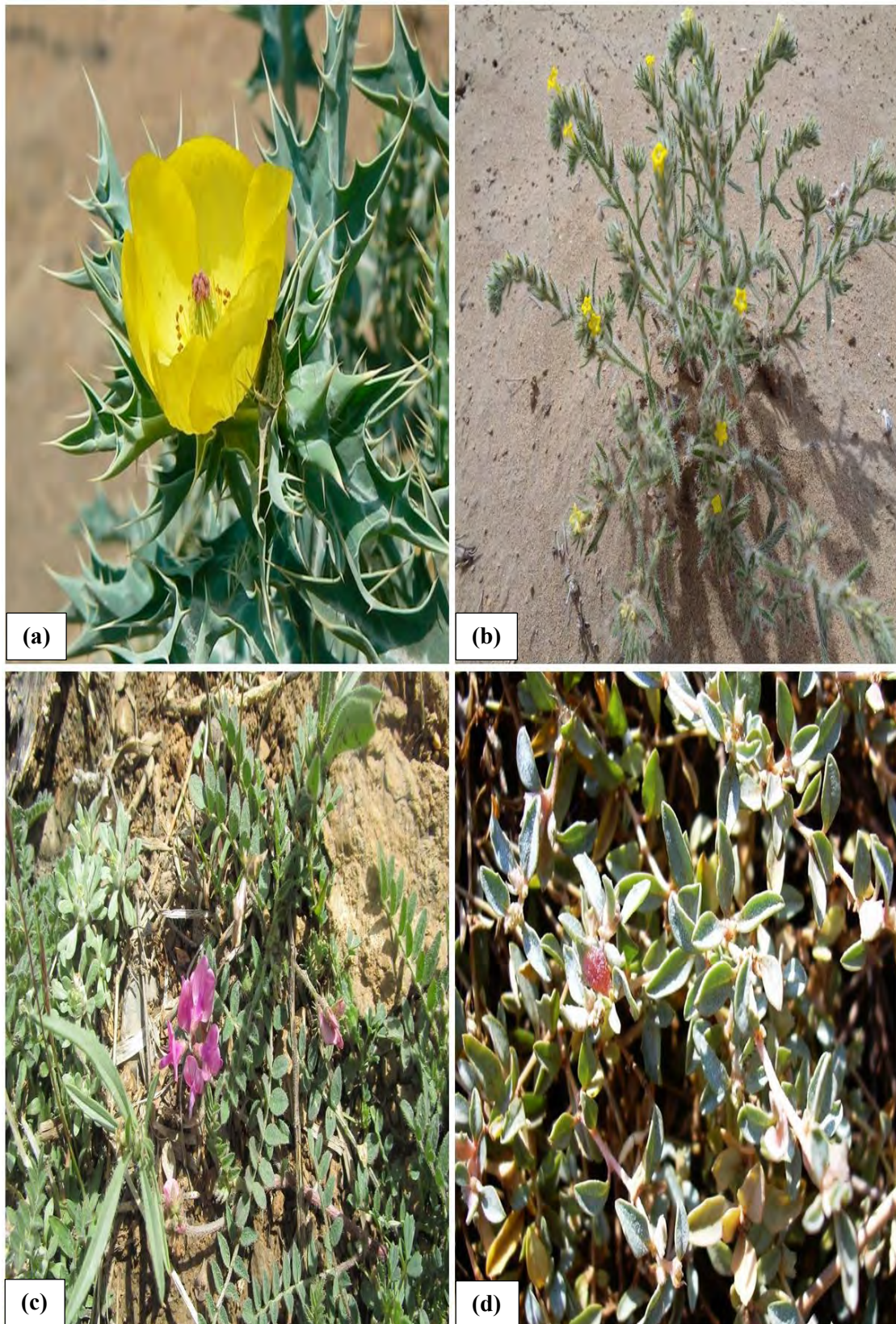


**Plate 12.** Field pictorial view of (a) *Argemone mexicana*; showy bright yellow flower, (b) *Arnebia hispidissima*; annual sub-erect stem, (c) *Astragalus hamosus*; imparipinnate compound leaves, (d) *Atriplex stocksii*; rhombic leafy and floral parts

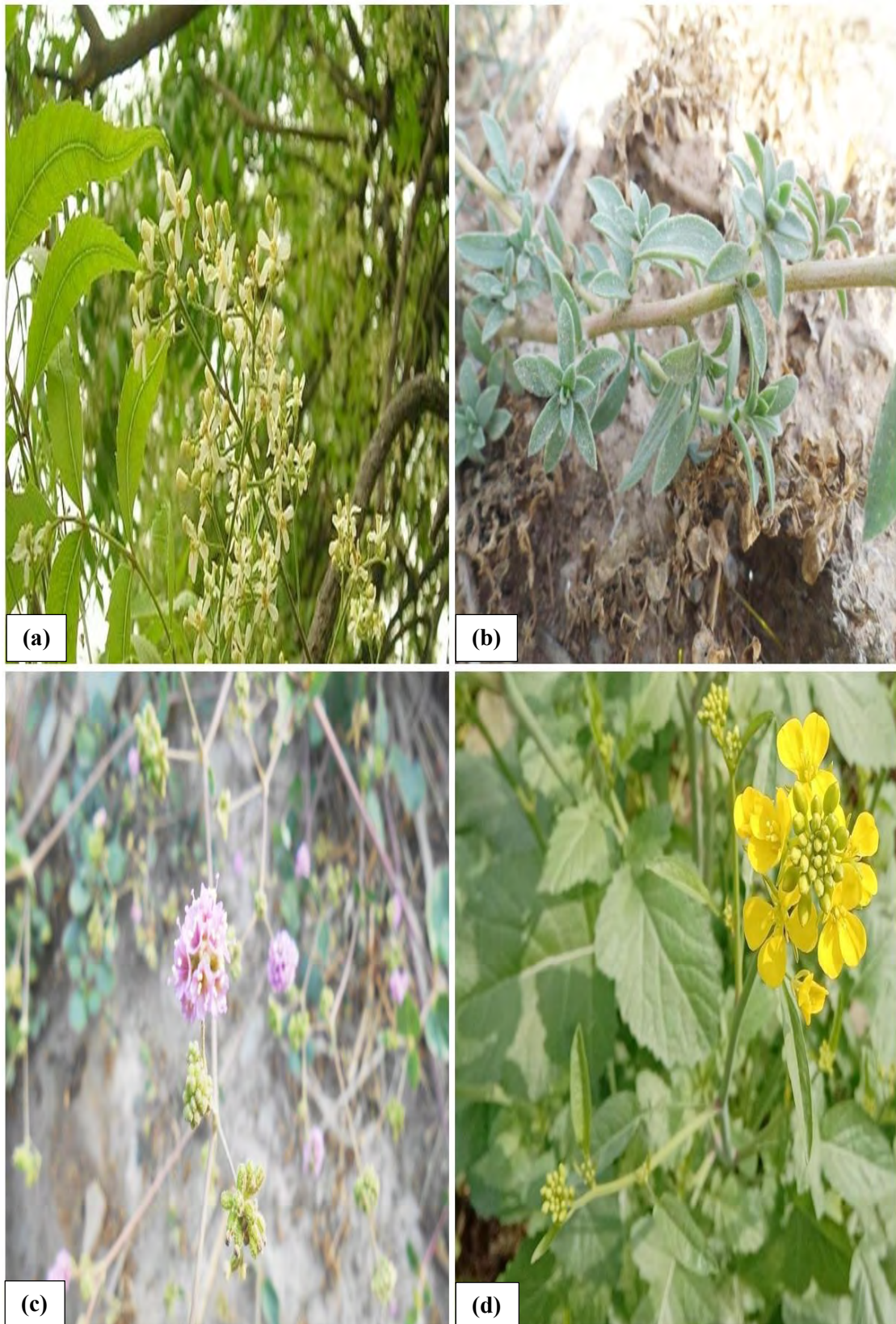


**Plate 13.** Field pictorial view of (a) *Azadirachta indica*; white floral branches, (b) *Bassia indica*; sub-glabrous leafy branches, (c) *Boerhavia procumbens*; axillary panicle flowers, (d) *Brassica nigra*; bright yellow flower with leafy branches

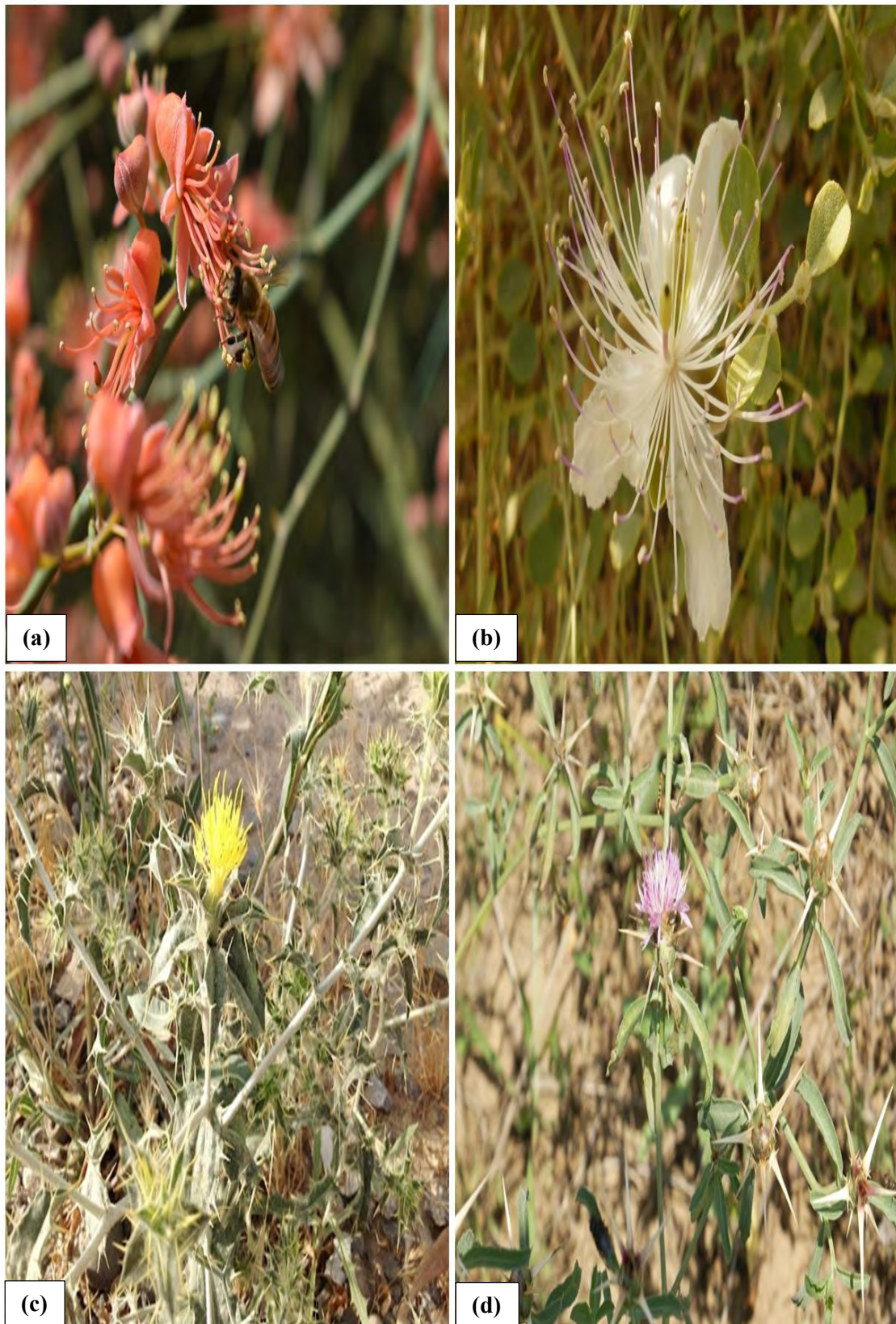


**Plate 14.** Field pictorial view of (a) *Capparis decidua*; brick red flowers, (b) *Capparis spinosa*; flowers solitary, (c) *Carthamus oxyacantha*; spiny branches with head, (d) *Centaurea iberica*; simple broad leaves with light pinkish capitulum

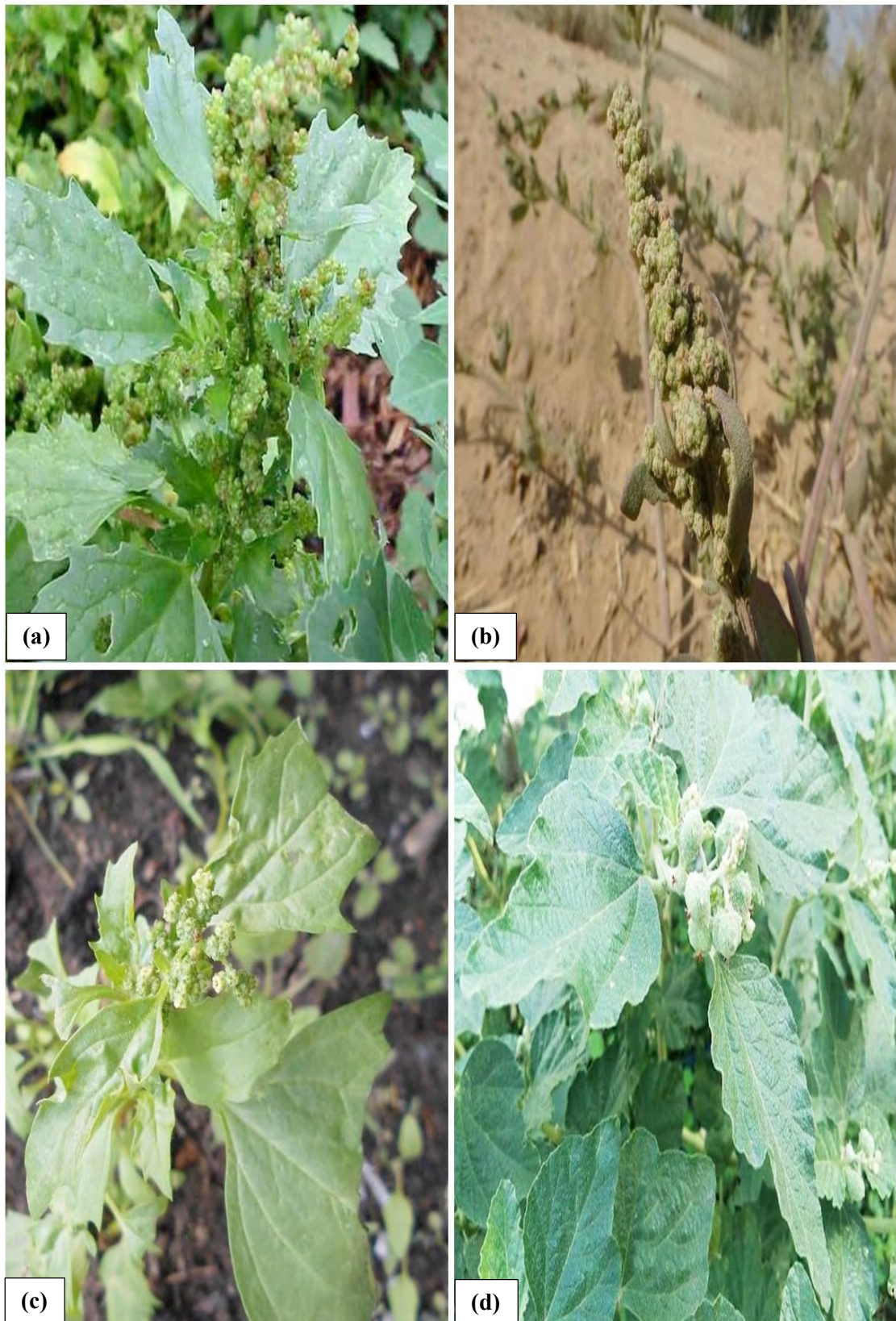


**Plate 15.** Field pictorial view of (a) *Chenopodium album*; cymosely branched panicle, (b) *Chenopodium ficifolium*; terminal panicles, (c) *Chenopodium murale*; olive green leafy branch, (d) *Chrozophora plicata*; triangular ovate leaf.

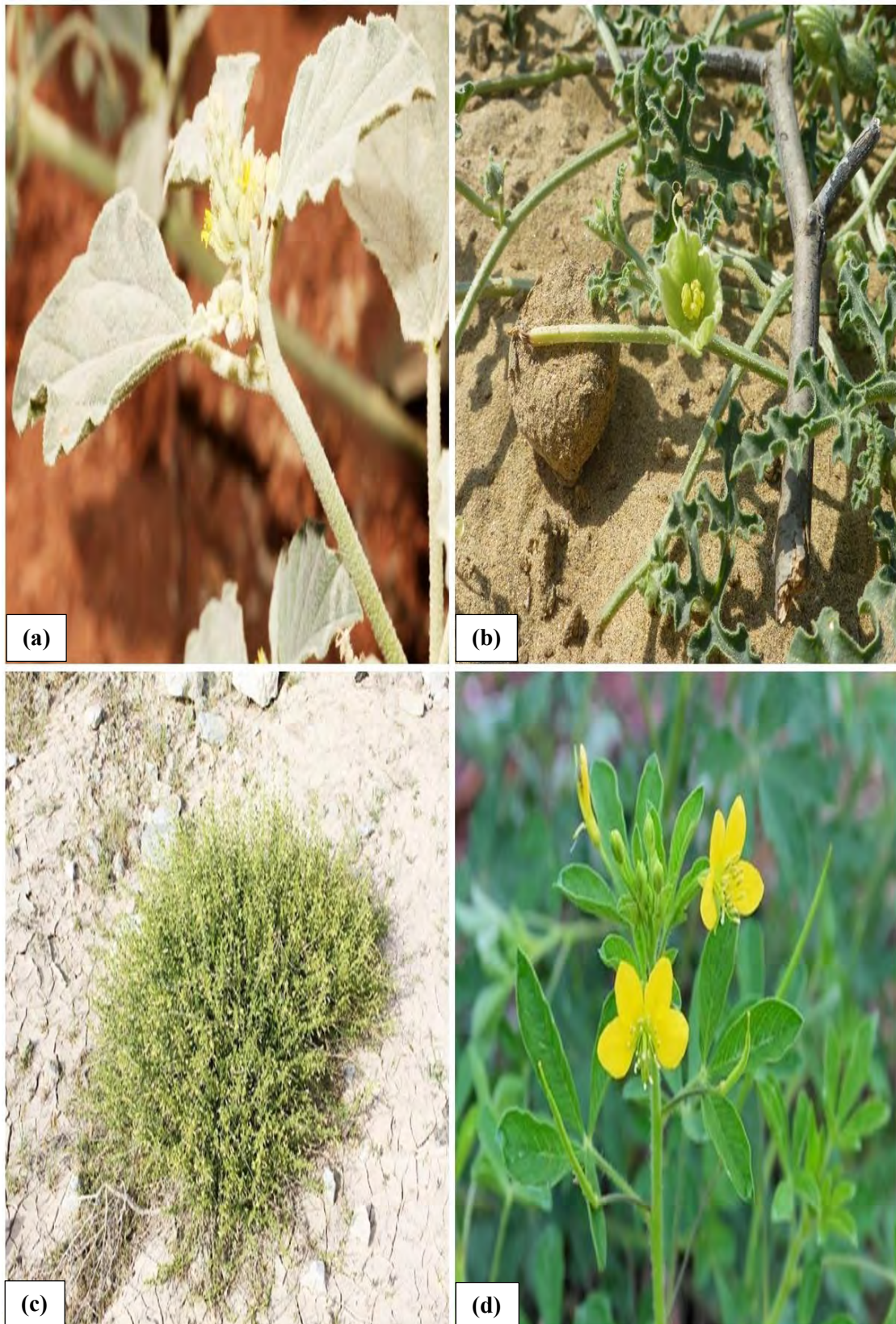


**Plate 16.** Field pictorial view of (a) *Chrozophora tinctoria*; leaf-blades broadly ovate-rhombic, (b) *Citrullus colocynthis*; elongate leaf and yellowish flower, (c) *Cleome brachycarpa*; sub-erect herb, (d) *Cleome viscosa*; foliolate leaf and yellow

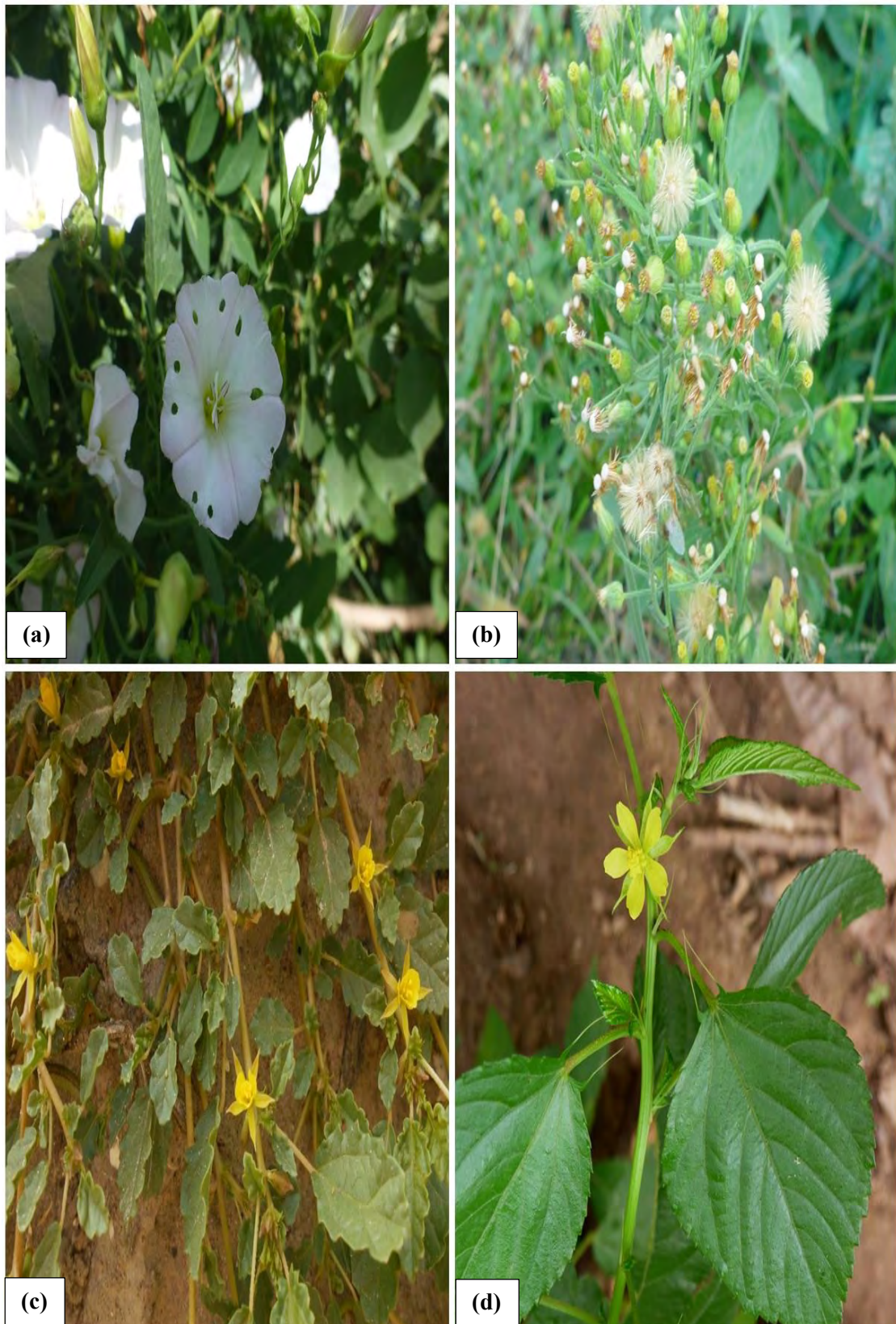


**Plate 17.** Field pictorial view of (a) *Convolvulus arvensis*; campanulate whitish flower, (b) *Conyza candensis*; flower head with tiny phyllaries, (c) *Corchorus depressus*; floral branches, (d) *Corchorus olitorius*; lanceolate leaf



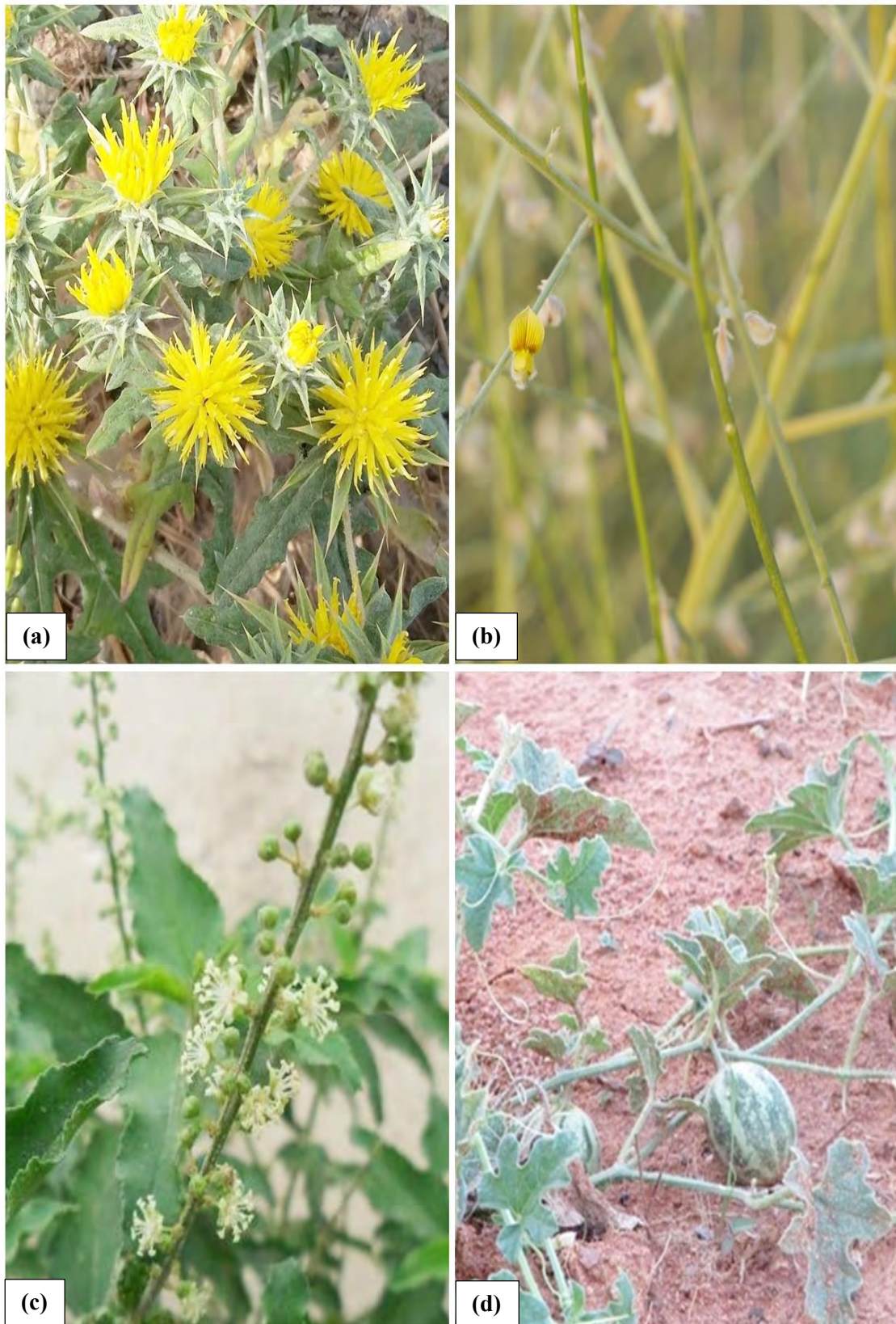


**Plate 18.** Field pictorial view of (a) *Cousinia prolifera*; dense floral heads, (b) *Crotalaria burhia*; floral branches with yellow corolla, (c) *Croton bonplandianus*; pedicels with male flower, (d) *Cucumis melo*; trailing angular stem with fruit.

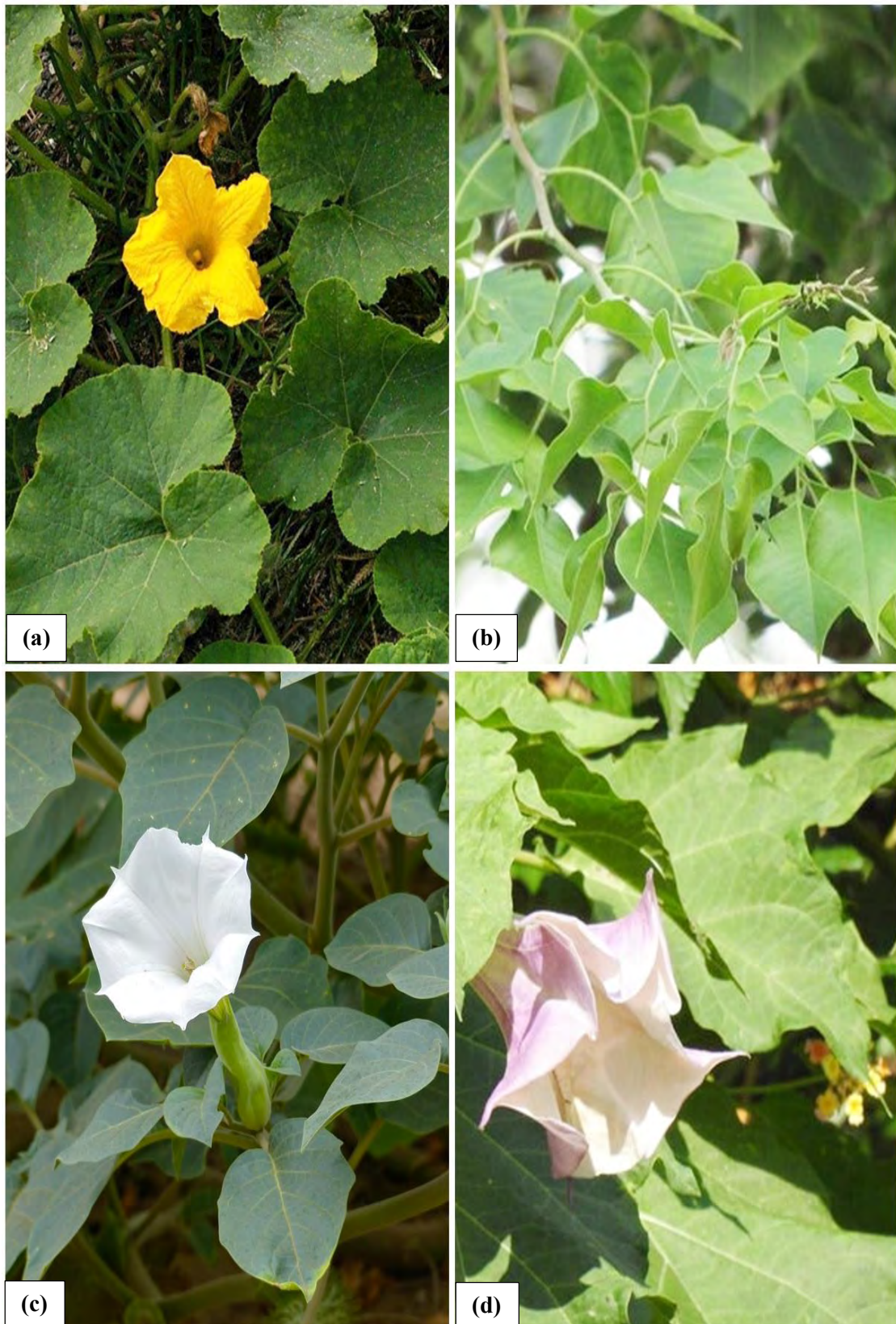


**Plate 19.** Field pictorial view of (a) *Cucurbita maxima*; 5-lobed leaves, (b) *Dalbergia sissoo*; imparipinnate leaves, (c) *Datura innoxia*; broadly ovate leaves with showy flower, (d) *Datura stramonium*; purplish suffused flower.

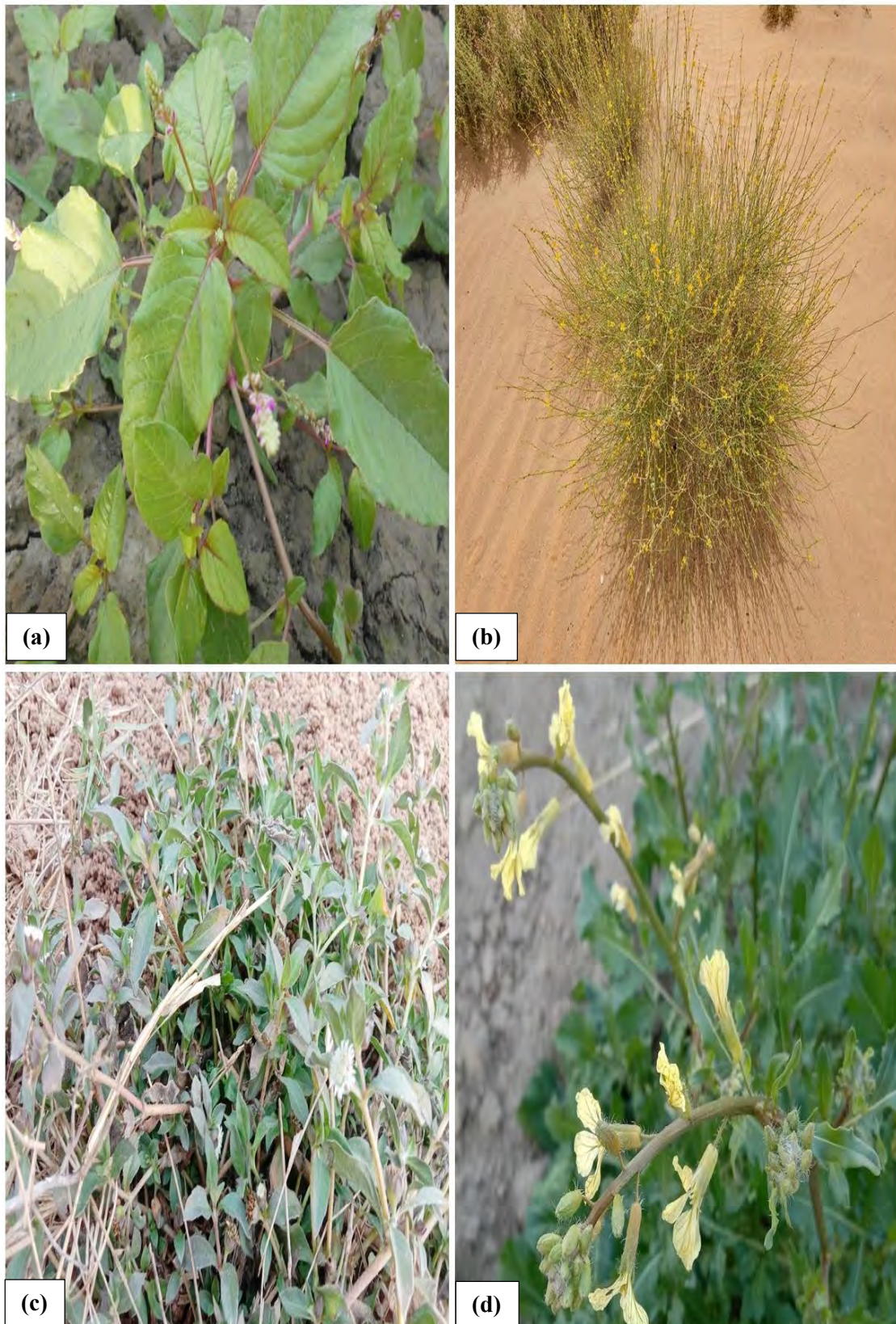


**Plate 20.** Field pictorial view of (a) *Digera muricata*; leafy branches with immature inflorescence, (b) *Dipterygium glaucum*; branched undershrub, (c) *Eclipta prostrata*; lanceolate leaves, (d) *Eruca vesicaria*; dull yellow large flower.

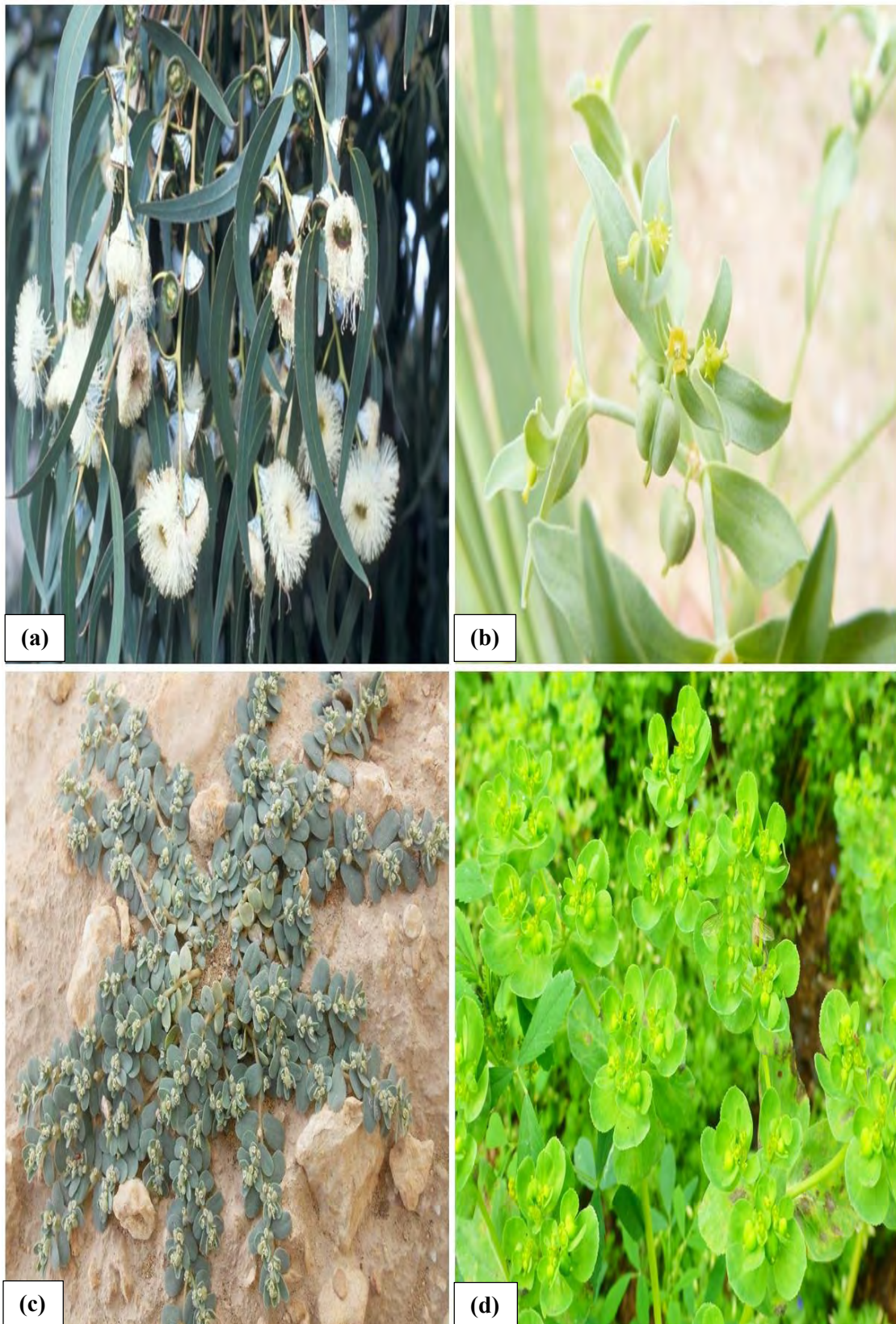


**Plate 21.** Field pictorial view of (a) *Eucalyptus globulus*; umbel inflorescence, (b) *Euphorbia dracunculoides*; subglobose fruit, (c) *Euphorbia granulata*; ephemeral herbaceous habitat, (d) *Euphorbia helioscopia*; pseudo-umbel inflorescence.

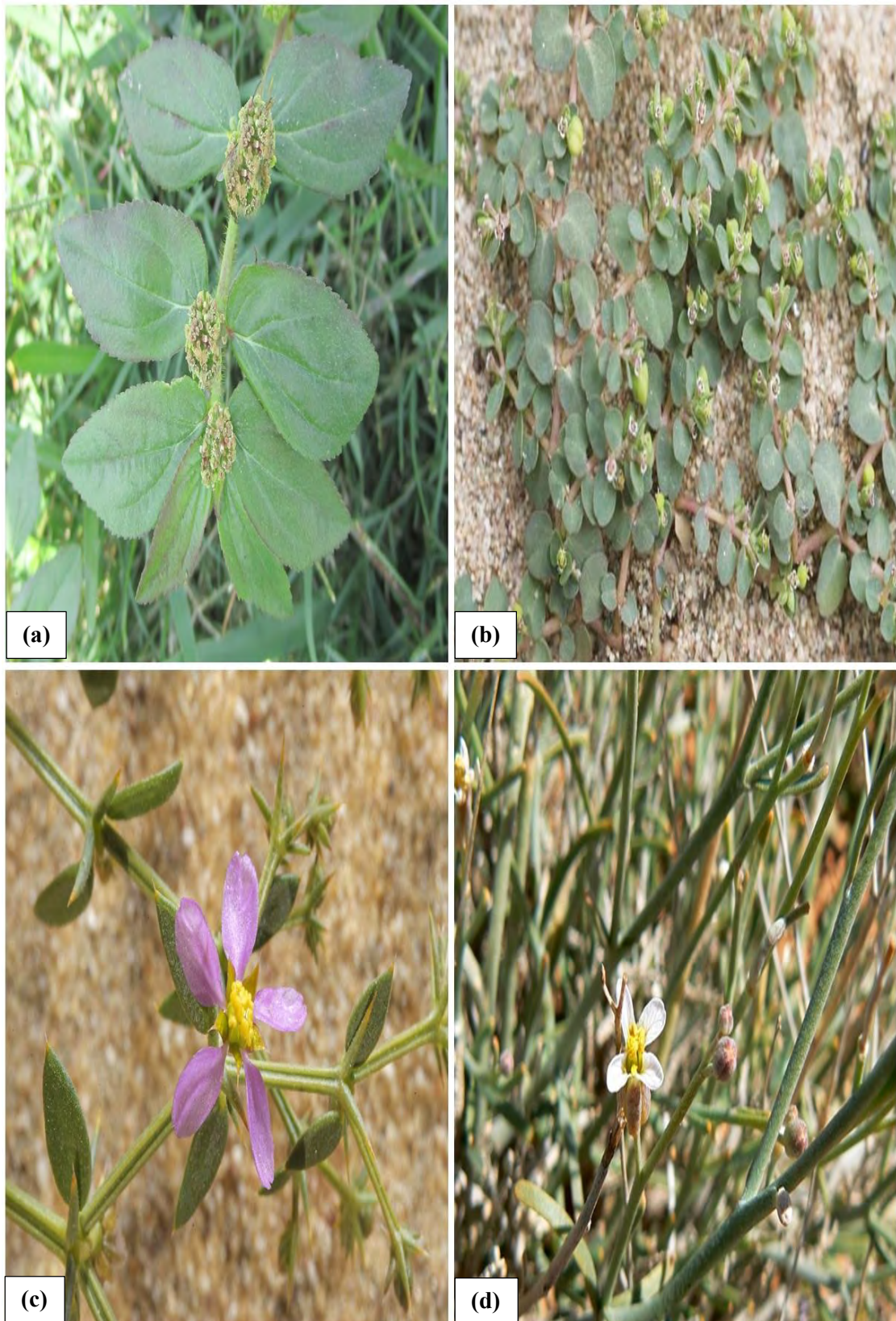


**Plate 22.** Field pictorial view of (a) *Euphorbia hirta*; opposite leaves with cyathia, (b) *Euphorbia serpens*; prostrate growth habitat, (c) *Fagonia bruguieri*; pale pink flower, (d) *Farsetia stylosa*; whitish flower with vegetative branches.

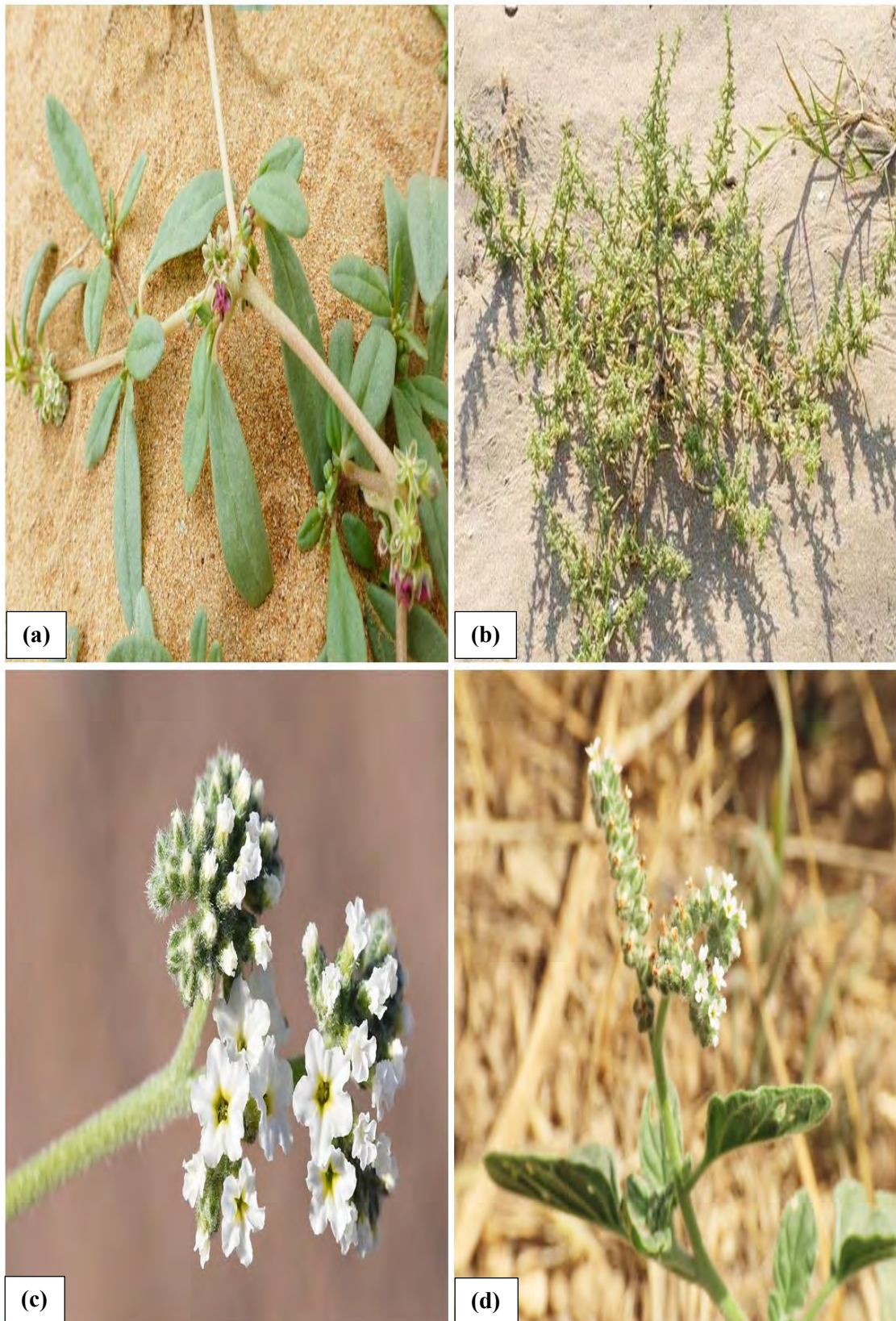


**Plate 23.** Field pictorial view of (a) *Gisekia pharnaceoides*; lanceolate leaves, (b) *Haloxylon stocksii*; divaricate shrub, (c) *Heliotropium bacciferum*; white corolla flower, (d) *Heliotropium europaeum*; obovate leaves with terminal inflorescence.

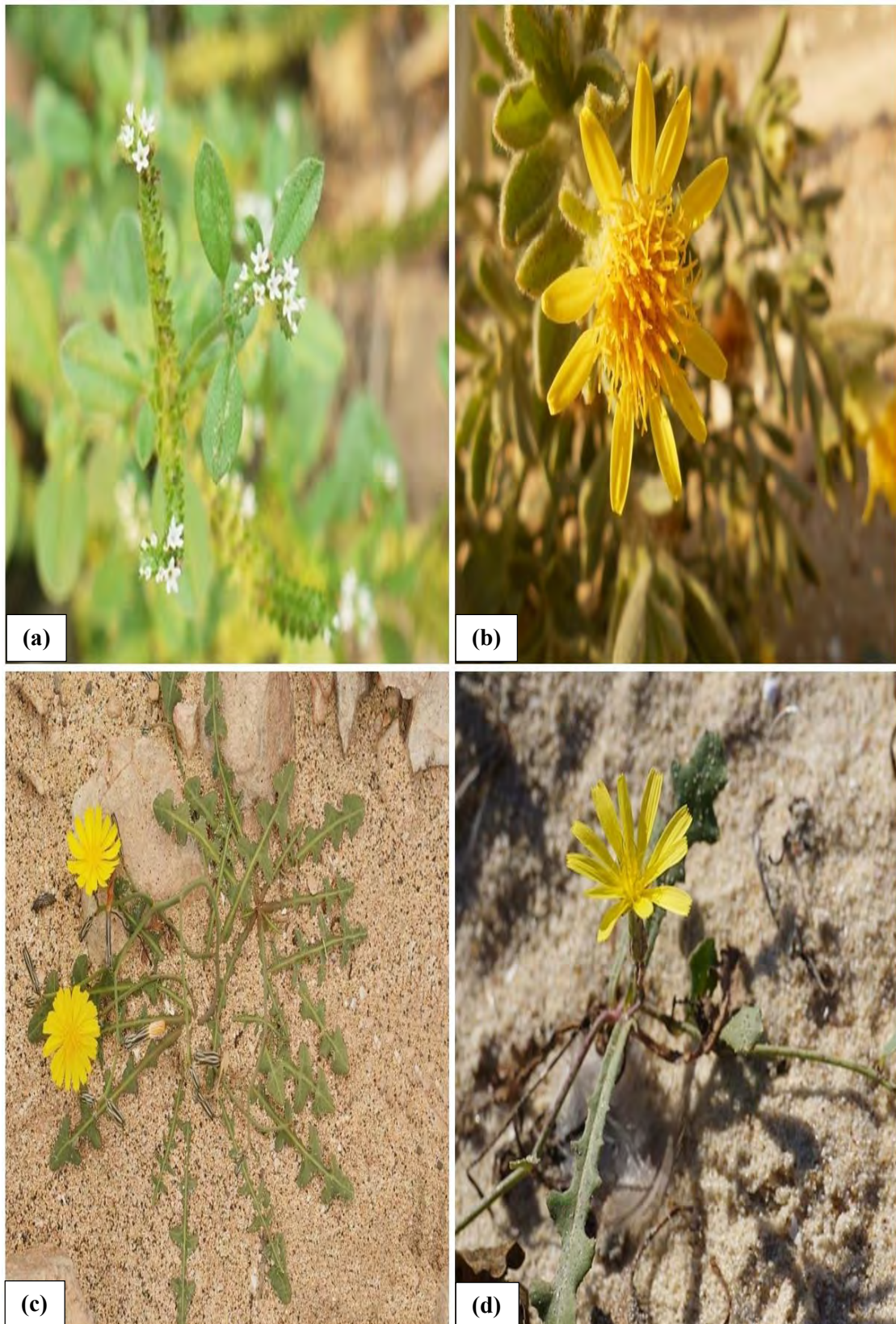


**Plate 24.** Field pictorial view of (a) *Heliotropium strigosum*; bracteates inflorescence, (b) *Iphiona grantioides*; yellowish flower head, (c) *Launaea nudicaulis*; habit growth with floral parts, (d) *Launaea procumbens*; yellow flower-

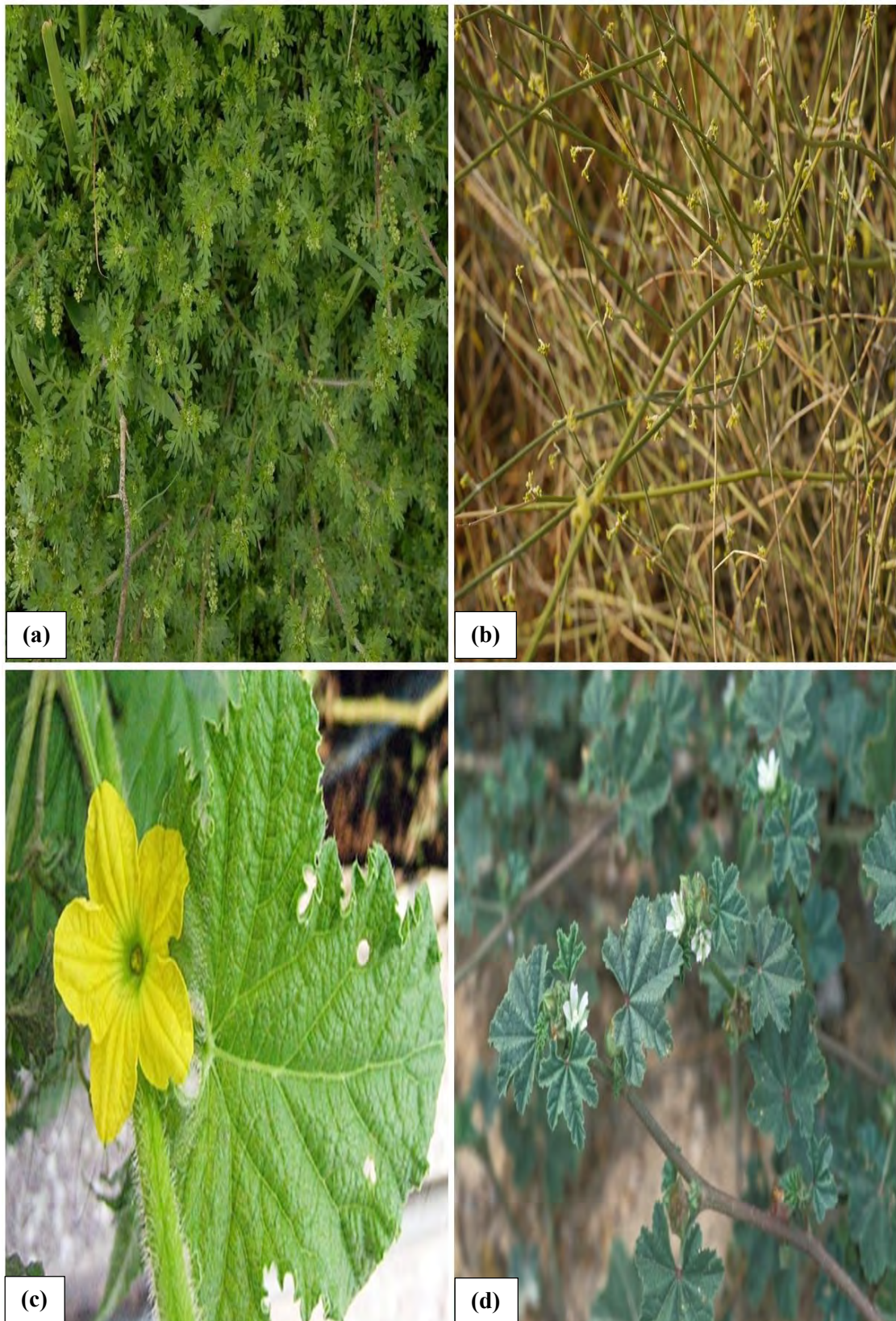


**Plate 25.** Field pictorial view of (a) *Lepidium didymum*; glabrous decumbent stem, (b) *Leptadenia pyrotechnica*; branched leafless shrub, (c) *Luffa cylindrica*; palmately leaf with bright yellow flower, (d) *Malva parviflora*; orbicular leaves.



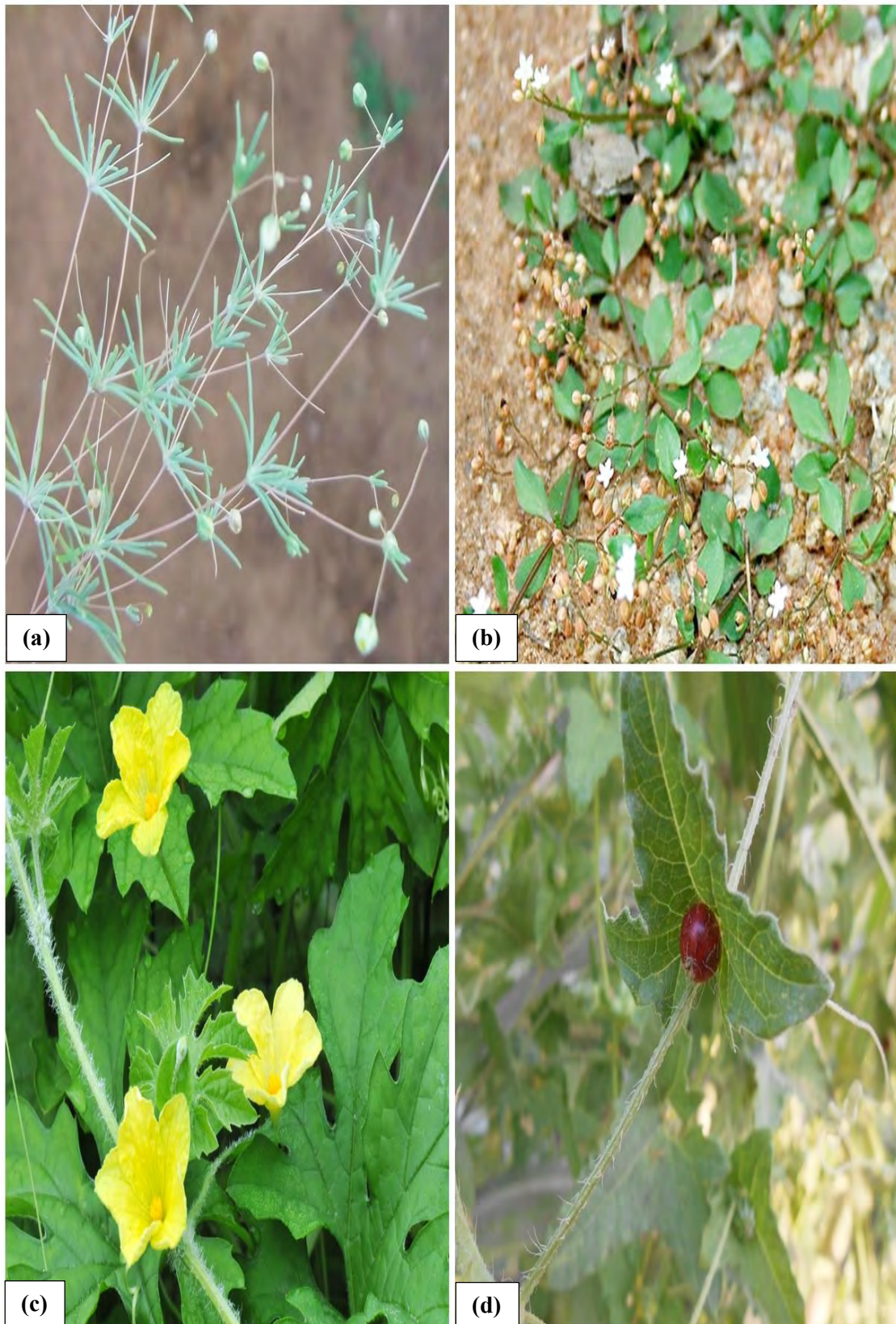


**Plate 26.** Field pictorial view of (a) *Mollugo cerviana*; whorled leaves, (b) *Mollugo nudicaulis*; basal leafy branches habit growth, (c) *Momordica charantia*; orbicular leaves with yellow flower, (d) *Mukia maderaspatana*; sagittate leaves with berry.

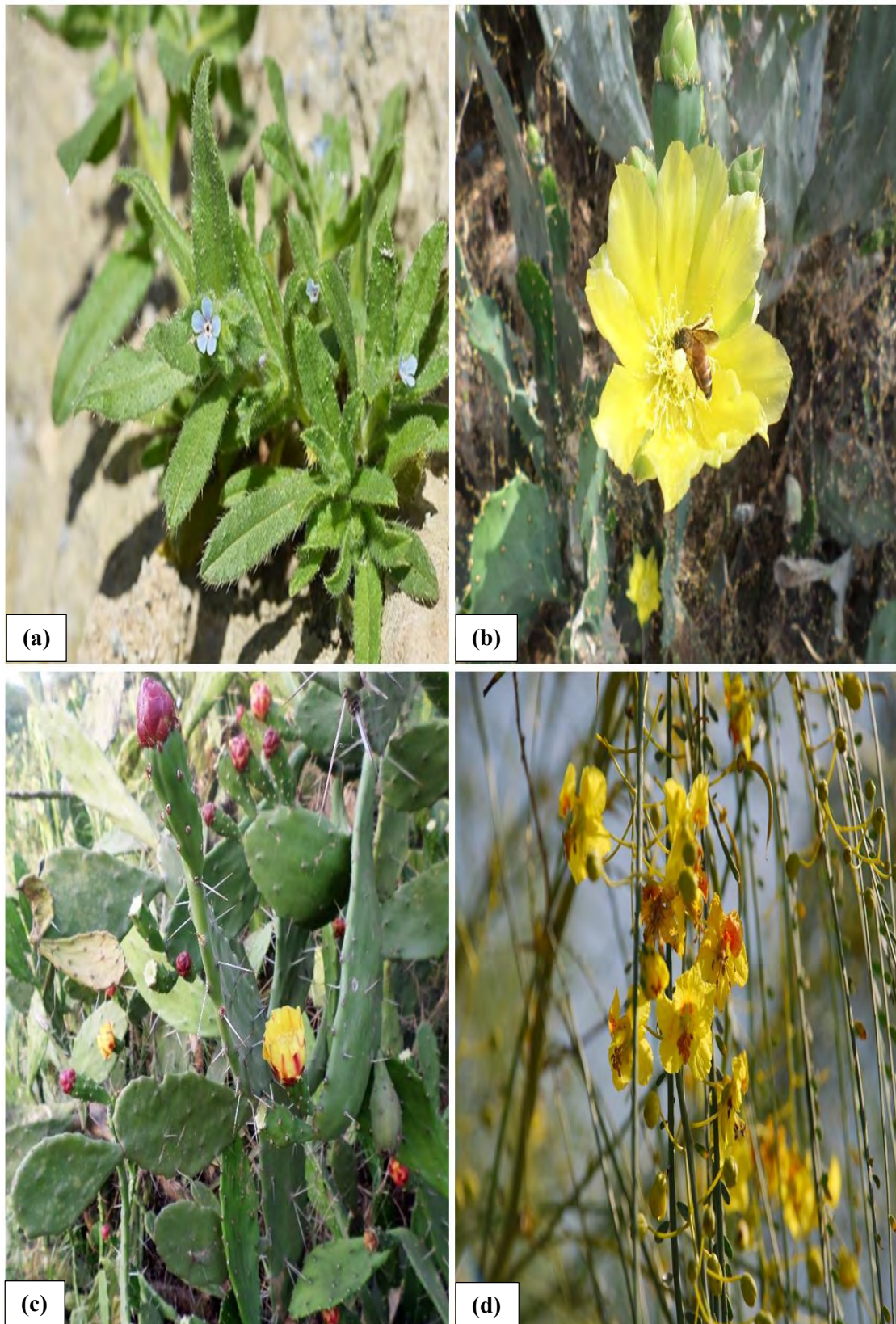


**Plate 27.** Field pictorial view of (a) *Nonea micrantha*; hispid leaf with flowers, (b) *Opuntia dillenii*; showy yellow flower, (c) *Opuntia monacantha*; flattened cladodes with yellow reddish flower, (d) *Parkinsonia aculeata*; floral branches with stamens.

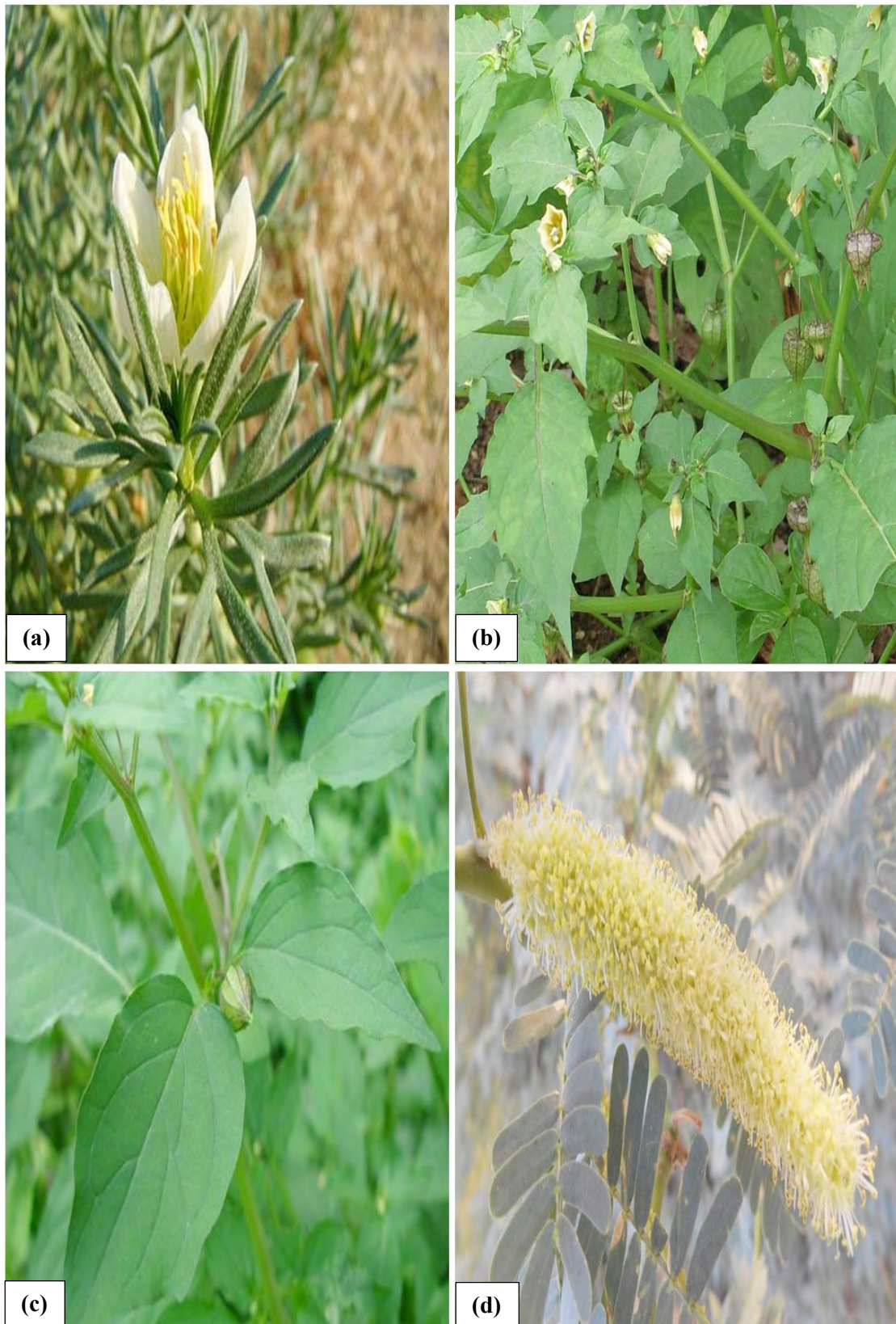


**Plate 28.** Field pictorial view of (a) *Peganum harmala*; scabrous leaf with whitish flower, (b) *Physalis divaricata*; vegetative branches, (c) *Physalis minima*; sinuate leaves with berry, (d) *Prosopis cineraria*; creamy white pedunculate spike.

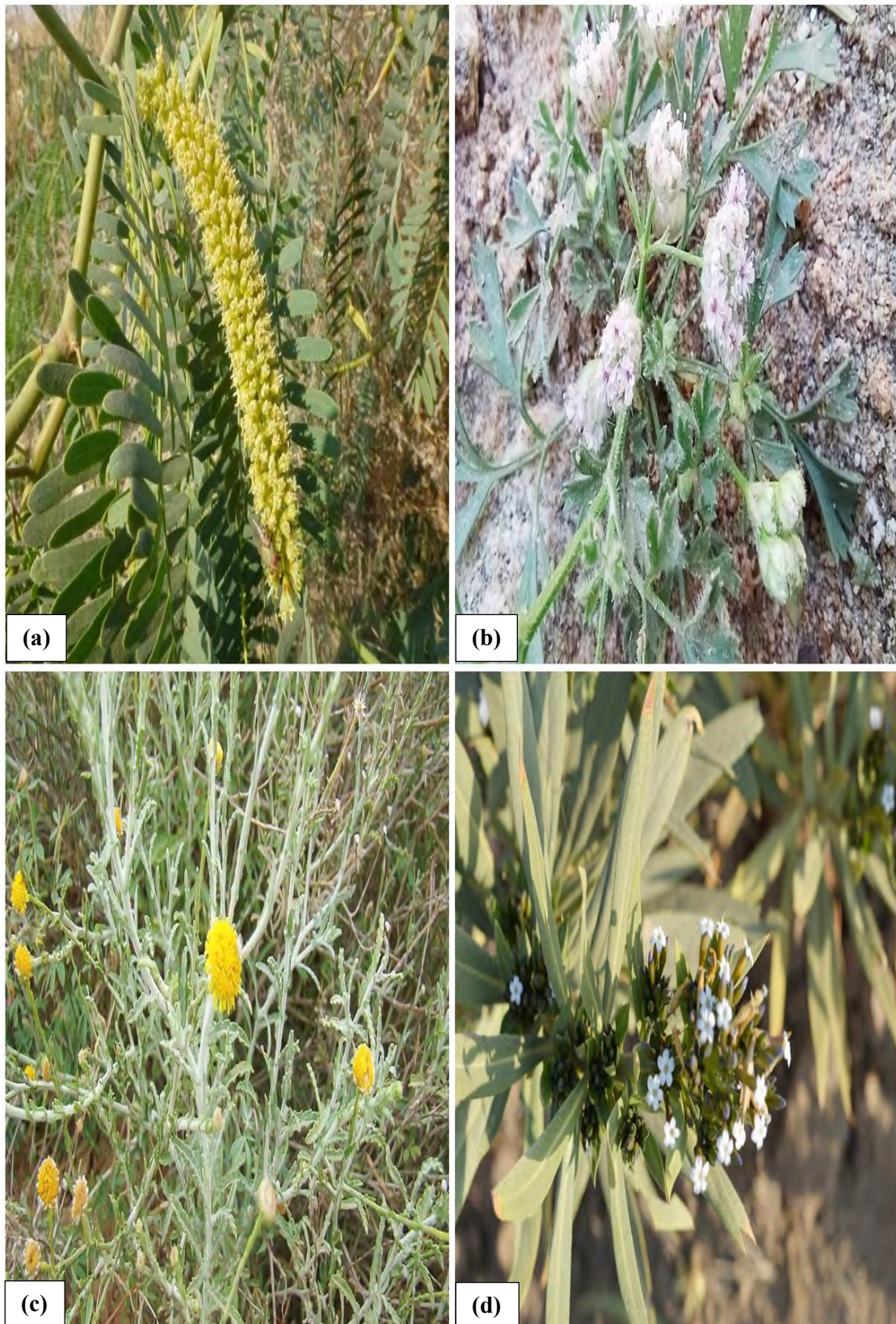


**Plate 29.** Field pictorial view of (a) *Prosopis juliflora*; pinnate leaves with axillary spike, (b) *Psammogeton biternatum*; vegetative branches, (c) *Pulicaria boissieri*; floral branches with capitulum, (d) *Rhazya stricta*; white foliaceous flowers.

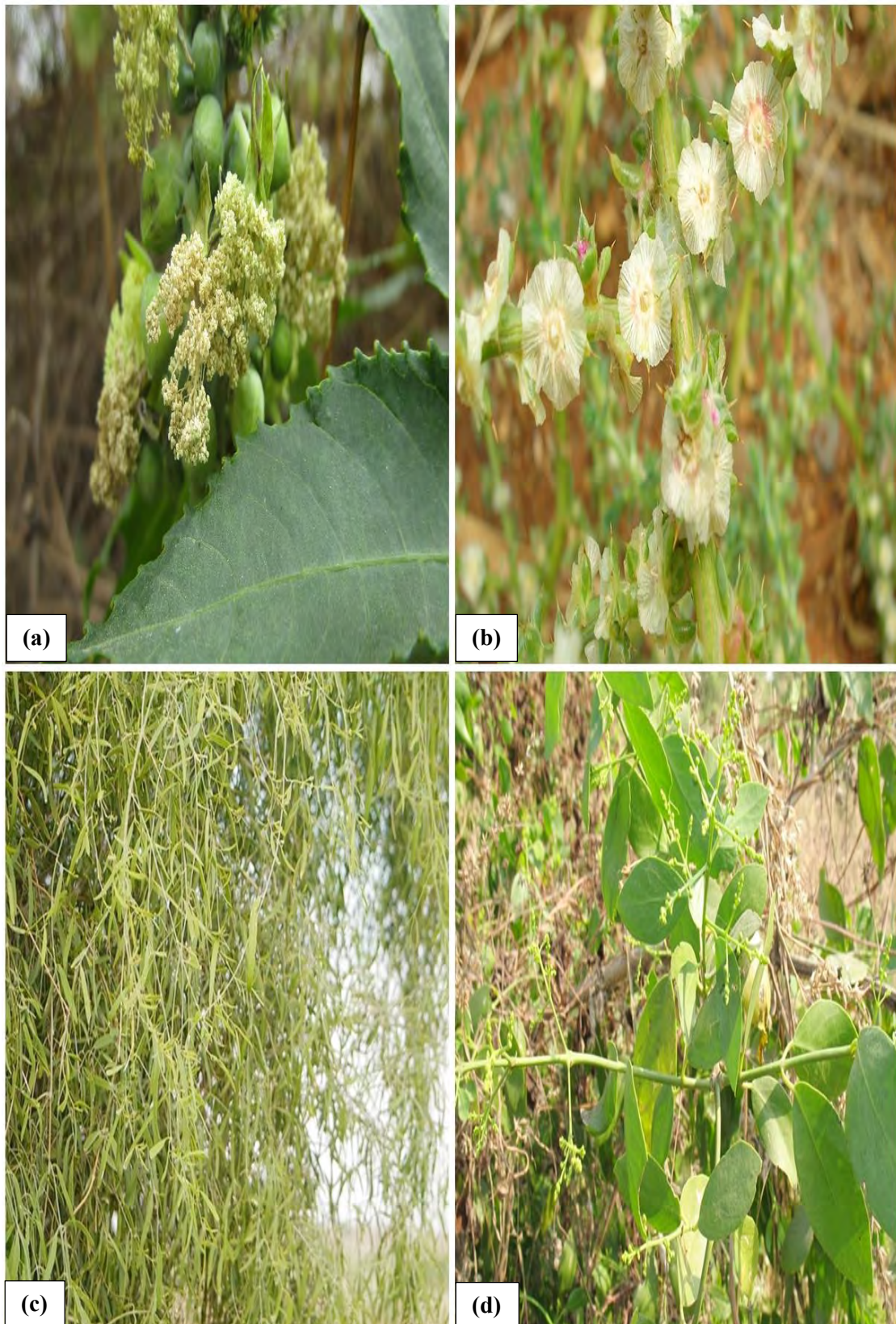


**Plate 30.** Field pictorial view of (a) *Ricinus communis*; inflorescence with calyx lobes, (b) *Salsola tragus*; solitary floral branch, (c) *Salvadora oleoides*; Leaves coriaceous, (d) *Salvadora persica*; sub-fleshy elliptic ovate leaves.

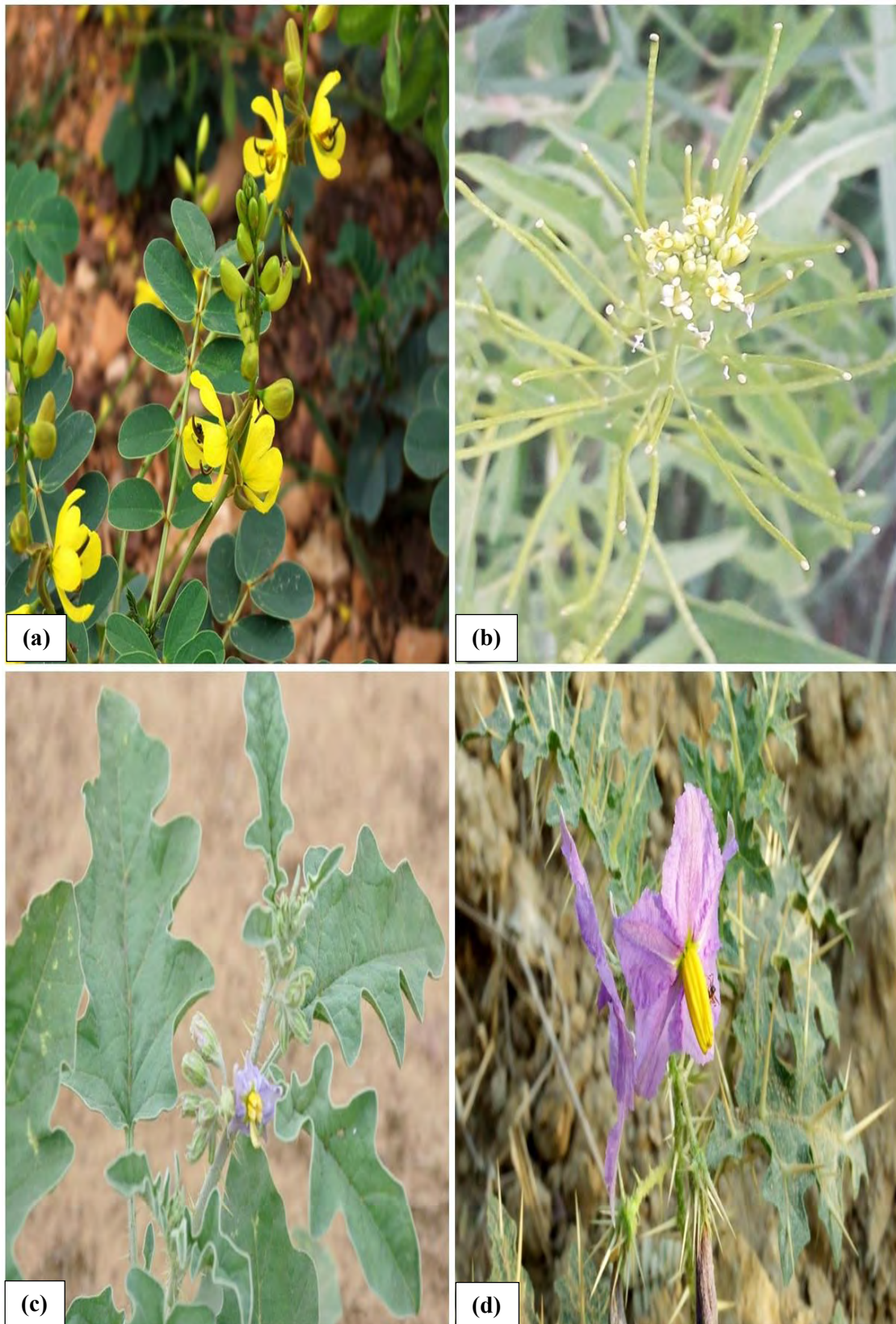


**Plate 31.** Field pictorial view of (a) *Senna italica*; obovate leaves with yellow flowers, (b) *Sisymbrium irio*; yellow pedicel, (c) *Solanum incanum*; sinuate leaves, (d) *Solanum surattense*; purple flower with elongated anther.

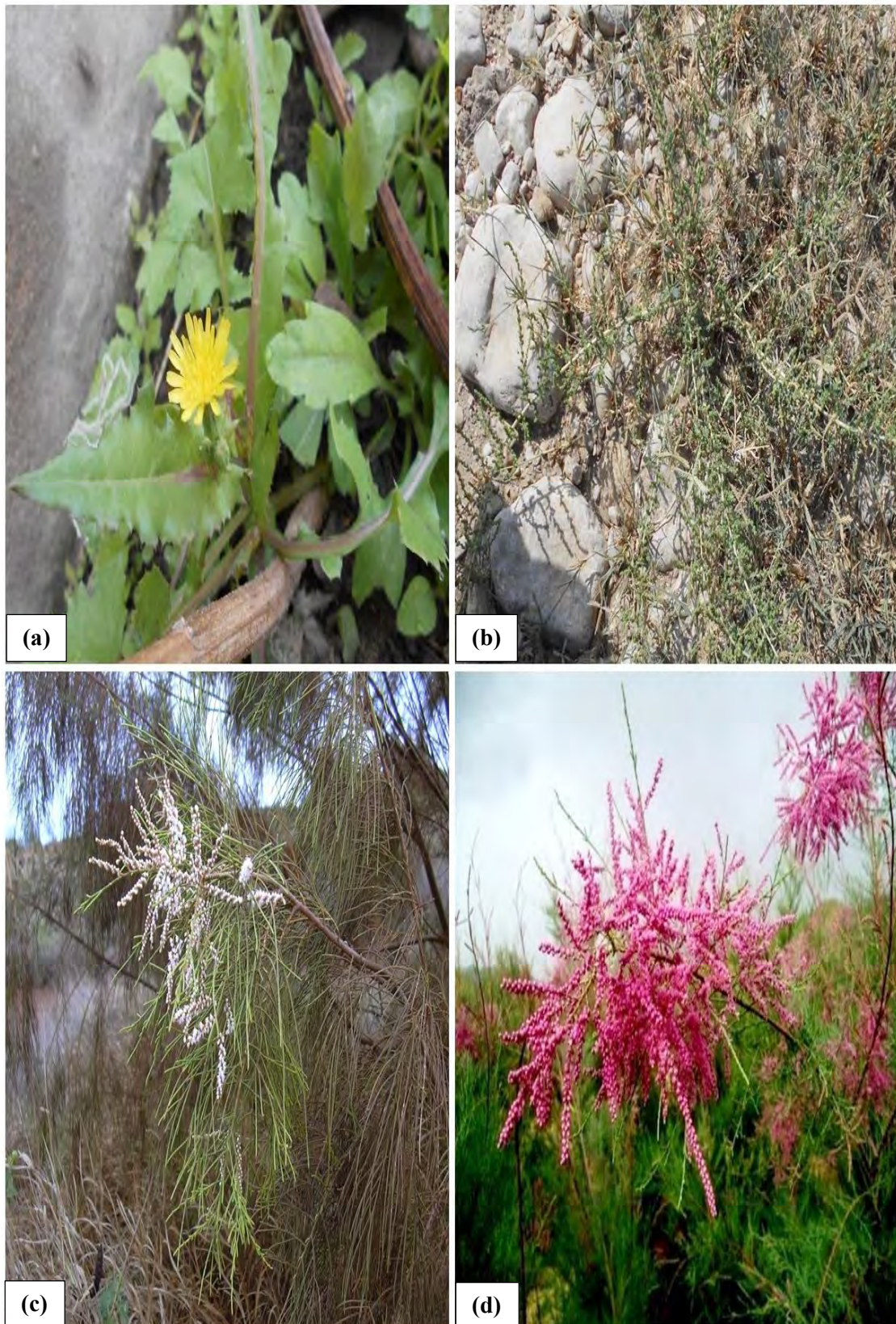


**Plate 32.** Field pictorial view of (a) *Sonchus asper*; lanceolate leaves with capitulum, (b) *Suaeda fruticosa*; shrubby bush, (c) *Tamarix aphylla*; subsessile pinkish white flower, (d) *Tamarix dioica*; purplish pink subsessile flower

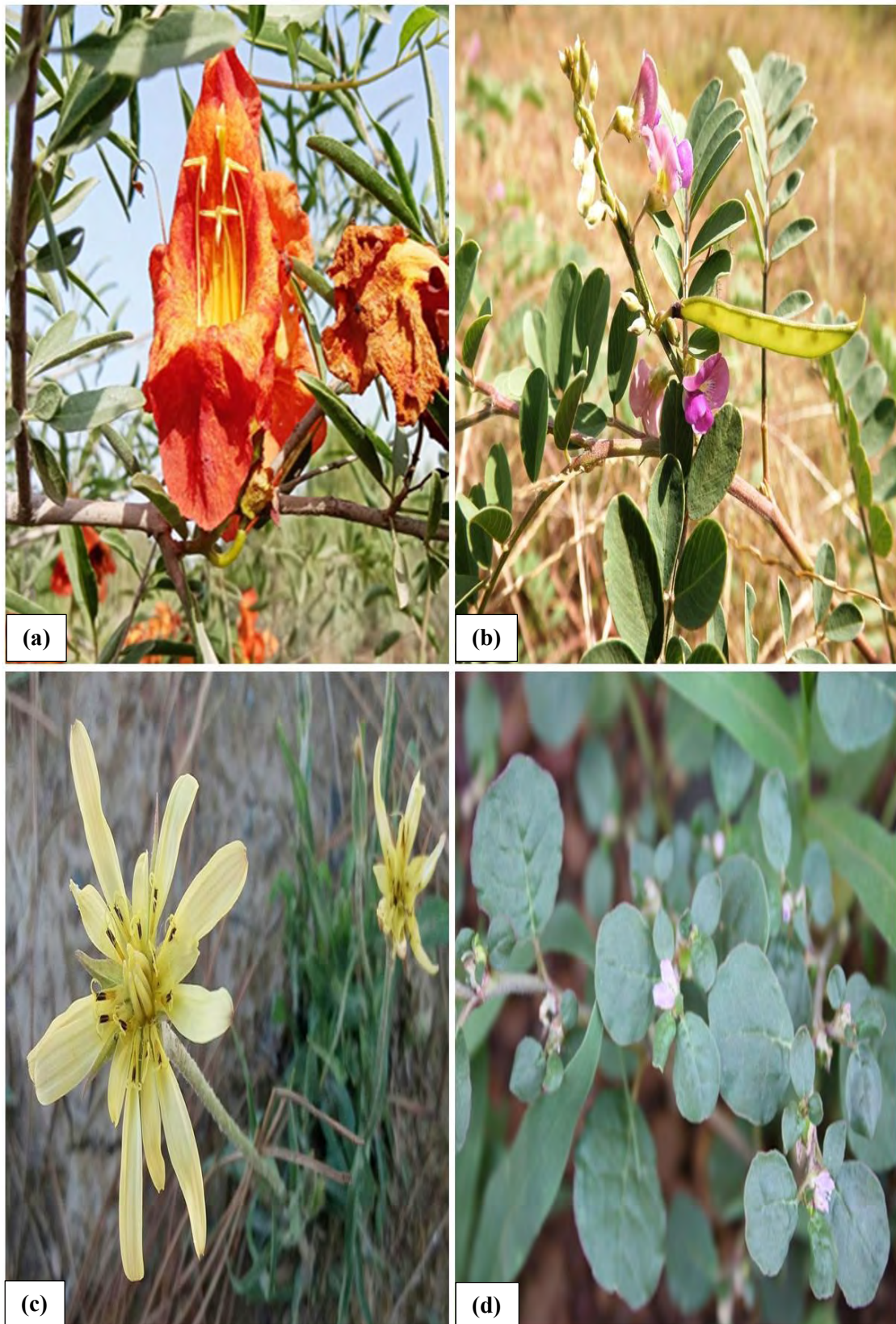


**Plate 33.** Field pictorial view of (a) *Tecomella undulata*; filaments of longer stamens, (b) *Tephrosia purpurea*; leaf imparipinnate, (c) *Tragopogon gracilis*; flower-heads phyllaries, (d) *Trianthema portulacastrum*; sub-orbicular leaves



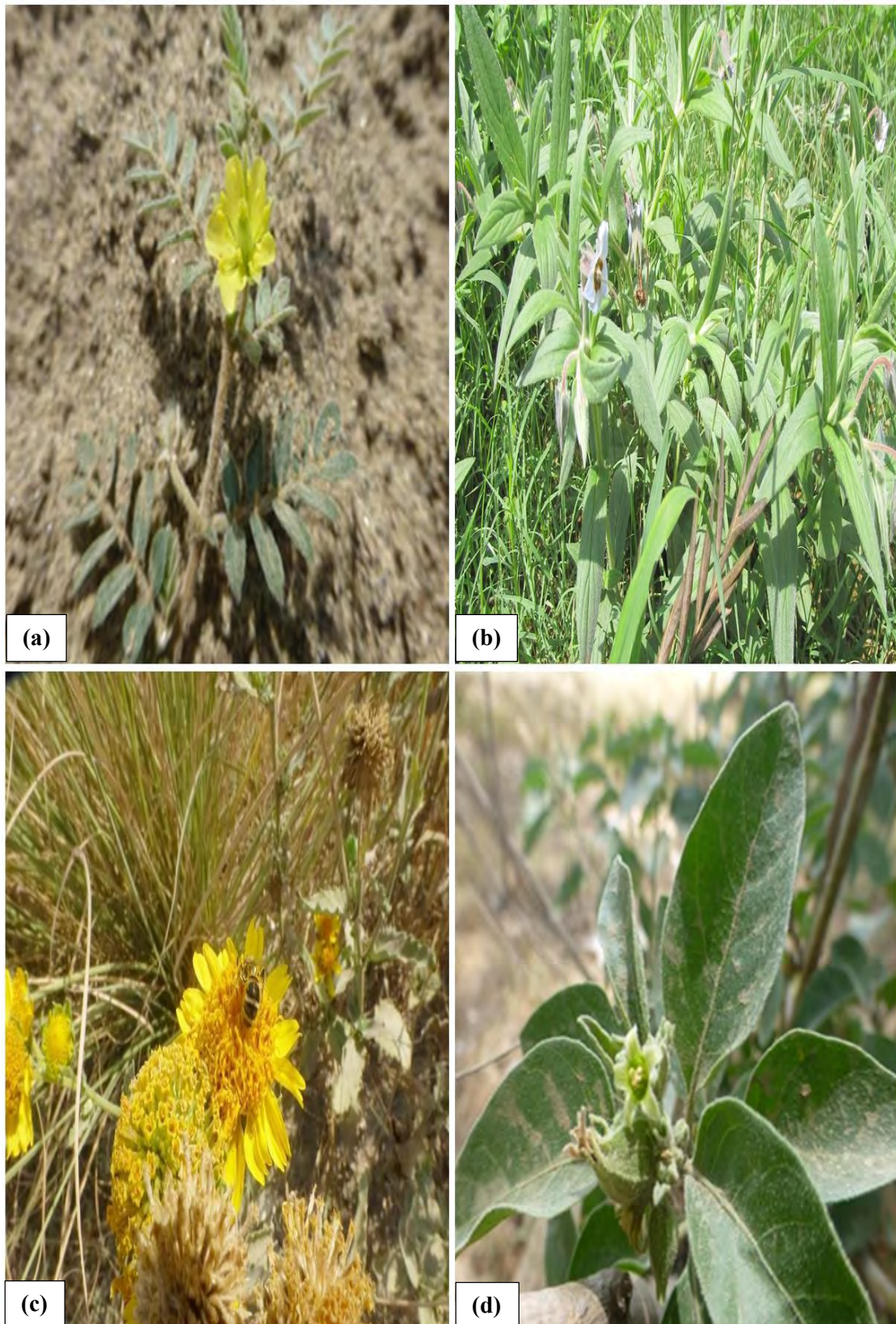


**Plate 34.** Field pictorial view of (a) *Tribulus terrestris*; paripinnate leaves with yellow flower, (b) *Trichodesma indicum*; densely hairy branches, (c) *Verbesina encelioides*; yellow flower-heads, (d) *Withania coagulans*; elliptic-ovate leaves

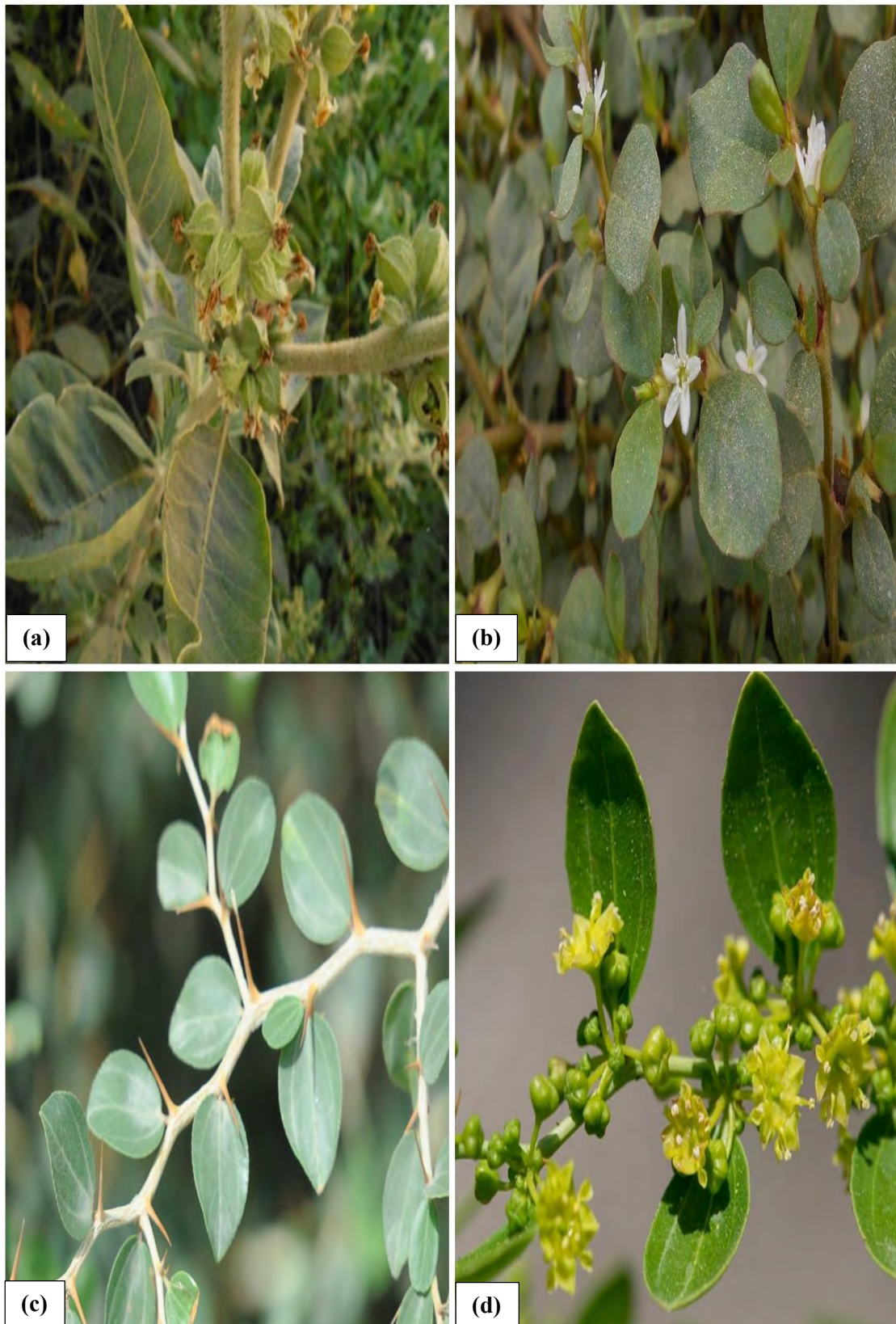
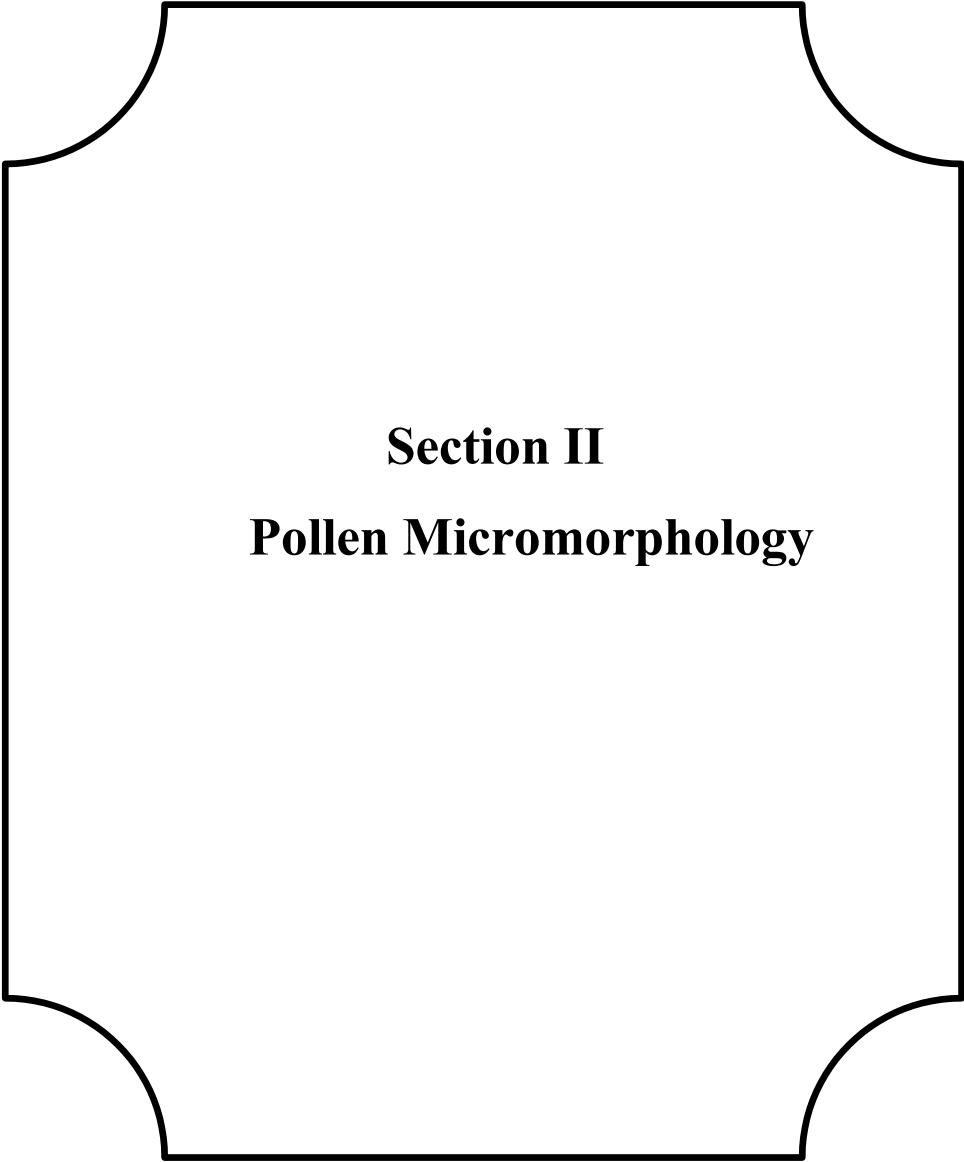


**Plate 35.** Field pictorial view of (a) *Withania somnifera*; axillary cluster flower, (b) *Zaleya pentandra*; oblong leaves, (c) *Ziziphus nummularia*; orbicular leaves, (d) *Ziziphus spina-christi*; ovate-elliptic leaves with axillary tomentose inflorescence



**Section II**  
**Pollen Micromorphology**

### 3.2 Pollen Micromorphological Studies of Dicot flora

Here we describe in this section, the detailed pollen micro-morphology of 77 Dicot angiosperm species belonging to 22 families using scanning electron microscopy from the Thal Desert. Among them, Amaranthaceae (14 species) was the most dominating family having maximum no. of species followed by Asteraceae (13 species), Fabaceae (nine species), Solanaceae (eight species), Boraginaceae (five species), Brassicaceae (four species), Aizoaceae, Cactaceae, Capparaceae, Cucurbitaceae, Euphorbiaceae, Rhamnaceae, Tamaricaceae and Zygophyllaceae (each with two species), Apiaceae, Apocynaceae, Bignoniaceae Malvaceae, Myrtaceae, Nitrariaceae, Nyctaginaceae and Papaveraceae (one species each).

Pollen micromorphological characters of Dicot angiosperms analyzed here include pollen type, shape, size, sculpturing, apertural membrane, mesoporia, pore density, echini and spines features, lacunate grains, colpus orientation, mesocolpium distance, exine thickness, P/E ratio, pore number, polarity, dispersal unit, operculum, ektexinuous bodies, pollen diameter, colpi size and pollen fertility and sterility determination.

### 3.2.1 Micromorphological Pollen Structure of Amaranthaceous taxa

Amaranthaceous pollen visualization using scanning microscopy and used pollen characters like pores, shape, size and mesoporia as key characters. From this study of the palynology from the family Amaranthaceae for 14 species, nine genera are observed by scanning electron microscopy. Chenopodiaceae and Amaranthaceae constitute a stenopalynologic group which contains similar pollen grains were classified following Erdtman (1966). A pollen-type definition based on different pollen characters, especially the pore numbers and pore structure, may help in inferring more precise environmental information from Amaranthaceous pollen, one of the most dominant components of pollen assemblages in arid regions. The means and standard deviations of pollen character measurements from LM and SEM are presented in Table 5. A summary of pollen morphological results and important findings for each genus is also provided in the table. The pollen morphological structures were illustrated in Plate 36, 37 & 38.

#### a) Pollen size

Small as in nine species, small to medium in three species, and medium in the rest studied in two species. Perveen and Qaiser (2012) used pollen size as diagnostic character to differentiate between pollen types. However, Pan (1993) reported that it influenced by humidity in various habitats.

#### b) Pollen shape

Prolate-spheroidal as dominant shape in *Achyranthes aspera*, *Aerva javanica*, *Amaranthus graecizans*, *Amaranthus retroflexus*, *Amaranthus viridis*, *Chenopodium album*, *Chenopodium ficifolium*, *Chenopodium murale*, *Haloxylon stocksii* and *Suaeda fruticosa*, oblate-spheroidal in *Aerva lanata*, *Bassia indica*, *Digera muricata* and *Salsola tragus* (Table 3).

#### c) Pore number

12-16 in *A. aspera*, 25-27 in *A. javanica*, 9-13 in *A. lanata* and *S. tragus*, 22-28 in *A. graecizans*, 16-19 in *A. retroflexus*, 33-35 in *A. viridis*, 20-24 in *B. indica*, 14-17 in *C. album* and *S. fruticosa*, 8-12 in *C. ficifolium*, 23-26 in *C. murale* and *H. stocksii*, 32-36 in *D. muricata*. El Ghazali (2021) mentioned that pore size, pore number, and spinules shape are considered valuable characteristics in Amaranthaceous taxa.

#### **d) Operculum**

The pollen grains of the Amaranthaceae may be operculate or nonoperculate. The presence/absence of opercula, may occur even within the same genus (Dehghani et al., 2021). Opercula present in nine taxa and absent in the rest five species.

#### **e) Sculpturing Elements**

Smooth sparsely granulate as in *A. aspera*, scabrate-spinulose in *A. javanica*, micro-spinulose perforate in *C. album*, micro-echinate scabrate to meta-reticulate in *D. muricata*, granulate, nano-spinulate in *S. tragus*, granulate-spinulose perforate in *S. fruticosa*, granulate-perforate echinate in *A. graecizans* and *A. viridis* and micro-echinate perforate in the rest six species (Plate 36, 37 & 38, Table 4). The term metareticulate sculpture used for *D. muricata* was proposed by Borsch and Barthlott (1998) to describe pantoporate pollen with a reticulum-like structure of vaulted mesopori and sunken pores with width to the height ratio of mesopori less than one.

#### **f) Tectum**

High resolution scanning electron microscopy (SEM) revealed punctate tectum (Borsch et al., 2018). Punctate in *B. indica*, *D. muricata* and *H. stocksii* and not punctate in the rest 11 taxa.

#### **g) Ektexinous Bodies**

The pores are covered by ektexinous bodies of different number and shape, they may be closely adjoined to each other or separated from each other. The sculpture of pore membranes were described as having hook-shaped stellately arranged ektexinous bodies, with ektexinous bodies arranged in a mosaic-like pattern (Zumaya et al., 2013). Absent in four species and present in the rest of 10 taxa. Borsch (1998) reported that differences in ektexinous bodies shapes in Chenopodiaceae less variable than in Amaranthaceae but their number, and the number of microspines are characteristic for some species.

#### **h) Aperture Group**

The pollen in this study can be divided into three groups based on the character of the aperture, i.e., convex-shaped circular group, collapsed-shaped circular group, and deeply collapsed circular group.

### i) Mesoporia

The mesoporia is an area of a pollen grain surface delimited by lines between the apices of adjacent colpi or the margins of adjacent pores also named mesh. The mesoporia refers to the tectate areas surrounding two sunken pores (Punt et al., 2007). Sánchez-del Pino et al., (2016) introduced the concepts of meta-reticulate pollen, mesoporia, conjunction points and structural elements to describe the ornamentation of the amaranthoid pollen and changed the whole understanding of pollen morphology in the family. The pollen in this study can be divided into three groups based on the mesoporia, i.e., mesoporia broadly flat, mesoporia moderately and broadly vaulted, and mesoporia narrow and highly vaulted.

### j) Quantitative Attributes

Pollen diameter variations in polar view ranged from (12.2  $\mu\text{m}$ ) in *C. album* to (26.3  $\mu\text{m}$ ) in *A. retroflexus*. While equatorial diameter measured minimum for *C. album* (11.5  $\mu\text{m}$ ) and maximum for *B. indica* (26.5  $\mu\text{m}$ ) as illustrate in Figure 5. Polar to equatorial ratio (P/E) index was determined highest for *S. fruticosa* (1.12) and lowest for *D. muricata* (0.94) as shown in Figure 6. The pore diameter ranged from 0.7  $\mu\text{m}$  (found in *A. retroflexus*) to 1.64  $\mu\text{m}$  (found in *S. tragus*) as mentioned in Figure 8. Pore density was also calculated found maximum for *A. retroflexus* 5.37  $\mu\text{m}$  and minimum for *H. stocksii* 2.34  $\mu\text{m}$  (Figure 9). Interporal distance was calculated largest for *C. ficifolium* (4.94  $\mu\text{m}$ ) and shortest for *A. javanica* (1.42  $\mu\text{m}$ ) (Figure 10). The exine thickness of the pollen was noted to be minimum (0.78  $\mu\text{m}$ ) in *A. graecizans* and maximum (2.15  $\mu\text{m}$ ) in *S. tragus* (Figure 7).

### k) UPGMA Dendrogram and PCA Clustering

The dendrogram distributed the Amaranthaceous species into two major clusters (Figure 11). Cluster 1 includes species *A. retroflexus*, *S. fruticosa*, *B. indica*, *D. muricata*, and *S. tragus* which are entirely distinct from other species. Cluster II is divided into two further clades; *H. stocksii* and *A. javanica* in clade 1 while clade 2 further divided into sub-clusters I (*A. graecizans* and *C. album*) while sub-cluster II with *A. lanata*, *C. ficifolium*, *A. viridis*, *C. murale* and *A. aspera*. The highest similarities were observed among *A. viridis* and *C. murale* in sub-cluster II due to the non-punctate tectum surface, and *B. indica* and *D. muricata* in cluster I with convex-shaped circular group aperture group and punctate tectum.

Principal component analysis (PCA) is one of the most important statistical tool used for factor calculations among groups to represent the variations. Typically, it is visualized by two-dimensional projections of sample data with principal axes (Zhao et al., 2016). In the present work, PCA was performed to examine pollen variability among 14 desert-inhabited Amaranthaceous taxa using variables like polar diameter, equatorial distance, P/E index, pore diameter, pore density, exine thickness and interpore distance. Variable loadings for the seven components have been illustrated in Table 2. A total of 71.23% of the accumulative variance was summarized in our present study. Eigenvalues were found higher than 1 in PC1 PC2 and PC3 hence, are considered as significant in the PCA analysis. Variable loadings analysis (Table 2) illustrated that PC1 holds about 39.105% of total data variation and delimited pollen of Amaranthaceous taxa. Interpore distance followed by pore density and pollen diameter was the most relevant variable in PC1. *A. graecizens* and *C. ficifolium* with higher values of pollen diameter and pore density were located on the positive side of the first axis whereas, *A. lanata*, *A. viridis*, *C. album* and *C. murale* on the negative side of the first axis (Figure 12). PCA second axis explained 23.70% variability separating pollen among Amaranthaceae species. The most significant variables in PC2 were pore diameter followed by exine thickness. *A. retroflexus*, *B. indica*, *D. muricata*, *S. fruticosa* and *S. tragus* were found on the positive side while *A. aspera* was placed on the negative side of the second axis.

**Table 2.** Cumulative variance and eigenvectors of principal component analysis (PCA) using quantitative palynological characters.

PC	Eigen Values	% variance
PC1	2.73	39.105
PC2	1.65	23.707
PC3	1.08	15.444
PC4	0.84	12.018
PC5	0.40	5.727
PC6	0.27	3.994
PC7	0.0002	0.004

**Keywords:** PC = Principal component



### 3.2.2 Taxonomic Key for Amaranthaceous Pollen Identification

- 1 + Operculum absent, broadly vaulted mesoporia, non-punctate.....*A. retroflexus*
- Narrow vaulted mesoporia, punctate tectum, ektexinuos bodies absent.....*B. indica*
- 2 + Broadly vaulted mesoporia, ektexinuos bodies present, non-punctate tectum.....*C. ficifolium*
- Ektexinuos bodies present, broadly vaulted mesoporia, non-punctate tectum, micro-echinate perforate .....*C. murale*
- 3 + Moderately broad vaulted mesoporia, granulate-spinulose perforate, non-punctate tectum, ektexinuos bodies present.....*S. fruticosa*
- 4 + Operculum present, sparsely granulate, non-punctate tectum.....*A. aspera*
- Highly vaulted mesoporia, scabrate-spinulose tectum.....*A. javanica*
- 5 + Narrow vaulted mesoporia, pantoaperturate, non-punctate tectum.....*A. lanata*
- Ektexinuos bodies present, granulate-spinulose, perforate tectum.....*A. graecizens*
- 6 + Moderately and broadly vaulted mesoporia, granulate-perforate, non-punctate tectum.....*A. viridis*
- Broadly flat mesoporia, echinate, granulate-perforate, ektexinuos bodies absent.....*C. album*
- 7 + Micro-echinate scabrate, meta-reticulate tectum, ektexinuos bodies absent.....*D. muricata*
- Densely micro-echinate perforate, ektexinuos bodies present, punctate tectum.....*H. stocksii*
- 8 + Granulate, nano-spinules tectum, narrow and highly vaulted mesoporia.....*S. tragus*

**Table 3.** Pollen morphological characters among desert inhabited Amaranthaceous species.

<b>Sr. No</b>	<b>Amaranthaceous taxa</b>	<b>Size</b>	<b>Amb/ Polar View</b>	<b>Operculum</b>	<b>Shape</b>	<b>Aperture character</b>	<b>Aperture group</b>
1.	<i>Achyranthes aspera</i> L.	Small	Circular	Present	Prolate-spheroidal	Periporate	Convex shaped circular group
2.	<i>Aerva javanica</i> (Burm.f.) Juss. ex Schult.	Small	Spheroidal	Present	Prolate-spheroidal	Periporate	Collapsed shaped circular group
3.	<i>Aerva lanata</i> (L.) Juss.	Small	Spheroidal	Present	Oblate-spheroidal	Periporate	Deeply collapsed circular group
4.	<i>Amaranthus graecizans</i> L.	Small	Rounded	Present	Prolate-spheroidal	Periporate	Convex shaped circular group
5.	<i>Amaranthus retroflexus</i> L.	Small to medium	Circular	Absent	Prolate-spheroidal	Periporate	Collapsed shaped circular group
6.	<i>Amaranthus viridis</i> L.	Small	Rounded	Present	Prolate-spheroidal	Periporate	Collapsed shaped circular group
7.	<i>Bassia indica</i> (Wight) A.J.Scot	Medium	Circular	Absent	Oblate-spheroidal	Periporate	Convex shaped circular group
8.	<i>Chenopodium album</i> L.	Small	Circular	Present	Prolate-spheroidal	Periporate	Deeply collapsed circular group
9.	<i>Chenopodium ficifolium</i> Sm.	Small	Spheroidal	Absent	Prolate-spheroidal	Periporate	Collapsed shaped circular group
10.	<i>Chenopodium murale</i> L.	Small	Rounded	Absent	Prolate-spheroidal	Periporate	Deeply collapsed circular group
11.	<i>Digera muricata</i> (L.) Mart.	Small to medium	Spheroidal	Present	Oblate-spheroidal	Periporate	Convex shaped circular group
12.	<i>Haloxylon stocksii</i> (Boiss.) Benth. & Hook. f.	Small	Spheroidal	Present	Prolate-spheroidal	Periporate	Collapsed shaped circular group
13.	<i>Salsola tragus</i> L.	Medium	Rounded	Present	Oblate-spheroidal	Periporate	Deeply collapsed circular group
14.	<i>Suaeda fruticosa</i> Forssk. ex J.F.Gmel.	Small to medium	Circular	Absent	Prolate-spheroidal	Periporate	Convex shaped circular group

**Table 4.** Qualitative pollen micromorphological features of desert inhabited Amaranthaceous taxa.

<b>Sr. No</b>	<b>Amaranthaceous taxa</b>	<b>Mesoporina</b>	<b>Ektexiniuos bodies</b>	<b>Pollen Surface</b>	<b>Exine Sculpture</b>	<b>Tectum</b>
1.	<i>Achyranthes aspera</i> L.	Broadly flat	Present	Psilate-scabrate	Smooth, sparsely granulate	Non punctate
2.	<i>Aerva javanica</i> (Burm.f.) Juss. ex Schult.	Narrow and highly vaulted	Present	Scabrate	Scabrate-spinulose	Non punctate
3.	<i>Aerva lanata</i> (L.) Juss.	Narrow and highly vaulted	Absent	Scabrate	Pantoaperturate, micro-echinate perforate	Non punctate
4.	<i>Amaranthus graecizans</i> L.	Moderately and broadly vaulted	Present	Psilate	Granulate-spinulose, perforate	Non punctate
5.	<i>Amaranthus retroflexus</i> L.	Moderately and broadly vaulted	Present	Scabrate	Micro-echinate perforate	Non punctate
6.	<i>Amaranthus viridis</i> L.	Moderately and broadly vaulted	Present	Scabrate	Echinate, evenly granulate, perforate	Non punctate
7.	<i>Bassia indica</i> (Wight) A.J.Scot	Narrow and highly vaulted	Absent	Scabrate	Microechinate-perforate	Punctate
8.	<i>Chenopodium album</i> L.	Broadly flat	Absent	Scabrate	Scabrate-micro-spinulose perforate	Non punctate
9.	<i>Chenopodium ficifolium</i> Sm.	Broadly flat	Present	Psilate-scabrate	Micro-echinate perforate	Non punctate
10	<i>Chenopodium murale</i> L.	Broadly flat	Present	Scabrate	Micro-echinate perforate	Non punctate
11	<i>Digera muricata</i> (L.) Mart.	Moderately and broadly vaulted	Absent	Scabrate	Micro-echinate scabrate, meta-reticulate	Punctate
12	<i>Haloxylon stocksii</i> (Boiss.) Benth. & Hook. f.	Broadly flat	Present	Scabrate	Densely micro-echinate perforate	Punctate
13	<i>Salsola tragus</i> L.	Narrow and highly vaulted	Present	Scabrate	Granulate, nano-spinules	Non punctate
14	<i>Suaeda fruticosa</i> Forssk. ex J.F.Gmel.	Moderately and broadly vaulted	Present	Scabrate	Granulate-spinulose perforate	Non punctate

**Table 5.** Pollen morphometric characters measurements among Amaranthaceous pollen.

S. No.	Amaranthaceous taxa	P/E ratio	ET (x ± SE µm)	PVD (x ± SE µm)	EVD (x ± SE µm)	PN	PD (x ± SE µm)	PDT (x ± SE µm)	IPD (x ± SE µm)	Fertility (%)	Sterility (%)
1.	<i>Achyranthes aspera</i> L.	1.05	1.04±0.07	15.6±0.13	14.8±0.2	12-16	1.23±0.21	3.1±0.13	3.27±0.62	89.4	10.5
2.	<i>Aerva javanica</i> (Burm.f.) Juss. ex Schult.	1.09	0.86±0.34	19.4±0.09	17.7±0.37	25-27	0.85±0.11	2.8±1.19	1.42±0.14	97.6	2.3
3.	<i>Aerva lanata</i> (L.) Juss.	0.98	1.25±0.16	16.9±0.23	17.2±0.17	10-13	1.12±0.53	4.45±0.32	2.73±0.33	93.2	6.7
4.	<i>Amaranthus graecizans</i> L.	1.07	0.78±0.08	13.5±0.11	12.6±0.21	22-28	1.58±0.24	2.61±0.49	4.15±1.24	95.6	4.3
5.	<i>Amaranthus retroflexus</i> L.	1.10	1.14±0.19	26.3±0.47	23.9±0.86	16-19	0.70±0.19	5.37±0.23	3.43±1.04	93.8	6.1
6.	<i>Amaranthus viridis</i> L.	1.04	1.30±0.26	14.4±0.18	13.8±0.08	33-35	1.34±0.12	4.76±1.26	2.12±0.46	88.4	11.5
7.	<i>Bassia indica</i> (Wight) A.J.Scot	0.96	1.74±0.37	25.1±0.63	26.1±0.36	20-24	0.92±0.36	3.54±0.87	1.85±0.74	98.3	1.6
8.	<i>Chenopodium album</i> L.	1.06	1.20±0.11	12.2±0.19	11.5±0.13	14-17	1.35±0.22	2.56±0.61	2.84±0.79	92.5	7.4
9.	<i>Chenopodium ficifolium</i> Sm.	1.05	0.97±0.08	17.3±0.39	16.4±0.27	8-12	1.16±0.09	5.13±1.83	4.62±0.93	90.8	9.1
10.	<i>Chenopodium murale</i> L.	1.03	1.47±0.64	15.1±0.07	14.6±0.16	24-26	0.80±0.17	4.32±0.41	2.45±0.32	94.2	5.7
11.	<i>Digera muricata</i> (L.) Mart.	0.94	1.20±0.28	23.8±0.2	25.2±0.11	32-36	1.10±0.44	3.68±0.29	1.78±0.18	89.3	10.6
12.	<i>Haloxylon stocksii</i> (Boiss.) Benth. & Hook. f.	1.06	1.85±0.48	20.4±0.26	19.2±0.33	23-26	1.43±0.32	2.34±0.16	4.94±1.41	92.1	7.8
13.	<i>Salsola tragus</i> L.	0.97	2.15±0.96	25.4±1.03	25.9±0.68	9-13	1.64±0.28	4.72±1.06	3.78±0.87	97.5	2.4
14.	<i>Suaeda fruticosa</i> Forssk. ex J.F.Gmel.	1.12	1.72±0.36	25.4±0.42	22.5±0.56	14-17	1.31±0.15	3.84±0.93	2.93±0.54	94.7	5.2

**Keywords:** P = Polar, E = Equatorial, PVD = Polar view diameter, EVD = Equatorial view diameter, PN = Pore number, PDT = Polar density, IPD = Inter poral distance, x = Mean, SE = Standard error, µm = micrometer

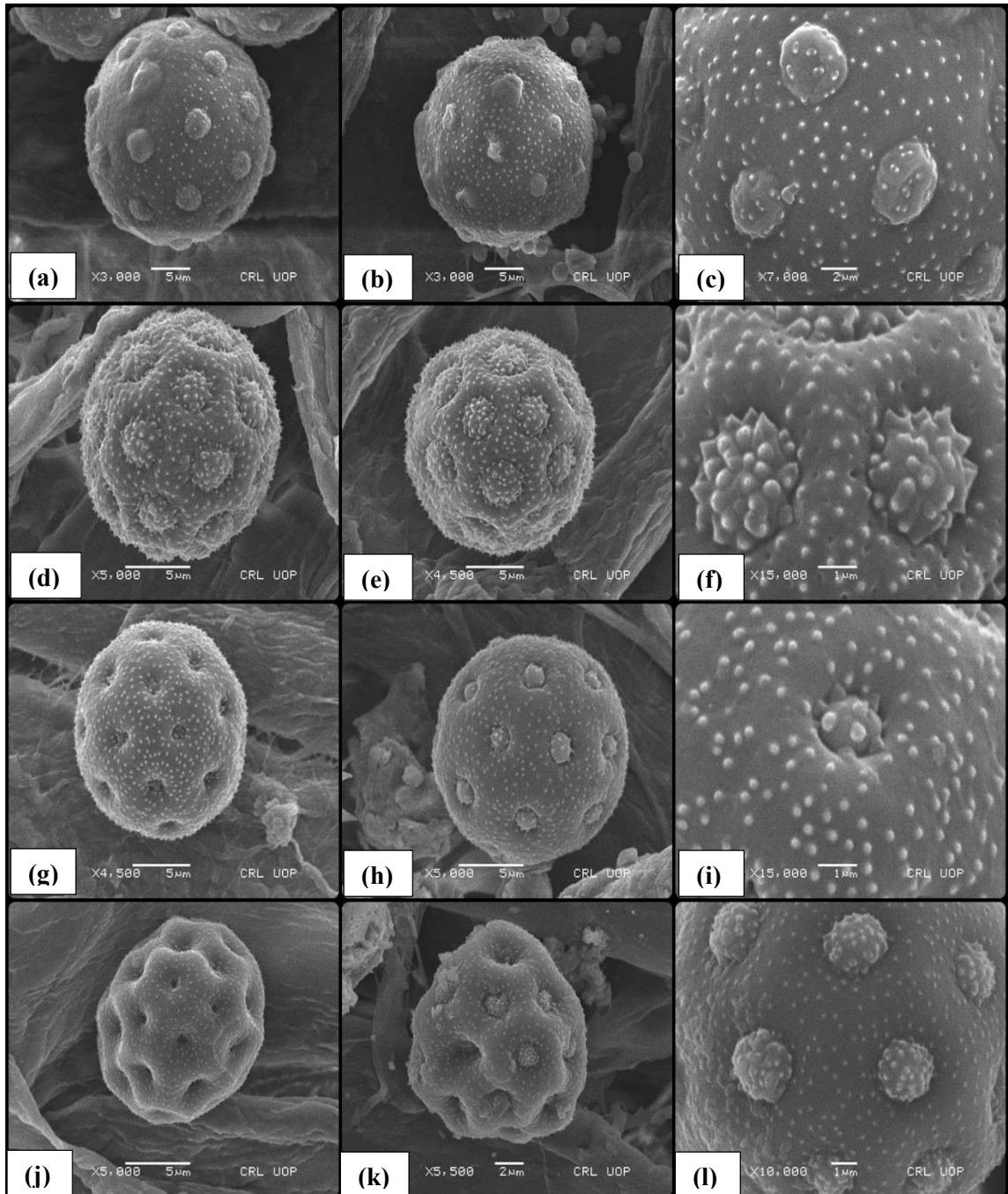


**Plate 36.** Scanning electron photomicrographs of pollen grains of Amaranthaceae. (a-c) *Achyranthes aspera*; sparsely granulate non punctate (Scale bar = 5  $\mu$ m, 2  $\mu$ m), (d-f) *Aerva javanicia*; Scabrate spiniulose and ektexiniuos bodies (Scale bar = 5  $\mu$ m, 1  $\mu$ m), (g-i) *Aerva lanata*; micro-echinate perforate, non-punctate (Scale bar = 5  $\mu$ m, 1  $\mu$ m), (j-l) *Amaranthus graecizans*; Granulate-spinulose exine (Scale bar = 5  $\mu$ m, 2  $\mu$ m, 1  $\mu$ m).

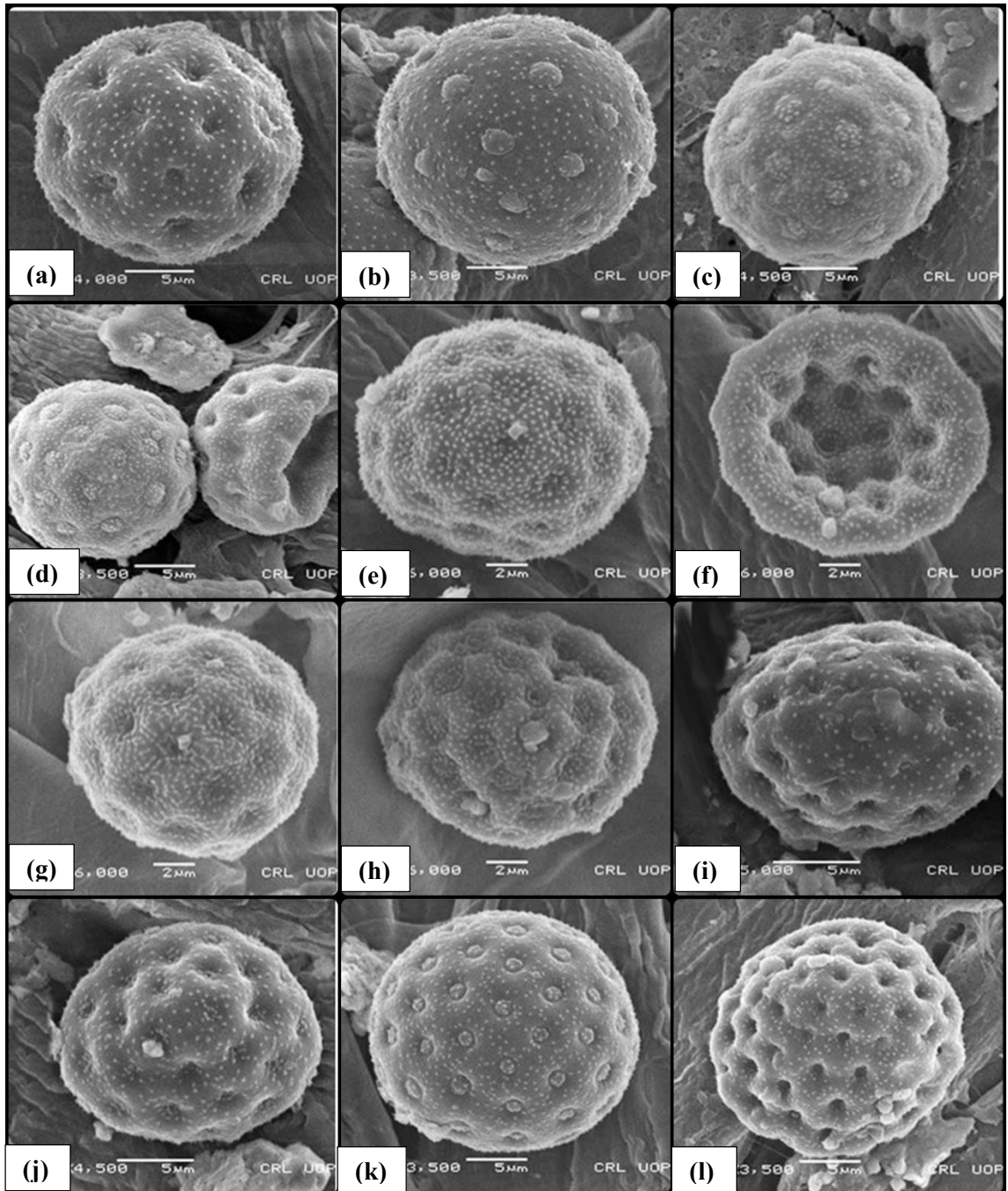


**Plate 37.** Scanning electron photomicrographs of pollen grains of Amaranthaceae. (a-b) *Achyranthes retroflexus*; micro-echinate perforate exine (Scale bar = 5  $\mu\text{m}$ ), (c-d) *Amaranthus viridis*; granulate perforate exine (Scale bar = 5  $\mu\text{m}$ ), (e-f) *Bassia indica*; micro-echinate perforate, mesoporia narrow (Scale bar = 2  $\mu\text{m}$ ), (g-h) *Chenopodium album*; Scabrate micro-spinulose exine (Scale bar = 2  $\mu\text{m}$ ), (i-j) *Chenopodium ficifolium*; Non-punctate, broad flat mesoporia (Scale bar = 5  $\mu\text{m}$ ), (j-l) *Chenopodium murale*; micro-echinate perforate sculpturing (Scale bar = 5  $\mu\text{m}$ ).

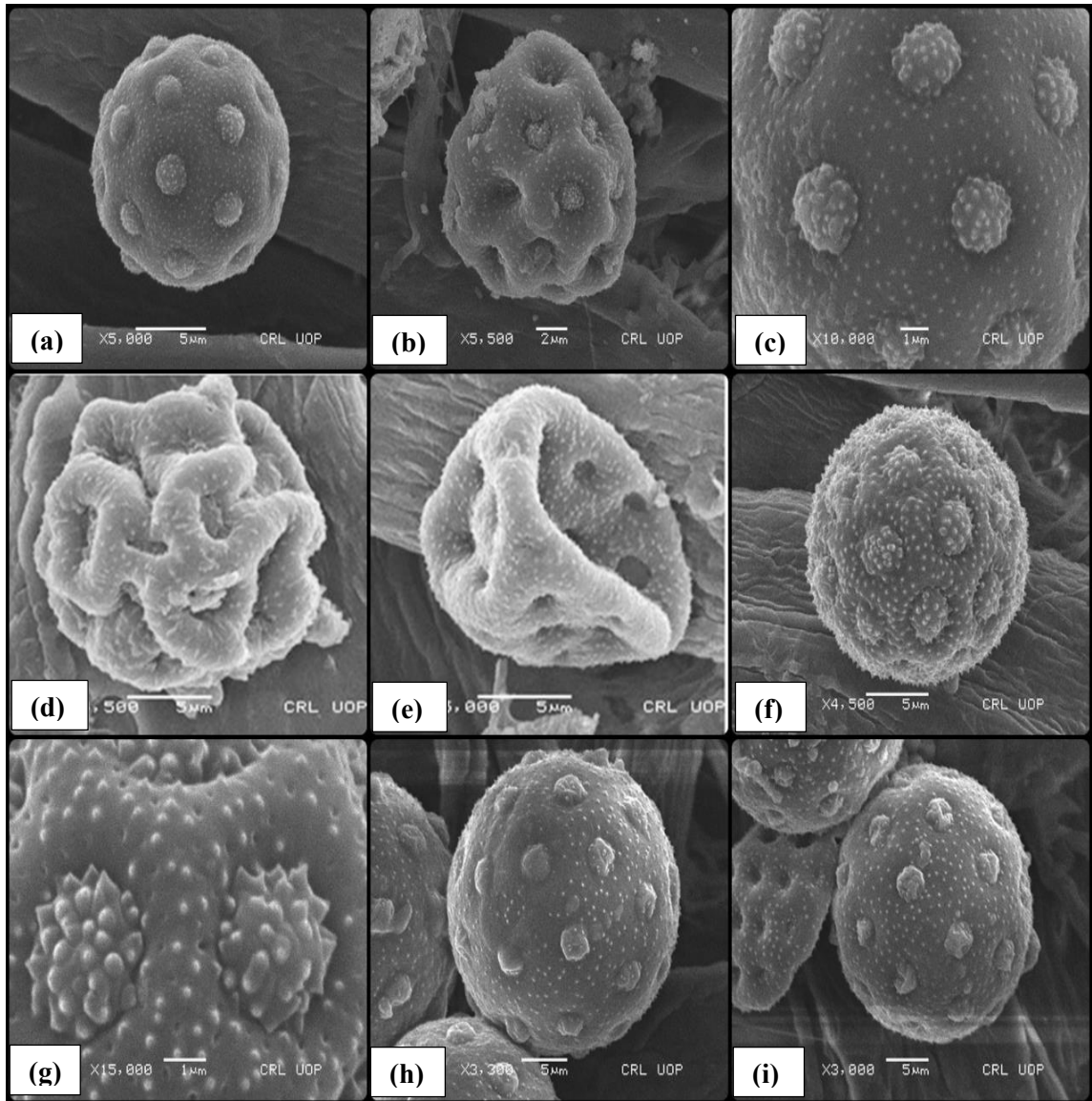


**Plate 38.** Scanning electron photomicrographs of pollen grains of Amaranthaceae. (a-c) *Digera muricata*; meta-reticulate exine (Scale bar = 5  $\mu$ m, 2  $\mu$ m, 1  $\mu$ m), (d-e) *Haloxylon stocksii*; dense micro-echinate exine (Scale bar = 5  $\mu$ m), (f-g) *Salsola tragus*; granulate nano spiniules, mesoporia narrow (Scale bar = 5  $\mu$ m, 1  $\mu$ m), (h-i) *Suaeda fruticosa*; granulate-spinulose perforate exine (Scale bar = 5  $\mu$ m)

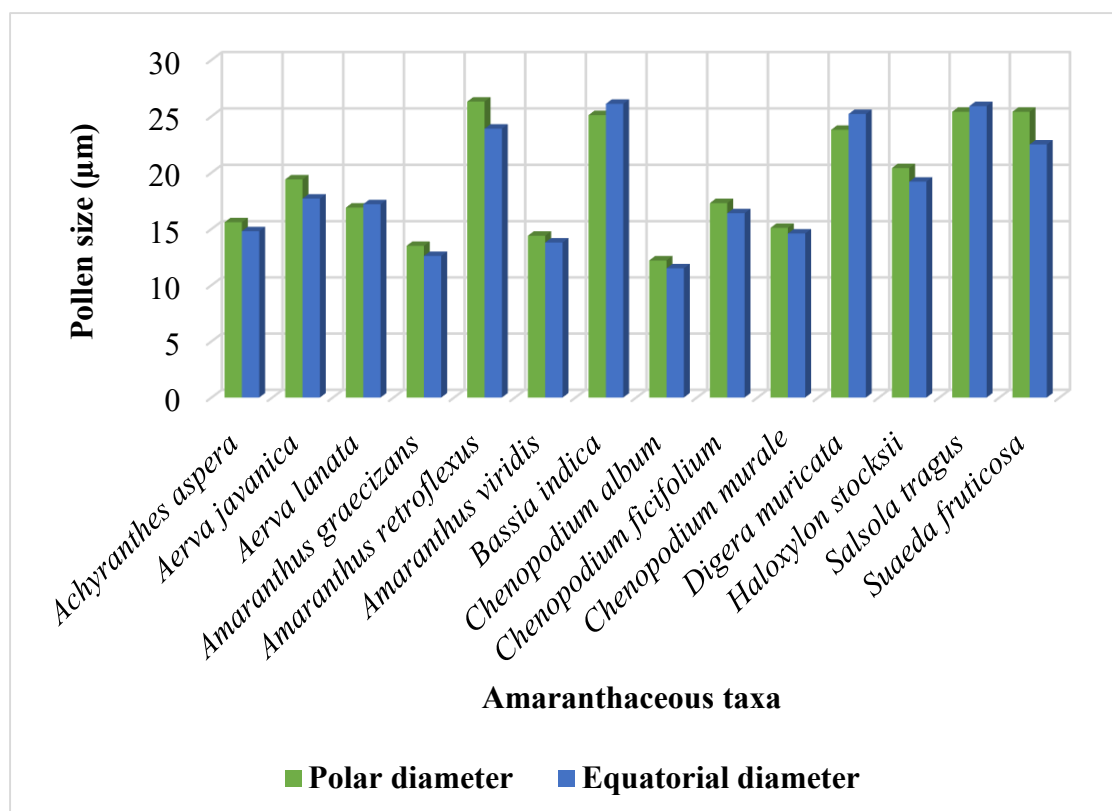


**Figure 5.** Average pollen size variability among Amaranthaceous taxa

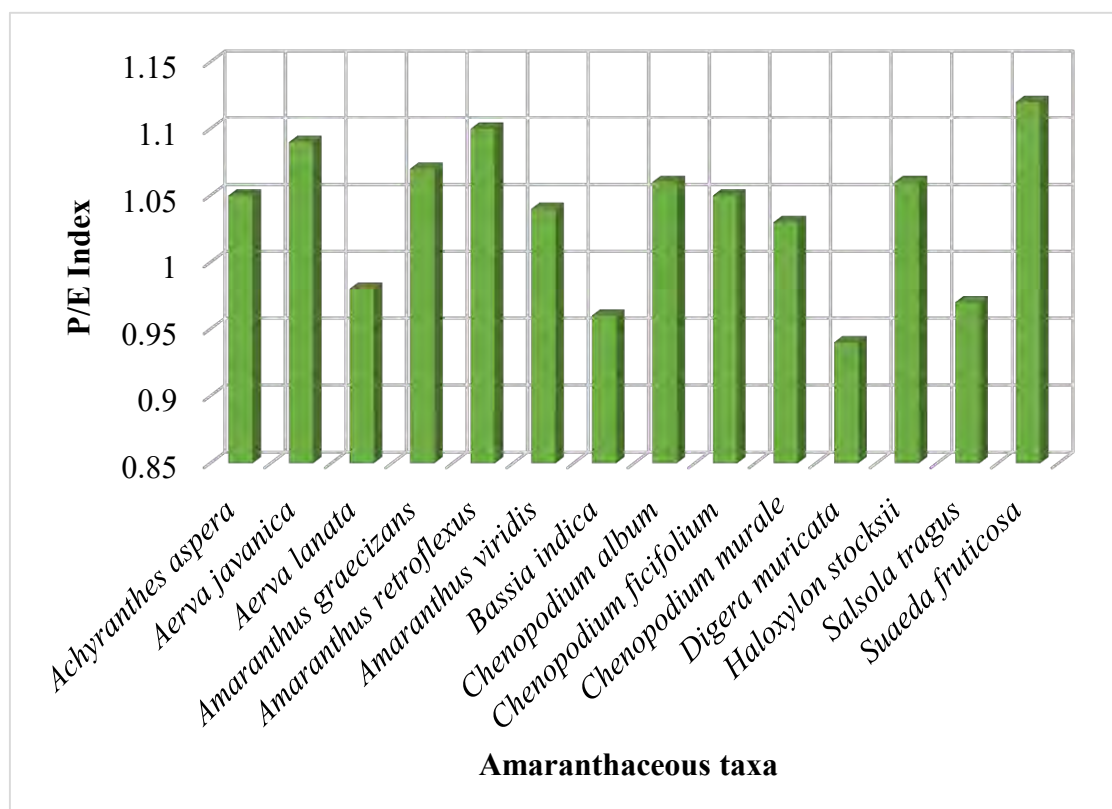


**Figure 6.** Polar to equatorial distance (P/E ratio) among Amaranthaceous taxa



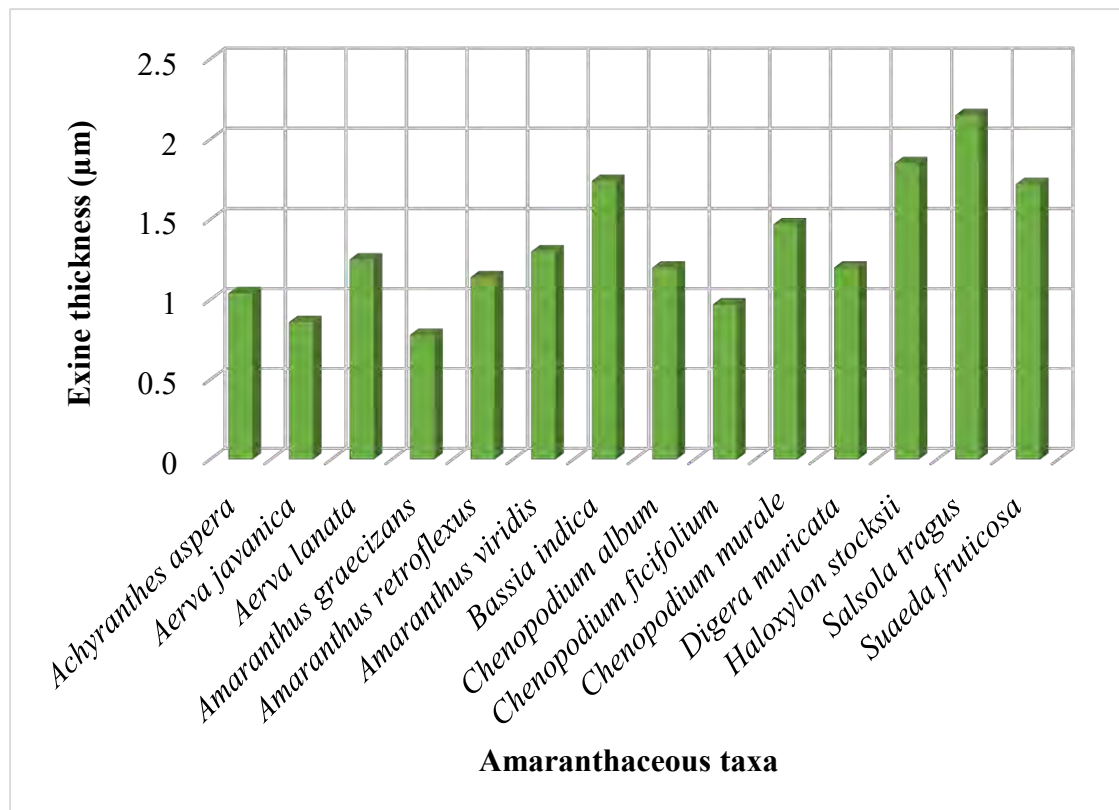


Figure 7. Mean exine thickness pollen measurements among Amaranthaceous taxa

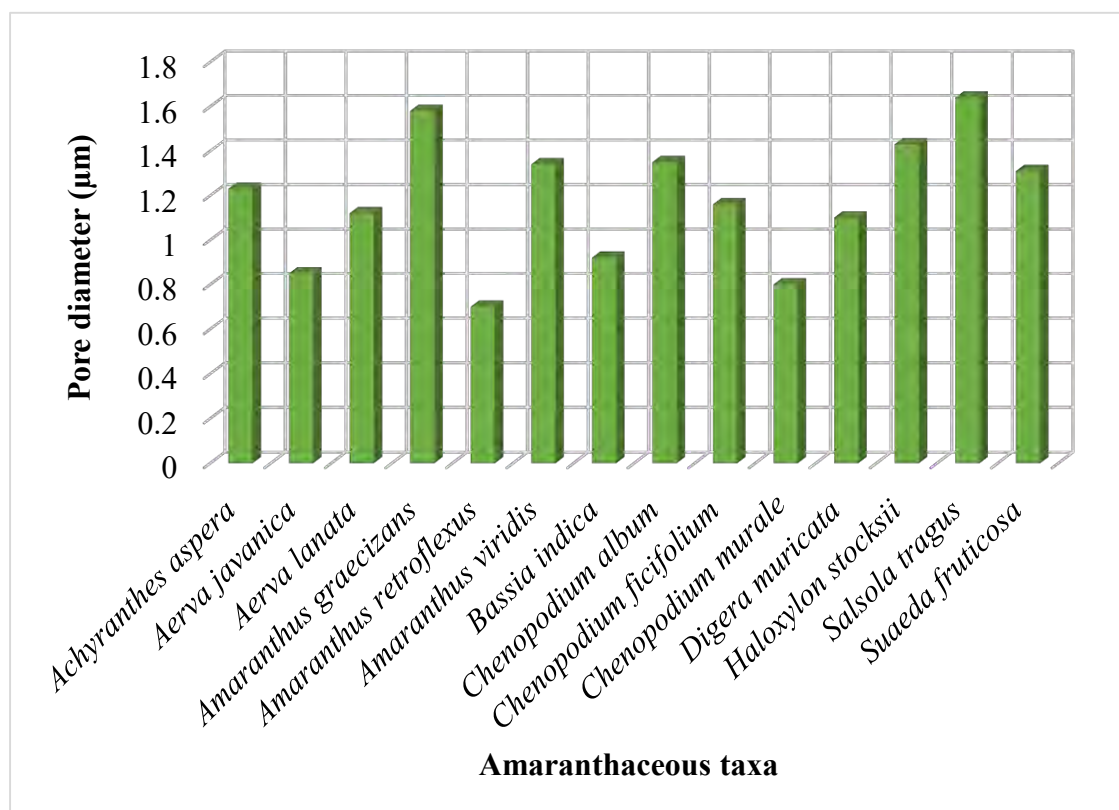
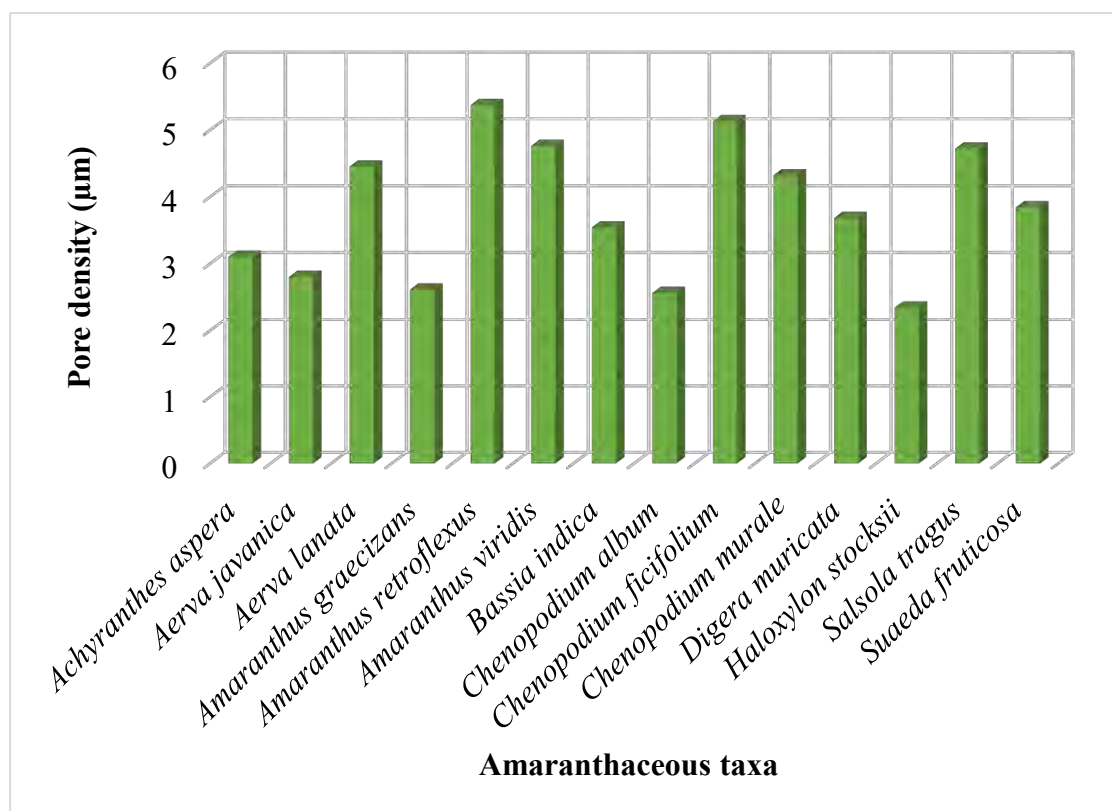
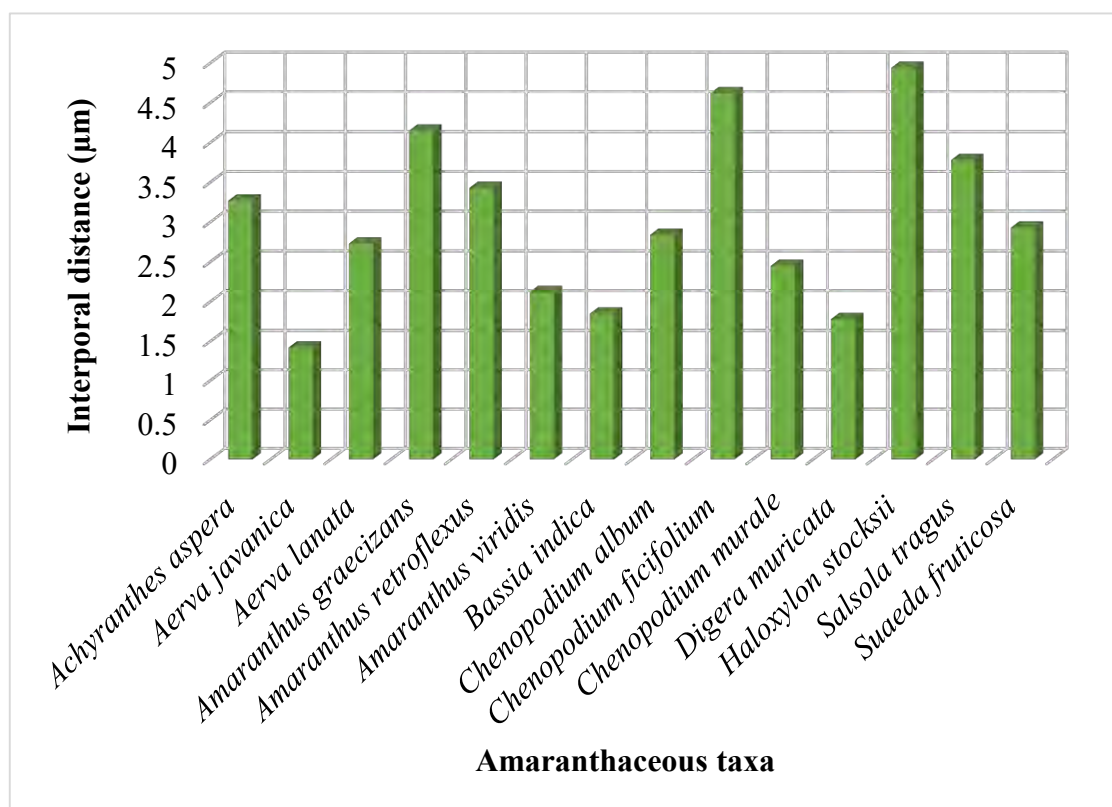


Figure 8. Average variations in pore diameter among Amaranthaceous taxa



**Figure 9.** Mean pore density variations among Amaranthaceous taxa



**Figure 10.** Average interporal distance variability among Amaranthaceous taxa

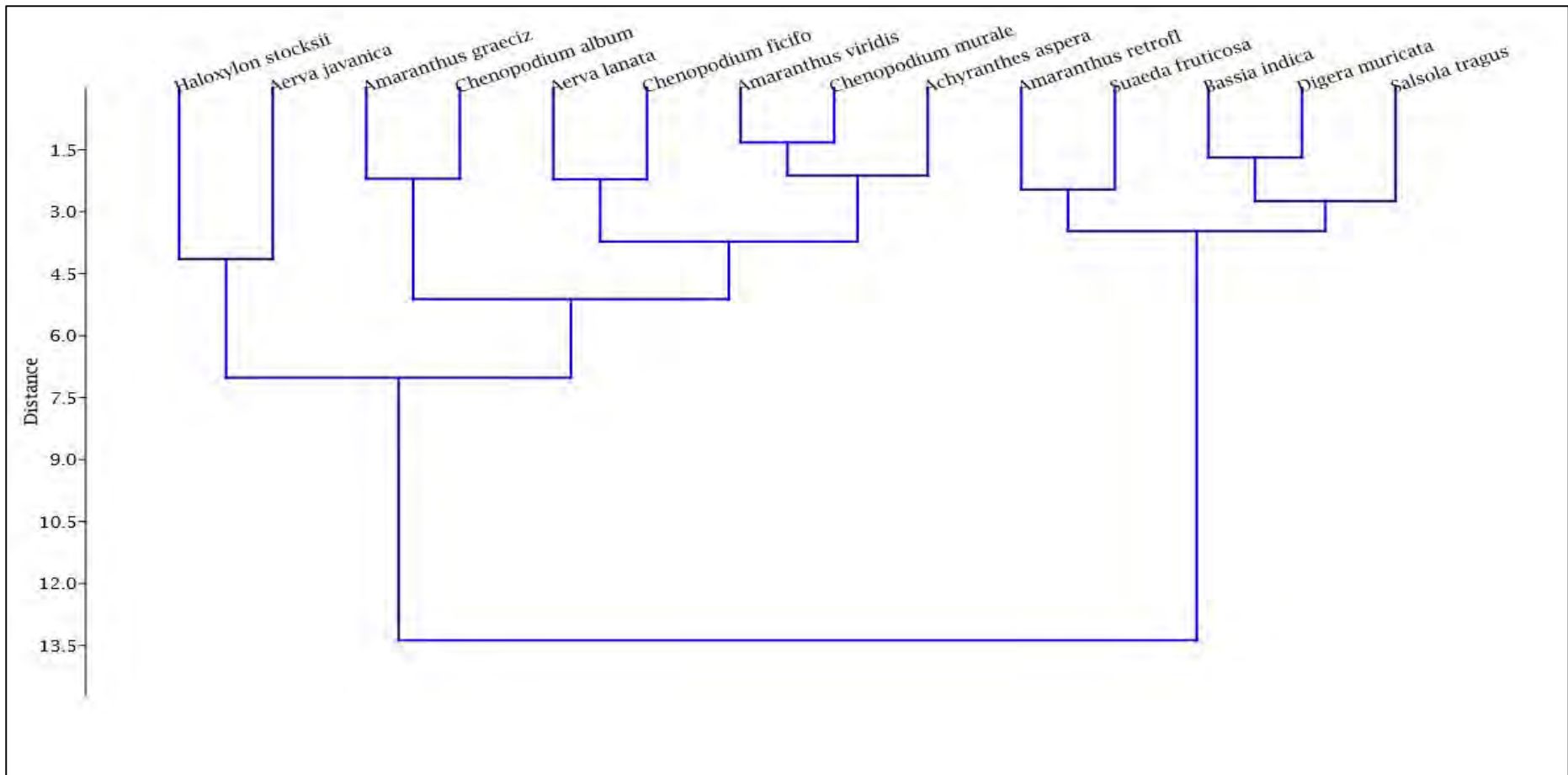


**Figure 11.** Dendrogram clustering showing relationship among different Amaranthaceous species

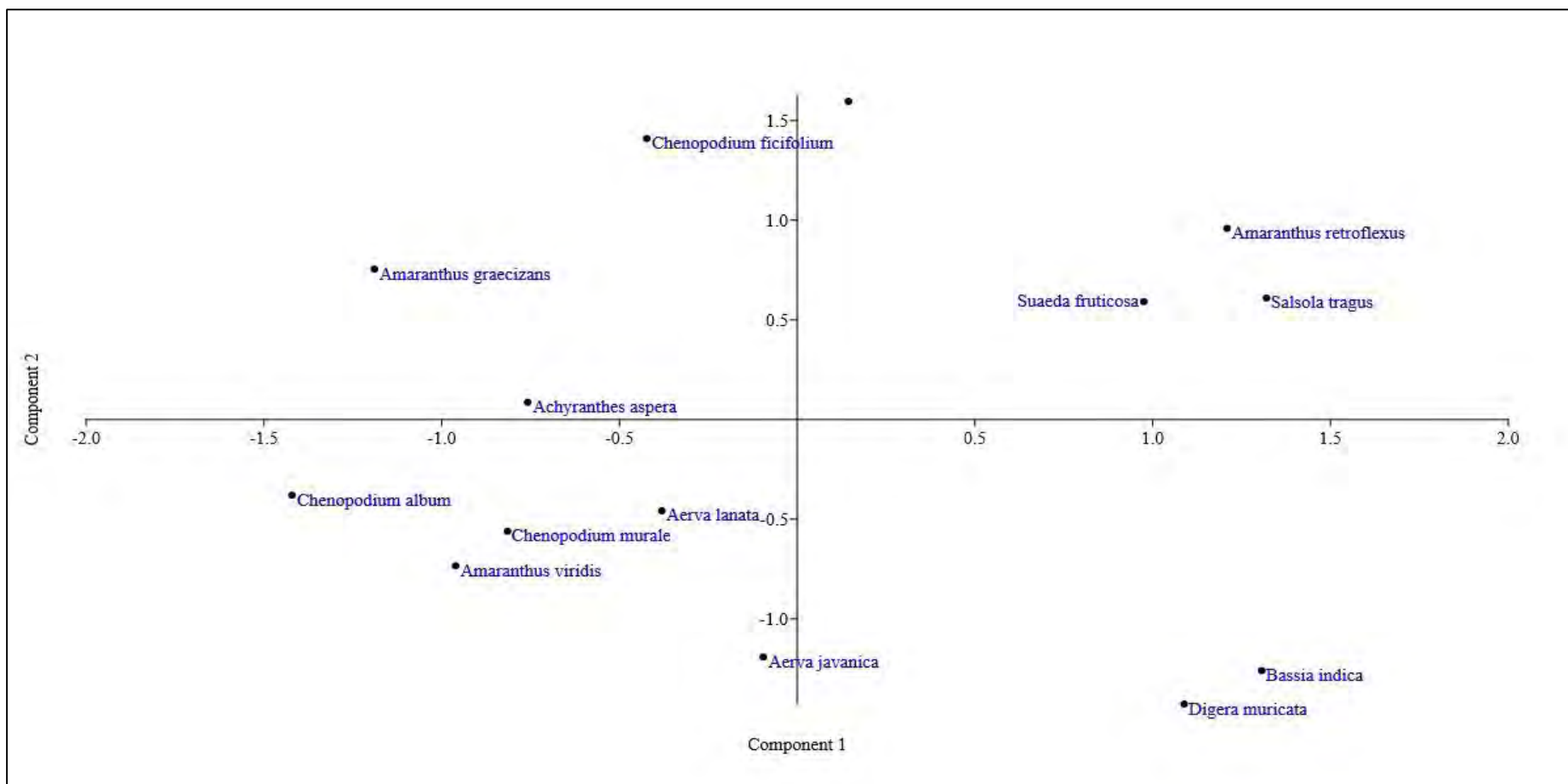


**Figure 12.** Principal component analysis (PCA) performed with the pollen quantitative data from Amaranthaceous species

### 3.2.3 Discussion

Pollen morphological similarities are evident at both generic and specific levels. Commonly the pollen grains of Amaranthaceae are periporate, the pollen grains shape differs from spheroidal to sub-spheroidal, and the exine is either perforate or imperforate and has a stimulating more or less similar sculpture, structures, and aperture with a persistent or a deciduous operculum. In the dimensions of the grains clear differences have been exhibited at the generic level by the biometric analysis, no severe deviation has been observed between the studied species of Amaranthaceae and this may validate the work of (Nowicke, 1975), who specified that pollen grains both of the same and closely related species tend to be like if they face constant environmental factors and the degree to which they are alike is a degree of their close relationship. (Nowicke and Skvarla, 1979), also apprehended the same estimation. For the family Amaranthaceae, the study of pollen morphology in the determination of generic affinity has proved very valuable, and the extensive classification of the family was undoubtedly highlighted by the general pollen survey (Hussain et al., 2018). Current studies have considered that pollen of Chenopodiaceae is mostly not distinguishable from species to species like from *Chenopodium album* to *Amaranthus graecizans*. From the studies on the pollen grains of Chenopodiaceae, it is well known that the grains are in general circular and polyporate. Palynological study has to be carried out in detail on the level of species. Only this can offer a way to note the part that pollen morphology can play in the systematic classification and identification of Amaranthaceous species at the microscopy level.

Amaranthaceae exhibits the highest pollen morphological diversity in the whole order Caryophyllales (Nowicke 1994). Pollen studies were carried out at different taxonomic ranks (from family to species), and several characters (both quantitative and qualitative) were considered. Qualitative characters include pollen and shape type, exine sculpturing, pore membrane sculpturing, pore borders, convexness of mesopori, shape of spines, etc. Quantitative characters include pollen diameter, pore number, diameter and density, exine thickness, interpore distance, punctate/spinules ratio, spinules height and density, punctae density, etc. These quantitative features show a broad range of overlap and as a consequence, they appear to be not good to distinguish taxonomic groups (Flores-Olvera et al., 2016). Pollen with a microspinose, punctate tectum is the rule, and rarely, the punctate are annulated. The variation in size, shape,

and number of, ektexinous bodies covering the pores provide most of the morphological variation observed in the pores of Amaranthaceae pollen (Müller and Borsch, 2005). Previous studies (Costea et al., 2004; Talebi et al., 2016) have confirmed that in *Amaranthus* taxa, flowers lack nectar glands and pollen grains are small (diameter 18 to 28  $\mu\text{m}$ ), usually with 30 to 45 pores uniformly distributed on their surface. Pollen grains of dioecious species have a larger number of apertures on the visible surface. However, three important parameters can be pointed out by Angelini et al., (2014): the first two are biometrical parameters (interporal distance and exine thickness) and the third one is a morphological microechini occurrence on pollen surface.

Pollen grains of *Achyranthes aspera* were monad, radial symmetry, spheroidal in shape, small in size with diameter  $12.48 \pm 1.25 \mu\text{m}$ , apolar, 32 apertures, aperture diameter 3.2  $\mu\text{m}$ , polyantoporate aperture, and aperture areas have membrane covering the aperture making it look more convex and circular-like shape covered with sparse granules, mesoporia broadly flat, without ridge, exine sculpturing smooth with sparsely distributed granulates. The character of this type is aperture areas with a membrane covering the aperture, making it look more convex and circular-like shape covered with sparse granules, mesoporia broadly flat, without ridge (Saensouk and Saensouk 2022). Periporate; exine 1  $\mu\text{m}$ , thick, tectate, tectum granulate; pores 47, annulus thick pore diameter 3  $\mu\text{m}$ , circular, interporium 2  $\mu\text{m}$ , wide; pore membrane granular, circular; grains spheroidal (Khan, 2004). Prabhakar and Ramakrishna (2014) examined scabrate type sculptural elements for *Achyranthes aspera*. The pollen of Amaranthaceae family were mostly uniform in morphological features which confirms its stenopalynous condition. According to Hussain et al., (2018) the pollen of *Achyranthes aspera* are small with large number of pores. Hence our results corroborated with the result description of Hussain et al., (2018). Recently in 2022 Saensouk and Saensouk explained exine sculpturing smooth with sparsely distributed granulates in *A. aspera* was contradicted with our results which shows micro-echinate perforate sculptured elements. The pollen description for *Amaranthus viridis* observed by us highly corroborated with the pollen morphological results of Sopaladawan et al., (2019) as prolate to spheroidal in shape with radial symmetry, peri-porate type grains. While Gasma et al., (2020) briefly visualized scabrate type ornamentation show dissimilarity with current findings revealed micro-echinate perforate ornamentation.

Singh and Chaturvedi (2016) analyzed rough exine type and scabrate ornamented grains for *Aerva* species. In spite of the fact that the term metareticulate gained acceptance by many authors and widely adopted, it is still not followed throughout, and descriptive phrases were used instead. Nowicke and Skvarla (1979) described the pollen grains of *Aerva* as with sunken pores and convex mesoporial exines (El Ghazali, 2022). Bayoumy et al., (2020) described punctate type tectum in *Aerva javanica* as consistent with our findings. The spectrum of allergenic pollen in Karachi including *Aerva javanica* a major allergen revealed also scabrate ornamentation (Perveen et al., 2015). Perveen and Qaiser (2002) elaborate finely scabrate densely type pollen and sexine thicker for *Aerva* species. Gosh and Mandal (2016) earlier observed pantoporate, psilate and spheroidal grains for *Aerva lanata* from Pollen Atlas of Santiniketan, West Bengal.

Pollen grains of *Amaranthus graecizans* have the thinnest exine, less than 70 pores and greatest interpore distances (Angelini et al., 2014). Pollen grain was apolar, spheroidal and polyantoporate in the genus *Amaranthus*. Grains were small in size, with spinulose tectum in *Amaranthus graecizans* from Southern Marshes (Iraq) of Dicots Wetland Plants (Al-Saadi and Al-Mayah, 2012). The pores, which are moderate in diameter, are superficial or protruded enriched by granules or echinae in different densities. Exine, thin tectate with granulate or echinate surfaces (Taia et al., 2020). Zhigila et al., (2014) provided evidence that *Amaranthus* species are eurypalynous (multipalynous) and that the genus is anemophilous. The pollen grains are generally small, rounded, smooth, thin-walled and dry but vary among species within this genus.

The currently existing morphological characteristics of pollen give grounds to classify it to *Amaranthus* type with pores type II typical of that type of pollen (Borsch, 1998). Our data largely confirm the already published ones. The pollen in *Amaranthus retroflexus* populations has typical spherical shape covered by numerous perforations. It is characterized by small size and a big number of pores (Terzieva and Grozeva, 2021). Terzieva et al., (2019) studied the pollen of seven species, including *Amaranthus retroflexus*. The characteristics published by them about the pollen of *Amaranthus retroflexus* were similar to those found by us. Borsch (1998), stepping on profound studies of pollen in Amaranthaceae, distinguished 11 different types of pores and 17 pollen types. The pore characteristics established in the present study of *Amaranthus retroflexus* correlate to Type II (pores 1-2  $\mu\text{m}$  in diameter, and sharply set off against

the tectum) and the pollen type described by the author as *Amaranthus* type (spheroidal, punctate tectum with numerous distributed microspines).

Gosh and Mandal (2016) described periporate, spheroidal and psilate surface nature grains in *Amaranthus viridis*. While our findings contradicts examined echinate, evenly granulate, perforate sculptural elements. Pollen grains of plant taxa *Amaranthus viridis* are pantoporate (stenopalynous plant) and they cannot be differentiated at species level, except for *Alternanthera*, which has pollen of distinctive character (Quamar et al., 2017). Previously Gasma et al., (2020) also mentioned scabrate sculpture grains with spheroidal shape from diverse ecozones of Nigeria. Pollen morphology has been studied previously by (Butt et al., 2021; Perveen, Qaiser, 2012) in which they reported that exine sculpturing of the Amaranthaceae family was scabrate to psilate, while in our study *Amaranthus viridis* have microechinate ultrasculpturing.

Pollen shape sub-prolate and densely scabrate ornamentation as in *Bassia eriophora* while sparsely scabrate peculiarities were analyzed for *Bassia arabica* from Egypt (Bayoumy et al., 2020). Study of pollen grains by SEM indicated the presence of differences represented in: density and distribution of spinules on the pollen surface, number of apertures, pollen exine punctate or smooth, and number of mesoporial spinules (Turki et al., 2006). The absence of ektexinous elements on the pores (non-operculate) were encountered in *Bassia* genus (El Ghazali, 2022) while our work also show similar observation.

Micrographs of pollen grains in *Chenopodium album* revealed perforate tectum at the proximal face in *Chenopodium album* subsp. *striatum*, and perforate ornamentation (Malekloo et al., 2010). Optical microscopic pollen was seen to be apolar, radially symmetrical, polipantoporate, with circular pores. While scanning electron microscope defined numerous uniformly distributed spinules were seen on the exine, both on the surface and also on the operculum. Numerous foreign particles attached to the surface of the grains were also observed (Bianchimano et al., 2014). *Chenopodium album* pollen is the smallest with a small size of 12.2  $\mu\text{m}$ . Whereas Punsalpaamuu et al., (2012) measured, the medium size of pollen of *Chenopodium album* in the Magnolia is 30.9  $\mu\text{m}$ .

Nazish et al., (2019) studied halophytic *Chenopodium facifolium* have pollen grains with pantoporate aperture, spheroidal shape, apolar and micro-echinate scabrate



sculptured elements Perveen and Qasier (2012) studied the apolar type pollen of Chenopodiaceae. While current findings broadly flat mesoporia and micro-echinate perforate peculiarities. The figure shows no correlation between pore number and pollen size of the specie examined. Therefore, previous study indicating that there are two holes types on pollen surface in Chenopodiaceae: foveat and perforate confirms this point of view the *Chenopodium ficifolium* has tendency to have larger pollen grains.

Grains observed peripolporate, radial symmetrical, faveat tectum at the proximal face with scabrate ornamentation of exine in *Chenopodium murale* (Hamdi et al., 2009). Whereas our examination revealed micro-echinate perforate exine structure was dissimilar to earlier studies. In another study (Ahmad et al., 2020) winter weeds honeybee flora performed optical microscopy of *Chenopodium murale* grains as polyporate, sub-oblate and psilate. However this research analyzed via SEM non punctate scabrate type exine.

*Digera muricata* pollen grains were monads, white, spheroidal, pantoporate, multiporate, dry, and fall as single grains (Aluri and Chappidi, 2018). Reticulate, circular, lobate and thin granular exine grains were illustrated for *Digera muricata* by Devarkar in (2011). Whereas Khan in (2004) described variations of tectum as metareticulate was consistent with our current findings.

In the *Haloxylon* type, the pollen grains have pore membranes with dense microechini and larger pore diameter. The new pollen classification of the Chenopodiaceae opens up the possibility of linking this pollen type to the desert vegetation types such as a temperate dwarf semi-arboreal desert (Lu et al., 2018). Chenopodiaceae pollen inventory from Pakistan was provided by Perveen and Qaiser in 2012 mentioned *Haloxylon stocksii* as densely scabrate type grains elements contradict the present examination of punctate and densely micro-echinate perforate pollen. Perveen et al., (2015) also reported the scabrate surface grains in *Haloxylon stocksii* similar to the current observation. Jalilzadeh et al., (2021) explained micromorphology of *Haloxylon ammodendron* had a high density of micro-echinate in exine ultrasculpture was somehow in accordance to present study.

The pollen morphology in genus *Salsola* was discussed only briefly in the previous publication of Toderich et al., (2000). General description of pollen grain of

*Salsola tragus* is given in the classical work of Toderich et al., (2010). The palynological data provided by Grozeva et al., (2018) showed from the five studied populations of *Salsola tragus* had pantoporate, spheroidal pollen with spinulose tectum. Our data showed that *Salsola tragus* had greater diameter and polar axis, bigger pore area and greater distance between them. Pollen grains of 12 species of the genus *Salsola* mentioned above, as pantoporate, the pore number vary within the limits small, very rarely of medium size, angular-rounded in outline and the surface of the pollen grain is wavy (Sonyan and Hayrapetyan 2021).

Nazish et al., (2019) examined micro-echinate exine surface of *Suaeda fruticosa* while microscopic palyno-morpho characters observed in this study illustrating granulate spinulose perforate stratification of exine with non-punctate tectum. Our ongoing study among different genera of Amaranthaceae including *Suaeda* showed inter-generic and even interspecific differences in pollen traits. The smooth surface of grains and density of spinules were similar in *Suaeda* species to be included in one separate section (Akhani et al., 2003). A study of 28 taxa of the genus *Suaeda* from the old world by Dehghani and Akhani (2009) showed apparently little difference in pollen characters between the studied species, however, a statistical study of the pollen characters was not undertaken. The pollen morphology of the new species was described as *Suaeda iranshahrii* from Southern Iran revealing periporate type and similar pollen diameter to other known species of the genus (Freitag et al., 2013).

### 3.2.4 Micromorphology of Asteraceous Pollen

The observed ranges are summarized and reported as mean values of the 20 pollen grains per species as obtained from the nine parameters from the 13 species measured using LM. The morpho-structural features measured in micrometers ( $\mu\text{m}$ ) diameter of polar and equatorial axis, echinae size, colpi size, mesocolpium distance, thickness of exine, number of echinae and P/E ratio were calculated. The summary of pollen morphometric traits are presented in Table 7, 8, 9 & 10 and the scanning bio imaging micrographs was shown in Plates 39, 40, 41 & 42.

The 13 desert-inhabited Asteraceous species were analyzed for pollen micromorphology. The species examined here were: *C. oxyacantha* (Plate 39 a-c), *C. iberica* (Plate 39 d-f), *C. prolifera* (Plate 39 g-i), *C. candensis* (Plate 40 a-c), *E. prostrata* (Plate 40 d-f), *I. grantioides* (Plate 40 g-i), *L. procumbens* (Plate 41 a-c), *L. nudicaulis* (Plate 41 d-f), *P. boissieri* (Plate 41 g-i), *S. asper* (Plate 42 a-c), *T. gracilis* (Plate 42 d-f), *V. encelioides* (Plate 42 g-i) and *X. strumarium* (Plate 42 j-l).

#### a) Shape and Size

The detailed scanning microscopic visualization indicated that pollen grains are iso-polar and radially symmetrical. In the equatorial view, dominant pollen shape was oblate-spheroidal in eight species followed by prolate-spheroidal (six species) and sub-oblate in one species. However, in the polar view, pollen were circular, slightly rounded, triangular, slightly circular, and oblique.

The polar diameter varied from 19.1  $\mu\text{m}$  in *P. boissieri*, to 47.2  $\mu\text{m}$  in *C. oxyacantha*, the equatorial distance ranged from minimum 21.6  $\mu\text{m}$  in *P. boissieri*, to maximum 51.1  $\mu\text{m}$  in *C. oxyacantha* (Figure 13), with correlation P/E index value varied from 0.83 in *L. procumbens* to 1.11  $\mu\text{m}$  in *C. candensis* (Figure 14). Accordingly, P/E ratio measures from 83 to 111, pollen are described sub-oblate to prolate-spheroidal types. The pollen grains are categorized as the dominant medium in size based on the length of the polar axis in eight species followed by small to medium-sized (three species) and medium to large and small sized one species each).

## b) Apertures Characteristics

The pollen grains of the 13 deserted Asteraceous species are aperturate. All of the species analyzed have both types of apertures, colpi and pores. Colpi are fissure-like openings but pores are mostly rounded. Each pollen features three colpi and three pores. The apertures of *C. prolifera* are oriented equidistantly all around the equator with trizonocolporate type grains. The orientations of the aperture were observed as sunken, slightly sunken, bulged, and slightly bulged.

In Asteraceous taxa, the colpi are pointed at both ends when visualized under a microscopic field. Colpus diameter, pore length and width, and mesocolpium distance varied between Asteraceous grains. The colpus length measured shortest from 3.61  $\mu\text{m}$  in *I. grantioides*, to largest 9.55  $\mu\text{m}$  in *T. gracilis*, whereas the width varies from 3.8  $\mu\text{m}$  in *C. candensis*, to 11.3  $\mu\text{m}$  in *T. gracilis* (Figure 15). Mesocolpium distance measurement ranged from minimum 5.6  $\mu\text{m}$  in *I. grantioides*, to 14.7  $\mu\text{m}$ , in *T. gracilis* (Figure 18).

## c) Pollen wall and Lacunate Grains

The exine sculpture was echino-perforate in *P. boissieri*, and *V. encelioides*, while it was echino-perforate fenestrate in *L. procumbens* and *S. asper*. Micro-perforate echinate type elements was observed in *C. oxycantha* and *E. prostrata*. Echino-perforate lophate fenestrate peculiarities were examined in *L. nudicaulis* and *T. gracilis*. While echino-perforate reticulate in *C. prolifera*, echino-perforate tectate in *I. grantioides*, echinate in *C. candensis* and scabrate in *C. iberica*. Exine surface was noted thinnest in *L. procumbens* while thick in *I. grantioides*. Exine wall thickness measured maximum 1.65  $\mu\text{m}$  in *L. procumbens* to minimum 4.2  $\mu\text{m}$  in *I. grantioides* (Figure 16).

The appearance of the abporal lacunae is directly affected by the lophate character state, which is less defined and more rounded. The poral and abporal lacunae are usually linked by inter-lacunar gaps, that are identified in both lophate and sub-lophate pollen. The pollen of *L. procumbens*, *L. nudicaulis* and *S. asper* has a lophate exine pattern that is nearly symmetrical. The pattern consists of a mixture of trigonal to pentagonal lacunae. The paraporal lacunae in *T. gracilis* are large and pentagonal

having scabrate peculiarities. The abporal lacunae were angular with narrow inter-lacunar gap.

#### **d) Taxonomy of Echini Features**

The analyzed features of spines including echini shape, arrangement, and spine size allowed the recognition of different patterns of exine and their taxonomical significance. The shape of the spine can be difficult to define in certain cases, but in the group under study, it can be broadly defined by the shape of the base and tip as well as tectal perforations; these traits seem to be effective for identifying stratification patterns among Asteraceous grains. Among asteraceous taxa, the echini shape was short with a narrow broad base surface, minute with a flattened base, micro-spinilues with flattened base, mucronate pointed tips spines, and bulged spines are substitutes with thick exine structural variation has taxonomic and evolutionary relevance. The pattern of sculpturing elements can be identified by closely examining micro-echinate and echinate pollen used as a diagnostic tool in palynomorphic studies. Spine length was measured shortest (1.8  $\mu\text{m}$ ) in *L. procumbens* and longest (3.9  $\mu\text{m}$ ) in *P. boissieri* (Figure 17).

#### **e) Numerical Statistics via UPGMA Dendrogram and PCA Analysis**

The Asteraceous species under examination were quantified to Cluster Analysis via Euclidian distance using statistic pollen data. The cluster analysis results are provided in (Figure 19). The two major clusters were seen, the first cluster comprise single species *C. oxycantha* is due to its unique slightly bulged aperture and short narrow spiny condition. The second cluster is divided into two sub-clusters. Sub-cluster I includes two species, namely; *C. prolifera* and *E. prostrata* are closely related and have similar small to moderate polar region and slightly sunken aperture orientation. The II sub-cluster comprises *C. iberica*, *V. encelioides*, *I. grantioides*, *L. procumbens*, *S. asper*, *C. candensis*, *L. nudicaulis*, *X. strumarium*, *P. boissieri* and *T. gracilis*. Sub-cluster revealed that *L. procumbens* and *S. asper* are closely placed with minimum Euclidean distance due to echino-perforate fenestrate grains sculpturing.

PCA analysis was performed to identify variables necessary to explain the percent variation in the nine quantitative features of the Asteraceous pollen. The values

of the eigen factor and the cumulative variance were summarized in Tables 6, and the pollen statistic data scatter plot was described in Figure 20. The PCA explains 55.626% variance among first four components of the Asteraceous pollen. The first component PC1 represent 31.313% variation, polar view axis and spine size being the most particular variables. Along PC1 the *C. iberica*, *T. gracilis* and *X. strumarium* was lie on the positive side. However, *I. grantioides*, *L. nudicaulis*, *L. procumbens* and *S. asper* placed on the negative side. The second principal component (PC2), accounts for 24.313% of the variation, with equatorial and mesocolpium distance as the most significant factors (Table 5). *C. oxycantha*, *E. prostrate*, *C. prolifera* and *V. encelioides* were present on the positive side in the second axis and *C. candensis* and *P. boissieri* on negative side of PC2.

**Table 6.** Eigenvalues, percentage of total variance explained by each axis among Asteraceous pollen.

PC	Eigen value	% variance
PC1	2.81	31.313
PC2	2.18	24.313
PC3	1.39	15.544
PC4	1.11	12.352
PC5	0.68	7.595
PC6	0.36	4.103
PC7	0.32	3.644
PC8	0.10	1.128
PC9	0.00057	0.006

### 3.2.5 Taxonomic Keys Based on Asteraceous Pollen Characters

1 + Lacunaes absent.....	2
- Lacunaes present.....	11
2 + Slightly bulged aperture, micro-perforate echinate, echini slightly regular.....	<i>C. oxycantha</i>
- Regular echini, long spines.....	3
3 + Echino-perforate, regular echini, small to moderate polar area.....	<i>V. encelioides</i>
- Bulged aperture, lacunaes absent.....	4
4 + scabrate, regular echini, moderately extensive polar area.....	<i>C. iberica</i>
- Bulged aperture, echini irregular.....	5
5 + Micro-perforate reticulate, echini irregular, micro-spiniules, small to moderate polar area.....	<i>C. prolifera</i>
- Bulged aperture, echini irregular.....	6
6 + Micro-echinate verrucate brevicolporus, moderate polar area.....	<i>X. strumarium</i>
- Echini slightly regular, slightly sunken aperture.....	7
7 + Echininate sculpturing, mucronate pointed tips spines, moderately extensive polar area.....	<i>C. candensis</i>
- Echini regular, slightly sunken aperture.....	8
8 + Echino-perforate, tectate, broad perforate base echini.....	<i>I. grantioides</i>
- Echini regular, aperture slightly sunken.....	9
9 + Echino-perforate, flattened based echini.....	<i>P. boissieri</i>
- Sunken aperture, lacunaes absent.....	10
10 + Micro-perforate echinate, echini with broad base, echini regular.....	<i>E. prostrata</i>
- Slightly bulged aperture, lacunaes present.....	11
11 + Echino-perforate, fenestrate lophate, trigonal to tetragonal lacunaes, narrow base echini.....	<i>L. procumbens</i>
- echini regular, bulged aperture.....	12
12 + Echino-perforate scabrate, fenestrate, pentagonal lacunaes present, echini bulged.....	<i>T. gracilis</i>
- Echini irregular, sunken aperture orientation.....	13
13 + Echino-perforate lophate and fenestrate, trigonal to pentagonal lacunaes, narrow tips echini.....	<i>L. nudicaulis</i>

**Table 7.** Qualitative palynological attributes among desert inhabited Asteraceous species.

<b>Sr. No</b>	<b>Asteraceous taxa</b>	<b>Size</b>	<b>Amb/ Polar View</b>	<b>Polar region</b>	<b>Shape</b>	<b>Pollen type</b>	<b>Aperture orientation</b>
3	<i>Carthamus oxyacantha</i> M.B ieb.	Medium to large	Circular	Small to moderate	Oblate-spheroidal	Tricolporate	Slightly Bulged
4	<i>Centaurea iberica</i> Trevir. ex Spreng.	Medium	Slightly rounded	Moderately extensive	Prolate-spheroidal	Tricolporate	Bulged
6	<i>Cousinia prolifera</i> Jaub. & Spach	Medium	Triangular	Small to moderate	Oblate-spheroidal	Trizonocolporate	Bulged
7	<i>Conyza candensis</i> (L.) Cronquist	Small to medium	Circular	Moderately extensive	Prolate-spheroidal	Tricolporate	Slightly sunken
8	<i>Eclipta prostrata</i> (L.) L.	Medium	Circular	Small to moderate	Oblate-spheroidal	Tricolporate	Sunken
9	<i>Iphiona grantioides</i> (Boiss.) Anderb.	Medium	Slightly circular	Small to moderate	Oblate-spheroidal	Tricolporate	Slightly sunken
10	<i>Launaea procumbens</i> (Rox b.) Ramayya & Rajagopal	Medium	Triangular	Small to moderate	Sub-oblate	Tricolporate	Slightly Bulged
11	<i>Launaea nudicaulis</i> (L.) Hook.f.	Medium	Slightly circular	Moderately extensive	Prolate-spheroidal	Tricolporate	Sunken
12	<i>Pulicaria boissieri</i> Hook.fil.	Small	Circular	Moderately extensive	Oblate-spheroidal	Tricolporate	Slightly sunken
13	<i>Sonchus asper</i> (L.) Hill	Medium	Slightly rounded	Small to moderate	Oblate-spheroidal	Tricolporate	Slightly sunken
14	<i>Tragopogon gracilis</i> D.Don	Small to Medium	Oblique	Small to moderate	Oblate-spheroidal	Tricolporate	Bulged
15	<i>Verbesina encelioides</i> (Cav.) Benth. & Hook.f. ex A.Gray	Medium	Circular	Small to moderate	Prolate-spheroidal	Tricolporate	Slightly bulged
16	<i>Xanthium strumarium</i> L.	Small to medium	Slightly rounded	Moderate	Oblate-spheroidal	Tricolporate	Bulged



**Table 8.** Qualitative pollen morphological features of desert inhabited Asteraceous species.

Sr. No	Asteraceous taxa	Pollen ornamentation	Echini shape	Echini arrangement	Interlacunar gap	Lacunar shape
1.	<i>Carthamus oxyacantha</i> M.Bi eb.	Echinate, Micro perforate	Short Spines, narrow broad bases	Slightly regular	Absent	Absent
2.	<i>Centaurea iberica</i> Trevir. ex Spreng.	Scabrate	Minute spine, flattened bases	Regular	Absent	Absent
3.	<i>Conyza candensis</i> (L.) Cronquist	Echinate	Short, narrow bases and mucronate pointed tips	Slightly regular	Absent	Absent
4.	<i>Cousinia prolifera</i> Jaub. & Spach	Echino-perforate, Reticulate	Base flattened and micro spiniules	Irregular	Absent	Absent
5.	<i>Eclipta prostrata</i> (L.) L.	Micro-perforate echinate	Broad base with pointed tips	Regular	Absent	Absent
6.	<i>Iphiona grantioides</i> (Boiss.) Anderb.	Echinate, perforate, tectate	Broad perforate base, sharp narrow tips	Slightly regular	Absent	Absent
7.	<i>Launaea nudicaulis</i> (L.) Hook.f.	Echinate scabrate, Perforate, Fenestrate	Short spine, broad bases, narrower tips	Irregular	Narrow	Trigonal to pentagonal
8.	<i>Launaea procumbens</i> (Roxb.) Ramayya & Rajagopal	Fenestrate, Echinoperforate	Spines short with narrow bases	Slightly regular	Slightly broad	Trigonal to tetragonal
9.	<i>Pulicaria boissieri</i> Hook.fil.	Echinate-perforate	Flattened base, sharp spines and circular pointed tips	Regular	Absent	Absent
10.	<i>Sonchus asper</i> (L.) Hill	Fenestrate, Echino-perforate	Spines broad base between lacunaes	Regular	Narrow	Trigonal to pentagonal
11.	<i>Tragopogon gracilis</i> D.Don	Fenestrate, Echino-perforate scabrate	Bulged spines, short narrow bases between lacunaes	Regular	Narrow to broad	Pentagonal
12.	<i>Verbesina encelioides</i> (Cav.) Benth. & Hook.f. ex A.Gray	Echinate-perforate	Long echini, broader base, pointed tips	Regular	Absent	Absent
13.	<i>Xanthium strumarium</i> L.	Micro-echinate verrucate and brevicolporus	Spines minute, bulged base	Irregular	Absent	Absent

**Table 9.** Quantitative measurements of Asteraceous pollen data among desert inhabited Asteraceous species (n = 20).

<b>S. No.</b>	<b>Asteraceous taxa</b>	<b>P/E ratio</b>	<b>PVD (x ± SE µm)</b>	<b>EVD (x ± SE µm)</b>	<b>CL (x ± SE µm)</b>	<b>CW (x ± SE µm)</b>
1.	<i>Carthamus oxyacantha</i> M.Bieb.	0.92	47.2±2.11	51.1±1.71	5.76±0.35	3.94±0.23
2.	<i>Centaurea iberica</i> Trevir. ex Spreng.	1.07	29.4±0.97	27.4±0.61	3.87±0.23	5.36±1.17
3.	<i>Conyza candensis</i> (L.) Cronquist	1.11	26.9±1.56	24.2±1.08	5.15±0.43	3.8±0.19
4.	<i>Cousinia prolifera</i> Jaub. & Spach	0.94	35.3±0.41	37.4±0.73	8.6±1.45	5.86±0.62
5.	<i>Eclipta prostrata</i> (L.) L.	0.89	34.5±0.64	38.7±0.89	3.80±0.14	5.27±0.32
6.	<i>Iphiona grantioides</i> (Boiss.) Anderb.	0.94	28.4±0.75	30.1±1.12	3.61±0.87	4.9±0.43
7.	<i>Launaea nudicaulis</i> (L.) Hook.f.	0.94	25.3±0.42	26.9±0.92	5.7±0.14	4.1±0.19
8.	<i>Launaea procumbens</i> (Roxb.) Ramayya & Rajagopal	0.83	26.6±0.52	31.8±1.04	7.43±0.78	5.76±0.61
9.	<i>Pulicaria boissieri</i> Hook.fil.	0.88	19.1±0.44	21.6±1.16	5.92±0.62	4.8±0.36
10.	<i>Sonchus asper</i> (L.) Hill	0.93	27.35±1.29	29.15±1.09	7.25±0.32	4.62±0.2
11.	<i>Tragopogon gracilis</i> D.Don	1.10	25.8±1.07	23.4±0.94	9.55±0.54	11.3±0.39
12.	<i>Verbesina encelioides</i> (Cav.) Benth. & Hook.f. ex A.Gray	0.91	29.2±0.49	31.8±0.3	6.5±0.21	7.2±0.56
13.	<i>Xanthium strumarium</i> L.	0.89	23.3±0.74	25.9±0.56	7.15±1.14	6.65±0.99

**Table 10.** Quantitative pollen measurements data of desert inhabited Asteraceous species (n = 20).

S. No.	Asteraceous Taxa	ET (x ± SE µm)	SL (x ± SE µm)	SW (x ± SE µm)	MC (x ± SE µm)	Fertility (%)	Sterility (%)
1.	<i>Carthamus oxyacantha</i> M.Bieb.	2.68±0.32	2.28±0.65	1.38±0.19	13.2±2.16	85.3	14.6
2.	<i>Centaurea iberica</i> Trevir. ex Spreng.	2.1±0.23	2.65±0.17	1.73±0.5	11.7±1.03	89.6	10.3
3.	<i>Conyza candensis</i> (L.) Cronquist	3.15±1.6	2.7±1.42	1.85±1.02	10.2±0.93	87.2	12.7
4.	<i>Cousinia prolifera</i> Jaub. & Spach	4.12±1.07	3.26±1.16	2.2±1.28	8.9±0.74	92.1	7.9
5.	<i>Eclipta prostrata</i> (L.) L.	3.48±0.71	3.1±0.62	2.32±0.26	7.3±1.05	90.3	9.6
6.	<i>Iphiona grantioides</i> (Boiss.) Anderb.	4.2±0.77	1.9±0.6	2.4±0.39	5.6±2.71	84.8	15.1
7.	<i>Launaea nudicaulis</i> (L.) Hook.f.	3.75±1.06	2.84±0.78	1.95±0.51	8.9±1.09	93.3	6.6
8.	<i>Launaea procumbens</i> (Roxb.) Ramayya & Rajagopal	1.65±0.18	1.8±0.09	1.35±0.58	7.23±0.29	95.4	4.5
9.	<i>Pulicaria boissieri</i> Hook.fil.	4.10±0.25	3.9±0.62	1.74±0.34	10.2±0.15	88.7	11.2
10.	<i>Sonchus asper</i> (L.) Hill	2.55±1.4	2.38±0.4	1.5±0.14	6.59 ±1.48	97.2	2.7
11.	<i>Tragopogon gracilis</i> D.Don	4±0.27	3.1±0.22	1.16±0.2	14.7±1.75	87.6	12.3
12.	<i>Verbesina encelioides</i> (Cav.) Benth. & Hook.f. ex A.Gray	3.2±0.72	2.2±1.1	1.24±0.8	10.95±1.8	96.3	3.6
13.	<i>Xanthium strumarium</i> L.	2.5±1.02	3.25±0.6	2.20±0.58	11.3±0.89	91.2	8.7

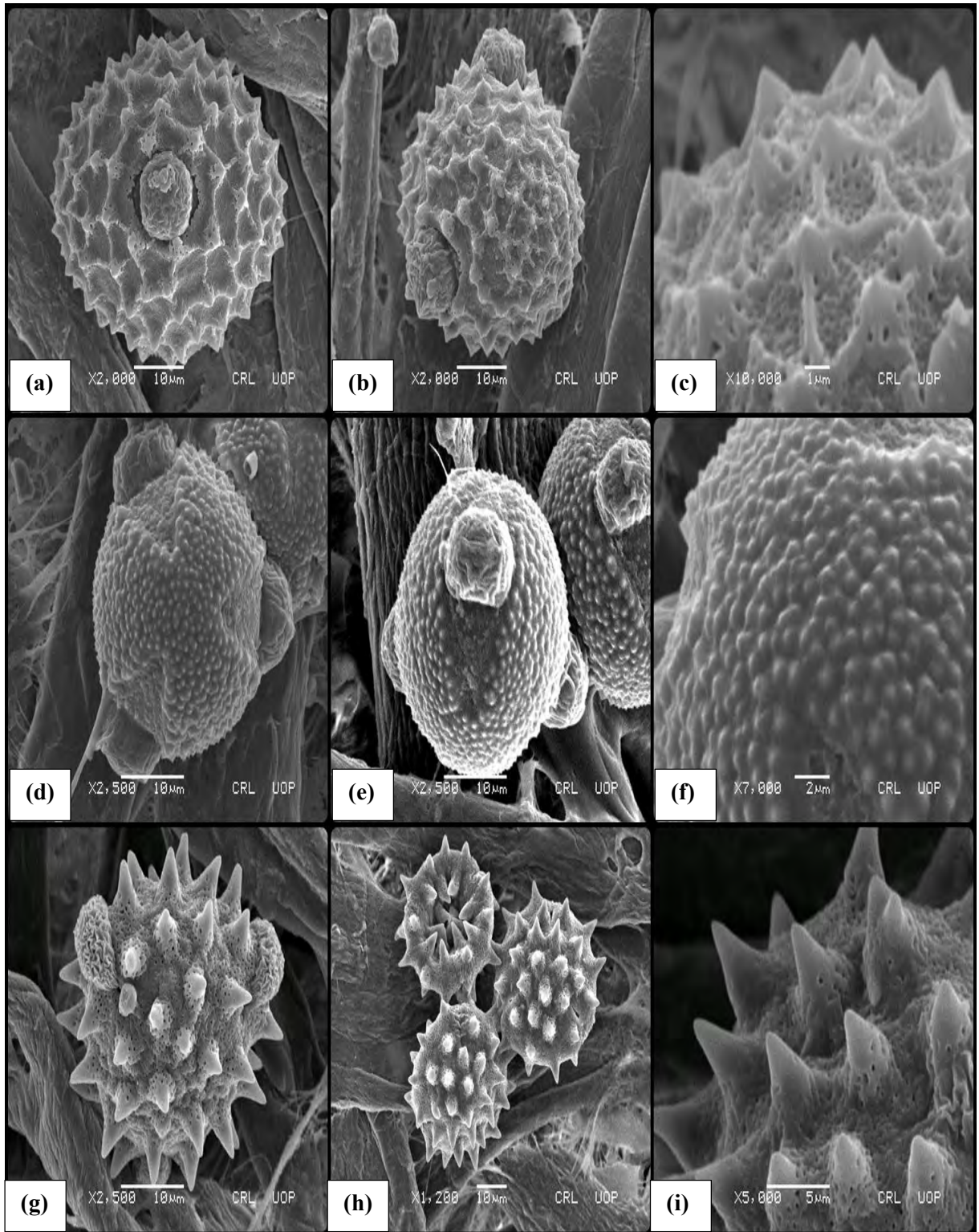


**Plate 39.** Scanning electron microscope photographs of Asteraceous taxa. (a-c) *Carthamus oxyacantha*; short spines and micro-perforate exine (Scale bar = 10  $\mu\text{m}$ , 1  $\mu\text{m}$ ), (d-f) *Centaurea iberica*; scabrate exine and regular flat based echini (Scale bar = 10  $\mu\text{m}$ , 2  $\mu\text{m}$ ), (g-i) *Conyza candensis*; echinate sculpture and mucronate pointed echini shape (Scale bar = 10  $\mu\text{m}$ , 5  $\mu\text{m}$ ).

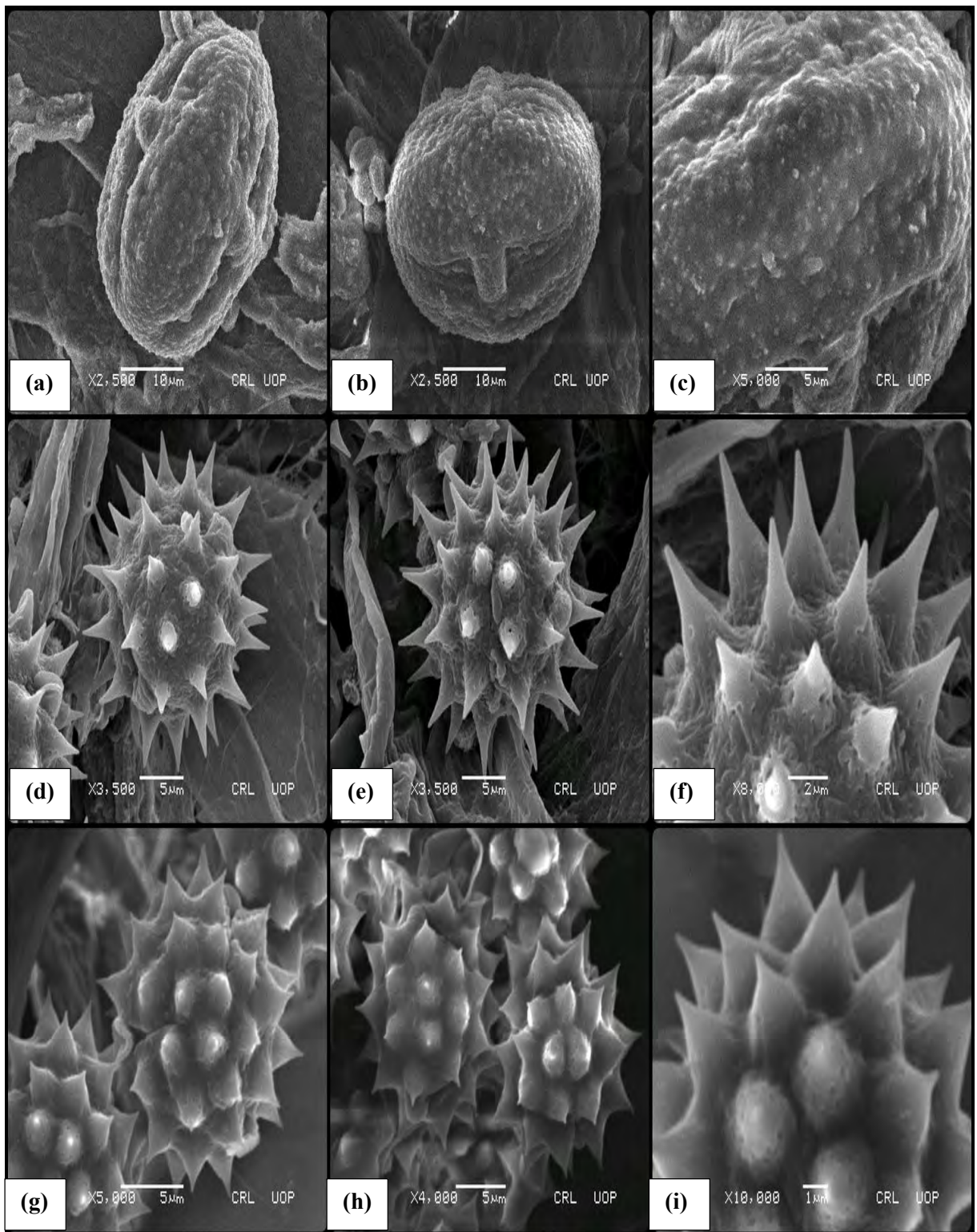


**Plate 40.** Scanning electron microscope photographs of Asteraceous taxa. (a-c) *Cousinia prolifera*; echino-perforate sculpture and micro spiniules (Scale bar = 10  $\mu\text{m}$ , 5  $\mu\text{m}$ ), (d-f) *Eclipta prostrata*; micro-perforate echinate exine and broad based echini (Scale bar = 5  $\mu\text{m}$ , 2  $\mu\text{m}$ ), (g-i) *Iphiona grantioides*; echino-perforate tectate exine and broad base perforate echini (Scale bar = 5  $\mu\text{m}$ , 1  $\mu\text{m}$ ).

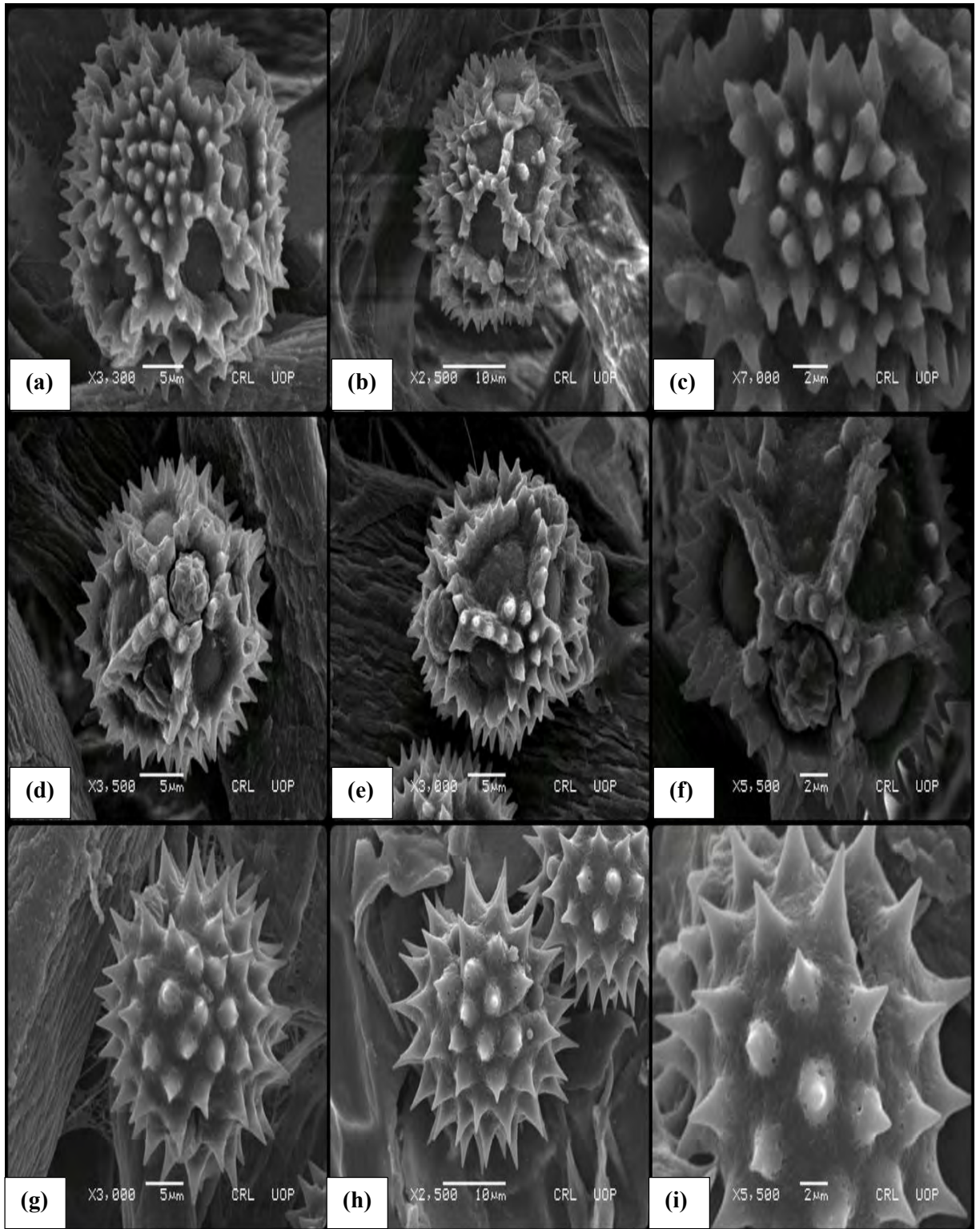


**Plate 41.** Scanning electron microscope photographs of Asteraceous taxa. (a-c) *Launaea procumbens*; fenestrate lophate sculpture and lacunate (Scale bar = 10  $\mu\text{m}$ , 5  $\mu\text{m}$ , 2  $\mu\text{m}$ ), (d-f) *Launaea nudicaulis*; Echino-perforate lophate exine and lacunate (Scale bar = 5  $\mu\text{m}$ , 2  $\mu\text{m}$ ), (g-i) *Pulicaria boissieri*; echino-perforate exine and sharp regular echini (Scale bar = 10  $\mu\text{m}$ , 5  $\mu\text{m}$ , 2  $\mu\text{m}$ ).

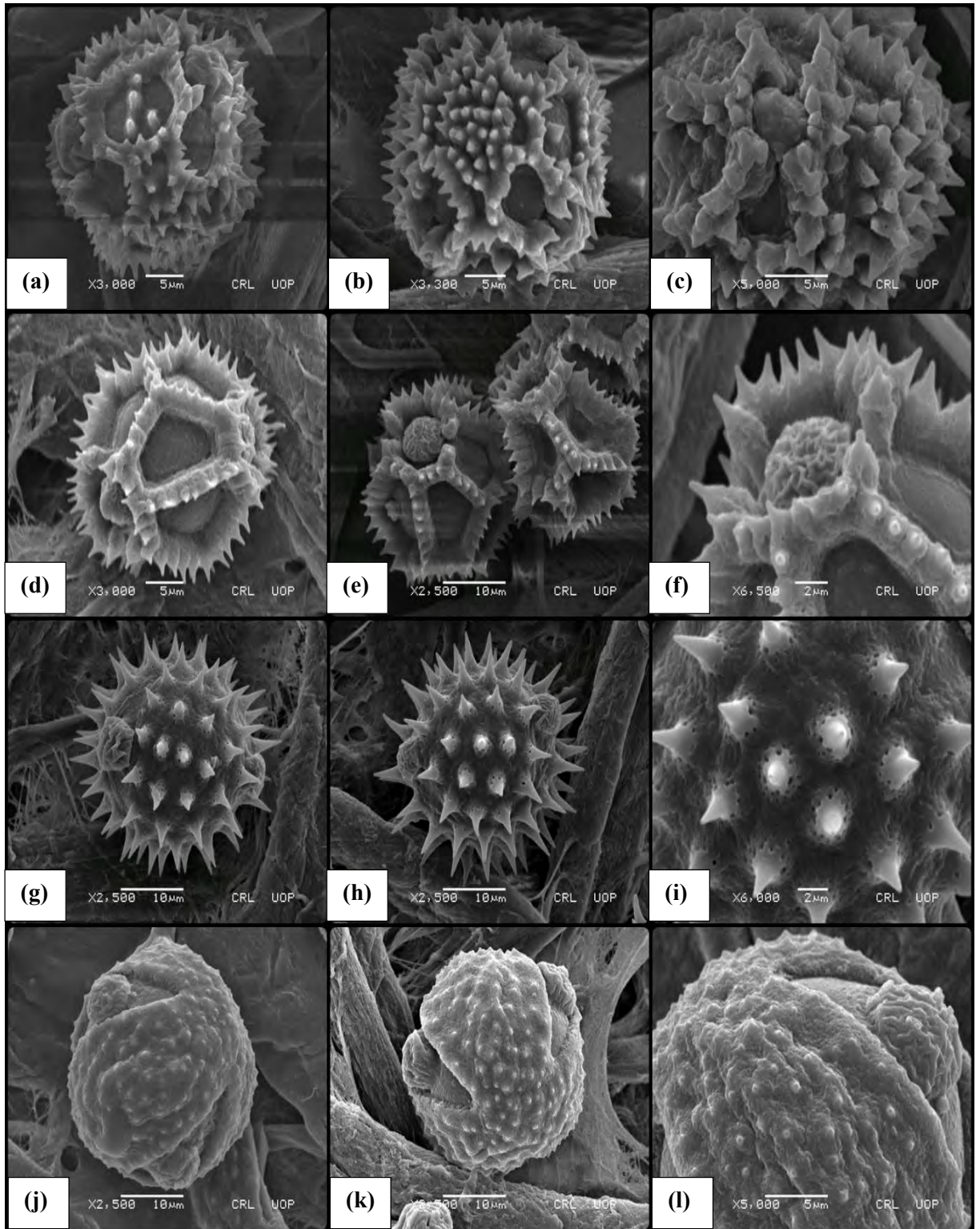


**Plate 42.** Scanning electron microscope photographs of Asteraceous taxa. (a-c) *Sonchus asper*; fenestrate lacunate (Scale bar = 5  $\mu\text{m}$ ), (d-f) *Tragopogon gracilis*; Echino-perforate scabrate and bulged echini (Scale bar = 10  $\mu\text{m}$ , 5  $\mu\text{m}$ , 2  $\mu\text{m}$ ), (g-i) *Verbesina encelioides*; echino-perforate exine and pointe tips spines (Scale bar = 10  $\mu\text{m}$ , 2  $\mu\text{m}$ ), (j-l) *Xanthium strumarium*; micro-echinate verrucate exine (Scale bar = 10  $\mu\text{m}$ , 5  $\mu\text{m}$ ).

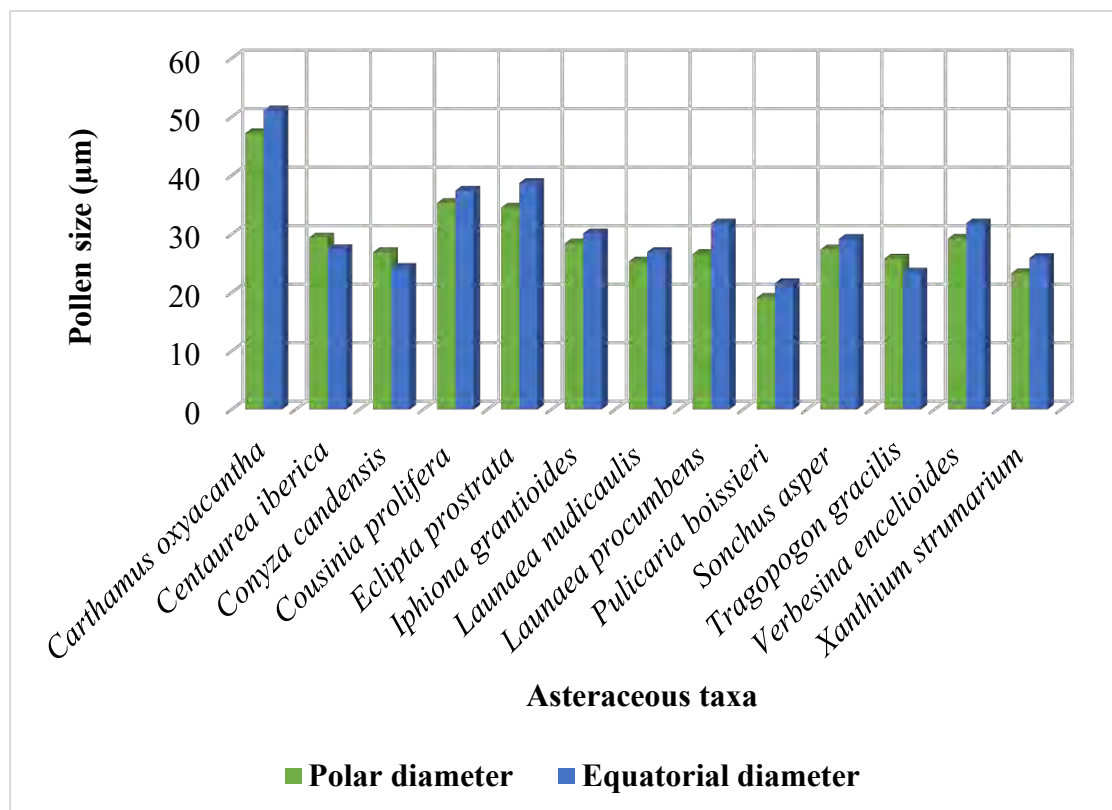


**Figure 13.** Mean pollen size variations among Asteraceous taxa

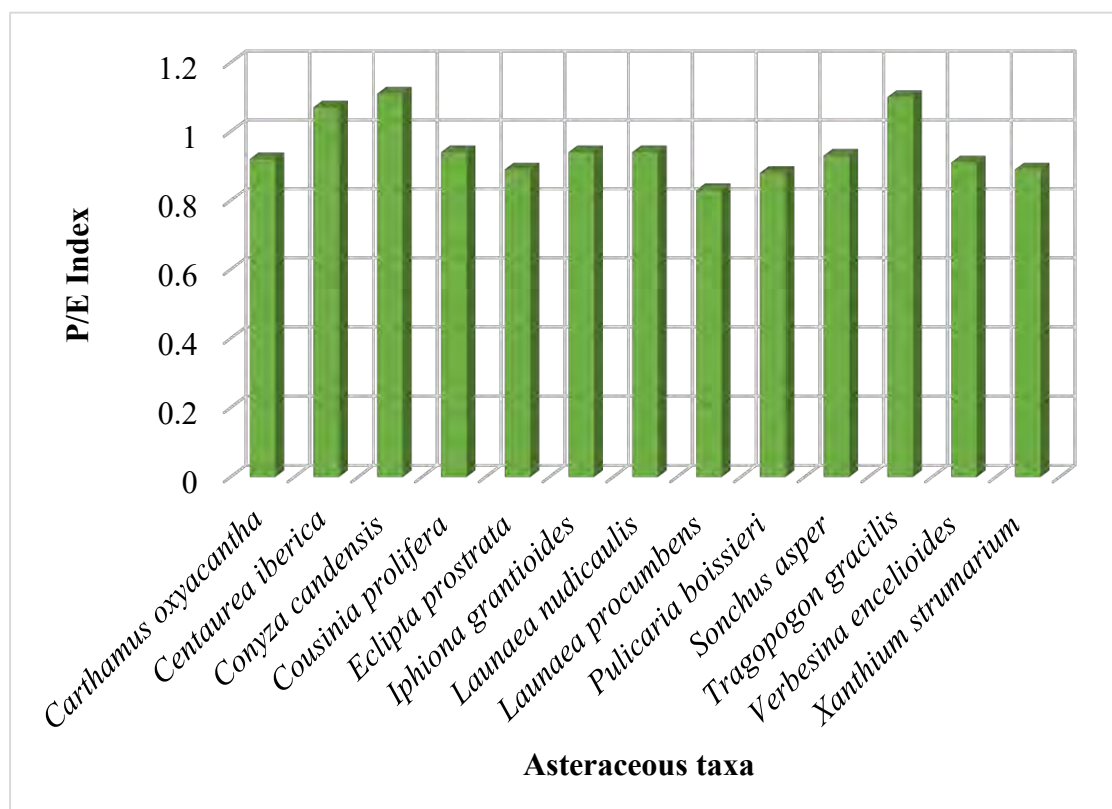


**Figure 14.** Polar to equatorial diameter index ratio among Asteraceous taxa



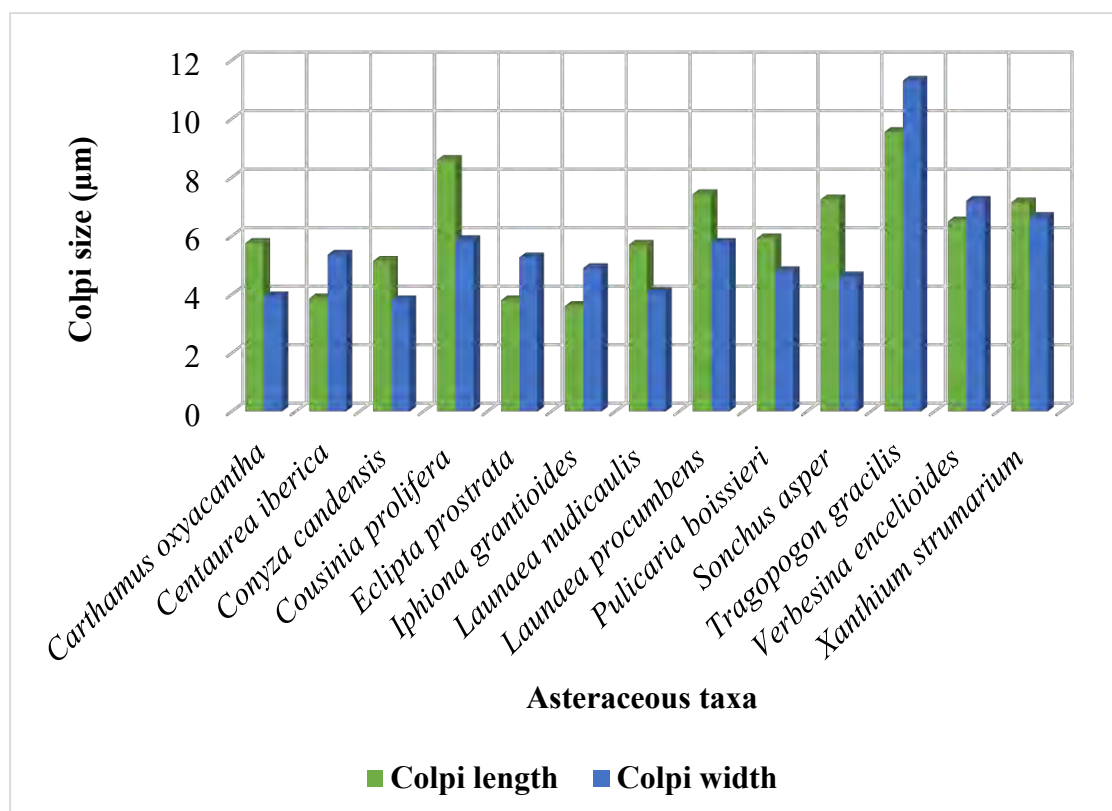


**Figure 15.** Average colpi length and width variations among Asteraceous taxa

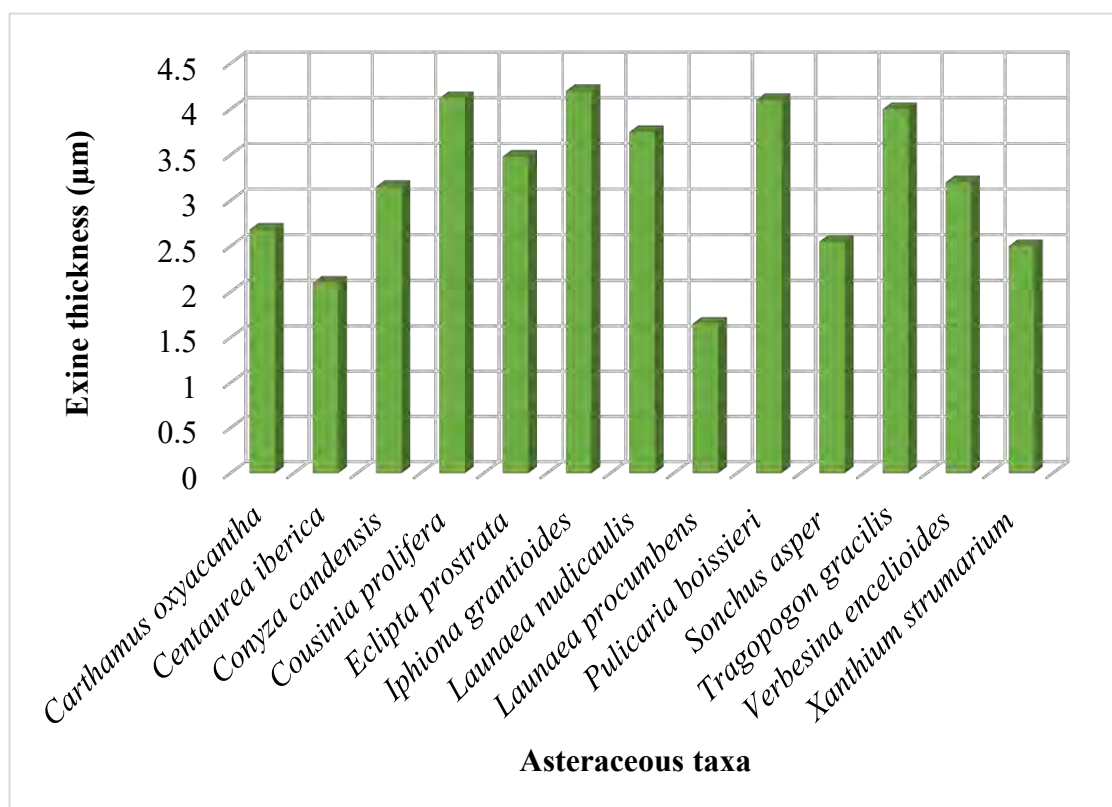


**Figure 16.** Mean exine thickness variations among Asteraceous taxa

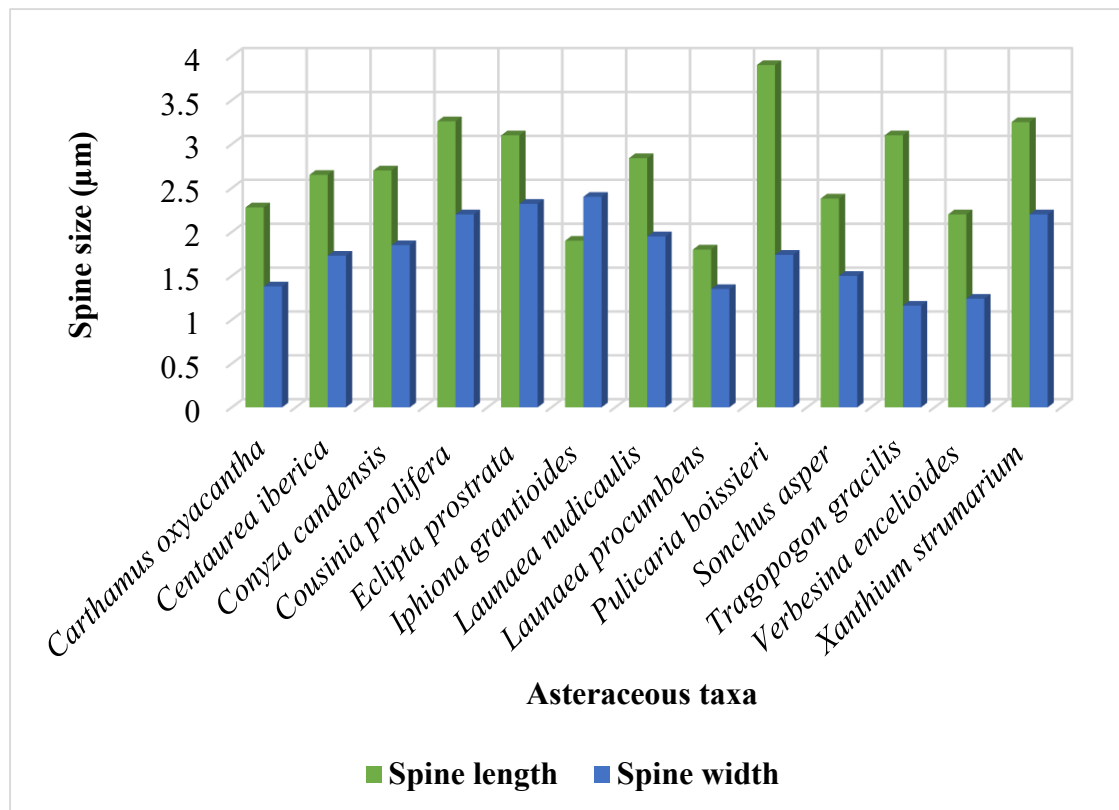


**Figure 17.** Spine measurement variations among Asteraceous taxa

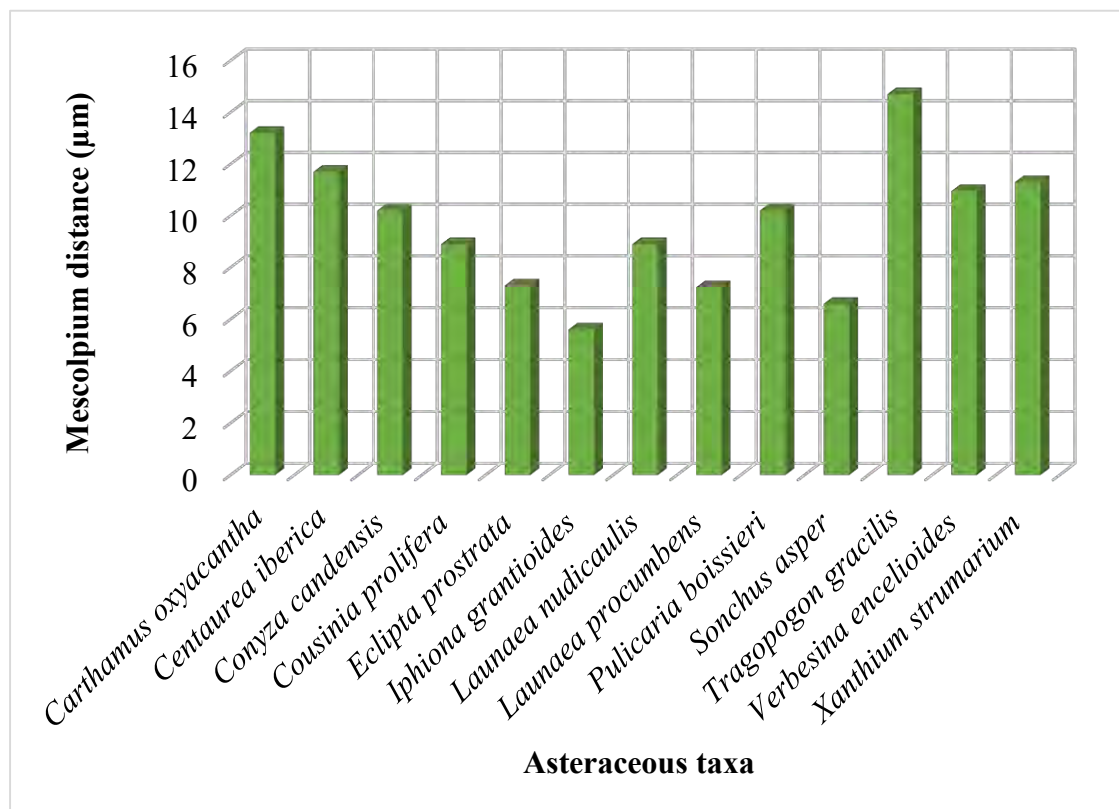


**Figure 18.** Mean distance variations of mesocolpium among Asteraceous taxa

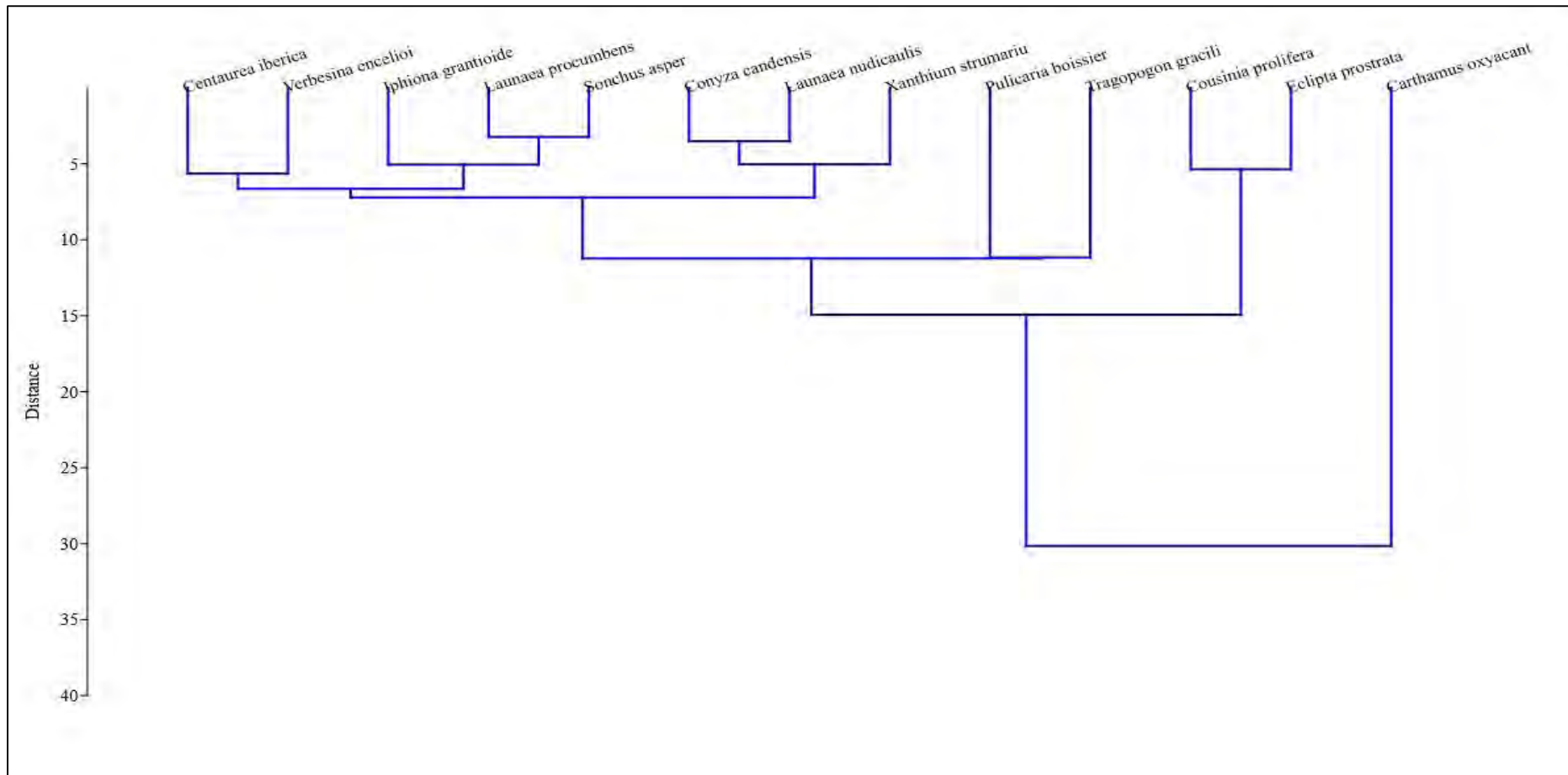


**Figure 19.** Cluster groupings through UPGMA dendrogram clustering among Asteraceous taxa based on quantitative pollen morphometrics

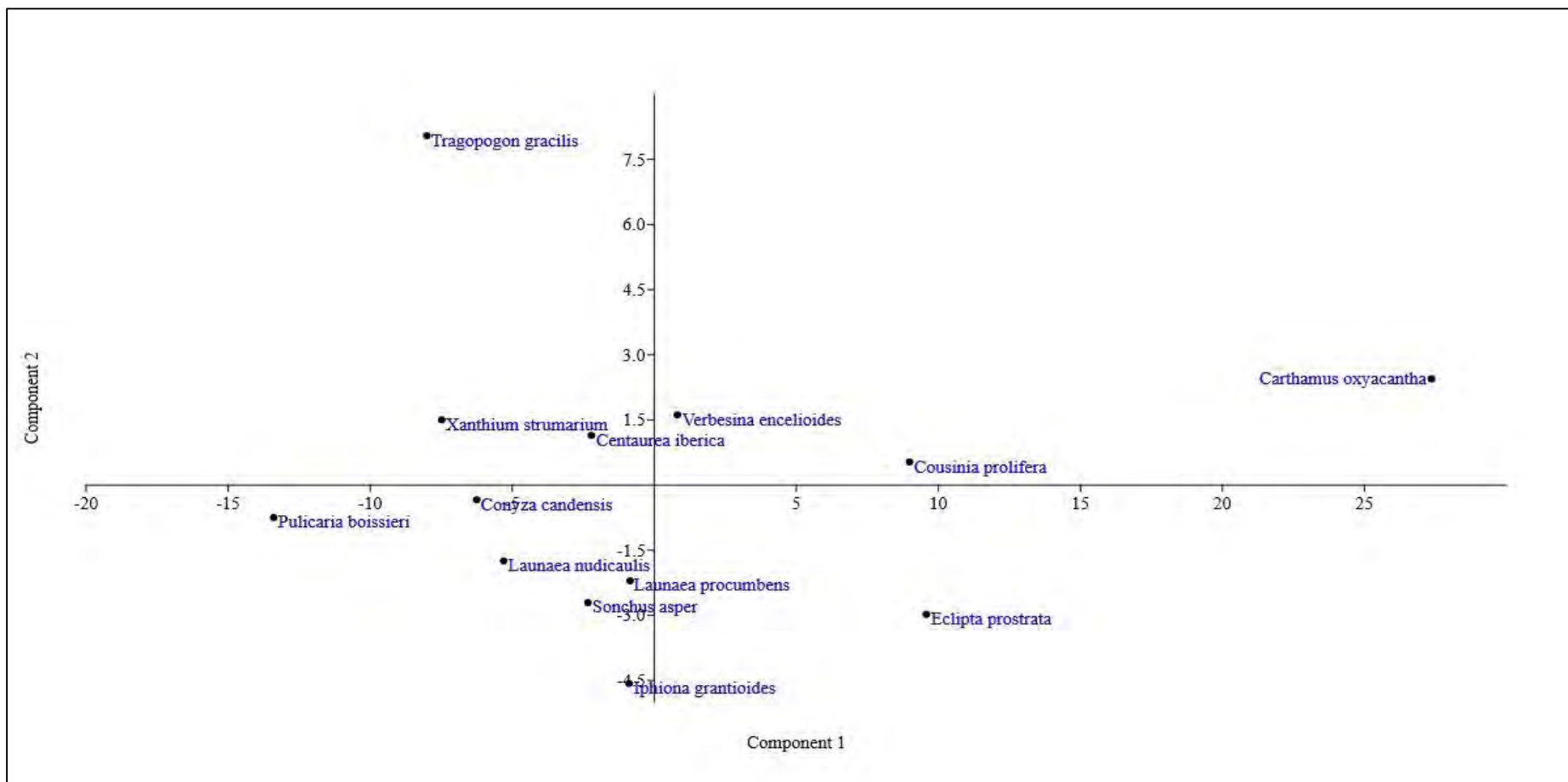


**Figure 20.** Principal component analysis (PCA) biplot of matrix variables of Asteraceae pollen

### 3.2.6 Discussion

There have been several morpho-taxonomic research carried on *Carthamus* species (Sehgal et al., 2009; Bowles et al., 2010, Hacıoğlu et al., 2012). Three species of *Carthamus* were focused at in the works by Vilatersana et al., (2001) and Bulbul et al., (2013), and echino-scabrate type pollen was identified. The diverse microscopic tools in our study sheds light on the morphometric variations on *Carthamus* grains. According to Vilatersana et al. (2005) pollen observation in the *Carthamus* complex, *Carthamus oxyacantha* pollen were trizonocolporate, isopolar, radial symmetry, subprolate, continuous echini with elevated tectum, and minute perforations between echini. There is a consistency among Vilatersana et al., (2005) and our findings, and the measures are comparable. In a different study, Ahmad et al., (2022) and Osman (2009) noted a little variation in the pollen of *Carthamus* spp., with trizonocolporate and spheroidal pollen that varies from oblate to prolate. Sexine tectate with imperforate reticulate and psilate-perforate stratification. *Carthamus oxyacantha* pollen was classified as sub-oblate by Gul et al., (2022). The pollen category was similar to that reported by Ahmad et al., (2013), Khan et al., (2021), and Reshmi and Rajalakshmi (2019).

One of the most important methods used in the taxonomy of *Centaurea* is pollen microstructure (Bancheva et al., 2014). In this respect, the aim was to describe in depth the pollen morpho-structure of Desert-inhabited *Centaurea* species, as well as to assess the taxonomic relevance. The pollen of the six *Centaurea* species was similar in size, shape, and aperture characters, polarity, and symmetry. Moreover, they diverse in color, exine structure, and density of the spines on the exine tectum (Joujeh et al., 2019) This study revealed that pollen wall aspects use to have a notable taxonomic significance in identifying between Asteraceous species. This finding is comparable with the earlier studies, which indicated that the ornamented pollen wall elements are useful in taxonomic inquiry of genus *Centaurea* (Ozler et al., 2009, Shabestari et al., 2013). Atar (2006) examined pollen of *Centaurea kileae* and *Centaurea cuneifolia*, Pinar (2007) visualized 5 sub-species of *Centaurea cariensis* using scanning bio imaging techniques (Biyiklioğlu et al., 2018). The pollen of such group was found to be isopolar, radially symmetric, and tricolporate, based on this research. The ornamentation was classified as echinate to echino-perforate. Gürdal and Özhatay (2019) also studied pollen of five *Centaurea* species from Turkey and one of them is

*Centaurea iberica*. According to their data exine peculiarities are scabrate to micro-echinate and the tectum is perforate. In our study the pollen shape and the exine sculpture are spheroidal and scabrate- micro-echinate. Micro-structure of 19 *Centaurea* taxa from Iran was examined using scanning microscopy showed tricolporate, isopolar, radially, sub-prolate, perforate tectal elements and scabrate surface. On the exine sculptured patterns two diverse nature pollen were visualized: (1) dense acute end spinules and (2) sparsely distributed spinules (Ismial and Shahbaz, 2020; Shabestari et al., 2013).

Most of Asteraceae genera possess zonocolporate pollen the study has shown on the position as well as the shape of colpi and most species of this family are with 3 colpus and distributed along the equatorial line, tri-zonocolporate, radically symmetrical, spheroidal, isopolar, exine spinulose as in *Erigeron canadensis*. Sadeq and Aliwy (2019) noticed a significant pattern in pollen features of *Erigeron canadensis* with a closely oblong shape, psilate, and straight thick exine, while Qureshi et al., (2019) identified a difference in shape that seems to be oblate-spheroidal. In this study, pollen from *Erigeron canadensis* was analyzed as prolate-spheroidal with the echinate surface, but the early report indicates spherical, scabrate-echinate, angular colpus in *Conyza bonariensis* (Khan et al., 2021; Umber et al., 2022). On the basis of exine sculpturing elements Perveen (1999) identified Type II exine peculiarities in *Conyza canadensis* which was easily determined from its echinate tectum costae; colpus structure sub-psilate and rarely granulate.

Pollen grains in *Cousinia* genera are tri-zonocolporate, with a columellate exine morphology (Wortley et al., 2012). Extensive research has been done on the pollen morphology of the tribe Cardueae. Except for *Cousinia*, each genus of the subtribe Carduinae has almost a uniform pollen structure. However, there are two forms of pollen in the genus *Cousinia*. Type I has triangular-spheroid grains with a short polar axis and spinulose exine peculiarities with small tubercles. Type II *Cousinia* pollen is defined by elliptic-oblong shape with a long polar axis and psilate-spinulose exine (Saber et al., 2009; Ulukuş and Tugay, 2020). Meo & Khan (2003) reported *Cousinia minuta* pollen are prolate to spheroidal. The pollen structure of this species is similar to that of *Cousinia prolifera*, which included in our study. Jafari and Ghanbarian (2007) noted that the grains of *Cousinia eriobasis* were sub-prolate and verrucated pattern

exine. Pollen grains from species in the *Cousinia* section, according to Ahmad et al., (2011), have a spherical to a circular shape. This study mentioned *Cousinia eleonorae* is sub-prolate, while *Cousinia humilis* is prolate-spheroidal. Our study argued that the pollen of *Cousinia prolifera* has verrucate-perforate stratified exine.

*Eclipta prostrata* had one member of tribe Heliantheae with rectangular pores (Salamah et al., 2019). El-Ghazaly (1993), Perveen (1999) and Sardar et al., (2013) previously examined the Ecliptinae tribe sculpturing described pollen of single species *Eclipta prostrata*. SEM micrographs of exine stratification of the *Eclipta prostrata* were described in fine details of the exine ultrastructure of this species. Spines were echinate with large bases and little, not sharpened tips were seen as pollen sculptures in both healthy and virus-infected *Eclipta alba* (Sonia et al., 2022). Data on pollen fertility is a preferred method for recognizing the potentially hybrids from the parents (Ahmad et al., 2010). In the latest research, pollen fertility of healthy *Eclipta alba* was 94%, whereas it was only 76% in virus-infected species. Perveen (1997) highlighted that the echinate tectum in *Eclipta prostrata* is easily identifiable by its radially symmetric, isopolar, oblate-spheroidal to rarely sub-oblate, tricolporate, and rarely tetracolporate grains. Our findings confirm the presence of an intermediate aperturate type in exine structure in this tribe. However, contrary to Coutinho and Dinis (2007), the mesoaperture does not intersect to the foot layer of exine for the Asteraceous species delimitation. Oblate-spheroidal (*Iphiaea grantioides*) pollen shape was observed which was not similar to the finding of Ahmad et al., (2013); Khan et al., (2021) and Reshmi and Rajalakshmi, (2019).

Tribe Lactuceae pollen micromorphology from the flora of Egypt revealed the outer exine of pollen types is either tectate or bulged in a series of ridges (lophae) around lacunae, with the ridges usually forming regular, magnificent patterns (Marzouk et al., 2021). We identified the same pollen attributes for this species in terms of aperture type and number; however, exine ornament was characterized as echino-perforate here. Mabel et al., (2014) studied earlier species in the same genus; *Launaea taraxacifolia* grains were acolpate, prolate spheroidal, medium-sized; minute spinules with sharp ends; and pores were widely placed and three in number, which varied from our current observation. Blackmore (1982) identified seven pollen types that were classified using a taxonomic key based on the number and orientation of the

lacunae. In addition, Blackmore (1984) examined the pollen structure of large number species belonging to the tribe Lactuceae and identified seven different pollen types, that were divided into sub groups based on particular exine features. Qureshi et al., (2002) counted pollen fertility of seven different species belongs to genus *Launaea* from Pakistan. Kilian (1997) analyzed radially symmetrical, isopolar, hexagonal and echino-lophate tectum in *Launaea nudicaulis*. Whereas our findings elaborated tricolporate, echinate scabrate to perforate-fenestrate type grains. In another study Azzazy (2011) examined hexagonal, fenestrate, 3-colporate, rounded ends colpi and lophate, echini with sharp conical apices in *Launaea nudicaulis* grains. Ragho (2020) provided detailed micromorphology of *Launaea procumbens* pollen with trichotomoporate aperture and verrucate reticulate sculptured pattern was inconsistent with our findings.

Light and scanning visualized microscopic tools to define exine stratified characters, with special emphasis on the spines variations, were the most significant characters in identifying *Pulicaria* pollen types from Iberian species. Coutinho et al., (2011) analyzed the pollen structure of seven *Pulicaria* species and described a tectum with acute spines and perforations on the entire exine membrane. The morphometry of the exine sculptural traits were explained in the subtribe Inulinae including *Pulicaria paludosa* with senecioid pattern. The tectal structure is made up of three primary layers that vary in thickness and morphometry: tectum, columellar layer, and a layer made up of the columellae's basal lamina. Type III pollen easily recognized by its 3-zonocolporate, in *Pulicaria Gaertn* (Padrón-Mederos and Serna-Ramos, 2011).

Similar to this, *Sonchus asper* has tricolporate or tetracolporate exine sculptures that have sunken colpi. The ridges on the elliptical or spherical apertures are lined with spines. These findings are similar to the reports of (Diez et al., 1999). Ahmad et al., (2020) draw similar conclusions regarding pollen shape and sculpturing but emphasized on broad and conical echini arrangement. Mallick (2017) defined pollen of *Sonchus asper* hexagonal, hexaporate, and echinate hexahedral, which did not agree with our findings. *Sonchus asper* pollen was found to be spheroidal, prolate, rectangular, and 3-coloporate to 4-coloporate (Mazari et al., 2012). *Sonchus asper* grains were trizonocolporate, but *Sonchus palustris* pollen were 4-zonocolporate (Ali et al., 2021; Qureshi et al., 2002).



According to Gültepe et al., (2018), the pollen grains of the *Tragopogon* species are sub-oblate to oblate-spheroidal in shape, and 3-zonocolporate with 15 lacunae. The pollen morphometric traits Wagenitz (1976) identified three evolution process in the Asteraceae: spines reduction, and absence of inner columellae; and formation of surface ridges (lophate or fenestrate pollen). Qureshi et al., (2008) reported sub-oblate and sub-prolate pollen for *Tragopogon gracilis*. The genus *Tragopogon* generally has trizonocolporate pollen grains, but dizonocolporate and tetrazonocolporate pollen grains were also reported by Azizi et al., (2022). According to ITS data, the species *Tragopogon porphyrocephalus*, *Tragopogon stroterocarpus*, and *Tragopogon jesdianus* belongs to the Rubriflori section, which is aligned with the pollen statistics of Azizi et al., (2021). Pollen grains are tricolporate and echinate with six abporeal, three equatorial, and six interapertural lacunae within the genus *Tragopogon*. The results also indicated that *Tragopogon artvinensis* and *Tragopogon vanensis* have tricolporate pollen grains as reported by Gültepe et al., (2016).

The pollen morphology of *Verbesina encelioides* in this study correspond to the investigation of Ullah et al., (2021), who also described prolate-spheroidal pollen with conical pointed spines. Previous studies of *Verbesina* have shown that pollen grain shape can vary from oblate-spheroidal to prolate-spheroidal, medium-sized, isopolar, monads, sub triangular amb as was reported by Moreira et al., (2019) who analyzed eight Brazilian species of *Verbesina*. Considering the new species *Verbesina barrancae* by Harker and Reyes (2002) from Mexico described echinate, tricolporate grains with small polar area. On the basis of spine length and shape of the spine base subtypes were recognized with spines longer than 4  $\mu\text{m}$ , commonly with narrower bases, as they emerge abruptly from the exine surface on *Verbesina encelioides* (Telleria, 2017). Pollen grains of *Verbesina* can be classified as the "Aspilia" type described by Radaeski et al. (2016), because they are medium to large in size, 3-colporate, and lalongate, with an endoaperture with a medium constriction, an echinate exine and conical spines with perforations at the base.

Concerning the exine ultrastructure of the sections *Xanthium*, our data are in very good agreement with those of Coutinho et al., (2020) in practically all points (e.g. the presence of pattern exine ultrastructure and the existence of a significant difference in the relative number of the columellae in the outer and inner layers of the sexine). The results of palynological analysis of this study are inconsistent with the results of

Coutinho et al., (2021) that showed the pollen grains of section *Xanthium* are clearly differed by their LM and SEM characters. However, no significant difference found between the pollen of *Xanthium strumarium*. According to the terminology of Punt and Hoen (2009), pollen type of the *Xanthium strumarium* L. complex overall seems to be similar to that of *Xanthium strumarium* type. Pollen grains are mainly 3-zonocolporate and rarely 4-zonocolporate with very short, narrow acutecolpus and sculpturing in the members is scabrate (Noedoost et al., 2021).

### 3.2.7 Micromorphological Description of Fabaceous Pollen

The pollen of selected desert-inhabited Fabaceous taxa was visualized using scanning imaging analysis, revealing diverse sculpturing patterns and exine types. Micromorphology of pollen described various ultrasculptural elements helpful to accurately identify species. Scanning micrographs of Fabaceous pollen were illustrated in Figures 10, 11 & 12.

All of the studied species show similarities in pollen shape as oblate-spheroidal, prolate-spheroidal, sub-prolate and prolate, isopolar, and monad except *A. jacquemontii*, *A. modesta*, and *A. nilotica* that show polyads type grains. Some species show variation in colpi ornamentation from the rest of the studies species e.g. *C. burhai*, *D. sissoo*, and *P. cineraria* appear with trizonocolporate pollen while the rest has tricolporate. Pollen oriented in two shapes i.e. polar and equatorial in the present study we observed that *A. jacquemontii*, *A. nilotica*, *P. aceulata*, *P. cineraria*, and *P. juliflora* shares the same polar view i.e. circular. Exine sculpturing was observed as scabrate regulate in *A. jacquemontii* while in *A. homosus* and *C. burhai*, it was regulated fossulate in *A. modesta*. The maximum polar and equatorial distance was calculated for *A. modesta* (39.5  $\mu\text{m}$ ) and (38.4  $\mu\text{m}$ ) respectively. P/E ratio was measured highest for *A. homosus* (1.59) and lowest for *A. jacquemontii* (0.93). Exine thickness was noted highest for *A. modesta* (4.7  $\mu\text{m}$ ) and minimum for *A. homosus* (0.37  $\mu\text{m}$ ). Pollen fertility was estimated to be highest for *D. sissoo* (95.2%) and lowest for *P. aceulata* (83%).

Pollen micro-morphological investigation of nine species of the family Fabaceae was examined under the scanning electron microscope (SEM) to reveal the ultra-picture of pollen of this family. We found some outstanding observations after the study of these selected leguminous species below.

#### a) *Acacia jacquemontii* Benth.

Pollen compound (12, 14 cells polyad) and medium-sized. Polar view semi-circular and equatorial view oblate-spheroidal. Colpi and pores absent. Exine sculpturing smooth to scabrate regulate and tectum verrucate. Polar diameter (33.7 $\pm$ 1.76  $\mu\text{m}$ ), equatorial view distance (36.14 $\pm$ 1.2  $\mu\text{m}$ ). P/E ratio 0.93. Exine thickness (2.05 $\pm$  0.13). Pollen fertility 89.5% and sterility 10.4%.

**b) *Acacia modesta* Wall.**

Pollen polyad, medium-sized, heteropolar and radically symmetrical. Polar view semi-circular and prolate-spheroidal equatorial view. Colpi and pores absent. Exine thicker than nexine and sculpturing regulate fossulate. Polar diameter ( $39.5 \pm 1.61 \mu\text{m}$ ) and equatorial distance ( $38.4 \pm 1.34 \mu\text{m}$ ). P/E ratio 1.02. Exine thickness ( $4.7 \pm 0.81 \mu\text{m}$ ). Pollen fertility 84% and sterility 15.9%.

**c) *Acacia nilotica* (L.) Delile**

Pollen 16-32 celled polyad, radically symmetrical, medium sized and heteropolar. Polar view circular and oblate-spheroidal equatorial view shape. Exine ornamentation sub-psilate. Colpi and pores absent. Exine thicker than nexine, tectum sub-psilate and foveolate. Polar view diameter ( $35.2 \pm 1.54 \mu\text{m}$ ) and equatorial view distance ( $36.3 \pm 1.14 \mu\text{m}$ ). P/E ratio 0.96. Exine thickness ( $2.50 \pm 0.39 \mu\text{m}$ ). Pollen fertility 88.4% and sterility 12.5%.

**d) *Astragalus homosus* L.**

Grains monad, small to medium, and tricolporate. Slightly circular polar view shape and equatorial view shape prolate. Exine sculpturing scabrate reticulate. Polar diameter and equatorial diameters were recorded as ( $34.58 \pm 0.13 \mu\text{m}$ ) and ( $21.66 \pm 0.23 \mu\text{m}$ ), respectively. P/E ratio 1.59. The width and length of colpi was 1.29 and  $0.50 \mu\text{m}$  while the quantitative values of mesocolpium and exine thickness were noted as 2.00 and  $0.37 \mu\text{m}$ . Pollen fertility 94.6% and sterility 5.3%.

**e) *Crotalaria burhia* Benth.**

Grains monad, medium sized and trizonocolporate. Semi angular polar view and equatorial view shape oblate-spheroidal. Exine sculpturing psilate to scabrate-reticulate. Polar diameter ( $25.4 \pm 1.43 \mu\text{m}$ ) and equatorial view distance ( $26.4 \pm 1.23 \mu\text{m}$ ). P/E ratio 0.96. Colpi length ( $4.25 \pm 0.46 \mu\text{m}$ ) and colpi width ( $4.65 \pm 0.28 \mu\text{m}$ ). Exine thickness ( $2.45 \pm 0.25 \mu\text{m}$ ). Mesocolpium distance ( $13.2 \pm 0.42 \mu\text{m}$ ). Pollen fertility 93.2% and sterility 6.71%.

**f) *Dalbergia sissoo* DC.**

Grains monad, medium sized and trizonocolporate. Semi angular polar view and equatorial view shape oblate-spheroidal. Exine sculpturing scabrate. Polar diameter ( $25.9 \pm 1.43 \mu\text{m}$ ) and equatorial view distance ( $26.7 \pm 1.23 \mu\text{m}$ ). P/E ratio 0.97. Colpi length ( $4.25 \pm 0.46 \mu\text{m}$ ) and colpi width ( $4.65 \pm 0.28 \mu\text{m}$ ). Exine thickness ( $2.12 \pm 0.25 \mu\text{m}$ ). Mesocolpium distance ( $13.2 \pm 0.42 \mu\text{m}$ ). Pollen fertility 93.2% and sterility 6.71%.

**g) *Parkinsonia aculeata* L.**

Pollen monad, medium sized and tricolporate. Polar view circular and equatorial view shape prolate-spheroidal. Exine peculiarities regulate, sexine thicker than nexine. Polar diameter ( $26 \pm 1.13 \mu\text{m}$ ) and Equatorial view distance ( $25.72 \pm 0.76 \mu\text{m}$ ). P/E 1.01. Colpi length ( $7.90 \pm 0.26 \mu\text{m}$ ). Colpi width ( $5.30 \pm 0.97 \mu\text{m}$ ). Mesocolpium distance ( $7.2 \pm 0.63 \mu\text{m}$ ). Exine thickness ( $1.9 \pm 0.54 \mu\text{m}$ ). Pollen fertility 83% and sterility 16.9%.

**h) *Prosopis cineraria* (L.) Druce**

Pollen monad, medium sized, and trizonocolporate. Circular polar view and equatorial view shape prolate-spheroidal. Exine sculpture pattern regulate. Polar diameter ( $31.7 \pm 0.65 \mu\text{m}$ ) and equatorial view distance ( $30.4 \pm 0.94 \mu\text{m}$ ). P/E ratio 1.04. Length of colpi ( $7.14 \pm 0.82 \mu\text{m}$ ), width of colpi ( $9.3 \pm 0.62 \mu\text{m}$ ). Exine thickness ( $2.65 \pm 0.48 \mu\text{m}$ ). Mesocolpium distance ( $5.8 \pm 1.48 \mu\text{m}$ ). Pollen fertility 94.7% and sterility 6.2%.

**i) *Prosopis juliflora* (Sw.) DC.**

Pollen grain monad, radially symmetrical, iso polar, medium sized, and tricolporate. Circular polar view and sub-prolate equatorial view shape. Colpi long and broad at base. Exine sculpturing scabrate-granulate. Polar diameter ( $32.3 \pm 4.52 \mu\text{m}$ ) and equatorial view distance ( $26.6 \pm 2.31 \mu\text{m}$ ). P/E ratio 1.24. Colpi length ( $4.55 \pm 0.25 \mu\text{m}$ ), colpi width ( $3.50 \pm 0.23 \mu\text{m}$ ), and mesocolpium distance ( $15.8 \pm 0.89 \mu\text{m}$ ). Exine thickness ( $3.65 \pm 0.46 \mu\text{m}$ ). Pollen fertility 94.6% and sterility 6.3%.

### j) Hierarchical UPGMA Clustering and PCA Analysis

Cluster analysis divided taxa into two main groups, namely, clusters A and B. Cluster A includes: *P. aculeata*; Cluster B is subdivided into two sub-cluster: sub-cluster I includes *A. modesta*, *A. nilotica* and *A. jacquemontii*; sub-cluster II includes: *A. homosus*, *C. burhia*, *D. sissoo*, *P. cineraria*, and *P. juliflora*. In sub-cluster II *C. burhia* and *D. sissoo* are closely related with the least euclidean distance due to shared intectate tectum and scabrate ornamentation. While in sub-cluster I *A. nilotica* and *A. jacquemontii* shared oblate-spheroidal shape and polyad typee grains as common features with a minimum of euclidean distance.

Principal component analysis was performed with the pollen metric variables from the two-dimensional plot of the first and second principal components (Fig. 1). The variance extracted was by variance and coordinates in a distance-based biplot. The six main components that were generated with significant biplots are represented in Table 4. The first two PCs explain 75.17% of the total variance of the analyzed data. The results of the PCA explained 53.85% of the variance for PC1 explained *A. jacquemontii*, *A. modesta* and *A. nilotica* lie on the positive side of the axis and *P. aculeata* on the negative side and away from the central position due to thicker sexine layer of component 1. The PC2 described *P. cineraria* and *P. juliflora* were on the positive side and *C. burhia* and *D. sissoo* on the negative side of the component 2 axis attributed to data variability among shape (P/E) and exine thickness.

**Table 11.** Principal component analysis (PCA) % variance loadings for the Fabaceous pollen.

Principal component	Eigen value	% variance
PC1	3.23	53.856
PC2	1.27	21.325
PC3	1.04	17.357
PC4	0.44	7.378
PC5	0.0043	0.072
PC6	0.00061	0.010

### 3.2.8 Taxonomic Keys based on Fabaceous Pollen Characters

- 1+ Prolate equatorial shape, exine scabrate reticulate.....*Astragalus hamosus*
- Equatorial shape other than prolate.....2
- 2+ Tectum striate, exine scabrate granulate, sub-prolate shape.....*Prosopis juliflora*
- Oblate-spheroidal equatorial shape.....3
- 3+ Exine sub-psilate, tectum foveolate .....*Acacia nilotica*
- Tectum intactate, exine psilate to scabrate-reticulate .....*Crotalaria burhia*
- 4+ Sculpturing scabrate.....*Dalbergia sissoo*
- Exine scabrate regulate, tectum verrucate.....*Acacia jacquemontii*
- 5+ Oblate-spheroidal, exine regulate.....*Prosopis cineraria*
- Sexine thicker, exine regulate.....*Parkinsonia aculeata*
- 6+ Sculpturing regulate fossulate.....*Acacia jacquemontii*

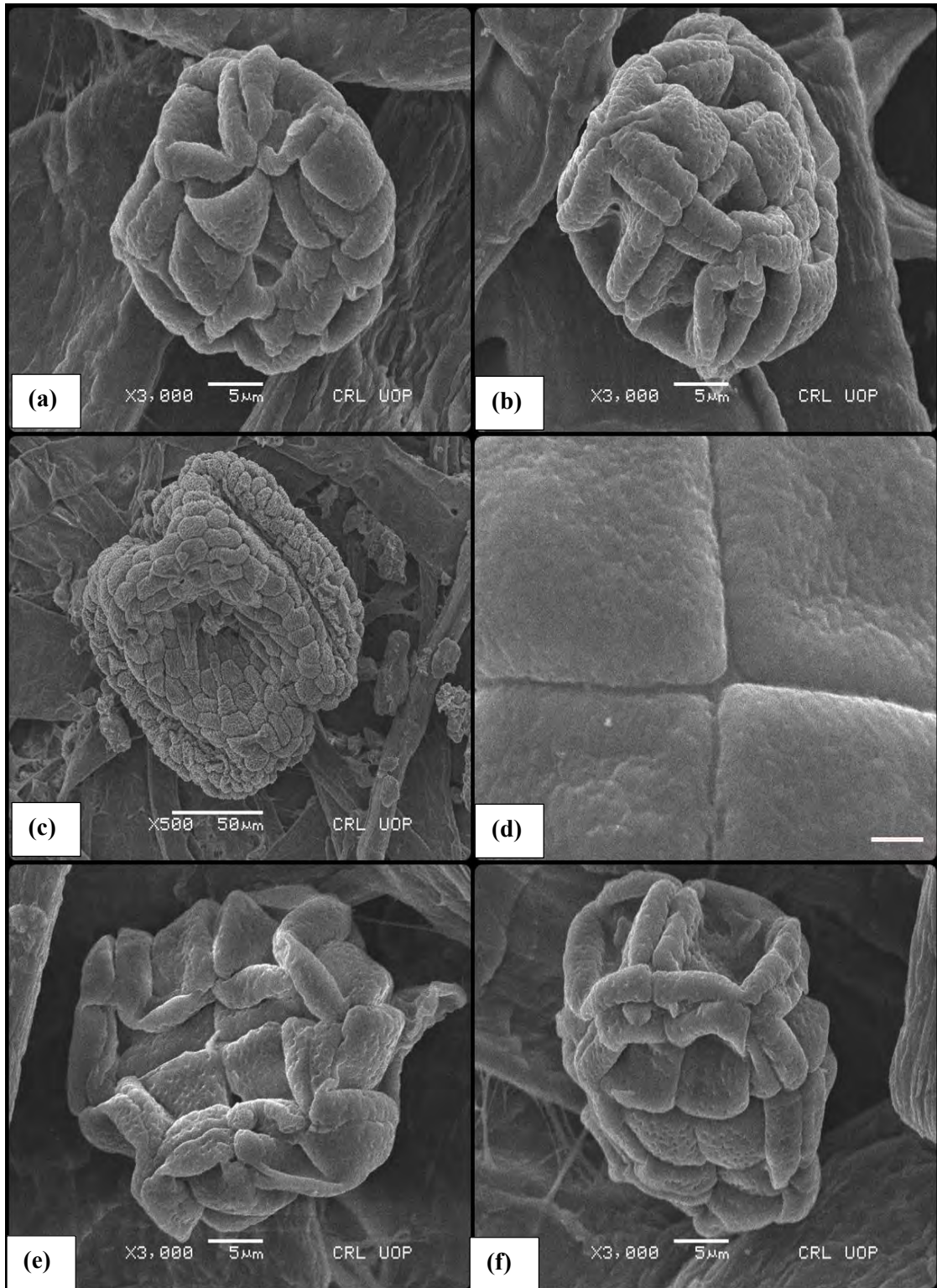


**Plate 43.** SEM micrographs of pollen grains, pollen surface pattern and exine peculiarities. (a-b) *Acacia jacquemontii* scale bar 5 μm, (c-d) *Acacia modesta* scale bar 50 μm & 2 μm, (e-f) *Acacia nilotica* scale bar 5 μm.



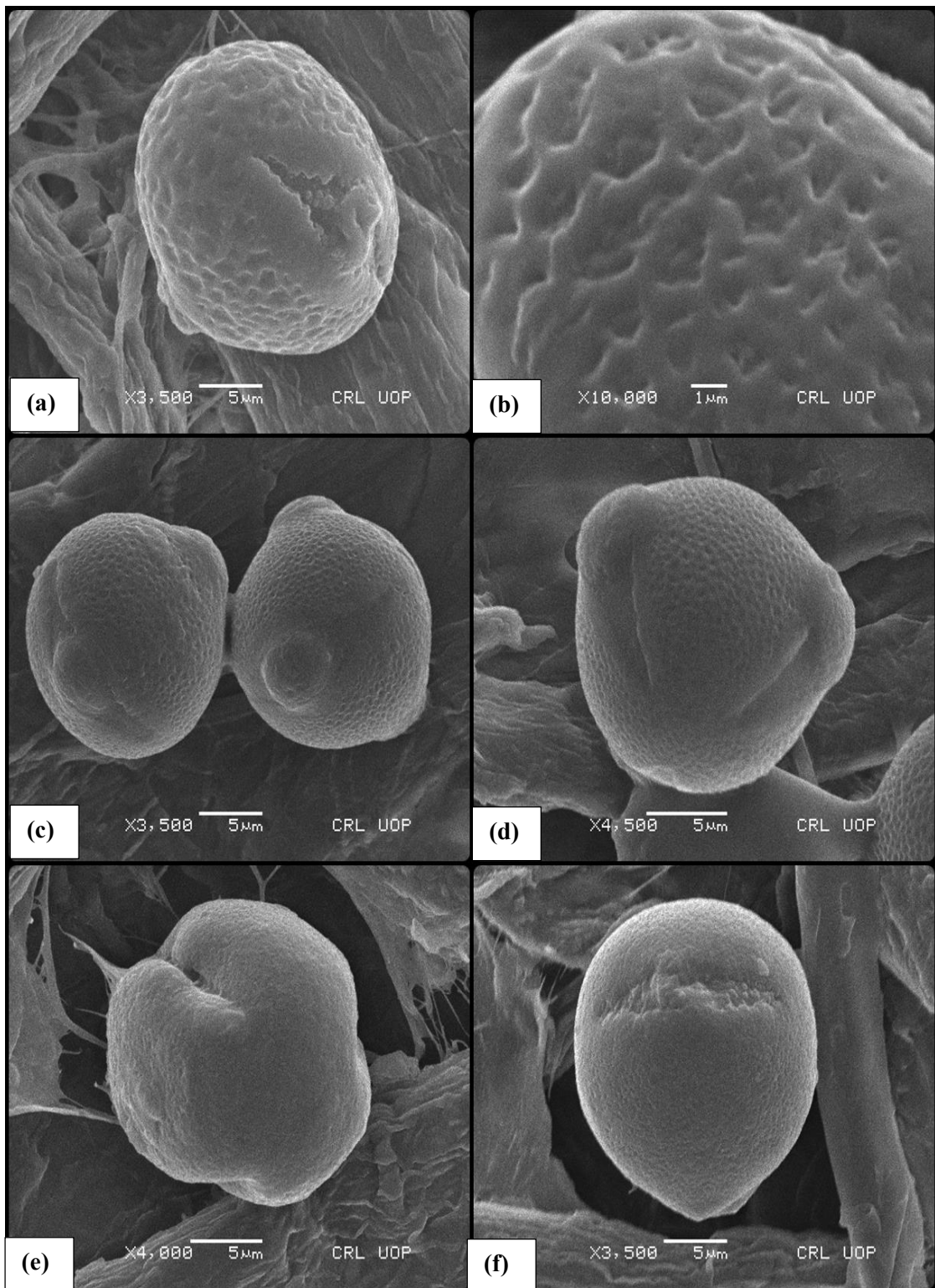


**Plate 44.** SEM micrographs of pollen grains, pollen surface pattern and exine peculiarities. (a-b) *Astragalus hamosus* scale bar 5  $\mu\text{m}$  & 1  $\mu\text{m}$ , (c-d) *Crotalaria burhia* scale bar 5  $\mu\text{m}$ , (e-f) *Dalbergia sissoo* scale bar 5  $\mu\text{m}$

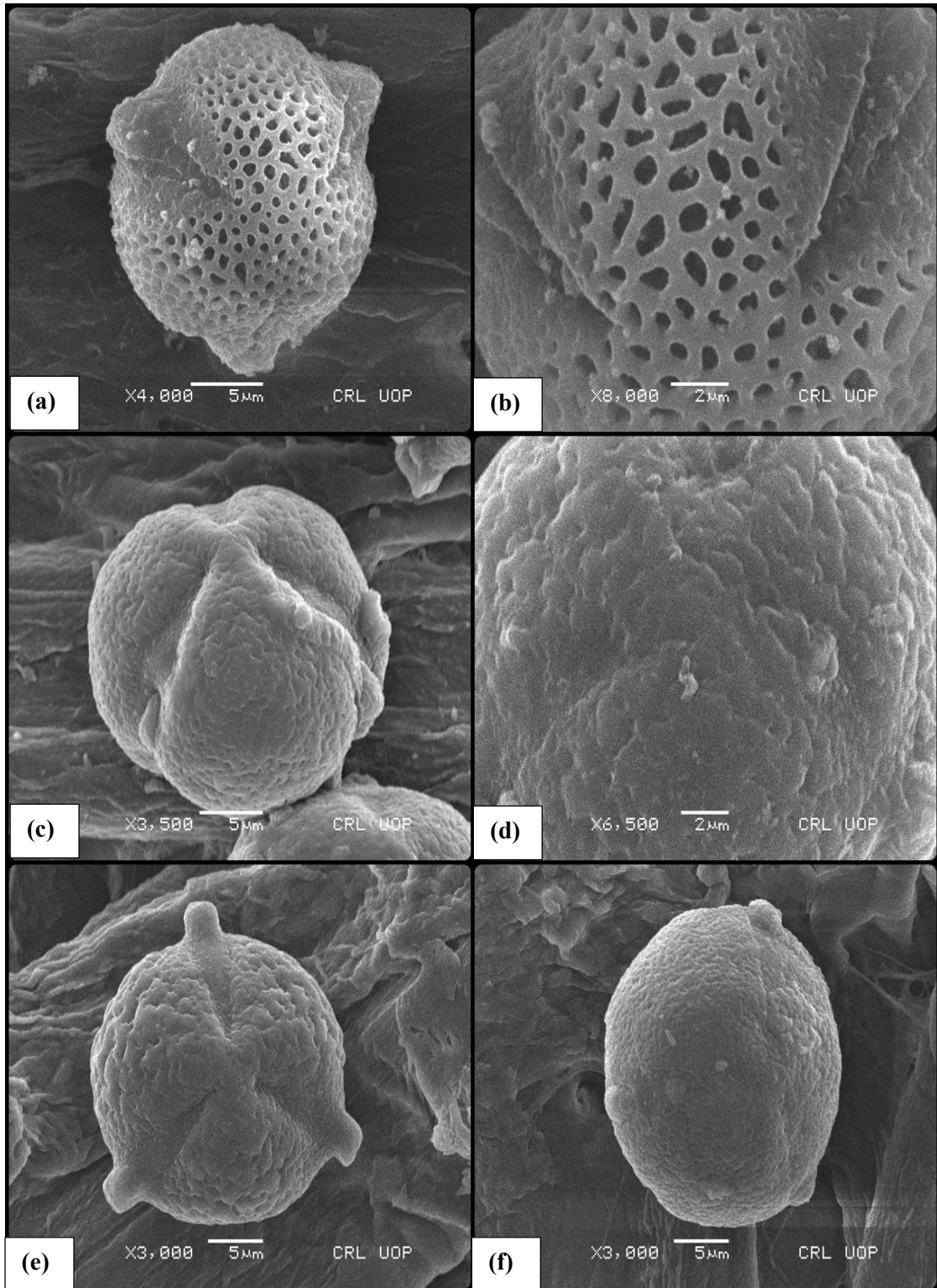


**Plate 45.** SEM micrographs of pollen grains, pollen surface pattern and exine peculiarities. (a-b) *Parkinsonia aculeata* scale bar 5 μm & 2 μm. (c-d) *Prosopis cineraria* scale bar 5 μm & 2 μm. (e-f) *Prosopis juliflora* scale bar 5 μm.

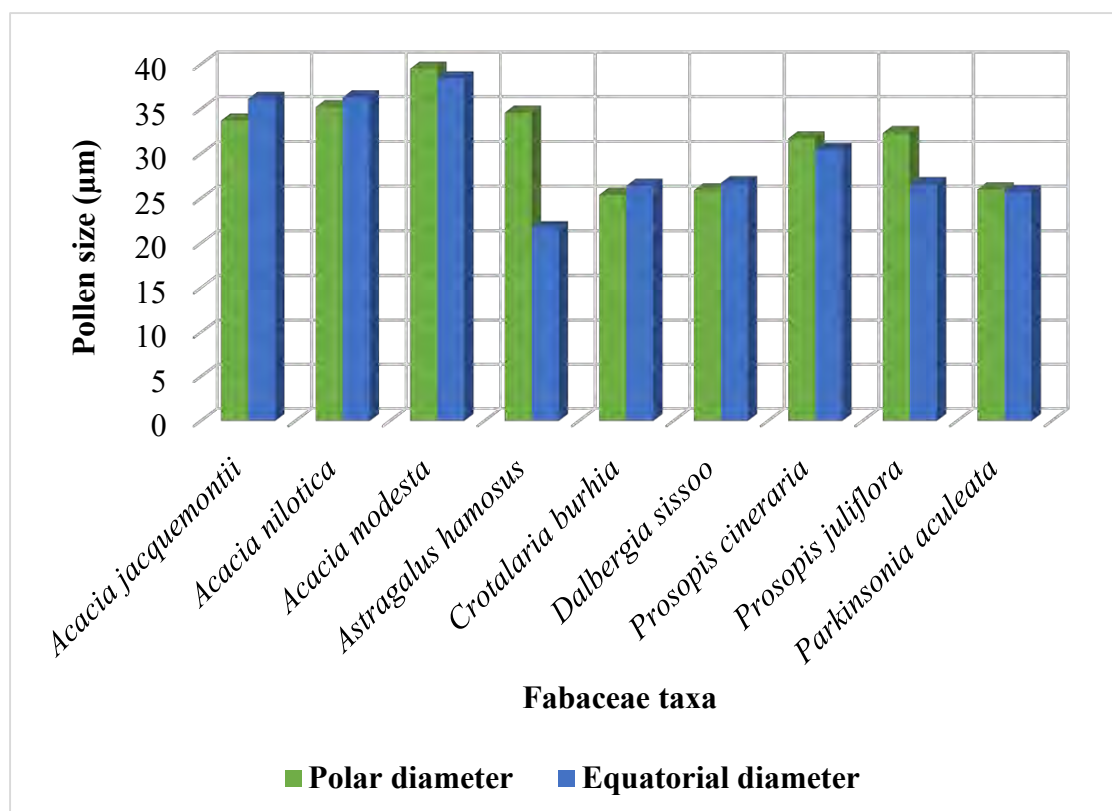


**Figure 21.** Mean pollen size variations among Fabaceous taxa.

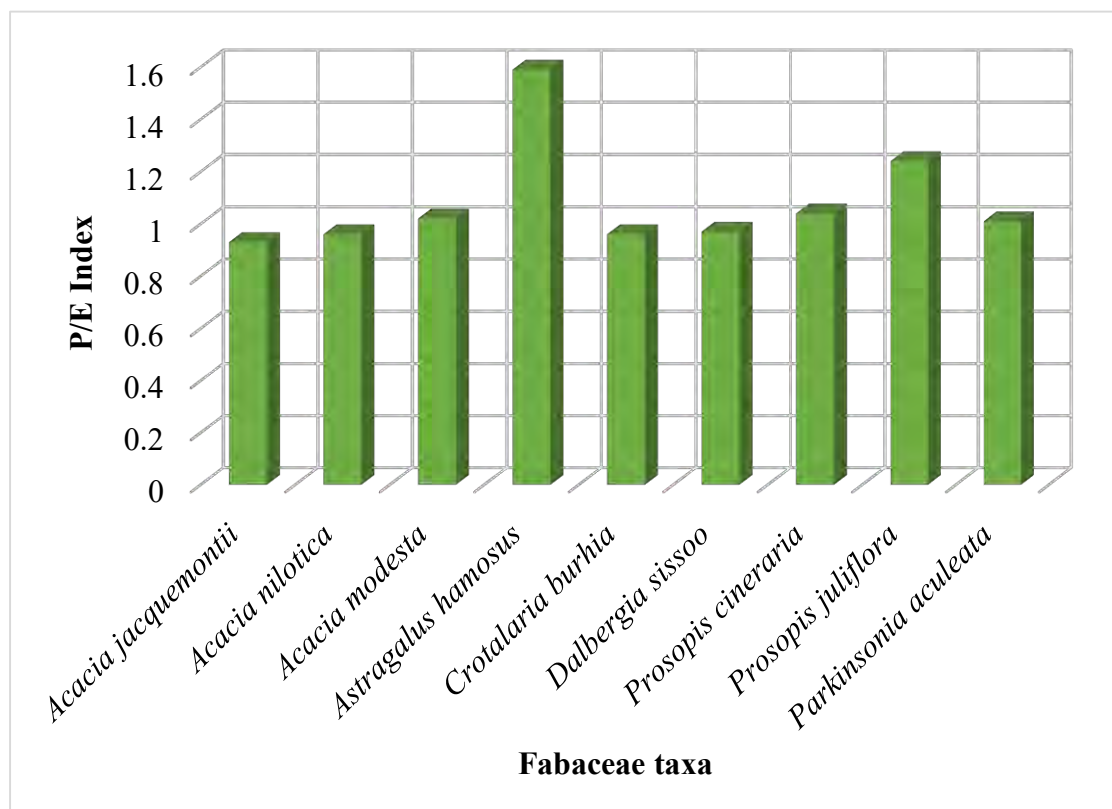


**Figure 22.** Polar to equatorial diameter ratio (P/E) among Fabaceous taxa.

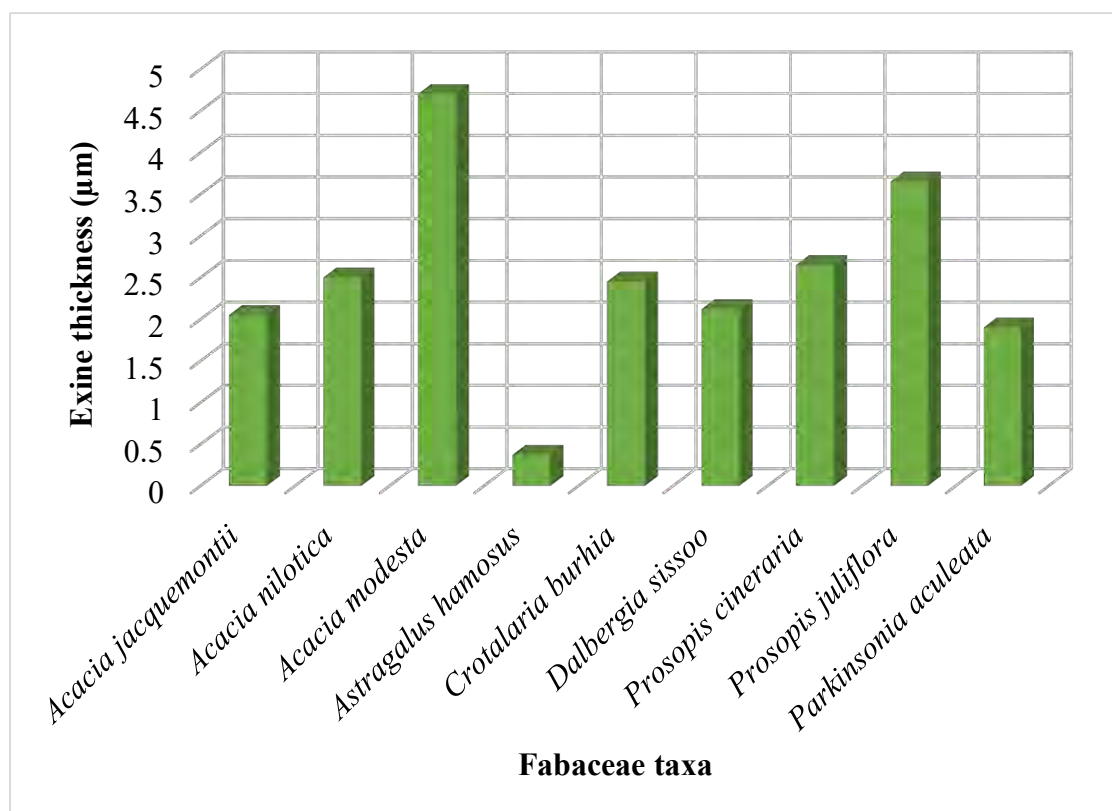


**Figure 23.** Average variations in exine thickness among Fabaceous taxa.

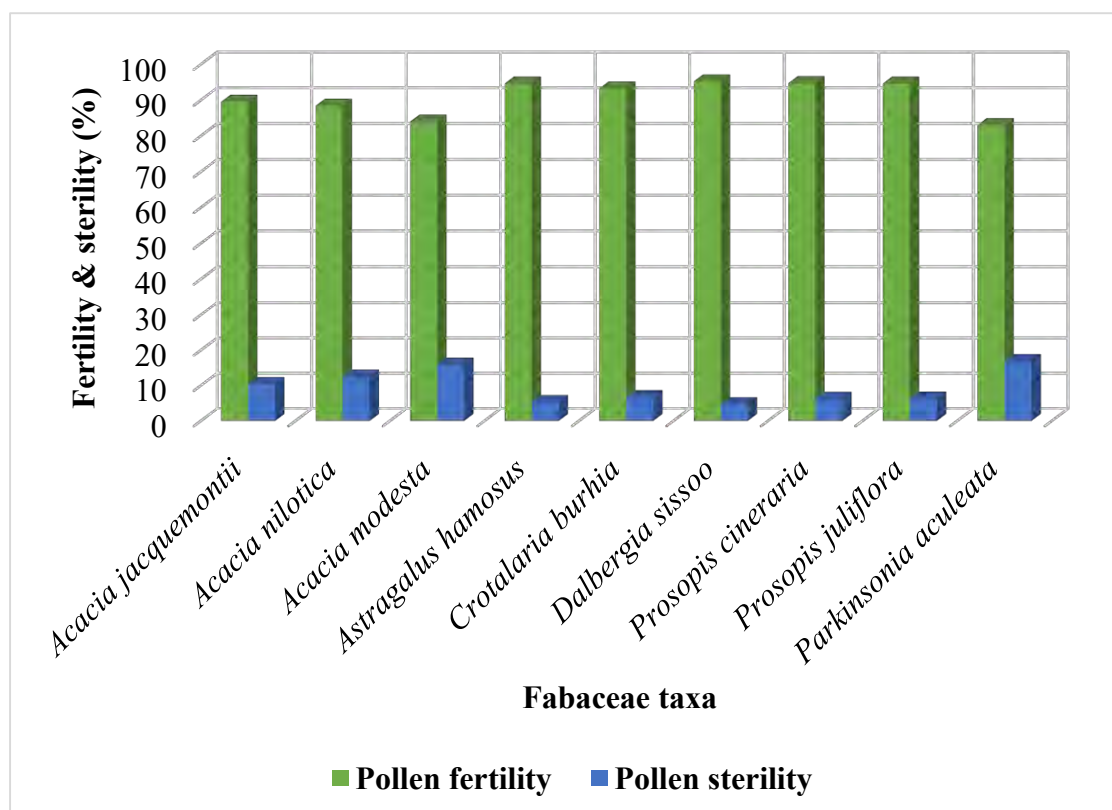


**Figure 24.** Pollen fertility and sterility percentage count among Fabaceous taxa.

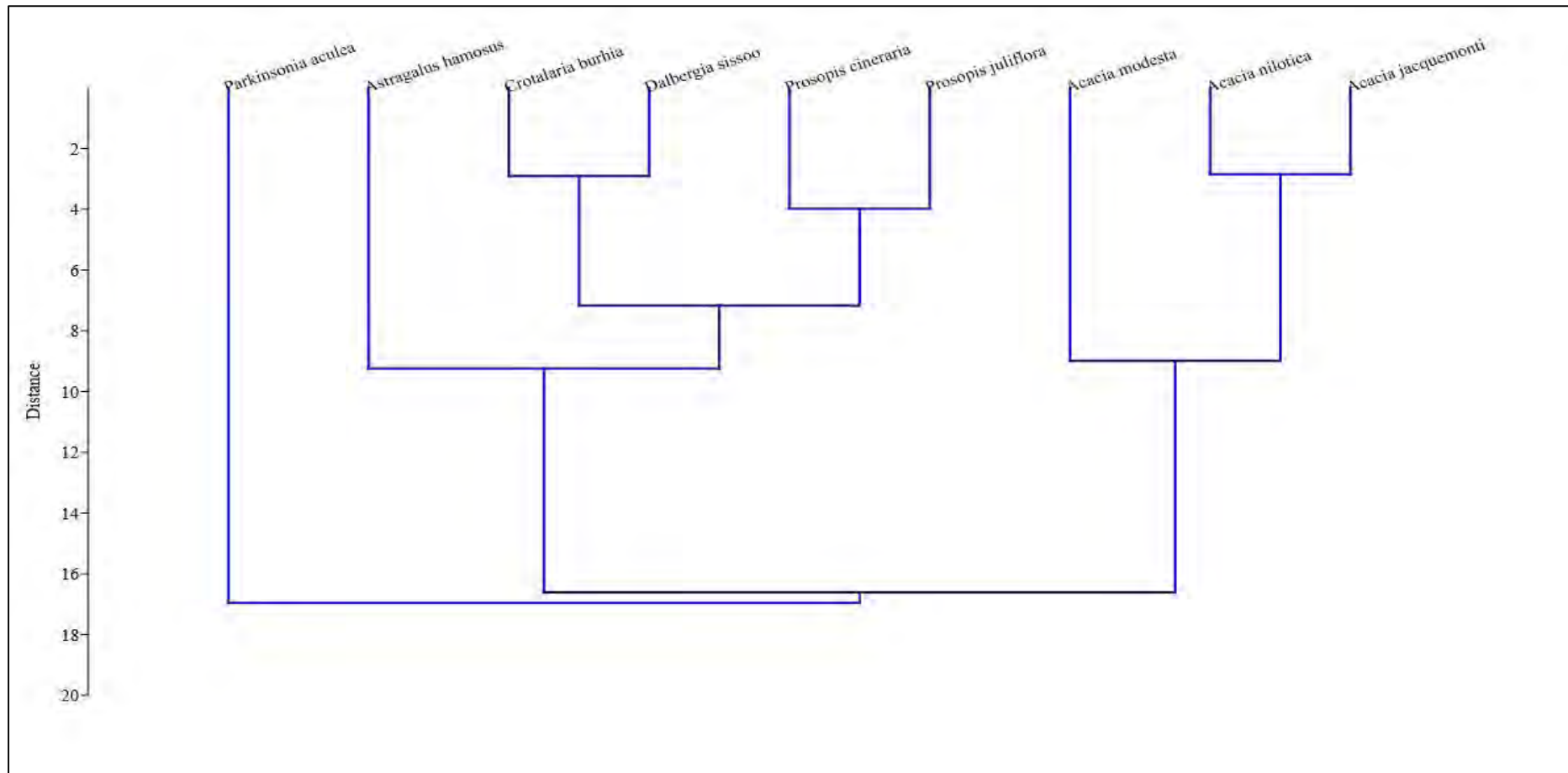


**Figure 25.** UPGMA tree of Fabaceous taxa based on pollen quantitative characters.

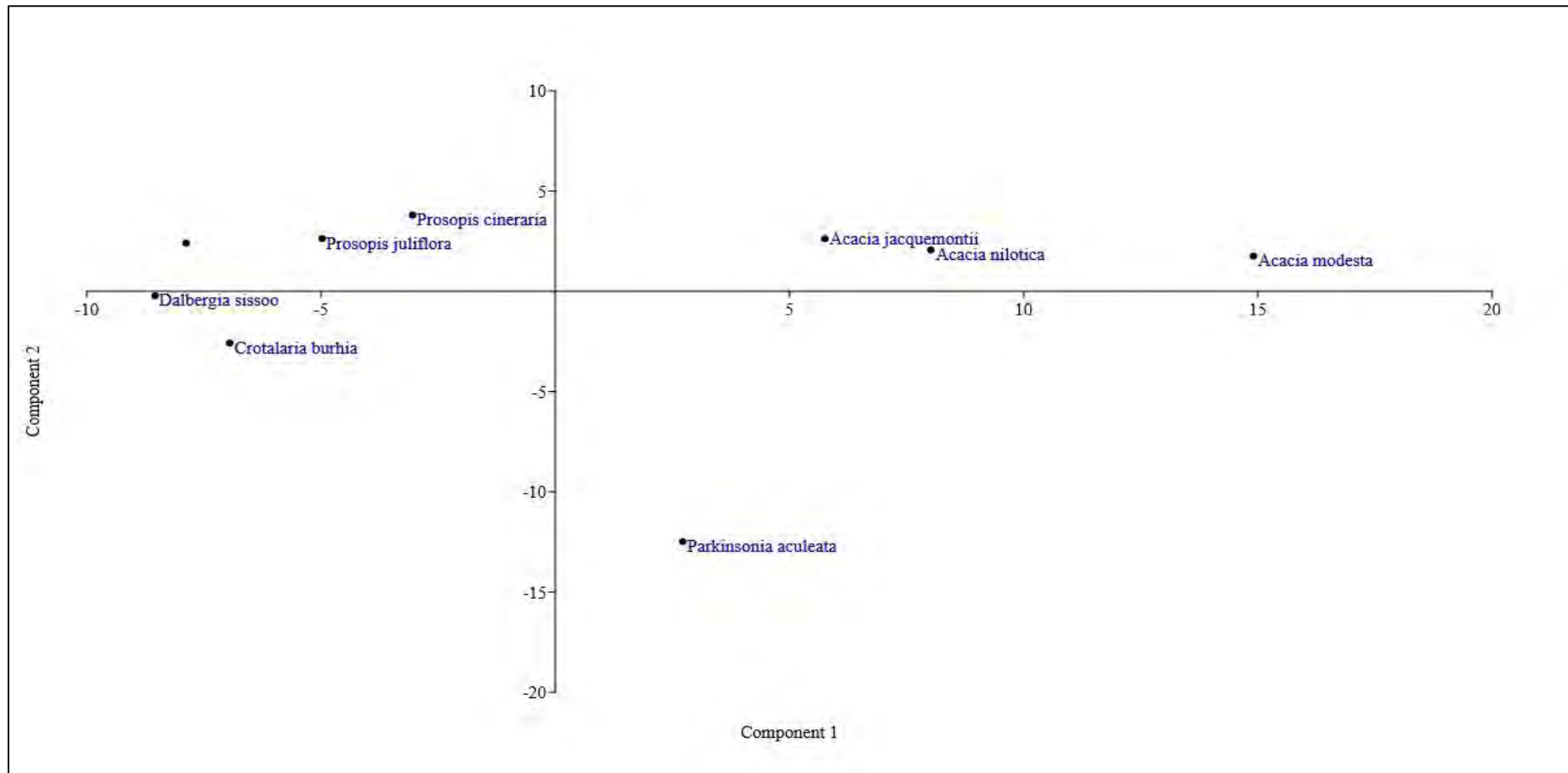


**Figure 26.** Principal component analysis (PCA) case scores of the palynological characters based on Fabaceous pollen traits.

### 3.2.9 Discussion

The findings demonstrate the pollen of nine desert-inhabited Fabaceous taxa. The pollen grains show little variations among the quantitative features. Pollen features were also described such as size, shape, symmetry and polarity, aperture condition, surface sculpturing, and peculiarities based on scanning microscopy. There are many disciplines related to systematic which are used by taxonomists as an aid to improve the identification, taxonomic position of various taxa (Erdtman, 1972). Like other disciplines one of the most valuable tool used by taxonomists is palynology. Application of palyno-morphology is very extensive and multidisciplinary as palynology is valuable in supporting taxonomic suggestions (Mallick, 2017).

The major features in Fabaceous taxa are pollen aperture shape, tectum pattern, and exine stratification. The palynological study may aid in solving taxonomic issues, the correct identification of species, and the identification of species at various taxonomic levels. Ultrastructural differences within Fabaceous species have been studied frequently across various geographical regions throughout the world (Bahadur et al., 2022; Khan et al., 2022; Rashid et al., 2022). The most frequent type of variation within the eudicots has been described as variations in the number and arrangement of apertures. There are two types of apertures: simple apertures with a single colpus or pore; and compound apertures with an ectocolpus and an endocolpus that cause the pollen to be colporate (Zhao et al., 2016). Trends in Fabaceous pollen are correlated with specialization in morphological traits. The most common type is tricolporate with a small lalongate endexine. Colpi covered with coarsely granulate operculum. Most common type of sculpturing is fine to coarse reticulate (Song, 2007).

The present research shows the polyad pollen of sub-spheroidal shapes and exine sculpture were found in *Acacia nilotica*, however the investigation for the same species by Khan et al., (2019) shows dissimilarities to our observations in pollen shape and ornamentation. The previous research findings of Begum et al., (2016) noticed 16-celled polyads oblate-spheroidal and psilate grains in *Acacia nilotica* that shows dissimilarity to the current study. According to Khan et al., (2021) member of Mimosaceae, *Acacia modesta* and *Acacia nilotica* polyad type of pollen were observed composed of 16 cells forming a polyad complex. Polyads were aggregate of eight units, eight grains centrally arranged in to two layers of four each and surrounded by eight

grains in periphery with psilate surface and rounded shapes which shows correlation with the present study. *Acacia modesta* was analyzed with regulate to fossulate ornamentation accordance with the findings of Khan et al., (2021). Attique et al., (2022) interpreted pollen of *Acacia modesta* having a polar diameter of 38.6  $\mu\text{m}$  possessing no pores and colpi. Our study measured the pollen of *Acacia modesta* as polyads, medium sized, heteropolar, polar diameter 39.5  $\mu\text{m}$  and exine thickness 9.7  $\mu\text{m}$ . Morphopalynological studies among *Crotalaria species* from India revealed reticulate and circular pollen type in *Crotalaria burhia* while we observed reticulate-scabrtae type sculptural features found dissimilar with the Gupta and Gupta (1979). Parveen and Qaiser (1997) elaborate on coarsely reticulated tectum in *Crotalaria medicaginea* somehow consistent with our study.

*Dalbergia sissoo* pollen morphotypes as triangular, small grains, tricolporate, isopolar, radially symmetric, and psilate tectum were visualized that were slightly dissimilar to Jamwal (2021). Raj and Reddy (2019) also analyzed the *Dalbergia sissoo* grains as euprolate, trizonoporate and psilate was accordance with our findings. *Prosopis juliflora* shows the tricolporate type, triangular and prolate to sub-prolate grains which show similarity to some extent with the previous findings of Rajurkur et al., (2013) having triangular and sub-oblate shape. Our demonstration stated that the pollen of *Prosopis cineraria* is sub-oblate, triangular with scabrate foveolate sculpture which was found different from the previous work of (Khan et al., 2021) in which psilate to scabrate peculiarities were examined. Ullah et al., (2022) described recently in *Parkinsonia aculeata* psilate, tectate, medium-sized and reticulate sculptured grains for their correct identification which confirms the current findings.

Whereas Maw et al., (2020) also elaborate reticulate ornamented lumina with heterobrochated features similar to our work. *Astragalus* identification at species level is exceedingly challenging due to its greater diversity and polymorphic nature. Previous literatures attempted to provide vital and useful palyno-morphological information on the taxa but remains poorly understood. Pollen in both species namely, *Astragalus hamosus* and *Astragalus glycyphyllos* were tricolporate having reticulate sculpturing (Dane et al., 2007). Our results were previously corroborated by reports of three types of exine peculiarities among tribe Astragaleae: reticulate, reticulate to perforate, and perforate (Rashid et al., 2022).



### 3.2.10 Micromorphological Details of Solanaceous Pollen

The palynological descriptions of Solanaceous grains are arranged according to the following pollen features: (a) dispersal unit and polarity and shape, (b) polar area, (c) size and polar area index (d) types of apertures and mesocolpium, and (f) sculpturing elements of exine wall. Images of pollen characteristics are presented in Plates 46 & 47, and described in Tables 12 & 13.

#### a) Polarity, Dispersal Unit, and Shape

Based on this selection of attributes, it was concluded that in the eight Solanaceous examined pollen grains were predominate with monads type unit. All of the species examined had iso-polar and radially symmetrical pollen grains. They are circular to semi-circular and triangular in polar view. Prolate spheroidal grains were observed in most species (four); oblate spheroidal grains were observed in *P. divaricate* and *P. minima*. Whereas sub-oblate pollen was examined in *S. surratense* and sub-prolate in *W. somnifera*. *D. stramonium* exhibited higher mean values, (39.4  $\mu\text{m}$ ) and 37.6  $\mu\text{m}$ ), for the polar axis and equatorial diameters. While lowest polar diameter and equatorial distance were measured for *S. surratense* (17.3  $\mu\text{m}$ ) and *W. somnifera* (19.6  $\mu\text{m}$ ) respectively (Figure 27). PD/ED values range between (0.81) for *S. surratense* and (1.18) for *W. somnifera* (Figure 28).

#### b) Polar Area

A polar area is a region at and around the pole of pollen grains. This polar area is called the apocolpium if the zonally arranged apertures are colpi, and apoporium if the zonally arranged apertures are pori. The denomination of the polar area with small size (*D. innoxia*, *D. stramonium*, *P. minima*, *S. surratense* and *W. coagulans*) to very small size in *P. divaricate*, *S. incanum* and *W. somnifera*.

#### c) Size and Polar Area Index (PAI)

According to Erdtman's (1952) pollen size classification, Small size; pollen diameter 17.3–24.8  $\mu\text{m}$  in *P. minima*, *S. incanum*, and *S. surratense*. *D. innoxia*, *D. stramonium* and *P. divaricate* showed the medium pollen grains (26.6–39.4  $\mu\text{m}$ ) while the small to medium was found in *W. coagulans* and *W. somnifera* (PD 19.6–26.35  $\mu\text{m}$ ).

Pollen grains were also classified in relation to the polar area index (PAI) which is given by the relationship between the ends of two adjacent apertures (or their margins) and the largest width of the pollen grain in the polar view. The highest polar area index was measured for *S. incanum* (0.38) and lowest for *D. innoxia* (0.21) as illustrated in Figure 32.

#### d) Apertures and Mesocolpium

Pollen grains 3-colporate; some specimens in *Solanum* showed 3-zonocolporate pollen grains but most were colporate. The colpus size was noted as a minimum ( $7.5 \times 4.9 \mu\text{m}$ ) for *W. somnifera* to a maximum ( $14.7 \times 11.3 \mu\text{m}$ ) for *P. minima* (Figure 29). The length, width and sunken and bulged degree of the colpus and the surface of the colpus membrane are different among Solanaceous species. Colpus short, very narrow, sunken was found in *D. innoxia* and *D. stramonium*; colpi long, narrow, sunken with tapering ends were visualized in *P. divaricate*, *S. incanum* and *W. coagulans*. colp orientation long, narrow, bulged in *P. minima*, *S. surratense* and *W. somnifera*. Colpi membranes are scabrate gemmate, scabrate regulate, verrucate, psilate to granulate, granulate-scabrate and tuberculate.

Mesocolpium is the distance measured between two apertures and the diagnostic traits to identify species. The highest mesocolpium distance was recorded for *D. stramonium* ( $9.23 \pm 1.21 \mu\text{m}$ ) and minimal for *P. minima* ( $5.9 \pm 0.87 \mu\text{m}$ ) as mentioned in Figure 31.

#### e) Sculpturing Elements

The exine ranged in thickness from 0.92–2.91  $\mu\text{m}$ . The maximum thickness of exine was measured for *D. innoxia* (2.91  $\mu\text{m}$ ) and the minimum for *S. incanum* (0.92  $\mu\text{m}$ ) as shown in Figure 30. Variations were observed in the main ornamentation types: Striate-psilate with longitudinal orientated (*D. innoxia*); reticulate with psilate muri (*D. stramonium*), granulate punctate in *P. divaricata*, granulate in *P. minima*, Homobrochate granulate type in *S. incanum*, scabrate psilate sculptured elements in *S. surratense*. *W. coagulans* and *W. somnifera* both has rugulate-striate ornamentation.

### 3.2.11 Taxonomic Keys Based Pollen Features of Solanaceous Species

1 + Trizonocolporate, homobrochate granulate-scabrate.....	<i>S. incanum</i>
- Tricolporate pollen.....	2
2 + Tricolporate, striate psilate exine, scabrate gemmate colpus.....	<i>D. innoxia</i>
- Scabrate regulate colpus membrane.....	3
3 + Reticulate psilate muri, narrow sunken colpi.....	<i>D. stramonium</i>
- Granulate scabrate colpus.....	4
4 + Scabrate psilate exine, long bulged colpus.....	<i>S. surratense</i>
- Psilate to granulate colpus surface.....	5
5 + Granulate tectum, bulged colpi.....	<i>P. minima</i>
- Verrucate colpus stratification.....	6
6 + Granulate punctate, narrow bulged colpi.....	<i>P. divaricata</i>
- Verrucate membrane, long bulged colpi.....	7
7 + Regulate-striate ornamentation.....	<i>W. somnifera</i>
- Tuberculate colpus membrane.....	8
8 + Regulate-striate exine, very small polar area.....	<i>W. coagulans</i>

**Table 12.** Micromorphological characters of Solanaceous pollen.

<b>Sr. No.</b>	<b>Solanaceous taxa</b>	<b>Size</b>	<b>Shape</b>	<b>Polar view</b>	<b>Aperture</b>	<b>Colpus</b>	<b>Colpus membrane</b>	<b>Polar area</b>	<b>Exine ornamentation</b>
1.	<i>Datura innoxia</i> Mill.	Medium	Prolate-spheroidal	Circular	Tricolporate	Colpus short, very narrow, sunken	Scabrate to gemmate	Small	Striate-psilate, longitudinal orientated
2.	<i>Datura stramonium</i> L.	Medium	Prolate-spheroidal	Circular	Tricolporate	Colpus short, very narrow, sunken	Scabrate regulate	Small	Reticulate; muri psilate
3.	<i>Physalis divaricata</i> D.Don	Medium	Oblate-spheroidal	Semi-Circular	Tricolporate	Colpus long, narrow, sunken	Verrucate	Very small	Granulate punctate
4.	<i>Physalis minima</i> L.	Small	Oblate-spheroidal	Triangular	Tricolporate	Colpus long, narrow, bulged	Psilate to granulate	Small	Granulate
5.	<i>Solanum incanum</i> L.	Small	Prolate-spheroidal	Circular	Trizonocolporate	Colpus long, narrow, sunken	Almost Psilate	Very small	Homobrochate Granulate scabrate
6.	<i>Solanum surattense</i> Burm. f.	Small	Sub-oblate	Circular	Tricolporate	Colpus long, narrow, bulged	Granulate scabrate	Small	Scabrate to psilate
7.	<i>Withania coagulans</i> (Stocks) Dunal	Small to medium	Prolate-spheroidal	Semi-triangular	Tricolporate	Colpus long, narrow, sunken	Tuberculate	Small	Rugulate-striate
8.	<i>Withania somnifera</i> (L.) Dunal	Small to medium	Sub-prolate	Triangular	Tricolporate	Colpus long, narrow, bulged	Verrucate	Very small	Rugulate-striate

**Table 13.** Measurements of the pollen diameter, colpus, exine layer, mesocolpium and polar area index (PAI), of pollen grains of Solanaceae (n=15).

Sr. No.	Solanaceous taxa	Pollen diameter		Colpus		P/E	ET (x ± SE μm)	MC (x ± SE μm)	PAI
		PDV (x ± SE μm)	EDV (x ± SE μm)	LOC (x ± SE μm)	WOC (x ± SE μm)				
1.	<i>Datura innoxia</i> Mill	35.5±0.61	34.7±0.32	8.3±0.14	6.7±0.17	1.02	2.91±0.93	7.16±1.4	0.21
2.	<i>Datura stramonium</i> L.	39.4±1.08	37.6±0.77	12.6±1.1	9.5±0.26	1.04	2.12±0.11	9.23±1.21	0.31
3.	<i>Physalis divaricata</i> D.Don	26.6±0.17	27.4±0.11	9.9±0.76	7.9±0.2	0.97	1.45±0.2	6.4±1.05	0.37
4.	<i>Physalis minima</i> L.	22.6±0.34	23.8±0.29	14.7±0.13	11.3±0.19	0.94	1.21±0.49	5.9±0.87	0.33
5.	<i>Solanum incanum</i> L.	24.8±0.8	22.9±0.94	10.4±0.23	8.8±0.26	1.08	0.92±0.27	6.8±0.96	0.38
6.	<i>Solanum surattense</i> Burm. f.	17.3±0.51	21.14±0.15	9.5±0.43	6.2±0.79	0.81	1.34±0.21	7.5±1.13	0.26
7.	<i>Withania coagulans</i> (Stocks) Dunal	26.35±0.12	24.7±1.03	8.9±0.19	5.62±0.47	1.06	1.84±0.07	8.3±1.41	0.23
8.	<i>Withania somnifera</i> (L.) Dunal	23.2±0.24	19.6±0.69	7.5±0.08	4.9±0.12	1.18	1.62±0.13	7.85±1.29	0.29

**Keywords:** PDV = Polar diameter view; EDV = Equatorial diameter view; LOC= Length of colpi; WOC = Width of colpi; ET = Exine thickness; MC = Mesocolpium; PAI = Polar Area Index; P = Polar; E = Equatorial; x = Mean; SE = Standard Error; μm = micrometer

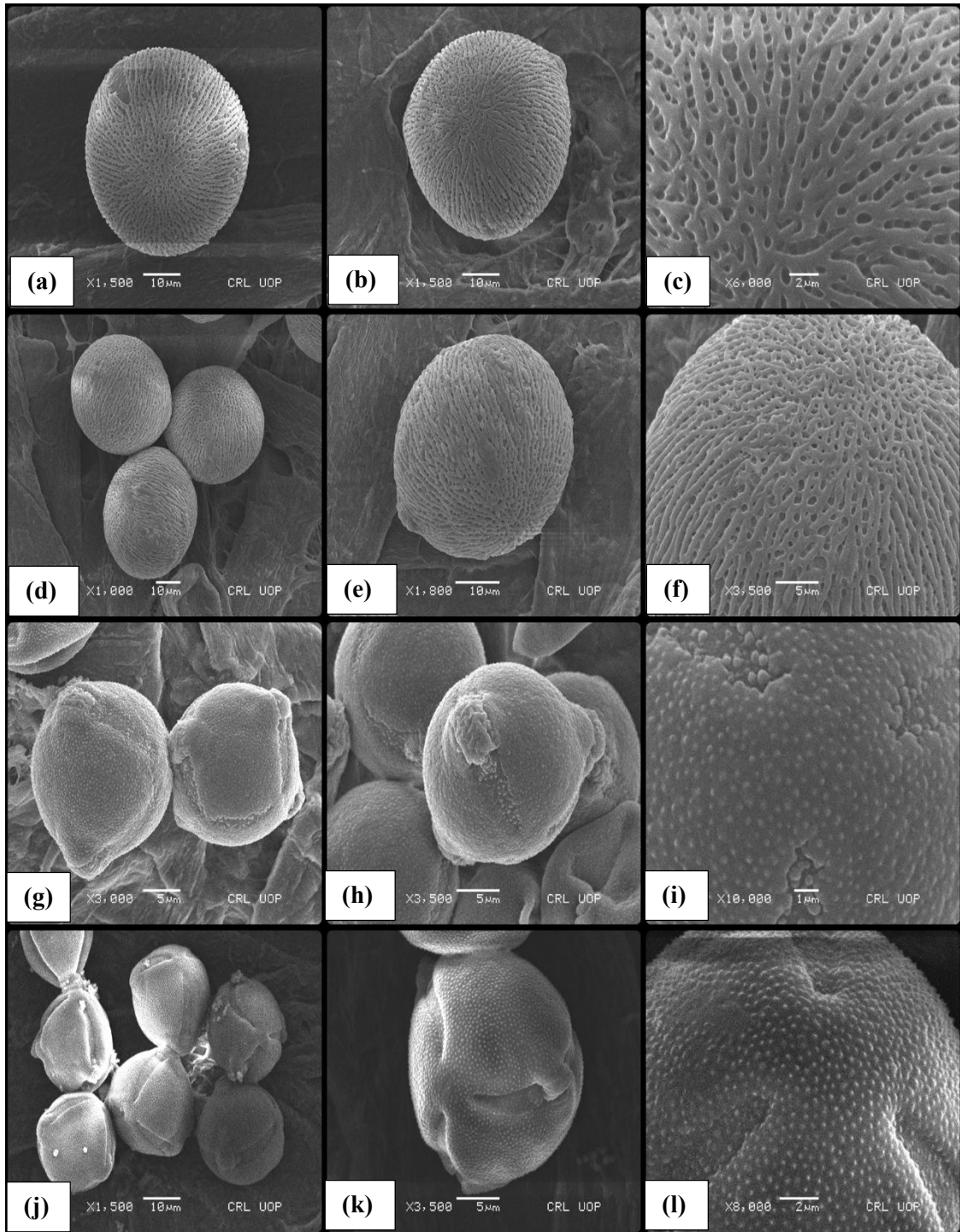


**Plate 46.** Scanning electron microphotographs of pollen and exine ornamentation types of Solanaceous grains. (a-c) *Datura innoxia*; striate psilate exine (scale bar = 10  $\mu\text{m}$ , 2  $\mu\text{m}$ ), (d-f) *Datura stramonium*; muri reticulate (scale bar = 10  $\mu\text{m}$ , 5  $\mu\text{m}$ ), (g-i) *Physalis divaricata*; verrucate colpus membrane (scale bar = 5  $\mu\text{m}$ , 1  $\mu\text{m}$ ), (j-l) *Physalis minima*; granulate sculptured (scale bar = 5  $\mu\text{m}$ , 2  $\mu\text{m}$ )

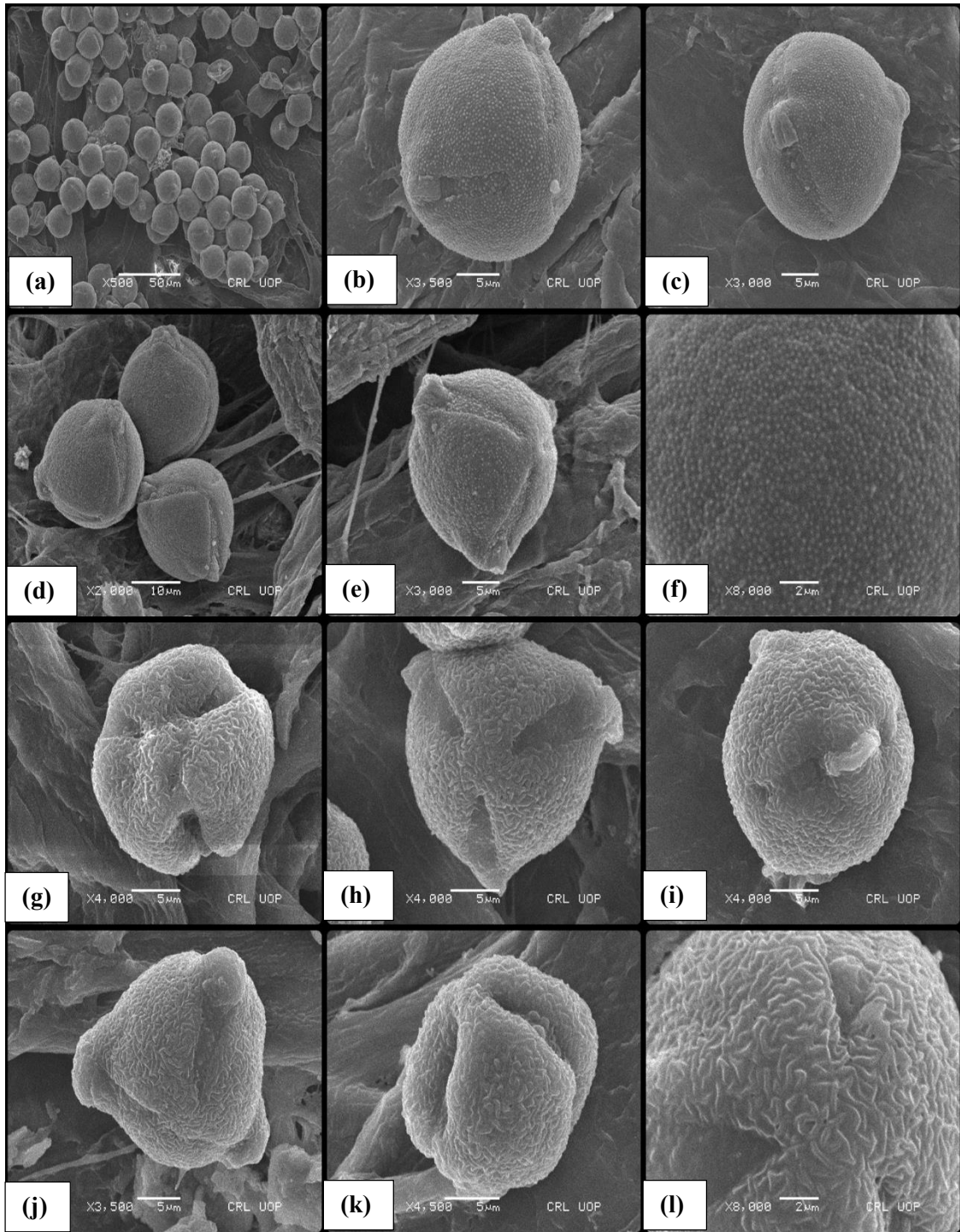


**Plate 47.** Scanning electron microphotographs of pollen and exine ornamentation types of Solanaceous grains. (a-c) *Solanum incanum*; homobrochate exine (scale bar = 10  $\mu\text{m}$ , 2  $\mu\text{m}$ ), (d-f) *Solanum surattense*; granulate scabrate (scale bar = 10  $\mu\text{m}$ , 5  $\mu\text{m}$ , 2  $\mu\text{m}$ ), (g-i) *Withania coagulans*; regulate striate exine (scale bar = 5  $\mu\text{m}$ ), (j-l) *Withania somnifera*; verrucate sculptured colpi (scale bar = 5  $\mu\text{m}$ , 2  $\mu\text{m}$ )

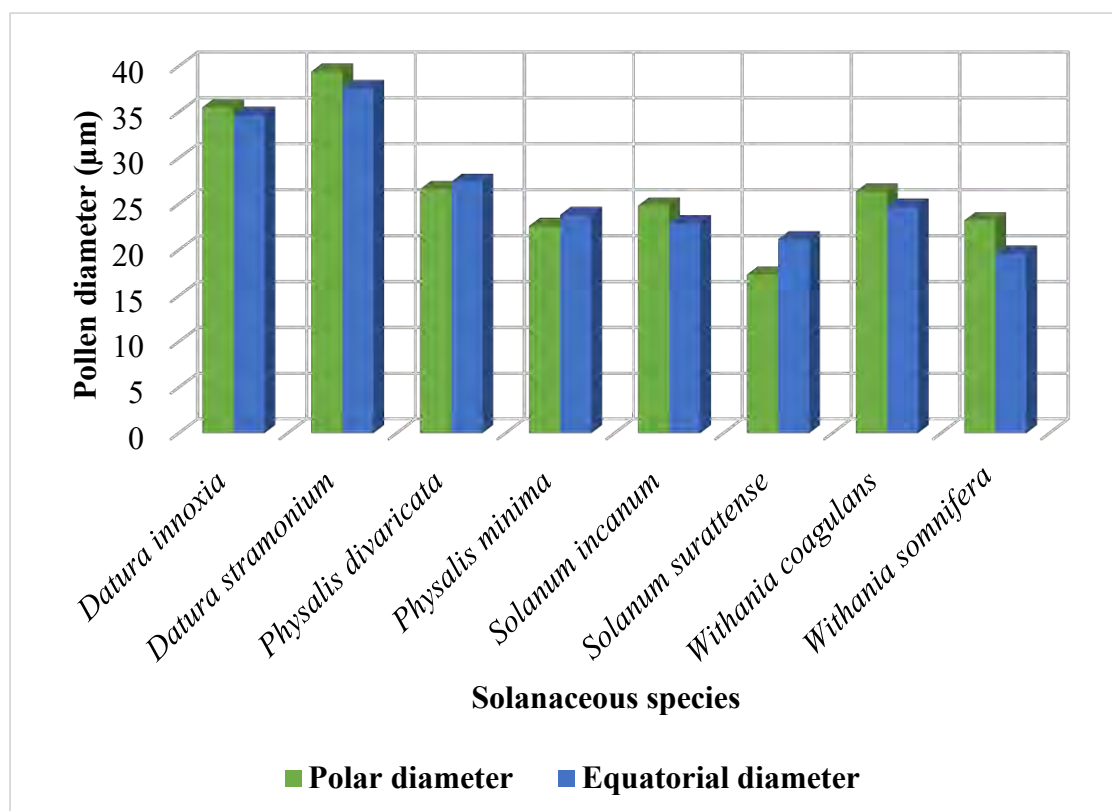


**Figure 27.** Average pollen size variations among Solanaceous taxa.

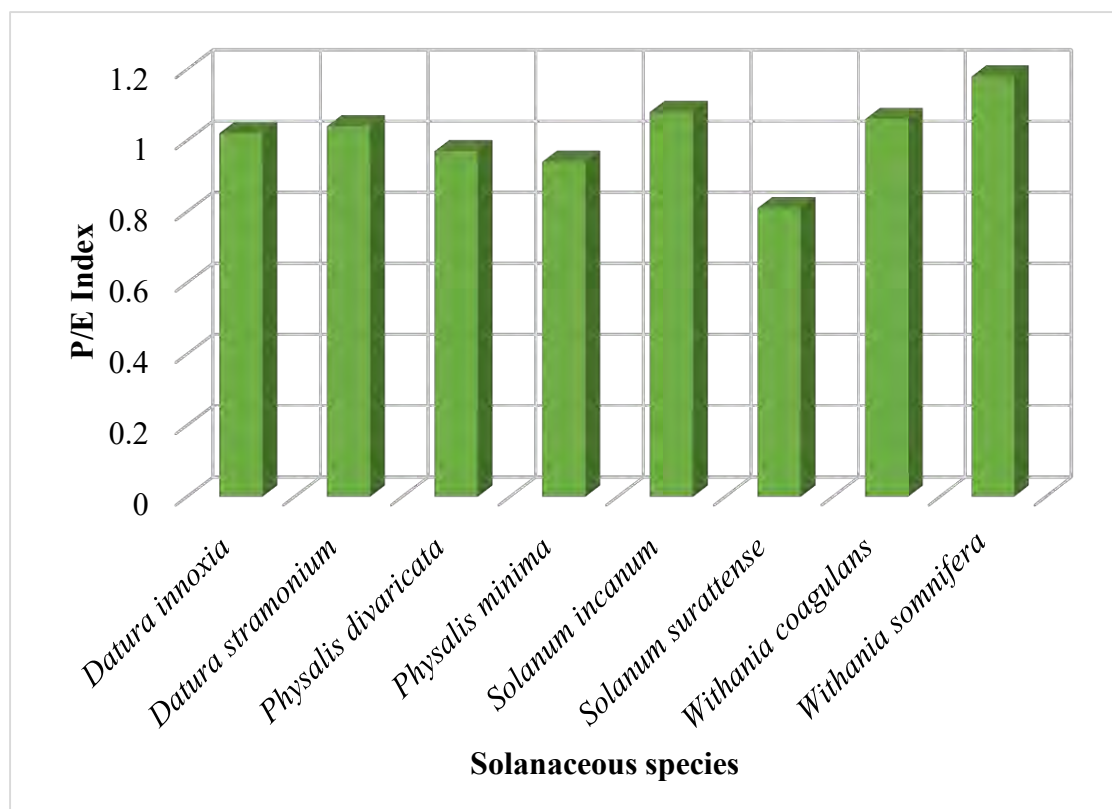


**Figure 28.** Polar to equatorial diameter index ratio (P/E) among Solanaceous taxa.



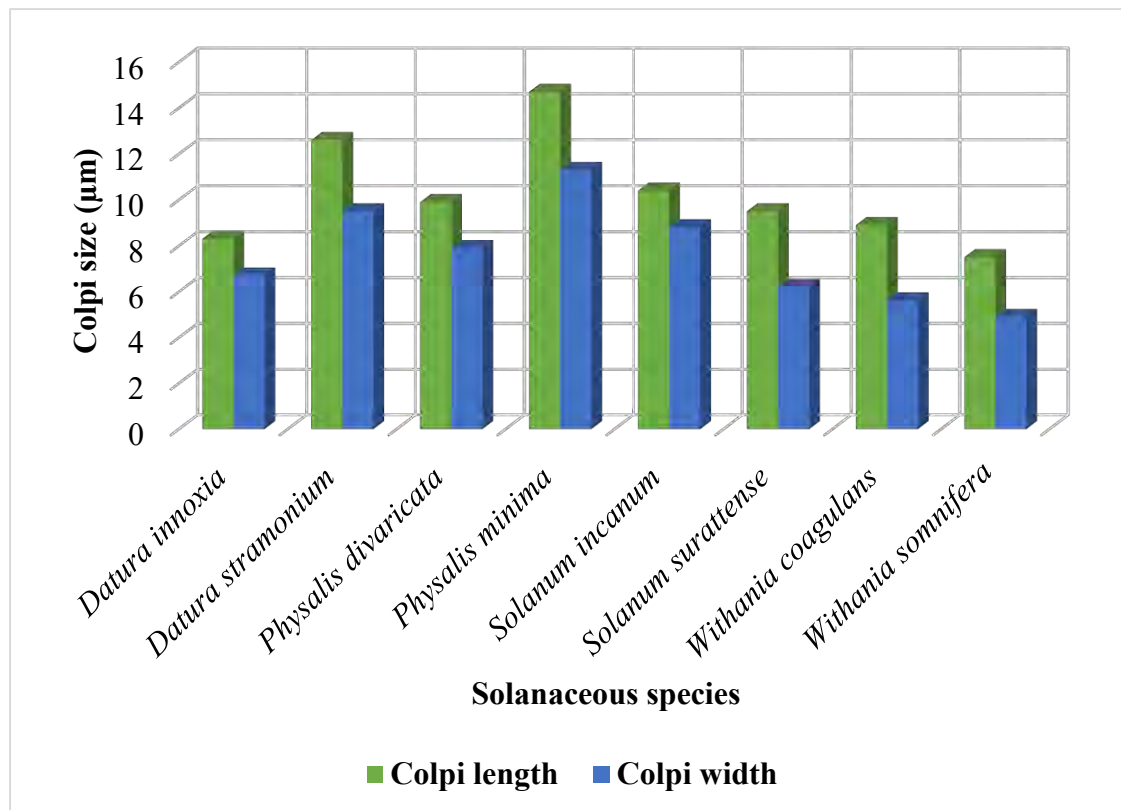


**Figure 29.** Mean colpi length and width variations among Solanaceous taxa.

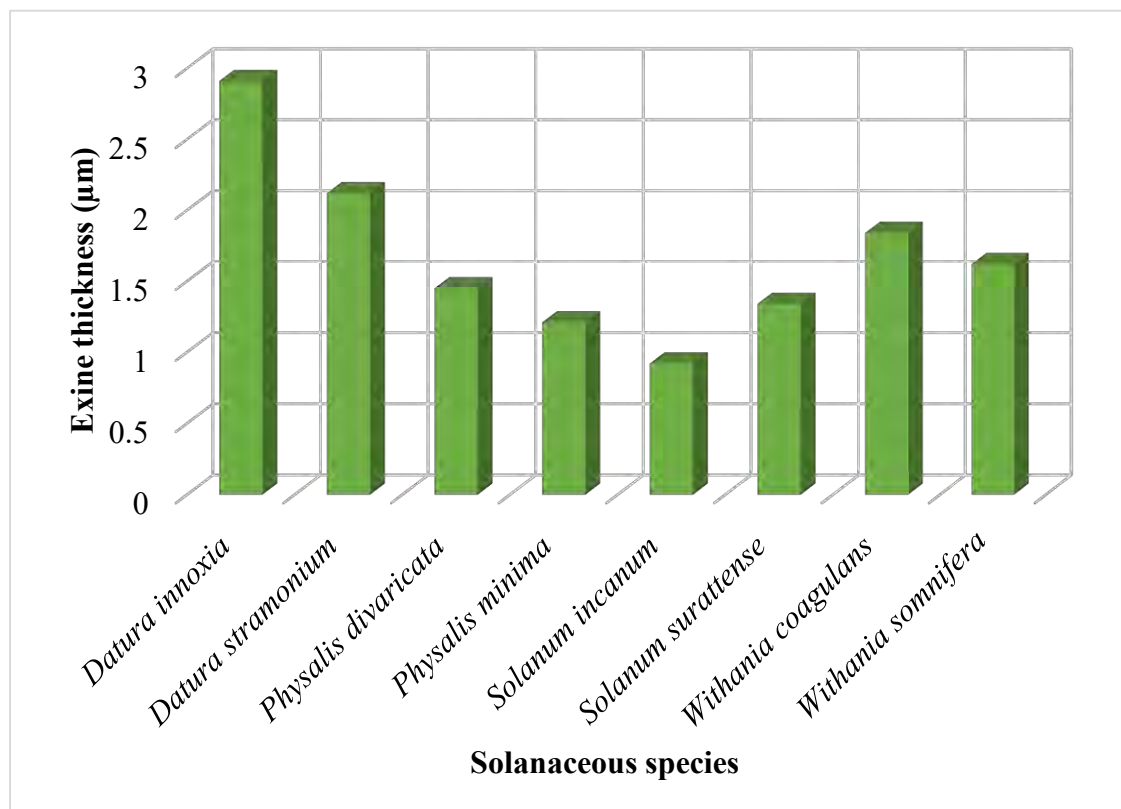


**Figure 30.** Average exine thickness measurements among Solanaceous taxa.

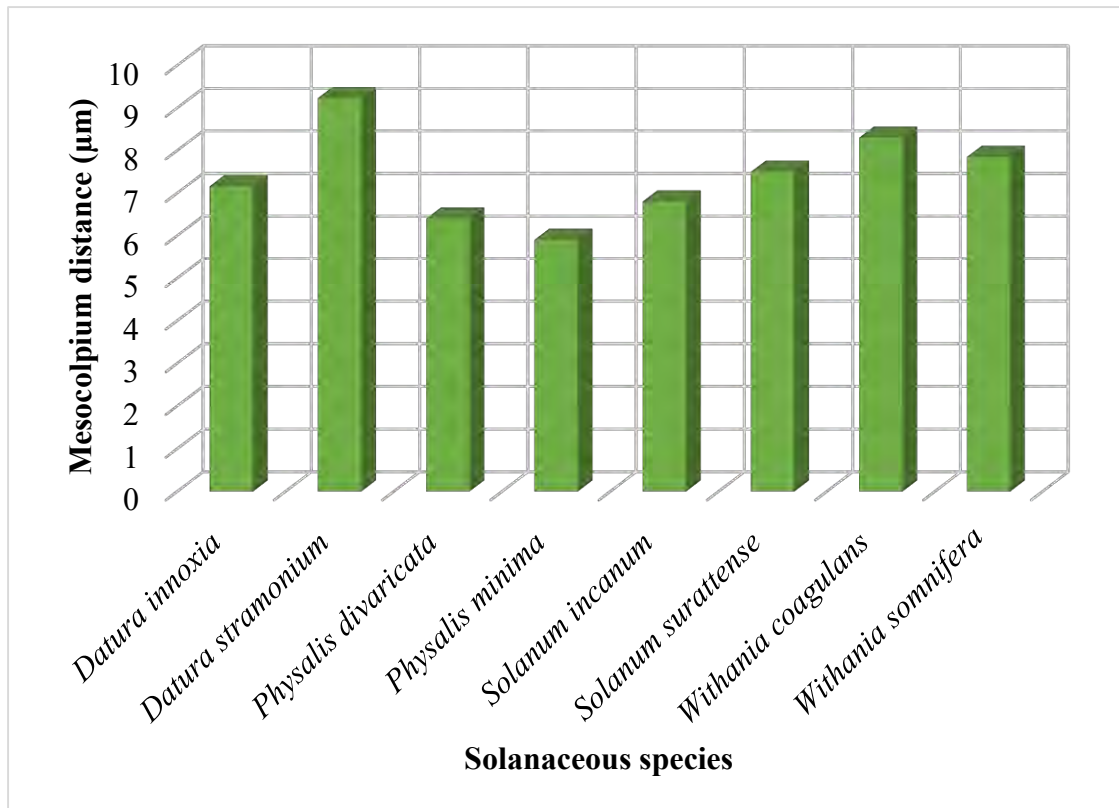


**Figure 31.** Mesocolpium distance mean variations among Solanaceous taxa.

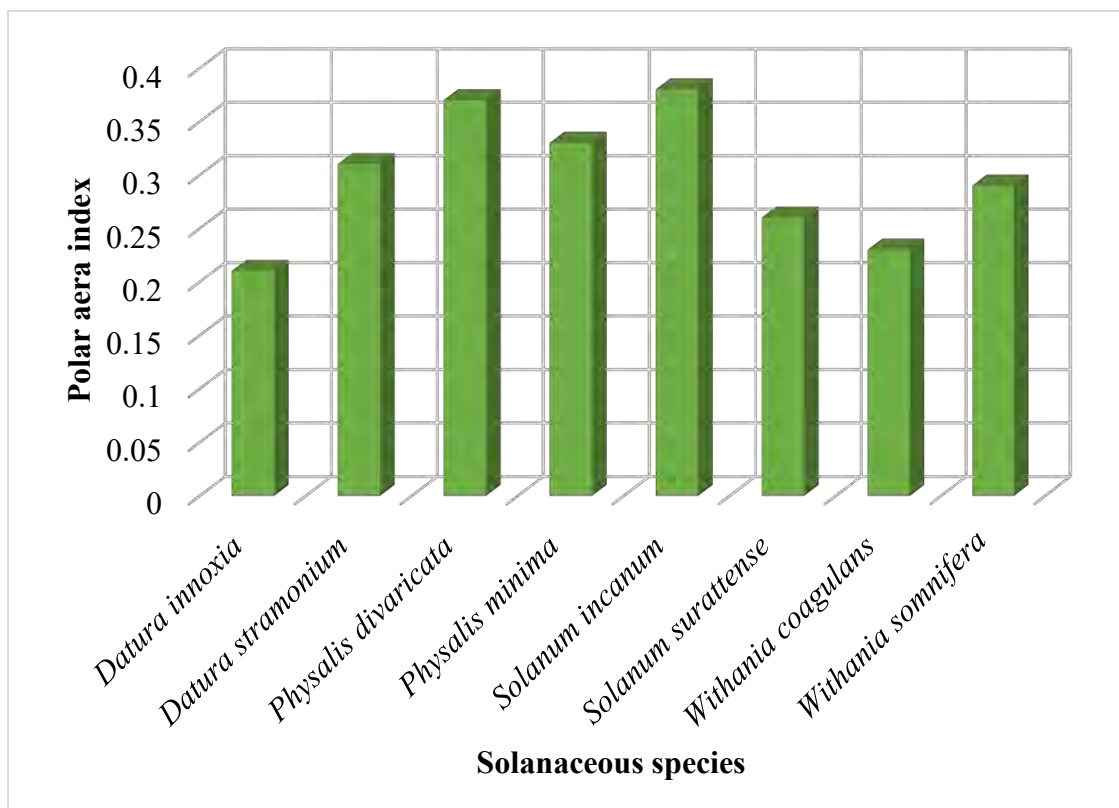


**Figure 32.** Average variations among polar area index in Solanaceous taxa.

### 3.2.12 Discussion

Wang and Wang (1983) argued that the pollen size of angiosperms is mostly small to medium. Pollen grains of Solanaceae basically comply with the general rules of angiosperm pollen in terms of size. However, Torres (2000) argued that pollen size cannot be inherited stably due to the impacts of multiple factors of physiology, morphology, and ecology, and lacks taxonomic significance. In this study, we found that *D. stramonium* is separated from the other species by a longer polar axis and *S. surratense* is separated from other species by a shorter polar axis. The other species cannot be separated by pollen size because of the overlapping ranges of polar and equatorial axis lengths. Our point of view is in line with that of Al-Quran (2004). Our results indicate that the pollen grains of Solanaceae are mainly prolate-spheroidal, rarely oblate-spheroidal, sub-oblate, and sub-prolate, which is in agreement with the results of previous studies. However, tricolporate pollen with scabrate tectum is more commonly found within the family (Perveen and Qaiser, 2007).

Ashfaq et al., (2020) indicate that striate-reticulate exine, colpus surface was scabrate to gemmate and sub-spheroidal shape was observed in *D. innoxia*. While our observation are quite similar in respect to colpus surface while exine surface was found with striate psilate type peculiarities. In another study, Song et al., (2019) found that exine ornamentation of pollen grains of *D. innoxia* is striate with psilate lirae which is in agreement with the previous work. *D. innoxia* pollen with more than one colpate; exine with lamellate thickening was discussed (Krishan and Gopi, 2018).

In our study reticulate with psilate muri pattern surface stratification and scabrate regulate colpus membrane was examined whereas El-Ghamery et al., (2018) explained irregular striate type sculpture pattern while Hassan and Amer (2019) elaborate regulate-reticulate exine in *D. stramonium*. Perveen and Qaiser (2007) provided detailed features such as tectum striate at mesocolpium with perforations, ornamentation coarsely reticulate-rugulate were inconsistent with our study. Kayani et al., (2019) reported the scabrate exine tectum for the same species, which is dissimilar to the present findings. Colpi were reported wider at the equator and gradually narrowing and deeply sunken towards the poles in *D. stramonium* form while exine sculpturing was semi-tectate, columellate with irregular rugulate-reticulate (Hassan and Amer, 2019).

Bhat et al., (2019) examined *Physalis* species grains were eurypalynous, trizonocolporate, and micro-echinate. Perveen and Qaiser (2007) described *Physalis divaricata* type pollen class elaborate ectoaperturate colpus, not sunken with long margin and tectum was verrucate. In our case granulate punctate type sculpturing was examined in *P. divaricata*. According to Prabhakar and Ramakrishna (2014) *P. minima* grains were prolate-spheroidal, triangular, trizonocolporate, colpi narrowly elliptic and exine sculptured psilate and micro-echinate (Ashfaq et al., 2020; Azeez et al., 2019). While our observation of stratification revealed granulate stratification of exine somewhat dissimilar to previous studies. Awachat (2015) analyzed *P. minima* grains as sub-prolate, colporate, psilate ornamented with thicker nexine, although granulate tectum was observed in our study.

Finot et al., (2018) explained that *Solanum* species showed scabrate sculpture under SEM while they appeared psilate under LM. Sculpture pattern of *Solanum* has been described as reticulate seen with LM and as granulate, granular and scabrate observed with SEM (Hayrapetyan 2008). Kumar et al., (2015) found a greater diversity of exine sculpture in *Solanum*, including spinulose, granulose, striate echinate, echinate, and micro-echinate. Al-Wadi and Lashin (2007) documented three different species of *Solanum* from the present study and reported pollen grains are tricolporate, zonoaperturates, generally radially symmetrical, prolate, isopolar, and with non-perforate tectum. Franklim and Esteves (2008) reported palynology of some other taxa of *Solanum* from the resting as of Rio de Janeiro State, Brazil and the result showed that the pollen grains are isopolar, sub-prolate to oblate spheroidal, tricolporate with granulate, regulate-granulate or scabrate sexine and pollen of these taxa are rather heterogeneous in shape.

Our results showed that *S. incanum* has the prolate-spheroidal, trizonocolporate with homobrochate granulate scabrate sculpture features whereas Ibrahim et al., (2021) also mentioned the same characteristics for *S. incanum*. Our findings also indicate that *S. incanum* has the smallest grains size is consistent with the findings of Mohsen and Badr (2019). Similarly, Ashfaq et al. (2020) also characterized scabrate to psilate ornamentation in *S. surattense* is accordance with our study. Perveen and Qaiser (2007) observed scabrate type tectum and sub-psilate end acute ectoaperture in *S. surattense*. Chaturvedi et al., (1999) observed palynomorphs of *S. surattense* variants explained grains are tri-zonocolporate, spheroidal and the exine peculiarities are finely granulose.

However, our elaboration revealed sub-oblate, tricolporate, and scabrate psilate sculptured grains for *S. surratense*. Our results suggest that the colpus of *Solanum* has bulged, long, short, narrow, and sunken, and that the surface of the colpus is scabrate, gemmate, verrucate, granulate, and tuberculate, consistent with the results of Du et al., (2017). Overall, we argued that the *Solanum* species studied demonstrated sufficient pollinic heterogeneity in their shapes, aperture feature, and exine ornamentation to enable their micromorphological pollen characterization.

Rodrigues et al., (2016) studied pollen morphology in (Withaniinae, Solanaceae), the analysis showed that the grains are very similar, differing in size-related characters and also reported monad pollen with varying morphology, small to medium-sized, lalongate apertures, and long colpi. The present study revealed semi triangular, tricolporate, tuberculate colpus membrane and regulate striate exine in *W. coagulans*. However earlier findings of Kayani et al., (2019) described sub-triangular, tricolporate, colpi tectate finely granulate, and finely granulate exine sculptural features which differ from the present finding. Song et al., (2019) also reported *W. somnifera* morphology of grains from China, and results suggested that the exine ornamentation of pollen grains could be rugulate-perforate while our case study examined regulated striate exine and verrucate sculptured colpus surface. Alwadie (2002) from Saudi Arabia performed scanning microscopic pollen observation of *W. somnifera* and showed that surface sculpturing is scabrate-granulate which contradicts our observation.

### 3.2.13 Pollen Micromorphology of Boraginaceous Species

#### a) *Arnebia hispidissima* (Lehm.) A. DC.

Pollen monad, iso polar, small-sized and stephanocolporate. Polygonal polar view and equatorial view sub-oblate. Aperture ornamented membrane and colporate. Exine sculpturing micro-echinate. Polar diameter (10.75-18.2)14.6±1.22 µm and equatorial view distance (11.15- 23)18.1±1.04 µm. P/E ratio 0.8. Polar area index (0.39). Colpi length (10.50-15.4)13.3±0.76 µm and colpi width (4.5-9.2)6.95±0.27 µm. Exine thickness (0.9-2.9)1.8±0.29 µm. Mesocolpium measurement (8.75-17.2)13.4±0.34 µm. Pollen fertility 96.1% and sterility 3.8%. EL Ghazaly (1995) characterized the pollen of *A. hispidissima* and reported prolate, isopolar, and 6-colpate often wider at the equator with tapering ends. Similar results about shape were reported by Perveen and Qaiser (1995). Gazer (2017) described the pollen of this specie as pre-prolate, isopolar, stephanoaperture, and psilate stratification. Our study shows mostly similarities to the results of Gazer (2017), but varies in shape sub-oblate and surface sculpturing. Our results are showing the difference in a number of colpi to the results described by Yousaf et al., (2022).

#### b) *Heliotropium bacciferum* Forssk.

Pollen are monad, medium-sized and hetracolpate. Rounded polar and sub-prolate equatorial shape. Mesocolpium with pseudocolpi, aperture membrane granular, smooth perforated sexine, colpi linear and sunken. Exine peculiarities rugulate. Polar diameter (28.25-30.5)29.4±0.43 µm, and equatorial view distance (20.75-23)22.05±0.44 µm. P/E ratio 1.33. Polar area index (0.49). Colpi length (0.5-1)0.7±0.09 µm and colpi width (0.75-1.25)1.05±0.09 µm. Exine thickness (2.2-3.5)2.82±0.2 µm. Mesocolpium distance (10.25-11.25)10.85±0.16 µm. Pollen fertility 86.7% and sterility 13.2%. Pollen grains of *H. bacciferum* were identified as prolate and 8-heterocolpate by Perveen and Qaiser in 1995. The pollen of this species was prolate, iso-polar, pseudo-colpate, and rugulate, according to Gazer et al., (2017). Kamel (2019) reported prolate, spheroidal, tetracolporate with alternate pseudocolporate, and perforate rugulate sculptured grains. We reported mainly comparable outcome to those given by Kamel (2019), apart from ornamentation that we refer to as verrucate.

**c) *Heliotropium europaeum* L.**

Pollen are monad, medium-sized and 6-Hetracolpate. Semi-circular polar and oblate-prolate equatorial shape. Thick intine, scabrate narrow colpi and deeply sunken. Exine psilate verrucate. Polar diameter (26.25-28.2)27.4±0.35 µm, and equatorial view distance (28.25-30.5)29.35±0.4 µm. P/E ratio 0.93. Polar area index (0.66). Colpi length (1.5-2.25)2±0.13 µm and colpi width (2.25-3)2.7±0.14 µm. Exine thickness (1.75-2.5)2.1±0.12 µm. Mesocolpium distance (18.5-20.75)19.6±0.43 µm. Pollen fertility 92.2% and sterility 8.7%. Perveen and Qaiser, (1995) reported the pollen of *H. europaeum* as prolate and 6-heterocolpate, whereas Saad-Limam (2005) revised the same facts as prolate, iso-polar, tricolpate, 3-pseudocolpate, and scabrate. The polarity and aperture type of the pollen in this study was identical to those of Saad-Limam (2005), however other pollen features such as 4-stephanocolporate and 4-pseudocolpate, verrucate were different.

**d) *Heliotropium strigosum* Willd.**

Pollen are monad, isopolar, small to medium and 6-Hetracolpate. Elliptical polar and prolate equatorial shape. Deeply sunken aperture orientation. Exine sculpturing psilate verrucate. Polar diameter (23.5-27.1)25.36±0.39 µm, and equatorial view distance (16.5-20.2)18.6±0.74 µm. P/E ratio 1.36. Polar area index (0.58). Colpi length (1.8-2.8)2.3±0.12 µm and colpi width (2.2-3.1)2.8±0.09 µm. Exine thickness (1.5-3.4)2.6±0.73 µm. Mesocolpium distance (13.6-19.15)16.1±0.34 µm. Pollen fertility 94.3% and sterility 5.6%. Kasem (2015) observed micromorphology of *Heliotropium* species from Saudi Arabia including *H. strigosum* pollen as the elliptical and prolate type was reported similar to our results. Kumar et al., (2020) observed specimens of *Heliotropium indicum* pollen were tricolpate, pentoporate aperture, and spinose tectum. Whereas in our case the spiny features were absent and hetracolpate pollen type was examined.

**e) *Nonea micrantha* Boiss. & Reut.**

Pollen are monad, small to medium and stephanocolporate. Circular polar and prolate-spheroidal equatorial shape. Oblique pollen orientation and sunken aperture condition. Exine sculpturing gemmate verrucate. Polar diameter (24.7-26.5)25.45±0.82 µm, and equatorial view distance (22.75-24)23.4±0.23 µm. P/E ratio 1.08. Polar area

index (0.46). Colpi length (3-4)3.4±0.16 µm and colpi width (3.75-4.5)4.2±0.14 µm. Exine thickness (2.25-3.25)2.8±0.16 µm. Mesocolpium distance (9-12)10.8±0.5 µm. Pollen fertility 92.9% and sterility 7%. Parveen and Qaiser (1995) cited that *N. capsica* with la-longate endoaperturate, finely reticulate, tectate grains, while our results analyzed *N. micrantha* as a stephano-aperturate gemmate perforate sculptured. Khatamsaz in 2001 also described pollen of *Nonea* species with tetra to hexacolporate aperture and foveolate to psilate ornamentation dose not find similarity to above reported features. The presence of suprategal elements such as gemmate and spinules occur in *N. obtusifolia* support our results with respect to exine surface (Bigazzi and Selvi, 1998).



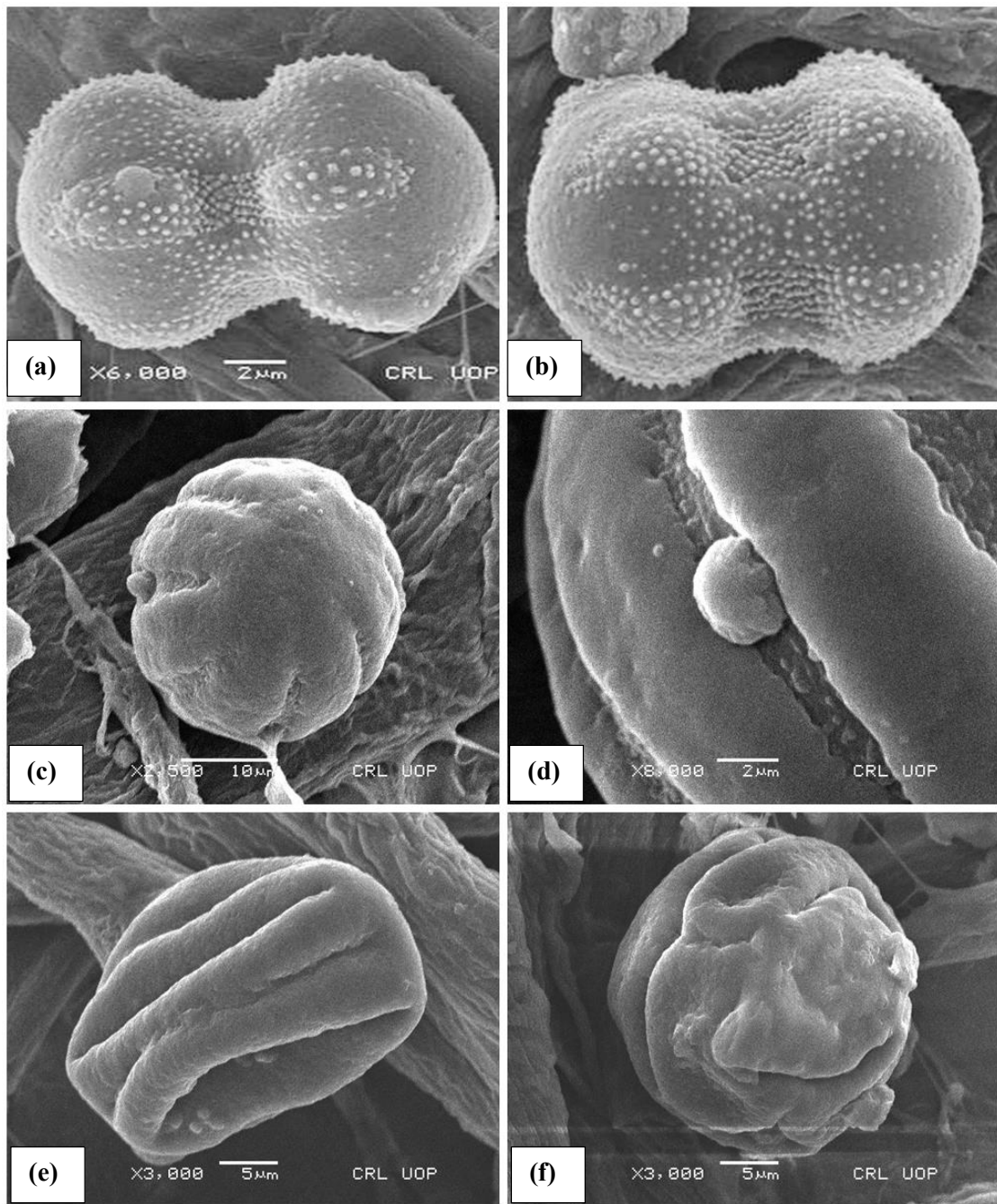


**Plate 48.** Scanning electron microscope photographs of Boraginaceae taxa. (a-b) *Arnebia hispidissima*; micro-echinate exine sculpture (Scale bar 2µm), (c-d) *Heliotropium bacciferum*; rugulate pollen wall (Scale bar = 10 µm, 2 µm), (e-f) *Heliotropium europaeum*; verrucate exine peculiarities (Scale bar = 5 µm)

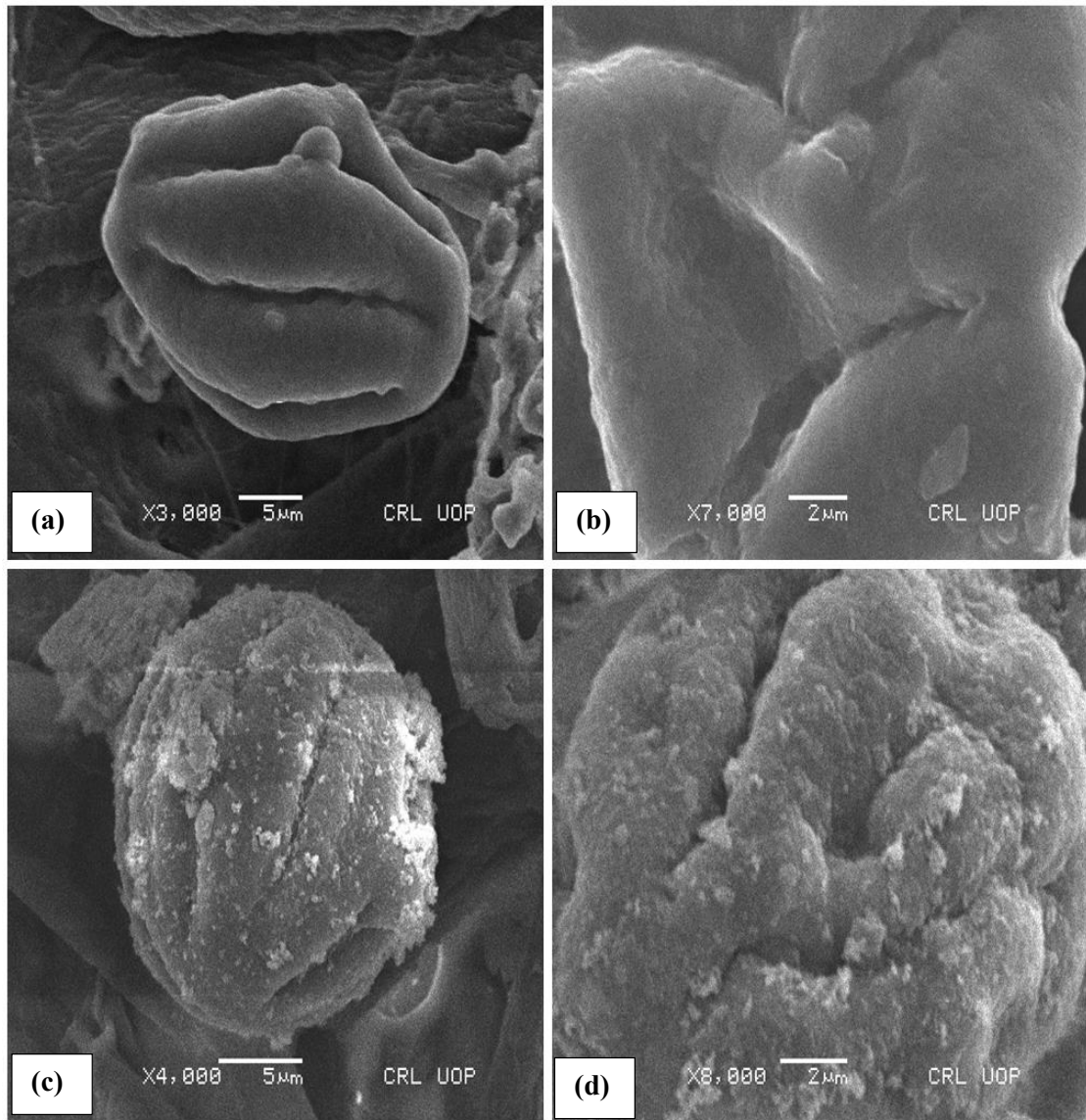


**Plate 49.** Scanning electron microscope photographs of Boraginaceae taxa. (a-b) *Heliotropium strigosum*; psilate verrucate exine (Scale bar = 5 μm, 2 μm), (c-d) *Heliotropium bacciferum*; rugulate pollen wall (Scale bar = 10 μm, 2 μm), (e-f) *Nonea micrantha*; verrucate gemmate exine wall (Scale bar = 5 μm, 2 μm)

### 3.2.14 Pollen Micromorphology of Brassicaceous Species

#### a) *Brassica nigra* (L.) K.Koch

Pollen monad, isopolar, medium-sized and tricolpate. Lobate in polar view and sub-prolate equatorial view. Aperture sunken oriented. Exine sculpturing elements compact and reticulate. Polar diameter (27-32)29.8±0.25 µm, equatorial distance (25.1-30)25.9±0.81 µm. P/E ratio 1.15. Polar area index (0.29). Colpi length (0.95-2.85)1.85±0.4 µm and colpi width (3.25-5.45)4.3±0.23 µm. Exine thickness (2.7-4.2)3.6±0.17 µm, mesocolpium distance (18.4-21.6)19.6±1.31 µm. Pollen fertility 93.8% and sterility was 6.1%. Perveen et al., (2004) described the pollen of *Brassica juncea* tricolpate as reticulate-ornamented, prolate-spheroidal, long sunken colpus with acute ends. According to our analysis, the pollen grains of *Brassica* species were prolate-spheroidal, sub-prolate, and prolate with tricolpate and finely reticulate exine. Saha and Begum (2020) performed a pollen character description of six varieties of *Brassica* from Bangladesh appears to be reticulate and coarsely reticulate sculpturing was corroborated with the current research.

#### b) *Eruca vesicaria* (L.) Cav.

Pollen monad, small and tricolpate. Circular polar view and equatorial view shape prolate-spheroidal. Colpi sunken and membrane ornamented. Exine stratification semi-tectate and reticulate. Polar diameter (18.2-24.2)21.4±1.06 µm and equatorial diameter (17.6-23.2)20.1±0.89 µm. P/E ratio 1.06. Polar area index (0.57). Colpi length (2.5-3.8)3.2±0.31 µm and width of colpi (2.6-5.5)4.12±0.37 µm. Exine thickness (1.85-4.6)3.1±0.74 µm. Mesocolpium distance (7.4-12.8)10.3±1.51 µm. Pollen fertility 86.7% and sterility 13.2%. Shakeel et al., (2021) evaluate the difference of pollinator's diversity and abundance around *E. vesicaria* and their relative abundance. Arora and Modi (2011) described sub-oblate, tricolpate and reticulate sculptured *E. vesicaria* pollen while this study identified prolate-spheroidal and semi tectate reticulate exine. Gabr (2018) show prolate, reticulate with irregular lumina for *E. vesicaria* grains which is different from the current report study. Recently, Umber et al., (2022) explained that 3-zonocolpate and reticulate pollen in *E. vesicaria* was similar to our observation.

**c) *Lepidium didymum* L.**

Pollen are monad, small sized, and tricolpate. Circular polar view, prolate-spheroidal equatorial view. Deeply sunken oriented colpi. Exine sculpturing reticulate. Polar view diameter (15.5-21.7)  $18.6 \pm 1.18$   $\mu\text{m}$  and equatorial view distance (14.2-18.3)  $17.9 \pm 1.63$   $\mu\text{m}$ . P/E ratio 1.03. Polar area index (0.25). Colpi length (0.9-3.2)  $1.85 \pm 0.53$   $\mu\text{m}$ , colpi width (1.2-3.4)  $2.15 \pm 0.58$   $\mu\text{m}$ , and mesocolpium length (10.7-16.6)  $13.2 \pm 0.67$   $\mu\text{m}$ . Exine thickness (1.5-5.8)  $3.65 \pm 0.68$   $\mu\text{m}$ . Pollen fertility 94.4% and sterility 5.5%. Monad, tricolpate, reticulated sculpture and polygonal luminate grains described by Gabr (2018) and Zafar et al., (2019) were coherent with our findings. Umer et al., (2022) illustrate palynology of *L. didymium* correctly identifies reticulate type stratification although the current study was also in line with this earlier study.

**d) *Sisymbrium irio* L.**

Pollen are monad, small and tricolpate. Circular polar view and oblate-spheroidal equatorial view. Colpi slightly sunken-oriented. Exine peculiarities reticulate. Polar diameter (21.5-24)  $22.8 \pm 1.01$   $\mu\text{m}$  and equatorial distance (22.6-24.7)  $23.6 \pm 1.18$   $\mu\text{m}$ . P/E ratio 0.96. Polar area index (0.68). Colpi length (5.5-7.2)  $6.3 \pm 1.05$   $\mu\text{m}$  and colpi width (4.8-6.7)  $5.65 \pm 1.24$   $\mu\text{m}$ . Mesocolpium distance (12.4-17.2)  $14.8 \pm 1.62$   $\mu\text{m}$ . Exine thickness (3.6-4.95)  $4.45 \pm 0.62$   $\mu\text{m}$ . Pollen fertility 91.4% and sterility 8.5%. According to Amina et al., (2020), *S. irio* grains have a spheroidal shape and reticulate sculpture. *S. irio* has a syncolpate acute end with a thicker sexine (Khan et al., 2005). Previously Azzazy (2011) reported the palynomorphs attributes with semi-tectate exine and micro-reticulate patterns.

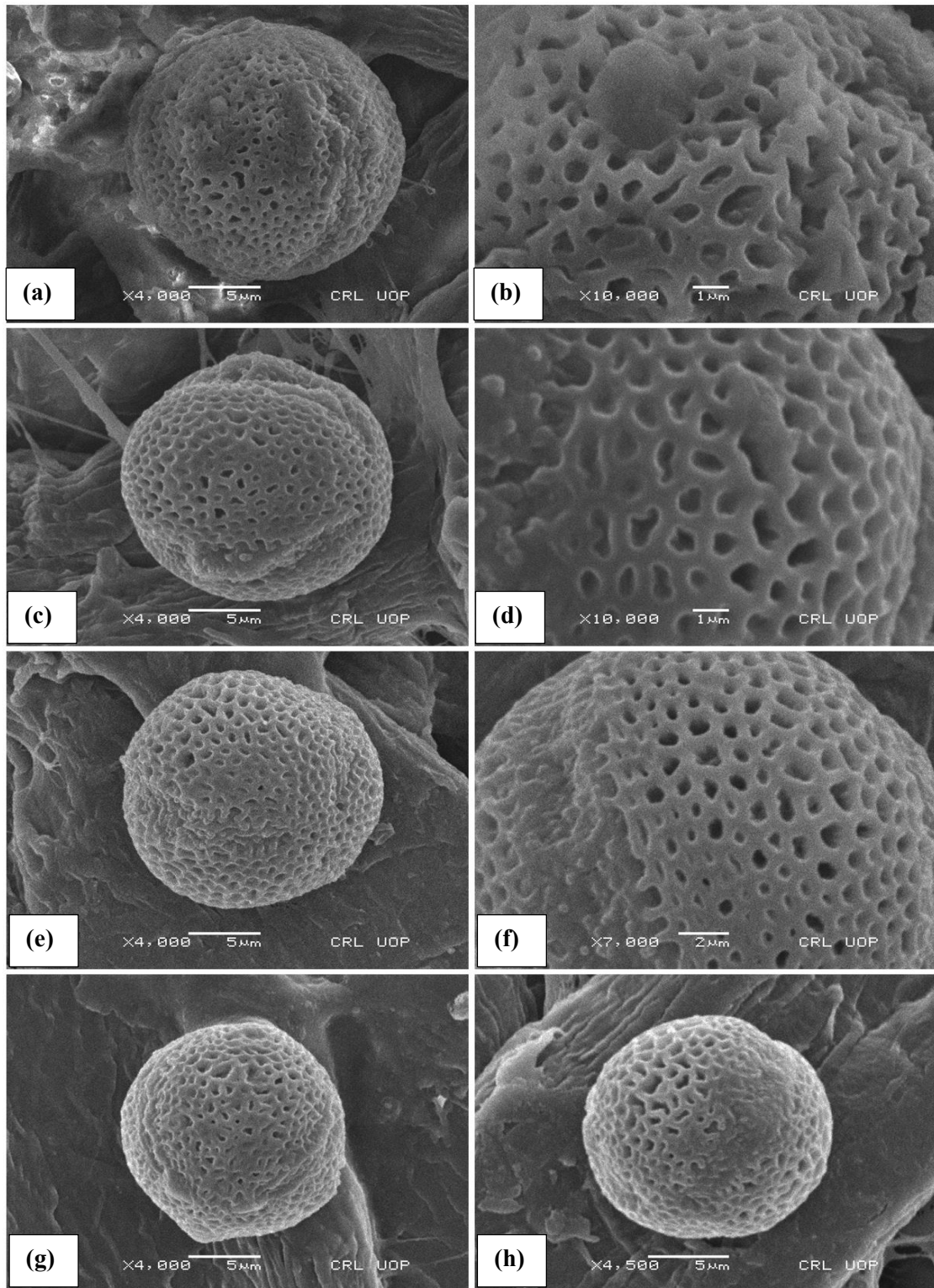


**Plate 50.** Scanning electron microscope photographs of Brassicaceous taxa. (a-b) *Brassica nigra*; compact reticulate exine (Scale bar = 5µm, 1 µm), (c-d) *Eruca vesicaria*; semi tectate pollen wall (Scale bar = 5 µm, 1 µm), (e-f) *Lepidium didymum*; reticulate sculpturing (Scale bar = 5 µm, 1 µm), (g-h) *Sisymbrium irio*; reticulated pollen stratification (Scale bar = 5 µm)

### 3.2.15 Pollen Micromorphology of Cactaceae Species

Literature also exists on pollen morphology of Cactaceae (Aguilar-García et al., 2012; dos Santos et al., 1997; Garralla and Cuadrado, 2007) but the understanding of cactus plants reproductive biology is mainly inadequate with respect to morphological, physiological, biochemical, and ethnobotanical features (Martins et al., 2016). The morphological diversity in the Cactaceae regarding stem, flower, fruit, and seed provided detailed description and discussion in previous research work and distinctive morphology for taxonomic classification in addition to monographs (Sánchez et al., 2018), but this is the first reference documentation in Pakistan on selected species of the *Opuntia* (Cactaceae) using diverse light and scanning electron microscopy. Palynological features of genus *Opuntia* in qualitative and quantitative state was examined scanning microscopic imaging visualization. The micro-morphological characteristics of pollen grains were provided with the use of SEM. The pollen grains of the studied taxa were pantoporate, prolate-spheroidal, and had perforate-reticulate tectate to reticulate semi-tectate ornamentation.

#### a) *Opuntia dillenii* (Ker-Gawl) Haw

Pollen large, monad, pantoporate and psilate. Shape of pollen was prolate spheroidal, pollen sculpturing reticulate, elongated pores, aperture ornamentation slightly sunken, exine ornamentation semi-tectate. Polar and equatorial diameter was found to be  $110.0(121.4\pm 2.31)132.50 \mu\text{m}$  and  $84.25(108.3\pm 4.63)132.5 \mu\text{m}$  respectively. Pore length was measured  $15(20.37\pm 1.30)27.25$  and width was  $12.50(18.50\pm 1.06)23.5 \mu\text{m}$ . Thickness of exine was calculated  $5.50(9.90\pm 0.79)13.50 \mu\text{m}$ . The ratio of polar to equatorial diameter (P/E) was found to be 1.12. No of fertile pollen measured was 137 and sterile pollen was 53. Pollen fertility estimated 72.10%. Cactaceae has pantoporate and tricolpate pollen grains which appears to be only two outlines within family Cactaceae as described previously (Cuadrado and Garralla, 2009; Garralla et al., 2013; Garralla and Cuadrado, 2007). This study also showed that the *Opuntia* species have prolate spheroidal, large size, and pantoporate pollen grains. While according to previous study (Garralla and Cuadrado, 2007) reported the pollen grains of spheroidal shape in genus *Opuntia*. The previous research work by (Miesen et al., 2015) demonstrated that in the family Cactaceae the pollen grains of large size diameter (40–100  $\mu\text{m}$ ) are present. But according to present findings

the *Opuntia* species were observed with large and very large size diameter (84–132  $\mu\text{m}$ ) of pollen grains.

**b) *Opuntia monacantha* (Willd.) Haw**

Pollen grain large, a polar, monad, pantoporate, psilate. Pollen shape prolate spheroidal, ornamentation perforate-reticulate, elongated pores, aperture ornamentation sunken, exine tectate. Polar diameter is  $97.50(112.08\pm 3.35)127 \mu\text{m}$ , equatorial diameter is  $90(101.65\pm 2.71)115 \mu\text{m}$ . Length and width of pore was measured  $17.50(22.10\pm 0.95)27.50 \mu\text{m}$  and  $7.50(13.22\pm 1.32)20 \mu\text{m}$  respectively. Exine thickness was noted  $5(8.57\pm 0.76)12.50 \mu\text{m}$ . P/E ratio was 1.10. No. of fertile and sterile pollen was calculated 78 and 23 respectively. Fertility of pollen was measured 77.22%. According to Kiesling, (1984), the differentiation of genus and species through the size of pollen cannot be occur, because the sizes of various species overlap. The ornamentation of pollen grains observed in present findings was reticulate, perforate reticulate and exine sculpturing was tectate and semi-tectate. While Garralla and Cuadrado (2007) also observed the same findings of pollen through SEM. Additionally, pollen grains of the studied species of *Opuntia* differ from those of other species of Cactaceae because of prominent exine thickness which was easily observed under light microscope.

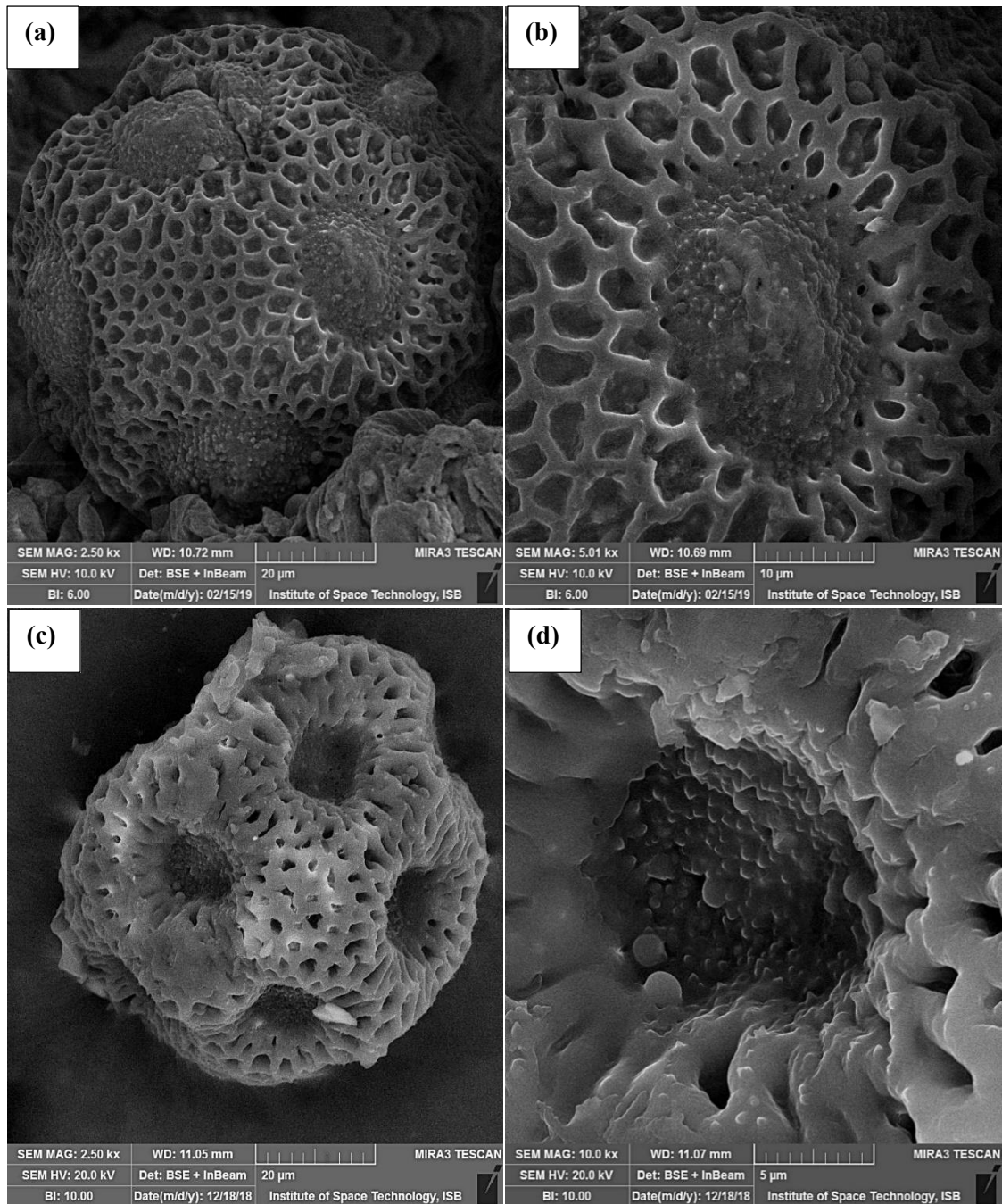


**Plate 51.** Scanning electron microscopic photographs of Cactus species (a) *Opuntia dillenii* polar view (20 µm), (b) *Opuntia dillenii* exine sculpturing (10 µm), (c) *Opuntia monacantha* polar view (20 µm), and (d) *Opuntia monacantha* exine surface



### 3.2.16 Pollen Micromorphology of Capparaceae Species

#### a) *Capparis decidua* (Forssk.) Edgew

Pollen grains small, monad, and tricolporate. Angular polar shape and sub-oblolate equatorial view shape. Deeply sunken aperture orientation, colpi sparsely granulated and reticulate tectum. Exine sculpturing reticulate striate. Polar diameter (22.5–19.7)  $21.4 \pm 0.41$   $\mu\text{m}$ . Equatorial diameter (19.7–14.5)  $15.6 \pm 0.5$   $\mu\text{m}$ . P/E ratio 1.37. Polar area index (0.67). Length of colpi (5–2.75)  $4.47 \pm 0.26$   $\mu\text{m}$  and width of colpi (10.0–7.5)  $8.52 \pm 0.32$   $\mu\text{m}$ . Mesocolpium (12.2–10.0)  $10.5 \pm 0.27$   $\mu\text{m}$ . Exine thickness (2.75–1.5)  $2.12 \pm 0.11$   $\mu\text{m}$ . Pollen fertility 87.4% and sterility 12.5%. Erdtman (1986) described the pollen of the Capparaceae as sub-prolate or prolate and colporoidate. For the genus *Capparis*, Ronse De Craene et al., (2002) described the grains as tricolporate and perforate. For sect. *Capparis*, Fici (2004) reported spindle-shaped, tricolpate grains, with smooth exine-bearing scattered hollows. The species investigated here, tricolporate, sub-oblolate pollen with sparsely granulated colpi has been observed. Mir et al., (2019) pointed out that the sculpturing in *C. decidua* is reticulate whereas in my finding sculpturing is reticulate striate.

#### b) *Cleome brachycarpa* (Forssk.) Vahl ex DC.

Pollen monad, small sized and tricolporate. Triangular polar view and oblate-spheroidal equatorial view. Colpus membrane densely granulate, tectum verrucate to spinulate and sunken aperture. Exine sculpturing spinulose verrucate. Polar diameter (15-18.8)  $17.5 \pm 0.47$   $\mu\text{m}$  and equatorial view distance (15.9-23.5)  $17.8 \pm 0.85$   $\mu\text{m}$ . P/E ratio 0.98. Polar are index (0.45). Colpi length (3.6-8.6)  $6.4 \pm 0.81$   $\mu\text{m}$ , colpi width (2.6-6.8)  $4.75 \pm 1.11$   $\mu\text{m}$ . Exine thickness (0.75-1.8)  $1.28 \pm 0.19$   $\mu\text{m}$ . Mesocolpium distance (7.5-9.25)  $8.15 \pm 0.17$   $\mu\text{m}$ . Pollen fertility 90.4% and sterility 9.5%. The spinulose verrucate type features in our characterization were found to be slightly divergent to Riaz et al., (2019) which revealed spinulose prolate pollen type in *C. brachycarpa*. Ahmad et al., (2010) observed palynomorphs of semi-desert species using light microscopy including *C. brachycarpa* with semi-angular and psilate sculptured grains. While our observation was different showing a triangular shape and verrucate exine surface.

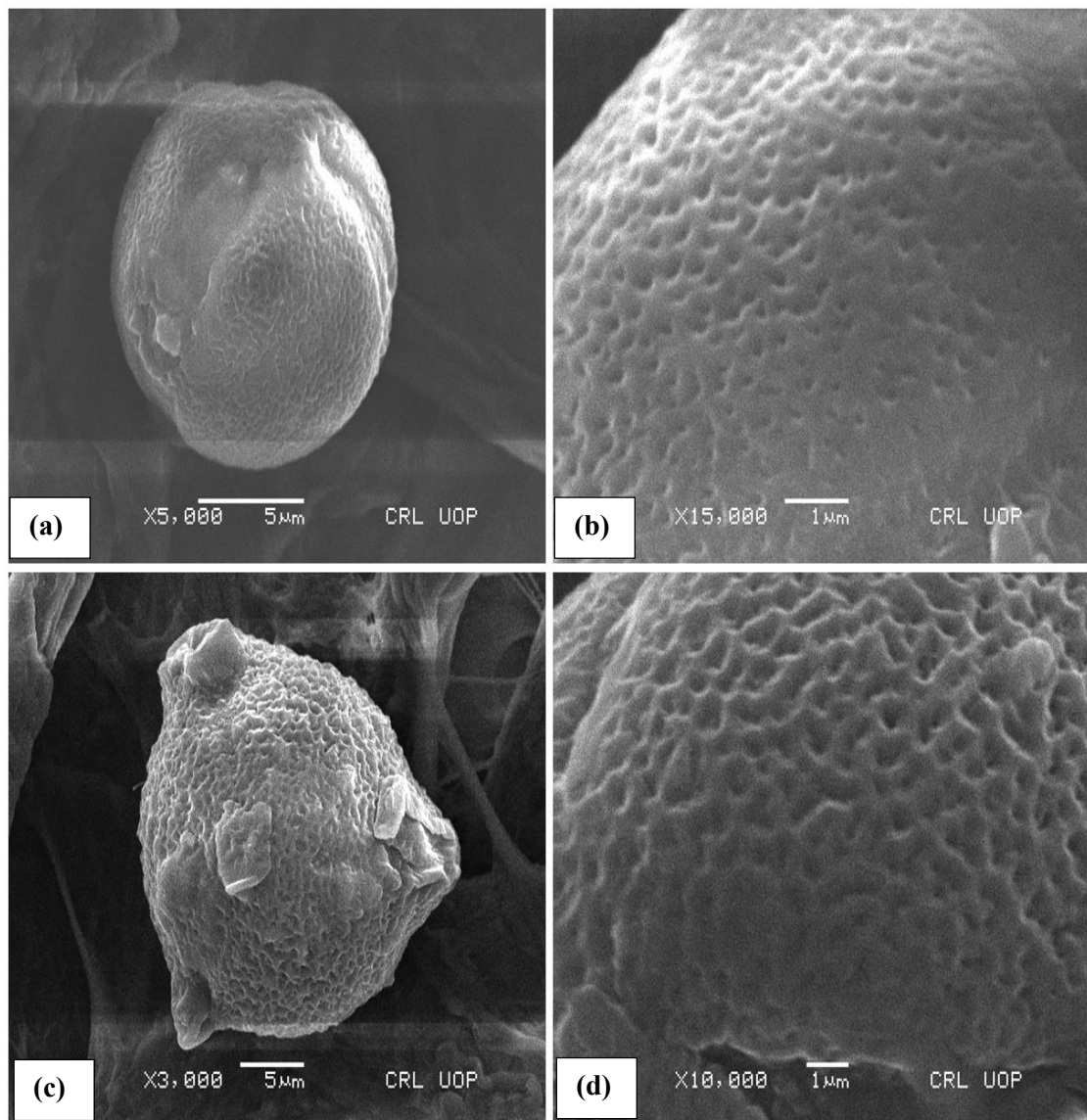


**Plate 52.** Scanning electron microscope photographs of Capparaceae species (a-b) *Capparis decidua*; reticulate striate exine (Scale bar = 5 μm, 1 μm), (c-d) *Cleome brachycarpa*; spinulose verrucate pollen wall (Scale bar = 5 μm, 1 μm)

### 3.2.17 Pollen Micromorphology of Aizoaceae Species

#### a) *Trianthema portulacastrum* L.

Pollen are monad, medium and tricolpate. Circular polar view and prolate-spheroidal equatorial shape. Ectocolpi narrow with scabrate surface and sunken aperture. Exine sculpturing foveolate-punctate. Polar diameter (35.5-43.2)40±1.39 µm equatorial view distance (34.5-39.7)36.4±0.94 µm. P/E ratio 1.09. Polar area index (0.74). Colpi length (2.75-5.25)4.3±0.42 µm, colpi width (6.75-8)7.35±0.23 µm and mesocolpium distance (24.5-30.7)27±1.14 µm. Exine thickness (4.75-6.25)5.4±0.24 µm. Pollen fertility 92.7% and sterility 7.2%. Abo El-Naga et al., (2014) defined sparsely punctate grains in *Trianthema portulacastrum* while this study showed dissimilarity in analyzed foveolate punctate pollen. Samina et al., (2003) also explained 3-colpate pollen in *T. portulacastrum* in accordance with our outcomes.

#### b) *Zaleya pentandra* (L.) C. Jeffrey

Pollen are monad, medium sized and tricolporate. Semi-angular polar view and sub-oblite equatorial shape. Slightly oriented sunken aperture. Exine sculpturing scabrate granulate. Polar diameter (29-33.6)32.5±1.14 µm equatorial view distance (23.7-32.6)27.5±1.07 µm. P/E ratio 1.18. Polar area index (0.46). Colpi length (5.1-8.2) 6.9±0.89 µm, colpi width (3.7-6.5)5.2±0.59 µm and mesocolpium distance (11.4-13.6)12.3±0.77 µm. Exine thickness (1.4-2.9)2.2±0.37 µm. Pollen fertility 95.2% and sterility 4.7%. The Aizoaceae family is defined as eurypalynous, pollen tri-colporate (tetracolporate and hexacolporate) isopolar with radial symmetry (Abo El-Naga et al., 2014). Based on the structure of the exine, the scabrate type was recognized in our case. Perveen and Qaiser (2000) studies based on using scanning microscopy indicate a striated stratified surface for some members of Aizoaceae.

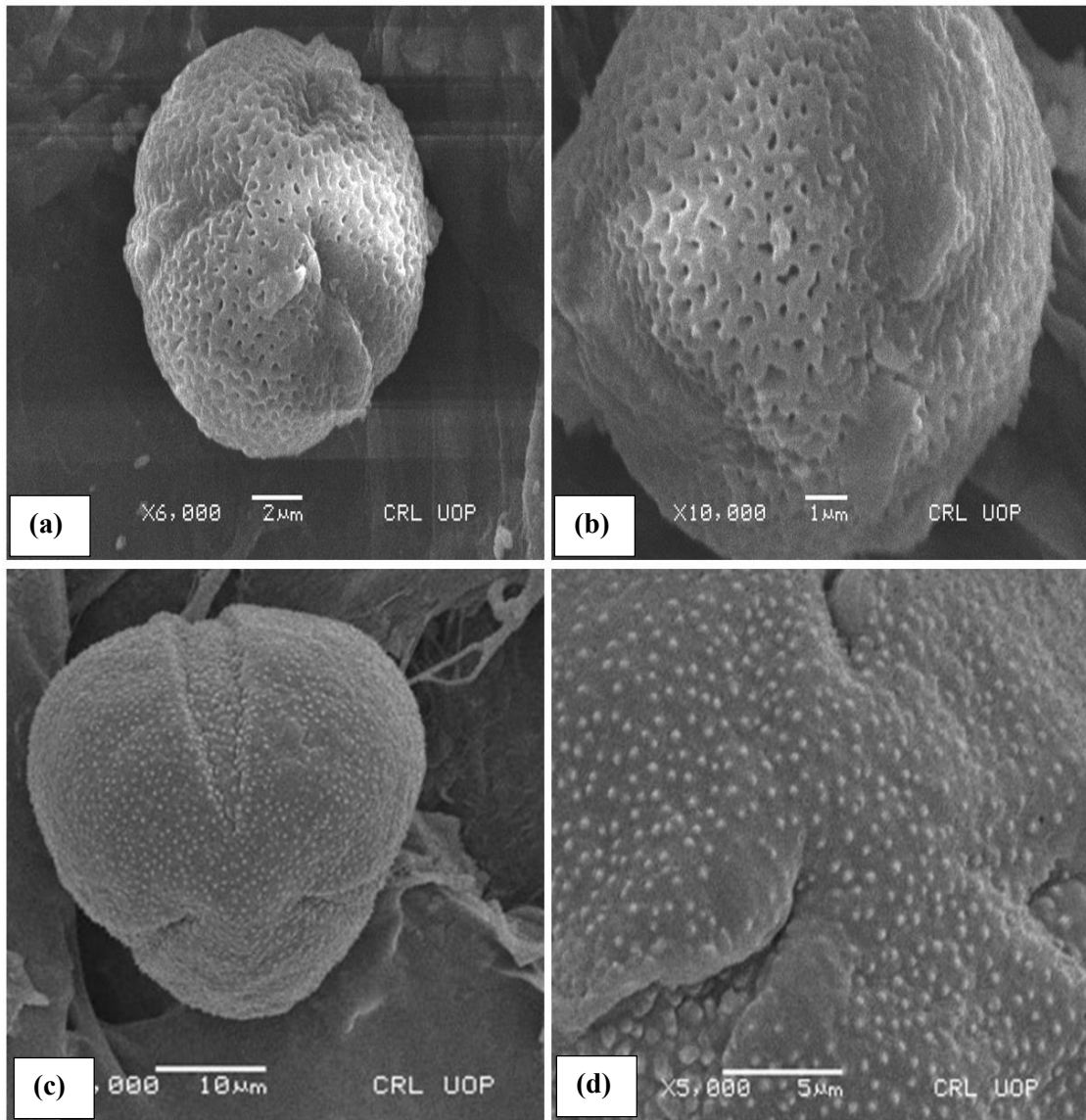


**Plate 53.** Scanning electron microscope photographs of Aizoaceae species (a-b) *Trianthema portulacastrum*; foveolate punctate sculpturing (Scale bar = 2  $\mu\text{m}$ , 1  $\mu\text{m}$ ), (c-d) *Zaleya pentandra*; scabrate granulate pollen tectum (Scale bar = 10  $\mu\text{m}$ , 5  $\mu\text{m}$ )

### 3.2.18 Pollen Micromorphology of Cucurbitaceous Species

#### a) *Citrullus colocynthis* (L.) Schrad.

Pollen monad, medium-sized, radially symmetrical and tricolporate. Circular polar view and sub-prolate equatorial view shape. Colpus long, radially symmetrical, acute ends and sunken oriented aperture. Exine ornamentation coarsely reticulate. Polar diameter (33.3–51)  $41.65 \pm 1.06$   $\mu\text{m}$  and equatorial diameter (29.5–43)  $34.9 \pm 1.57$   $\mu\text{m}$ . P/E ratio 1.19. Polar are index (0.40). Colpi length (0.85-1.7)  $1.2 \pm 0.02$   $\mu\text{m}$  and width of colpi (0.9-1.5)  $1.15 \pm 0.01$   $\mu\text{m}$ . Exine thickness (1.2–3.6)  $2.25 \pm 0.13$   $\mu\text{m}$ . Mesocolpium measurement (12.5-16.75)  $14.3 \pm 0.75$   $\mu\text{m}$ . Pollen fertility 93.9 % and sterility 6 %. Akhtar et al., (2019) reported that in *C. colocynthis* pollen was circular elliptic with coarsely reticulate ornamentation and a large exine thickness, however the results of our study elaborate polyhedral and psilate tectate grains. Perveen and Qaiser (2008) studied in detailed the pollen of Cucurbitaceous species from Pakistan analyzed *C. colocynthis* grains were similar microstructural characters as we observed in this study.

#### b) *Cucumis melo* L.

Pollen grains monad, medium to large and triporate. Rounded polar view and equatorial view shape prolate-spheroidal. Aperture deeply sunken, tectum coarsely reticulate and circular pores. Exine sculpturing reticulate-regulate. Polar diameter (48.25-60.3)  $53.2 \pm 1.95$   $\mu\text{m}$  and equatorial view distance (48-54.75)  $51.65 \pm 1.18$   $\mu\text{m}$ . P/E ratio 1.03. Polar are index (0.27). Pore length (11.5-13.7)  $12.5 \pm 0.52$   $\mu\text{m}$  and pore width (5.25-7.9)  $6.85 \pm 0.3$   $\mu\text{m}$ . Exine thickness (2.05-5.5)  $3.95 \pm 0.83$   $\mu\text{m}$ . Mesocolpium distance (10.5-17.2)  $14.35 \pm 1.62$   $\mu\text{m}$ . Pollen fertility 97.3% and sterility 2.6%. *Cucumis melo* has reticulate regulate exine sculptured elements and prolate-spheroidal grains Akhtar et al., (2019) and Perveen and Qaiser (2008) findings were dissimilar to above mentioned data with respect to circular elliptical shape and fine reticulated exine tectum. In another study by Levi et al., (2010) explained triangular, tricolpate and smooth surface grains in *C. melo*. Similar results with few differences were also reported by Ullah et al., (2021) on *C. melo* pollen as potential honeybee foraging resource.

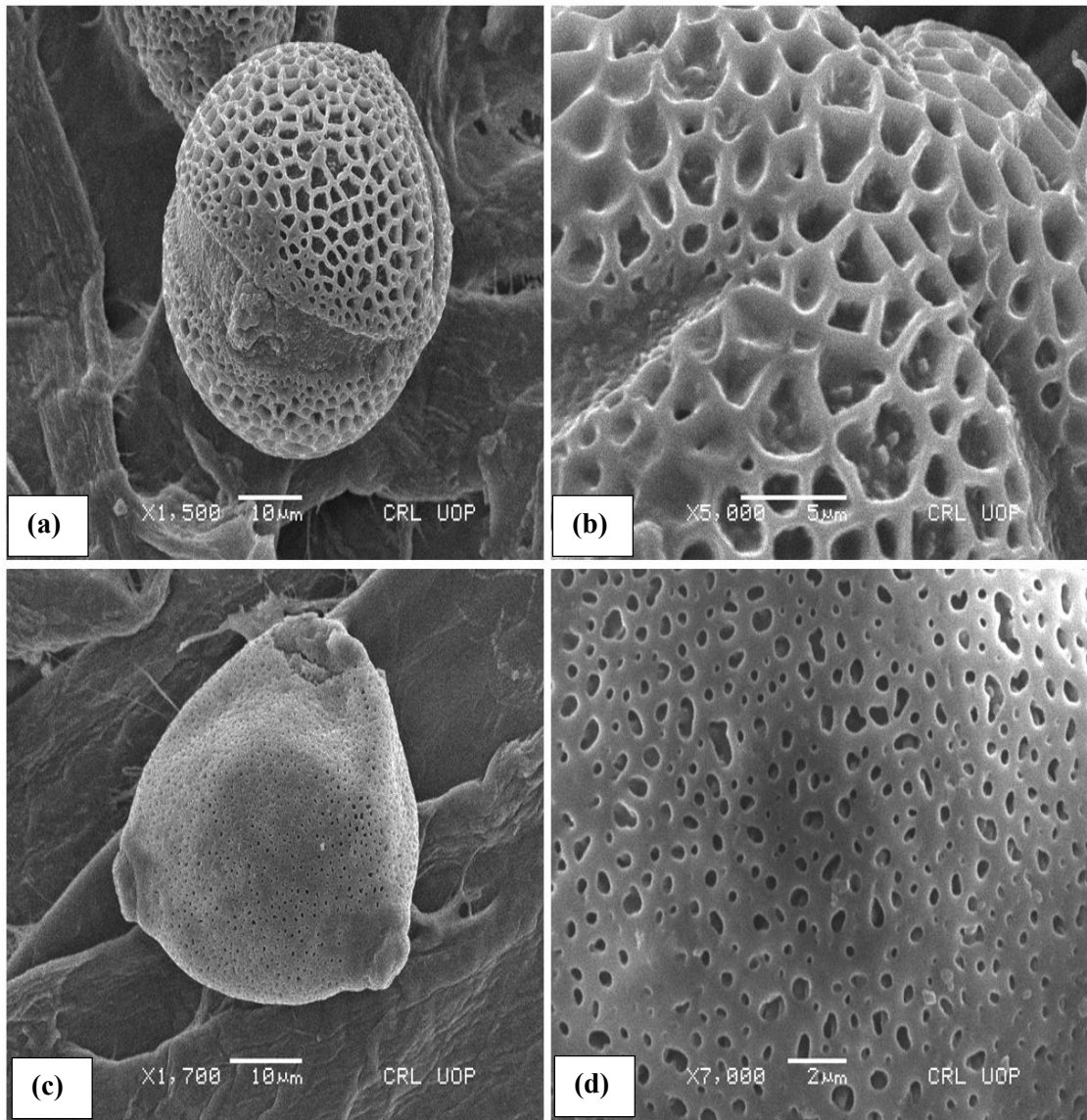


**Plate 54.** Scanning electron microscope photographs of Cucurbitaceae species (a-b) *Citrullus colocynthis*; coarsely reticulate exine wall (Scale bar = 10 μm, 5 μm), (c-d) *Cucumis melo*; reticulate-regulate pollen ornamentation (Scale bar = 10 μm, 2 μm)

### 3.2.19 Pollen Micromorphology of Euphorbiaceous Species

#### a) *Chrozophora plicata* (Vahl) A.Juss. ex Spreng.

Pollen monad, large sized, and hexacolporate. Rounded polar view and sub-oblately equatorial shape. Aperture orientation slightly bulged, ectocolpi long, narrow, acute and tectum coarsely reticulated. Exine sculpturing reticulate heterobrochate. Polar diameter (20.2-25.5)  $22.3 \pm 0.92$   $\mu\text{m}$  and equatorial diameter (22.2-28)  $25.1 \pm 1.08$   $\mu\text{m}$ . P/E ratio calculated 0.88. Colpi length (7.55-6.5)  $7.05 \pm 0.2$   $\mu\text{m}$ , colpi width (6.75-5.25)  $6.1 \pm 0.78$   $\mu\text{m}$ . Mesocolpium length (15.25-5.2)  $10.4 \pm 1.81$   $\mu\text{m}$ . Exine thickness (3.-4)  $3.52 \pm 0.15$   $\mu\text{m}$ . Pollen fertility 85.7% and sterility 14.2%. Previously *Chrozophora tinctoria* pollen were examined by Perveen and Qaiser, (2005) elaborates oblate-spheroidal, large-sized, and coarsely reticulate ornamented with exine thickness of 1.44  $\mu\text{m}$  was measured. Whereas our findings are similar to the earlier work mentioned above in the case of *C. plicata* pollen size. Whereas sub-oblately shape and reticulate heterobrochate and exine thickness (3.52  $\mu\text{m}$ ) are slightly deviating from previous work. Nowicke et al., (1999) conducted the SEM analysis of *Chrozophora* described 9-colporate and reticulate, which did not match our results in terms of shape, reticulate heterobrochate sculptured, and acute end colpi.

#### b) *Euphorbia dracunculoides* Lam.

Pollen monad, medium sized and tricolporate. Lobate polar view and prolate-spheroidal equatorial shape. Aperture sunken and obliquely oriented. Exine sculpturing perforate-gemmate. Polar diameter (25.1-28.6)  $27.1 \pm 0.95$   $\mu\text{m}$  and equatorial distance (25.4-27.7)  $26.7 \pm 0.39$   $\mu\text{m}$ . P/E ratio 1.01. Polar area index (0.73). Colpi length (1.5-2.6)  $2.05 \pm 0.41$   $\mu\text{m}$  and colpi width (1.8-3.7)  $2.9 \pm 1.03$   $\mu\text{m}$ . Exine thickness (2.15-3.5)  $2.8 \pm 0.93$   $\mu\text{m}$ . Mesocolpium distance (11.8-16.3)  $14.1 \pm 1.27$   $\mu\text{m}$ . Pollen fertility 91.5% and sterility 8.4%. *E. dracunculoides* showed variations in pollen quantitative measurements when compared with findings of Perveen and Qaiser (2005) while this study also revealed reticulate tectum grains found dissimilarity with our observation. *E. dracunculoides* with finely reticulated surface grains was illustrated and compared to the sculptured fine reticulation examined by Paul et al., (2014). In other studies, Basarkar (2017) examined tricolpate, reticulate, usually with long exine, finely reticulate grains.

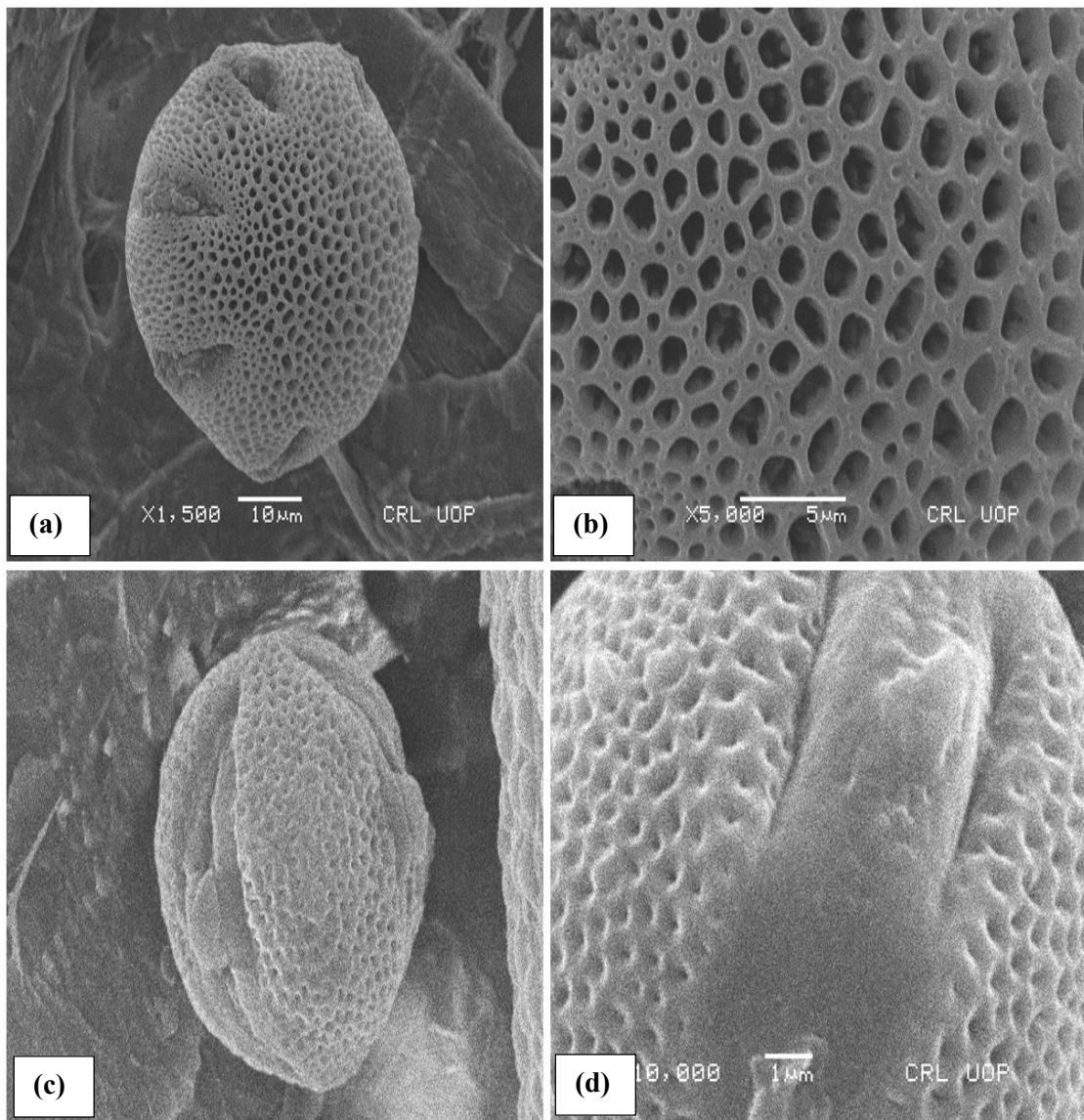


**Plate 55.** Scanning electron microscope photographs of Euphorbiaceous species (a-b) *Chrozophora plicata*; reticulate heterobrochate wall tectum (Scale bar = 10 μm, 5 μm), (c-d) *Euphorbia dracunculoides*; perforate gemmate exine stratification (Scale bar = 10 μm)



### 3.2.19 Pollen Micromorphology of Rhamnaceous Species

#### a) *Ziziphus nummularia* (Burm.f.) Wight

Pollen are monad, isopolar, medium and tricolporate. Triangular polar view and oblate-spheroidal equatorial shape. Colpus orientation bulged. Exine sculpturing rugulate. Polar diameter (25.7-29.8)27.4±0.84 µm and equatorial distance (26.4-30.9)28.6±1.01 µm. P/E ratio 0.95. Polar area index (0.56). Colpi length (2.3-5.5)4.1±0.63 µm and colpi width (3.15-6.2)5.15±0.78 µm. Mesocolpium distance (14.8-20.6)17.2±0.82 µm. Exine thickness (3.1-5.7)4.2±0.61 µm. Pollen fertility 89.6% and sterility 10.3%. Rhamnaceae is a stenopalynous family. Pollen grains are generally free, radially symmetrical, isopolar, colporate. Aftab and Perveen (2006) experimented morpho-palynology of cultivated tress described tricolporate, triangular and regulate striate tectum features in *Z. nummularia*. Naimat et al., (2012) observed palynomorphs features of selected Rhamnaceous taxa elaborate semi-angular and oblate-spheroidal pollen for *Z. nummularia*.

#### b) *Ziziphus spina-christi* (L.) Desf.

Pollen are monad, small, isopolar and tricolporate. Triangular polar view shape and oblate-spheroidal equatorial shape. Interapertural area sunken. Exine sculpturing rugulate. Polar diameter (19.6-24.5)22.1±1.65 µm and equatorial view distance (21.9-24.4)22.8±0.84 µm. P/E ratio 0.96. Polar area index (0.71). Colpi length (4.2-6.1)5.35±0.94 µm and colpi width (6.5-9.2)7.7±0.56 µm. Mesocolpium distance (10-16.3)13.4 ±1.23 µm. Exine thickness (0.8-1.9)1.4±0.26 µm. Pollen fertility 86.2% and sterility 13.7%. Grains with small pollen volume, tricolporate, and psilate exine features were examined for *Z. spina-christi* using optical microscopy (Gasma et al., 2020). In another study by (Lippi et al., 2007) analyzed pollen morphotypes from coastal zones of Oman and explained tricolporate, granulate colpus membrane, and irregular elliptical equatorial outline features in *Z. spina-christi*. However similar exine ornamentation to our visualization in scanning microscopy was observed.

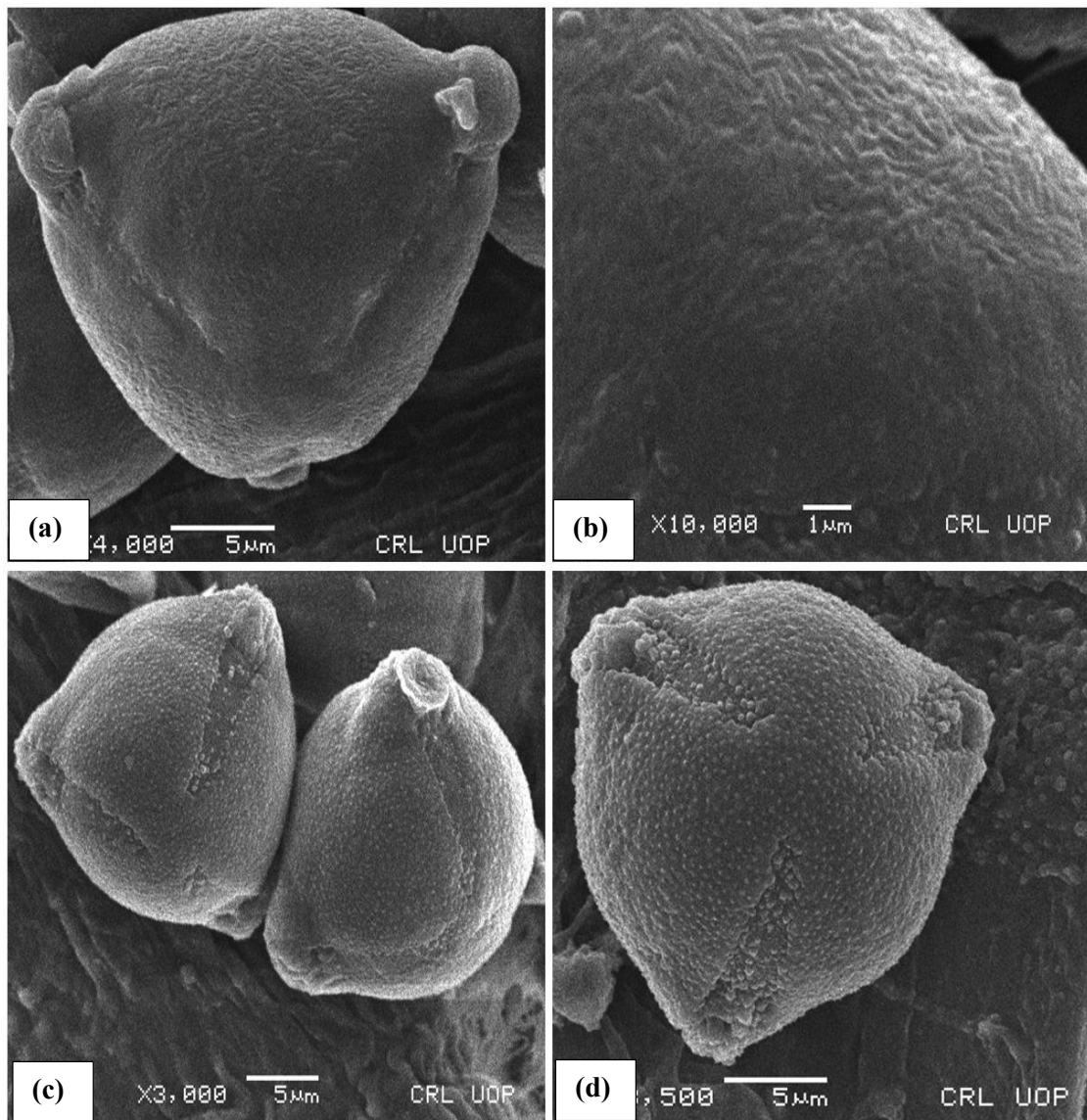


**Plate 56.** Scanning electron microscope photographs of Rhamnaceae species (a-b) *Ziziphus nummularia*; bulged colpus orientation (Scale bar = 5 μm, 1 μm), (c-d) *Ziziphus spina-christi*; rugulate exine stratification (Scale bar = 5 μm)

### 3.2.21 Pollen Micromorphology of Tamaricaceae Species

#### a) *Tamarix aphylla* (L.) H.Karst.

Pollen are monad, isopolar, small to medium and tricolpate. Lobate polar view and prolate-spheroidal equatorial shape. Apertural with long and sunken colpi. Exine sculpturing micro-reticulate. Polar diameter (19.2-35.7)  $26.7 \pm 0.45$   $\mu\text{m}$  equatorial distance (17.5-34.3)  $25.8 \pm 1.01$   $\mu\text{m}$ . P/E ratio 1.03. Polar area index (0.54). Colpi length (1.9-3.6)  $2.8 \pm 0.29$   $\mu\text{m}$ , colpi width (1.6-2.7)  $2.15 \pm 0.31$   $\mu\text{m}$  and mesocolpium distance (5.9-8.7)  $7.2 \pm 1.21$   $\mu\text{m}$ . Exine thickness (4.1-6.6)  $5.2 \pm 0.83$   $\mu\text{m}$ . Pollen fertility 91.8% and sterility 8.1%. *Tamarix* is known as a stenopalynous genus. The morphology of *T. aphylla* pollen is remarkably similar, especially together with the aspects of small, tricolpate and reticulate exine. These results show congruence with those of Elkorday and Faried (2017) who showed that the *T. aphylla* belong to monophyletic group based on molecular data from the nuclear ribosomal region (Gaskin et al., 2004).

#### b) *Tamarix dioica* Roxb. ex Roth

Pollen are monad, medium and tricolpate. Circular polar view and prolate-spheroidal equatorial shape. Membrane apertural features fine to medium coarse with long and sunken colpi. Exine sculpturing coarsely reticulate-perforate. Polar diameter (23.15-35.7)  $35.7 \pm 1.61$   $\mu\text{m}$  equatorial view distance (21.5-52)  $31.05 \pm 1.13$   $\mu\text{m}$ . P/E ratio 1.14. Polar area index (0.26). Colpi length (2.1-3.15)  $2.4 \pm 0.16$   $\mu\text{m}$ , colpi width (1.4-2.15)  $1.75 \pm 0.11$   $\mu\text{m}$  and mesocolpium distance (6.7-9.75)  $8.25 \pm 1.02$   $\mu\text{m}$ . Exine thickness (4.7-6.2)  $5.5 \pm 0.37$   $\mu\text{m}$ . Pollen fertility 93.3% and sterility 6.6%. Morphology of *Tamarix* pollen by Elkordy and Faried, (2017) reported reticulate type exine and prolate type pollen. Previous works by Qaiser and Perveen, (2004) described coarse to fine reticulate grains while our results showed that in *Tamarix dioica* reticulate perforate type sculptural surface was examined.

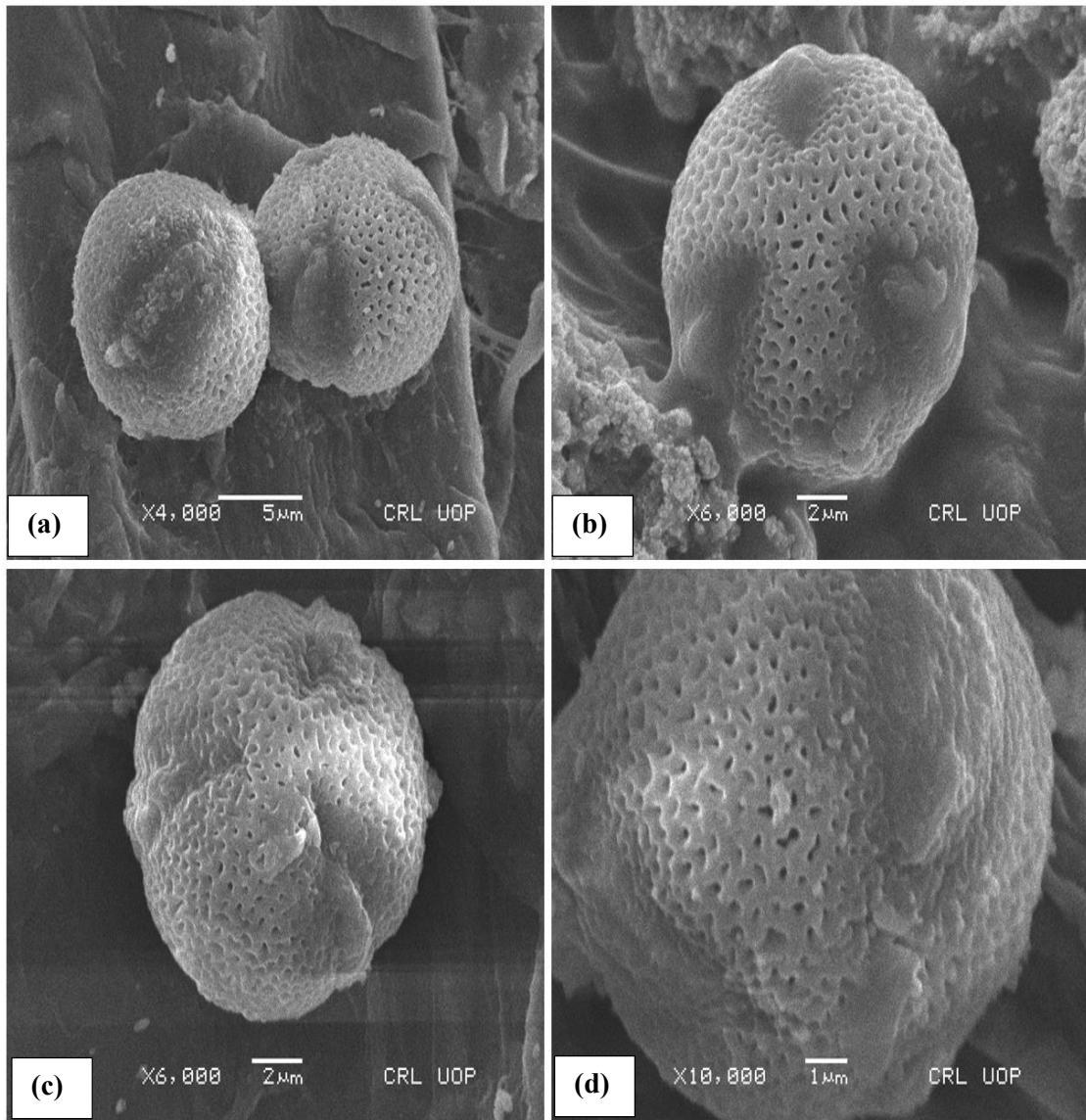


**Plate 57.** Scanning electron microscope photographs of Tamaricaceae species (a-b) *Tamarix aphylla*; micro-reticulate ornamentation (Scale bar = 5  $\mu\text{m}$ , 2  $\mu\text{m}$ ), (c-d) *Tamarix dioica*; reticulate perforate pollen wall stratification (Scale bar = 2  $\mu\text{m}$ , 1  $\mu\text{m}$ )

### 3.2.22 Pollen Micromorphology of Zygophyllaceous Species

#### a) *Fagonia bruguieri* DC.

Pollen are monad, medium-sized and tricolpate. Circular polar and prolate-spheroidal equatorial view shape. Irregular margins and acute ends apertures. Exine peculiarities reticulate. Polar diameter (19.7-80.2)36.7±4.83 µm, and equatorial view distance (18.0-75.2)34.5±4.65 µm. P/E ratio 1.06. Polar area index (0.71). Colpi length (2.7-5.5)4.1±0.18 µm and colpi width (1.7-6.75)4.51±0.4 µm. Exine thickness (2.5-8.2)6.1±0.91 µm. Mesocolpium distance (14.7-35)24.8±2.39 µm. Pollen fertility 96.1% and sterility 3.8%. *F. indica* shows long narrow ectocolpi with a reticulate-foveolate surface (Parveen and Qaiser, 2006), although our research analyzed reticulate exine with acute end aperture grains in *F. bruguieri*. *F. indica* pollen were sub-prolate, tricolporate, long colpus and micro-reticulate tectate represented by Taia et al., (2021) was somehow similar to our analysis.

#### b) *Tribulus terrestris* L.

Pollen are monad, medium to large and pantoporate. Circular polar view and sub-oblate equatorial shape. Radially symmetrical, pore oval shaped, exine thinner, obliquely placed sunken aperture orientation. Exine sculpturing coarsely reticulate. Polar diameter (54-57)55.25±1.32 µm equatorial view distance (39.75-42.75)41.55±1.26 µm. P/E ratio 1.32. Polar area index (0.32). Pore length (2-3.25)2.8±0.48 µm, pore width (1.5-2.75)2.15±0.45 µm and mesocolpium distance (13-14)13.45±0.37 µm. Exine thickness (2.25-3.25)2.8±0.48 µm. Pollen fertility 94.6% and sterility 5.3%. Linn (2020) recently described polyporate, medium-sized, circular, thick sexine, retipilate sculptured, and heterobrochate lumina in *Tribulus terrestris*. Praglowski (1987) explained that *Tribulus* sexine was thicker than nexine and fibrillar with small globular elements and reticulate type ornamentation (Semerdjieva et al., 2011). Our examination of pollen sculpture appearance was also reticulated, similar to previous work.

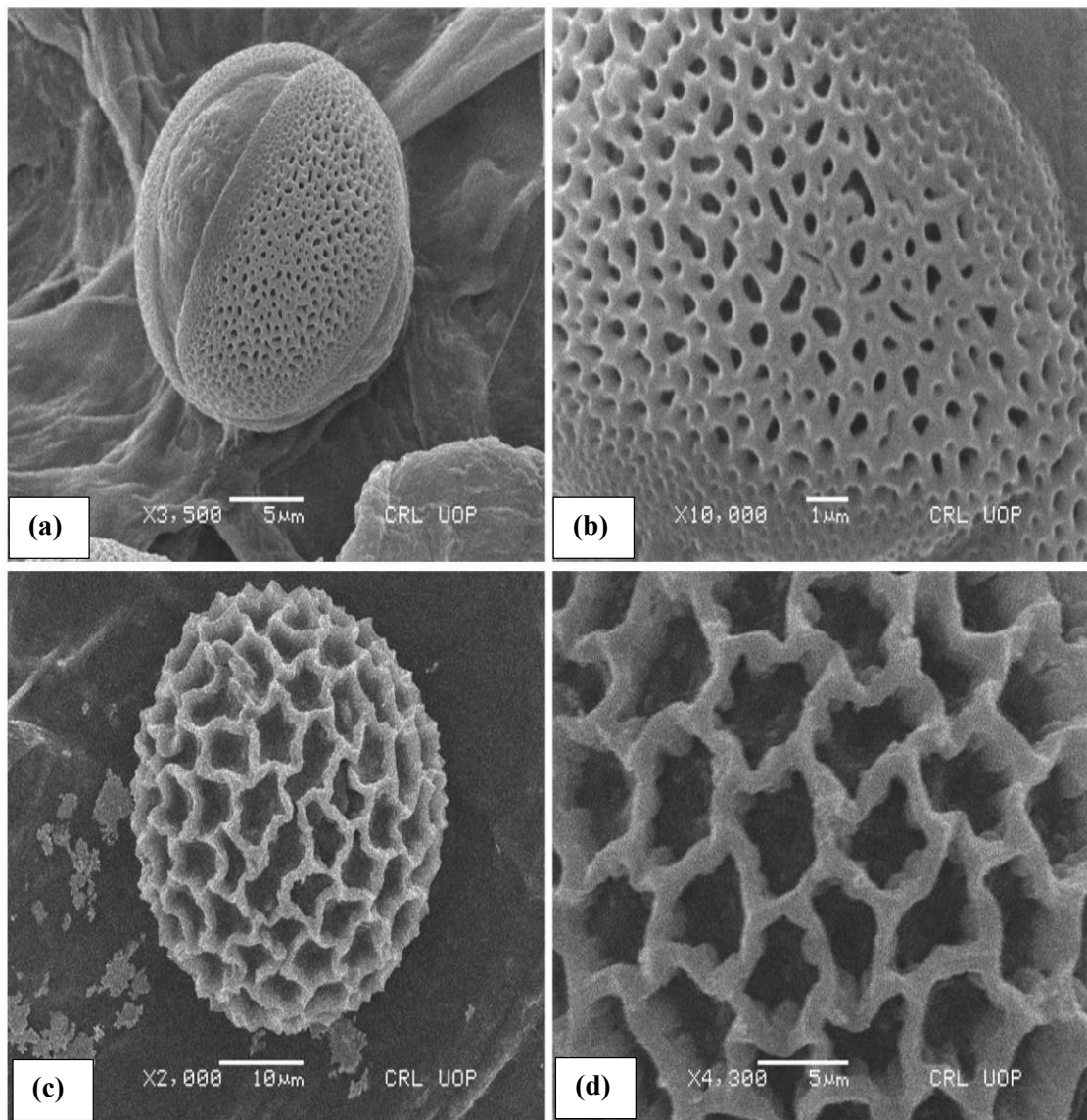


**Plate 58.** Scanning electron microscope photographs of Zygophyllaceous species (a-b) *Fagonia bruguieri*; acute end apertures and reticulate ornamentation (Scale bar = 5 μm, 1 μm), (c-d) *Tribulus terrestris*; micro-reticulate exine wall (Scale bar = 5 μm, 10 μm)

### 3.2.23 Pollen Micromorphology of Apiaceous Species

#### a) *Psammogeton biternatum* Edgew.

Pollen are monad, small to medium-sized and tricolpate. Elliptical polar view and equatorial view shape oblate. Striate and cerebroid apertural membrane with slightly bulged orientation. Exine sculpturing verrucate-gemmate. Polar diameter (14.25-16)15.15±0.3 µm and equatorial view distance (29.25-30.5)29.65±0.23 µm. P/E ratio 0.51. Polar area index (0.48). Colpi length (1.25-2)1.55±0.14 µm and colpi width (1.25-1.75)1.45±0.09 µm. Exine thickness (2.25-3.5)2.75±0.23 µm. Mesocolpium distance (13.75-15.25)14.45±0.26 µm. Pollen fertility 92.5% and sterility 7.4%. Perveen and Qaiser (2006) explained 3-zonocolporate, per-prolate, striate-rugulate tectum, ectoaperturate colpi with longer irregular margin and acute ends grains in *Psammogeton spp.*, whereas our outcome explained verrucate sculpture in *P. biternatum*.

### 3.2.24 Pollen micromorphology of Apocynaceous Species

#### a) *Rhazya stricta* Decne

Pollen are monad, isopolar, small to medium and tricolporate. Circular lobate polar view and sub-prolate equatorial view. Sunken apertural condition. Psilate-scabrate exine sculpturing. Polar diameter (22.8-27.5)24.7±0.89 µm and equatorial distance (17.2-19.8)18.6±0.61 µm. P/E ratio 1.32. Polar area index (0.53). Colpi length (3.1-5.4)4.05±0.67 µm and colpi width (2.3-3.7)2.9±0.43 µm. Mesocolpium distance (6.2-9.4)7.8±1.09 µm. Exine thickness (1.3-3.6)2.52±0.92 µm. Pollen fertility 89.6% and sterility 10.3%. Differences in exine stratification such as psilate pollen was examined for *R. stricta* in the reported study of Khan et al., (2021) was dissimilar to our work. Nilsson (1990) analyzed the ultrastructure of exine stratification of *R. stricta* define outer compact perforated and granular tectum.

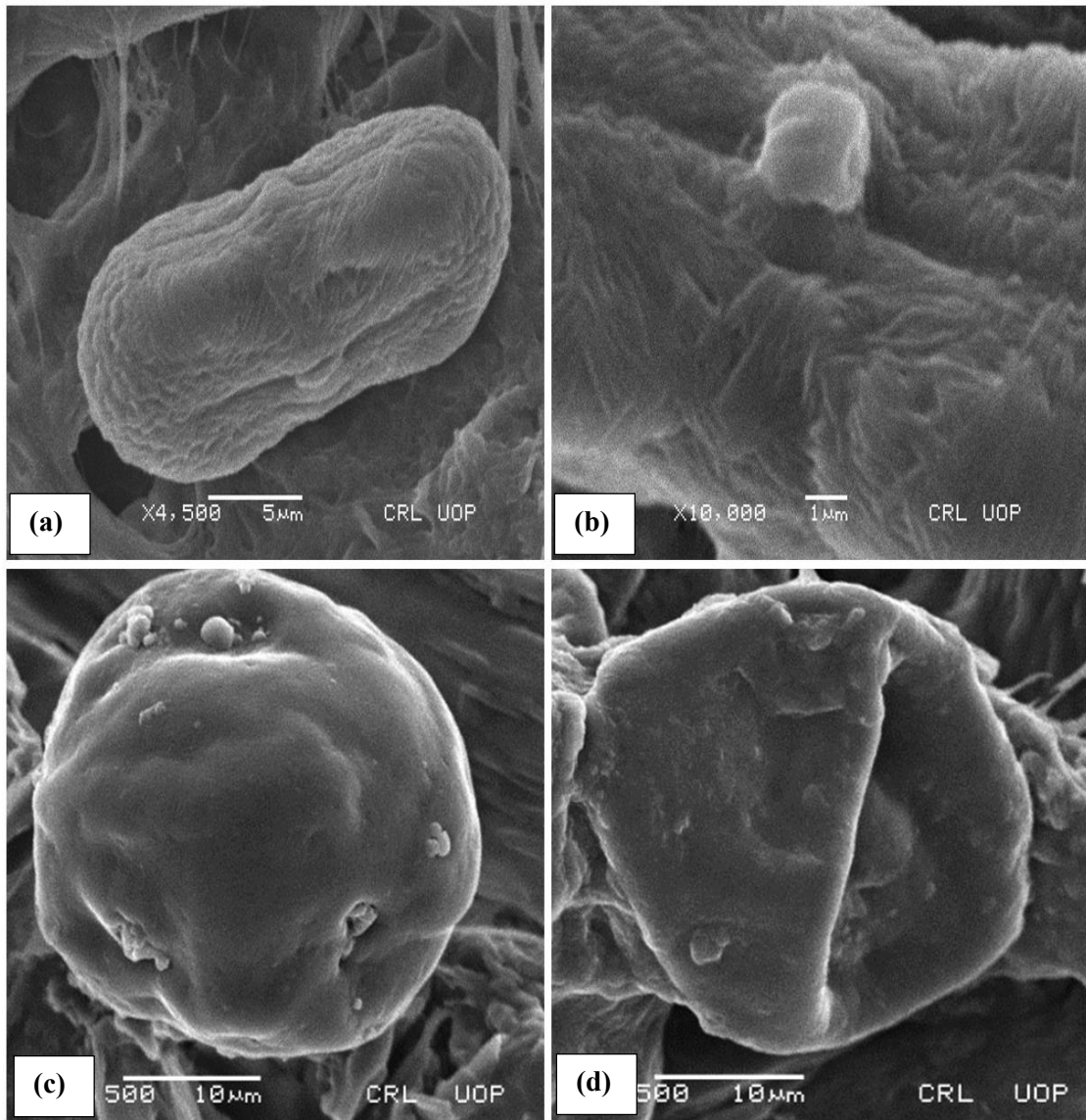


**Plate 59.** Scanning electron microscope photographs of Apiaceous and Apocynaceous taxa (a-b) *Psammogeton biternatum*; verrucate gemmate peculiarities (Scale bar = 5  $\mu\text{m}$ , 1  $\mu\text{m}$ ), (c-d) *Rhazya stricta*; psilate scabrate exine sculpturing (Scale bar = 10  $\mu\text{m}$ )



### 3.2.25 Pollen Micromorphology of Bignoniaceous Species

#### a) *Tecomella undulata* (Sm.) Seem.

Pollen are monad, medium and tricolporate. Semi-circular polar view and prolate-spheroidal equatorial shape. Sexine thicker, tectum reticulate with slightly sunken aperture. Exine sculpturing rugulate-reticulate. Polar diameter (34-37.25)34.45±0.57 µm equatorial view distance (28-35.25)31.7±1.24 µm. P/E ratio 1.08. Polar area index (0.51). Colpi length (4-5.25)4.65±0.23 µm, colpi width (3.25-4.75)4.05±0.26 µm and mesocolpium distance (15.25-18)16.45±0.44 µm. Exine thickness (1.5-2.75)2.2±0.21 µm. Pollen fertility 96.5% and sterility 3.4%. Rezanejad and Hakemi (2017) examined tricolpate pollen being widely represented and the reticulate sculpture pattern among various Bignoniaceous species. *Tecomella undulata* scanning micrographs revealed rugulate–reticulate ultrasculpture was accordance with our findings. In another study by Aftab and Perveen (2006), they also observed reticulate tectum and tricolporate grains.

### 3.2.26 Pollen Micromorphology of Malvaceous Species

#### a) *Malva parviflora* L.

Pollen are monad, apolar, large sized, and periporate. Rounded polar view and prolate-spheroidal equatorial shape. Exine sculpturing echinate. Polar diameter (59.2-83.2)70.2±2.78 µm and equatorial view distance (54.2-.82.2)68.78±2.32 µm. P/E ratio 1.02. Polar area index (0.46). Pore numbers varies 32 to 43. Pore length (2.95-5.1)4.2±1.71 µm and pore width (1.8-4.45)2.25±0.63 µm. Average spines number per pollen 65 to 80. Spine length (1.1-1.65)1.34±0.83 µm, spine width (1.4-4.2)2.85±0.97 µm. Exine thickness (2.45-5.1)3.9±0.56 µm. Pollen fertility 93.8% and sterility 6.1%. The present findings are in accordance with Bibi et al., (2010) that pollen in *M. parviflora* are usually pantoporate, spherical and reniform. Granulate, perforated, punctuate tectum and micro verrucate sculptural features. Naggar (2004) reported that micro-reticulate verrucate sculpturing in spiny *M. parviflora* grains disagree with our findings.

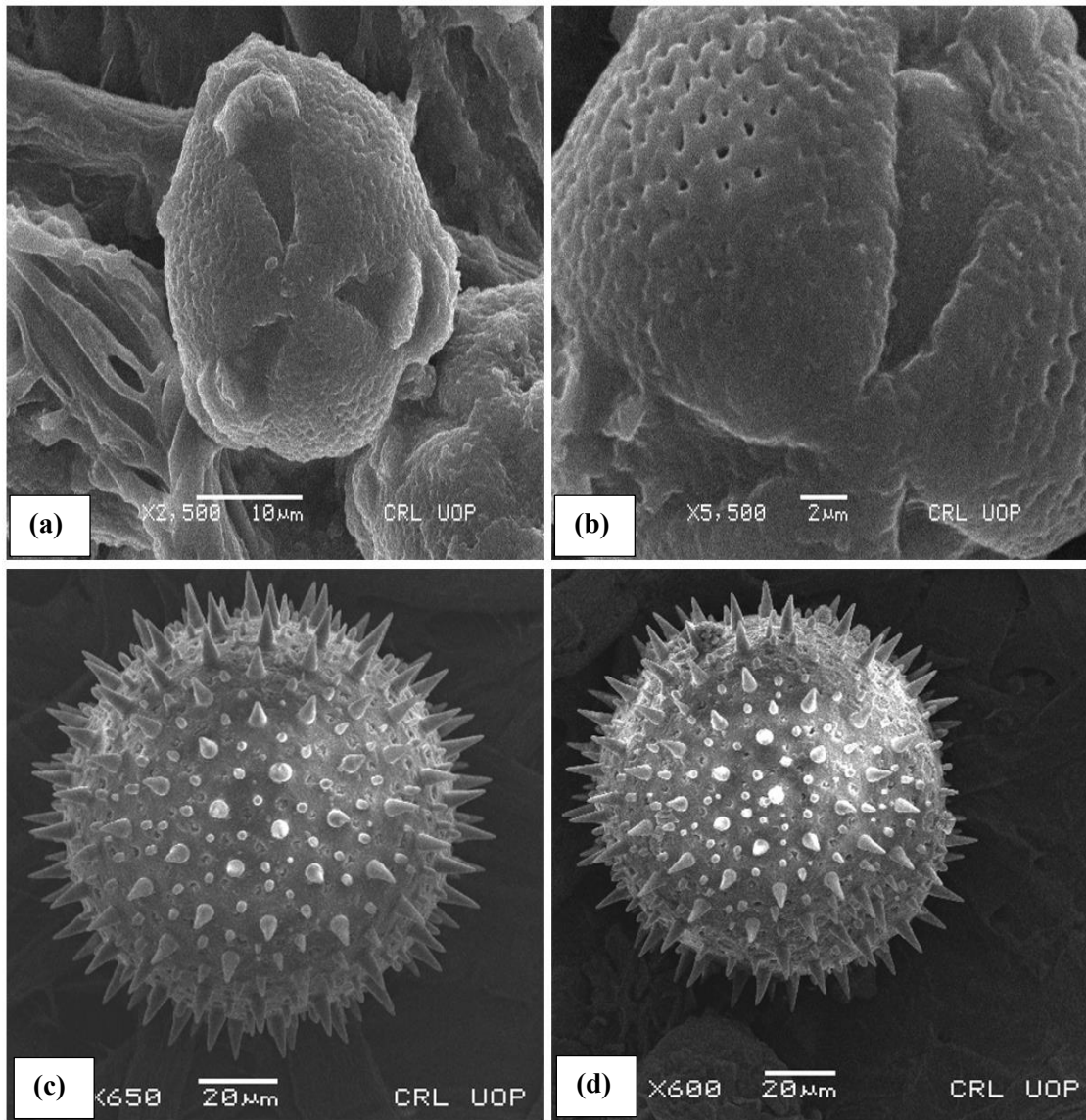


**Plate 60.** Scanning electron microscope photographs of Bignoniaceous and Malvaceous taxa (a-b) *Tecomella undulata*; rugulate reticulate pollen stratification (Scale bar = 10 μm, 2 μm), (c-d) *Malva parviflora*; echinate sculpturing (Scale bar = 20 μm)

### 3.2.27 Pollen Micromorphology of Myrtaceae Species

#### a) *Eucalyptus globulus* Labill.

Pollen grains monad, small to medium, and tricolporate. Triangular polar view and equatorial view shape oblate-spheroidal. Aperture obliquely oriented. Exine ornamentation scabrate-verrucate. Polar diameter (19.2-28.7)24.2±1.39 µm and equatorial view distance (23.6-29.4)26.1±1.334 µm. P/E ratio 0.92. Polar area index (0.43). Colpi length (5.7-7.5)6.4±1.09 µm and colpi width (3.5-8.7)5.3±1.12 µm. Exine thickness (3.15-6.5)4.9±1.26 µm. Mesocolpium distance (10.5-17.1)13.4±1.49 µm. Pollen fertility 88.6% and sterility 11.3%. Myrtaceae pollen morphotypes explained by Adeleye et al., (2020) define scabrate to psilate exine, parasyncolpate aperture and large apocolpial field. Typically, *Eucalyptus* pollen is triangular, radial symmetric, 3-parasyncolpate, apocolpial edges, surface peculiarities that define and separate a number of *E. globulus* pollen types (Eliseu and Dinis, 2008). While this study revealed variability in *E. globulus* pollen grains wall as scabrate verrucate. Azzazy (2016) explained the environmental impact on *E. globulus* pollen examined the reticulate sculpture surface.

### 3.2.28 Pollen Micromorphology of Nitrariaceae Species

#### a) *Peganum harmala* L.

Pollen are monad, small and tricolporate. Oval/Oblate polar view and sub-oblate equatorial view shape. Narrow long ectocolpus, colpi border thickened, sexine thicker, and slightly sunken aperture orientation. Exine sculpturing rugulate perforate. Polar diameter 15.7-17.75)16.8±0.79 µm equatorial view distance 19-20.75)19.95±0.64 µm. P/E ratio 0.83. Polar area index (0.84). Colpi length (1.75-2.75)2.25±0.39 µm, colpi width 3(1.75-3)2.35±0.51 µm and mesocolpium distance (15.5-17.75)16.45±0.99 µm. Exine thickness (0.5-1.25)0.75±0.3 µm. Pollen fertility 97.1% and sterility 2.8%. The study of Lu et al., (2018) on pollen morphological description of *Peganum harmala* described spheroidal, reticulate ornamentation which differs from present findings, which elucidate sub-oblate and regulate perforate grains. Semerdjieva and Yankova-Tsvetkova (2017) uncovered pollen traits in *P. harmala*, including multilayered apocolpium, and reticulate and heterobrochate pollen. In our study, dissimilarities in reticulate scabrate exine peculiarities were identified.

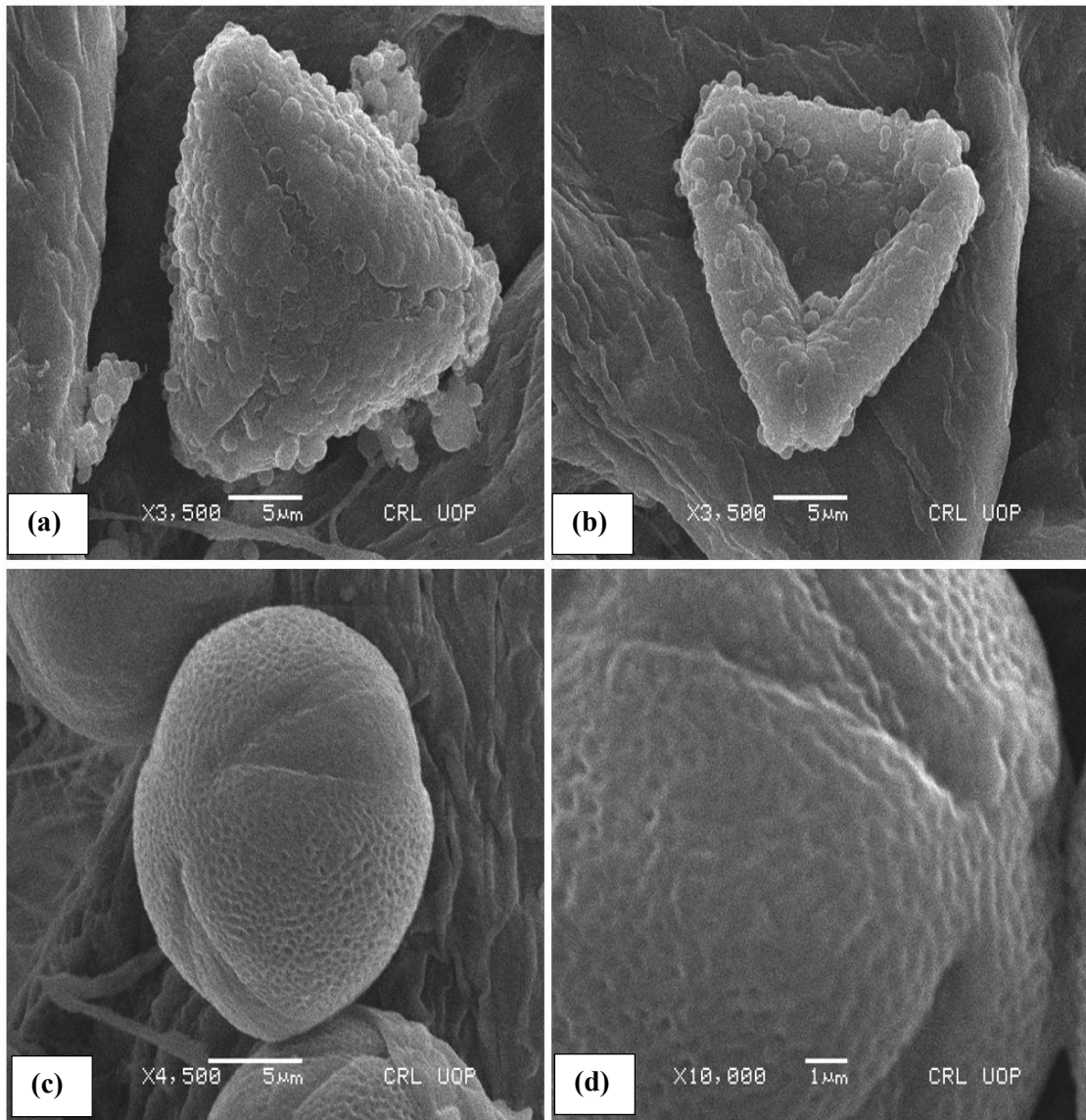


**Plate 61.** Scanning electron microscope photographs of Myrtaceous and Nitrariaceae taxa (a-b) *Eucalyptus globulus*; scabrate verrucate exine tectum (Scale bar = 5 μm), (c-d) *Peganum harmala*; rugulate perforate wall stratification (Scale bar = 5 μm, 1 μm)

### 3.2.29 Pollen Micromorphology of Nyctaginaceous Species

#### a) *Boerhavia procumbens* Banks ex Roxb.

Pollen grains monad, radially symmetric, large sized, apolar and polyporate. Polar view spheroidal and prolate-spheroidal equatorial view shape, sexine thicker than nexine. Pore orientation sunken. Exine tectum sculpture spinulose. Polar diameter (50.2-74.2)62.3±4.5 µm and equatorial view distance (51.2-70.4)60.9±3.11 µm, P/E ratio 1.02. Polar area index (0.44). Pore length (2.15-4.9)3.6±0.35 µm and pore width (1.4-4.5)2.9±0.67 µm. Exine thickness (3.5-8.4)5.7±0.73 µm. Pollen fertility 89.2% and sterility 10.7%. Perveen and Qaiser (2001) studied the morphology-palynology of the Nyctaginaceae in Pakistan and included species, namely *B. procumbens*. The present study confirms the pollen shape and sculpturing of this species given by Perveen and Qaiser (2001), but in some instances, the diameter of the pollen grains, the pore diameter, and the exine thickness differ. Slight differences in measurements between this study and the previous one can be ascribed to natural variation between geographical areas. Perveen and Qaiser (2001) elaborate oblate-spheroidal, pantoporate, circular sunken, granulate poral membrane, and spinulose tectum in *B. procumbens* were similar to our current examination. However, Singh and Dixit (2018) also visualized the echinate surface tectum. Basir and Khan (2003) briefly elaborate on the 5-colporate pollen type in *B. procumbens* was inconsistent with present findings.

### 3.2.30 Pollen Micromorphology of Papaveraceous Species

#### a) *Argemone mexicana* L.

Pollen monad, medium-sized and tricolpate. Circular polar view and equatorial view prolate-spheroidal. Rounded end colpi, obliquely oriented and slightly sunken aperture. Exine sculpturing reticulate-verrucate gemmate. Polar diameter (35-36)35.45±0.16 µm and equatorial view distance (34-35.25)34.55±0.21 µm. P/E ratio 1.02. Polar area index (0.64). Colpi length (3.5-4.25)3.95±0.14 µm and colpi width (4.25-5.5)4.95±0.21 µm. Exine thickness (2-3)2.4±0.2 µm. Mesocolpium distance (21.75-23)22.45±0.21 µm. Pollen fertility 93.2% and sterility 6.7%. Chaturvedi et al., (1999) explained Pollen of *A. mexicana* are tri to tetra-zonocolpate aperture type, small to medium, with reticulate scanning ornamentation, with closely packed muri regions and crustate colpus membrane. The pollen grains are distinguishable on the basis of pollen size only, the grains being small to medium in *A. mexicana* (24 × 27 µm) as

compared to our findings revealed a difference. Noor Almousawi and Alwan (2011) dealt with the morphology of 22 species of *Argemone* and pollen structure in the Papaveraceae. They described *A. mexicana* pollen sub-prolate, small to medium, and obscurely reticulate sculpturing as dissimilar to our observation.

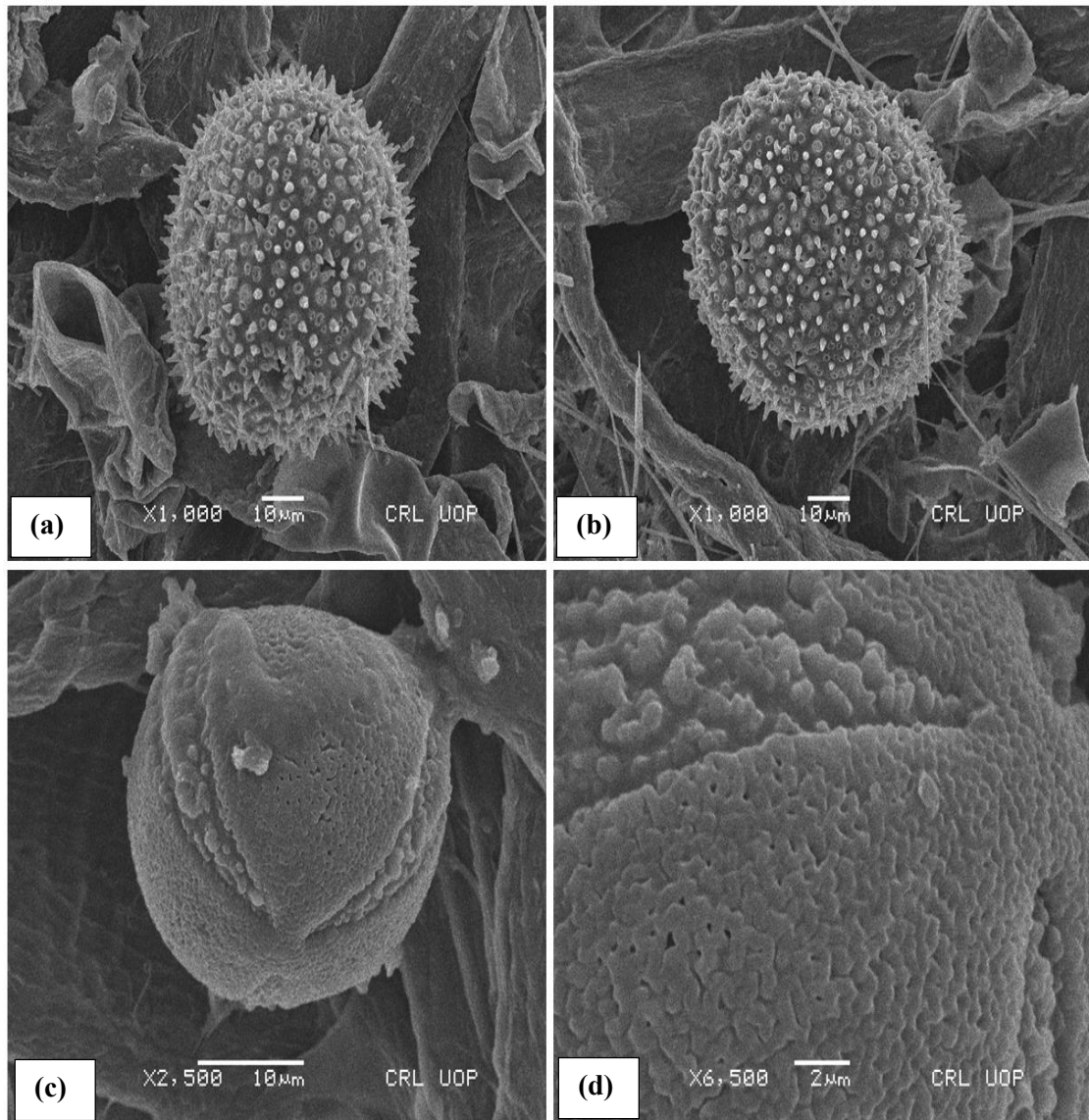


**Plate 62.** Scanning electron microscope photographs of Nyctaginaceus and Papaveraceous taxa (a-b) *Boerhavia procumbens*; spinulose tectum (Scale bar = 10 µm), (c-d) *Argemone mexicana*; reticulate-verrucate gemmate exine stratification (Scale bar = 10 µm, 2 µm)



**Section III**  
**Seed Micromorphology**

### 3.3 Seed Micromorphology of Dicot Angiosperms

An overview of the general parameters regarding seed micromorphology, followed by family, class, habit, status and studied region of the species are provided (Table 14). We found a total of 30 publications describing 200 angiosperm species from Pakistan, representing 25 botanical families. Two families of gymnosperms (two species) and 23 families of angiosperms were reported. Amongst angiosperms, three families of monocots (35 species) and 22 dicot families (165 species) were mentioned, representing 18% and 82% of the total, respectively (Figure 33). We then constructed a database that includes information about the seed morphometric parameters identified in the literature. The following families have the most seed morphotypes: Fabaceae (54), Poaceae (33), Amaranthaceae (18), Asteraceae (15), Caryophyllaceae (14), Clemoaceae and Myrtaceae (10 species each), and Verbenaceae (six species) as shown in Figure 34. The status of the angiosperm plants revealed that 90 species were herbs, followed by trees (45), shrubs (33), and grasses (32). The habit of plant species was listed as mostly annuals, followed by perennials and biennials.

In this study dicot angiosperm species were determined based on the field survey and interviews with the indigenous communities with regards to those angiosperm species most commonly grown in this desert rangeland. Micromorphological features such as shape, color, texture, apex, hilum, sculpturing, anticlinal wall, cell outline, epicuticular projections, texture crudeness, and periclinal wall pattern were extremely variable among dicot species (Table 15 & 16). Seed ultra-sculptured micrographs for 30 desert angiosperm species are shown in Plates 63 to 71.

#### 3.3.1 Seed Shape and Color Variations

Variation has been observed in the shape of seeds. *C. burhia*, *M. nudicaulis* and *W. coagulans* had reniform shapes, whereas *A. jacquemontii*, *A. nilotica*, *A. indica*, *C. colocynthis*, *P. juliflora* and *S. italic* had obovate and *D. sissoo*, *F. stylosa*, *P. cineraria* and *T. purpurea* had oblong shapes. *A. hamosus* has a reniform-globose, whereas *A. lebbek* (elliptical depressed), *B. nigra* (round), *C. decidua* (ovoid), *C. album* (oblate), *F. bruguieri* (broadly ovoid), *H. europaeum* (curved), *L. pyrotechnica* (ovoid flattened), *M. cerviana* (D-shaped), *A. modesta* and *P. aculeata* (ellipsoidal), *P. harmala* (rhomboid), *P. biternatum* (oval) and *T. terrestris* have an ovate flattened shape. A



rounded seed apex shape was observed in most species, followed by the elliptical, oval, oblong and pointed apex shape.

The variation in seed color ranged from dark brown to yellowish. Most of the species had yellowish brown seeds (*F. stylosa*, *P. biternatum* and *T. purpurea*), while dark brown was observed in *A. modesta*, *A. nilotica*, *F. bruguieri* and *S. italica*, black in *C. decidua* and *C. album*, brown in *A. lebbeck*, *B. nigra*, *D. sissoo*, *M. cerviana* and *P. cineraria*, greenish brown in *A. jacquemontii*, *A. homosus* and *T. terrestris*, light brown in *C. colocynthis* and *H. europaeum*, yellowish orange in *A. indica*, brown green in *C. burhia*, brown in *L. pyrotechnica*, greyish black in *P. aculeate*, blackish brown in *P. hermala* and yellowish in *W. coagulans*.

### 3.3.2 Seed Surface Pattern

The seed texture pattern of the desert species analyzed indicated significant variations that proved to be taxonomically significant (Table 15). The seed texture showed different patterns: rough texture cells were observed in *A. modesta*, *C. decidua*, *F. bruguieri*, *M. cerviana*, *P. cineraria*, *P. juliflora*, *S. italica* and *W. coagulans*, while they were scabrous in *A. jacquemontii*, *A. lebbeck*, *A. indica*, *B. nigra*, *C. album*, *C. burhia*, *H. europaeum*, *L. pyrotechnica*, and *P. hermala*, smooth in *A. homosus*, *C. colocynthis*, *D. sissoo*, *M. nudicaulis*, *P. aculeata* and *T. purpurea*, rough pitted in *A. nilotica*, glabrous in *F. stylosa*, spiny in *P. biternatum* and scabrous spiny in *T. terrestris*.

Three types of seeds were observed based on hilum position: terminal, sub-terminal, and central. *A. jacquemontii*, *A. modesta*, *A. nilotica*, *A. lebbeck*, *A. indica*, *C. decidua*, *C. album*, *C. burhia*, *F. bruguieri*, *L. pyrotechnica*, *M. cerviana*, *M. nudicaulis*, *P. aculeata*, *P. cineraria*, *P. juliflora*, *S. italica*, *T. terrestris* and *W. coagulans* had terminal hilum. *A. homosus*, *C. colocynthis*, *D. sissoo*, *H. europaeum*, *P. hermala*, and *T. purpurea* had nearly sub-terminal hilum, while *B. nigra*, *F. stylosa*, and *P. biternatum* had a central type. The hilum level was observed to be mostly depressed, followed by raised and undetermined.

### 3.3.3 Seed Surface Ultrastructure

Anticlinal wall patterns in seed coat epidermal cells in dicot angiosperm can be categorized into 21 types: striate foveolate, striate regulate, striate, foveolate rugose, reticulate, foveolate, foveolate striate, papillate, papillate rugose, papillate scabrate,

papillate foveolate, rugose, rugose papillate, rugose scabrate, striate reticulate, rugose striate, papillate smooth, undulated granulate and wrinkled spiny (Table 16). Papillate smooth surface features were observed only in *T. purpurea* and wrinkled spiny in *T. terrestris*. Therefore, we should not consider these anticlinal sculpture elements as prominent types but rather as unique features. While periclinal wall patterns were flat, concave, slightly concave, flat to convex, deeply convex, flat to concave, slightly convex, protuberance, flat to slightly convex, and convex type. The majority of the species have thick ornamented walls. Observed epicuticular projections vary from glabrous to bulges, prickles, glabrous and prickles, multicellular spiny, and bulges to prickles. *A. jacquemontii*, *A. modesta*, *A. nilotica*, *A. lebbeck*, *C. burhia*, *D. sissoo*, *P. cinraria* and *S. italica* has a unique fracture line continuous pattern, while *P. aculeata* has an irregular reticulate pattern. Cell outlines were mostly random, with in-rows, raised, flattened, and protuberant. Cells in the majority of dicot species were irregularly arranged. Diverse forms of coarseness were observed; coarse (17 species), very fine, and medium (four species each), medium (three species) and fine sinuate in *A. nilotica* and fine texture in *T. purpurea*.

### 3.3.4 Variations in Quantitative Parameters

Mean seed length ranged from a minimum of  $1.5 \pm 0.07$  mm for *M. cerviana* to a maximum of  $15.2 \pm 0.21$  mm for *A. nilotica*. Seed width varied from a minimum of  $0.6 \pm 0.05$  mm for *M. cerviana* to a maximum of  $13.7 \pm 0.1$  mm for *A. nilotica* (Figure 35). The length to width ratio ranged from 1.1 to 2.52 in *A. nilotica* and *A. hamosus*, respectively (Figure 36). The weight of the seeds revealed considerable variation. Among dicot species, *A. modesta* had the largest seed weight (0.93 mg), while *C. album* had the lowest (0.09 mg) (Table 15).

### 3.3.5 Dendrogram and PCA Clustering

UPGMA provided an insight into the degree of similarity among the species and showed whether they formed groups or clusters, indicating the range of variations. PCA indicated which characters were important on the axes, which were the most significant based on the highest factor loading.

The numerical findings of the seed morphology via UPGMA Euclidean distances using 15 characters and 109 character-states resulted in the formation of a

dendrogram (Table 17, 18 and Figure 37). The dendrogram shows similarities and differences in the traits of the dicot angiosperms, grouping the tree into two clusters, cluster I and cluster II. Cluster I has 24 species, while Cluster II contains three species. Hilum position accounts for the majority of the difference between these two clusters. Cluster I species reveal terminal, sub-terminal, and central positions hilum, whereas the species in cluster II show terminally raised hilum. Cluster I is divided into IA and IB, IA with seven species and IB with 17 species. Cluster IA is divided further into two subclusters, IA1 and IA2. There are two further sub-groups in Cluster IA1; one group, *C. burhia*, *A. modesta* and *A. jacquemontii* linked with a *L. pyrotechnica*, *P. cineraria* and *T. terrestris*, and a second group, comprising *W. coagulans*. In the first group, the similarity between *A. jacquemontii*, *A. modesta* and *C. burhia* was compared with their hilum position, epicuticular projection, and periclinal wall pattern. Similarly, cluster IA2 also has two groups; one containing *A. homosus*, *B. nigra*, *C. decidua* and *C. album*, linked with *F. bruguieri* and *A. nilotica*, and the second one comprising *D. sissoo*, *M. cerviana*, *F. stylosa*, *M. nudicaulis* linked to *H. europaeum*, *T. purpurea*, *P. aceulata*, *P. hermala*, *A. lebbeck* and *P. biternatum*. In cluster IA1, *C. decidua* and *C. album* have similar correlated features of hilum occurrence and epicuticular projections.

Principal component analysis (PCA) is one of the most fundamental statistical tools for assessing a group of elements and attempting to describe the variance. PCA is often visualized using two-or three-dimensional projections of sample data with principal axes. The same 15 characters and 109 state characteristics used in UPGMA clustering were used for PCA. PCA was performed to evaluate seed micro-morphological variability among dicot angiosperms by measuring seed color, shape, texture, apex, hilum, peculiarities, and periclinal and anticlinal wall. The variable loadings for each component are seen in Table 19. PC1 to PC15 showed eigenvalues greater than one were of maximum significance. Multivariate analysis among 15 variance components was 99.93% (Table 17 and 18). PC1 accounts for approximately 17.42 % of the variance in the data. The eigenvalues range between 0.10 and 2.10. PCA analysis of qualitative seed morphological aspects revealed a link between dicot angiosperms (Figure 38).

**Table 14.** Comprehensive review literature on seed micro-morphological features of angiosperms.

Sr. No	Angiosperm species	Family	Class	Common name	Habit	Status	Seed Micro-morphological Characters	Study Region	Citation
1.	<i>Acacia ampliceps</i> Maslin	Fabaceae	Dicot	Salt wattle	Perennial	Shrub	Grayish brown, shiny black in color, Hilum terminal, texture glabrous, O-shape pleurogram, and irregular shape fracture line reticulate ridges	FR Bannu/KPK	(Alam et al., 2018)
2.	<i>Acacia catechu</i> (L.f.) Willd.	Fabaceae	Dicot	Senegalia catechu	Perennial	Tree	Dark grey in color, Hilum sub-terminal, texture medium, U-shape pleurogram, and fracture line parallel ridges	Faisalabad/Punjab	
3.	<i>Acacia farnesiana</i> (L.) Willd.	Fabaceae	Dicot	Needle bush	Perennial	Shrub	Deep brown in color, Hilum terminal, texture medium, O-shaped pleurogram, and irregular fracture line pattern.	Mardan/KPK	
4.	<i>Acacia modesta</i> Wall.	Fabaceae	Dicot	Phulai	Perennial	Tree	Greenish outer color, brown, yellow internal color, hilum level elliptical and raised. Seed spherical, sculpture rugose, coarse texture and pleurogram lunar shape and fracture lines with parallel ridges.	Karak/KPK, Pakistan	(Alam et al., 2018; Arshad et al., 2019)
5.	<i>Acacia nilotica</i> (L.) Delile	Fabaceae	Dicot	Gum Arabic tree	Perennial	Tree	Blackish brown seed color hilum of dome shape and raised. Elliptical shape, rugose ornamentation, coarse texture, O-shape pleurogram and reticulate fracture lines.	Dikhan/Punjab, Pakistan	
6.	<i>Acacia stenophylla</i> Benth.	Fabaceae	Dicot	Shoestring acacia	Perennial	Tree	Dark brown in color, Hilum sub-terminal, texture coarse, elliptic pleurogram, and irregular reticulate fracture line.	Peshawar/KPK	(Alam et al., 2018)
7.	<i>Acacia tortilis</i> (Forssk.) Hayne	Fabaceae	Dicot	Umbrella thorn acacia	Perennial	Tree	Brown in color, Hilum terminal, texture coarse, O-shape pleurogram, and dispersed ridges in fracture line.	Bannu/KPK	
8.	<i>Acrachne racemose</i> (B.Heyne ex Roth) Ohwi	Poaceae	Monocot	Goose grass	Perennial	Grass	Oblong-elliptic, smooth and Light gray. Striate sculpture Irregular Straight wall pattern.	Dera Ghazi Khan, Pakistan	(Ahmad et al., 2019)
9.	<i>Aerva javanica</i> (Burm.f.) Juss. ex Schult.	Amaranthaceae	Dicot	Kapok Bush	Perennial	Shrub	Seeds compressed, hilum sub-central, surface colliculate or punctulate	Pakistan	(Kanwal and Abid, 2017)
10.	<i>Aerva sanguinolenta</i> (L.) Blume	Amaranthaceae	Dicot	Karadia	Perennial	Herb	Seeds black shiny, not compressed, hilum sub-basal and surface favulariate		
11.	<i>Albizia lebbeck</i> (L.) Benth.	Fabaceae	Dicot	Indian siris	Perennial	Tree	Seed color brown yellowish. Hilum; elliptical and raised. Ovate shape and rugose sculpture.	Loon Khan/ district Sanghar, Pakistan	(Arshad et al., 2019; Waheed et al., 2021)

						Pleurogram O- shape, thin ornamentation wall and irregular fracture line pattern.		
12.	<i>Alternanthera paronychioides</i> A.St.-Hil.	Amaranthaceae	Dicot	Smooth joyweed	Perennial	Herb	Seed orbicular, lateral hilum and surface reticulate and punctulate	Pakistan (Kanwal and Abid, 2017)
13.	<i>Alternanthera pungens</i>	Amaranthaceae	Dicot	Khaki weed	Perennial	Herb	Seeds obovate with retuse apex and undulate rugose sculpture pattern	
14.	<i>Alternanthera sessilis</i> Kunth	Amaranthaceae	Dicot	Sessile joyweed	Perennial	Herb	Seed orbicular, compressed surface colliculate, favulariate and granulate	
15.	<i>Amaranthus caudatus</i> L.	Amaranthaceae	Dicot	Pendant amaranth	Annual	Herb	Seed obovate, hilum sub-basal and surface colliculate and favulariate	
16.	<i>Amaranthus graecizans</i> L.	Amaranthaceae	Dicot	Short-tepalled pigweed	Annual	Herb	Seed surface colliculate, reticulate or punctulate.	
17.	<i>Amaranthus hybridus</i> L.	Amaranthaceae	Dicot	Smooth pigweed	Annual	Herb	Seed obovate/orbicular and surface colliculate and reticulate or reticulate and punctulate	
18.	<i>Amaranthus retroflexus</i> L.	Amaranthaceae	Dicot	Redroot pigweed	Annual	Herb	Seeds with sub-central hilum, obovate and faintly reticulate.	
19.	<i>Amaranthus spinosus</i> L.	Amaranthaceae	Dicot	Spiny pigweed	Annual	Herb	Seed surface reticulate at edges, obovate, compressed and sub-basal hilum.	
20.	<i>Amaranthus tricolor</i> L.	Amaranthaceae	Dicot	Edible amaranth	Annual	Herb	Seeds black, surface undulate, orbicular and marginal hilum.	
21.	<i>Amaranthus viridis</i> L.	Amaranthaceae	Dicot	Green amaranth	Annual	Herb	Seeds dark brown, surface verrucate	
22.	<i>Arenaria leptoclados</i> (Rchb.) Guss.	Caryophyllaceae	Dicot	Lesser thyme-leaved sandwort	Annual	Herb	Seed color dark, hilum sub-central, cell surface tuberculate	Rawalpindi/Punjab (Ullah et al., 2019)
23.	<i>Arenaria neelgherrensis</i> Wight & Arn.	Caryophyllaceae	Dicot		Annual	Herb	Rounded shape seed, brownish color, anticlinal wall very deep and tuberculate cell surface.	Mardan/KPK
24.	<i>Arenaria orbiculata</i> Royle ex Edgew. & Hook.f.	Caryophyllaceae	Dicot	Roundleaf Sandwort	Annual	Herb	Epidermal cell wavy/elongated, slightly convex and echinate sculpture.	Muzaffarabad/Azad Kashmir
25.	<i>Arenaria serpyllifolia</i> L.	Caryophyllaceae	Dicot	Thyme-leaved sandwort	Annual	Herb	Color blackish, hilum sub-central, anticlinal wall deep and echinate.	Swat/KPK
26.	<i>Argemone ochroleuca</i> Sweet	Papaveraceae	Dicot	Pale Mexican prickly poppy			Blackish, subspherical, ellipsoid, concave depression, reticulations radial and entire wall structure. Sculpturing smooth helium basal, and outer periclinal wall flat.	Pakistan (Munir et al., 2019)
27.	<i>Argemone Mexicana</i> L.	Papaveraceae	Dicot	Mexican prickly poppy	Annual	Herb	Smooth walled, thin, elongated, polygonal, rectangular shaped cells; parallel arranged and slightly projected outwards.	Pakistan (Fatima et al., 2018)

28.	<i>Astragalus graveolens</i> Benth.	Fabaceae	Dicot	N/A	Annual	Shrub	Bean shaped, oblong, smooth and gray. Reticulate sculpture and wavy anticlinal wall.	Quetta (Baluchistan)	(Rashid et al., 2021)
29.	<i>Astragalus lasiosemius</i> Boiss.	Fabaceae	Dicot	N/A	Perennial	Shrub	Flat, elliptic, smooth and grayish black. Granulate sculpture and wavy anticlinal wall.	Quetta (Baluchistan)	
30.	<i>Astragalus leucocephalus</i> Bunge	Fabaceae	Dicot	N/A	Perennial	Shrub	Flat, oblong, smooth and grayish black. Granulate sculpture and straight anticlinal wall.	Bagh (Azad Kashmir)	
31.	<i>Astragalus psilocentros</i> Fisch.	Fabaceae	Dicot	N/A	Perennial	Shrub	Oval-flat, oblong, smooth and gray. Reticulate sculpture and wavy anticlinal wall.	Quetta (Baluchistan)	
32.	<i>Astragalus rhizanthus</i> Benth.	Fabaceae	Dicot	N/A	Perennial	Herb	Bean shaped, ovate, smooth and grayish black. Reticulate sculpture and wavy anticlinal wall.	Quetta (Baluchistan)	
33.	<i>Avena fatua</i> L.	Poaceae	Monocot	Common wild oat	Annual	Grass	Hairy and Gray. Smooth ornamentation.	Dera Ghazi Khan, Pakistan	(Ahmad et al., 2019)
34.	<i>Avena sativa</i> L.	Poaceae	Monocot	Oat	Annual	Grass	Yellowish brown, widely elliptic, reticulate and style persistent.	Chakwal/Punjab	(Usma et al., 2019)
35.	<i>Averrhoa carambola</i> L.	Oxalidaceae	Dicot	Carambola	Annual	Tree	Chocolate off white color, Hilum raised. Ovate in shape, rugose ornamentation, fine texture crudeness, O shape pleurogram and irregular fracture line.	Pakistan	(Arshad et al., 2019)
36.	<i>Azadirachta indica</i> A.Juss.	Meliaceae	Dicot	Neem	Perennial	Tree	Color shiny black and creamy. Hilum level elliptical and depressed. Shape; Elliptical, sculpture levigate, texture glabrous, pleurogram O shaped and irregular reticulate ridges pattern of fracture lines.		
37.	<i>Bauhinia purpurea</i> L.	Fabaceae	Dicot	Purple bauhinia	Perennial	Tree	Seed color dark brown, reticulate irregular surface ornamentation	Faisalabad/Punjab	(Ullah et al., 2019)
38.	<i>Bauhinia variegata</i> L.	Fabaceae	Dicot	Mountain ebony	Perennial	Tree	Golden color seed, reticulate regular surface ornamentation and depressed periclinal wall elevation	Islamabad/Pakistan	(Dawood et al., 2019; Ullah et al., 2019)
39.	<i>Beaumontia grandiflora</i> Wall.	Apocynaceae	Dicot	Nepal trumpet flower	Perennial	Shrub	Off white seed, flattened shape, Seed wing surface ornamentation aculeate ornamentation, hilum surface show irregular cells. Seed wing with thick to thin anticlinal wall.	Pakistan	(Cheema et al., 2021)
40.	<i>Brachiaria brizantha</i> (A.Rich.) Stapf	Poaceae	Monocot	Bread grass	Annual	Grass	Pale green, obovate, papillate and style persistent.	Chakwal/Punjab	(Usma et al., 2019)
41.	<i>Brachychiton populneus</i> (Schott & Endl.) R.Br.	Sterculiaceae	Dicot	Kurrajong	Perennial	Tree	Yellowish to brown-dark brown, reticulate surface and wavy anticlinal wall protuberance,	Pakistan	(Dawood et al., 2019)

						random cell outline, course periclinal wall surface and depressed periclinal wall elevation.		
42.	<i>Brassica Oleracea</i> L.	Brassicaceae	Dicot	Wild cabbage	Biennial	Herb	Pitch black, rounded seeds, glabrous surface, anticlinal walls identical, wings absent, ornamentation fabricated pattern, and rift and wax like pellicle on the surface.	Pakistan (Cheema et al., 2021)
43.	<i>Calotropis gigantea</i> (L.) Dryand.	Apocynaceae	Dicot	Giant calotrope	Perennial	Shrub	Blackish brown, obviate, ornamentation striate irregularly, minute granules, tiny apertures, anticlinal walls thin and smooth, periclinal walls elevated and thick and irregular cell arrangement.	Pakistan (Aziz et al., 2021)
44.	<i>Carthamus oxyacantha</i> M.Bieb.	Asteraceae	Dicot	Wild Safflower	Annual	Herb	Grayish, elliptic to oblong achene, smooth surface, anticlinal walls thick, seed surface cells elongated with rough texture. Seed ornamentation; ruminant-glebulate.	Pakistan (Cheema et al., 2021)
45.	<i>Carthamus tinctorius</i> L.	Asteraceae	Dicot	Safflower	Annual	Herb	Yellowish white, narrow obovate achene, shiny surface, anticlinal walls thin. Seed sculpture fine variegated and obovate hilum	
46.	<i>Cassia fistula</i> L.	Fabaceae	Dicot	Golden shower	Perennial	Tree	Ovate, Light brown color, hilum oval, lunar shaped pleurogram, reticulate surface ornamentation, fine texture line and thin ornamentation wall.	Loon Khan/district Sanghar, Bannu/KPK (Ullah et al., 2019; Waheed et al., 2021)
47.	<i>Celastrus paniculatus</i> Willd.	Celastraceae	Dicot	Intellect plant	Perennial	Shrub	Elongated, brownish color, flattened, polygonal, elliptic shaped and asymmetric. Periclinal wall protuberance, smooth, reticulate, irregular, papillae absent, cell margins straight to angular, anticlinal wall slightly deep and periclinal wall flat to slightly concave.	Pakistan (Munir et al., 2019)
48.	<i>Celosia argentea</i> L.	Amaranthaceae	Dicot	Silver cock's comb	Annual	Herb	Seeds orbicular-sub orbicular, compressed, black and shiny, surface foveate and reticulate. Hilum conspicuous and marginal.	Pakistan (Kanwal and Abid, 2017)
49.	<i>Cenchrus ciliaris</i> L.	Poaceae	Monocot	Buffel grass	Perennial	Grass	Elliptic-linear, hairy and light gray. Reticulate striate sculpture with wavy-irregular, striate and style base persistent and undulate epidermal wall.	Dera Ghazi Khan, Pakistan, Chakwal/Punjab (Ahmad et al., 2019; Usma et al., 2019)
50.	<i>Cenchrus echinatus</i> L.	Poaceae	Monocot	Spiny sandbur	Annual	Grass	Green, obovate, striate surface and style base persistent on stylopodium.	Chakwal/Punjab (Usma et al., 2020)

51.	<i>Cenchrus pennisetiformis</i> Steud.	Poaceae	Monocot	White or slender buffel grass	Annual	Grass	Green, widely obovate, rugose and style base persistent.	Rawalpindi/Punjab	(Usma et al., 2019)
52.	<i>Cenchrus setiger</i> Vahl	Poaceae	Monocot	Birdwood grass	Perennial	Grass	Elliptic, smooth and gray. Smooth sculpturing and Irregular to slightly undulate walls.	Dera Ghazi Khan, Pakistan	(Ahmad et al., 2019)
53.	<i>Cerastium fontanum</i> Baumg.	Caryophyllaceae	Dicot	Mouse-ear chickweed	Perennial	Herb	Anticlinal wall thin, cell surface tuberculate, margins dome Shapes.	Lower Dir/KPK	(Ullah et al., 2019)
54.	<i>Cerastium glomeratum</i> Thuill.	Caryophyllaceae	Dicot	Sticky mouse-ear chickweed	Annual	Herb	Seed color brownish, hilum nearly basal and echinate ornamented wall.	Islamabad/Capital territory	(Ullah et al., 2019)
55.	<i>Ceratonia siliqua</i> L.	Fabaceae	Dicot	Carob	Perennial	Tree	Ovoid seed shape, invisible pleurogram and rugose surface ornamentation.	Peshawar/KPK	(Ullah et al., 2019)
56.	<i>Cestrum nocturnum</i> L.	Solanaceae	Dicot	Night-blooming jasmine		Shrub	Triangular and black color seeds. Striate, wrinkled pattern sculpture, rough cell outline, reticulate cell arrangement, wavy thick depressed anticlinal wall and smooth and raised periclinal wall	Pakistan	(Rozina et al., 2021)
57.	<i>Chamaerops humilis</i> L.	Arecaceae	Monocot	European fan palm	Perennial	Shrub	Light yellowish, ovate, surface ornamentation reticulate irregular, bulging protuberance outlines, cell arrangement irregular, cell shape pentagonal, thick and rough anticlinal walls, and periclinal walls thin and depressed	Pakistan	(Aziz et al., 2021)
58.	<i>Chenopodium album</i> L.	Amaranthaceae	Dicot	White goosefoot	Annual	Herb	Seeds obovate, smooth and marginal conspicuous hilum	Pakistan	(Kanwal and Abid, 2017)
59.	<i>Chenopodium ambrosioides</i> L.	Amaranthaceae	Dicot	Mexican tea	Perennial	Shrub	Seeds obovate, compressed and surface punctuate with appressed ruminant lines		
60.	<i>Chenopodium murale</i> L.	Amaranthaceae	Dicot	Nettle-leaved Goosefoot	Annual	Herb	Surface compressed, orbicular, favulariate and hilum with marginal position.		
61.	<i>Cicer arietinum</i> L.	Fabaceae	Dicot	Chickpea	Annual	Herb	Seed shape bean shaped, texture smooth and striate ornamented wall	Chakwal, Rawalpindi	(Rashid et al., 2018)
62.	<i>Cichorium balaricum</i> Porta	Asteraceae	Dicot	Chicory	Perennial	Herb	Cuneiform shaped with yellow color seeds. Rugose, papillate sculpturing, narrow elliptic and layered cell shape, regular cell arrangement, raised, curved anticlinal wall and depressed, glabrous periclinal wall.	Pakistan	(Rozina et al., 2021)
63.	<i>Cichorium intybus</i> L.	Asteraceae	Dicot	Bunk Chicory	Perennial	Herb	Brown mottled to brown, obovoid to cylindrical, scabrous surface, rugose papillate surface	Chitral/KPK	(Ayaz et al., 2019)



						pattern and undeveloped angular ring shaped carpodium.		
64.	<i>Cissus trifoliata</i> (L.) L.	Vitaceae	Dicot	Possum grape	Perennial	Vine	Seed margins ellipsoidal pyriform and sculpturing slightly rugose. Grooved and thin anticlinal wall. Polygonal elongated integument cell shape.	Islamabad (Lubna et al., 2018)
65.	<i>Citharexylum spinosum</i> L.	Verbenaceae	Dicot	Spiny fiddlewood	Perennial	Shrub	Seeds triangular, rough and black color. Reticulate cell outline, striate cell arrangement, reticulate with nonporous protuberances. Anticlinal walls raised and rough.	Central library QAU, Islamabad (Kanwal et al., 2021)
66.	<i>Citrullus colocynthis</i> (L.) Schrad.	Cucurbitaceae	Dicot	Desert gourd	Perennial	Herb	Brown, clavate, ornamentation rugose, bulging protuberance, cell arrangement irregular, reticulate, anticlinal walls thick, depressed and periclinal thick and elevated.	Pakistan (Aziz et al., 2021)
67.	<i>Citrus paradisi</i> Macfad.	Rutaceae	Dicot	Grapefruit	Perennial	Tree	Broad ovate, yellow in color, reticulate sculpturing, granular projections and irregular cell arrangement, thick and smooth anticlinal walls and elevated flat periclinal walls.	Pakistan (Rozina et al., 2021)
68.	<i>Citrus aurantium</i> L.	Rutaceae	Dicot	Bitter orange	Perennial	Tree	Seeds ovate, greenish, perforate, semi-tectate surface, bulging protrusions, cells spherical to oval in shape, crooked cell arrangement, depressed, anticlinal wall wavy and periclinal walls with thick elevation.	
69.	<i>Citrus medica</i> L.	Rutaceae	Dicot	Citron	Perennial	Tree	Semi deltoid and greenish. Reticulate sculpturing, cells arranged in irregular fascicles, longitudinal lines in sulcate to ribbed pattern, smooth anticlinal walls and deep elevated periclinal wall.	
70.	<i>Cleome ariana</i> Hedge & Lamond	Cleomaceae	Dicot	N/A	Annual	Herb	Seeds light brown, Ob-elliptic pyriform, small groove present, sculpture papillate and hilum lateral.	Pakistan (Riaz and Abid, 2018)
71.	<i>Cleome brachycarpa</i> (Forssk.) Vahl ex DC.	Cleomaceae	Dicot	Ponwar	Annual	Herb	Seeds rust brown, elliptic-pyriform or ovoid, very small groove present and sculpture element reticulate to favulariate.	
72.	<i>Cleome dolichostyla</i> Jafri	Cleomaceae	Dicot	N/A	Annual	Herb	Seeds appressed, light brown, reticulate, glabrous, hilum lateral, Reniform and extreme narrow groove.	

73.	<i>Cleome fimbriata</i> Vicary	Cleomaceae	Dicot	N/A	Annual	Herb	Seeds reniform, mustard brown, hilum lateral, reticulate and pusticulate , magnesium absent		
74.	<i>Cleome oxypetala</i> Boiss.	Cleomaceae	Dicot	N/A	Annual	Herb	Seeds obovate, golden brown, tomentose hairy surface and groove very short		
75.	<i>Cleome pakistanica</i> (Jafri) Khatoon & A.Perveen	Cleomaceae	Dicot	N/A	Annual	Herb	Seeds orange brown, angular, densely pubescent surface and elliptic pyriform		
76.	<i>Cleome rupicola</i> Vicary	Cleomaceae	Dicot	N/A	Perennial	Shrub	Seeds reniform, dust brown, pillose hairy surface, groove long and hilum lateral.		
77.	<i>Cleome scapose</i> DC.	Cleomaceae	Dicot	N/A	Annual	Herb	Seeds metal green or black, reniform with narrow groove, alveolate surface and lateral hilum level.		
78.	<i>Cleome spinosa</i> Jacq.	Cleomaceae	Dicot	Spiny spider flower	Annual	Herb	Seeds angular, blackish brown, retortiform, wide rectangular groove and faintly reticulate sculpturing.		
79.	<i>Cleome viscosa</i> L.	Cleomaceae	Dicot	Asian spider flower	Annual	Herb	Seeds dark brown, retortiform beaked, widen groove and foveate sculpture surface.		
80.	<i>Corylus colurna</i> L.	Corylaceae	Dicot	Turkish filbert	Perennial	Tree	Brownish creamy color seeds with Subspherical, elliptic, ovate, orbicular outline, cells isodiametric polygonal, smooth rough surface, margins undulate, slightly dentate, anticlinal wall deep, and periclinal wall flat to slightly concave.	Pakistan	(Munir et al., 2019)
81.	<i>Cucumis pubescens</i> Willd.	Cucurbitaceae	Dicot	Cucumber	Perennial	Herb	Yellow, cuneiform, sculpturing pentagonal, cells elevata, cell arrangement regular layered, elevata flat anticlinal walls and periclinal walls are looped thick.	Pakistan	(Aziz et al., 2021)
82.	<i>Cymbopogon jwarancusa</i> (Jones) Schult.	Poaceae	Monocot	Oil grass	Perennial	Grass	Elliptic-linear, hairy and gray. Reticulate ornamentation, scabridulous and stylopodium absent, with irregular straight anticlinal wall.	Dera Ghazi Khan, Pakistan, Chakwal/Punjab	(Ahmad et al., 2019; Usma et al., 2019)
83.	<i>Dactyloctenium aegyptium</i> (L.) Willd.	Poaceae	Monocot	Egyptian crowfoot	Perennial	Grass	Circular, smooth and light gray. Granulate sculpture with wavy wall pattern and style base persistent on stylopodium.	Dera Ghazi Khan, Pakistan, Islamabad	
84.	<i>Dactyloctenium scindicum</i> Boiss.	Poaceae	Monocot	Sind Crowfoot Grass	Perennial	Grass	Hairy, light gray and elliptic. Striate wall pattern, style persistent with tuft of hairs on stylopodium and wavy wall.	Dera Ghazi Khan, Pakistan, Salt range area/Punjab	

85.	<i>Dalbergia sissoo</i> DC.	Fabaceae	Dicot	Shisham	Perennial	Tree	Kidney, brown, hilum oblong, Kidney shaped pleurogram and thick ornamentation wall.	Botar lake/ district Sanghar	(Waheed et al., 2021)
86.	<i>Datura innoxia</i> Mill.	Solanaceae	Dicot	Angel's trumpet	Perennial	Herb	Pyriiform, dull brownish, ellipsoid, reniform-sub reniform, comma shaped, and cells elongated polygonal. Sculpturing smooth rough, deeply dentate, anticlinal wall slightly deep and periclinal wall is flat to concave.	Pakistan	(Munir et al., 2019)
87.	<i>Delonix regia</i> (Hook.) Raf.	Fabaceae	Dicot	Royal poinciana	Perennial	Tree	Raised hilum level and lugose surface ornamentation.	Faisalabad/Punjab	(Ullah et al., 2019)
88.	<i>Desmostachya bipinnata</i> (L.) Stapf	Poaceae	Monocot	Big cordgrass	Perennial	Grass	Yellow, ovate, papillate rugose surface and style base with persistent on stylopodium.	Chakwal/Punjab	(Usma et al., 2020)
89.	<i>Dichanthium annulatum</i> (Forssk.) Stapf	Poaceae	Monocot	Marvel grass	Perennial	Grass	Purplish, oblong, papillate striate surface and style base persistent on stylopodium.	Islamabad	
90.	<i>Digera muricata</i> (L.) Mart.	Amaranthaceae	Dicot	False amaranth	Annual	Herb	Seeds orbicular and beaked at both sides, not compressed, greenish brown and shiny, surface and hilum basal	Pakistan	(Kanwal and Abid, 2017)
91.	<i>Duranta erecta</i> L.	Verbenaceae	Dicot	Golden dewdrop	Perennial	Shrub	Spheroid, rough with thin testa, dark brown and dull surface. Cell shape asymmetrical, cell outline faintly raised and webbed cell arrangement. Sculpturing granular reticulate.	Botanical research garden QAU, Islamabad	(Kanwal et al., 2021)
92.	<i>Echinochloa colona</i> (L.) Link	Poaceae	Monocot	Jungle rice	Annual	Grass	Smooth, gray and oval in shape. Smooth sculpture and anticlinal wall not visible	Dera Ghazi Khan, Pakistan	(Ahmad et al., 2019)
93.	<i>Echinochloa crus-galli</i> (L.) P.Beauv.	Poaceae	Monocot	Barnyard millet	Annual	Grass	Oval-elliptic, smooth and light gray. Ornamentation smooth and Irregular to straight epidermal wall.	Dera Ghazi Khan, Pakistan, Chakwal/Punjab	(Ahmad et al., 2019 Usma et al., 2019)
94.	<i>Eleusine indica</i> (L.) Gaertn.	Poaceae	Monocot	Yard grass	Annual	Grass	Oval, smooth and gray. Papillate sculpture, style base persistent on stylopodium and irregular to straight wall pattern.	Dera Ghazi Khan, Pakistan, Rawalpindi/Punjab	
95.	<i>Enneapogon persicus</i> Boiss.	Poaceae	Monocot	N/A	Perennial	Grass	Yellow, widely obovate, papillate surface and style base persistent on stylopodium.	Chakwal/Punjab	(Usma et al., 2020)
96.	<i>Eruca sativa</i> Mill.	Rosaceae	Dicot	Garden rocket	Annual	Herb	Very thick cell wall, with ridge around. Lumina, cells are slightly regular, circular, or somewhat triangular in shape	Pakistan	(Fatima et al., 2018)
97.	<i>Eucalyptus amplifolia</i> Naudin	Myrtaceae	Dicot	Cabbage gum	Perennial	Tree	Cuboid seed with black color, glabrous periclinal wall protuberance and puzzled anticlinal wall.	Baffa/Manshera	(Luqman et al., 2018)

98.	<i>Eucalyptus camaldulensis</i> Dehnh.	Myrtaceae	Dicot	River red gum	Perennial	Tree	Cuboid seed with yellowish brown color, wavy anticlinal wall and glabrous periclinal protuberance.	Damai/Bannu	
99.	<i>Eucalyptus citriodora</i> Hook.	Myrtaceae	Dicot	Lemon-scented gum	Perennial	Tree	Yellowish brown to light yellow in color. Hilum grooved and cuboid shaped, Oblong sculpture, texture glabrous, elliptical pleurogram and fracture line reticulate.	Pakistan	(Arshad et al., 2019)
100.	<i>Eucalyptus globulus</i> Labill.	Myrtaceae	Dicot	Tasmanian blue gum	Perennial	Tree	Surface cells diamond in shape with irregular arrangement	QAU/Islamabad	(Luqman et al., 2018)
101.	<i>Eucalyptus kitsoniana</i> Maiden	Myrtaceae	Dicot	Bog gum	Perennial	Tree	Seed shape elliptic, diamond surface cell shape and wavy anticlinal wall.	PFI/Faisalabad	
102.	<i>Eucalyptus melanophloia</i> F.Muell.	Myrtaceae	Dicot	Silver leaved iron bark	Perennial	Tree	Irregular surface cells, chocolate color seed and medium periclinal wall protuberance.	PFI/Peshawar	
103.	<i>Eucalyptus microtheca</i> F.Muell.	Myrtaceae	Dicot	Coolibah	Perennial	Tree	Elliptic surface cells, serrate anticlinal wall pattern and fine periclinal wall		
104.	<i>Eucalyptus pellita</i> F.Muell.	Myrtaceae	Dicot	Red mahogany	Perennial	Tree	Anticlinal wall puzzled, fine periclinal wall protuberance, surface cells oblong.	PFI/Faisalabad	
105.	<i>Eucalyptus pruinose</i> Schauert	Myrtaceae	Dicot	Silver leaf box	Perennial	Tree	Wavy anticlinal wall pattern, Bullate periclinal wall granulation.		
106.	<i>Eucalyptus tereticornis</i> Sm.	Myrtaceae	Dicot	Forest red gum	Perennial	Tree	Anticlinal wall pattern undulate, coarse periclinal wall, concave surface cells level.	PFI/Peshawar	
107.	<i>Faidherbia albida</i> (Delile) A.Chev.	Fabaceae	Dicot	Apple ring acacia	Perennial	Tree	Chocolate brown in color, Hilum terminal, texture coarse, elliptical pleurogram, and dispersed in ridges fracture line.	Faisalabad/Punjab	(Alam et al., 2018)
108.	<i>Gleditsia triacanthos</i> L.	Fabaceae	Dicot	Honey locust	Perennial	Tree	Levigata surface ornamentation and U-shaped pleurogram.	Faisalabad/Punjab	(Ullah et al., 2019)
109.	<i>Haematoxylon campechianum</i> L.	Fabaceae	Dicot	Log wood	Perennial	Tree	Central hilum position, rhombus surface ornamentation	Lahore/Punjab	
110.	<i>Imperata cylindrica</i> (L.) Raeusch.	Poaceae	Monocot	Cogon grass	Perennial	Grass	Brown, linear, papillate and tuft of hairs	Islamabad	
111.	<i>Isachne himalaica</i> Hook.f.	Poaceae	Monocot	N/A	Perennial	Grass	Light green, oblate, papillate and style base persistent.	Muzaffarabad/AJ K	
112.	<i>Lactuca dissecta</i> D.Don	Asteraceae	Dicot	Split leaf lettuce	Annual	Herb	Oblanceolate shape seeds and dark brownish in color. Cypselas with 3 prominent ribs on each side and muricate sculpture pattern.	Pakistan and Kashmir	(Abid and Qaiser, 2015)
113.	<i>Lactuca glaucifolia</i> Boiss.	Asteraceae	Dicot	N/A	Annual	Herb	Oblanceolate shape, yellow golden brown color seeds with muricate papillate ornamentation.		

						Cypsela long including beak, Beak; filiform without appendages		
114.	<i>Lactuca sativa</i> L.	Asteraceae	Dicot	Lettuce	Annual	Herb	Cypsela blackish oblanceolate; Carpodium with extensive interruption and scabrid pilose sculpturing.	
115.	<i>Lactuca serriola</i> L.	Asteraceae	Dicot	Prickly Lettuce	Annual	Herb	Cypsela brown and oblanceolate obovate. Scabrid pilose to verrucose papillate ornamentation and carpodium; U shaped with 2-narrow interruption.	Pakistan and Kashmir, Peshawar/KPK (Abid and Qaiser, 2015; Ayaz et al., 2019)
116.	<i>Lactuca undulata</i> Ledeb.	Asteraceae	Dicot	N/A	Annual	Herb	Shape; oblanceolate obovate and yellowish brown color. Papillate type sculpture. Cypsela up to 18 mm long including beak, Beak capillary basally with 2 white, pendent appendages	Pakistan and Kashmir (Abid and Qaiser, 2015)
117.	<i>Lantana camara</i> L.	Verbenaceae	Dicot	Tick berry, Spanish flag, Lantana,	Perennial	Shrub	Broadly ovate, rough, brownish black and shiny pubescence. Striate surface sculpturing, rectangular cell shape, cell outline smooth with layered and regular cell arrangement. Anticlinal walls depressed, smooth, and thick.	Hostel road, Islamabad Capital Territory Pakistan (Kanwal et al., 2021)
118.	<i>Lantana urticoides</i> Hayek	Verbenaceae	Dicot	Kunth, Texas lantana,	Perennial	Shrub	Shape ovoid, rough texture and hard, light to dark brown color. Asymmetrical cells, faintly raised cell outline. Cell arrangement irregular, reticulate surface pattern with granular projections. Anticlinal walls smooth and elevated and periclinal walls thin, flat, and faintly raised.	University road, Islamabad Capital territory
119.	<i>Lathyrus aphaca</i> L.	Fabaceae	Dicot	Yellow Pea	Annual	Herb	Seed outline slightly rounded, seed base round and striate	Near Mangla dam, Mirpur (Rashid et al., 2018)
120.	<i>Lathyrus emodi</i> (Fritsch) Ali	Fabaceae	Dicot	Himalayan Golden Pea	Annual	Herb	Seed texture hairy, color grayish black and striate sculpture	Chitral
121.	<i>Lathyrus odoratus</i> L.	Fabaceae	Dicot	Sweet pea	Annual	Herb	Seed shape oval, texture smooth and striate ornamentation	Chak Shezad, Islamabad
122.	<i>Launaea procumbens</i> (Roxb.) Ramayya & Rajagopal	Asteraceae	Dicot	Dandelion Creeping Launaea	Perennial	Herb	Greyish to brownish, narrowly lanceolate, glabrous surface, striated sculpture and carpodium of undeveloped circular ring shaped.	Peshawar/KPK (Ayaz et al., 2019)
123.	<i>Lens culinaris</i> Medik.	Fabaceae	Dicot	Lentil	Annual	Herb	Seed apex round, anticlinal wall pattern undulate and papillate sculpture.	Chakwal, Rawalpindi (Rashid et al., 2018)

124.	<i>Lepidium perfoliatum</i> L.	Brassicaceae	Dicot	Clasping pepper weed	Annual	Herb	Oblong-ovate, dark brownish seeds, slight projection, cells elongated, polygonal and irregular, sculpturing rough, margins undulate, wax warty granules, periclinal wall deep, outer wall convex, some elevated portions and sessile central.	Pakistan	(Munir et al., 2019)
125.	<i>Leucaena leucocephala</i> (Lam.) de Wit	Fabaceae	Dicot	River tamarind	Perennial	Tree	Dark brown, ovate, irregular polygonal, smooth surface pattern, puzzled cell outlines, wavy, dentate, deep anticlinal walls and thin, rough, slightly depressed periclinal walls.	Pakistan	(Aziz et al., 2021)
126.	<i>Luffa cylindrica</i> (L.) M.Roem.	Cucurbitaceae	Dicot	Vietnamese luffa	Annual	Herb	Blackish, Rugose sculpturing, in rows cell outline, regular cell arrangement, thick anticlinal wall, wavy anticlinal wall protuberance, smooth periclinal wall and elevated periclinal wall elevation	Pakistan	(Dawood et al., 2019)
127.	<i>Medicago lupulina</i> L.	Fabaceae	Dicot	Black Medic	Annual	Herb	Oval-round, ovate, hairy and gray. Slightly striate and straight sculpture and wavy anticlinal wall.	Bara Gali (Murree, Punjab)	(Rashid et al., 2021)
128.	<i>Medicago monantha</i> (C.A.Mey.) Trautv.	Fabaceae	Dicot	Single-flowered medick	Annual	Herb	Oval-round, oblong, smooth and gray. Smooth sculpture and straight anticlinal wall.	Chitral	
129.	<i>Medicago polymorpha</i> L.	Fabaceae	Dicot	Burr medic	Annual	Herb	Oval-round, ovate, smooth and gray. Striate sculpture and straight anticlinal wall.	Rawalpindi (Punjab)	
130.	<i>Melia azedarach</i> L.	Meliaceae	Dicot	Chinaberry	Perennial	Tree	Green yellowish, ovate elliptic, sculpturing striate, bulged reticulate projections, irregular cell arrangement, narrow elliptic smooth cell shape, flat and thin anticlinal walls and depressed elevated periclinal walls.	Pakistan	(Aziz et al., 2021)
131.	<i>Melilotus indicus</i> (L.) All.	Fabaceae	Dicot	Annual yellow sweet clover	Annual	Herb	Oval-round, ovate, smooth and dark gray. Papillate sculpture and undulate anticlinal wall.	Mirpur (Azad Kashmir)	(Rashid et al., 2021)
132.	<i>Melilotus officinalis</i> (L.) Pall.	Fabaceae	Dicot	Yellow sweet clover	Annual	Herb	Oval-round, ovate, smooth and gray. Reticulate sculpture and undulate anticlinal wall.	Chitral	
133.	<i>Minuartia kashmirica</i> (Edgew. & Hook. f.) Mattf.	Caryophyllaceae	Dicot	Kashmir Sandwort	Perennial	Herb	Anticlinal wall thick, margins convex and echinate sculpture surface.	Nellum valley/Azad Kashmir	(Ullah et al., 2019)
134.	<i>Minuartia meyeri</i> (Boiss.) Bornm.	Caryophyllaceae	Dicot	N/A	Annual	Herb	Seed color brownish, reniform and deep anticlinal wall with echinate sculpture.	Chitral/KPK	
135.	<i>Minuartia picta</i> (Sm.) Bornm.	Caryophyllaceae	Dicot	N/A	Annual	Herb	Hilum nearly basal and cell surface echinate.	Zhob/Baluchistan	

136.	<i>Momordica charantia</i> L.	Cucurbitaceae	Dicot	Bitter melon	Annual	Herb	Light brown color seeds, reticulate sculpture, granular projection, random cell outline, thin anticlinal wall, conspicuous protuberance, smooth periclinal wall surface and flat periclinal wall elevation.	Pakistan	(Dawood et al., 2019)
137.	<i>Oryza sativa</i> L.	Poaceae	Monocot	Asian rice	Perennial	Grass	White, linear, reticulate surface and style base persistent on stylopodium.	Jhelum/Punjab	(Usma et al., 2020)
138.	<i>Parthenocissus Semicordata</i> (Wall.) Planch.	Vitaceae	Dicot	Himalayan Woodbine	Perennial	Shrub	Seed margins obovoid and reticulate sculpturing. Raised and thin anticlinal wall. Polygonal integument cell shape.	Ayubia National Park track / Donga gali	(Lubna et al., 2018)
139.	<i>Parthenocissus quinquefolia</i> (L.) Planch.	Vitaceae	Dicot	Virginia creeper	Perennial	Shrub	Seed margins obovoid and reticulate sculpturing. Grooved and thin anticlinal wall. Polygonal integument cell shape.	Kaghan bazaar /Kaghan	
140.	<i>Parthenocissus tricuspidata</i> (Siebold & Zucc.) Planch.	Vitaceae	Dicot	Virginia Creeper	Perennial	Shrub	Seed margins obovoid and reticulate sculpturing. Raised and thick anticlinal wall. Polygonal integument cell shape.	Jinnah Abad / Abbottabad	
141.	<i>Paspalidium flavidum</i> (Retz.) A.Camus	Poaceae	Monocot	Yellow water crown Grass	Perennial	Grass	Green, widely obovate, papillate and style base persistent	Islamabad	(Usma et al., 2019)
142.	<i>Pennisetum glaucum</i> (L.) R.Br.	Poaceae	Monocot	Pearl millet	Annual	Grass	Yellowish brown, obovate, scabrate and style persistent.	Chakwal/Punjab	
143.	<i>Phalaris minor</i> Retz.	Poaceae	Monocot	Little seed canary grass	Annual	Grass	Elliptic, hairy and light gray. Striate ornamentation with wavy epidermal wall features.	Dera Ghazi Khan, Pakistan	(Ahmad et al., 2019)
144.	<i>Pistacia chinensis</i> Bunge	Anacardiaceae	Dicot	Chinese pistache	Perennial	Tree	Greenish color seeds, Irregular and polygonal shaped, dentate margins, deep anticlinal wall, outer periclinal wall flat to concave-slightly convex.	Pakistan	(Munir et al., 2019)
145.	<i>Pisum sativum</i> L.	Fabaceae	Dicot	Pea	Perennial	Herb	Seed shape round, texture hairy, and ornamentation papillate.	Bagh, Azad Kashmir	(Rashid et al., 2018)
146.	<i>Pithecellobium dulce</i> (Roxb.) Benth.	Fabaceae	Dicot	Madras Thorn	Perennial	Tree	Deformed, Dark black, dome and raised hilum, lunar shaped pleurogram and thick ornamentation wall.	Panhal/ district Sanghar	(Waheed et al., 2021)
147.	<i>Platyclusus orientalis</i> (L.) Franco	Cupressaceae	Monocot	Oriental arbor vitae	Annual	Tree	Brown, narrow elliptic, striate layered, regular surface sculpturing, rectangular cells cell outline, thin flat anticlinal walls, and depressed thick periclinal walls.	Pakistan	(Aziz et al., 2021)
148.	<i>Poa angustifolia</i> L.	Poaceae	Monocot	Narrow leaved meadow grass	Perennial	Grass	Green, obovate, reticulate surface and style base persistent with tuft of hairs on stylopodium.	Islamabad	(Usma et al., 2020)

149.	<i>Poa annua</i> L.	Poaceae	Monocot	Annual bluegrass	Annual	Grass	Brown, rounded, rugose surface and style base persistent on stylopodium.	Chakwal/Punjab	
150.	<i>Polypogon monspeliensis</i> (L.) Desf.	Poaceae	Monocot	Annual beard-grass	Annual	Grass	Elliptic, hairy and light gray in color. Granulate sculpture element and Irregular Straight wall.	Dera Ghazi Khan, Pakistan	(Ahmad et al., 2019)
151.	<i>Pongamia pinnata</i> (L.) Pierre	Fabaceae	Dicot	Pongame oil tree	Perennial	Tree	Chocolate to off white in color. Hilum level raised. Elliptic shape, sculpture rugose type, texture medium, pleurogram elliptical, Irregular fracture line and thick ornamentation wall.	Sanghar City/ district Sanghar Pakistan	(Arshad et al., 2019; Waheed et al., 2021)
152.	<i>Prosopis cineraria</i> (L.) Druce	Fabaceae	Dicot	Jand	Perennial	Shrub	Brown Yellowish color, elliptical and convex hilum, ovoid, Polygonal discoid sculpture, texture rudeness coarse, pleurogram elliptical and irregular reticulate fracture line.	Pakistan	(Arshad et al., 2019)
153.	<i>Prosopis glandulosa</i> Torr.	Fabaceae	Dicot	Honey mesquite	Perennial	Shrub	Obovate, Yellow-brown, hilum oval, hilum terminal, U shaped pleurogram and thin and irregular pattern wall.	Bakhoro	(Waheed et al., 2021)
154.	<i>Prosopis juliflora</i> (Sw.) DC.	Fabaceae	Dicot	Mesquite	Perennial	Shrub	Obovate, light yellowish, U shaped pleurogram and medium wall with irregular pattern wall.	Panhal/ district Sanghar	
155.	<i>Prunus bokhariensis</i> Royle ex C.K.Schneid.	Rosaceae	Dicot	Prune	Perennial	Tree	Orange brown color, striate surface ornamented, random cell outline, bulges projection, thick anticlinal wall, anticlinal wall protuberance, medium periclinal wall surface and flat periclinal wall elevation.	Pakistan	(Dawood et al., 2019)
156.	<i>Prunus domestica</i> L.	Rosaceae	Dicot	Plum Tree	Perennial	Tree	hick smooth walled elongated cells lie parallel to each other	Pakistan	(Fatima et al., 2018)
157.	<i>Prunus persica</i> (L.) Batsch	Rosaceae	Dicot	Peach	Perennial	Tree	Cell wall is smooth, elongated, irregular shape; cells are elongated and slightly undulate		
158.	<i>Raphanus raphanistrum</i> L.	Brassicaceae	Dicot	Wild radish	Annual	Herb	Light brown color, globose to ovate, cells irregular to polygonal, sculpturing smooth, elongated cells, margins straight to undulate, anticlinal wall deep, outer periclinal wall flat to slightly concave.	Pakistan	(Munir et al., 2019)
159.	<i>Ricinus communis</i> L.	Euphorbiaceae	Dicot	Castor bean	Perennial	Shrub	Dark red to dark brownish, ovate, spherical, granular, rough sculpturing, reticulate cell arrangement, with glabrous projection, spherical ovate cells to undulate margins, thick random anticlinal walls and smooth thin periclinal walls.	Pakistan	(Aziz et al., 2021)



160.	<i>Saccharum spontaneum</i> L.	Poaceae	Monocot	Wild sugarcane	Perennial	Herb	Linear-elliptic, smooth and gray. Reticulate ornamentation, style base with tuft of hairs on stylopodium with Irregular straight epidermal wall.	Dera Ghazi Khan, Pakistan, Chakwal/Punjab	(Ahmad et al., 2019; Usma et al., 2019)
161.	<i>Salvadora oleoides</i> Decne.	Salvadoraceae	Dicot	Large toothbrush tree	Perennial	Tree	Globular and brown in color. Seed surface reticulated pattern with small pits. Cells regularly or irregularly arranged in circular rows	Sindh	(Korejo et al., 2010)
162.	<i>Salvadora persica</i> L.	Salvadoraceae	Dicot	Toothbrush tree	Perennial	Tree	Globular, dark brown, shinny surface. Seed surface shows scabrate pattern. Cells arranged; irregular and regular circular rows, and mostly pitted with defined lines.		
163.	<i>Senna alata</i> (L.) Roxb.	Fabaceae	Dicot	Candle bush	Perennial	Shrub	Kite like, dark brown, hilum elliptic, lunar shaped pleurogram and thin ornamentation wall.	Bakhoro/ district Sanghar	(Waheed et al., 2021)
164.	<i>Senna obtusifolia</i> (L.) H.S.Irwin & Barneby	Fabaceae	Dicot	Chinese senna	Annual	Herb	Shiny surface, rhombus shaped fracture line pattern and levigate surface ornamentation.	Rawalpindi/Punjab	(Ullah et al., 2019)
165.	<i>Senna occidentalis</i> (L.) Link	Fabaceae	Dicot	Coffee weed	Perennial	Shrub	Continuous reticulate fracture line pattern, fine texture crudeness and papillate, depressed periclinal wall elevation, and reticulate sculpture.	Islamabad, Pakistan	(Aziz et al., 2021; Ullah et al., 2019)
166.	<i>Sesbania grandiflora</i> (L.) Pers.	Fabaceae	Dicot	Vegetable hummingbird	Perennial	Tree	Oblong, red, hilum oblong, rectangular shaped pleurogram and thin ornamented wall.	Panhal/ district Sanghar	(Waheed et al., 2021)
167.	<i>Sesbania sesban</i> (L.) Merr.	Fabaceae	Dicot	Egyptian river hemp	Perennial	Shrub	Oblong, greenish brown, hilum oblong, rectangular shaped pleurogram and thin ornamentation wall.	Bakhoro/ district Sanghar	
168.	<i>Setaria glauca</i> (L.) P.Beauv.	Poaceae	Monocot	Golden foxtail	Annual	Grass	Green obovate, reticulate and style base persistent.	Chakwal/Punjab	(Usma et al., 2019)
169.	<i>Setaria pumila</i> (Poir.) Roem. & Schult.	Poaceae	Monocot	Yellow foxtail	Annual	Grass	Oval, hairy and gray. Papillate wall peculiarities and Irregular straight wall pattern.	Dera Ghazi Khan, Pakistan	(Ahmad et al., 2019)
170.	<i>Sinapis arvensis</i> L.	Brassicaceae	Dicot	Charlock mustard	Annual	Herb	Seeds brownish white with rounded, elongated, polygonal, wavy cells, sculpturing; wrinkled with some ridges, margins dentate and granulate, deep anticlinal wall, outer wall convex and central tubercle.	Pakistan	(Munir et al., 2019)
171.	<i>Sonchus arvensis</i> L.	Asteraceae	Dicot	Perennial sow thistle	Perennial	Herb	Yellowish brown, oblanceolate and glabrous surface seeds. Striated sculpturing, Incompletely developed circular ring with interruption carpodium and Depressed, glabrous periclinal wall.	Mardan/KPK	(Ayaz et al., 2019)

172.	<i>Sonchus asper</i> (L.) Hill	Asteraceae	Dicot	Spiny sow thistle	Annual	Herb	Seeds chestnut-brown and Striated ornamented with developed circular ring with Interruption carpodium.	Oblanceolate. Incompletely	Peshawar/KPK	
173.	<i>Sonchus oleraceus</i> (L.) L.	Asteraceae	Dicot	Common sow thistle	Annual	Herb	Yellowish to dull brown, obovoid and scabrous surface. Verrucose papillate and Incompletely developed U-shaped with interruption		Mardan/KPK	
174.	<i>Sorghum bicolor</i> (L.) Moench	Poaceae	Monocot	Broom corn	Annual	Grass	White-brown, oblate, reticulate and style persistent.		Chakwal/Punjab	(Usma et al., 2019)
175.	<i>Sorghum halepense</i> (L.) Pers	Poaceae	Monocot	Johnson grass	Perennial	Grass	Elliptic, hairy and gray. Smooth sculpture, style base with tuft of hairs on stylopodium and epidermal wall not visible		Dera Ghazi Khan, Pakistan, Chakwal/Punjab	(Ahmad et al., 2019; Usma et al., 2019)
176.	<i>Spergularia marina</i> (L.) Besser	Caryophyllaceae	Dicot	Lesser sea spurrey	Annual	Herb	Ovate in shape, tuberculate surface pattern at periphery and central portion granulate. Beads; compact at the tips of projections, surface sculpture striate and papilliformis protuberances		Khairpur/Sindh	(Memon et al., 2010)
177.	<i>Stellaria alsinoides</i> Boiss. & Buhse	Caryophyllaceae	Dicot	N/A	Annual	Herb	Seed color blackish, sub-central hilum and echinate wall pattern.		Rawalpindi/Punjab	(Ullah et al., 2019)
178.	<i>Stellaria kotschyana</i> Fenzl ex Boiss.	Caryophyllaceae	Dicot	N/A	Annual	Herb	Anticlinal wall deeply undulate and cell irregular.		Abbottabad/KPK	(Ullah et al., 2019)
179.	<i>Stellaria media</i> (L.) Vill.	Caryophyllaceae	Dicot	Chickweed	Annual	Herb	Seed shape sub-reniform, color dark brown, margins convex and tuberculated surface.		Lower Dir/KPK	
180.	<i>Stellaria uliginosa</i> Murray	Caryophyllaceae	Dicot	Bog stitchwort	Perennial	Herb	Seed shape elliptical pyriform, color shiny brownish, margins dome shape		Rawalpindi/Punjab	
181.	<i>Suaeda fruticose</i> Forssk. ex J.F.Gmel.	Amaranthaceae	Dicot	Seablite	Annual	Shrub	Seed reniform, compressed, marginal hilum and surface smooth centrally and lineate towards the base		Pakistan	(Kanwal and Abid, 2017)
182.	<i>Tamarindus indica</i> L.	Fabaceae	Dicot	Tamarind	Perennial	Tree	Deformed, dark brown, depressed hilum, lunar shaped pleurogram, – irregular shaped seed, stony texture and thick ornamentation wall.		Loon Khan/ district Sanghar, Lahore/Punjab	(Ullah et al., 2019; Waheed et al., 2021)
183.	<i>Taraxacum campylodes</i> G.E.Haglund	Asteraceae	Dicot	Dandelion	Perennial	Herb	Green to brownish ob lanceolate and glabrous surface. Sculpture verrucose papillate and completely developed circular ring without interruption carpodium shape.		Peshawar/KPK	(Ayaz et al., 2019)

184.	<i>Thevetia peruviana</i> (Pers.) K.Schum.	Apocynaceae	Dicot	Yellow Oleander	Perennial	Shrub	White brown in color, striate surface pattern, crystalloids projection, irregular cell arrangement, thick anticlinal wall, pentagonal periclinal wall surface, and depressed periclinal wall elevation.	Pakistan	(Dawood et al., 2019)
185.	<i>Tribulus terrestris</i> L.	Zygophyllaceae	Dicot	Bindii	Biennial	Herb	Light green, triangular ovate, striate ornamentation irregular, reticulate bulging projection, straight cell margins, thick curved anticlinal walls, convex thick periclinal walls and uniform cell arrangement.	Pakistan	(Aziz et al., 2021)
186.	<i>Trifolium alexandrinum</i> L.	Fabaceae	Dicot	Annual clover	Annual	Herb	Oval, oblong, smooth and light gray. Granulate sculpture and straight anticlinal wall.	Abbottabad (Khyber Pakhtunkhwa)	(Rashid et al., 2021)
187.	<i>Trigonella foenum-graecum</i> L.	Fabaceae	Dicot	Fenugreek	Annual	Herb	Oval, oblong, smooth and gray. Papillate sculpture and straight anticlinal wall.	Chakwal (Rawalpindi, Punjab)	
188.	<i>Triticum aestivum</i> L.	Poaceae	Monocot	Common wheat	Annual	Grass	Brown, widely obovate, striate surface and style base with tuft of hairs on stylopodium.	Chakwal/Punjab	(Usma et al., 2020)
189.	<i>Verbena officinalis</i> L.	Verbenaceae	Dicot	Common verbena	Perennial	Herb	Oblong, dorsal side rough, ventral side smooth, dorsal surface dark brown and ventral surface light brown. Dorsal surface dull, ventral surface Shiny. Cell shape is irregular; cell outline is webby with regular cell arrangement. Surface sculpturing reticulate.	Pharmacy department QAU, Islamabad	(Kanwal et al., 2021)
190.	<i>Verbena tenuisecta</i> Briq.	Verbenaceae	Dicot	Moss verbena	Perennial	Herb	Linear shape with rough and Brownish black color. Cell shape spherical; cell outline smooth, striate, and wrinkled cell arrangement. Raised anticlinal wall with thin smooth pattern, and wavy raised periclinal wall	Department of Chemistry QAU, Islamabad	
191.	<i>Vicia hirsute</i> (L.) Gray	Fabaceae	Dicot	Tiny vetch	Annual	Herb	Seed outline elliptic, ornamentation reticulate.	Chitral	(Rashid et al., 2018)
192.	<i>Vicia monantha</i> Retz.	Fabaceae	Dicot	Bam vetch	Annual	Herb	Seed shape circular, testa cells radiate and papillate sculpturing.	Near Mangla dam, Mirpur	
193.	<i>Vicia narbonensis</i> L.	Fabaceae	Dicot	Narbon vetch	Annual	Herb	Seed texture smooth, color grayish black and striate sculpture.	Neelum Valley, Azad Kashmir	
194.	<i>Vicia sativa</i> L.	Fabaceae	Dicot	Garden Vetch	Annual	Herb	Seed shape oval, anticlinal wall pattern wavy. Sculpturing papillate.	Rawalpindi	
195.	<i>Vicia tenuifolia</i> Roth	Fabaceae	Dicot	Cow vetch	Perennial	Herb	Seed margin ovate, color grayish black and papillate ornamentation		

196.	<i>Vicia tetrasperma</i> (L.) Schreb.	Fabaceae	Dicot	Smooth vetch	Annual	Herb	Seed shape oval and papillate sculpture wall.	Nakyal, Kotli	
197.	<i>Vitis vinifera</i> L.	Vitaceae	Dicot	Common grape vine	Perennial	Shrub	Seed margins pyriform, ovoid and sculpturing smooth/rugose. Raised and thick anticlinal wall. Elongated integument cell shape.	Baidra / Mansehra	(Lubna et al., 2018)
198.	<i>Xanthoxylum armatum</i> Druce	Rutaceae	Dicot	Winged prickly ash	Perennial	Shrub	Seed rounded and black. Rugose to reticulate ornamentation, finer small pits, elliptic to ovate cell outline and asymmetrical cell arrangement. Convex ventral and dorsal wall side, thick, deep anticlinal walls and puzzled periclinal walls.	Pakistan	(Rozina et al., 2021)
199.	<i>Youngia japonica</i> (L.) DC.	Asteraceae	Dicot	Oriental false hawkbeard	Annual	Herb	Brownish red, obovate and scabrous surface type. Verrucose papillate sculpture and shape of carpopodium completely developed circular ring without interruption.	Islamabad	(Ayaz et al., 2019)
200.	<i>Zea mays</i> L.	Poaceae	Monocot	Corn	Annual	Grass	Yellow, rounded, shallowly ob-triangular, reticulate and style persistent.	Chakwal/Punjab	(Usma et al., 2019)

**Keywords:** N/A= Not available

**Table 15.** Qualitative and quantitative seed micro-morphological attributes among Desert Dicot Angiosperms.

Dicot Species	Seed colour	Seed shape	Seed texture	Seed apex	Hilum			L (mm) (Range) x ± SD	W (mm) (Range) x ± SD	L/W Ratio	Average weight (mg)
					Occurrence	Position	Level				
<i>Acacia jacquemontii</i> Benth.	Greenish brown	Obovate	Scabrous	Round	Not visible	Terminal	Depressed	(4.9-7.8)6.4±1.33	(3-5.9)4.6±0.97	1.39	0.62
<i>Acacia modesta</i> Wall.	Dark brown	Ellipsoidal	Rough	Elliptic	Visible	Terminal	Depressed	(3.6-6.1)5.3±1.76	(2.9-5.5)4.2±0.88	1.26	0.93
<i>Acacia nilotica</i> (L.) Delile	Dark brown	Obovate	Rough pitted	Elliptic	Visible	Terminal	Depressed	(12.5-18.5)15.2±0.21	(11.4-15.5)13.7±0.1	1.1	0.74
<i>Albizia lebbeck</i> (L.) Benth.	Brown	Elliptical depressed	Scabrous	Round	Visible	Terminal	Depressed	(4.7-6.1)6.6±1.53	(4.2-6.6)±5.7±1.04	1.15	0.69
<i>Astragalus hamosus</i> L.	Greenish brown	Reniform-globose	Smooth	Oblong	Not visible	Sub-terminal	Depressed	(7-11.5)9.1±0.32	(1.8-4.2)3.6±0.14	2.52	0.53
<i>Azadirachta indica</i> A.Juss.	Yellowish orange	Obovate	Scabrous	Round	Not visible	Terminal	Undetermined	(6.5-9.6)8.4±1.04	(2.7-5.1)4.1±0.81	2.04	0.37
<i>Brassica nigra</i> (L.) K.Koch	Brown	Round	Scabrous	Round	Not visible	Central	Undetermined	(2.2-4.8)3.7±0.12	(0.6-2.9)1.7±0.18	2.17	0.17
<i>Capparis decidua</i> (Forssk.) Edgew.	Black	Ovoid	Rough	Oval	Visible	Terminal	Depressed	(1.3-2.9)2.1±0.08	(0.8-1.9)1.3±0.22	1.61	0.61
<i>Chenopodium album</i> L.	Black	Oblate spheroidal	Scabrous	Round	Visible	Terminal	Raised	(0.8-2.4)1.7±0.05	(0.5-1.4)0.8±0.04	2.12	0.09
<i>Citrullus colocynthis</i> (L.) Schrad.	Light brown	Obovate	Smooth	Round	Visible	Sub-terminal	Raised	(3.1-4.7)3.7±0.52	(1.7-3.8)2.9±0.39	1.2	0.45
<i>Crotalaria burhia</i> Benth.	Brown green	Reniform	Scabrous	Oblong	Visible	Terminal	Undetermined	(5.1-7.6)6.4±0.78	(4.5-6.7)5.8±1.13	1.10	0.29
<i>Dalbergia sissoo</i> DC.	Brown	Oblong	Smooth	Round	Not visible	Sub-terminal	Undetermined	(7.2-10)8.7±1.71	(4.6-7.2)5.9±0.96	1.47	0.17
<i>Fagonia bruguieri</i> DC.	Dark brown	Broadly Ovoid	Rough	Round	Visible	Terminal	Raised	(1.4-3.6)2.4±0.17	(1.1-2.3)1.5±0.13	1.6	0.58

<i>Farsetia stylosa</i> R.Br.	Yellowish brown	Oblong	Glabrous	Round	Not Visible	Central	Undetermined	(2.6-6.3)4.8±0.36	(2.4-3.8)3.1±0.29	1.54	0.21
<i>Heliotropium europaeum</i> L.	Light brown	Curved	Scabrous	Elliptic	Visible	Sub-terminal	Depressed	(1.5-3.1)2.3±0.14	(0.7-1.6)1.2±0.1	1.91	0.29
<i>Leptadenia pyrotechnica</i> (Forssk.) Decne.	Light brown	Ovoid flattened	Scabrous	Elliptic	Not Visible	Terminal	Undetermined	(3.9-6.1)5.2±1.23	(1.8-4.3)3.15±0.63	1.65	0.26
<i>Mollugo nudicaulis</i> Lamk.,	Dark red	Reniform	Smooth	Round	Visible	Terminal	Raised	(0.9-2.4)1.6±0.19	(0.4-1.4)0.8±0.09	2	0.12
<i>Mollugo cerviana</i> (L.) Ser.	Brown	D-shaped	Rough	Round	Visible	Terminal	Undetermined	(1-2.2)1.5±0.07	(0.3-1)0.6±0.05	2.5	0.15
<i>Parkinsonia aculeata</i> L.	Greyish black	Ellipsoidal	Smooth	Oval	Visible	Terminal	Depressed	(3-3-4.9)4.1±0.15	(1.8-3.7)2.9±0.32	1.41	0.41
<i>Peganum harmala</i> L.	Blackish brown	Rhomboid	Scabrous	Oblong	Not visible	Sub-terminal	Undetermined	(1.2-2.7)2.1±0.23	(0.6-1.5)0.9±0.03	2.33	0.38
<i>Prosopis cineraria</i> (L.) Druce	Brown	Oblong compressed	Rough	Elliptic	Visible	Terminal	Depressed	(3.3-4.8)3.9±0.86	(2.1-4.2)3.4±0.73	1.14	0.52
<i>Prosopis juliflora</i> (Sw.) DC.	Light Yellowish	Obovate	Rough	Elliptic	Visible	Terminal	Raised	(7.5-14.2)10.3±0.79	(4.8-9)6.7±0.56	1.53	0.63
<i>Psammogeton biternatum</i> Edgew.	Yellowish brown	Oval	Spiny	Pointed	Not visible	Central	Undetermined	(1.9-5.4)3.8±0.51	(1.9-3.5)2.6±0.25	1.46	0.19
<i>Senna italica</i> Mill.	Dark brown	Obovate	Rough	Pointed	Visible	Terminal	Depressed	(2.9-5.6)4.2±0.35	(2.4-4.9)3.5±1.07	1.2	0.83
<i>Tephrosia purpurea</i> (L.) Pers.	Yellowish brown	Oblong	Smooth	Round	Visible	Sub-terminal	Depressed	(2.2-6.8)4.6±0.44	(1.5-3.3)2.4±0.2	1.91	0.23
<i>Tribulus terrestris</i> L.	Greenish brown	Ovate flattened	Scabrous spiny	Pointed	Not visible	Terminal	Undetermined	(5.8-9)7.3±0.74	(1.7-3.8)3.1±0.08	2.35	0.16
<i>Withania coagulans</i> (Stocks) Dunal	Yellowish	Reniform	Rough	Oblong	Visible	Terminal	Depressed	(1.8-8.5)5.3±0.67	(2.5-3.8)3.1±0.17	1.7	0.56

**Keywords:** L=length, W=width, x=mean, SD=standard deviation, mm=millimetre, mg=milligram

**Table 16.** SEM ultrastructural seed coat micro-morphological features of selected Desert Dicot Angiosperms.

<b>Dicot Species</b>	<b>Ornamentation wall</b>	<b>Epicuticular Projections</b>	<b>Facture line pattern</b>	<b>Cell outline</b>	<b>Cell Arrangement</b>	<b>Texture crudeness</b>	<b>Periclinal Wall</b>	<b>Surface Anticlinal Wall pattern</b>
<i>Acacia jacquemontii</i> Benth.	Thick	Bulges	Continuous	Random	Irregular	Coarse	Flat to convex	Striate foveolate
<i>Acacia modesta</i> Wall.	Very thick	Glabrous	Continuous	Random	Regular	Very fine	Slightly convex	Striate rugulate
<i>Acacia nilotica</i> (L.) Delile	Thick	Glabrous	Continuous	Random	Irregular	Fine sinuate	Flat	Striate
<i>Albizia lebbeck</i> (L.) Benth.	Thick undulated	Bulges	Continuous	In-rows	Irregular	Coarse	Slightly concave	Rugose
<i>Astragalus homosus</i> L.	Thick	Bulges	Absent	Random	Irregular	Coarse	Concave	Foveolate Rugose
<i>Azadirachta indica</i> A.Juss.	Thick	Glabrous	Absent	Random	Regular	Coarse	Convex	Foveolate
<i>Brassica nigra</i> (L.) K.Koch	Thick	Prickles	Absent	Random	Irregular	Very fine	Slightly concave	Rugulate
<i>Capparis decidua</i> (Forssk.) Edgew.	Very thick	Bulges	Absent	In-rows	Regular	Coarse	Flat to Convex	Foveolate Striate
<i>Chenopodium album</i> L.	Thick	Bulges	Absent	Random	Irregular	Coarse	Slightly concave	Papillate
<i>Citrullus colocynthis</i> (L.) Schrad.	Medium flat	Glabrous	Absent	In-rows	Regular	Medium	Convex	Striate psilate
<i>Crotalaria burhia</i> Benth.	Very thick	Prickles	Continuous	In-rows and flattened	Regular	Coarse	Slightly flat to convex	Papillate rugose
<i>Dalbergia sissoo</i> DC.	Medium to thick	Glabrous and Prickles	Continuous	In-rows and flattened	Irregular	Medium	Deeply convex	Rugose
<i>Fagonia bruguieri</i> DC.	Thick	Prickles	Absent	In-rows	Regular	Coarse	Deeply convex	Striate
<i>Farsetia stylosa</i> R.Br.	Thick	Glabrous	Absent	In-rows	Regular	Coarse	Flat to concave	Reticulate

<i>Heliotropium europaeum</i> L.	Very thick	Glabrous	Absent	Random	Irregular	Coarse	Flat	Foveolate
<i>Leptadenia pyrotechnica</i> (Forssk.) Decne.	Thick	Bulges and prickles	Absent	Random	Regular	Coarse	Protuberance	Papillate scabrate
<i>Mollugo nudicaulis</i> Lamk.,	Thick	Glabrous	Absent	In-rows and protuberant	Regular	Medium	Slightly convex	Papillate foveolate
<i>Mollugo cerviana</i> (L.) Ser.	Very thick	Glabrous and Prickles	Absent	In-rows and raised	Irregular	Coarse	Protuberance	Reticulate
<i>Parkinsonia aculeata</i> L.	Thick	Glabrous	Irregular reticulate	In-rows and flattened	Regular	Very fine	Flat	Rugose
<i>Peganum harmala</i> L.	Very thick	Glabrous	Absent	Random	Irregular	Coarse	Deeply convex	Striate reticulate
<i>Prosopis cineraria</i> (L.) Druce	Thick	Bulges and glabrous	Continuous	In-rows	Irregular	Very fine and medium	Flat to convex	Rugose papillate
<i>Prosopis juliflora</i> (Sw.) DC.	Medium to thick	Bulges	Absent	In-rows and flattened	Irregular	Medium	Flat to slightly convex	Rugose striate
<i>Psammogeton biternatum</i> Edgew.	Very thick	Multicellular spines	Absent	Random	Irregular	Coarse	Protuberance	Rugulate
<i>Senna italica</i> Mill.	Thin	Glabrous	Continuous	Random	Irregular	Coarse	Deeply convex	Rugose scabrate
<i>Tephrosia purpurea</i> (L.) Pers.	Thick	Glabrous	Absent	In-rows	Irregular	Fine	Flat	Papillate smooth
<i>Tribulus terrestris</i> L.	Thick	Spiny glabrous	Absent	Random	Irregular	Coarse	Protuberance	Wrinkled spiny
<i>Withania coagulans</i> (Stocks) Dunal	Very thick	Bulges to Prickles	Absent	In-rows and raised	Irregular	Coarse	Convex	Undulate granulate



**Table 17.** Matrix of qualitative morphological features coding used for the statistics.

Dicot Species	Seed color	Seed shape	Seed texture	Seed apex	Hilum		
					Occurrence	Position	Level
<i>Acacia jacquemontii</i>	2	1	3	3	2	1	1
<i>Acacia modesta</i>	1	11	4	1	1	1	1
<i>Acacia nilotica</i>	1	1	1	1	1	1	1
<i>Albizia lebbeck</i>	3	14	3	3	1	1	1
<i>Azadirachta indica</i>	12	1	3	3	2	1	2
<i>Astragalus hamosus</i>	2	2	2	2	2	2	1
<i>Brassica nigra</i>	3	3	3	3	2	3	2
<i>Capparis decidua</i>	4	4	4	4	1	1	1
<i>Chenopodium album</i>	4	5	3	3	1	1	3
<i>Citrullus colocynthis</i>	6	1	2	3	1	2	3
<i>Crotalaria burhia</i>	2	9	3	2	1	1	2
<i>Dalbergia sissoo</i>	3	7	2	3	2	2	2
<i>Fagonia bruguieri</i>	1	6	4	3	1	1	3
<i>Farsetia stylosa</i>	5	7	5	3	2	3	2
<i>Heliotropium europaeum</i>	6	8	3	1	1	2	1
<i>Leptadenia pyrotechnica</i>	6	15	3	1	2	1	2
<i>Mollugo nudicaulis</i>	7	9	2	3	1	1	3
<i>Mollugo cerviana</i>	3	10	4	3	1	1	2
<i>Parkinsonia aculeata</i>	8	11	2	4	1	1	1
<i>Peganum harmala</i>	9	12	3	2	2	2	2
<i>Prosopis cineraria</i>	3	17	4	1	1	1	1
<i>Prosopis juliflora</i>	10	1	4	1	1	1	3
<i>Psammogeton biternatum</i>	5	13	6	5	2	3	2
<i>Senna italica</i>	1	1	4	5	1	1	1
<i>Tephrosia purpurea</i>	5	7	2	3	1	2	1
<i>Tribulus terrestris</i>	2	16	7	5	2	1	2
<i>Withania coagulans</i>	11	10	4	2	1	1	3

**Character: Character state**

**Seed color:** 1= Dark brown; 2= Greenish Brown; 3 = Brown; 4 = Black; 5 = Yellowish brown; 6 = Light brown; 7 = Dark red; 8 = Greyish black; 9 = Blackish brown; 10 = Light yellowish; 11 = Yellowish; 12 = Yellowish orange

**Seed shape:** 1 = Obovate; 2 = Reniform-globose; 3 = Round; 4 = Ovoid; 5 = Oblate spheroidal; 6 = Broadly Ovoid; 7 = Oblong; 8 = Curved; 9 = Reniform; 10 = D-shaped; 11 = Ellipsoidal; 12 = Rhomboid; 13 = Oval; 14 = Elliptical depressed; 15 = Ovoid flattened; 16 = Ovate flattened; 17 = Oblong compressed

**Seed texture:** 1 = Rough pitted; 2 = Smooth; 3 = Scabrous; 4 = Rough; 5 = Glabrous; 6 = Spiny; 7 = Scabrous spiny

**Seed apex:** 1 = Elliptic; 2 = Oblong; 3 = Round; 4 = Oval; 5 = Pointed

**Hilum occurrence:** 1 = Visible; 2 = Not visible

**Hilum position:** 1 = Terminal; 2 = Sub-terminal; 3 = Central

**Hilum level:** 1 = Depressed; 2 = Undetermined; 3 = Raised

**Table 18.** Matrix with qualitative seed morphological ultrastructure features coding used for the UPGMA dendrogram and PCA analysis

<b>Dicot Species</b>	<b>Ornamentation wall</b>	<b>Epicuticular Projections</b>	<b>Facture line</b>	<b>Cell outline</b>	<b>Cell Arrangement</b>	<b>Texture crudeness</b>	<b>Periclinal Wall</b>	<b>Anticlinal Wall</b>
<i>Acacia jacquemontii</i>	1	2	1	1	1	2	4	14
<i>Acacia modesta</i>	2	1	1	1	2	7		15
<i>Acacia nilotica</i>	1	1	1	1	1	1	1	1
<i>Albizia lebbeck</i>	4	2	1	2	1	2	3	9
<i>Astragalus hamosus</i>	1	2	2	1	1	2	2	2
<i>Azadirachta indica</i>	1	1	2	1	2	2	10	7
<i>Brassica nigra</i>	1	3	2	1	1	3	3	3
<i>Capparis decidua</i>	2	2	2	2	2	2	4	4
<i>Chenopodium album</i>	1	2	2	1	1	2	3	5
<i>Citrullus colocynthis</i>	5	1	2	2	2	4	10	16
<i>Crotalaria burhia</i>	2	3	1	5	2	2	11	17
<i>Dalbergia sissoo</i>	3	4	1	4	1	4	5	9
<i>Fagonia bruguieri</i>	1	3	2	2	2	2	5	1
<i>Farsetia stylosa</i>	1	1	2	2	2	2	6	6
<i>Heliotropium europaeum</i>	2	1	2	1	1	2	1	7
<i>Leptadenia pyrotechnica</i>	1	6	2	1	2	2	8	18
<i>Mollugo nudicaulis</i>	1	1	2	3	2	4	7	8
<i>Mollugo cerviana</i>	2	4	2	4	1	2	8	6
<i>Parkinsonia aculeata</i>	1	1	3	5	2	3	1	9
<i>Peganum harmala</i>	2	1	2	1	1	2	5	10
<i>Prosopis cineraria</i>	1	8	1	2	1	3	4	17
<i>Prosopis juliflora</i>	3	2	2	5	1	4	9	11
<i>Psammogeton biternatum</i>	2	5	2	1	1	2	8	3
<i>Senna italica</i>	6	1	1	1	1	2	5	19
<i>Tephrosia purpurea</i>	1	1	2	2	1	5	1	12

<i>Tribulus terrestris</i>	1	7	2	1	1	2	8	20
<i>Withania coagulans</i>	2	6	2	4	1	2	10	13

**Character: Character states**

**Ornamentation wall:** 1 = Thick; 2 = Very thick; 3 = Medium to thick; 4 = Thick undulated; 5 = Medium flat; 6 = Thin

**Epicuticular projections:** 1 = Glabrous; 2 = Bulges; 3 = Prickles; 4 = Glabrous and Prickles; 5 = Multicellular spines; 6 = Bulges to Prickles; 7 = Spiny glabrous; 8 = Bulges and glabrous

**Fracture line pattern:** 1 = Continuous; 2 = Absent; 3 = Irregular reticulate

**Cell outline:** 1 = Random; 2 = In-rows; 3 = In-rows and protuberant; 4 = In-rows and raised; 5 = In-rows and flattened

**Cell arrangement:** 1 = Irregular; 2 = Regular

**Texture crudeness:** 1 = Fine sinuate; 2 = Coarse; 3 = Very fine; 4 = Medium; 5 = Fine

**Periclinal wall:** 1 = Flat; 2 = Concave; 3 = Slightly concave; 4 = Flat to convex; 5 = Deeply convex; 6 = Flat to concave; 7 = Slightly convex; 8 = Protuberance; 9 = Flat to Slightly convex; 10 = Convex; 11 = Slightly flat to convex

**Anticlinal wall:** 1 = Striate; 2 = Foveolate rugose; 3 = Rugulate; 4 = Foveolate striate; 5 = Papillate; 6 = Reticulate; 7 = Foveolate; 8 = Papillate foveolate; 9 = Rugose; 10 = Striate reticulate; 11 = Rugose striate; 12 = Papillate smooth; 13 = Undulate granulate; 14 = Striate foveolate; 15 = Striate regulate; 16 = Striate psilate; 17 = Papillate rugose; 18 = Papillate scabrate; 19 = Rugose scabrate; 20 = Wrinkled spiny

**Table 19.** Variance for seed morphological metric variables of the first and the second axis of PCA component analysis.

PC	Eigen Values	% variance
PC1	2.61	17.42
PC2	2.41	16.12
PC3	2.14	14.28
PC4	1.55	10.37
PC5	1.33	8.86
PC6	1.10	7.34
PC7	1.01	6.76
PC8	0.71	4.74
PC9	0.62	4.17
PC10	0.41	2.76
PC11	0.36	2.4
PC12	0.28	1.88
PC13	0.16	1.13
PC14	0.14	0.98
PC15	0.10	0.72

**Keywords:** PC = Principal component

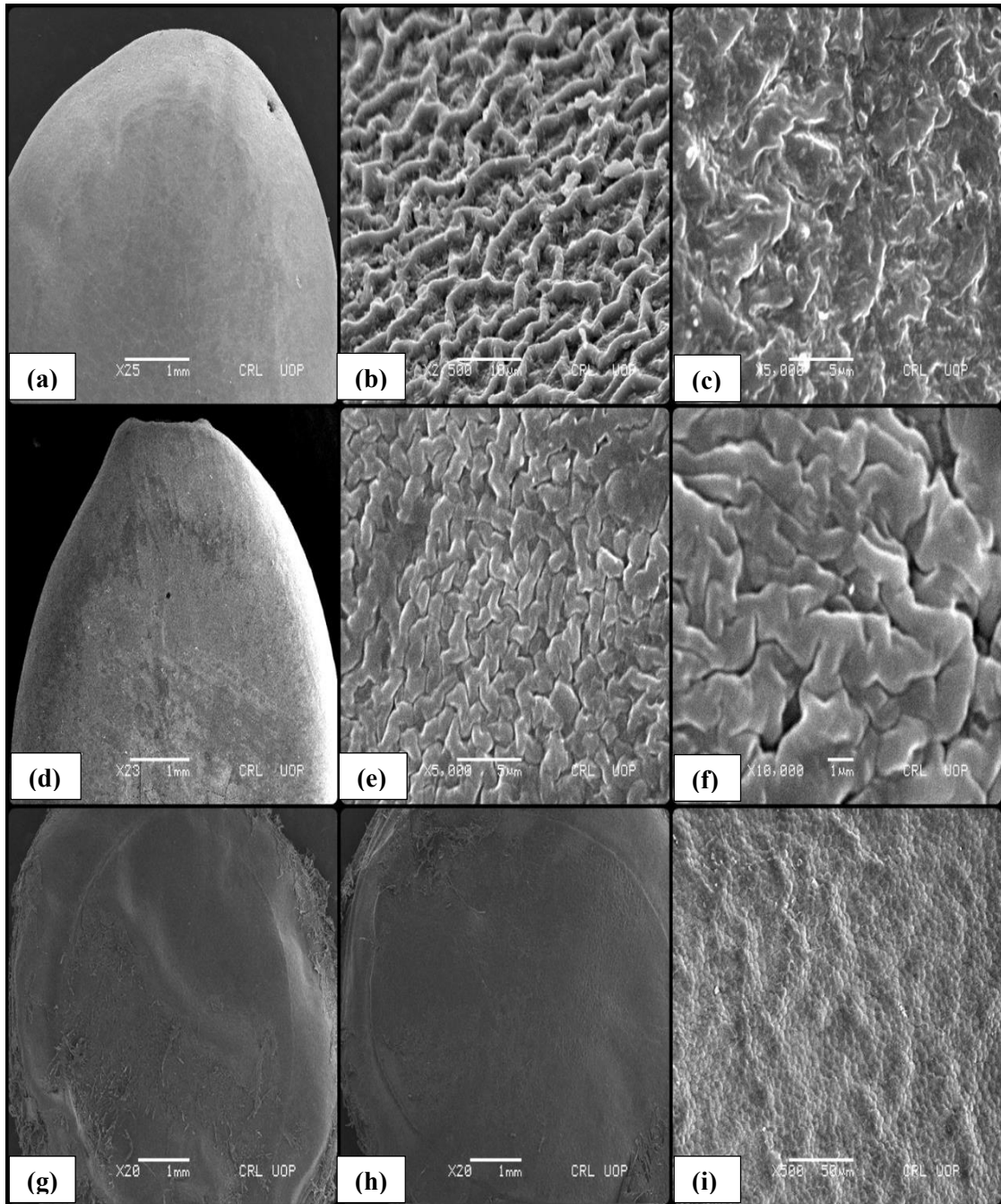


**Plate 63.** Scanning electron micrographs of seed micromorphology; (a-c) *Acacia jacquemontii* (a) shape (b) texture (c) striate foveolate sculpture. (d-f) *Acacia modesta* (d) terminal hilum (e) very fine texture (f) striate-regulate sculpture (g-i) *Acacia nilotica* (g) shape (h) fracture line (i) striate sculpture.

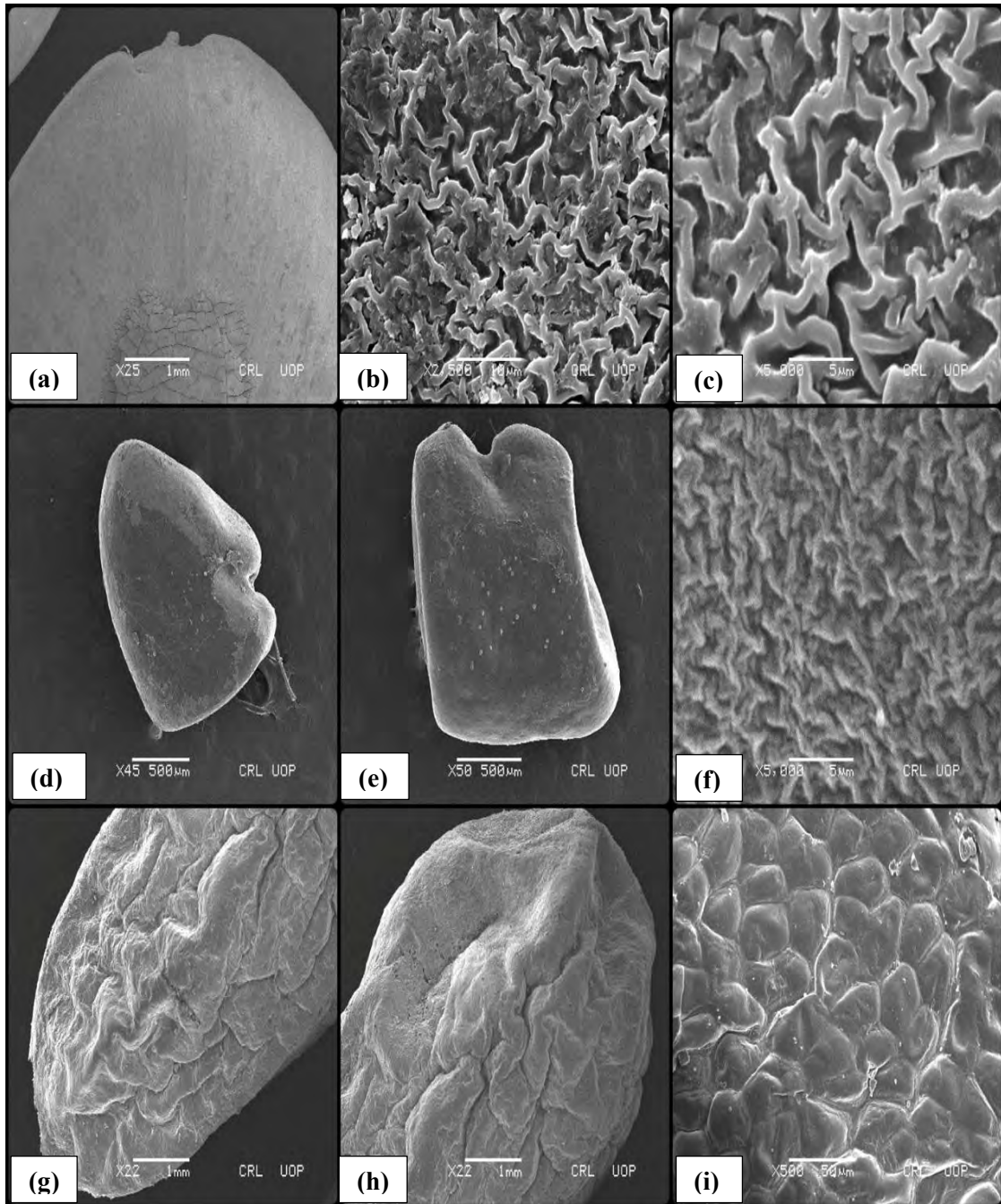


**Plate 64.** Scanning electron micrographs of seed micromorphology; (a-c) *Albizia lebbeck* (a) terminal hilum (b) coarse texture (c) rugose sculpture. (d-f) *Astragalus homosus* (d) sub-terminal hilum (e) coarse texture (f) foveolate rugose sculpture (g-i) *Azadirachta indica* (g) shape (h) coarse texture (i) foveolate sculpture.

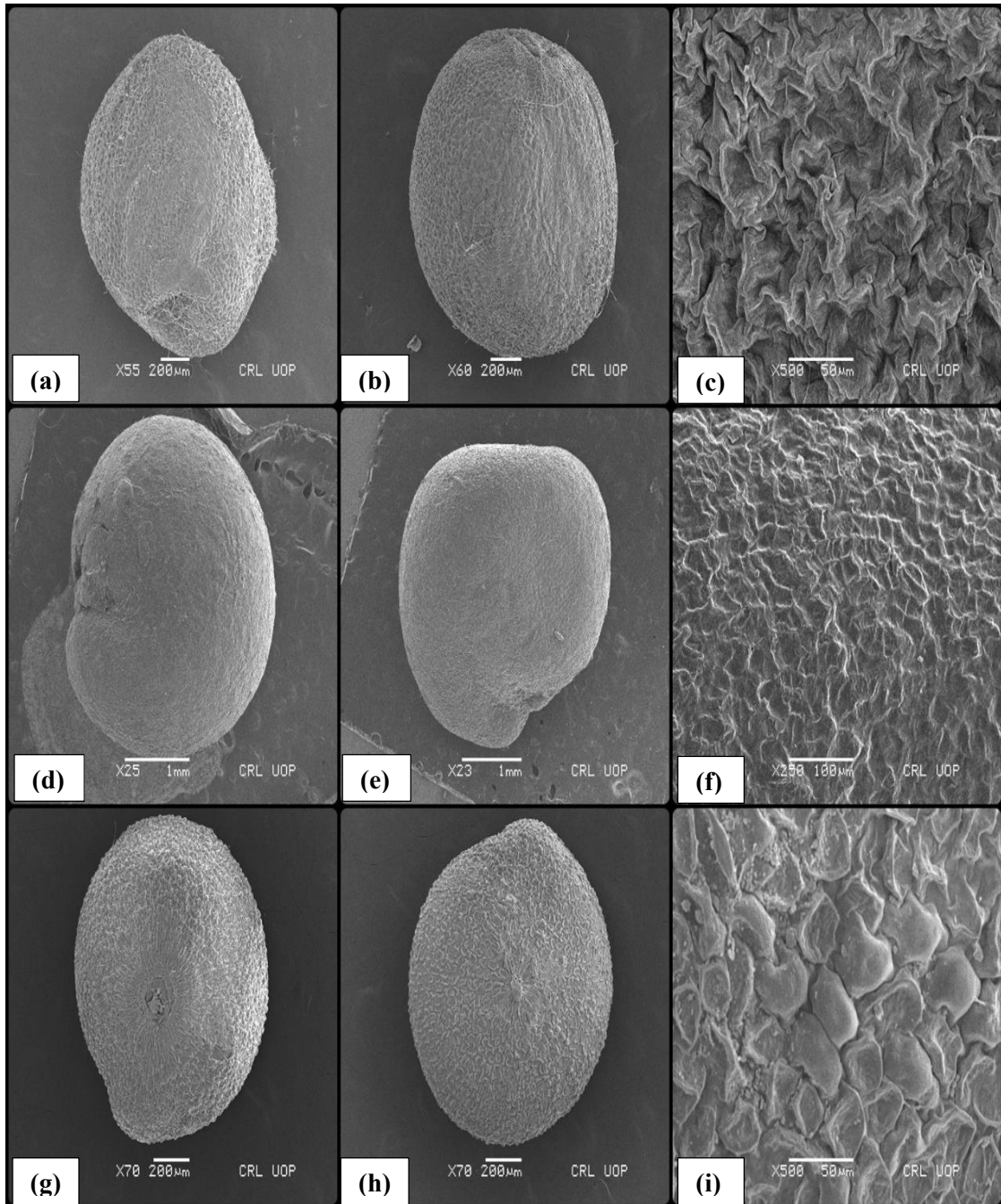


**Plate 65.** Scanning electron micrographs of seed micromorphology; (a-c) *Brassica nigra* (a) central hilum (b) very fine texture (c) rugulate sculpture. (d-f) *Capparis decidua* (d) depressed hilum (e) very fine texture (f) foveolate striate sculpture (g-i) *Chenopodium album* (g) raised hilum (h) coarse texture (i) papillate sculpture.

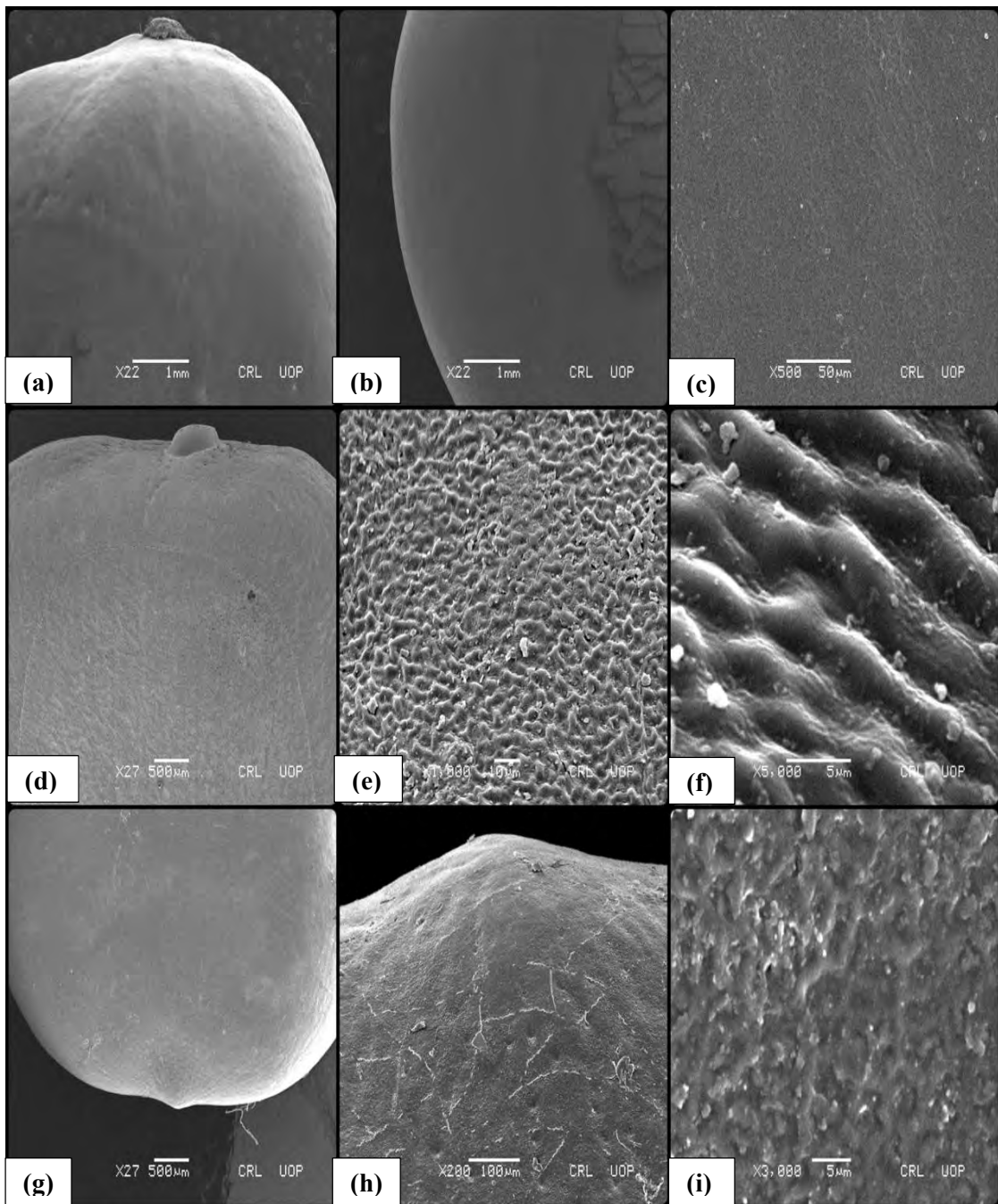


**Plate 66.** Scanning electron micrographs of seed micromorphology; (a-c) *Citrullus colocynthis* (a) raised hilum (b) medium texture (c) striate psilate sculpture. (d-f) *Crotalaria burhia* (d) terminal hilum (e) coarse texture (f) papillate rugose sculpture (g-i) *Dalbergia sissoo* (g) sub-terminal hilum (h) medium texture (i) rugose sculpture.



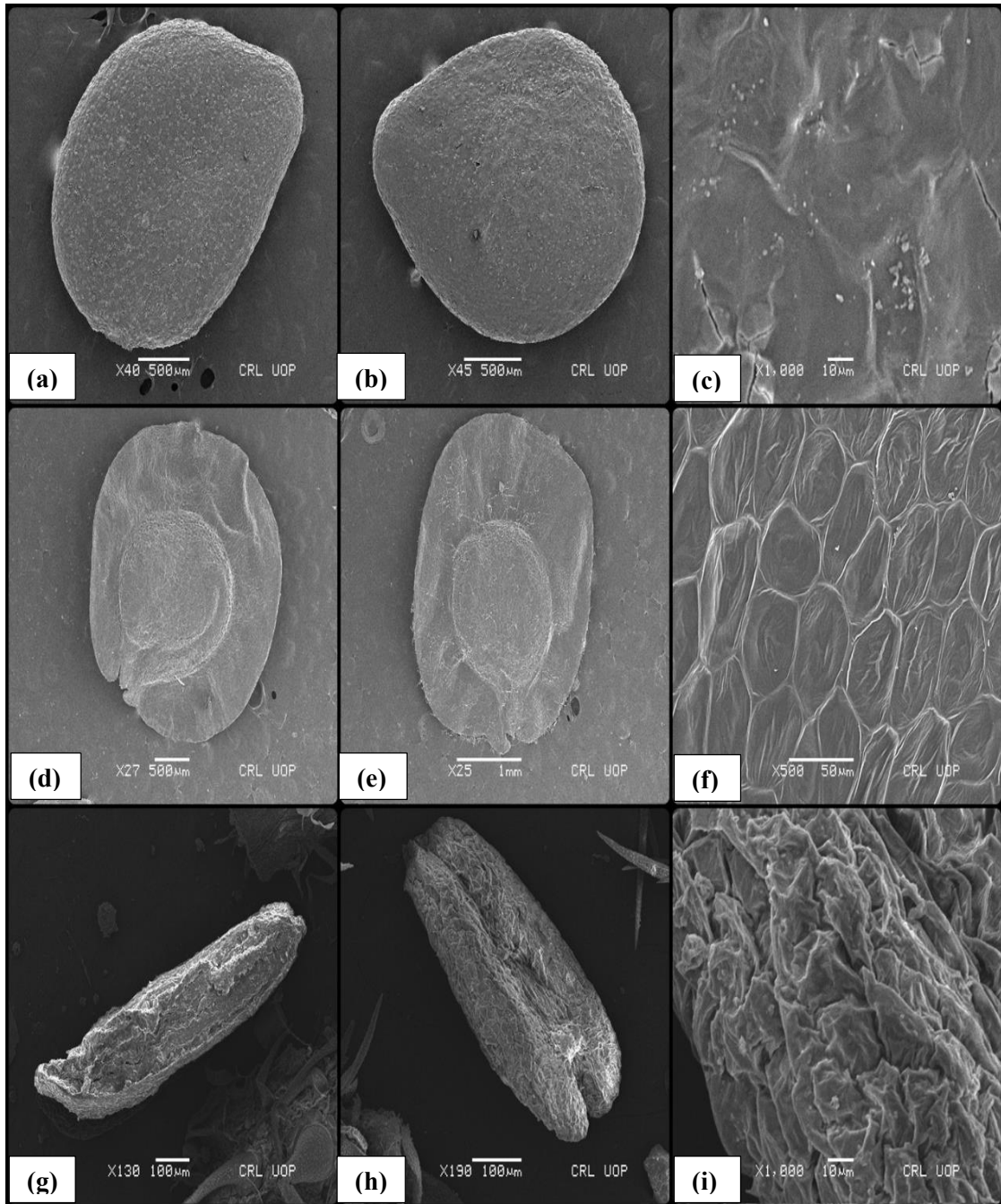


**Plate 67.** Scanning electron micrographs of seed micromorphology; (a-c) *Fagonia bruguieri* (a) raised hilum (b) coarse texture (c) striate sculpture. (d-f) *Farsetia stylosa* (d) central hilum (e) coarse texture (f) reticulate sculpture (g-i) *Heliotropium europaeum* (g) general view (h) sub-terminal depressed hilum (i) foveolate sculpture.

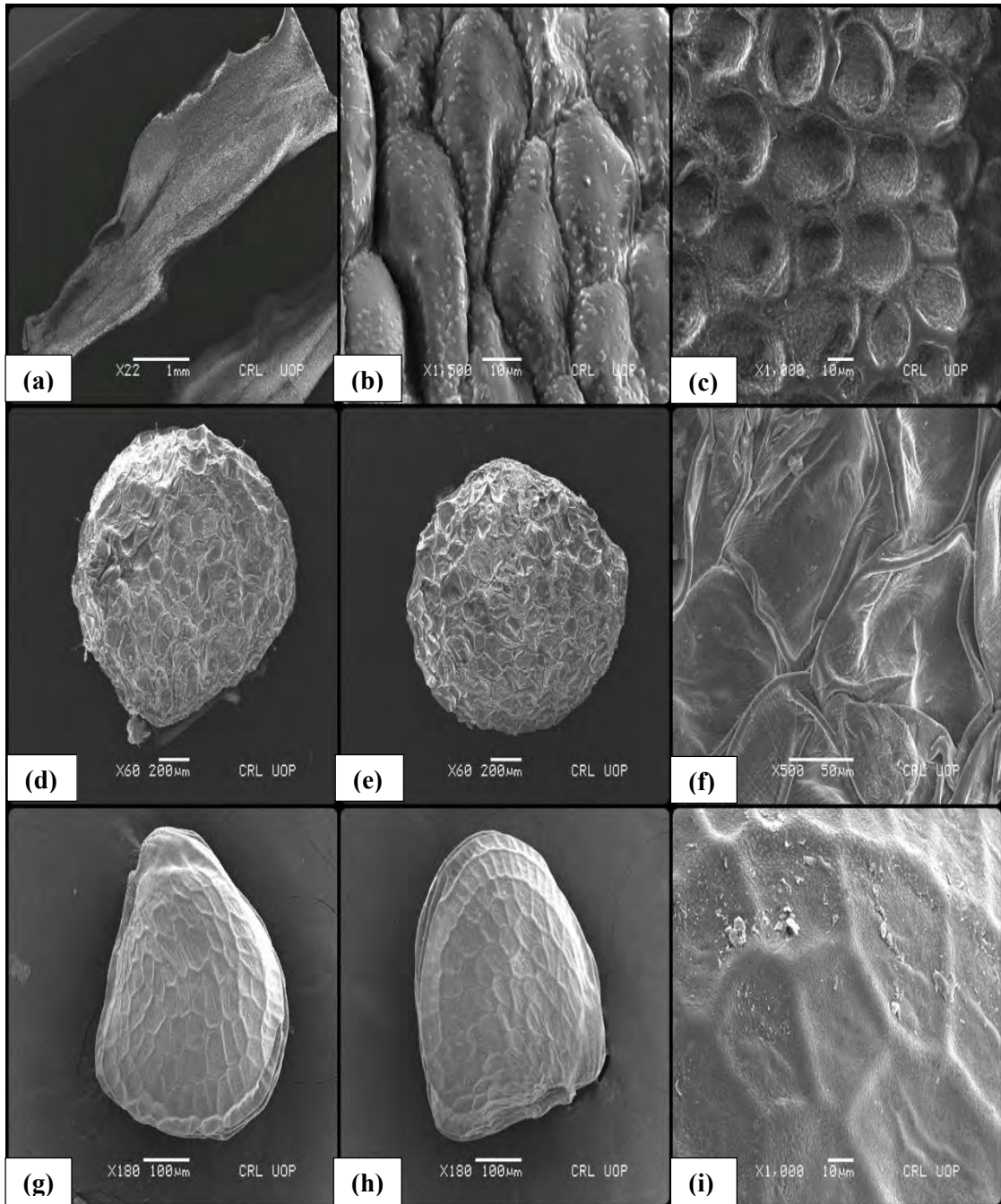


**Plate 68.** Scanning electron micrographs of seed micromorphology; (a-c) *Leptadenia pyrotechnica* (a) terminal hilum (b) coarse texture (c) papillate scabrate sculpture. (d-f) *Mullago cerviana* (d) raised hilum (e) coarse texture (f) reticulate sculpture (g-i) *Mullago naudicaulis* (g) general shape (h) raised hilum (i) papillate foveolate sculpture.

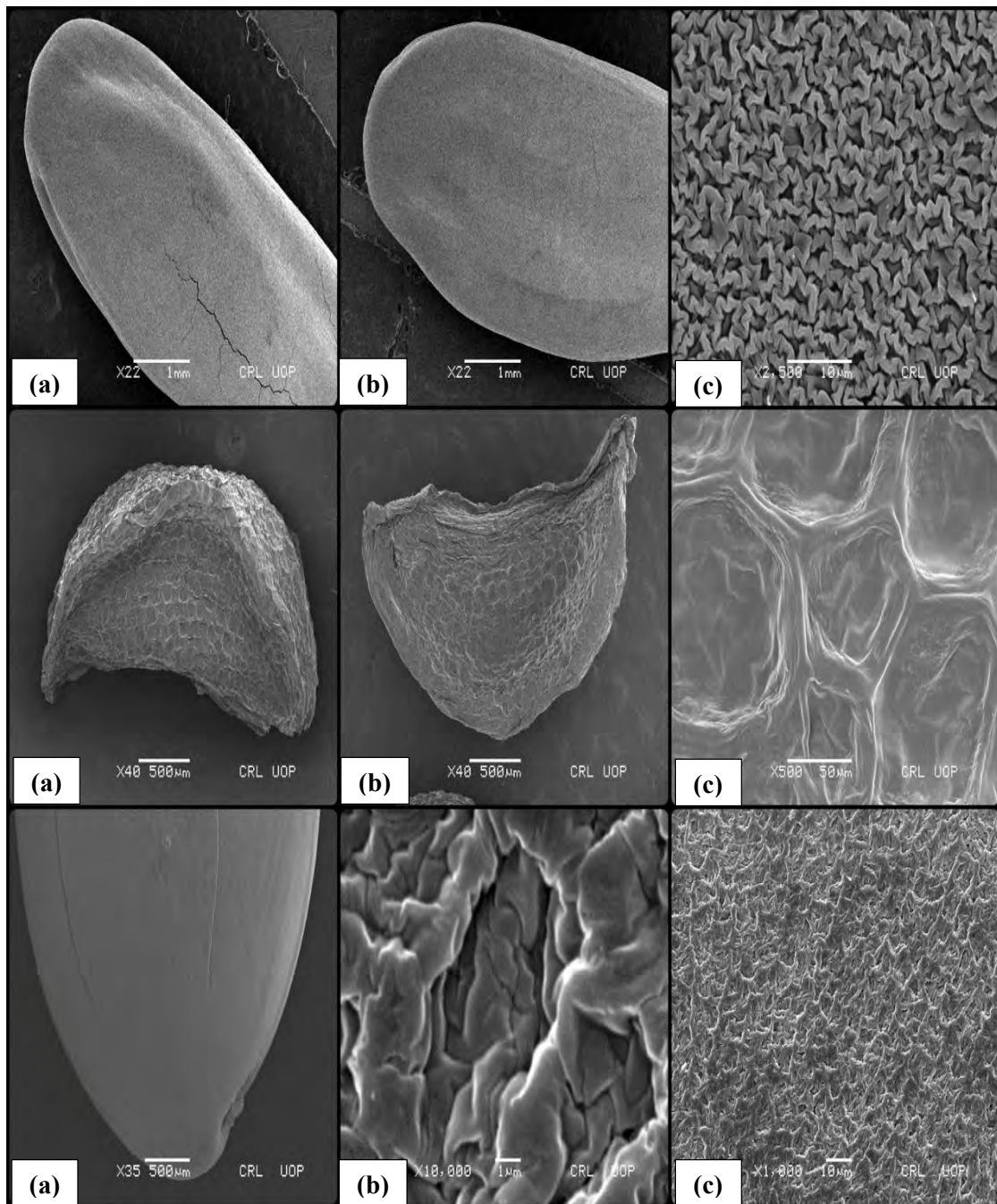


**Plate 69.** Scanning electron micrographs of seed micromorphology; (a-c) *Parkinsonia aculeata* (a) shape (b) irregular fracture line (c) rugose sculpture (d-f) *Peganum harmala* (d) shape (e) deeply convex periclinal wall (f) striate reticulate sculpture (g-i) *Prosopis cineraria* (g) oblong shape (h) depressed hilum (i) Rugose papillate sculpture.

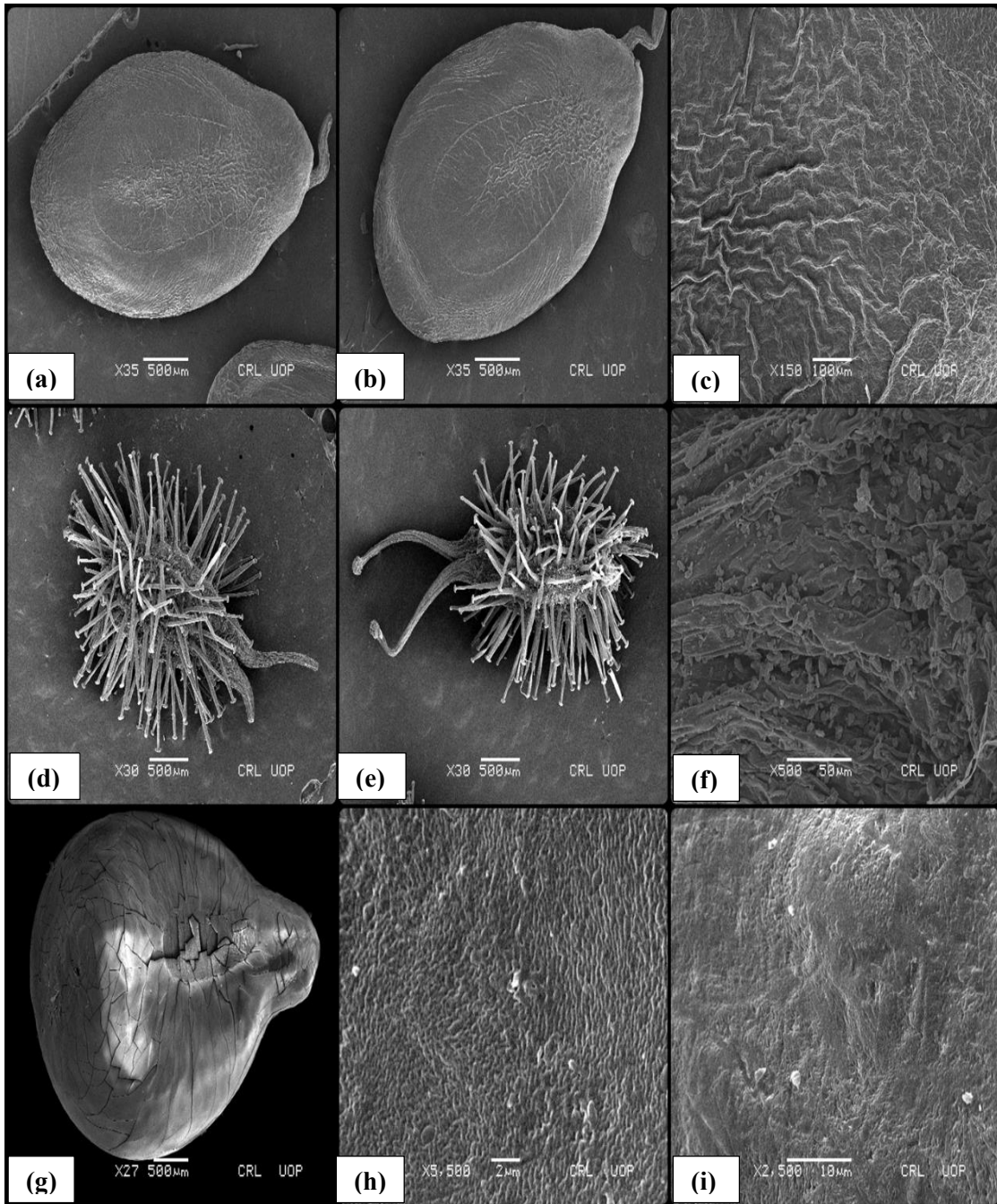


**Plate 70.** Scanning electron micrographs of seed micromorphology; (a-c) *Prosopis juliflora* (a) shape (b) U shape pleurogram (c) rugose sculpture (d-f) *Psammogeton biternatum* (d) shape (e) spiny projections (f) rugulate (g-i) *Senna italica* (g) obovate shape (h) coarse texture (i) Rugose scabrate sculpture.

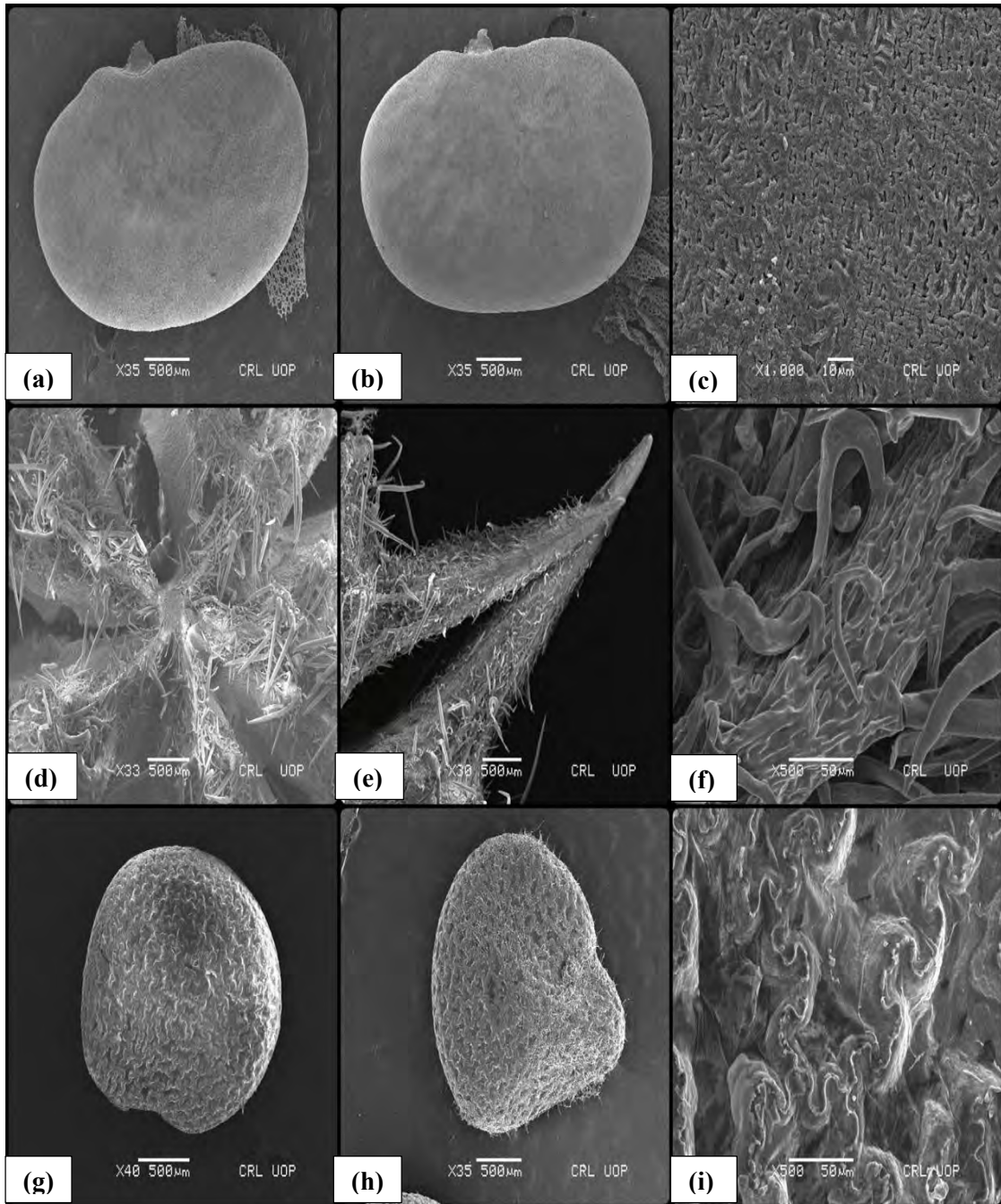


**Plate 71.** Scanning electron micrographs of seed micromorphology; (a-c) *Tephrosia purpurea* (a) shape (b) visible depressed hilum (c) smooth papillae sculpture (d-f) *Tribulus terrestris* (d) spiny scabrous shape outline (e) coarse spiny texture (f) wrinkled spiny sculpture (g-i) *Withania coagulans* (j) shape (k) coarsely rough texture (l) undulate granulate sculpture.

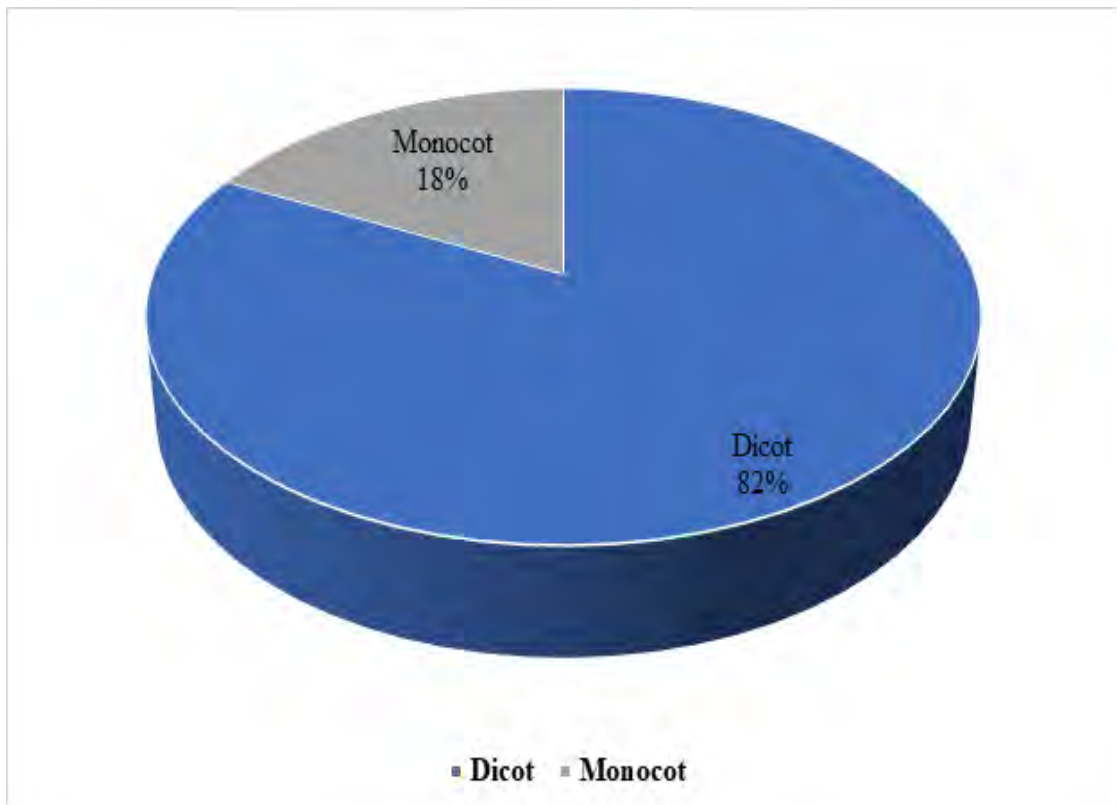


**Figure 33.** Pie chart showing percentages of overviewed dicot and monocot.

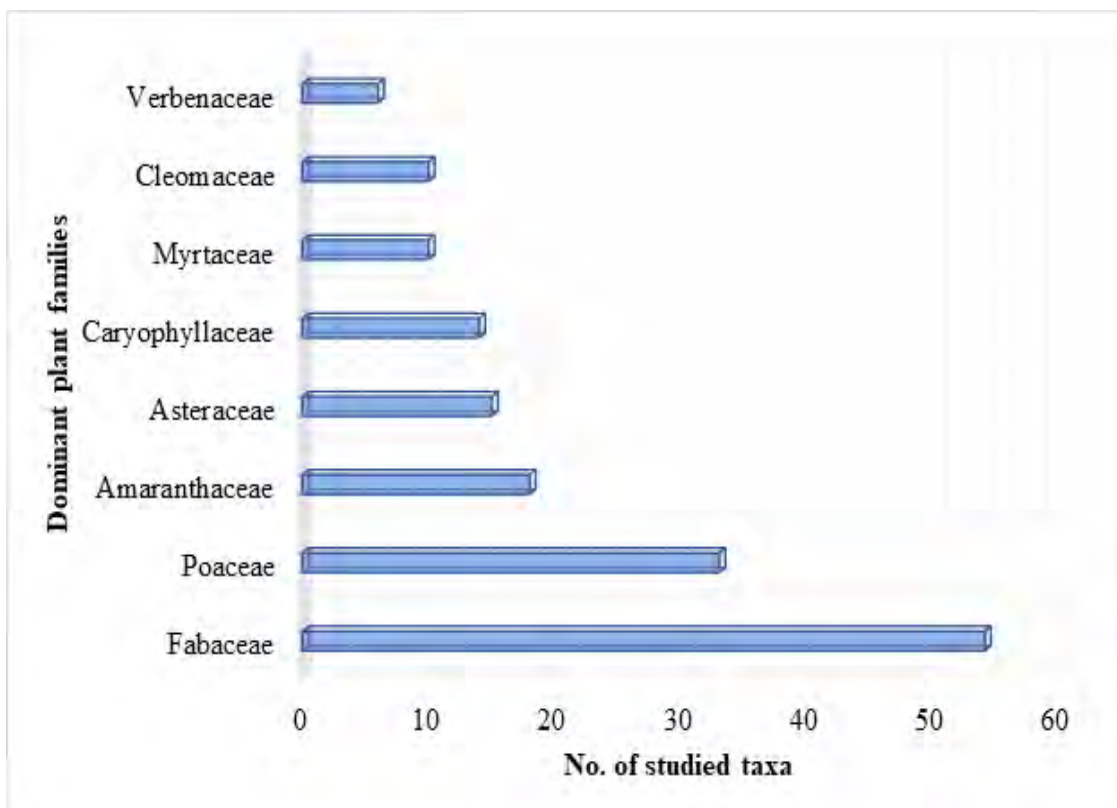


**Figure 34.** Graphical representation of number of taxa within different angiosperm families whose seed morphology has been published.

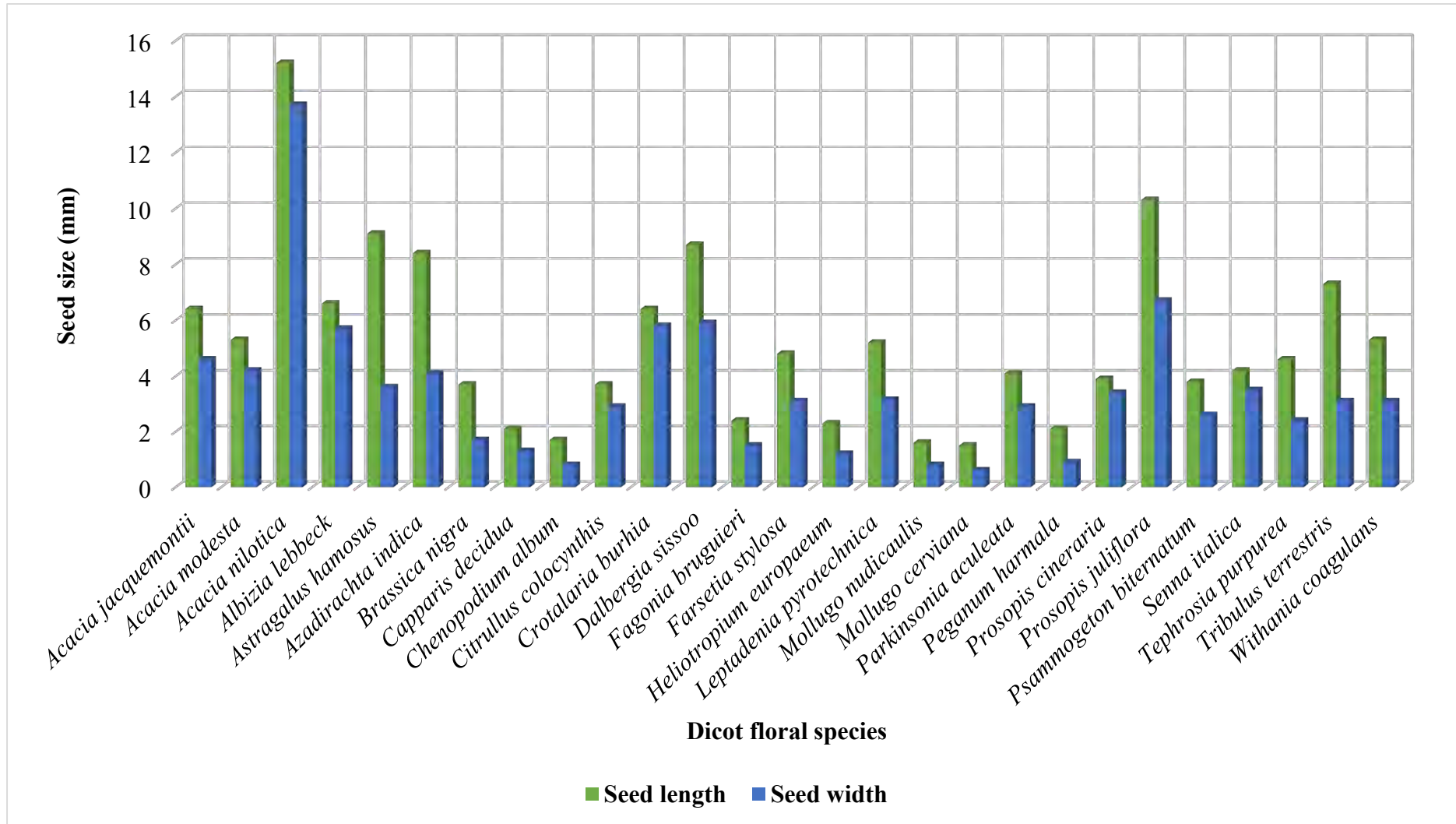


**Figure 35.** Comparison of mean seed length and width in dicot angiosperm species

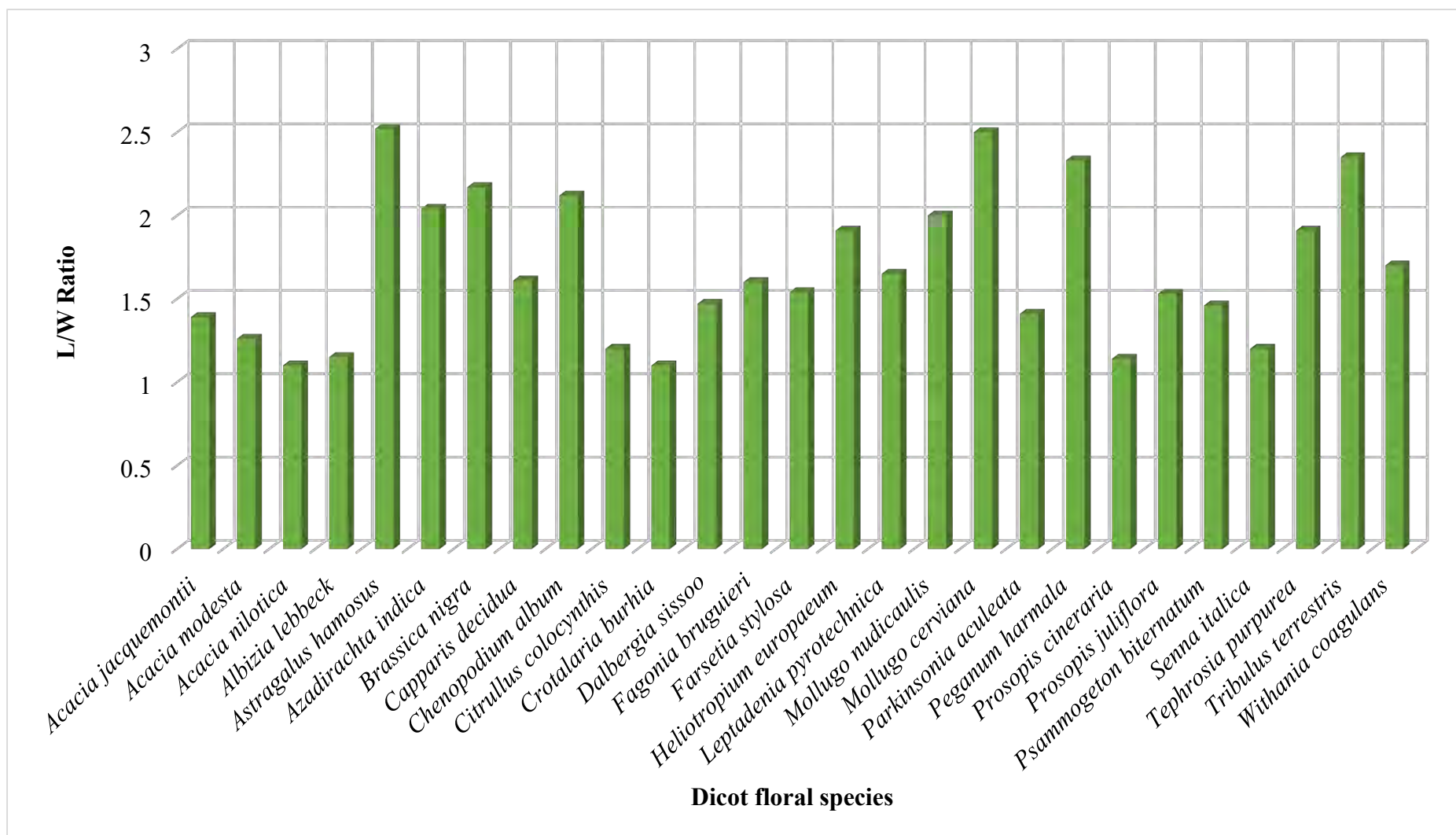


**Figure 36.** Graph showing seed length-to-width (L/W) ratios in studied dicot species.



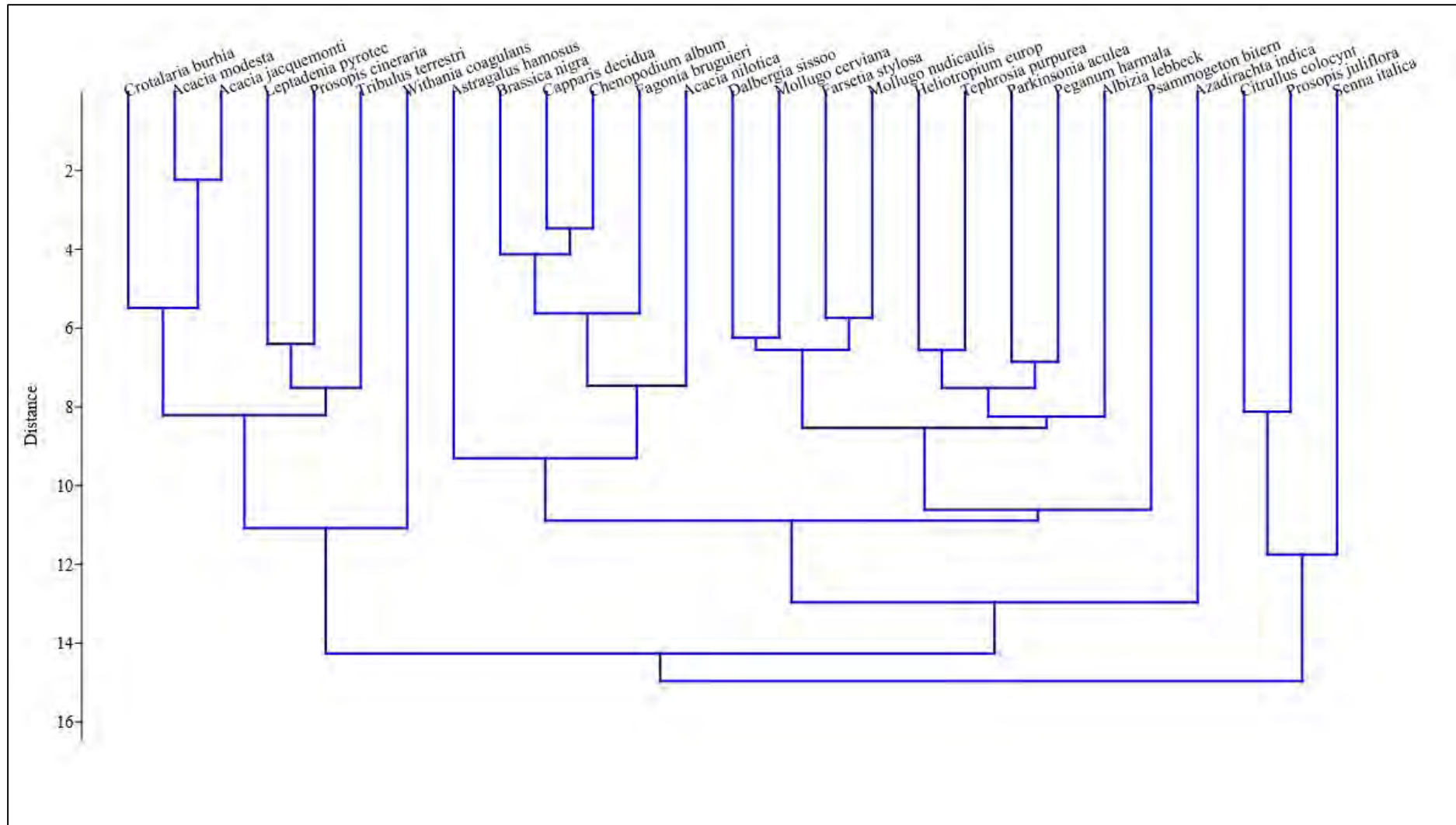


**Figure 37.** Cluster groupings through dendrogram of dicot angiosperm desert species based on qualitative seed morphological traits.

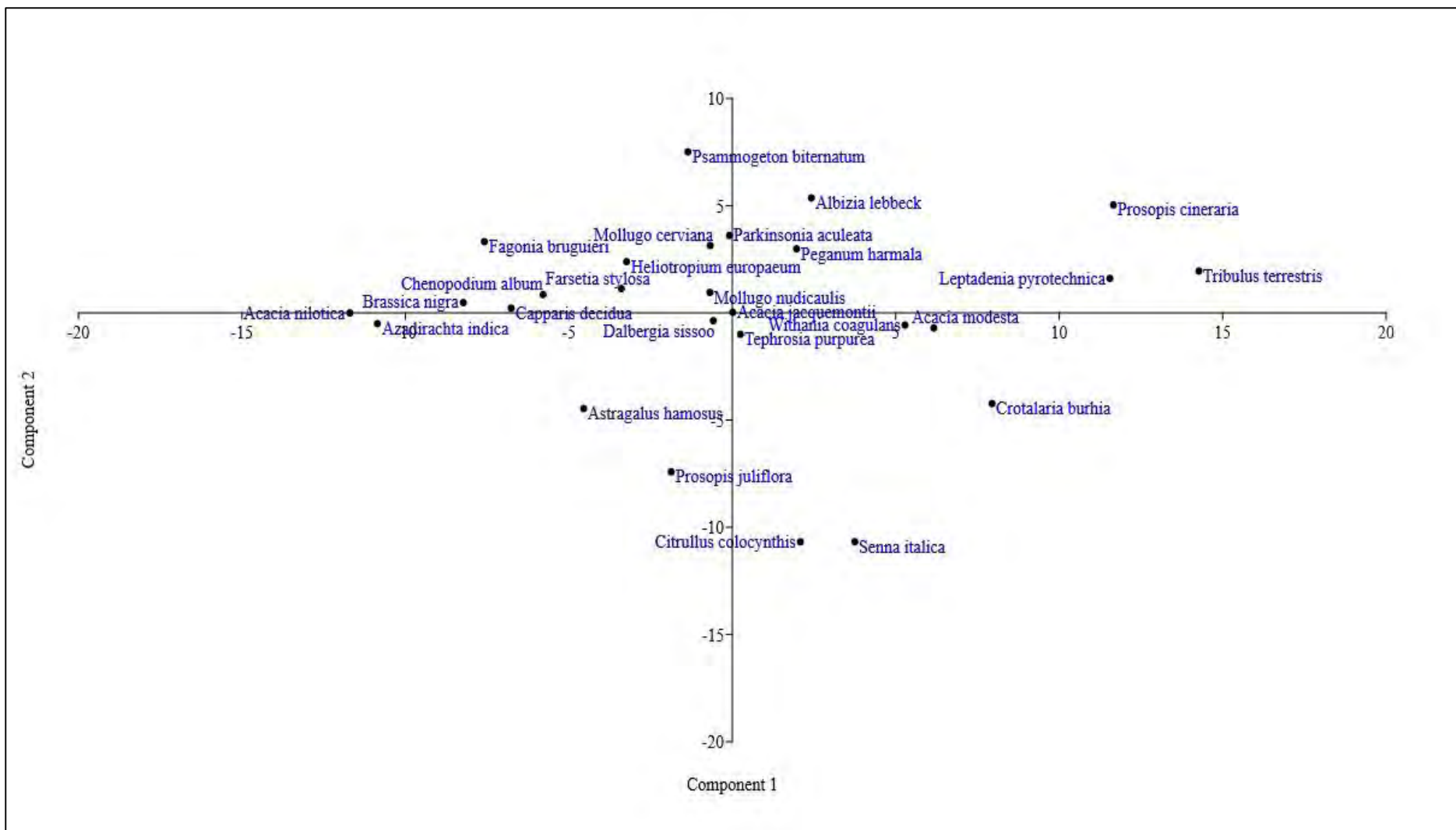


**Figure 38.** Principal component analysis (PCA) biplot of matrix variables of seeds of dicot taxa.

### 3.3.6 Discussion

Seed characteristics were analyzed among desert species and include shape, size, color, weight, wall patterns, hilum region, and surface architecture. These features were quantified statistically by UPGMA dendrogram and PCA, both of which allowed to accurately identify the dicot angiosperms. The seed surface ultrastructure, visualized as a micro-level character, has taxonomic significance for identification and classification.

Previous research identified species based on seed micromorphology and assessed taxonomic affinity using cluster analysis (Abdel Khalik and Osman 2007; Arai et al., 2011; Kaya et al., 2011; Davitashvili and Karrer 2010; de Queiroz et al., 2013; Kasem et al., 2011; Pahlevani et al., 2015; Song and Hong 2020). Seed coat sculpturing in dicot species is not confined to a specific genus or subfamily. However, significant variations in ultra-sculpturing were species specific and of taxonomic relevance. Previously, seed surface orientations and patterns of anticlinal and periclinal walls were proven useful in determining inter-species linkages (Karaismailoğlu 2018).

Many researchers have previously highlighted the remarkable variation in the shape of angiosperm seeds and demonstrated their importance in taxonomic study (Corner 1976; Hassan et al., 2005; Luqman et al., 2018; Nalawade et al., 2020). Seed characteristics, according to Cutler and Brandham (1977), are less influenced by environmental factors and often reflect genetic variations. Seed attributes can be highly effective in distinguishing taxa with similar floral and vegetative aspects (Poulsen and Nordal 2005).

Seed texture metrics evaluated using electron microscope images were categorized, as done previously for other legumes. Spermoderm attributes are genetically determined and are the primary source of intra-or interspecific variations (Al-Ghamdi and Al-Zahrani 2010; Zoric et al., 2010; Gunes and Ali 2011; Kahraman et al., 2014; Ozbek et al., 2014; Umdale et al., 2017). Earlier findings revealed that spermoderm features, wall status (thin or thick), texture crudeness, secondary sculpturing, papillae or tubercles, and fracture line pattern was analyzed to correctly identify *A. nilotica* (Karakish et al., 2013; Alam et al., 2018). SEM visualization identified a depressed hilum, continuous fracture line pattern, sinuate texture, and striate anticlinal wall for *A. nilotica*. Recently, Aboulela et al., (2021) provided

phylogenetic insights for multivariate analysis to compare morphological seed traits within the three tribes of subfamily Papilionoideae.

Corner (1976) emphasized dicotyledonous seeds micromorphology and could accurately identify *Tephrosia candida* based on the number of seed features. Key diagnostic features identified by Kirkbride et al., (2003) in *Tephrosia spp.*, were the cotyledon with a wrinkled inner face, an embryonic axis perpendicular to the length, a reticulate testa, and a hilum inside the corona. Ekici et al., (2005), Vural et al., (2008), and Shemetova et al., (2018) described reticulate, multi-reticulate, striate, and rugose seed patterns among different *Astragalus* species. Astragaleae seed aspects were poorly reported, and there were few standard references on their surface shape and ultra-sculpture elements (Rashid et al., 2021). Seed coat surface peculiarities have phylogenetic implications and are important in resolving relations among the tribes, genera, and species (Ghimire et al., 2015). This study supports earlier findings by exhibiting elliptic-oblong seed outlines in *Astragalus hamosus*. Recently, Kashyap et al. (2021) provided additional micromorphological features in *Astragalus* species, revealing that surface sculpturing has evolved differently in *A. hamosus*, helpful in accurate identification.

Koul et al., (2000) mentioned that seed coat micro-sculpturing of *Brassica* provides evidence for the close relationship of polyphyletic origin among various taxa in the subtribe Brassicinae. Recently, Gabr (2018) gave detailed of morphological parameters in subtribe Brassicinae to elucidate the phylogenetic relationships. Seed morphological findings of Tlili et al., et al., (2011) and Saadaoui et al., (2013) reported the differences between subspecies of *C. spinosa*. Franceschini and Tressens (2004) explained three types of seeds among *Capparis* species: chartaceous glabrous, coriaceous fibrous, and pilose coat sculpturing. *Capparis* phylogenetic relationships are still unknown, but differentiation based on seed morphology clarifies the position of the family Capparaceae (Mahmoud El Sayd and Amar 2020). However, seed characters evolved within the two populations of *C. album* using scanning imaging revealed that the testa of black seeds were more than twice as thick as those of brown seeds (Yao et al., 2010). Earlier observations made by Sukhorukov and Zhong (2013) explained seed characters (color, testa, and embryo orientation) evolution in chenopods to reconstruct the phylogeny.

The ovoid seeds, slightly concave and smooth periclinal and pyriform secretory cells in *F. bruguieri* were useful for classification, but do not support the natural groupings (Khalik and Hassan 2012). Cluster analysis revealed that *F. bruguieri* was characterized by a broadly ovoid shape, rough texture, round apex, and deep convex striate wall sculpture. Beier et al., (2004) performed molecular studies using trnL and ITS DNA sequences to explore phylogeny and showed no support for the clusters linkages among *Fagonia* species. Khalik and Hassan (2012) elaborate smooth seed architecture in *Fagonia* as a diagnostic character. The micro-structure of the seed shape and surface of *F. stylosa* was the same as reported by Kasem et al., (2011) and Gabr (2018) for *Farsetia burtonae* Oliv. and *Farsetia aegyptia* Turra. This research analyzed that the hilum position was central, which contradicted previous studies that described a sub-terminal hilum. Based on molecular and phylogenetic findings, clustering analysis revealed that tribe Alysseae (*Farsetia*) is found to be closely placed with Brassicaceae tribes (Liu et al. 2012). Swamy et al., (2015) showed that seed structure of *Heliotropium amplexicaule* Vahl distinguished it easily from *H. europaeum* with respect to texture, hilum and sculpturing pattern. Our study revealed reticulate anticlinal sculpturing with a protuberant periclinal wall and papillate foveolate in *M. cerviana*, whereas Sukhorukov and Kushunina (2017) described reticulate surface with raised boundaries along cell margins. Earlier research based on molecular phylogeny suggests a close relationship among *Mollugo* species displaying homoplastic papillate ornamentation (Sukhorukov and Kushunina, 2017). Phylogenetic reconstructions based on seed color in Molluginaceae were highly homoplastic in several lineages (Sukhorukov et al., 2018).

Waheed et al., (2021) recently identified psilate regular ridges in *P. aculeata*, but our findings revealed a glabrous irregular reticulate pattern. The outer seed surface in *Parkinsonia* was reported to have very few irregularities and no open fractures (Scott 2006). Seed peculiarities observation among seed of *P. harmala* make species-specific criteria. *P. harmala* micro-sculpturing at the sub-microscopic level exhibit significant surface variations, as the tabular to slightly concave type opposes the present interpretation of the deeply convex striate reticulate type. Current seed morphometric research placed *Peganum* in the Peganiaceae family, in terms of evolutionary trends based on SEM structural features (Semerdjieva and Yankova-Tsvetkova 2017). Scanning imaging analysis by Soliman et al., (2010) described regular reticulate

sculpture, thick anticlinal walls, finely striated texture, and concave periclinal walls. Reticulate surface and fine medium sinuate texture were observed for *P. juliflora* by Waheed et al., (2021), while our results are dissimilar showing striate rugose and medium texture crudeness. Ghimire et al., (2011) observed in *Withania somnifera* (L.) Dunal reticulated primary structure, cells irregularly shaped and undulating anticlinal walls, while in our work we observed thick undulating granulate anticlinal walls in *W. coagulans*.

Venier et al., (2012) studied the seed coat structure through histochemical analysis in five Neotropical *Acacia* species from xerophytic forests of central Argentina. In spite of the importance and stability of seed characters in systematic, very little work seems to have been done on seed anatomy of *A. jacquemontii*. Seeds are dark brown in color, smooth, compressed while our experimentation analyzed greenish brown, obovate and striate foveolate type seed coat structure. Due to its poor germination and biotic interference have caused depletion of shrubby *Acacia jacquemontii* in Thal desert rangelands (Rasool et al., 2016). Waly et al., 2012 outlined the morphology and anatomy of the seeds of 11 species of *Acacia* comprising *A. modesta* and constructed an artificial key indicating that seed micro characters contribute in the classification of *Acacia* species (Mustafa et al., 2017). Scanning electron microscope investigation of the seed surface shows variation between *Acacia* species; different types of seed surface stratification are recognized *A. jacquemontii* is flat to convex striate, *A. modesta* is striate regulate, *A. nilotica* is with striate fine sinuate texture features. Our results agree with Waly et al., (2012) who investigate 11 species of *Acacia* grown in the western region of Saudi Arabia, to standardize a procedure for identifying the seeds via scanning surface features of seeds.

The seeds of *A. lebbeck* are pale brown in color, shining, nearly round in outline, and compressed disk-like. Both sides of the seeds with faveolate-type sculptured elements (Khan, 2020). Whereas current findings contradict to previous work brown color, elliptical depression, and rugose surface ornamentation were analyzed. In this study, we observed variation in seed micromorphology of *A. lebbeck* seeds as brown, scabrous with terminal position hilum was observed while Khirade and Dudhe (2022) examined ovate, light brown, and centrally placed hilum.

The family Cucurbitaceae is a eurospermous family as considerable variation has been observed in seed characters, especially in seed shape and surface patterns

(Wimalasiri et al., 2016). Abid et al., (2015) examined *C. colocynthis* has obovate seeds with punctuate surface sculpturing while this work described obovate, smooth, sub-terminal raised hilum with striate psilate ornamentation. Heneidak and Khalik (2015) represented *C. colocynthis* seeds with yellow-brown; not arillate; sculpture of periclinal wall smooth to fine folds. Ali et al., (2013) explained that *C. colocynthis* spermoderm seed pattern was thin polygonate reticulate, compactly arranged reticulate cells have been extensively utilized as a secondary taxonomic characters.

Our observation revealed seeds of *C. burhia* species are generally reniform, compressed, flat and asymmetric. Seed color is an adaptive strategy since the brown seeds of *C. burhia*, are dispersed and reach the ground, and are not visible to predators, such as birds and insects, thereby promoting the reproductive success of the species (Subramaniam et al., 2015). Seed morphology of 19 *Crotalaria* species from Thailand was studied by Ninkaew et al., (2017) using stereo and scanning microscopy display seeds varied significantly with colliculate peculiarities, and ruminant features.

Waheed et al., (2021) described oblong and sub-terminal placed hilum in *D. sissoo* while this study also explained the same features but the hilum level is undetermined. Upadhyay et al., (2016) focused on 15 varieties of *D. sissoo* seed source explained variability in seed morphometric traits. Screening the variations in seed source provides a great opportunity for success of afforestation, besides providing information on the raw material for breeding and evolving improved planting stock.

Hilum position, seed wing sculpturing, and anticlinal wall pattern were recorded for *L. pyrotechnica* from Egypt using high-resolution microscopic techniques that recognized semi-depressed hilum, reticulate sculptural elements, and undulation of the anticlinal wall (Gabr, 2014). In our work dissimilarity exist regarding terminal place hilum and papillate scabrate anticlinal wall micro-structural traits. Based on the exomorphic seed characters, Al Nawaihi et al., (2006) reached the conclusion that *L. pyrotechnica* has long ovate seeds with surface hairy features that were missing and reticulation in the surface seed coat was examined.

Arshad et al., (2006) reported seeds of *P. cineraria* are rhomboidal, compressed, brown, and smooth. In this study, we evaluated the terminally depressed hilum and rugose papillate anticlinal wall ornamentation. *P. cineraria* has a wide range of variability within the population of trees for various seed characteristics including seed

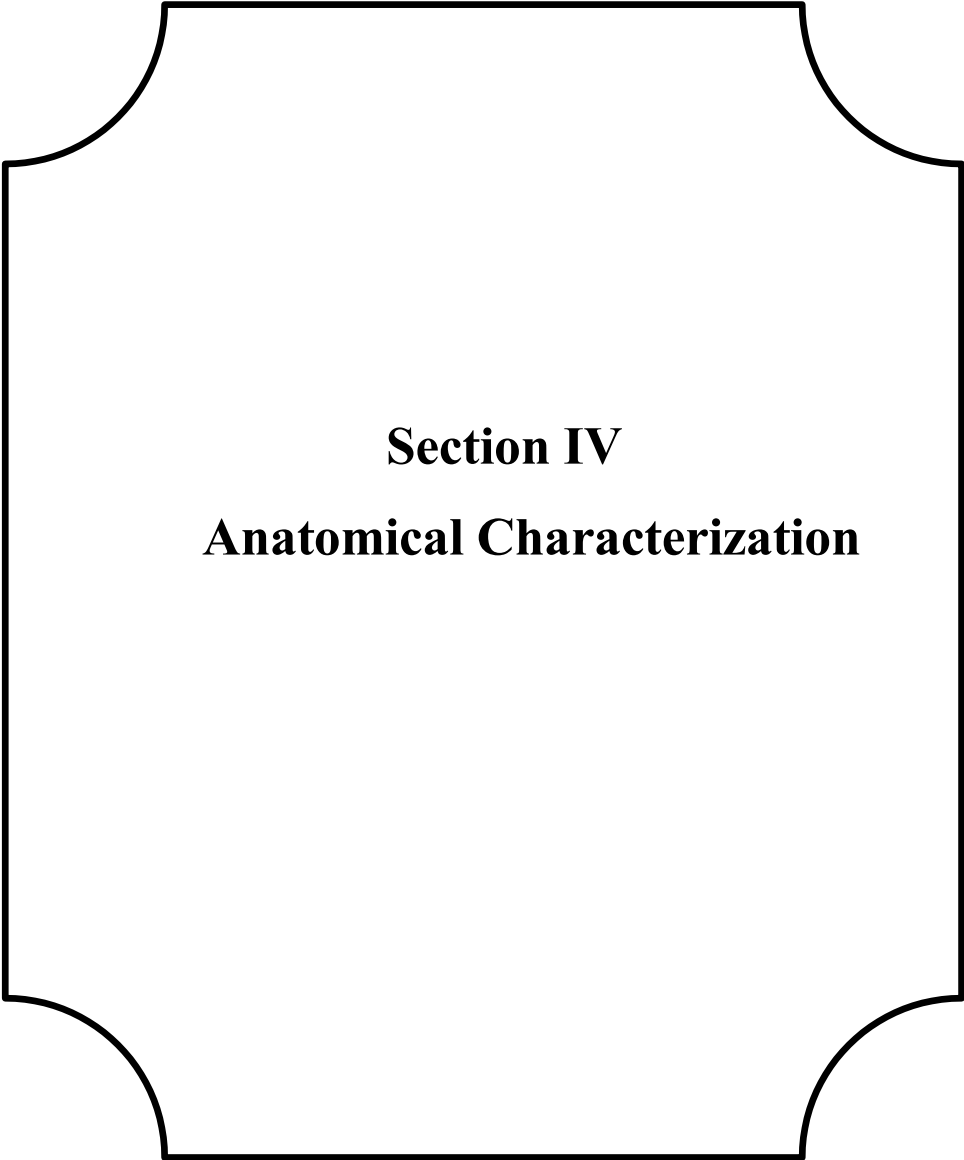
size can be used as a parameter for predicting germination and seedling growth rate (Noor et al., 2018). Karakish et al., (2013) discussed the electrophoretic seed protein profiles combined with morphological seed traits of 27 *Prosopis* species to explore their systematic relevance.

Fawzi et al., (2015) elucidate numerical taxonomic work on *S. italica* seeds provides detailed structure as a pod on both sides with elevated projections along the middle. However this study analyzed obovate shape with pointed apex and depressed hilum in *S. italica*. Mao et al., (2018) assessed the populations of *S. obtusifolia* using ISSR and SCot molecular markers was supported by micromorphological seed traits variations. Pod portioning separating the longitudinally, usually vertically compressed seeds with areoles among *Senna* species whereas deeply convex periclinal wall, visible terminal hilum and rugose scabrate sculpture was identify in this work.

Semerdjieva et al., (2011) recognized seed sculpture as tubular type, with polygonal cells and straight arched anticlinal walls, whereas the periclinal ones are wavy with dense cuticular folds. He also recognized *Tribulus* section including species whose mericarp is covered with several spines. Rozina et al., (2022) recently gives detailed micromorphology of *T. terrestris* seed demonstrated striate surface ornamentation with uniform cell arrangement, thick curved anticlinal walls and convex thick periclinal walls. However our results deviate with respect to sculpturing pattern of wrinkled spiny surface and protuberant periclinal wall.

The significance of seed micromorphology in identifying dicot angiosperms has been recognized in key taxonomic exploration of the desert flora. This research describes the seed micromorphology of 27 species that are mostly widespread in the tropical Thal desert. The SEM results showed significant taxonomic scorable diversity among various species and give useful data on seed surface shape in the context of phylogeny.





**Section IV**  
**Anatomical Characterization**

### 3.4 Anatomical Characterization of Dicot flora

This study, therefore, takes into account the foliar and petiole microcharacters with the aim of providing useful diagnostic characters to complement existing taxonomic information primarily for the identification of the Desert dicot species. In view of their taxonomic status and the difficulty in identifying species morphologically, this study, therefore, set out to describe the leaf and petiole anatomy of selected Dicot floral species using light and scanning electron microscopy. The microstructural features observed providing useful information for the delimitation, subsequent identification, and the taxonomy with respect to the characters viz, nature of epidermis, size of upper and lower epidermis, number of layers of collenchyma cells and length, number of layers of parenchymatous cells, type of vascular bundles, the occurrence of stomata their size, and trichomes.

Foliar epidermal micromorphology and sculpturing patterns of epidermis representing 37 Dicot floral species revealed stable foliar anatomical characters that are diagnostic and are important in separating the taxa. The comparative studies on foliar epidermal features of 14 Amaranthaceous taxa followed by Fabaceae (10 species), Cucurbitaceae (six species), Capparaceae (five species) and Cactaceae (two species) was carried out.

Petiole anatomy of 22 selected Dicot species belonging to family Amaranthaceae (14 species) and Euphorbiaceae (eight species) was investigated with a view to exploit its systematic and taxonomic significance. Specimens of the selected species were obtained from Thal desert and subjected to standard procedures for microscopic observation and micrographic documentation.

### 3.4.1 Foliar Epidermal Micromorphology of Amaranthaceous taxa

Leaf epidermal micro-morphology of fourteen Amaranthaceous species from the Thal desert was investigated using light and scanning microscopic (LM and SEM) techniques. In current findings, both qualitatively and quantitatively, foliar anatomical characters of amphistomatic and hypostomatic leaves have shown substantial variation. (Table 20, 21, 22 & 23). The leaf surface light and scanning micrographs were illustrated in Plates 72 to 79.

#### a) Epidermal Morphology

Significant differences in foliar epidermis structure were observed on both the adaxial and abaxial sides of the Amaranthaceous taxa. The epidermis cells differ in size depending on the species being examined. Diverse epidermal cell types were observed; irregular, rectangular, polygonal, undulated, isodiametric, and uniseriate (Table 20 & 21). Various types of anticlinal wall patterns were observed, i.e., angular, wavy, straight, undulating, slightly straight, rounded, curved, sinuous, and deeply sinuate. Average number of epidermal cells ranges from 16 to 110 were observed on both surfaces. Similarly, the number of lobes per cell differs from 3 to 14 among *Amaranthus* taxa. A minimum of 3 to 6 lobes per cell was observed in *Amaranthus retroflexus* along the adaxial surface, whereas a maximum 6 to 14 along the abaxial surface was observed in *Chenopodium album*. The largest epidermal cell length and width were measured on the adaxial side of *Aerva lanata* (55.5  $\mu\text{m}$ ) and (22.5  $\mu\text{m}$ ), respectively. Whereas on the abaxial surface, maximum length (38.5  $\mu\text{m}$ ) and width (21  $\mu\text{m}$ ) are found in *Alternanthera ficoidea*. The shortest epidermal cell length (L = 9.94  $\mu\text{m}$ ) and width (W = 4.8  $\mu\text{m}$ ) were measured in *Digera muricata* on the adaxial surface, while on the abaxial side, minimum length (L = 5.02  $\mu\text{m}$ ) and width (W = 3.06  $\mu\text{m}$ ) were noted in *Achyranthes aspera* (Figure 39). Subsidiary cells have also been found in all species with considerable variations. Four subsidiary cell arrangement types were examined; margin sinuous, enclosing guard cells in most Amaranthaceous taxa, followed by lobed margins, wavy, enclosing guard cells, and lobed margins, wavy and partly enclosing guard cell shapes. On the abaxial side of *Amaranthus graecizans*, the largest subsidiary cell length (62  $\mu\text{m}$ ) along the adaxial side and the maximum length (64  $\mu\text{m}$ ) on the abaxial side were noted. The width of the largest subsidiary cell

was noted in *Salsola tragus* (41  $\mu\text{m}$ ) on the adaxial surface, while in *Amaranthus graecizans* on the abaxial surface (41.5  $\mu\text{m}$ ), as summarized in Table 23.

### b) Morphological Parameters of Stomatal Complex

In the present study, stomata were observed on leaf surfaces in all deserted Amaranthaceous species. Six species have anomocytic types of stomata, followed by anisocytic types (4 species) and paracytic stomata (3 species), while in *Alternanthera ficoidea* and *Alternanthera philoxeroides*, the diacytic type of stomata on the epidermal surface was examined. Stomatal shape differences were observed as elliptic, elongate elliptic, and broad elliptic were observed in *Alternanthera philoxeroides*, *Atriplex stocksii*, and *Digera muricata*. The difference in stomatal size varied among species, and on the lower surface, the largest stomatal size was observed than on the upper surface. Lengthwise, the largest stomata were noted in *Alternanthera sessilis* (29.5  $\mu\text{m}$ ) and the maximum width along the adaxial surface (19.2  $\mu\text{m}$ ) was measured for *Aerva lanata*. Whereas maximum length (33  $\mu\text{m}$ ) and width (20  $\mu\text{m}$ ) along abaxial side was calculated in *Salsola tragus* (Figure 40).

The guard cells were mostly examined with a kidney shape, while some species with broad kidney shaped guard cells were examined. Guard cells mean variations in length ranged from 6.08  $\mu\text{m}$  in *Digera muricata* to 33  $\mu\text{m}$  in *S. tragus*. Quantitatively stomatal pore showed variations as shown in Table 23, on both sides length was observed maximum in *A. graecizans* (22.9  $\mu\text{m}$ ) and (16.8  $\mu\text{m}$ ) respectively. Whereas minimum length was noted for *D. muricata* on adaxial side (5.08  $\mu\text{m}$ ) and along abaxial surface (4.96  $\mu\text{m}$ ). On the adaxial side, maximum width was observed in *A. graecizans* (11.7  $\mu\text{m}$ ), while on the abaxial in *A. lanata* (6.5  $\mu\text{m}$ ). *Chenopodium album* had a minimum width of 1.05  $\mu\text{m}$  on the adaxial surface and 1.02  $\mu\text{m}$  on the abaxial surface. For each species, the stomatal index was measured on both the adaxial and abaxial surfaces of the epidermis. Stomatal index was measured maximum and minimum along adaxial and abaxial sides in *Atriplex stocksii* (28% and 7.29%), respectively. While stomatal index on abaxial surface was calculated (42.93%) in *Amaranthus graecizans*, whereas minimum along adaxial surface (8%) in *Digera muricata* (Figure 41).

### c) Trichome Diversity

Table 2 presents 10 species out of 14 that have trichomes on both surfaces of various forms, i.e. slender, unicellular, uniseriate, biseriate, multicellular, stellate,

capitate, glandular, and non-glandular. Selected light and scanning micrographs of different types of trichomes are shown in Plates 72 to 79. On both surfaces, densely distributed e-glandular, long and unbranched trichomes were recorded on the epidermis of most of the Amaranthaceous species. SEM examination confirmed the presence of only one type of unicellular, glandular, and conical trichome in *Bassia indica*. The longest trichome was found on the adaxial surface in *Alternanthera sessilis* (127  $\mu\text{m}$ ), while the smallest was examined for *Aerva lanata* (33.5  $\mu\text{m}$ ). On the abaxial surface, maximum length was measured for *Amaranthus graecizans* (117.5  $\mu\text{m}$ ), whereas the shortest in *Atriplex stocksii* was (59.5  $\mu\text{m}$ ). Differences were also observed in the trichome width along the adaxial side, with a maximum in *A. graecizans* (38.5  $\mu\text{m}$ ) and a minimum in *D. muricata* (6.1  $\mu\text{m}$ ). While the abaxial surface of *A. retroflexus* has a maximum width of 34.8  $\mu\text{m}$ , whereas the minimum examined in *D. muricata* is 5.16  $\mu\text{m}$ , as shown in Figure 42.

Trichome index was recorded highest 15.9 % on the adaxial surface of *Amaranthus retro flexus* and lowest 2.65 % for *Aerva lanata*. Whereas on abaxial side maximum was measured for *Amaranthus graecizans* (37.93 %) and minimum (2.46 %) for *Alternanthera sessilis* shown in (Figure 43).

### 3.4.2 UPGMA Dendrogram Statistics

The construction of a dendrogram using numerical taxonomic data analysis illustrates the differences and similarities among Amaranthaceous species (Karaismailoğlu et al. 2018). Dendrogram cluster analysis supports the specific status of various groups of plants (Thadeo et al. 2014; Santos et al. 2020; Guven et al. 2021). Based on Euclidean distance clustering (UPGMA) analysis among 16 quantitative anatomical features, Amaranthaceous species were placed into three major clusters (Figure 44). *Amaranthus graecizans*, which is individually separate from other species, belongs to C1 (cluster 1). The C2 (cluster 2) contained *Alternanthera sessilis* and *Salosla tragus*, whereas the C3 (cluster 3) is further subdivided into two sub-clusters; the first sub-cluster (C3-I) retains *Alternanthera philoxeroides*, *Chenopodium ficifolium*, *Bassia indica*, *Amaranthus retroflexus*, *Amaranthus viridis*, *Digera muricata*, and *Achyranthus aspera*, and the second sub-cluster (C3-II) includes *Alternanthera ficoidea*, *Atriplex stocksii*, *Chenopodium album*, and *Aerva lanata*. The highest similarities were observed

among *Alternanthera philoxeroides* and *Chenopodium ficifolium* in the third cluster (C3-D).

### 3.4.3 Taxonomic Keys Based on Amaranthaceous Foliar Anatomy

- 1 + Trichomes absent epidermal cell irregular, wavy anticlinal wall, stomata diacytic..... *Alternanthera philoxeroides*
- Trichomes absent, epidermal cell undulate to irregular, straight and wavy anticlinal wall, stomata anomocytic to anisocytic ..... 2
- 2 + Epidermal cell undulate, anticlinal wall straight, stomata anomocytic abaxial, trichome absent ..... *Salsola tragus*
- Epidermal cell irregular, anticlinal wall sinuate and deeply sinuate, stomata anomocytic ..... 3
- 3 + Epidermal cell irregular with wavy anticlinal wall, stomata anomocytic, trichome absent.....*Chenopodium ficifolium*
- Epidermal cell rectangular, anticlinal wall rounded .....4
- 4 + Epidermal cell uniseriate to rectangular, anticlinal wall rounded, stomata anisocytic, trichome absent..... *Amaranthus viridis*
- Epidermal cell irregular, anticlinal wall undulated, trichomes present..... 5
- 5 + Epidermal cell irregular to isodiametric, anticlinal wall undulated, stomata diacytic, trichome non-glandular (adaxial).....*Alternanthera ficoidea*
- Epidermal cell polygonal, stomata paracytic..... 6
- 6 + Epidermal cell polygonal, anticlinal wall deeply sinuate, stomata paracytic, trichome glandular capitate (abaxial)..... *Chenopodium album*
- Epidermal cell polygonal, anticlinal wall straight..... 7
- 7 + Epidermal cell polygonal, stomata anomocytic, anticlinal wall straight, trichome unicellular non-glandular (abaxial)..... *Atriplex stocksii*
- Epidermal cell rectangular, stomata paracytic..... 8

- 8** + Epidermal cell rectangular, stomata paracytic (abaxial), anticlinal wall rounded, trichome long slender, conical..... *Bassia indica*
- Epidermal cell polygonal, anticlinal wall sinuate..... **9**
- 9** + Epidermal cell polygonal, stomata paracytic (abaxial), anticlinal wall curved to deeply sinuate, trichome multicellular falcate..... *Amaranthus retroflexus*
- Epidermal cell irregular, stomata anisocytic ..... **10**
- 10** + Epidermal cell irregular, stomata anisocytic (abaxial), anticlinal wall undulate, trichome unicellular glandular..... *Achyranthes aspera*
- Epidermal cell polygonal, stomata elongate elliptic..... **11**
- 11** + Epidermal cell polygonal to rectangular, stomata anomocytic, anticlinal wall sinuate, smooth and angular, trichome stellar glandular..... *Aerva lanata*
- Epidermal cell irregular, trichome multicellular glandular..... **12**
- 12** + Epidermal cell polygonal to irregular, stomata anomocytic, anticlinal wall smooth to angular, trichome uniseriate to biseriate..... *Amaranthus graecizans*
- Epidermal cell round isodiametric, stomata elliptic shape..... **13**
- 13** + Epidermal cell polygonal, stomata anomocytic, anticlinal wall straight, trichome unicellular to multicellular capitate..... *Alternanthera sessilis*
- Epidermal cell round undulate, stomata broad elliptic shape..... **14**
- 14** + Epidermal cell irregular to undulate, stomata anomocytic to anisocytic, anticlinal wall sinuous, trichome glandular multicellular..... *Digera muricata*

**Table 20.** Qualitative analysis of leaf adaxial and abaxial surface among Amaranthaceous taxa.

<b>Amaranthaceous taxa</b>	<b>Leaves Condition</b>	<b>Ad × Ab</b>	<b>ECS</b>	<b>AWP</b>	<b>NES</b>	<b>LPC</b>
<i>Achyranthes aspera</i> L.	Hypostomatic	Ad	Irregular	Undulate	Numerous unicellular hairs, multi cellular and glandular hairs	11-13
		Ab	Irregular	Undulate		7-10
<i>Aerva lanata</i> (L.) Juss.	Amphistomatic	Ad	Polygonal	Sinuate	Epidermis has wide and thin walled cells	4-8
		Ab	Rectangular	Smooth, angular		5-9
<i>Alternanthera ficoidea</i> (L.) Sm.	Amphistomatic	Ad	Isodiametric, irregular	Undulated	Uniseriate row of compactly arranged cells	6-9
		Ab	Isodiametric, irregular	Undulated		7-12
<i>Alternanthera philoxeroides</i> (Mart.) Griseb.	Amphistomatic	Ad	Irregular	Curved	Hair simple and unbranched, Composed of compactly set of rectangular cells	5-9
		Ab	Irregular	Strightly curved		6-10
<i>Alternanthera sessilis</i> (L.) R.Br. ex DC.	Amphistomatic	Ad	Polygonal	Straight	Single layered epidermis on both surface, covered with striated thin-walled round isodiametric cells	6-8
		Ab	Polygonal	Straight		4-7
<i>Amaranthus graecizans</i> L.	Amphistomatic	Ad	Polygonal	Smooth, angular	Uniseriate with radial or pueblos cells	9-13
		Ab	Irregular	Smooth, angular		8-11



<i>Amaranthus retroflexus</i> L.	Hypostomatic	Ad	Polygonal	Slightly curved	Longitudinal cuticular folds or striate cells	3-6
		Ab	Polygonal	Deeply sinuate		5-9
<i>Amaranthus viridis</i> L.	Amphistomatic	Ad	Uniseriate	Rounded	Leaf epidermal cells on both sides with smooth walls	5-10
		Ab	Rectangular	Rounded		7-11
<i>Atriplex stocksii</i> Boiss.	Amphistomatic	Ad	Polygonal	Straight	Vesicular hairs present in surface cells	4-9
		Ab	Polygonal	Straight		5-7
<i>Bassia indica</i> (Wight) A.J.Scott	Hypostomatic	Ad	Rectangular, Isodiametric	Rounded	Regular arrangement of cells in rows	8-13
		Ab	Rectangular	Rounded		5-11
<i>Chenopodium album</i> L.	Amphistomatic	Ad	Polygonal	Deeply sinuate	Thin walled polygonal cells arranged in rows	6-14
		Ab	Polygonal	Deeply sinuate		4-8
<i>Chenopodium ficifolium</i> Sm.	Amphistomatic	Ad	Irregular	Wavy	Uniseriate, rectangular epidermal cells	7-12
		Ab	Irregular	Wavy		3-8
<i>Digera muricata</i> (L.) Mart.	Amphistomatic	Ad	Undulate	Sinuuous	Multicellular cells arrangement	6-11
		Ab	Irregular	Sinuuous		7-9
<i>Salsola tragus</i> L.	Hypostomatic	Ad	Undulate	Straight	High longitudinal folds of cells in rows	6-10
		Ab	Undulate	Straight		5-8

**Keywords:** Ad=Adaxial, Ab=Abaxial, ECS=Epidermal cell size, AWP=Anticlinal wall pattern, NES=Nature of epidermal cells, LPC=Lobes per cell,

**Table 21.** Qualitative observation of leaf adaxial and abaxial surface among Amaranthaceous taxa.

<b>Amaranthaceous taxa</b>	<b>Ad × Ab</b>	<b>St (P/A)</b>	<b>ST</b>	<b>SS</b>	<b>GCS</b>	<b>SCS</b>	<b>Tri (P/A)</b>	<b>Trichome</b>	<b>DT</b>
<i>Achyranthes aspera</i> L.	Ad	A	A	A	A	A	P	Glandular, Unicellular	Coastal zone
	Ab	P	Anisocytic	Elongate elliptic	Kidney shape	Margin sinuous, enclosing GC	P	Glandular, Unicellular, medium sized	Coastal zone
<i>Aerva lanata</i> (L.) Juss.	Ad	P	Anomocytic	Elongate elliptic	Kidney shape	Lobed margins, wavy, partly enclosing GC	P	Glandular, branched, Stellar, Unicellular. long	Intercostal zone
	Ab	P	Anomocytic	Elongate elliptic	Kidney shape	Margin sinuous, enclosing GC	P	Glandular, Stellar, Unicellular. long	Intercostal zone
<i>Alternanthera ficoidea</i> (L.) Sm.	Ad	P	Diacytic	Elliptic	Kidney shape	Lobed margins, wavy, enclosing GC	P	E-glandular and basal cells isodiametric	Costal zone
	Ab	P	Diacytic	Elliptic	Kidney shape	Lobed margins, wavy, enclosing GC	A	A	A
<i>Alternanthera philoxeroides</i> (Mart.) Griseb.	Ad	P	Diacytic	Broad Elliptic	Broad kidney shape	Margin sinuous, enclosing GC	A	A	A
	Ab	P	Diacytic	Elongate elliptic	Broad kidney shape	Lobed margins, wavy, enclosing GC	A	A	A
<i>Alternanthera sessilis</i> (L.) R.Br. ex DC.	Ad	P	Anomocytic	Elliptic	Broad kidney shape	Lobed margins, wavy, enclosing GC	P	Multicellular, non-glandular	Intercostal zone
	Ab	P	Anomocytic	Elliptic	Broad kidney shape	Margin lobed slightly enclosing GC	P	Capitate, unicellular, with ellipsoid head	Intercostal zone

<i>Amaranthus graecizans</i> L.	Ad	P	Anomocytic	Elongate elliptic	Kidney shape	Margin sinuous, enclosing GC	P	Uniseriate, glandular, multicellular, un-branched	Intercostal zone
	Ab	P	Anomocytic	Elongate elliptic	Broad kidney shape	Margin lobed slightly enclosing GC	P	Biseriate, multicellular, glandular	Intercostal zone
<i>Amaranthus retroflexus</i> L.	Ad	A	A	A	A	A	P	Glandular, Multicellular	Intercostal zone
	Ab	P	Paracytic	Elliptic	Broad kidney shape	Lobed margins, wavy, enclosing GC	P	E-glandular, falcate	Costal zone
<i>Amaranthus viridis</i> L.	Ad	P	Anisocytic	Elongate elliptic	Kidney shape	Lobed margins, wavy, enclosing GC	A	A	A
	Ab	P	Anisocytic	Elongate elliptic	Kidney shape	Margin lobed slightly enclosing GC	A	A	A
<i>Atriplex stocksii</i> Boiss.	Ad	P	Anomocytic	Broad Elliptic	Kidney shape	Lobed margins, wavy, partly enclosing GC	A	A	A
	Ab	P	Anomocytic	Elongate elliptic	Broad kidney shape	Lobed margins, wavy, partly enclosing GC	P	Unicellular, glandular	Non Intercostal zone
<i>Bassia indica</i> (Wight) A.J.Scott	Ad	A	A	A	A	A	P	Slender, Unicellular, E-glandular	Intercostal zone
	Ab	P	Paracytic	Elliptic	Kidney shape	Lobed margins, wavy, partly enclosing GC	P	Glandular, conical	Intercostal zone
<i>Chenopodium album</i> L.	Ad	P	Paracytic	Elliptic	Broad kidney shape	Margin sinuous, enclosing GC	A	A	A

	Ab	P	Paracytic	Elliptic	Kidney shape	Margin sinuous, enclosing GC	P	Glandular, Unicellular, capitate	Coastal zone
<i>Chenopodium ficifolium</i> Sm.	Ad	P	Anisocytic	Elongate elliptic	Kidney shape	Margin wavy, lobed partly enclosing GC	A	A	A
	Ab	P	Anisocytic	Elongate elliptic	Kidney shape	Margin lobed slightly enclosing GC	A	A	A
<i>Digera muricata</i> (L.) Mart.	Ad	P	Anisocytic	Elongate elliptic	Broad kidney shape	Margin lobed slightly enclosing GC	P	Multicellular glandular	and Intercostal zone
	Ab	P	Anomocytic	Broad Elliptic	Broad kidney shape	Margin lobed wavy partly enclosing GC	P	Multicellular, glandular	Intercostal zone
<i>Salsola tragus</i> L.	Ad	A	A	A	A	A	A	A	A
	Ab	P	Anomocytic	Elongate elliptic	Kidney shape	Margin sinuous, enclosing GC	A	A	A

**Keywords:** Ad=Adaxial, Ab=Abaxial, St= Stomata ; ST=Stomata type, SS=Stomata shape, GCS=Gaurd cells shape, SSC=Subsidiary cell shape, Tri=Trichome, DT=Distribution of trichomes, A=Absent, P=Present

**Table 22.** Quantitative measurements of leaf epidermal cells, stomata and trichomes of Amaranthaceous taxa.

Amaranthaceous Taxa	Ad × Ab	L × W	Average No. of Epidermal cell	Epidermal cell (Min-Max = Mean + SE)	No. of Stomata (Avg)	Stomata (Min-Max = Mean + SE)	SI (%)	Trichome Number Per unit area	Trichome (Min-Max = Mean + SE)	TI (%)
<i>Achyranthes aspera</i> L.	Ad	L	66	12.8-13.5 = 13.2±0.12	A	A	A	2	84-96 = 91.4±2.13	2.94
		W		5-5.7 = 5.34±0.12					8-12 = 10.6±0.7	
	Ab	L	49	4.7-5.2 = 5.02±0.08	9	10-12.1 = 11.42±0.38	15.51	4	84-102 = 94.2±3.29	7.54
		W		2.9-3.3 = 3.06±0.06		4.8-5.1 = 5±0.05			9-15 = 12.2±1.01	
<i>Aerva lanata</i> (L.) Juss.	Ad	L	110	27.5-855 = 55.5±10.73	11	24.75-28.7 = 26.2±0.81	9.09	3	25-47.5 = 33.5±3.92	2.65
		W		12.5-30 = 22±2.1		15-22.75 = 19.2±1.31			12.5-32.5 = 21.5±6.96	
	Ab	L	76	12.5-25.5 = 18.4±7	6	23.7-27 = 25.7±0.74	7.37	5	47.5-97.5 = 73.5±7.7	6.17
		W		10-20 = 15.5±1.6		17.5-20 = 18.85±0.46			12-42.5 = 29±4	
<i>Alternanthera ficoidea</i> (L.) Sm.	Ad	L	131	22.5-37.5 = 28±2.6	13	12.5-17.5 = 15.5±0.8	9.02	6	22.5-52.5 = 34.7±6.76	4.37
		W		12.5-20 = 16±1.27		7.5-8 = 7.65±0.1			12.5-15 = 13.5±0.6	
	Ab	L	71	25-62.5 = 38.5±6.35	7	12.5-17.5 = 14.5±0.9	8.97	A	A	A
		W		12.5-27.5 = 21±3.02		5-10 = 7.5±0.79				
<i>Alternanthera philoxeroides</i> (Mart.) Griseb.	Ad	L	37	14.8-20.3 = 17.8±1.04	5	10.3-12.8 = 11.86±0.46	11.9	A	A	A
		W		8.7-13.3 = 10.56±0.84		6.9-9.8 = 8.22±0.56				
	Ab	L	63	20.5-15.6 = 13.5±1.09	16	9.7-10.9 = 10.1±0.22	20.25	A	A	A
		W		6.5-8.9 = 7.34±0.4		6.8-8.3 = 7.48±0.3				
<i>Alternanthera sessilis</i> (L.) R.Br. ex DC.	Ad	L	32	42.5-57.5 = 50.8±1.1	12	27.5-32.5 = 29.5±0.9	27.27	3	87.5-175 = 127±17.16	8.57
		W		12.5-17.5 = 15±1.1		15-17.5 = 16.5±0.6			10-25 = 16.5±3.02	
	Ab	L	79	15-29.5 = 21.5±1.64	14	27.5-30 = 28.5±0.6	15.05	2	35-100 = 70.5±14.1	2.46
		W		12.5-25 = 17±2.29		17.5-20 = 19±0.6			7.5-12.5 = 10.5±0.9	
<i>Amaranthus graecizans</i> L.	Ad	L	59	11.2-15 = 13.1±0.25	9	10.25-14.75 = 12.5±0.7	13.23	8	87.5-150 = 122.7±6.25	11.94
		W		17.5-27.5 = 21.9±5.66		7.5-12.5 = 9.6±1.19			22.5-62.5 = 38.5±6.96	
	Ab	L	18	10.2-14.7 = 12.5±1.13	13	26.76-30 = 28±0.62	41.93	11	80-152 = 117.5±19.66	37.93
		W		4.5-6.25 = 5.6±2.69		9.5-12.5 = 10.85±0.55			25-47.5 = 33.5±3.92	
<i>Amaranthus retroflexus</i> L.	Ad	L	37	20.5-23.5 = 21.8±1.2	A	A	A	7	60-90 = 76±11.4	15.9
		W		11.5-11.5 = 10.8±0.41					30-35 = 32.6±2.5	
	Ab	L	16	26.5-28.5 = 27.8±0.83	9	10-10.8 = 10.46±0.29	36	3	75-100 = 90±10.6	15.78
		W		10.3-11 = 10.58±0.25		6.4-6.5 = 6.44±0.05			30-38 = 34.8±3.42	
<i>Amaranthus viridis</i> L.	Ad	L	86	25-26 = 25.36±0.18	8	12.3-12.5 = 12.42±0.03	8.51	A	A	A
		W		10-11 = 10.36±0.18		8.3-8.5 = 8.42±0.03				
	Ab	L	26	18.5-19.2 = 18.8±0.12	12	14.9-15.5 = 15.22±0.11	31.57	A	A	A
		W		9.5-9.7 = 9.58±0.03		8.5-8.9 = 8.74±0.06				

<i>Atriplex stocksii</i> Boiss.	Ad	L	36	$25-35 = 27.5 \pm 1.9$	14	$15-20 = 16.5 \pm 1$	28	A	A	A
		W		$17.5-25 = 21.5 \pm 1.3$		$10-12.5 = 11 \pm 0.61$				
	Ab	L	89	$12.5-25 = 19 \pm 2.17$	7	$15-17.5 = 17 \pm 0.5$	7.29	4	$35-87.5 = 59.5 \pm 7.3$	4.3
		W		$10-17.5 = 13.5 \pm 1.3$		$10-15 = 12 \pm 0.93$			$12.5-15 = 13.5 \pm 0.6$	
<i>Bassia indica</i> (Wight) A.J.Scott	Ad	L	95	$11-13 = 12.2 \pm 0.75$	A	A	A	6	$50-60 = 54 \pm 4.18$	5.94
		W	41	$6.3-7 = 6.54 \pm 0.28$					$10-19 = 16 \pm 3.67$	
	Ab	L	31	$17-18.5 = 17.9 \pm 0.65$	4	$11.5-12.5 = 12.1 \pm 0.41$	11.42	A	A	A
		W		$6.5-10.5 = 8.28 \pm 1.92$		$6-7.5 = 6.8 \pm 0.67$				
<i>Chenopodium album</i> L.	Ad	L	65	$25-40 = 32 \pm 2.89$	13	$7.5-12.5 = 10.5 \pm 0.9$	16.66	A	A	A
		W		$12.5-2.5 = 18.5 \pm 2.3$		$4.7-6.25 = 5.45 \pm 0.32$				
	Ab	L	95	$22-27 = 24.8 \pm 0.86$	9	$10-17.5 = 14 \pm 1.5$	8.65	5	$50-90 = 68.5 \pm 1.68$	5
		W		$10-15.5 = 12.7 \pm 1.21$		$5-7.5 = 6.25 \pm 0.5$			$7.5-20 = 14 \pm 3.3$	
<i>Chenopodium ficifolium</i> Sm.	Ad	L	55	$25-28.6 = 27.06 \pm 0.64$	5	$9.8-10.7 = 10.16 \pm 0.16$	8.33	A	A	A
		W		$15-16.6 = 15.86 \pm 0.28$		$5.8-6.5 = 6.22 \pm 0.13$				
	Ab	L	28	$15-16 = 15.66 \pm 0.18$	8	$7.8-8.8 = 8.28 \pm 0.17$	22.22	A	A	A
		W		$10-12 = 11.1 \pm 0.34$		$6.4-6.8 = 6.54 \pm 0.07$				
<i>Digera muricata</i> (L.) Mart.	Ad	L	69	$9.6-10.2 = 9.94 \pm 0.1$	6	$10-12 = 11.1 \pm 0.37$	8	3	$80-94 = 86 \pm 2.75$	4.16
		W		$4.5-5.2 = 4.8 \pm 0.13$		$5-6 = 5.42 \pm 0.22$			$4-8 = 6.1 \pm 0.71$	
	Ab	W	24	$10-12 = 11.4 \pm 0.38$	12	$10.7-13 = 11.76 \pm 0.43$	33.33	9	$62-74 = 66.8 \pm 2.26$	27.27
				$5-6.1 = 5.6 \pm 0.21$		$8-8.5 = 8.2 \pm 0.08$			$4.5-6 = 5.16 \pm 0.26$	
<i>Salsola tragus</i> L.	Ad	L	124	$17.5-36.5 = 28.5 \pm 5.2$	A	A	A	A	A	A
		W		$12.5-17.5 = 14.5 \pm 0.9$						
	Ab	L	63	$15-37.5 = 25 \pm 2.1$	16	$27.5-37.5 = 33 \pm 2.29$	20.25	A	A	A
		W		$12.5-20 = 16 \pm 1.5$		$17.5-22.5 = 20 \pm 1.11$				

**Keywords:** Ad=Adaxial, Ab=Abaxial, L=Length, W=Width, M=Mean, SE=Standard Error, Max=Maximum, Min=Minimum, SI=Stomatal Index, TI=Trichome Index; Avg=Average; A=Absent.

**Table 23.** Quantitative measures of stomatal pore, guard and subsidiary cells of Amaranthaceous taxa.

<b>Amaranthaceous Taxa</b>	<b>Ad × Ab</b>	<b>L×W</b>	<b>Stomatal pore (Min-Max = Mean + SE)</b>	<b>Guard cell (Min-Max = Mean + SE)</b>	<b>Subsidiary cell (Min-Max = Mean + SE)</b>
<i>Achyranthes aspera</i> L.	Ad	L	A	A	8.1-87 = 8.44±0.09
		W	A	A	5.2-5.7 = 5.48±0.08
	Ab	L	6-7.5 = 6.92±0.25	19.1-20 = 19.8±0.25	9.5-10.5 = 10±0.17
		W	2.2-2.5 = 2.34±0.06	8.30-95 = 8.82±0.21	3.8-4.5 = 4.06±0.12
<i>Aerva lanata</i> (L.) Juss.	Ad	L	10-15 = 13.2±0.91	7.20-7.7 = 7.5±0.83	50-65 = 57.5±25
		W	4.75-6.5 = 5.5±0.36	4.30-4.6 = 4.4±0.04	17.5-37.5 = 27.5±3.25
	Ab	L	10-14.2 = 12.2±0.67	7-8.00 = 7.6±0.18	50-62.5 = 54.5±2.54
		W	5.25-7.5 = 6.5±0.43	3.50-4 = 3.8±0.09	17.5-27.5 = 22.5±1.76
<i>Alternanthera ficoidea</i> (L.) Sm.	Ad	L	10-15 = 12.5±0.8	12.5-17.5 = 15±0.79	15-22.5 = 19±1.5
		W	1.25-2.5 = 1.85±0.2	2.5-3 = 2.85±0.1	5-7.5 = 6.6±0.6
	Ab	L	10-12.5 = 11.5±0.6	12-17.5 = 14.5±0.9	15-25 = 18±1.8
		W	1-1.5 = 1.25±0.1	2.5-3.25 = 2.8±0.15	5-7.5 = 6.5±0.6
<i>Alternanthera philoxeroides</i> (Mart.) Griseb.	Ad	L	7.9-10.9 = 9.22±0.55	14.6-18 = 16.8±0.76	9.9-11.7 = 10.98±0.31
		W	1.2-3.3 = 2.42±0.3	6.7-10.7 = 8.8±0.64	2.6-3.9 = 3.34±0.25
	Ab	L	4.7-7.9 = 6.16±0.61	13.6-18.7 = 16±0.88	7.8-9.2 = 8.34±0.25
		W	4.2-7.3 = 6.03±0.13	7.1-9.7 = 8.2±0.6	5.8-8.3 = 7.1±0.17
<i>Alternanthera sessilis</i> (L.) R.Br. ex DC.	Ad	L	20-25 = 22±0.9	27-32.5 = 29.5±0.9	37.5-87.5 = 62±9.02
		W	1-1.25 = 1.2±0.06	7.5-10 = 8±0.5	12.5-17.5 = 14.5±0.9
	Ab	L	15-17.5 = 16.5±0.6	27.5-30 = 28.5±0.6	35-51 = 42.4±3.09
		W	1.25-1.75 = 1.4±0.09	10-12.5 = 11.5±0.6	12.5-15 = 13.5±0.6
<i>Amaranthus graecizans</i> L.	Ad	L	20.2-25 = 22.9±1.16	9.5-9.90 = 9.7±0.06	42.5-65 = 51.5±3.92
		W	7.5-15 = 11.7±1.34	3.8-4.20 = 3.9±0.06	25-37.5 = 32.95±2.19
	Ab	L	14.7-18.5 = 16.8±0.8	8.50-9.0 = 8.7±0.09	52.5-75 = 64±4.3
		W	4.75-7.5 = 6.2±0.55	3.50-4.0 = 3.6±0.09	32.5-47.5 = 41.5±2.57
<i>Amaranthus retroflexus</i> L.	Ad	L	A	A	8.3-8.5 = 8.42±0.08
		W	A	A	3.4-3.6 = 3.48±0.08
	Ab	L	7.5-8.5 = 8.06±0.4	15.5-17.5 = 16±0.82	8.3-8.5 = 8.44±0.08

<i>Amaranthus viridis</i> L.	Ad	W	2-2.5 = 2.28±0.19	8.5-10.3 = 9.3±0.64	3-3.5 = 3.22±0.19
		L	10-10.5 = 10.24±0.1	18-18.9 = 18.5±0.06	9-9.5 = 9.32±0.09
	Ab	W	23.-2.5 = 2.44±0.04	9.7-10 = 9.86±0.06	4.3-4.5 = 4.38±0.04
L		10-10.5 = 10.3±0.09	19.5-20.8 = 20±0.26	11.4-11.7 = 11.5±0.05	
<i>Atriplex stocksii</i> Boiss.	Ad	W	2.3-2.5 = 2.44±0.04	15-16 = 15.6±0.18	5.4-5.6 = 5.5±0.03
		L	10-12.5 = 11±0.61	12.5-17.5 = 14±1	15-35 = 22.5±3.53
	Ab	W	1.25-2.5 = 2.05±0.27	2.5-5 = 4±0.61	11-23 = 17.5±3.5
L		10-12.5 = 11±0.61	12.5-15 = 13.5±0.61	20-27.5 = 24.5±1.22	
<i>Bassia indica</i> (Wight) A.J.Scott	Ad	W	1.25-2.50 = 1.7±0.22	2.5-5 = 3±0.5	10-15 = 12±0.93
		L	A	A	10-10.6 = 10.32±0.25
	Ab	W	A	A	6-6.7 = 6.28±0.31
L		8-9.5 = 8.56±0.65	9.5-11.1 = 10.5±0.63	10.2-10.5 = 10.3±0.13	
<i>Chenopodium album</i> L.	Ad	W	2.3-2.7 = 2.48±0.14	7.5-8.5 = 8±0.5	5.3-6.2 = 5.66±0.33
		L	5-7.5 = 6±0.6	7.5-12.5 = 10.5±0.9	20-25 = 23.5±1
	Ab	W	0.7-1.25 = 1.05±0.09	2.5-3 = 2.65±0.1	10-12.5 = 11.5±0.6
L		5-10 = 7±1.2	10-17.5 = 14±1.5	15-27.5 = 20±2.6	
<i>Chenopodium ficifolium</i> Sm.	Ad	W	0.7-1.25 = 1.05±0.09	2.5-3 = 2.7±0.1	7.5-10 = 8.5±0.6
		L	5.5-6.2 = 5.9±0.13	18-19.2 = 18.9±0.1	7.5-8.8 = 8.08±0.23
	Ab	W	2.3-2.8 = 2.5±0.1	12.5-13.3 = 12±0.12	4-4.6 = 4.3±0.1
L		5.9-6.6 = 6.22±0.12	11.8-12.1 = 11±0.11	8.2-8.9 = 8.58±0.12	
<i>Digera muricata</i> (L.) Mart.	Ad	W	2.9-3.2 = 3.02±0.05	7.8-8.7 = 8.24±0.16	6.5-7.1 = 6.84±0.1
		L	4.8-5.4 = 5.08±0.09	14-15.3 = 14.7±0.2	9.6-10.1 = 9.86±0.08
	Ab	W	2.8-3.2 = 3.04±0.06	7.8-8.8 = 8.38±0.17	3-3.5 = 3.18±0.08
L		4.7-5.1 = 4.96±0.07	5.7-6.4 = 6.08±0.11	7.5-8.8 = 8.06±0.22	
<i>Salsola tragus</i> L.	Ad	W	1.9-2.8 = 2.34±0.15	2.9-3.4 = 3.16±0.09	4.3-4.8 = 4.54±0.09
		L	A	A	37.5-62.5 = 49.5±4.43
	Ab	W	A	7.5-10 = 8.5±0.6	30-50 = 41±4.2
L		15-20 = 17±0.9	27.5-37.5 = 33±2.3	52.5-72.5 = 61±4.2	
		W	1-2.5 = 1.5±0.2	7.5-12.5 = 10±1.1	17.5-25 = 20.5±1.2

**Keywords:** Ad=Adaxial, Ab=Abaxial, L=Length, W=Width, M=Mean, SE=Standard Error, Max=Maximum, Min=Minimum, A=Absent



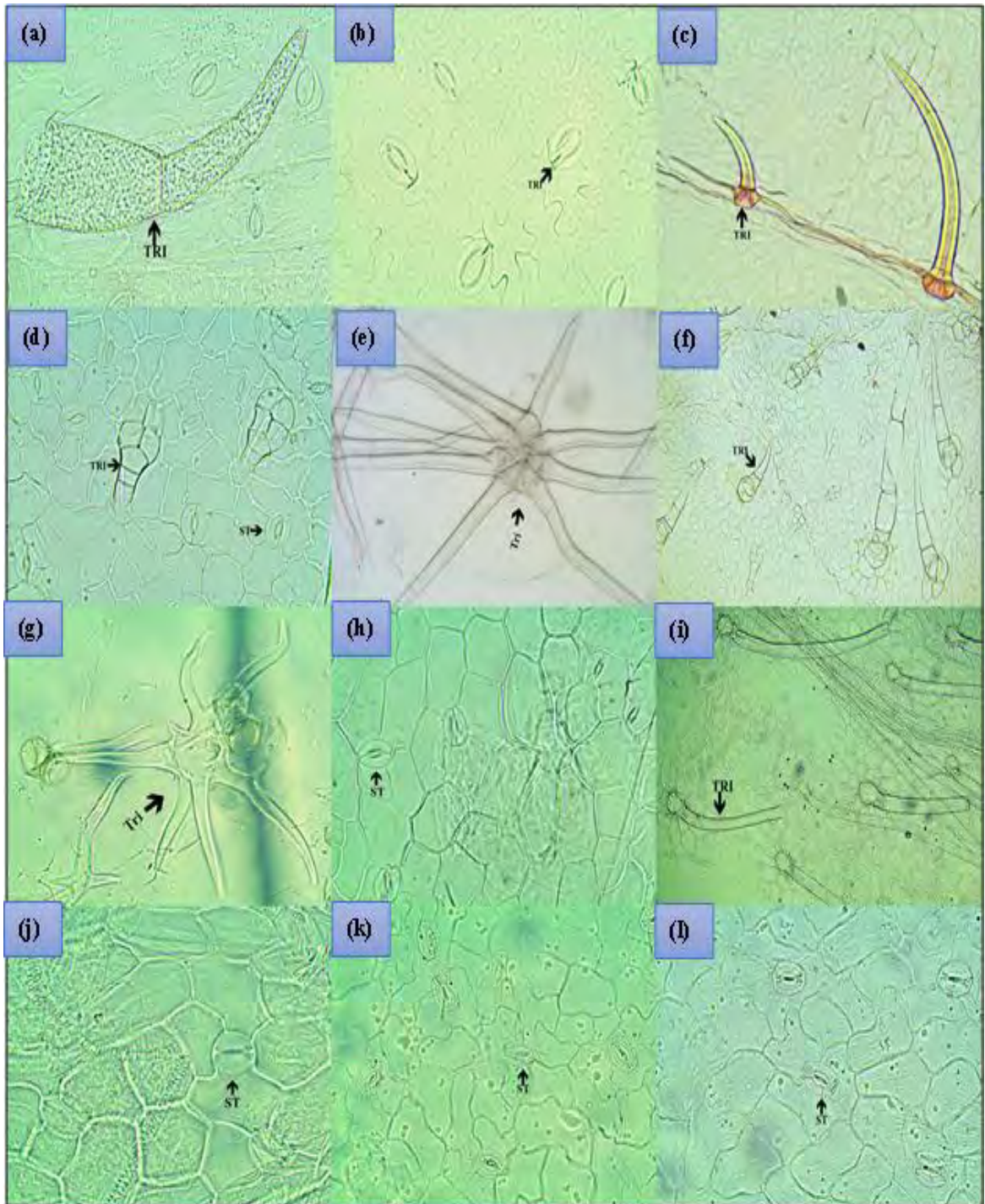


**Plate 72.** Light Micrographs (LM) illustrated stomata, shape of cells and wall pattern and trichomes of Amaranthaceae species; *Achyranthes aspera* (a) Abaxial surface showing trichome (b) Abaxial surface showing stomata (c) Adaxial surface showing trichome; *Aerva lanata* (d) Abaxial surface showing stomata (e) Abaxial surface showing trichome (f & g) Adaxial surface showing trichomes; *Alternanthera ficoidea* (h) Abaxial surface showing stomata (i) Adaxial surface showing trichome (j) Adaxial surface showing stomata; *Alternanthera philoxeroides* (k) Abaxial surface showing stomatal (l) Adaxial surface showing stomata.

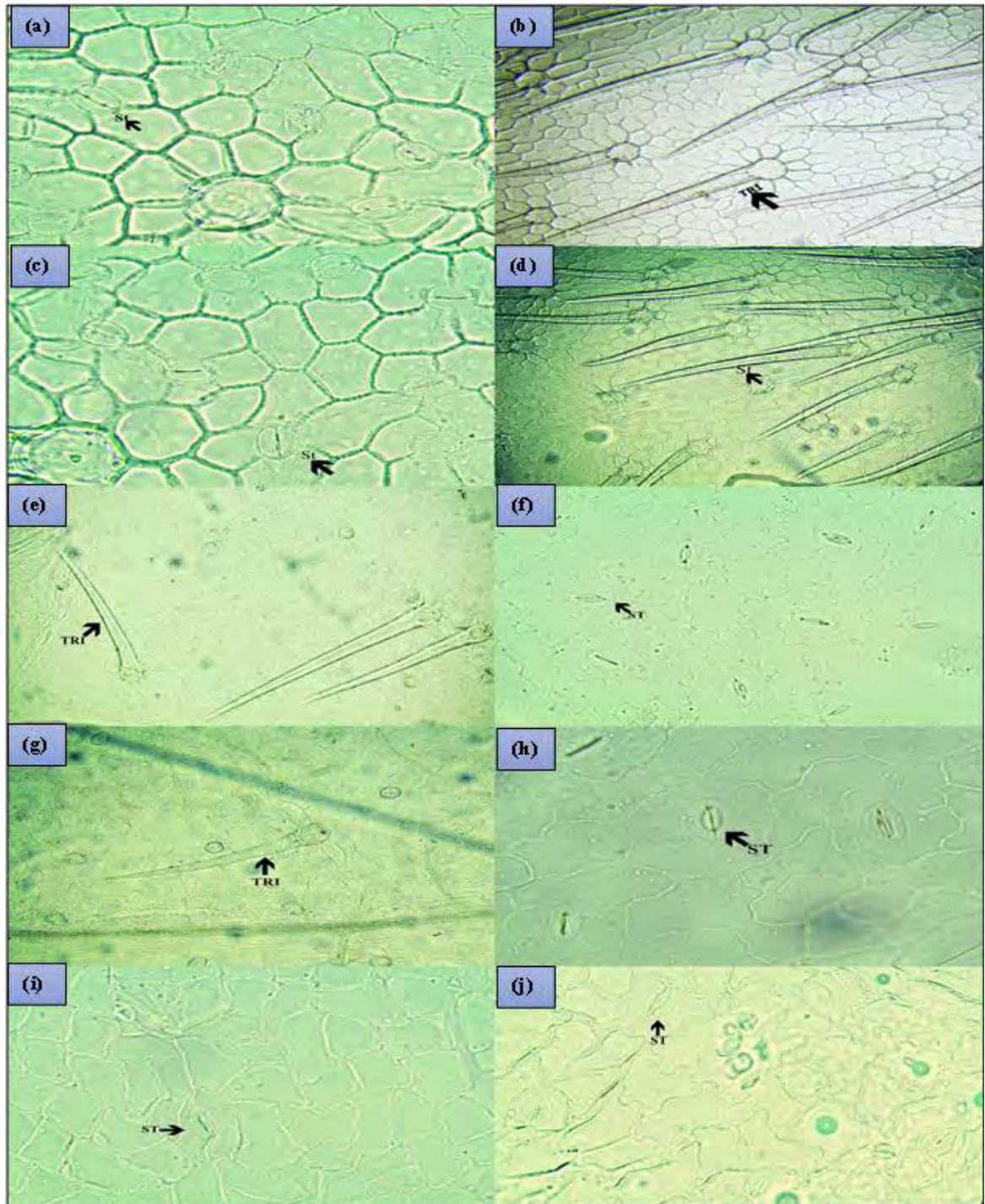


**Plate 73.** Light Micrographs (LM) illustrated stomata, shape of cells and wall pattern and trichomes of Amaranthaceous species; *Alternanthera sessilis* (a) Abaxial surface showing stomata (b) Abaxial surface showing trichome (c) Adaxial surface showing stomata (d) Adaxial surface showing trichome; *Amaranthus graecizans* (e) Abaxial surface showing trichome (f) Abaxial surface showing stomata (g) Adaxial surface showing trichome (h) Adaxial surface showing stomata; *Amaranthus viridis* (i) Abaxial surface showing stomata (j) Adaxial surface showing stomata.

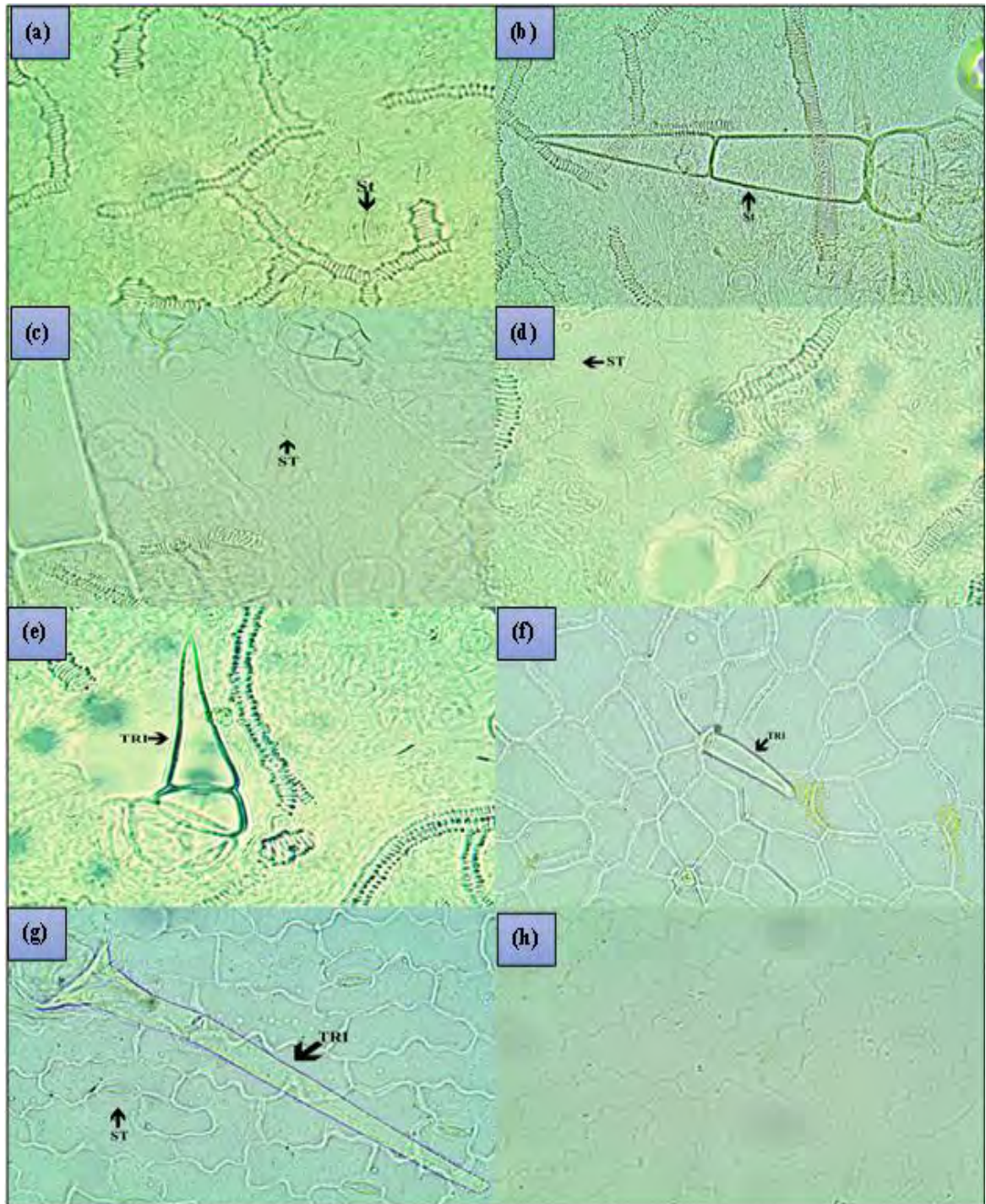


**Plate 74.** Light Micrographs (LM) illustrated stomata, shape of cells and wall pattern and trichomes of Amaranthaceous species; *Atriplex stocksii* (a) Abaxial surface showing stomata (b) Abaxial surface showing trichome (c) Adaxial surface showing stomata; *Bassia indica* (d) Abaxial surface showing stomata (e) Abaxial surface showing trichome (f) Adaxial surface showing trichome; *Chenopodium album* (h) Abaxial surface showing stomata & trichome (i) Adaxial surface showing epidermis cells

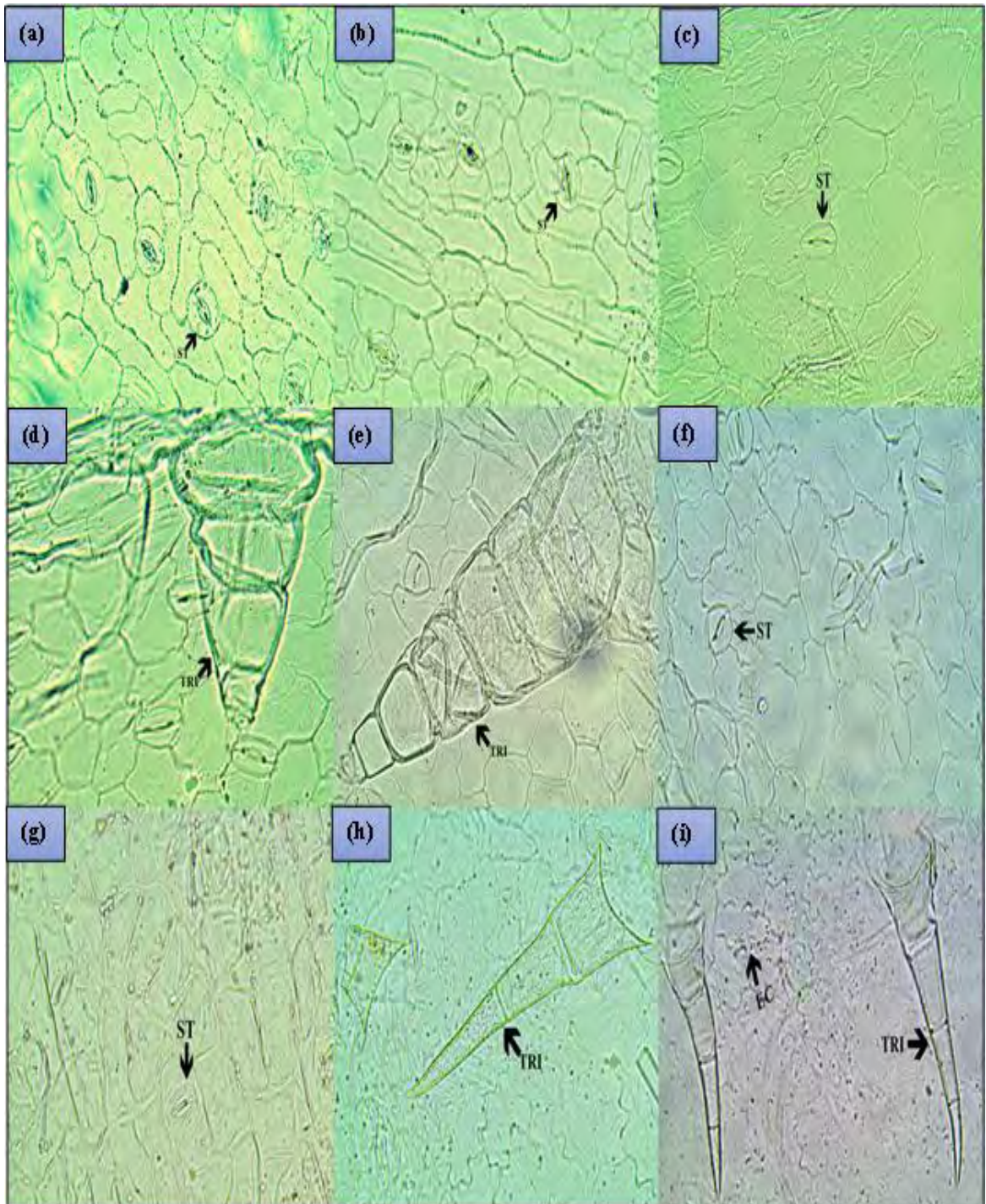


**Plate 75.** Light Micrographs (LM) illustrated stomata, shape of cells and wall pattern and trichomes of Amaranthaceous species; *Chenopodium ficifolium* (a) Abaxial surface showing stomata (b) Adaxial surface showing stomata *Digera muricata* (d) Abaxial surface showing stomata (e) Abaxial surface showing trichome (f) Adaxial surface showing trichome (g) Adaxial surface showing stomata; *Amaranthus retroflexus* (h) Abaxial surface showing stomata (i) Abaxial surface showing trichome (j) Adaxial surface showing trichome and epidermal cells.

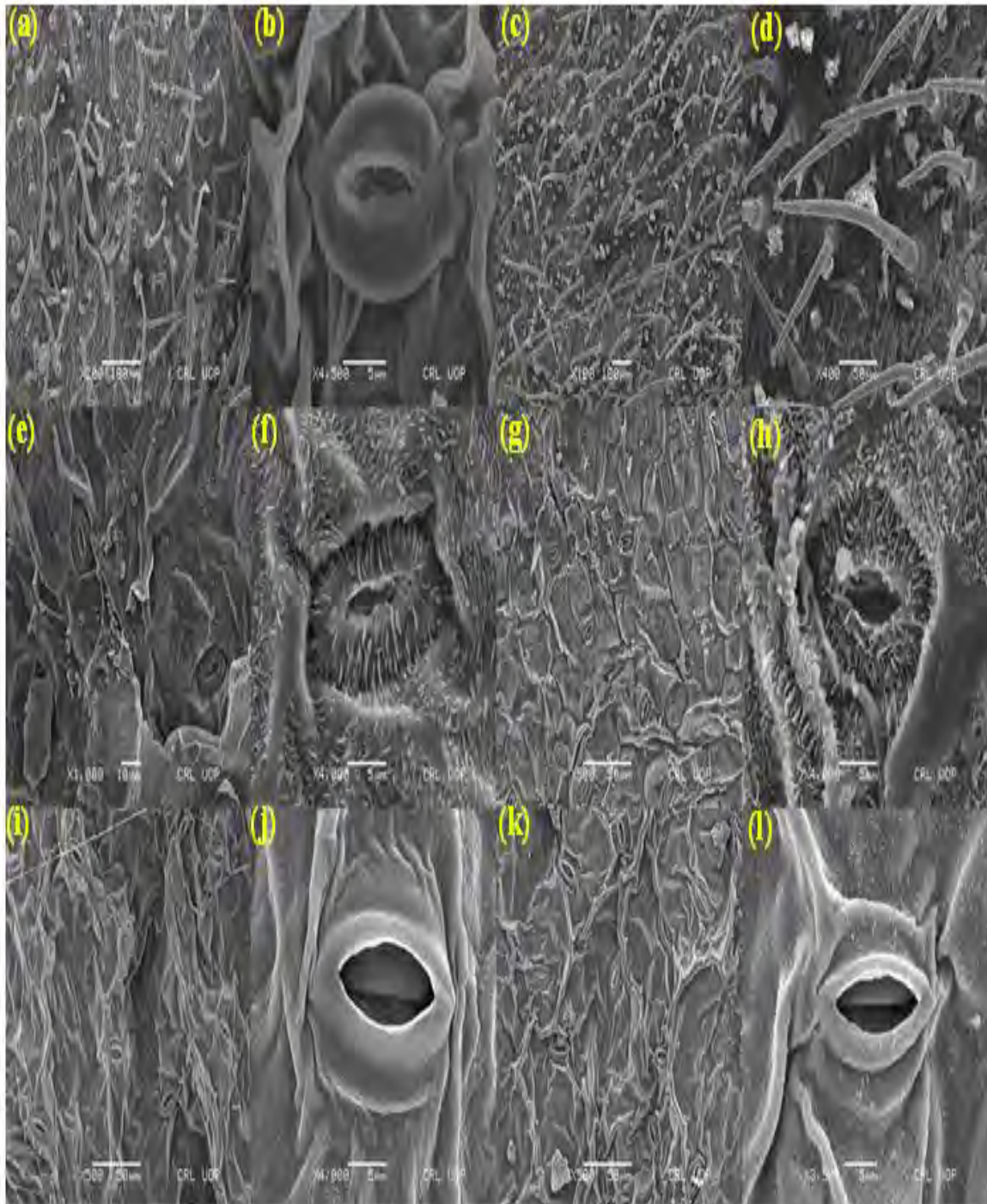


**Plate 76.** SEM micrograph of Amaranthaceous taxa showing shape of cell, pattern of anticlinal wall, trichomes and stomata type; *Achyranthes aspera* (a-b) Abaxial surface (scale bar = 100  $\mu\text{m}$ , 5  $\mu\text{m}$ ), (c-d) Abaxial surface (scale bar = 100  $\mu\text{m}$ , 50  $\mu\text{m}$ ); *Atriplex stocksii* (e-f) Abaxial surface (scale bar = 10  $\mu\text{m}$ , 5  $\mu\text{m}$ ), (g-h) Adaxial surface (scale bar = 50  $\mu\text{m}$ , 5  $\mu\text{m}$ ); *Alternanthera ficoidea* (i-j) Abaxial surface (scale bar = 50  $\mu\text{m}$ , 5  $\mu\text{m}$ ), (k-l) Adaxial surface (scale bar = 50  $\mu\text{m}$ , 5  $\mu\text{m}$ ).

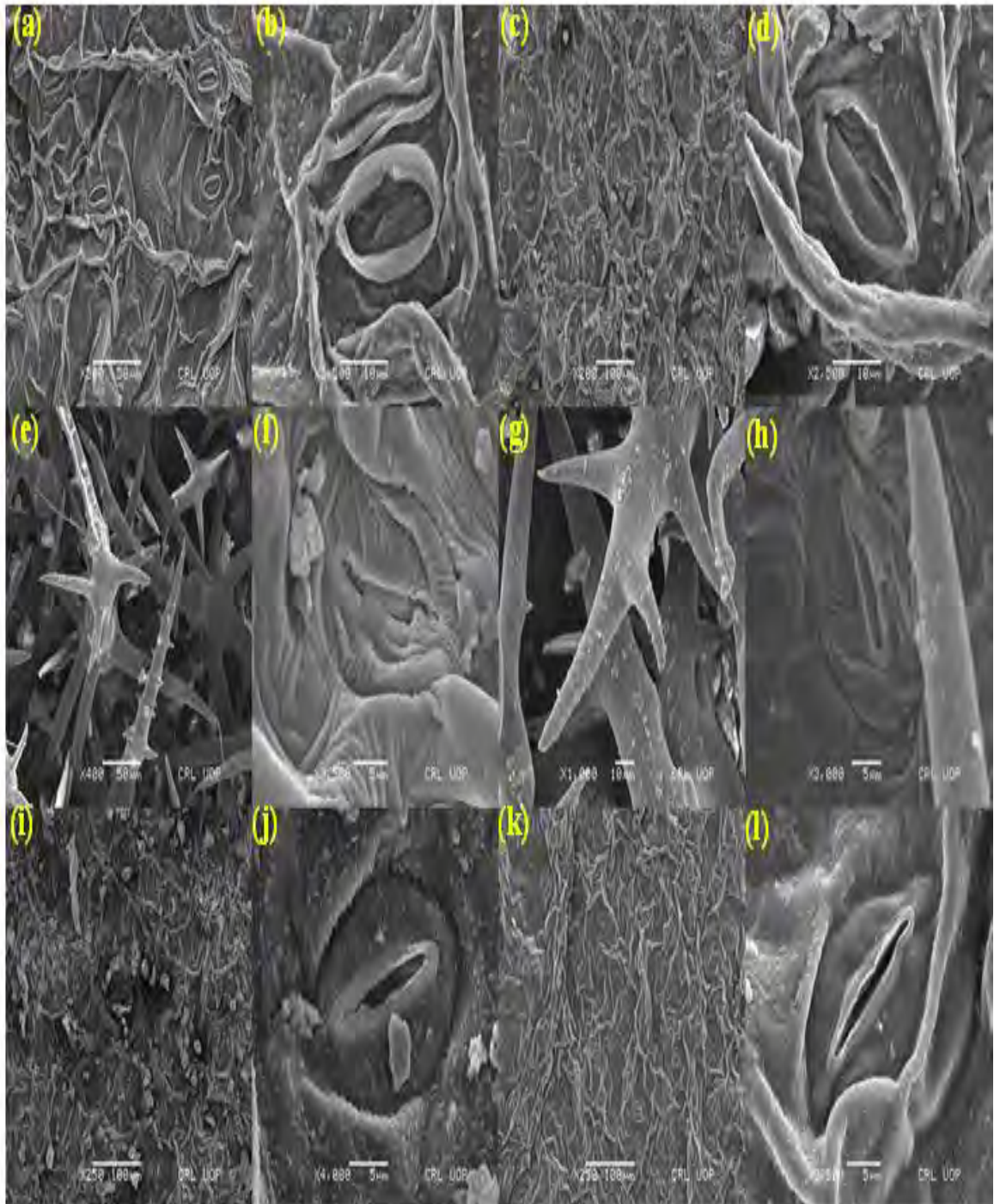


**Plate 77.** SEM micrograph of Amaranthaceous taxa showing shape of cell, pattern of anticlinal wall, trichomes and stomata type; *Amaranthus graecizans* (a-b) Abaxial surface (scale bar = 50  $\mu\text{m}$ , 10  $\mu\text{m}$ ), (c-d) Abaxial surface (scale bar = 100  $\mu\text{m}$ , 10  $\mu\text{m}$ ); *Aerva lanata* (e-f) Abaxial surface (scale bar = 50  $\mu\text{m}$ , 5  $\mu\text{m}$ ), (g-h) Adaxial surface (scale bar = 10  $\mu\text{m}$ , 5  $\mu\text{m}$ ), *Alternanthera sessilis* (i-j) Abaxial surface (scale bar = 100  $\mu\text{m}$ , 5  $\mu\text{m}$ ), (k-l) Adaxial surface (scale bar = 120  $\mu\text{m}$ , 5  $\mu\text{m}$ ).

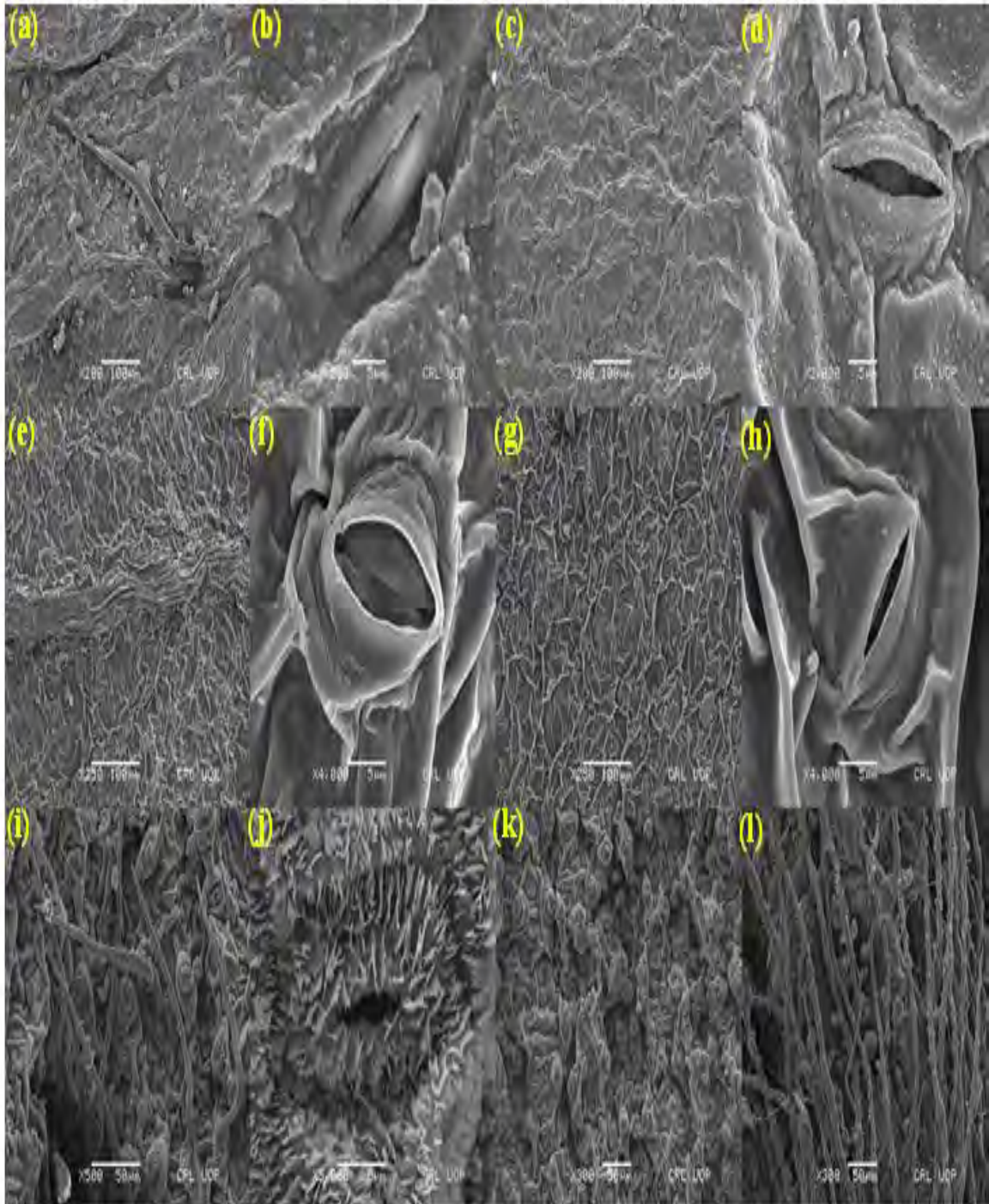


**Plate 78.** SEM micrograph of Amaranthaceous taxa showing shape of cell, pattern of anticlinal wall, trichomes and stomata type; *Alternanthera philoxeroides* (a-b) Abaxial surface (scale bar = 100  $\mu\text{m}$ , 5  $\mu\text{m}$ ) (c-d) Abaxial surface (scale bar = 100  $\mu\text{m}$ , 5  $\mu\text{m}$ ), *Amaranthus viridis* (e-f) Abaxial surface (scale bar = 100  $\mu\text{m}$ , 5  $\mu\text{m}$ ). (g-h) Adaxial surface (scale bar = 100  $\mu\text{m}$ , 5  $\mu\text{m}$ ), *Bassia indica* (i-j) Abaxial surface (scale bar = 50  $\mu\text{m}$ , 5  $\mu\text{m}$ ), (k-l) Adaxial surface (scale bar = 5  $\mu\text{m}$ , 50  $\mu\text{m}$ ).

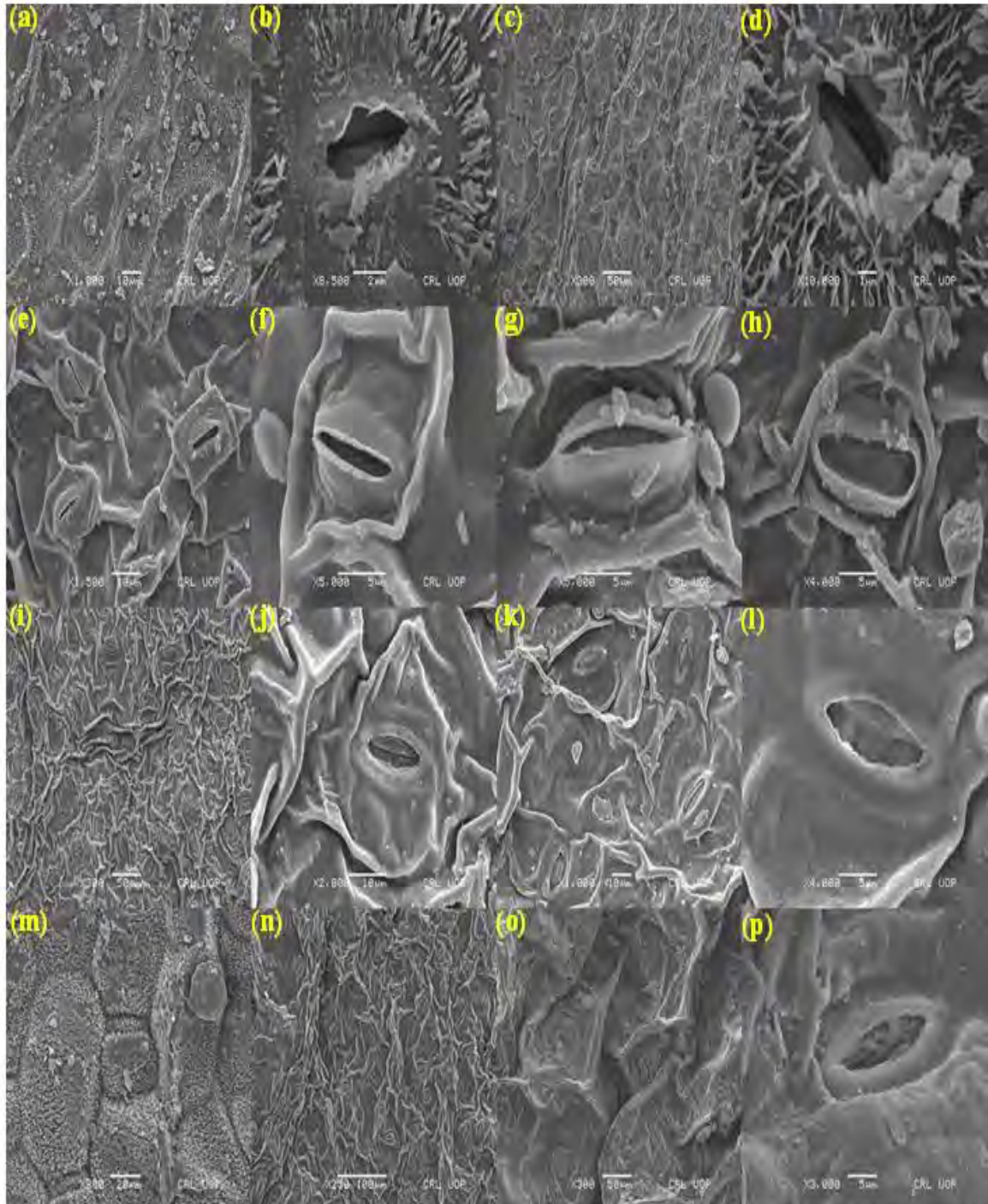


**Plate 79.** SEM micrograph of Amaranthaceous taxa showing shape of cell, pattern of anticlinal wall, trichomes and stomata type; *Chenopodium album* (a-b) Abaxial surface (scale bar = 10  $\mu\text{m}$ , 2  $\mu\text{m}$ ), (c-d) Abaxial surface (scale bar = 50  $\mu\text{m}$ , 1  $\mu\text{m}$ ), *Chenopodium ficifolium* (e-f) Abaxial surface (scale bar = 10  $\mu\text{m}$ , 5  $\mu\text{m}$ ), (g-h) Adaxial surface (scale bar = 5  $\mu\text{m}$ ), *Digera muricata* (i-j) Abaxial surface (scale bar = 50  $\mu\text{m}$ , 10  $\mu\text{m}$ ), (k-l) Adaxial surface (scale bar = 10  $\mu\text{m}$ , 5  $\mu\text{m}$ ), *Amaranthus retroflexus* (m & n) Abaxial and adaxial surfaces (scale bar = 20  $\mu\text{m}$ , 100  $\mu\text{m}$ ).; *Salsola tragus* (o & p) Abaxial and adaxial surface (scale bar = 50  $\mu\text{m}$ , 5  $\mu\text{m}$ ).



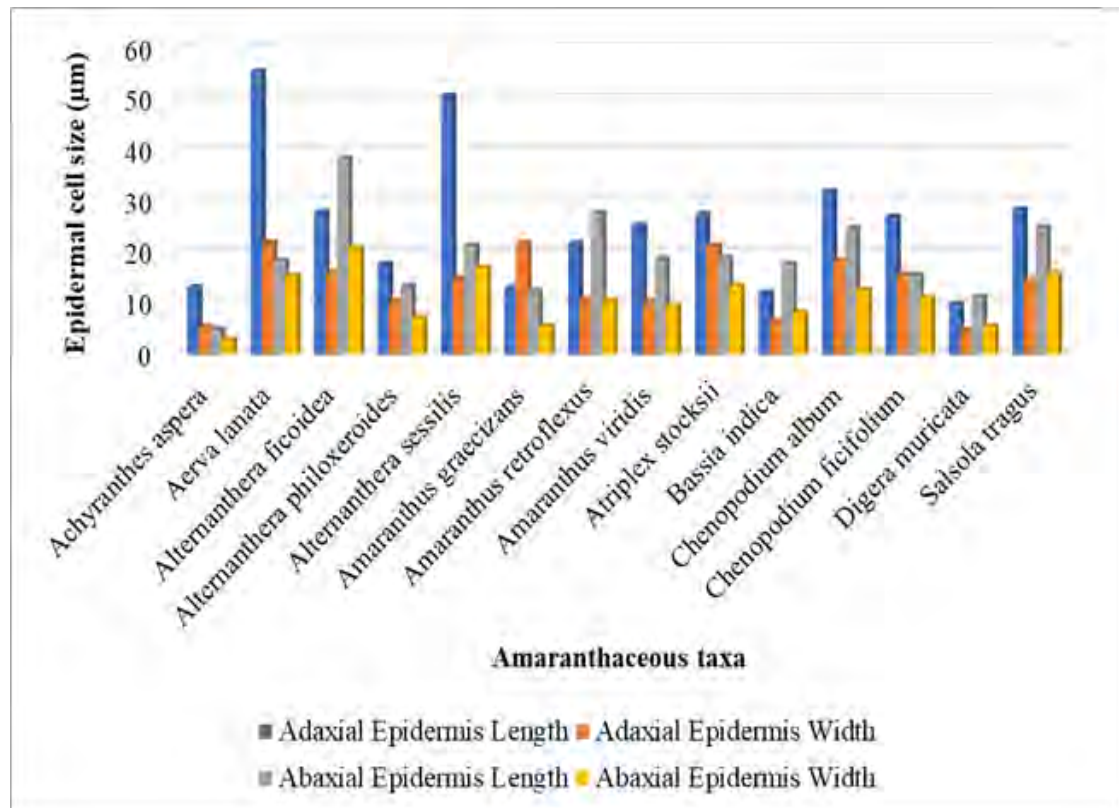


Figure 39. Mean size variation of epidermal cells along adaxial and abaxial surfaces

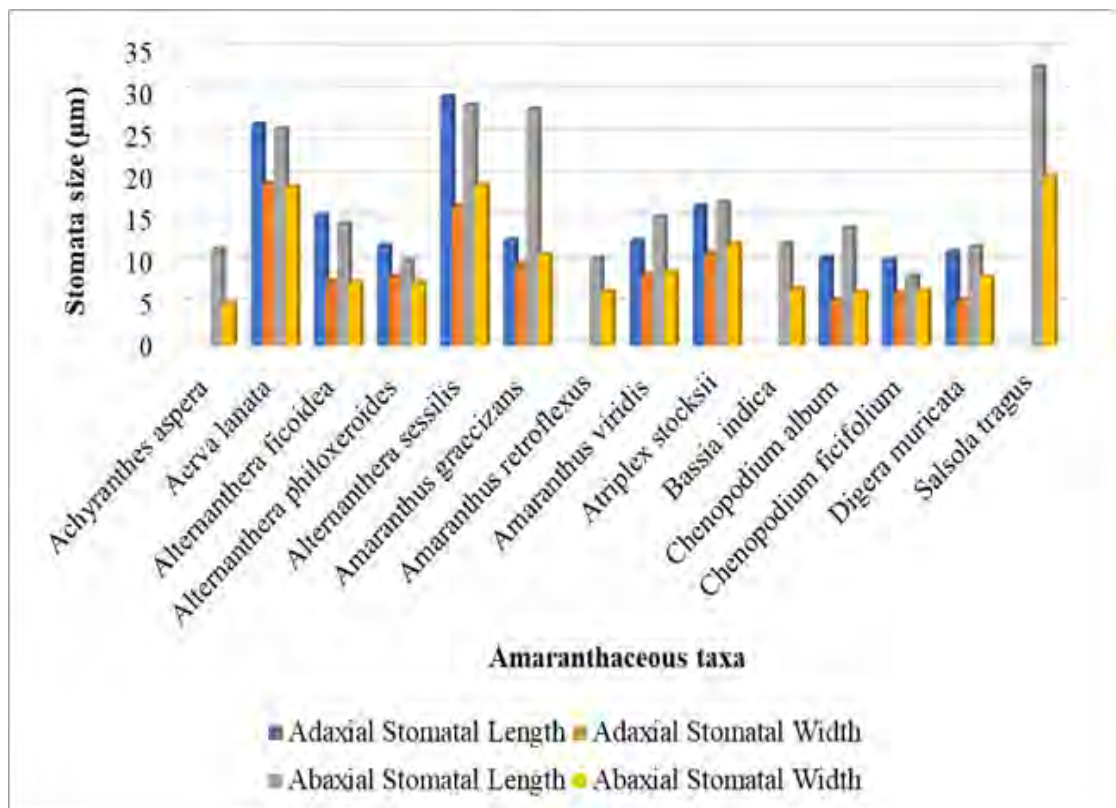
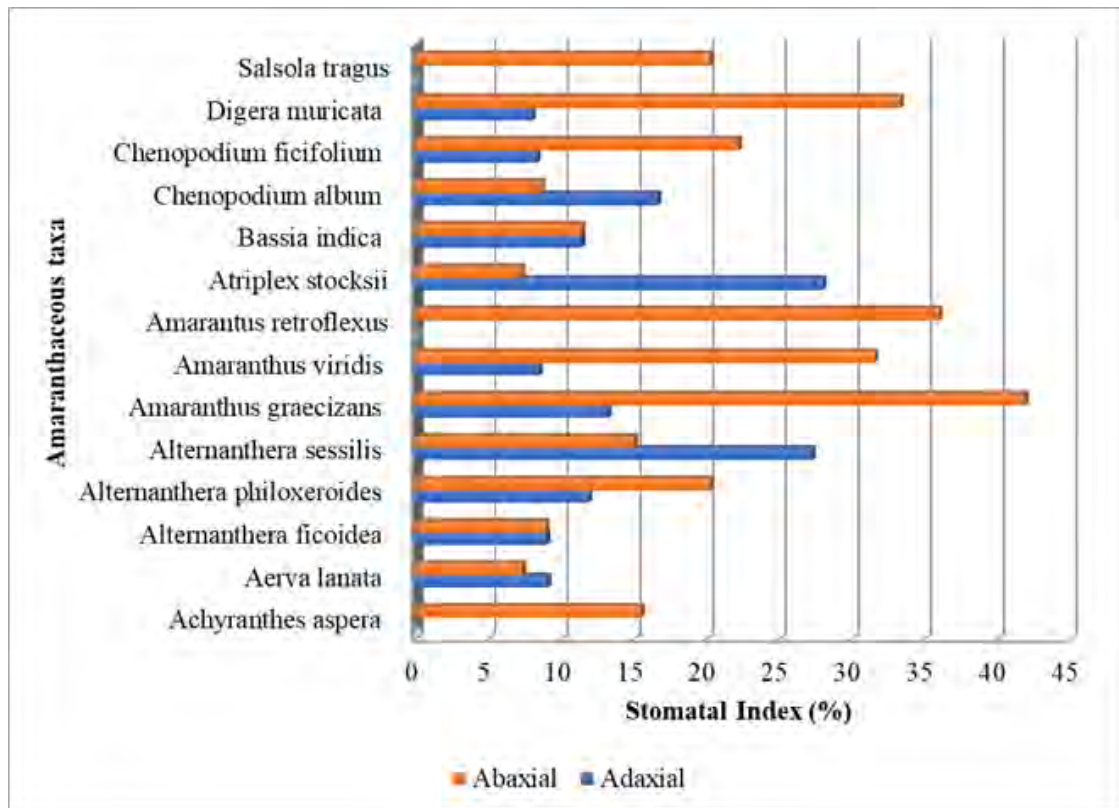
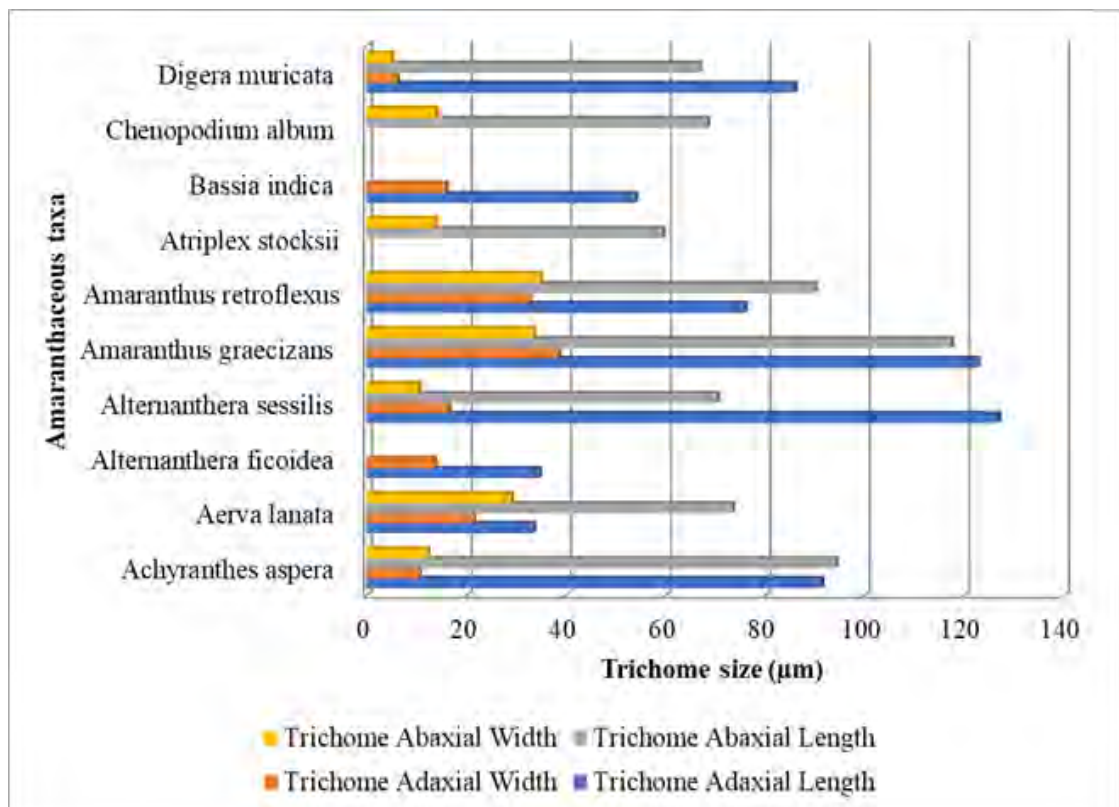


Figure 40. Stomatal length and width comparison along adaxial and abaxial sides



**Figure 41.** Average variation in stomatal Index on adaxial and abaxial surface



**Figure 42.** Mean variations of trichome size along epidermis surface

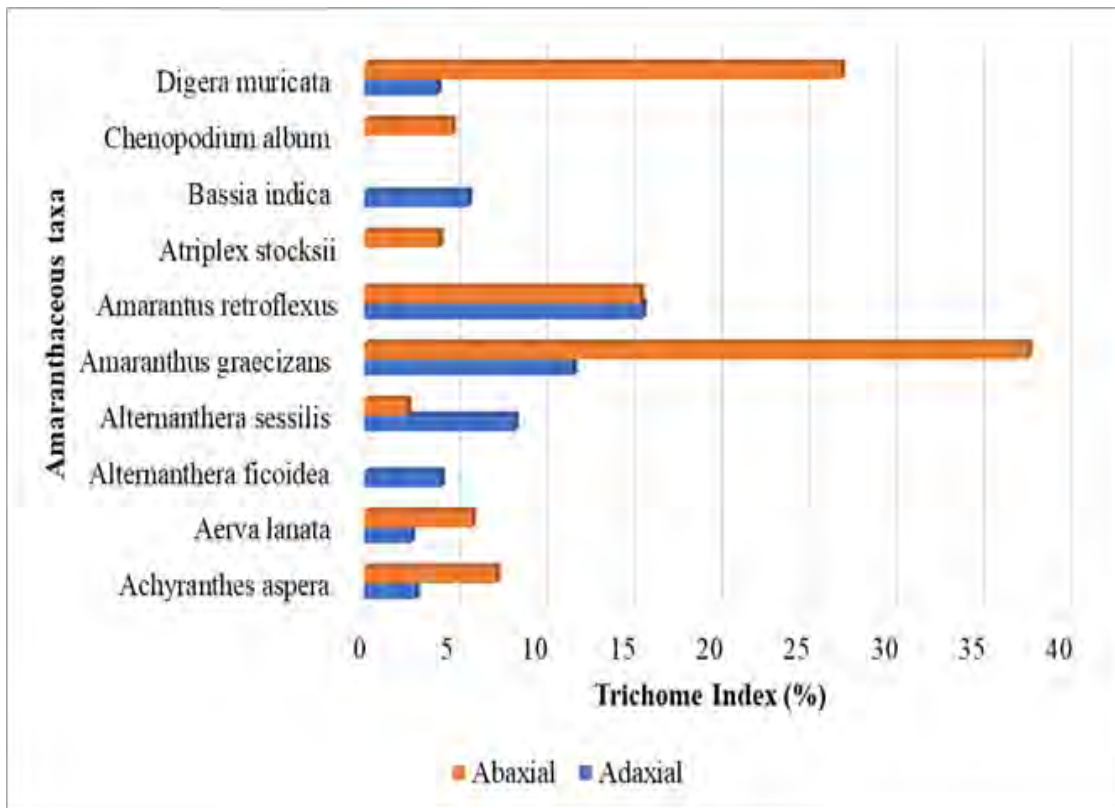


**Figure 43.** Variation in trichome index on adaxial and abaxial surface

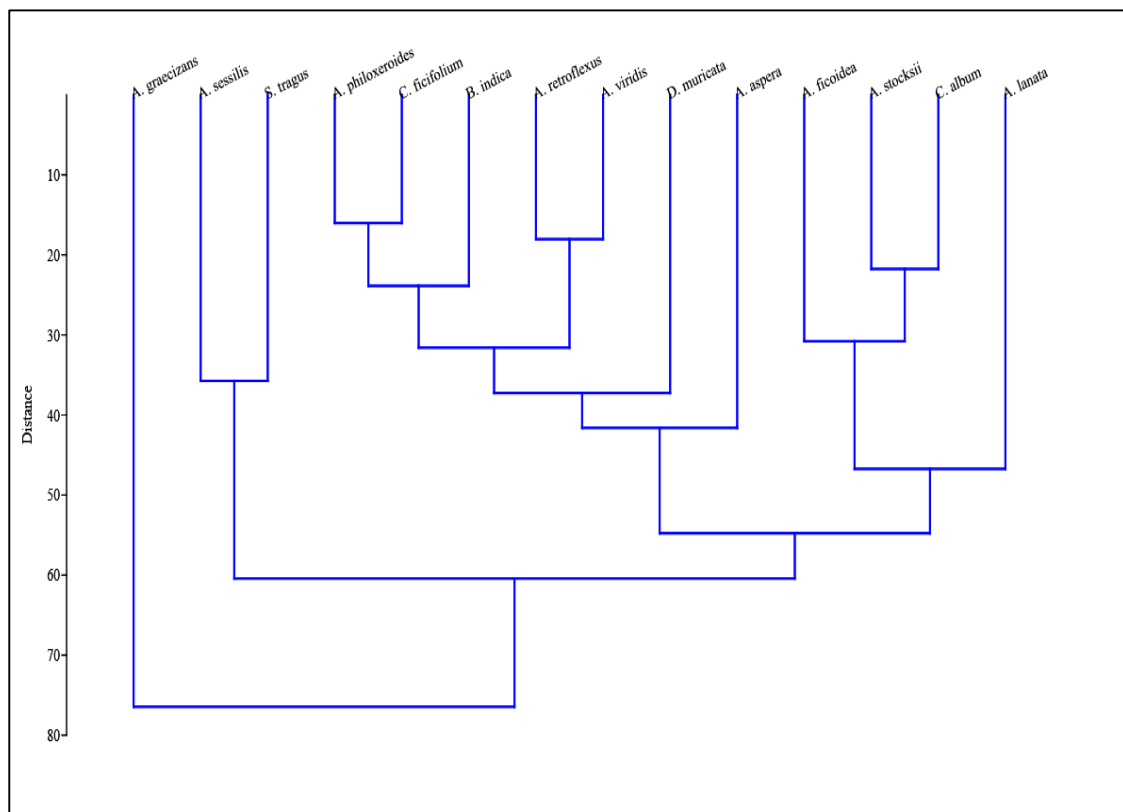


**Figure 44.** Dendrogram based hierarchical clustering of foliar anatomical features.

### 3.4.4 Discussion

In the present study, the anatomical and surface foliar epidermal characteristics of the leaves belonging to nine genera (*Achyranthes*, *Aerva*, *Alternanthera*, *Amaranthus*, *Atriplex*, *Bassia*, *Chenopodium*, *Digera*, and *Salsola*) of Amaranthaceae were examined using LM and SEM. The SEM has been shown to be quite useful for observing the surface morphology of plant material due to its better depth of field and high resolution, which are not attainable with the LM (Bahadur et al., 2019). The purpose of the study was to identify diagnostic traits that may be used to distinguish among Amaranthaceous genera and species. Based on both quantitative and qualitative anatomical traits, cluster analysis via dendrogram and PCA ordination of analyzed species revealed taxonomic importance. This study provides comprehensive micro-morphological information among 14 xeric Amaranthaceous taxa using botanical techniques. The micro-morphological attributes basically coincide slightly with the descriptions of other Amaranthaceous species previously studied using an optical microscope (Ahmad et al., 2009; Hussain et al., 2018; Khan et al., 2013; Nazish et al., 2020).

Leaf epidermal micro-morphological traits of 14 species belonging to nine genera, which were not previously explored using a scanning electron microscopy approach, have demonstrated significant taxonomic significance for their accurate identification and relationships among them. Earlier, a few studies on the micro-morphological characters of various species of Amaranthaceae were carried out in Pakistan by Sadia et al., (2020), Hussain et al., (2018), and Nazish et al., (2020). However, no comprehensive study of the leaf microstructure of amaranthaceous species in the Thal desert has been conducted. Therefore, the current report was undertaken with the aim of providing an identification guide based upon foliar micro-morphology using scanning microscopy.

The leaf epidermis is the subject of most taxonomic studies, and the foliar epidermal structure is one of the most significant taxonomic aspects in biosystematics. Epidermal cells, stomata, and trichome sizes, lengths, distribution, orientation, and frequency, as well as their distribution, orientation, and frequency, are all significant phylogenetic indicators (James et al., 2021). However, according to Akinsulire et al., (2020), the leaf possesses a range of anatomical traits that are taxonomically significant.

Certain epidermal characteristics, such as the morphology of subsidiary cells of the stomata, micro hairs, trichomes, and prickles, are of systematic relevance, according to Metcalfe (1968). The size, shape, and orientation of stomata, guard cells and subsidiary cells, structural peculiarities of epidermal cells, and frequency of stomata are just a few of the significant diagnostic features found in the epidermis that can aid in identification. Akinsulire et al., (2018) also stated that data recorded in leaf micro-morphological studies were taxonomically useful and the characters elaborated include the stomatal distribution, which is largely hypostomatous, though sometimes amphistomatous as documented. Plant species that have anticlinal walls of epidermal cells that are curved or straight are features of plant species that flourish in dry environments (Munir et al., 2011). According to Fajuke et al., (2018), the stomatal index and guard cell area offer values that may be used as comparison parameters among taxa, which can be valuable for taxon identification.

Foliar epidermal features are often regarded as a useful technique for establishing taxonomic relationships. In the case of taxonomic resolutions in the Amaranthaceae, SEM is preferable to other traditional microscopic methods because it reveals different characteristics of significant microstructural features (Hayat et al., 2010). Many researchers have used plant anatomical methods to resolve identification problems among groups of plants from diverse phytogeographic regions of Pakistan. Such studies include the works of Gul et al., (2019) on Lamiaceous species, Rashid et al., (2019) on some species of tribe *Trifolieae*, Shah et al., (2018) and (2019) on selected species of ferns from family Pteridaceae and Dryopteridaceae, Ullah et al., (2018) on the Caryophyllaceae species., Raza et al., (2021) and (2022) on selected *Acanthus* species, Ashfaq et al., (2019) on Convolvulaceous taxa and Khan et al., (2019) on identification of Gymnosperms.

Alwadie (2005) showed in *Aerva javanica* the uniseriate, multiarticulate, and stellate base trichomes, which are close to current findings where only unicellular stellate trichomes are present on the adaxial surface. Hussain et al., (2018) previously noted that the length and width of epidermal cells of *Aerva javanica* are 28  $\mu\text{m}$  and 34.5  $\mu\text{m}$  on the adaxial side, whereas on the abaxial surface, length and width are 31.5  $\mu\text{m}$  and 37.5  $\mu\text{m}$ , respectively. The length and width of epidermal cells in *A. javanica* were measured in current research is 28  $\mu\text{m}$  and 16.5  $\mu\text{m}$  on the adaxial surface, respectively.

However, the abaxial surface length is 38.5  $\mu\text{m}$  and the cell width is 21  $\mu\text{m}$ . The varieties of *Achyranthes aspera* represent similar types of unicellular trichomes while the number of trichomes varies with species. Two types of stomata, amphistomatic and anomocytic, were found in three varieties of *Achyranthes aspera*, whereas the stomatal index varies among these varieties. All these morphological features indicate that all the three varieties of *Achyranthes aspera* are quite different from each other (Teena and Yadav 2007). Similarly, the findings of Hussain et al. (2018) also supported our findings of elongated, irregular, paracytic, anomocytic, non-glandular trichomes of *Achyranthes aspera* and *Amaranthus viridis*.

In the specie *Alternanthera sessilis*, the uniseriate layer of epidermis, non-glandular trichome, anomocytic and diacytic stomata on both surfaces of the leaf were observed. Hussain et al., (2018) reported previously the irregular epidermal cell, anomocytic stomata on the abaxial and adaxial surface, and multicellular capitate trichomes present only on the abaxial surface. We found straight epidermal cells with multicellular trichomes in *Alternanthera ficoidea*, which is similar to the findings of Patil and Kore (2018). Hence, anatomical attribute sensitivity in *Alternanthera philoxeroides* could change to adapt to the water regime reflected in stoma density on leaf surfaces (Tao et al., 2009). While our findings explain irregular hairy unbranched epidermis and diacytic stomata, Bona (1993) observed two different non-glandular trichomes in *A. philoxeroides*.

The resultant characters from the anatomical features of *Amaranthus retroflexus*; paracytic stomata, glandular or non-glandular stellar and falcate trichomes, were not similar to those reported by El-Ghamery et al., (2017), who reported anomocytic type stomata and multicellular, uniseriate to biseriate glandular and unbranched trichomes. The current findings in *Amaranthus viridis* show the absence of trichomes on both sides, rectangular epidermal cells, and anisocytic stomata; hence they are consistent with those of Hussain et al., (2018). Recently Nazish et al., (2020) examined *Atriplex* species have anomocytic stomata and glandular capitate trichomes, while this study investigates unicellular non-glandular trichomes present in the intercostal zone.

According to Turki et al., (2008), *Bassia indica* comprises straight to curved walls, but rounded anticlinal walls on both surfaces of the epidermal cells have been

identified in the present research. The anticlinal wall of *Amaranthus graecizans* investigated was entirely different from those of Taia et al., (2020), which indicated a curved, undulating (elevated) anticlinal wall, whereas our results indicated a smooth angular wall. The present findings show that the *Chenopodium album* has mostly paracytic types of stomata, which is dissimilar to the earlier work of Zarinkamar (2006) and Khan et al., (2013) who reported staurocytic and anomocytic types of stomata, respectively. According to the recent work of Gaafar (2019), *Chenopodium ficifolium* had papillose shaped epidermal cells and undulate subsidiary cells. In accordance with our findings, the species has irregular shaped cells and lobed margin wavy type subsidiary cells.

Khan et al., (2013) described trichome and stomatal diversity in *Digera muricata* with an anomocytic uniseriate type on the abaxial side, while our research shows dissimilarities in multicellular, e-glandular, and capitate trichomes. Stem anatomy in *Salsola* species revealed a uniseriate with square to triangular and elliptic shapes in the epidermis. Munir et al., (2014) stated that multicellular hairs were small in the case of *Salsola tragus*.

### 3.4.5 Foliar Epidermal Micromorphology of Fabaceous taxa

Our research focus on 10 Fabaceous taxa belonging to seven genera were selected for palyno-anatomical examination with the help of light and scanning electron microscopy. The genera that were analyzed include *Acacia*, *Astragalus*, *Crotalaria*, *Dalbergia*, *Prosopis*, *Parkinsonia*, and *Tephrosia*. Significant variations in micromorphological foliar epidermal characters were analyzed (Table 24, 25 & 26). The field pictorial view, light and scanning micrographs of Fabaceous taxa were illustrate in Plate 80, 81, 82 and 83.

#### a) Foliar Epidermis

The shape of epidermal cells is polygonal or wavy with entire, slightly wavy, or sinuate walls. The shape of epidermal cells was the same on both abaxial and adaxial surfaces except in *Acacia modesta* and *Parkinsonia aculeata*. Where it was tetra to pentagonal in *Acacia modesta* while wavy in *Parkinsonia aculeata* on both sides. The pattern of anticlinal wall was entire, slightly wavy, sinuate, and deeply sinuate. The pattern of the wall was similar on both abaxial and adaxial surfaces. The length of epidermal cell ranges from  $(38.5 \pm 6.35 \mu\text{m})$  in *Prosopis cineraria* to  $(17.5 \pm 1.0 \mu\text{m})$  in *Astragalus homosus* on the abaxial surface. On the adaxial surface it varies from  $(47.5 \pm 2.5 \mu\text{m})$  in *Dalbergia sisso* to  $(17.5 \pm 1.76 \mu\text{m})$  in *Tephrosia purpurea* (Figure 45). Subsidiary cells have also been found in all species with considerable variations. Three types of subsidiary cell arrangement were noted; margin sinuous, enclosing guard cells, followed by lobed margins enclosing guard cells, and lobed wavy margins, partly enclosing guard cell shapes. The largest subsidiary cell length  $(42 \pm 6.49 \mu\text{m})$  along the adaxial side and the maximum length  $(40 \pm 4.67 \mu\text{m})$  on the abaxial side were noted in *Dalbergia sisso*. The width of the largest subsidiary cell was noted in *Acacia jacquemontii*  $(22 \pm 3.5 \mu\text{m})$  on the adaxial surface, while in *Dalbergia sisso* on the abaxial surface  $(13 \pm 1.2 \mu\text{m})$ , as mentioned in Figure 45.

#### b) Stomatal Complex

Fabaceous taxa examined were all amphistomatic except *Acacia modesta*, *Crotalaria burhia*, *Parkinsonia aculeata* and *Tephrosia purpurea* which are hypostomatic. Stomata of paracytic type were observed in all species except *Prosopis juliflora* where stomata were anisocytic. The stomatal length varies from  $(24.9 \pm 0.06$



$\mu\text{m}$ ) in *Dalbergia sisso* to  $(8.2 \pm 0.5 \mu\text{m})$  in *Prosopis juliflora* on the abaxial surface. On the adaxial surface, it ranges from  $(24 \pm 0.6 \mu\text{m})$  in *Dalbergia sisso* to  $(8.8 \pm 0.61 \mu\text{m})$  in *Prosopis juliflora* (Figure 46). The stomatal index ranges between 41.2-4.28% on the abaxial surface and 31.4-8.5% on the adaxial surface. On the abaxial surface, it is highest in *Acacia nilotica* (41.2%) and lowest in *Dalbergia sissoo* (4.28). Whereas on the adaxial surface, it is highest in *Dalbergia sissoo* (31.4) and lowest in *Acacia nilotica* (8.5) as illustrated in Figure 47.

### c) Trichomes

Unicellular, glandular trichomes are present on both surfaces in *Crotalaria burhia*, *Prosopis cineraria*, *Prosopis juliflora*, and *Tephrosia purpurea*. Trichomes are absent in the other six species. The length of trichomes ranges from  $(355 \pm 44.3 \mu\text{m})$  in *Prosopis juliflora* to  $(67.5 \pm 2.09 \mu\text{m})$  in *Crotalaria burhia* on the abaxial surface. On the adaxial surface, it ranges from  $(347 \pm 67.6 \mu\text{m})$  in *Prosopis cineraria* to  $(75 \pm 8.83 \mu\text{m})$  in *Crotalaria burhia*.

### 3.4.6 Identification Keys based on Foliar Anatomy of Fabaceous taxa

- 1 + Trichomes absent epidermal cell polygonal, entire anticlinal wall, stomata paracytic.....*Acacia jacquemontii*
- Trichomes absent, epidermal cell irregular..... 2
- 2 + Epidermal cell irregular, anticlinal wall entire, stomata paracytic, trichome absent.....*Acacia nilotica*
- Epidermal cell tetragonal, anticlinal wall entire and sinuate, stomata paracytic..... 3
- 3 + Epidermal cell tetragonal to pentagonal with sinuate anticlinal wall, stomata paracytic abaxial, trichome absent.....*Acacia modesta*
- Epidermal cell rectangular, anticlinal wall rounded .....4
- 4 + Epidermal cell polygonal, anticlinal wall sinuate, stomata paracytic, trichome absent.....*Astragalus hamosus*

- Epidermal cell polygonal, anticlinal wall entire, trichomes present.....**5**
- 5** + Epidermal cell polygonal isodiametric, abaxial paracytic stomata, trichome non-glandular unicellular.....*Crotalaria burhia*
- Epidermal cell polygonal, stomata paracytic, anticlinal wall wavy.....**6**
- 6** + Epidermal cell polygonal, anticlinal wall entire and slightly wavy, stomata paracytic, trichomes absent.....*Dalbergia sissoo*
- Anticlinal wall entire, trichome present.....**7**
- 7** + Epidermal cell tetragonal, stomata paracytic, trichome unicellular non-glandular.....*Prosopis cineraria*
- Epidermal cell polygonal, stomata paracytic.....**8**
- 8** + Epidermal cell polygonal, anticlinal wall entire, trichomes unicellular.....*Tephrosia purpurea*
- Stomata paracytic, anticlinal wall sinuate..... **9**
- 9** + Epidermal cell wavy, stomata paracytic (abaxial), anticlinal wall sinuate, trichome absent.....*Parkinsonia aculeata*
- Epidermal cell polygonal, stomata anisocytic ..... **10**
- 10** + Epidermal cell polygonal, stomata anisocytic, anticlinal wall entire, trichome unicellular glandular.....*Prosopis juliflora*

**Table 24.** Foliar qualitative characters of epidermis among Fabaceous species.

Fabaceous taxa	Ad/ Ab	Shape of epidermal cells	Anticlinal walls	Stomata type	Trichomes
<i>Acacia jacquemontii</i> Benth.	Ad	Polygonal	Entire	Paracytic	Absent
	Ab	Polygonal	Entire	Paracytic	Absent
<i>Acacia nilotica</i> (L.) Delile	Ad	Polygonal	Entire	Paracytic	Absent
	Ab	Irregular	Entire	Paracytic	Absent
<i>Acacia modesta</i> Wall	Ad	Tetragonal to Pentagonal	Entire	Absent	Absent
	Ab	Tetragonal to Pentagonal	Entire	Paracytic	Absent
<i>Astragalus hamosus</i> L.	Ad	Polygonal	Sinuate and deeply sinuate	Paracytic	Absent
	Ab	Polygonal	Sinuate and deeply sinuate	Paracytic	Absent
<i>Crotalaria burhia</i> Benth.	Ad	Polygonal	Entire	Absent	Unicellular
	Ab	Polygonal	Entire	Paracytic	Unicellular
<i>Dalbergia sissoo</i> DC.	Ad	Polygonal	Entire and Slightly wavy	Paracytic	Absent
	Ab	Polygonal	Entire and Slightly wavy	Paracytic	Absent
<i>Prosopis cineraria</i> (L.) Druce	Ad	Tetragonal	Entire	Paracytic	Unicellular
	Ab	Tetragonal	Entire	Paracytic	Unicellular
<i>Prosopis juliflora</i> (Sw.) DC.	Ad	Polygonal	Entire	Anisocytic	Glandular
	Ab	Polygonal	Entire	Anisocytic	Glandular
<i>Parkinsonia aculeata</i> L.	Ad	Wavy	Sinuate	Absent	Absent
	Ab	Wavy	Sinuate	Paracytic	Absent
<i>Tephrosia purpurea</i> (L.) Pers.	Ad	Polygonal	Entire	Absent	Unicellular
	Ab	Polygonal	Entire	Paracytic	Unicellular

**Keywords:** Ad = Adaxial, Ab = Abaxial

**Table 25.** Quantitative data analysis for stomatal index among Fabaceous species.

Fabaceous taxa	Ad /Ab	Stomata P/A	Av. No. of Tri. per unit area	Av. No. of Ep. cells per unit area	Av. No. of St. per unit area	Stomatal Index (%) $S/(S+E) \times 100$
<i>Acacia jacquemontii</i> Benth.	Ad	P	-	193	23	10.73
	Ab	P	-	247	52	17.5
<i>Acacia nilotica</i> (L.) Delile	Ad	P	3	92	8	8.18
	Ab	P	-	69	22	91.2
<i>Acacia modesta</i> Wall	Ad	A	-	45	-	-
	Ab	P	-	46	11	19.16
<i>Astragalus hamosus</i> L.	Ad	P	-	88	15	14.86
	Ab	P	2	30	26	21.9
<i>Crotalaria burhia</i> Benth.	Ad	A	3	200	-	-
	Ab	P	17	81	39	32.39
<i>Dalbergia sissoo</i> DC.	Ad	P	7.6	61	28	31.4
	Ab	P	5	80	3	4.28
<i>Prosopis cineraria</i> (L.) Druce	Ad	P	3	145	17	10.49
	Ab	P		106	70	40.04
<i>Prosopis juliflora</i> (Sw.) DC.	Ad	A	-	191	-	-
	Ab	P	-	94	29	24.07
<i>Parkinsonia aculeata</i> L.	Ad	P	-	57	21	27.15
	Ab	P	-	94	59	38.75
<i>Tephrosia purpurea</i> (L.) Pers.	Ad	A	7	151	-	-
	Ab	P	-	92	30	24.55

**Keywords:** (Ad) = Adaxial, (Ab) = Abaxial, (P) = Present, (A) = Absent, (S) = Stomata, (E) = Epidermal cells, (%) = Percentage, (Av.) = Average, (No) = Number

**Table 26.** Quantitative measurements of foliar epidermal anatomical characters among Fabaceous taxa.

Fabaceous taxa	Ad/Ab	Epidermal cells		Subsidiary cells (µm)		Stomata (µm)		Guard cells (µm)		Stomatal pore (µm)		Trichome (µm)	
		L	W	L	W	L	W	L	W	L	W	L	W
		Min-Max (Mean±SE)											
<i>Acacia jacquemontii</i> Benth.	Ad	25-35 (27.5±1.9)	17.5-25 (21.5±1.3)	15-35 (22.5±3.53)	15-35 (22.5± 3.5)	15-20 (16.5±1)	10-12.5 (11±0.61)	12.5-17.5 (14±1)	2.5-5 (4±0.61)	10-12.5 (11±0.61)	1.25-2.5 (2.05±0.27)	-	-
	Ab	12.5-25 (19±2.17)	10-17.5 (13.5±1.3)	20-27.5 (24.5±1.22)	10-15 (12±0.93)	15-17.5 (17±0.5)	10-15 (12±0.93)	12.5-15 (13.5±0.61)	2.5-5 (3±0.5)	10-12.5 (11±0.61)	1.25-2.50 (1.7±0.22)	-	-
<i>Acacia nilotica</i> (L.) Delile	Ad	22.5-37.5 (31±2.9)	10-25 (18±2.89)	12.5-15 (14.1±0.5)	5-5.5 (5.25±0.1)	10-15 (12±0.9)	6-8.7 (7.2±0.49)	10-15 (12±0.9)	2.5-3.25 (2.8±0.14)	6.75-10 (7.8±0.5)	0.25-1 (0.6 ±0.1)	117-275 (223±28)	10-12.5 (11.2±0.6)
	Ab	17.5-50 (31.5±5.4)	10-17.5 (14±1.5)	15-17.5 (16.1±0.57)	5-5.5 (5.15±0.1)	14-17 (15.9±0.6)	6.7-10 (8.3±0.6)	14.7-17.5 (15.9±0.6)	2.5-3 (2.7±0.1)	7.5-12.5 (9.5±0.9)	0.25-1 (0.7±0.14)	-	-
<i>Acacia modesta</i> Wall	Ad	27.5-50 (36±3.84)	17.5-22.5 (19.5±0.9)	-	-	-	-	-	-	-	-	-	-
	Ab	17.5-27.5 (22±2.0)	10-15 (12.5±0.8)	15-22.5 (19±1.27)	4.25-7.50 (5.6±0.57)	15-20 (17±0.93)	15-20 (17±0.93)	12.5-17.5 (14.5±0.93)	2.75-3.25 (2.9±0.09)	7.5-12.5 (10±0.79)	0.75-1.25 (1±0.11)	-	-
<i>Astragalus hamosus</i> L.	Ad	25-32.5 (29±1.27)	10-15 (12.8±0.8)	15-20 (17.5±1.11)	5-7.5 (6.25±0.5)	12.5-13 (12.6±0.1)	9.25-10 (9.8±0.14)	10-13 (12.1±0.53)	2.5-3.75 (3.35±0.2)	9.25-10.5 (9.9±0.2)	0.04-0.25 (0.14±0.04)	-	-
	Ab	15-20 (17.5±1.1)	12.25-13.75 (13.1±0.8)	15-17.5 (16.5±0.61)	6.25-7.75 (7.15±0.3)	10-15 (13±0.93)	6.25-8 (7.2±0.3)	10-12.5 (11.5±0.61)	2.5-3.5 (2.9±0.2)	5-10 (7.45±0.8)	0.04-0.25 (0.10±0.03)	-	-
<i>Crotalaria burhia</i> Benth.	Ad	17.5-30 (25±2.09)	12.5-25 (20.5±2.1)	-	-	-	-	-	-	-	-	50-100 (75± 8.83)	7.5-11.25 (9.25±0.6)
	Ab	17.5-37.5 (27±3.39)	12.5-25 (20.5±2.2)	15-22.5 (20±1.36)	5-7.5 (6.4±0.4)	15-22.5 (19±1.27)	7-8.25 (7.6±0.20)	12.5-20 (16.5±1.27)	2.50-3.25 (2.85±0.2)	10-15 (12±0.93)	0.5-1 (0.75±0.11)	62.5-75 (67.5±2.09)	7.5-12.5 (10.05±0.8)
<i>Dalbergia sissoo</i> DC.	Ad	37.5-50 (47.5±2.5)	25-37.5 (27.5±2.5)	25-62.5 (42±6.49)	10-17.5 (14±1.5)	22.5-25 (24±0.6)	17.5-22.5 (20.5±0.9)	22.5-25 (24±0.6)	6.25-7.5 (7.05±0.3)	12.5-17.5 (14±1)	3.75-5 (4.5±0.3)	-	-

	<b>Ab</b>	12.5-50 (30±6.37)	20-25 (23.5±1)	25-50 (40±4.67)	10-17.5 (13±1.2)	24.7-25 (24.9±0.06 )	17.25- 17.5 (17±0.05)	24.7-25 (24.9±0.06)	7.25-7.5 (7.45±0.0 5)	15-17.5 (16.9±0.5 )	2.5-5 (3.9±0.59)	-	-
<i>Prosopis cineraria</i> (L.) Druce	<b>Ad</b>	22.5-37.5 (28±2.6)	12.5-20 (16±1.27)	15-22.5 (19±1.5)	5-7.5 (6.5±0.6)	12.5-17.5 (15.5±0.8)	7.5-8 (7.65± 0.1)	12.5-17.5 (15.05± 0.79)	2.5-3 (2.85± 0.1)	10-15 (12.5±0.8 )	1.25-2.5 (1.85±0.2)	225-525 (347±67.6)	12.5-15 (13.5±0.6)
	<b>Ab</b>	25-62.5 (38.5±6.35)	12.5-27.5 (21±3.02)	15-25 (18±1.8)	5-7.5 (6.5±0.6)	12.5-17.5 (14.5±0.9)	5-10 (7.5±0.79)	12.5-17.5 (14.5±0.9)	2.5-3.25 (2.8±0.15)	10-12.5 (11.5±0.6 )	1-1.5 (1.25±0.1)	150-550 (335±79.7)	5-17.5 (12.5±2.1)
<i>Prosopis juliflora</i> (Sw.) DC.	<b>Ad</b>	23-47 (35.5±3.09)	10-22.5 (14±2.17)	10-15 (12.5±1.11)	5-6.25 (5.35± 0.3)	7.7-10.2 (8.8±0.58)	5.7-7.3 (6.5±0.59)	7.2-10.1 (8.6±0.66)	2.8-3.4 (3.1±0.23)	5.3-6.2 (5.9±0.76 )	0.56-2.2 (1.7±0.32)	180-320 (252±45.8)	15-30 (19±2.80)
	<b>Ab</b>	24.5-52 (36.3±3.27)	11.3-26 (16±2.31)	9.7-16.3 (12.7±0.87)	5.4-7.3 (6.1±0.82)	7.4-9.3 (8.2±0.54)	5.3-7.2 (6.4±0.39)	7-10.3 (8.8±0.58)	2.4-3.3 (2.7± 0.21)	5-7.3 (6.4±0.41 )	1-1.5 (1.3±0.09)	225-450 (355±44.3)	25-50 (38.5±4.1)
<i>Parkinsonia aculeata</i> L.	<b>Ad</b>	10-30 (21.5±3.5)	7.5-17.5 (12.5±1.7)	-	-	-	-	-	-	-	-	-	-
	<b>Ab</b>	15-37 (24±3.9)	7.5-15 (12±1.2)	12.5-25 (19.5±2.42)	5-7.5 (6.5±0.6)	15-22.5 (18.5±1.5)	7.5-10 (8.5±0.6)	12.5-20 (16±1.5)	3.75-5 (4.5±0.27)	7.5-15 (11.5±1.3 )	1.5-2.5 (2.05±0.2)	-	-
<i>Tephrosia purpurea</i> (L.) Pers.	<b>Ad</b>	12.5-22.5 (17.5±1.76)	12.5-17.5 (14±1)	-	-	-	-	-	-	-	-	95-142.5 (111±8.38)	10-15 (11.5±1)
	<b>Ab</b>	22.5-45 (35±4.13)	12.5-22.5 (17.5±1.7)	12.5-22.5 (17.5±1.76)	5-10 (8±0.93)	10-17.5 (14±1.5)	7.5-10 (8.5±0.61)	10-17.5 (14±1.5)	2.75-3.25 (2.9±0.09)	7.5-12.5 (10.5±0.9 )	1-1.75 (1.35±0.12)	-	-

**Keywords:** (L) = Length, (W) = Width, (Ad) = Adaxial, (Ab) = Abaxial, (Min) = Minimum, (Max) = Maximum, (SE) = Standard error, (µm) = Micromete

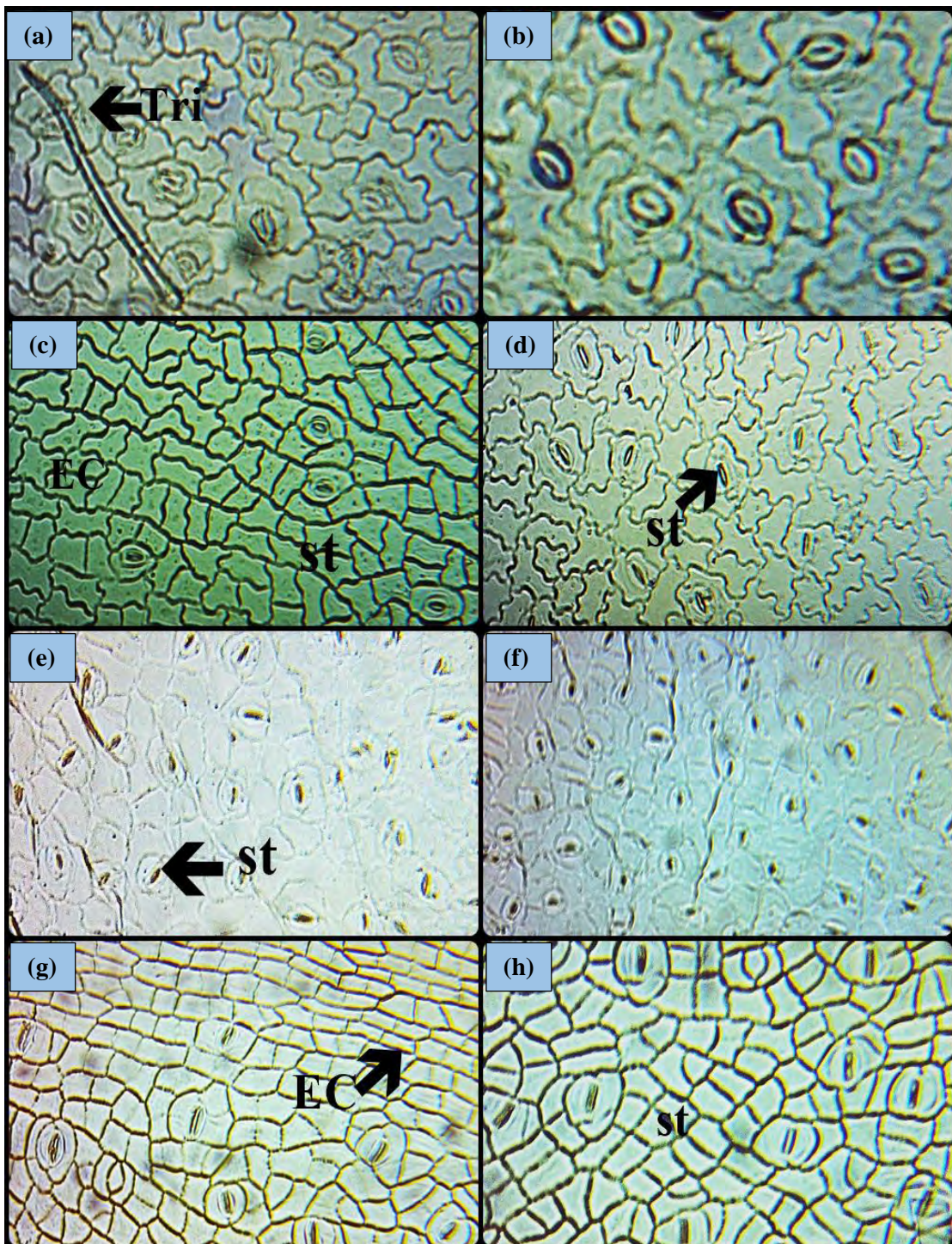


**Plate 80.** Light microscopic anatomical photographs, scale bar 10  $\mu$ m: *Acacia jacquemontii* Benth. (a) Adaxial surface 40x, (b) Abaxial surface 40x; *Acacia modesta* Wall. (c) Adaxial surface 40x, (d) Abaxial surface 40x; *Acacia nilotica* (L.) Delile (e) Adaxial surface 40x, (f) Abaxial surface 40x,; *Astragalus hamosus* L. (g) Adaxial surface 40x, (h) Abaxial surface 40x.

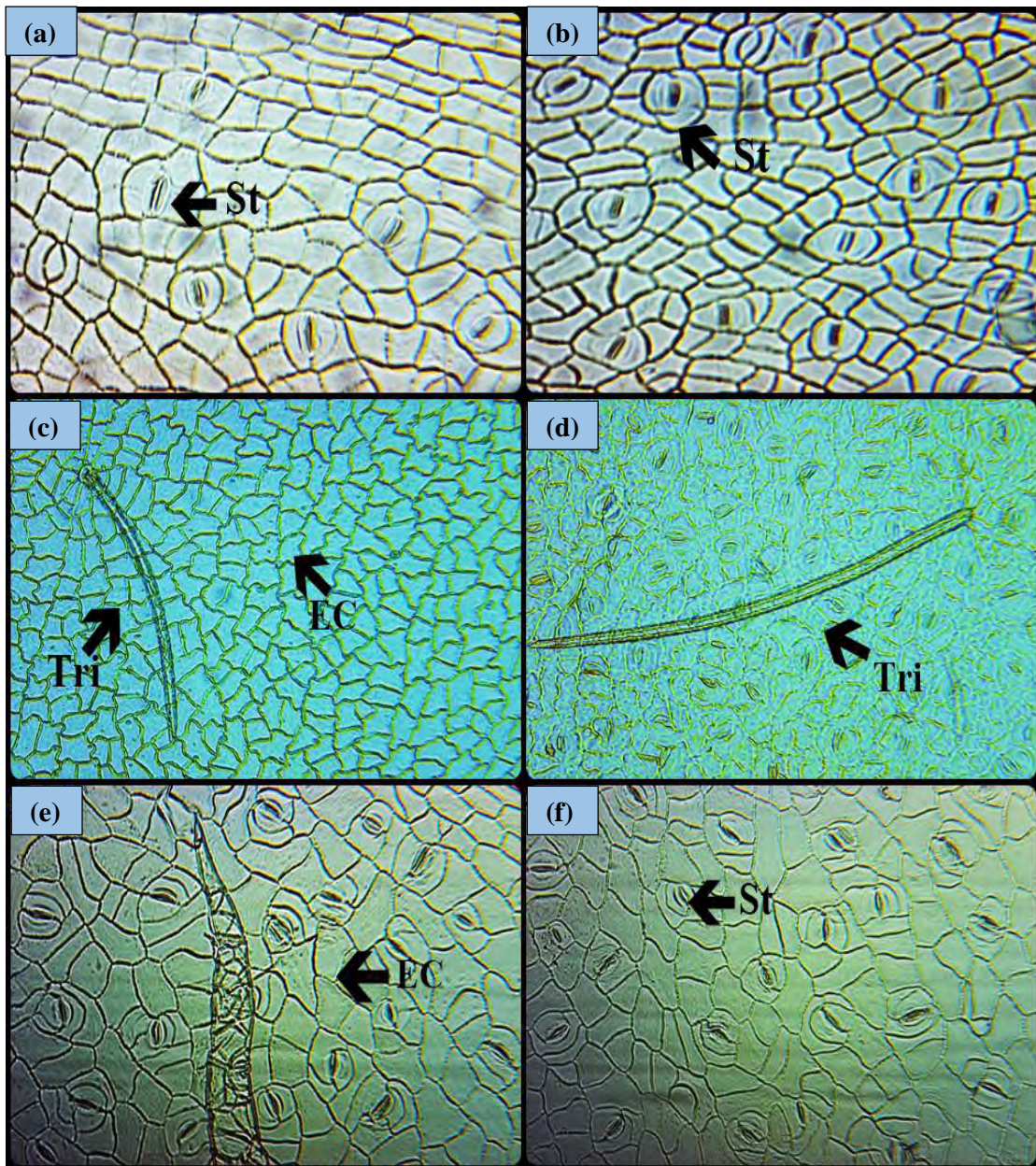


**Plate 81.** Light microscopic anatomical photographs, scale bar 10  $\mu$ m: *Crotalaria burhia* Benth. (a) Adaxial surface 40x, (b) Abaxial surface 40x; *Dalbergia sissoo* DC. (c) Adaxial surface 40x, (d) Abaxial surface 40x; *Parkinsonia aculeata* L. (e) Adaxial surface 40x, (f) Abaxial surface 40x.



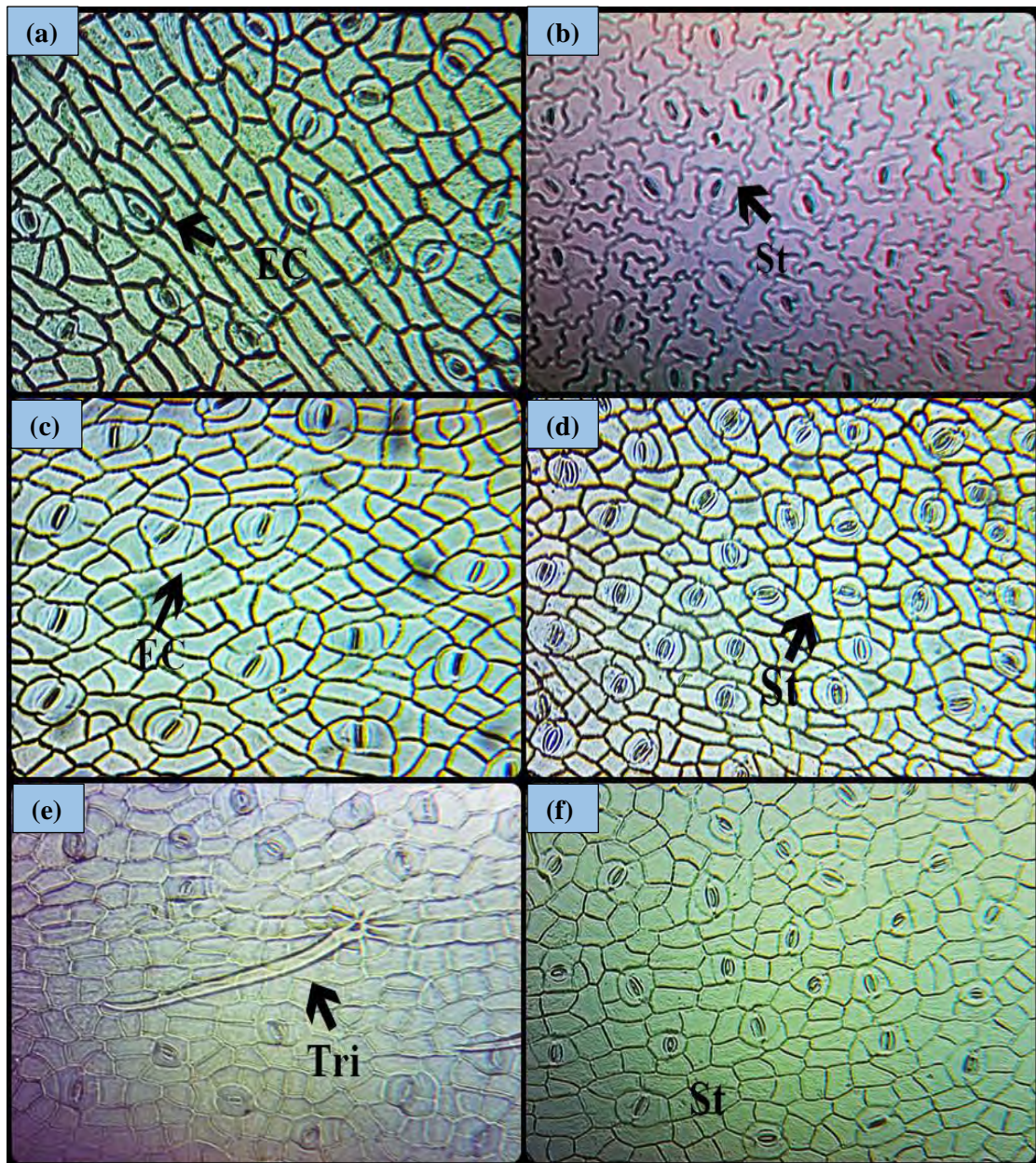


**Plate 82.** Light microscopic anatomical photographs, scale bar 10  $\mu$ m: *Prosopis cineraria* (L.) Druce (a) Adaxial surface 40x, (b) Abaxial surface 40x; *Prosopis juliflora* (Sw.) DC. (c) Adaxial surface 40x, (d) Abaxial surface 40x; *Tephrosia purpurea* (L.) Pers. (e) Adaxial surface 40x, (f) Abaxial surface 40x.

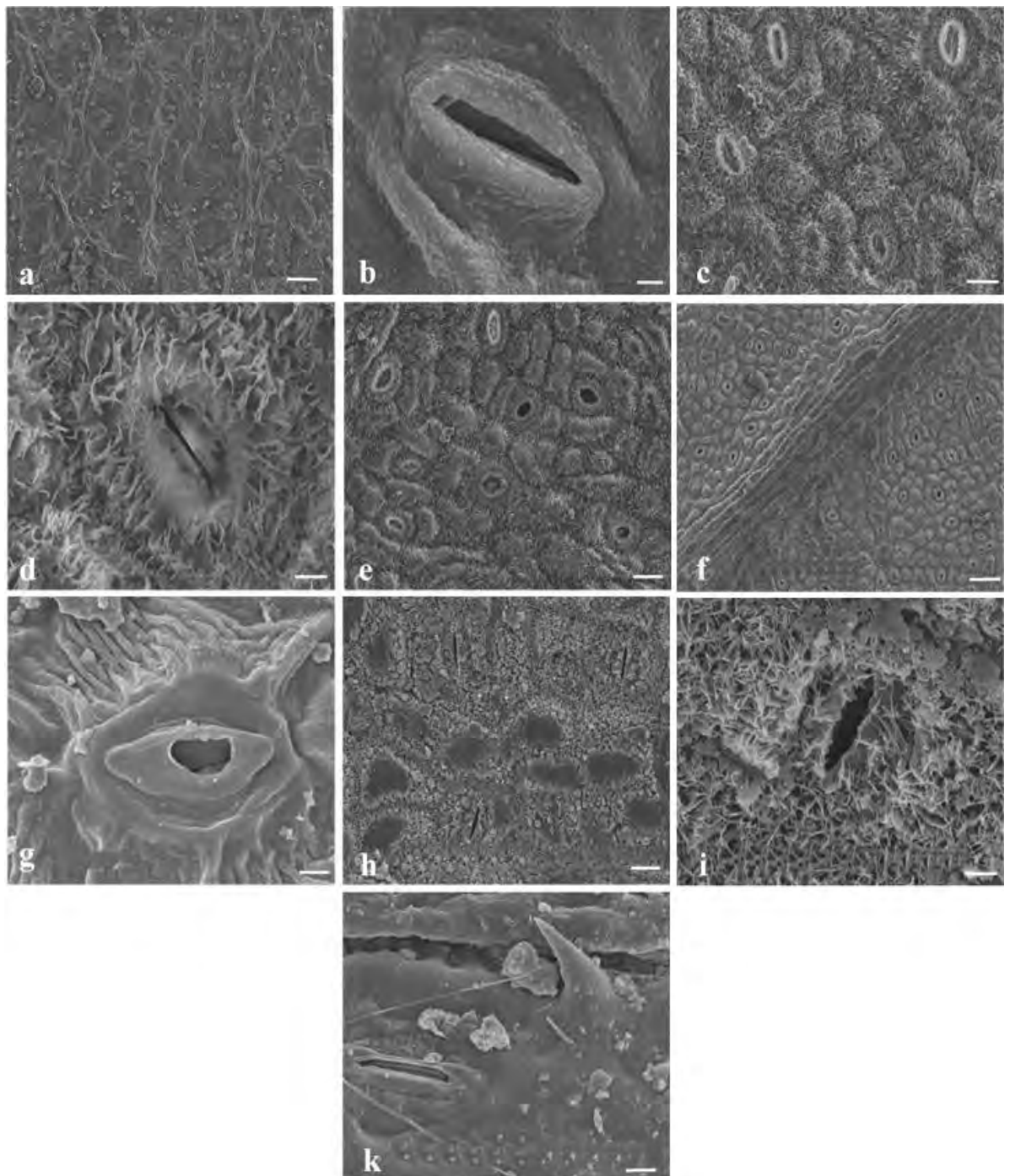


**Plate 83.** Scanning microscopic anatomical micrographs: (a) *Acacia jacquemontii*, SEM epidermis surface scale bar 100 µm; (b) *Acacia modesta*, epidermis and stomata scale bar 5 µm; (c) *Acacia nilotica*, SEM stomatal view scale bar 10 µm; (d) *Astragalus hamosus*, SEM stomatal view scale bar 5 µm; (e) *Crotalaria burhia*, epidermis surface scale bar 20 µm; (f) *Dalbergia sisso*, stomatal view scale bar 100 µm; (g) *Parkinsonia aculeata*, epidermis and stomata scale bar 5 µm; (h) *Prosopis cineraria*, epidermis surface scale bar 20 µm; (i) *Prosopis juliflora*, stomatal view scale bar 5 µm; (j) *Tephrosia purpurea*, epidermis and stomata scale bar 10 µm.

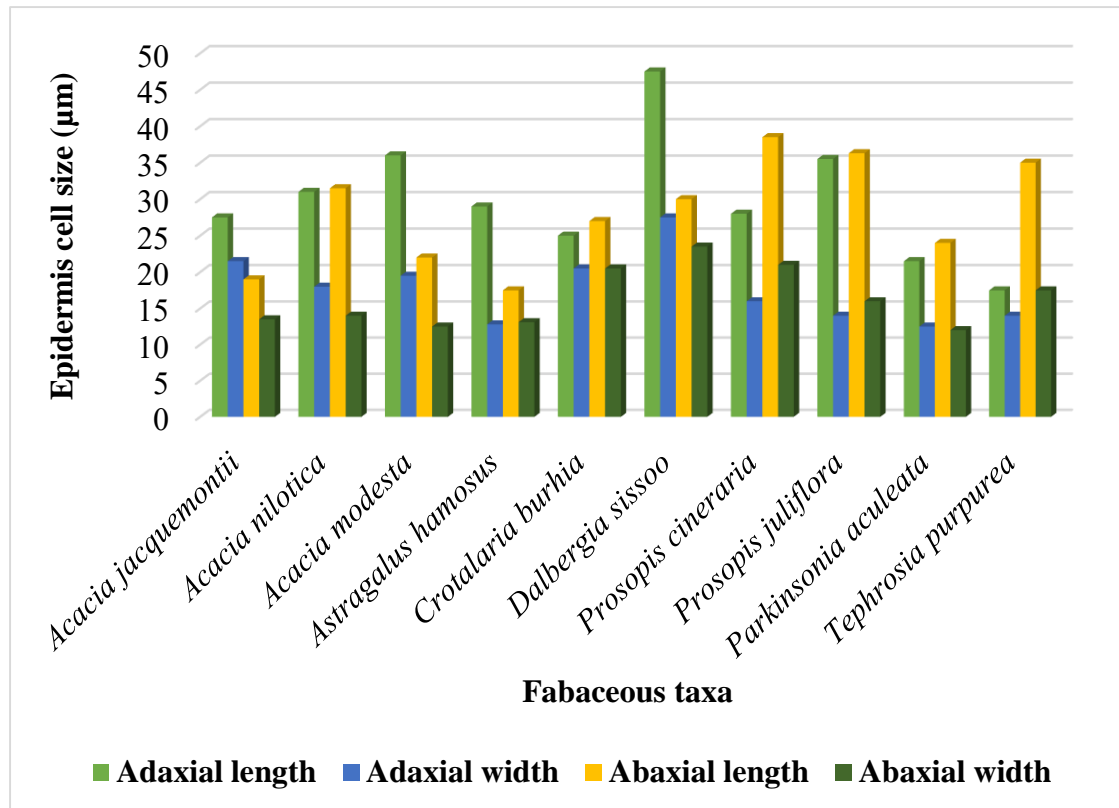


Figure 45. Epidermal cell size variations among Fabaceous taxa.

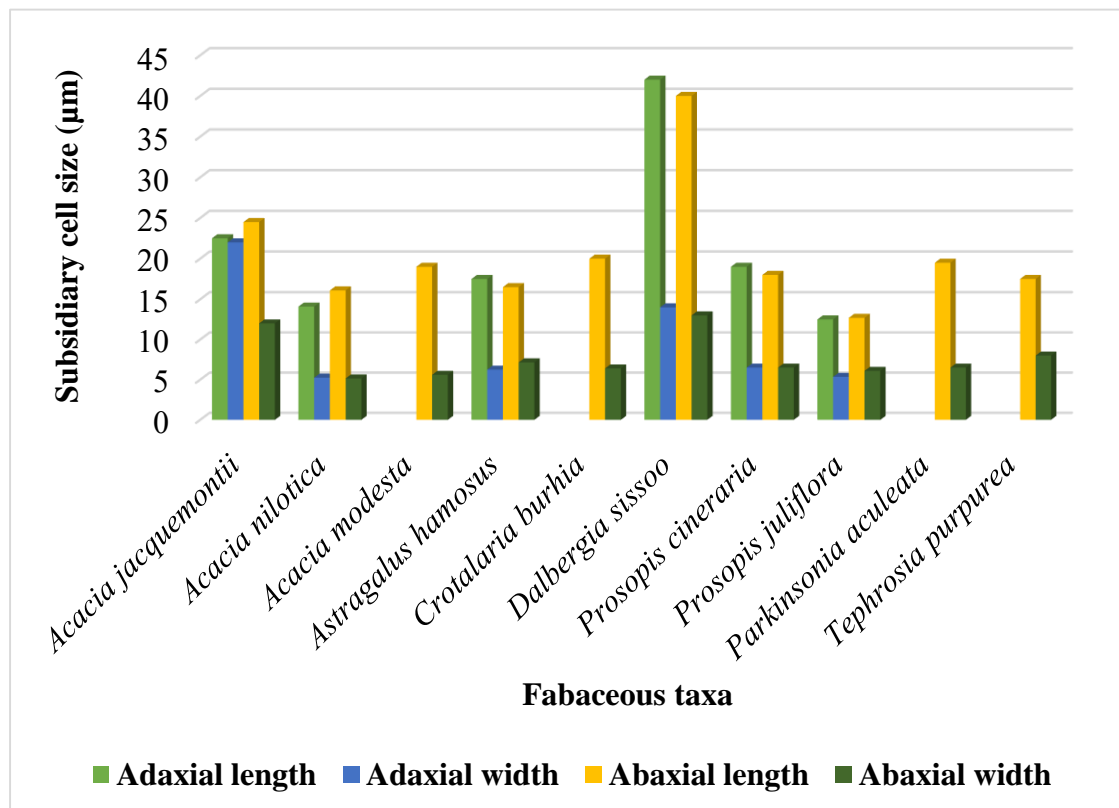
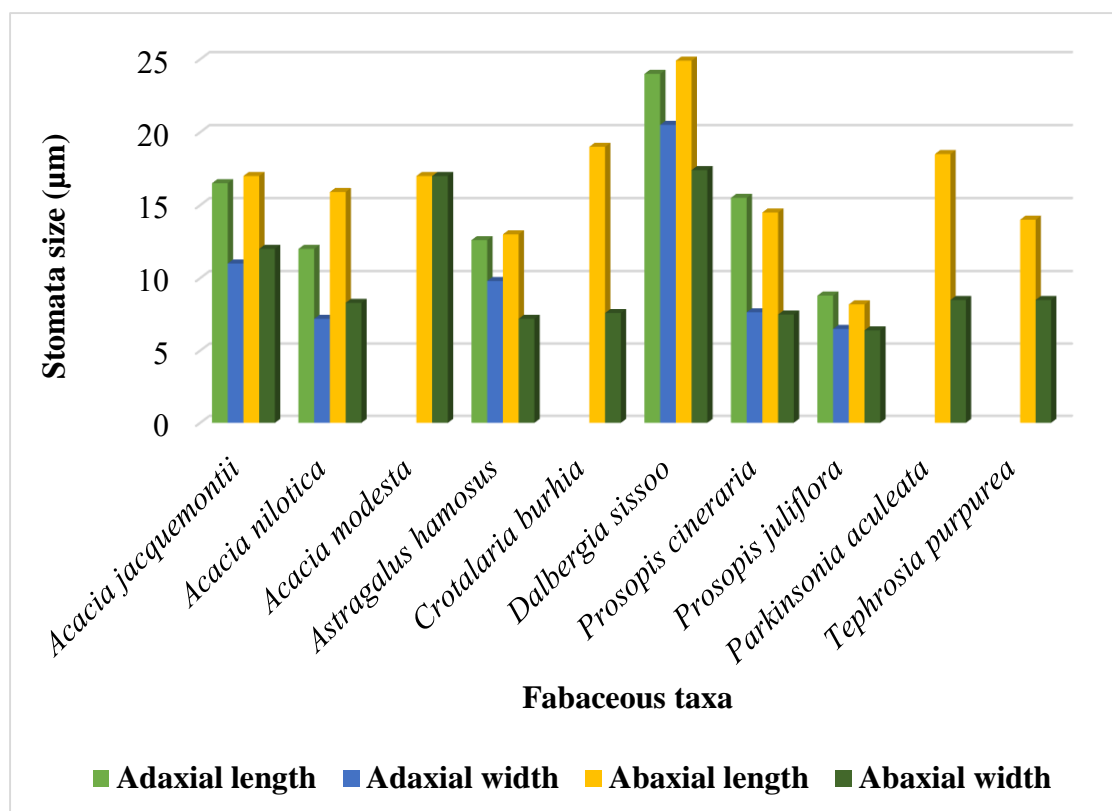
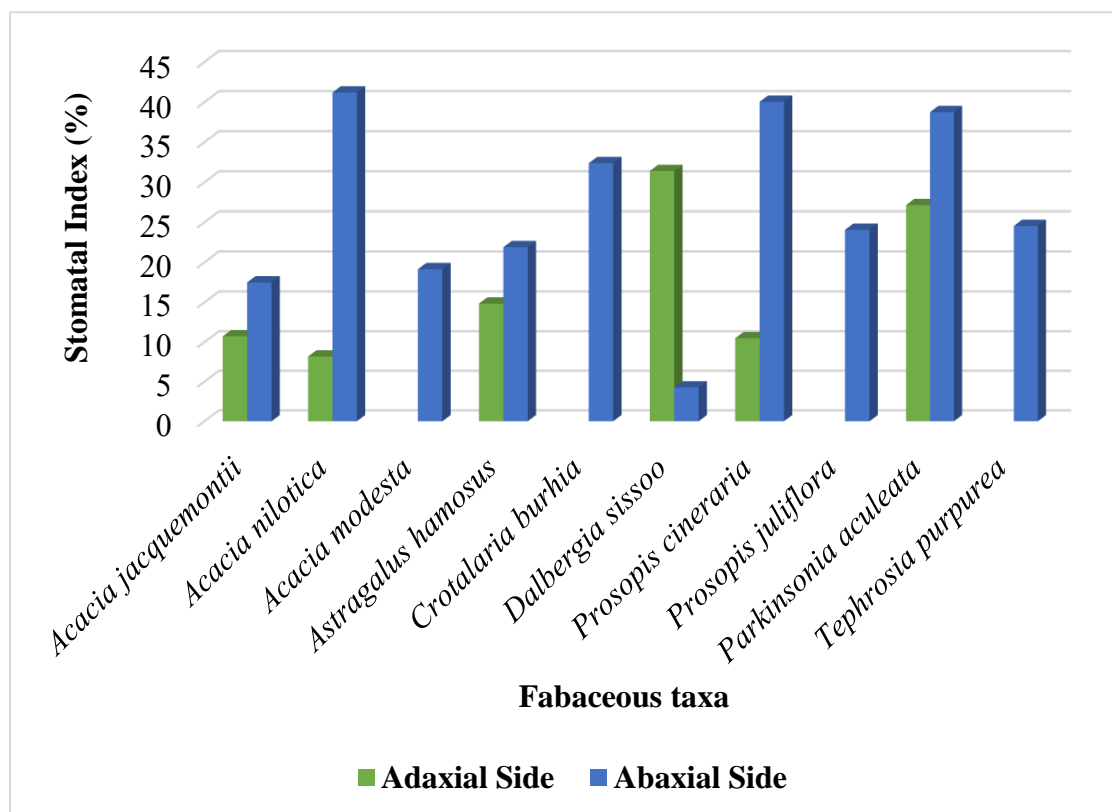


Figure 46. Subsidiary cell size variations along among Fabaceous taxa.



**Figure 47.** Stomatal size variations along epidermal surface among Fabaceous taxa.



**Figure 48.** Stomatal index variations along epidermis among Fabaceous taxa.

### 3.4.7 Discussion

The present study was based on light and scanning microscope visualization to observe the microstructural characteristics of the Fabaceous taxa from the different localities of the Thal desert. The micromorphological features (LM and SEM) are useful for the identification of plant species at various taxonomic levels. In the current research, the plant species were examined on the basis of epidermal cell size and shape, stomatal presence and absence along with stomatal type and size and presence and absence of trichomes and their size and type. Micromorphology of Fabaceous pollen was also observed to identify the range of pollen characters using scanning microscopy.

In the taxonomy of angiosperms, the use of leaf epidermal features is expanding and has been used for many years. The use of leaf epidermal traits in systematic botany is becoming more frequent, as is the use of other markers like DNA sequences and chemical compositions (Hameed et al., 2020). Foliar epidermal anatomical characters are valuable tools for anatomical studies. Although considerable work has been conducted on wood anatomy and gross morphology for identification purposes but without foliar epidermal morphology identification criteria would be incomplete (Endress et al., 2000; Zafar et al., 2019). One of the significant features of taxonomic classification is anatomical leaf study that is of boundless position from taxonomical assessment. That is why most families have research on the basis of anatomical leaf study (Birjees et al., 2022; Shaheen et al., 2010). Countless stress has been laid on leaf epidermal micro-morphology for the purpose of classification (Metcalf and Chalk, 1979). Although there exists a lot of literature on Angiospermic families from a taxonomic viewpoint (Sahreem et al., 2010).

Leaf epidermis is an important taxonomic feature and taxonomic analysis of many families is done with the help of leaf epidermis (Sadia et al., 2020; Shaheen et al., 2009). The use of microscopic imaging tools can be quite useful in examining foliar epidermal micromorphology and quantifying the idea that glandular trichome density reduces with increasing aridity in dry lands. The impact of the microenvironment on plants can be seen at the morpho-anatomical level by examining the composition of trichomes as well as the microstructure of stomata (Belmonte et al., 2022). The majority of morphological and anatomical adaptations made by desert plants in saline habitats include thinner cuticles, smaller leaves, fewer stomata per unit leaf area,

higher succulene, and wax deposition (Abd Elhalim et al., 2016). Foliar epidermal micromorphology is particularly important, and earlier reports highlight its importance in the identification of diverse plant groups (Attar et al., 2019; Bano et al., 2019; Esfandani-Bozchaloyi et al., 2018; Kandemir et al., 2019; Mamoona et al., 2011; Shah et al., 2019; Ullah et al., 2019). The anatomical properties of the Fabaceous species and their significance for the taxonomic classification have been presented by some earlier studies (Rashid et al., 2019; Yousaf et al., 2022).

Cildir et al., (2017) analyzed the leaf anatomical and micromorphological implications of *Lathyrus* species using light and scanning microscopy. Variations were observed in the epidermal cell shape of the selected plant species of Fabaceae. Polygonal, tetragonal, pentagonal, and wavy-shaped epidermal cells were reported in the present study. Duarte and Wolf (2005) reported polygonal epidermal cells in *Acacia* species which is in accordance with the present study. Variations were also recorded in epidermal cell size with the largest epidermal cell size reported in *Prosopis cineraria* with epidermal cell length ( $38.5 \pm 6.35 \mu\text{m}$ ) and the smallest in *Astragalus homosus* ( $17.5 \pm 1.11 \mu\text{m}$ ) on abaxial surface. While the abaxial surface largest and smallest epidermal cell ( $47.5 \pm 2.5 \mu\text{m}$ ) ( $17.5 \pm 1.76 \mu\text{m}$ ) in *Dalbergia sissoo* and *Tephrosia purpurea*, respectively. In Fabaceous taxa: *Acacia nilotica* and *Acacia modesta* observed epidermal cell shape is polygonal and tetragonal to pentagonal which was not in accordance with Saini et al., (2008). Epidermal cell shape in *Dalbergia sissoo* is polygonal and irregular which was in accordance with the previous findings of Shaheen et al., (2013).

The stomatal frequency is very most importantly use in taxonomy (Krishnamurthy and Kannabiran 1975). The foliar anatomical remaining persistent no change of environmental stress according to Davis and Heywood (1963). In *Acacia nilotica* the straight anticlinal wall and paracytic stomata are observed and anticlinal wall straight are also observed by Sahreen et al., (2010). In *Acacia nilotica* paracytic type of stomata were observed while Baretta-Kuipers (1981) observed both paracytic and anomocytic type of stomata. Stomatal frequency, size, and distribution are regarded as important tools in phylogeny and taxonomy (Albert and Sharma 2013). Gill et al., (1982) studied 21 species of Fabaceae and reported paracytic type stomata. In the order of Legume family, paracytic, anisocytic and anomocytic stomata were examined and Bano et al., (2019) discovered stomatal complex on both the adaxial and abaxial side

of *Astragalus*. The *Astragalus homosus* was also found to have amphistomatic and polygonal epidermal cells with deeply sinuate anticlinal walls in the current study.

The majority of Fabaceae members have paracytic stomata as their primary stomata type, according to earlier study of Ju (2020) whereas *Crotalaria* species have stomata that are paracytic, anisocytic, diacytic, or have one subsidiary cell (Ekeke et al., 2020). Paracytic stomata were reported in all the species except *Prosopis juliflora*. Martínez Quesada (1997) reported anisocytic stomata in *Prosopis juliflora* that does not coincide with the present study. Epidermal cells shape observed irregular in *Prosopis juliflora* were coincide with the findings of Shaheen et al., (2020). In order to assess the efficacy of the features defining the botanical identity (Robertson et al., 2010) proposed microscopic standards to distinguish the leaves of *Prosopis cineraria* with petiole micromorphological sectioning.

The research on the epidermal cells of *Tephrosia* species reveal that the abundance of epidermal cells varies from the leaf of one species to another within genera and that the size of stomata is significant taxonomic character. However, *Tephrosia purpurea* stomata complex type was paracytic, which conflicts with the observations made by Robertson et al., (2010). The stomatal index varied accordingly to the number of epidermal cells and stomata on both leaf surfaces. The maximum stomatal index was observed in *Acacia nilotica* (41.2%) on abaxial side while the along adaxial surface (31.4%) was observed for *Dalbergia sisso*. Munir et al., (2011) confirmed the presence of stomata on adaxial and abaxial sides. Nazish et al., (2022) reported a significant decrease in stomata number per unit leaf area when they grow in more arid land habit.

Presence of trichomes is an additional astonishing character in leaf epidermal micromorphology which have significance role in classification of various taxa. Trichomes are an important taxonomic tool and can be used to delimit taxa. Unicellular trichomes were observed in *Crotalaria burhia* while glandular trichomes were seen in *Prosopis juliflora* and *Tephrosia purpurea*. Bijauliya et al., (2017) reported simple uniseriate trichomes that coincides with our study.

### 3.4.8 Foliar Epidermal Micromorphology of Cucurbitaceous Species

Comparative foliar anatomy of selected species belonging to the Cucurbitaceae from Thal desert is performed to visualize the micromorphology. The six species, *Citrullus colocynthis*, *Cucumis melo*, *Cucurbita maxima*, *Luffa cylindrica*, *Momordica charantia* and *Mukia maderaspatana* were analyzed that are economically important from medicinal point of view. The foliar micro-structural features both qualitative and quantitative including epidermis cell size and types, stomata distribution and size and trichomes. The variations observed among quantitative features was illustrated in graphical form in Figure 49, 50, 51, 52, 53 & 54.

#### a) *Citrullus colocynthis* (L.) Schrad

Leaves are amphistomatic.

##### Adaxial surface

Epidermal cells are polygonal in shape. Stomata are Diacytic and trichomes are absent. No. of epidermal cells observed is 59 mm<sup>2</sup> on average. Length of cell is (91±4.5 µm). Width of epidermal cell is (53±2.8 µm). Number of stomata per average is 7. Length of stomata is (42.5±1.7 µm) and width of stomata is (23±1.4 µm). Length of Stomatal pore observed is (23.5±1.2 µm) and width of Stomatal pore is (6±0.6 µm). Length of guard cell is (29.5±2.8 µm) and width of guard is (19±2.3 µm). Length of subsidiary cell observed is (50±1.7 µm). Width of subsidiary cell is (39±3.9 µm). Stomatal index is 10% (Plate 81a, Table 27, 28 & 29).

##### Abaxial surface

Epidermal cells are irregular in shape. Stomata are cyclocytic and trichomes are SCT and glandular in shape. No. of epidermal cells observed is 57 mm<sup>2</sup> on average. Length of epidermal cell is (86±4.6 µm). Width of epidermal cell is (42±4.1 µm). Number of trichomes present on average is 4 mm<sup>2</sup>. Length of trichome is (53±2.8 µm) and width of trichome is (30.5±2.6 µm). Number of stomata per average is 9 mm<sup>2</sup>. Length of stomata is (41±4.2 µm) and width of stomata (19±2.5 µm) on average. Length of stomatal pore measured as (16±1.2 µm) and width (6.5±1.2 µm). Length of guard cell is (38±4.1 µm) width of guard is (16.5±2.3 µm). Length of subsidiary cell observed



is ( $36.5 \pm 3.7 \mu\text{m}$ ) width of subsidiary cell is ( $21 \pm 1.8 \mu\text{m}$ ). Stomatal index is 13.6% (Plate 84b, Table 27, 30 & 31).

#### **b) *Cucumis melo* L.**

Leaves are amphistomatic.

##### **Adaxial surface**

Epidermal cells are irregular in shape. Stomata are anisocytic and trichomes are SCT in shape. No. of epidermal cells observed is  $84 \text{ mm}^2$  on average. Length of cell is ( $49.5 \pm 1.6 \mu\text{m}$ ). Width of epidermal cell is ( $23 \pm 2.4 \mu\text{m}$ ). Number of trichomes present on average is  $8 \text{ mm}^2$ . Length of trichome is ( $92.5 \pm 8.6 \mu\text{m}$ ) and width of trichome is ( $34.5 \pm 3.3 \mu\text{m}$ ). Number of stomata per average is  $22 \text{ mm}^2$ . Length of stomata is ( $18.5 \pm 1.27 \mu\text{m}$ ) and width of stomata is ( $11 \pm 1.27 \mu\text{m}$ ). Length of stomatal pore observed is ( $8 \pm 0.93 \mu\text{m}$ ) and width of stomatal pore is ( $5 \pm 0.7 \mu\text{m}$ ). Length of guard cell is ( $19 \pm 1.27 \mu\text{m}$ ) and width of guard cell is ( $7.5 \pm 1.1 \mu\text{m}$ ). Length of subsidiary cell measured is ( $45 \pm 3.39 \mu\text{m}$ ) and width is ( $16.5 \pm 1.27 \mu\text{m}$ ). Stomatal index is 20.7% (Plate 84c, Table 27, 28 & 29).

##### **Abaxial surface**

Epidermal cells are polygonal in shape. Stomata are anisocytic and trichomes are absent. No. of epidermal cells observed is  $62 \text{ mm}^2$  on average. Length of epidermal cell is ( $48 \pm 3.1 \mu\text{m}$ ). Width of epidermal cell is ( $36 \pm 2.5 \mu\text{m}$ ). Number of stomata per average is  $18 \text{ mm}^2$ . Length of stomata is ( $21.5 \pm 1.27 \mu\text{m}$ ) and width of stomata ( $13.5 \pm 1.27 \mu\text{m}$ ) on average. Length of stomatal pore observed is ( $10.5 \pm 0.5 \mu\text{m}$ ) and width is ( $5.5 \pm 0.93 \mu\text{m}$ ). Length of guard cell is ( $18.5 \pm 1.27 \mu\text{m}$ ) width of guard cell is ( $9 \pm 1.27 \mu\text{m}$ ). Length of subsidiary cell calculated is ( $35 \pm 3.06 \mu\text{m}$ ) and width is ( $18 \pm 1.45 \mu\text{m}$ ). Stomatal index is 22.1% (Plate 84d, Table 27, 30 & 31).

#### **c) *Cucurbita maxima* Duchesne**

Leaves are hypostomatic.

##### **Adaxial surface**

Epidermal cells are irregular in shape. Stomata are absent and trichomes are present. No. of epidermal cells observed is 58 mm<sup>2</sup> on average. Length of cell is (77±8 µm). Width of epidermal cell is (27.5±1.7 µm). Number of trichomes present on average is 4 mm<sup>2</sup>. Length of trichome is (147±2.8 µm) and width of trichome is (172±3.1 µm) (Plate 84e, Table 27, 28 & 29).

#### **Abaxial Surface**

Epidermal cells are irregular in shape. Stomata are absent and trichomes are multicellular in shape. No. of epidermal cells observed is 59 mm<sup>2</sup> on average. Length of epidermal cell (72.5±3.7 µm) and width of epidermal cell (22.5±1.7 µm). Number of trichomes present on average is 5 mm<sup>2</sup>. Length of trichome is (148±2.3 µm) and width of trichome is (180±4.7 µm) (Plate 84f, Table 27, 30 & 31).

#### **d) *Luffa cylindrica* (L.) M.Roem**

Leaves are amphistomatic.

#### **Adaxial surface**

Epidermal cells are polygonal in shape. Stomata are actinocytic and trichomes are SCT in shape. No of epidermal cells observed is 117 mm<sup>2</sup> on average per unit area. Length of cell is (10±3.7 µm). Width of epidermal cell is (10±3.1 µm). No. of trichomes present on average is 3 mm<sup>2</sup> per unit area. Length of trichome is (24±1.3 µm) and width of trichome is (10±1.5µm). Number of stomata per average is 11 mm<sup>2</sup> per unit area. Length of stomata is (11.2±1.9 µm) and width of stomata is (7.2±1.3 µm). Length of stomatal pore observed is (5.8±0.8 µm) and width of stomatal pore is (1.4±0.5 µm). Length of guard cell is (8±1.5 µm) and width of guard is (3.2±0.83 µm). Length of subsidiary cell observed is (9.2±1.9 µm). Width of subsidiary cell is (4.6±1.1 µm). Stomatal index is 8.5% (Plate 84g, Table 27, 28 & 29).

#### **Abaxial surface**

Epidermal cells are irregular in shape. Stomata are Staurocytic and trichomes are multicellular conical trichome. No of epidermal cells observed are 121 mm<sup>2</sup> on average per unit area. Length of epidermal cell is (10±3.1 µm). Width of epidermal cell is (10±1.5 µm). Number of trichomes present on average is 4 mm<sup>2</sup>. Length of trichome

is (26.4±4.8 µm) and width of trichome is (12±2.5 µm). Number of stomata per average is 17 mm<sup>2</sup> per unit area. Length of stomata is (4.4±1.1 µm) and width of stomata (5.4±1.1 µm) on average. Length of stomatal pore observed is (11±1.5 µm) and width of stomatal pore is (1.8±0.8 µm). Length of guard cell is (8.2±1.9 µm) width of guard is (2.8±0.8 µm). Length of subsidiary cell observed is (9.2±1.9 µm) and width of subsidiary cell is (5±1.5 µm). Stomatal index is 12.3% (Plate 84h, Table 27, 30 & 31).

**e) *Momordica charantia* L.**

Leaves are hypostomatic.

**Adaxial surface**

Epidermal cells are irregular in shape. Stomata are absent and trichomes are multicellular colonial in shape. No of epidermal cells are 81 mm<sup>2</sup> on average per unit area. Length of epidermal cell is (60±5.2 µm) and width is (37.5±5 µm). Number of trichomes present are 6 mm<sup>2</sup> per unit area. Length of trichome is (161±6 µm) and width is (35±3.0 µm) (Plate 84i, Table 27, 28 & 29).

**Abaxial surface**

Epidermal cells are polygonal in shape. Stomata are Diacytic and trichomes are absent. No. of epidermal cells observed is 84 mm<sup>2</sup> on average. Length of epidermal cell is (59±7.3 µm) and width of epidermal cell is (44±5.7 µm). Number of stomata per average is 24 mm<sup>2</sup>. Length of stomata is (49.5±7.6 µm) and width of is (41.5±2.6 µm) on average. Length of stomatal pore observed is (20.5±4.4 µm) and width of pore is (11±1.27 µm). Length of guard cell is (9.5±0.93 µm) width of guard is (5±0.7 µm). Length of subsidiary cell observed is (34±2.3 µm) width of cell is (22±2.1 µm). Stomatal index is 22.2% (Plate 84j, Table 27, 30 & 31).

**f) *Mukia maderaspatana* (L.) M.Roem**

Leaves are amphistomatic.

**Adaxial surface**

Epidermal cells are irregular in shape. Stomata are Paracytic and trichomes are cortical in shape. No of epidermal cells observed is 64 mm<sup>2</sup> on average. Length of cell

is ( $46.5 \pm 3.3 \mu\text{m}$ ). Width of epidermal cell is ( $26.5 \pm 5.1 \mu\text{m}$ ). Number of trichomes present on average is  $2 \text{ mm}^2$ . Length of trichome is ( $75 \pm 11.2 \mu\text{m}$ ) and width of trichome is ( $34 \pm 3.0 \mu\text{m}$ ). Number of stomata per average is  $12 \text{ mm}^2$ . Length of stomata is ( $29 \pm 2.3 \mu\text{m}$ ) and width of stomata is ( $16 \pm 1.2 \mu\text{m}$ ). Length of stomatal pore observed is ( $7.5 \pm 1.3 \mu\text{m}$ ) and width of stomatal pore is ( $4.5 \pm 0.9 \mu\text{m}$ ). Length of guard cell is ( $22 \pm 2.1 \mu\text{m}$ ) and width of guard cell is ( $8.5 \pm 1.27 \mu\text{m}$ ). Length of the subsidiary cell observed is ( $57 \pm 4.9 \mu\text{m}$ ). Width of subsidiary cell is ( $29.5 \pm 2.6 \mu\text{m}$ ). Stomatal index is 12% (Plate 84k, Table 27, 28 & 29).

### **Abaxial surface**

Epidermal cells are irregular in shape. Stomata are paracytic and trichomes are MCT in shape. No. of epidermal cells observed is  $70 \text{ mm}^2$  on average. Length of the epidermal cell is ( $57 \pm 2.8 \mu\text{m}$ ). Width of the epidermal cell is ( $43 \pm 2.8 \mu\text{m}$ ). Number of trichomes present on average is  $2 \text{ mm}^2$ . Length of trichome is ( $82.5 \pm 13.4 \mu\text{m}$ ) and width of trichome is ( $36.5 \pm 3.0 \mu\text{m}$ ). Number of stomata per average are  $17 \text{ mm}^2$ . Length of stomata is ( $26 \pm 1.27 \mu\text{m}$ ) and width of stomata ( $14 \pm 1.27 \mu\text{m}$ ) on average. Length of stomatal pore observed is ( $6 \pm 0.6 \mu\text{m}$ ) and width of stomatal pore is ( $3.5 \pm 0.6 \mu\text{m}$ ). Length of guard cell is ( $22 \pm 1.7 \mu\text{m}$ ) width of guard is ( $7 \pm 0.93 \mu\text{m}$ ). Length of subsidiary cell observed is ( $52.5 \pm 2.9 \mu\text{m}$ ) width of subsidiary cell is ( $30.5 \pm 2.5 \mu\text{m}$ ). Stomatal index is 19.5% (Plate 84l, Table 27, 30 & 31).

**Table 27.** Qualitative foliar anatomical characters of Cucurbitaceous species.

Sr. No.	Cucurbitaceous species	Surface of epidermis	Epidermal cell shape	Status of stomata (P/A)	Type of stomata	Status of Trichome (P/A)	Type of Trichome
1.	<i>Citrullus colocynthis</i> (L.) Schrad.	Adaxial	Polygonal	Present	Diacytic	Absent	Absent
		Abaxial	Irregular	Present	Cyclocytic	Present	Short conical Trichome
2.	<i>Cucumis melo</i> L.	Adaxial	Irregular	Absent	Absent	Present	Short conical Trichome
		Abaxial	Irregular	Absent	Absent	Present	Short conical Trichome
3.	<i>Cucurbita maxima</i> Duchesne	Adaxial	Irregular	Present	Anisocytic	Present	Short Conical Trichome
		Abaxial	Polygonal	Present	Anisocytic	Absent	Absent
4.	<i>Luffa cylindrica</i> (L.) M.Roem.	Adaxial	Polygonal	Present	Actinocytic	Present	Long Conical Trichome
		Abaxial	Irregular	Present	Staurocytic	Present	Multicellular Conical Trichome
5.	<i>Momordica charantia</i> L.	Adaxial	Irregular	Absent	Absent	Present	Multicellular Conical Trichome
		Abaxial	Irregular	Present	Diacytic	Absent	Absent
6.	<i>Mukia maderaspatana</i> (L.) M.Roem.	Adaxial	Polygonal	Present	Paracytic	Present	Multicellular conical Trichome
		Abaxial	Polygonal	Present	Paracytic	Present	Multicellular conical Trichome

**Table 28.** Quantitative foliar anatomical features of adaxial side epidermis and trichomes among Cucurbitaceous species.

Sr. No.	Cucurbitaceous species	No. of epidermal cells (mm <sup>2</sup> )	Epidermal cell size (µm)		Trichome no. (mm <sup>2</sup> )	Trichome/glands (µm)	
			(Average)	L		W	(Average)
1.	<i>Citrullus colocynthis</i> (L.) Schrad.	59	75(91±4.5)100	45(53±2.8)62.5	-	-	-
2.	<i>Cucumis melo</i> L.	84	45(49.5±1.6)55	15(23±2.4)30	8	62.5(92.5±8.6)112.5	25(34.5±3.3)45
3.	<i>Cucurbita maxima</i> Duchesne	58	50(77±8)100	22.5(27.5±1.7)55	4	137.5(147±2.8)155	125(172±3.1)25
4.	<i>Luffa cylindrica</i> (L.) M.Roem.	117	6(12±3.7)15	6(10±3.1)14	3	15(24±1.3)32	8(10±1.5)12
5.	<i>Momordica charantia</i> L.	81	47.5(60±5.3)60	25(37.5±5)52	6	142.5(161±6)177	27.5(35±3.0)45
6.	<i>Mukia maderaspatana</i> (L.) M.Roem.	64	35(46.5±3.3)55	20(26±2.5)35	2	45(75±11.2)107	27(34±3.0)45

**Table 29.** Quantitative foliar anatomical features of adaxial side stomata among Cucurbitaceous species.

Sr No.	Cucurbitaceous species	L/W	No. of stomata	Stomata (µm)	Stomatal pore (µm)	Guard cells (µm)	Subsidiary cells (µm)	S. I (%)
1.	<i>Citrullus colocynthis</i> (L.) Schrad.	L	7	37.5(42.5±1.7)47.5	20(23.5±1.2)27.5	22.5(29.5±2.8)37	45(50±1.7)55	10
		W		20(23±1.4)27	5(6±0.6)7.5	12.5(19±2.3)25	27.5(39±3.9)50	
2.	<i>Cucumis melo</i> L.	L	22.2	15(18.5±1.27)	5(8±0.93)10	15(19±1.27)	35(45±3.39)54	20
		W		7.5(11±1.27)1	2.5(5±0.7)7	5(7.5±1.1)7.5	12.5(16.5±1.27)20	
3.	<i>Luffa cylindrica</i> (L.) M.Roem.	L	11	9.0(11.2±1.9)14	5(5.8±0.8)7	6(8±1.5)10	7(9.2±1.9)12	8.5
		W		6.0(7.2±1.3)9	1(1.4±0.5)2	2(3.2±0.83)4	3(4.6±1.1)6	
4.	<i>Mukia maderaspatana</i> (L.) M.Roem.	L	12	22.5(29±2.3)35	2.5(7.5±1.3)10	15(22±2.1)27	45(57±4.9)75	15
		W		12.5(16±1.2)20	2.5(4.5±0.9)7.5	5(8.5±1.27)12.5	22.5(29.5±2.6)37.5	

**Table 30.** Quantitative foliar anatomical features of abaxial side epidermis and trichomes among Cucurbitaceous species.

Sr. No.	Cucurbitaceous species	Epidermal cell (mm <sup>2</sup> ) (Average)	Epidermal cell (µm)		Trichome no. (mm <sup>2</sup> ) (Average)	Trichome (µm)	
			L	W		L	W
1.	<i>Citrullus colocynthis</i> (L.) Schrad.	57	72.5(86±4.6)97	30(42±4.1)52.5	4	45(53±2.8)62.5	22.5(30.5±2.6)37
2.	<i>Cucumis melo</i> L.	62	37(48±3.1)55	30(36±2.5)45	-	-	-
3.	<i>Cucurbita maxima</i> Duchesne	59	62.5(72.5±3.7)85	17.5(22.5±1.7)27	5	130(148±2.3)177	142(180±4.7)222
4.	<i>Luffa cylindrica</i> (L.) M.Roem.	121	6(13±3.1)14	6(8±1.5)10	4	21(26.4±4.8)32	9(12±2.5)15
5.	<i>Momordica charantia</i> L.	84	37.5(59±7.3)80	30(44±5.7)62.5	-	-	-
6.	<i>Mukia maderaspatana</i> (L.) M.Roem.	70	50(57±2.8)65	35(43±2.8)50	2	50(82.5±13.4)125	30(36.5±3.0)47.5

**Table 31.** Quantitative foliar anatomical features of abaxial side stomata among Cucurbitaceous species.

Sr. No.	Cucurbitaceous species	Stomata (mm <sup>2</sup> )	L/W	Stomata (µm)	Stomatal pore (µm)	Guard cells (µm)	Subsidiary cells (µm)	S.I (%)
1.	<i>Citrullus colocynthis</i> (L.) Schrad.	9	L	27.5(41±4.2)50	12(16±1.2)20	27.5(38±4.1)50	27(36.5±3.7)47.5	13.6
			W	10(19±2.5)25	2.5(6.5±1.2)10	10(16.5±2.3)22.5	17.5(21±1.8)27.5	
2.	<i>Cucumis melo</i> L.	17.6	L	17.5(21.5±1.27)25	7.5(10.5±0.5)12.5	15(18.5±1.27)22.5	27.5(35±3.06)45	22.1
			W	10(13.5±1.27)17.5	2.5(5.5±0.93)7.5	5(9±1.27)12.5	15(18±1.45)22.5	
3.	<i>Luffa cylindrica</i> (L.) M.Roem.	17	L	7.0(9.6±2.07)12	3(4.4±1.1)6	5(8.2±1.9)10	7(9.2±1.9)12	12.3
			W	4.0(5.4±1.1)7	1(1.8±0.8)3	2(2.8±0.8)4	3(5±1.5)7	
4.	<i>Momordica charantia</i> L.	24	L	20(49.5)7.6)62.5	12.5(20.5±4.4)37.5	7.5(9.5±0.93)12.5	27(34±2.3)40	22.2
			W	35(41.5±2.6)50	7.5(11±1.27)15	2.5(5±0.7)7.5	15(22±2.1)27	
5.	<i>Mukia maderaspatana</i> (L.) M.Roem.	17	L	22.5(26±1.27)30	5(6±0.6)17.5	17.5(22±1.7)27.5	45(52.5±2.9)62.5	19.5
			W	10(14±1.27)17.5	2.5(3.5±0.6)7.5	5(7±0.93)10	25(30.5±2.5)37.5	



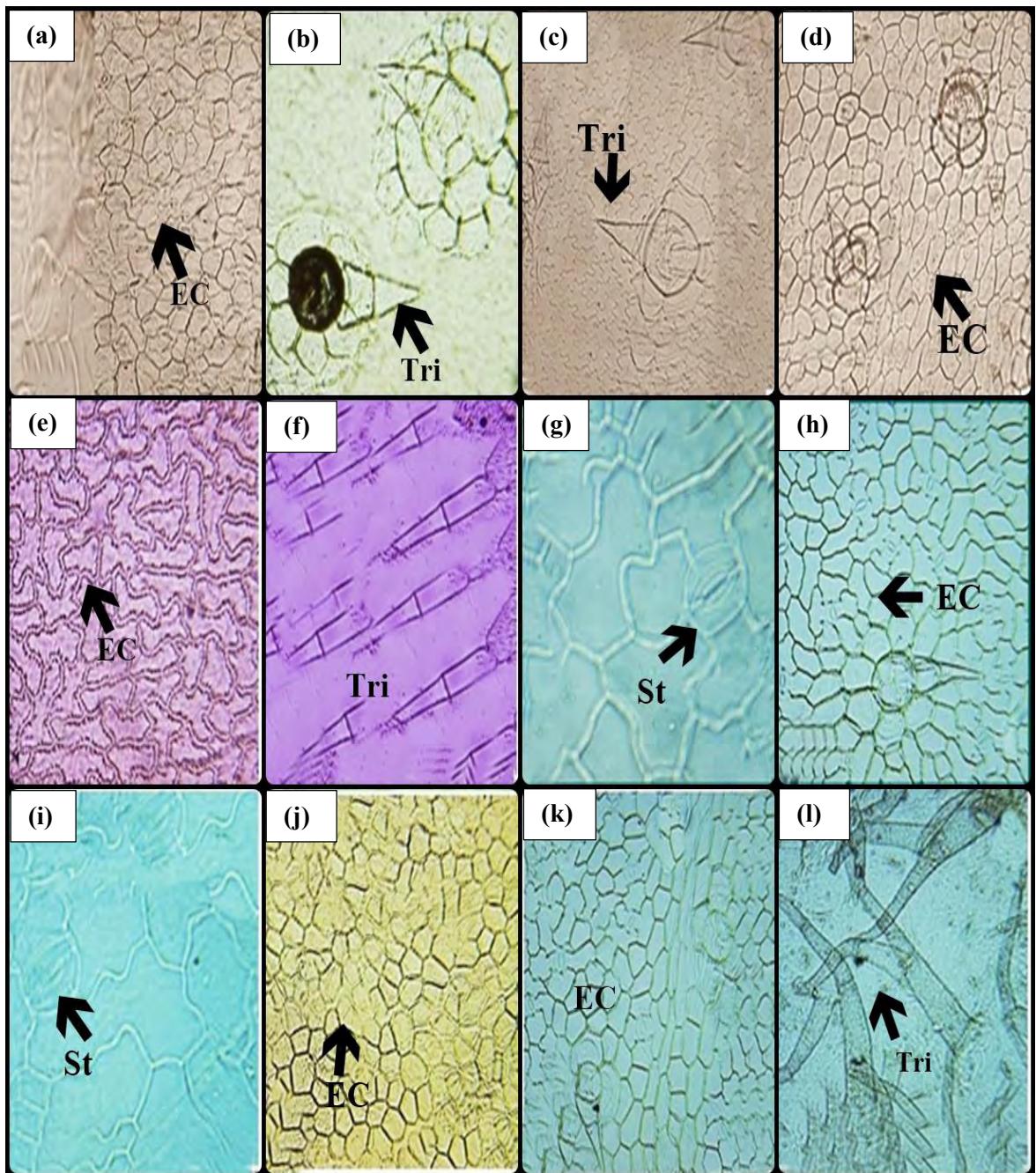


**Plate 84.** Light Micrographs (LM) illustrated stomata, epidermal cells and trichomes of Cucurbitaceous species; *Citrullus colocynthis* (a) Adaxial surface showing epidermis (b) Abaxial surface showing trichomes, *Cucumis melo* (c) Adaxial surface showing trichome (d) Abaxial surface showing epidermal cells, *Cucurbita maxima* (e) Adaxial surface showing epidermal cells (f) Abaxial surface showing trichomes, *Luffa cylindrica* (g) Adaxial surface showing stomata (h) Abaxial surface showing cells and glandular trichome, *Momordica charantia* (i) Adaxial surface showing stomata (j) Abaxial surface showing epidermis, *Mukia maderaspatana* (k) Adaxial surface showing epidermal cells (l) Abaxial surface showing multicellular trichomes.

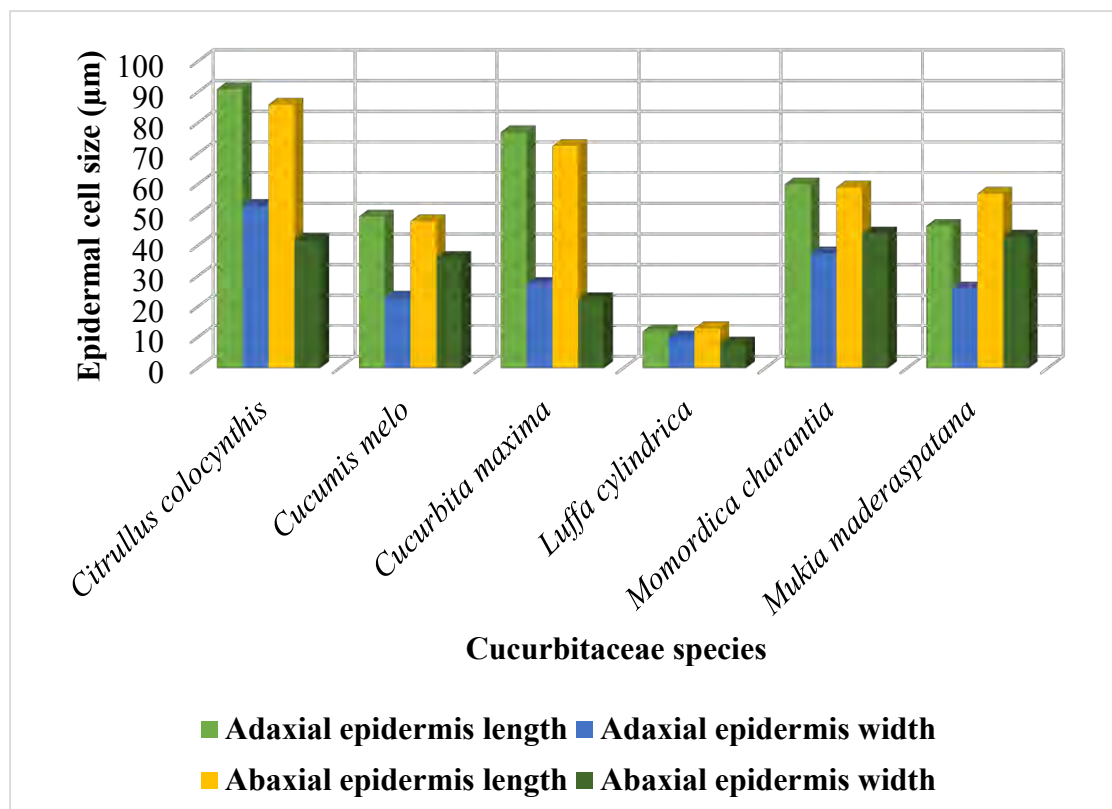


**Figure 49.** Mean size variation of epidermal cells among Cucurbitaceous species

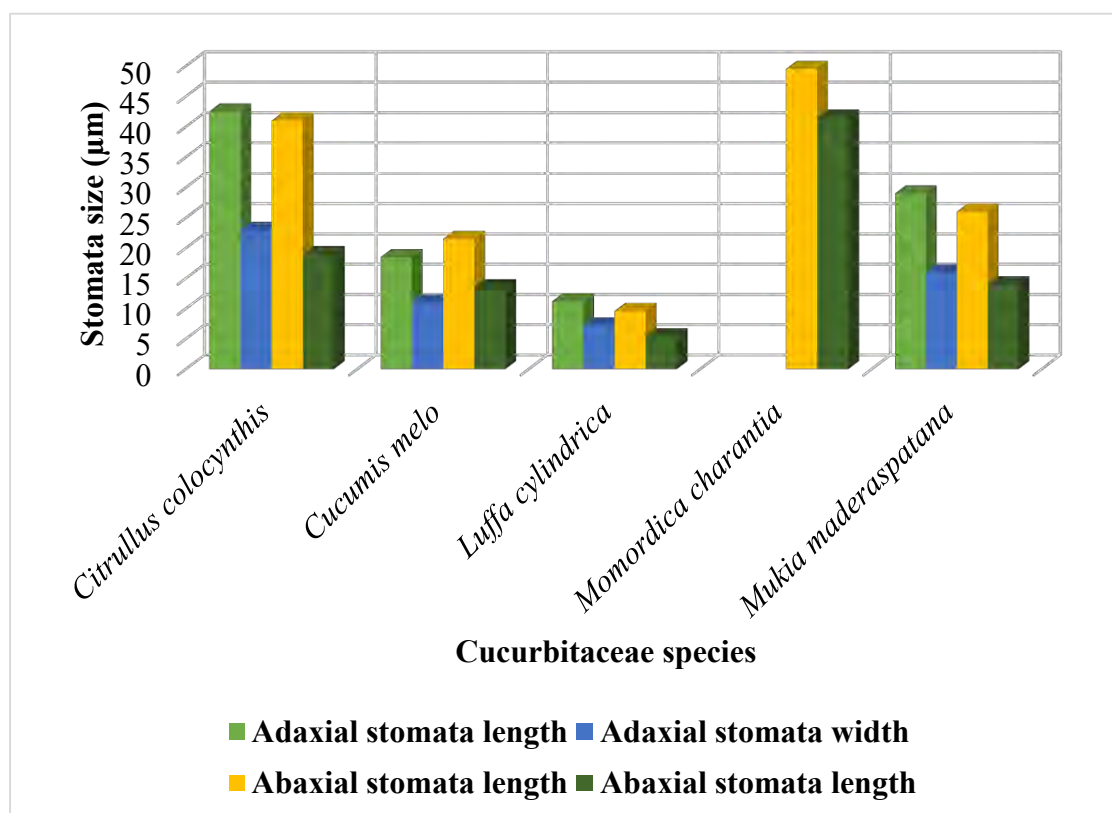


**Figure 50.** Average stomatal size variations among Cucurbitaceous species

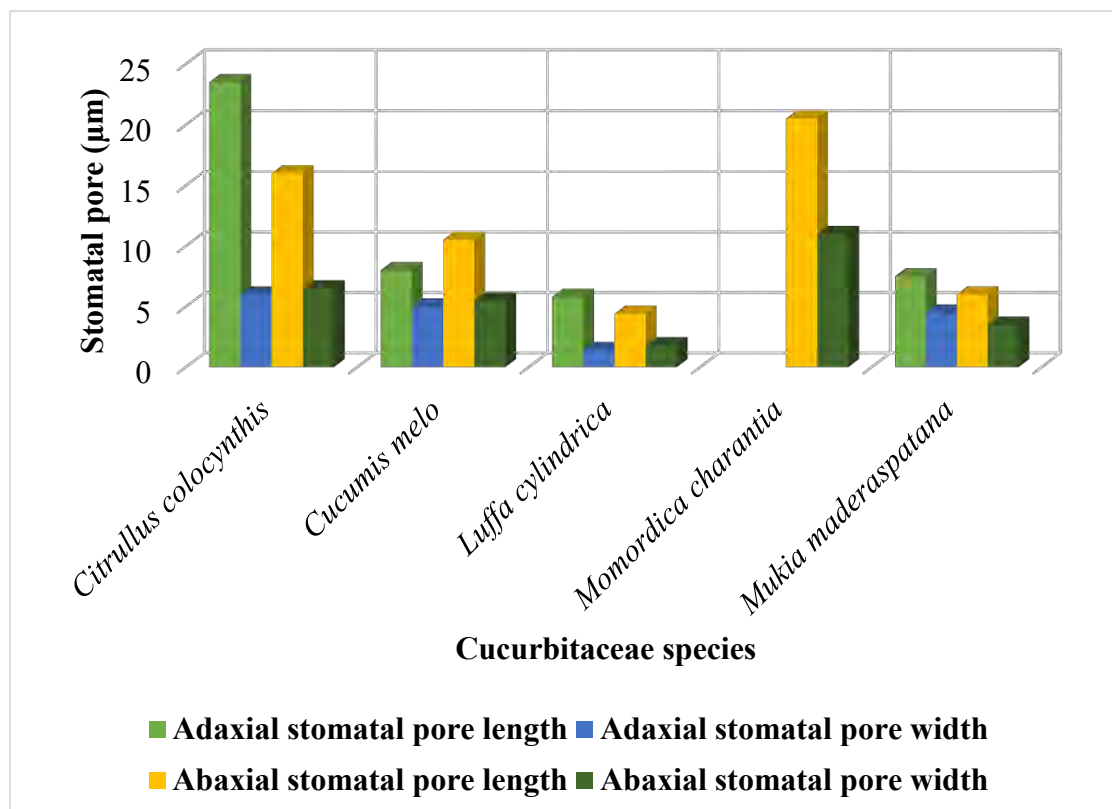


**Figure 51.** Stomatal pore mean size variations among Cucurbitaceous species

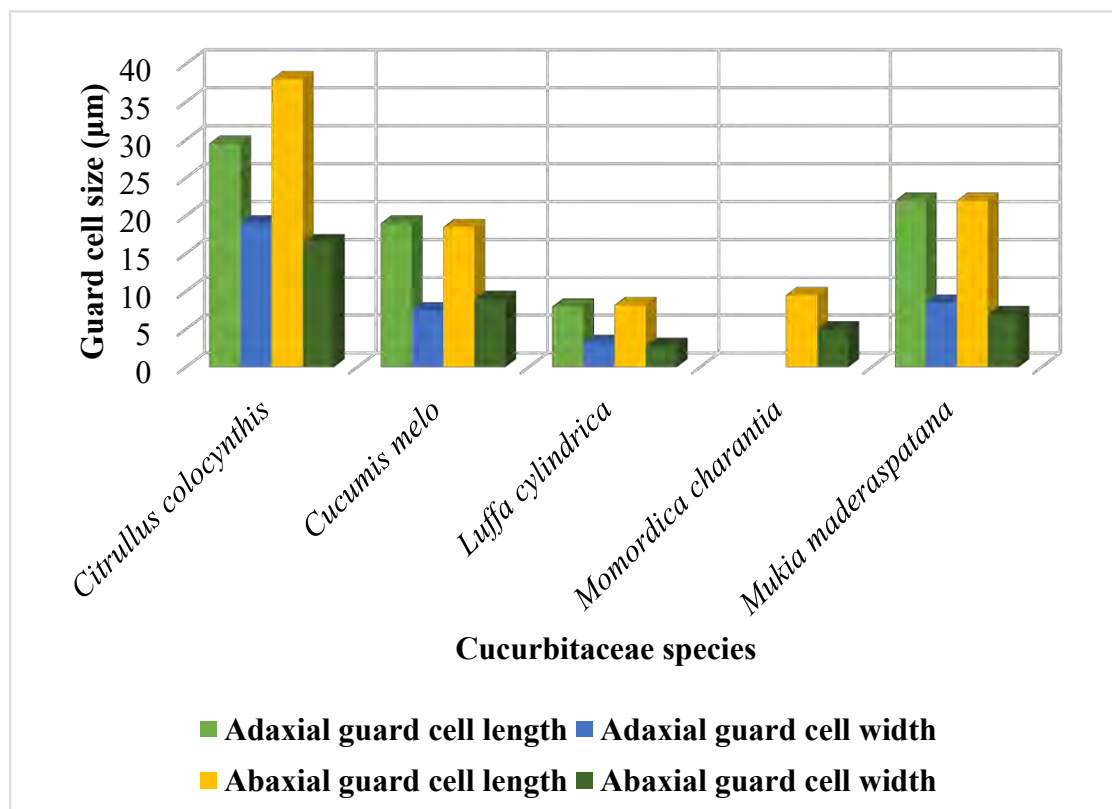


**Figure 52.** Average guard cell size variations among Cucurbitaceous species

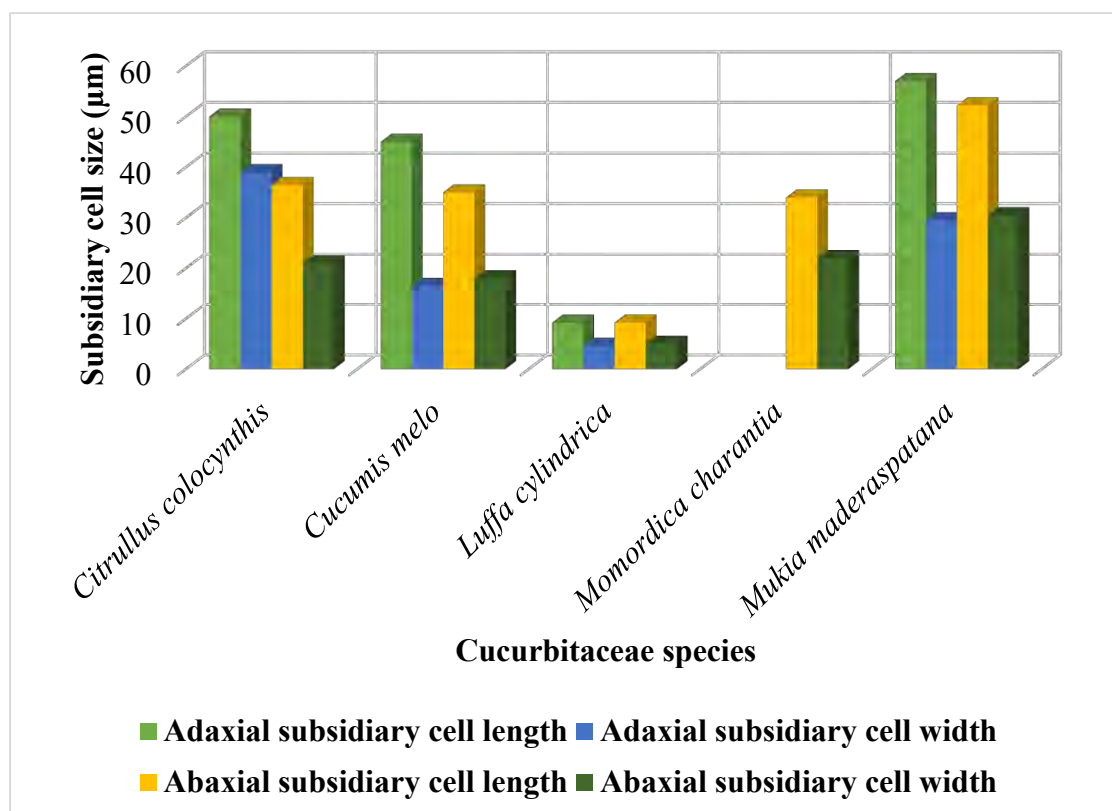


**Figure 53.** Subsidiary cell size variations among Cucurbitaceous species

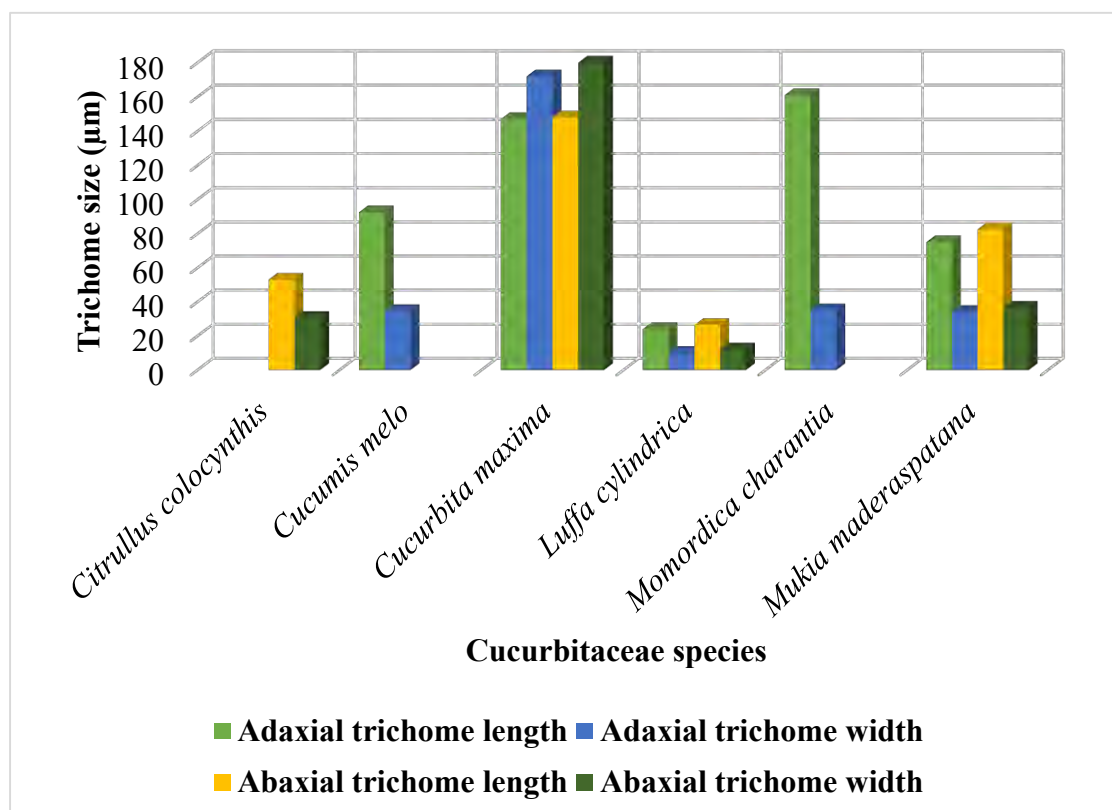


**Figure 54.** Mean trichome size variations among Cucurbitaceous species

### 3.4.9 Discussion

The previous study showed that the anatomical characteristics of fruit stalks and tendrils can be used to distinguish among species within Cucurbitaceae (Ekeke et al. 2015). Variations of stomatal types among some Cucurbitaceae members are paracytic, diacytic, anisocytic, actinocytic, cyclocytic, and staurocytic (Abdulrahman et al., 2011). The stomata type and variation in a stomatal index can be used to distinguish among species within Cucurbitaceae (Jibril and Bello 2016). Presence of trichomes and cuticular wax under different environmental condition has beneficial role particularly for imparting increased resistance against water loss and reflecting light, for the removal of pathogens and pollutants and creation of hydrophobic leaf surfaces (Singh et al., 2020). These studies shows that there is a remarkable variation in the taxonomy and systematics of family Cucurbitaceae and many astonishing things are observed. This study not only delimitate the taxa but also helpful in distinguishing upper and lower surface of leaves in family. There is variation in trichomes morphology in the family Cucurbitaceae, they fluctuate in form from single cell to many cell, they may be conical or may be elongated, or it may be thin or thick, it may be blunt at apex or may be curved. Trichome characters in the family Cucurbitaceae estimated that in the present days these characters are credible to verify the medicinal value of Cucurbitaceae and its contaminant (Ali and Al-Hemaid 2011). The current study evidently imitates that the variety of trichomes in Cucurbitaceae is very helpful in resolving the many problems related to taxonomy of barely encircled taxa, moreover this can be used in infrageneric classification. Hasson et al., (2019) found glandular trichomes with various tiers in *Momordica* species. The glandular trichomes have been implicated for storage (Akram et al., 2020). Green and Horsefall (2008) pointed that the non-glandular trichomes were useful as defense organs for the plants that possess them.

Center (2013) visualized scanning micrograph of the upper surface in *Cucurbita maxima* leaf blade shows paracytic stomata with raised level and reticulate foveate sculpture pattern, whereas the lower surface shows paracytic and anomocytic stomata with raised level and reticulate sculpture pattern. Trichomes of non-glandular and glebulate ornamentation are present on both surface. Whereas our findings revealed multicellular trichomes on abaxial surface and stomata was absent along adaxial side.

According to Kadiri et al., (2013) in the abaxial surface of *Momordica charantia* do not have trichomes in it, which is in accordance with the present studies. In *Luffa cylindrica* long conical trichomes were present in adaxial and abaxial surfaces (Kadiri et al., 2013). But in current findings short conical trichomes are present in adaxial surfaces and multicellular trichomes present in abaxial surface. In *Citrullus colocynthis* trichomes were absent in the earlier study by Abdulrahman et al., (2011) while our work describe unicellular glandular trichomes along abaxial surface of *Citrullus colocynthis*. In *Cucumis melo* short thick walled conical trichomes were present (Ali and Al-Hemaid 2011), and these findings demonstrates that short capitate trichome is present in *Cucumis melo*. Trichomes diversity help to distinguish between different species' in the family. By having this data on trichomes morphology one can easily distinguish between different species.

*Mukia maderaspatana* has wavy with wide U-shaped curve epidermal cell wall pattern on the abaxial side, whereas, *Cucumis* L. has wavy with very deep curve epidermal cell wall pattern on the abaxial side (Pratami et al., 2019). While this study explained irregular shape epidermal cells and paracytic type stomata in *Mukia maderaspatana*. The non-glandular trichomes are uniseriate and multicellular and the glandular trichomes has uniseriate pedicel and multicellular head in *Mamordica charantia*. In frontal view via optical microscopy, the leaf blade of is hypostomatic, with anomocytic stomata on the abaxial surface. The epidermal cells have strongly sinuous walls on both sides (Sa et al., 2018). Whereas our examination found for *Mamordica charantia* diacytic stomata and multicellular colonial trichomes.

The observed anatomical similarities among the Cucurbitaceous species studied indicate phylogenetic relatedness of the taxa. These anatomical differences observed in each species must have been as a result of evolution, conferring heritable variation that could be exploited for taxonomic purposes.

### 3.4.10 Foliar Epidermal Micromorphology of Capparaceae Species

Following anatomical features were studied viz. shape of epidermal cells, type of trichomes/glands, shape and type of stomata, stomatal index, no. of epidermal cells, stomata and trichomes, their length and width both on adaxial and abaxial surface (Table 32, 33 & 34). All examined species of Capparaceae are amphistomatic (stomata both on the adaxial and abaxial surface) as shown in Plate 85 and 86.

The maximum number of epidermal cells on the adaxial surface was observed in *Cleome viscosa* (81) and on the abaxial surface in *Capparis decidua* (80). Minimum epidermal cells number on the adaxial surface were observed in *Capparis decidua* (43) and on the abaxial surface in *Dipterygium glaucum* (64). Maximum no. of stomata on the adaxial surface was observed in *Capparis decidua* (23) and on the abaxial surface in *Capparis spinosa* (46), while minimum on the adaxial side (15) and abaxial surface (16) was calculated in *Cleome viscosa* (Table 33). While the quantitative statistical graphics for foliar anatomical parameters of epidermal cells, stomata, subsidiary cells, guard cells and stomatal pore were illustrated in for adaxial surface in Figure 55, 56, 57, 58 and 59 and for abaxial surface in Figure 60, 61, 62, 63 & 64.

#### a) *Capparis decidua* (Forssk.). Edgew.

Leaves are amphistomatic.

##### Adaxial surface

Shape of epidermal cells is irregular, anticlinal wall is smooth, thin-walled. Epidermal cells length is ( $42 \pm 4.70 \mu\text{m}$ ) and width is ( $45.5 \pm 6.72 \mu\text{m}$ ). Stomata type is Paracytic. Stomata length is ( $16.6 \pm 0.95 \mu\text{m}$ ) and width is ( $7.50 \pm 0.79 \mu\text{m}$ ). Length of subsidiary cells is ( $23.6 \pm 1.72 \mu\text{m}$ ) and width is ( $4.90 \pm 0.06 \mu\text{m}$ ). Length of guard cells is ( $16.6 \pm 2.13 \mu\text{m}$ ) and width is ( $3.35 \pm 1.44 \mu\text{m}$ ). Length of stomatal pore is ( $11.5 \pm 0.99 \mu\text{m}$ ) and width is ( $2.65 \pm 0.39 \mu\text{m}$ ). Stomatal index is 34.5%. Trichomes are unicellular with gradually tapering at both ends. Trichomes length is ( $306 \pm 47.9 \mu\text{m}$ ) and width is ( $19 \pm 2.03 \mu\text{m}$ ) (Plate 85a, Table 32 & 34).

##### Abaxial surface

Shape of epidermal cells is irregular, anticlinal wall is smooth, thin walled.

Epidermal cells length is ( $38.5 \pm 1.87 \mu\text{m}$ ) and width is ( $33 \pm 4.35 \mu\text{m}$ ). Stomata type is Paracytic. Stomata length is ( $12.6 \pm 0.79 \mu\text{m}$ ) and width is ( $8.40 \pm 0.43 \mu\text{m}$ ). Length of subsidiary cells is ( $19 \pm 1.00 \mu\text{m}$ ) and width is ( $4.15 \pm 0.43 \mu\text{m}$ ). Length of guard cells is ( $12.6 \pm 1.78 \mu\text{m}$ ) and width is ( $2.75 \pm 0.46 \mu\text{m}$ ). Length of stomatal pore is ( $9.5 \pm 0.93 \mu\text{m}$ ) and width is ( $1.60 \pm 0.39 \mu\text{m}$ ). Stomatal index is 32.2%. Trichomes are unicellular with gradually tapering at both ends. Trichomes length is ( $300 \pm 47.7 \mu\text{m}$ ) and width is ( $19 \pm 2.31 \mu\text{m}$ ) (Plate 85b, Table 32 & 34).

#### **b) *Capparis spinosa* L.**

Leaves are amphistomatic.

##### **Adaxial surface**

Shape of epidermal cells is Square, triangular, hexagonal, rarely irregular and anticlinal wall is smooth, thin-walled. Epidermal cells length is ( $39 \pm 5.09 \mu\text{m}$ ) and width is ( $23 \pm 3.74 \mu\text{m}$ ). Stomata type is paracytic. Stomata length is ( $15.3 \pm 0.98 \mu\text{m}$ ) and width is ( $8 \pm 0.93 \mu\text{m}$ ). Length of subsidiary cells is ( $24.0 \pm 0.61 \mu\text{m}$ ) and width is ( $8.30 \pm 1.23 \mu\text{m}$ ). Length of guard cells is ( $13.8 \pm 1.22 \mu\text{m}$ ) and width is ( $3.05 \pm 0.48 \mu\text{m}$ ). Length of stomatal pore is ( $3.45 \pm 0.63 \mu\text{m}$ ) and width is ( $2.31 \pm 0.33 \mu\text{m}$ ). Stomatal index is 27.4%. Trichomes are multicellular, hydathode and stellate. Trichomes is ( $87.5 \pm 2.50 \mu\text{m}$ ) and width is ( $7.35 \pm 0.43 \mu\text{m}$ ) (Plate 85c, Table 32 & 34).

##### **Abaxial surface**

Shape of epidermal cells is Irregular to triangular or square, anticlinal wall is thick-walled, undulate to slightly smooth. Epidermal cells length is ( $43 \pm 4.35 \mu\text{m}$ ) and width is ( $24 \pm 2.57 \mu\text{m}$ ). Stomata type is paracytic. Stomata length is ( $10.6 \pm 0.92 \mu\text{m}$ ) and width is ( $5 \pm 0.79 \mu\text{m}$ ). Length of subsidiary cells is ( $23 \pm 1.83 \mu\text{m}$ ) and width is ( $9.15 \pm 1.43 \mu\text{m}$ ). Length of guard cells is ( $9.5 \pm 0.50 \mu\text{m}$ ) and width is ( $2.5 \pm 0.13 \mu\text{m}$ ). Length of stomatal pore is ( $4.8 \pm 0.12 \mu\text{m}$ ) and width is ( $1.8 \pm 0.12 \mu\text{m}$ ). Stomatal index is 40.4%. Trichomes are multicellular, hydathode and stellate. Trichome length is ( $85 \pm 2.85 \mu\text{m}$ ) and width is ( $7.25 \pm 0.27 \mu\text{m}$ ) (Plate 85d, Table 32 & 34).

#### **c) *Cleome brachycarpa***

Leaves are amphistomatic.



**Adaxial surface**

Shape of epidermal cells is Polygonal and anticlinal wall is smooth, thin-walled. Epidermal cells length is  $(48 \pm 5.88 \mu\text{m})$  and width is  $(49.5 \pm 4.56 \mu\text{m})$ . Stomata type is Paracytic. Stomata length is  $(17.3 \pm 0.81 \mu\text{m})$  and width is  $(12 \pm 1.58 \mu\text{m})$ . Length of subsidiary cells is  $(28.2 \pm 2.44 \mu\text{m})$  and width is  $(6.6 \pm 0.79 \mu\text{m})$ . Length of guard cells is  $(15.8 \pm 0.64 \mu\text{m})$  and width is  $(4.65 \pm 0.63 \mu\text{m})$ . Length of stomatal pore is  $(12 \pm 0.73 \mu\text{m})$  and width is  $(2.5 \pm 0.22 \mu\text{m})$ . Stomatal index is 27.4%. Trichomes are Multicellular with broad base. Length of trichomes is  $(189 \pm 46.1 \mu\text{m})$  and width is  $(27.5 \pm 4.74 \mu\text{m})$  (Plate 85e, Table 32 & 34).

**Abaxial surface**

Shape of epidermal cells is Polygonal, anticlinal wall is smooth, Slightly thick-walled. Epidermal cells length is  $(41.5 \pm 4.58 \mu\text{m})$  and width is  $(35 \pm 4.33 \mu\text{m})$ . Stomata type is Paracytic. Stomata length is  $(17.8 \pm 1.05 \mu\text{m})$  and width is  $(11.9 \pm 1.82 \mu\text{m})$ . Length of subsidiary cells is  $(27.1 \pm 1.66 \mu\text{m})$  and width is  $(7.75 \pm 0.65 \mu\text{m})$ . Length of guard cells is  $(17.3 \pm 0.94 \mu\text{m})$  and width is  $(4.85 \pm 0.16 \mu\text{m})$ . Length of stomatal pore is  $(13.4 \pm 0.42 \mu\text{m})$  and width is  $(2.20 \pm 0.09 \mu\text{m})$ . Stomatal index is 33.5%. Trichomes are Multicellular with broad base. Trichomes length is  $(216 \pm 43.9 \mu\text{m})$  and width is  $(27.5 \pm 4.54 \mu\text{m})$  (Plate 85f, Table 32 & 34).

**d) *Cleome viscosa* L.**

Leaves are amphistomatic.

**Adaxial surface**

Shape of epidermal cells is irregular and anticlinal wall is smooth, thin-walled. Epidermal cells length is  $(30.5 \pm 1.22 \mu\text{m})$  and width is  $(22.5 \pm 2.50 \mu\text{m})$ . Stomata type is anomocytic. Stomata length is  $(18.5 \pm 0.61 \mu\text{m})$  and width is  $(14.9 \pm 0.71 \mu\text{m})$ . Length of subsidiary cells is  $(41 \pm 6.10 \mu\text{m})$  and width is  $(19.5 \pm 0.93 \mu\text{m})$ . Length of guard cells is  $(14.1 \pm 0.57 \mu\text{m})$  and width is  $(5.6 \pm 0.65 \mu\text{m})$ . Length of stomatal pore is  $(12 \pm 0.61 \mu\text{m})$  and width is  $(2.35 \pm 0.12 \mu\text{m})$ . Stomatal index is 15.2%. Trichomes are Multicellular. Length of trichomes is  $(151 \pm 24.4 \mu\text{m})$  and width is  $(24.5 \pm 2 \mu\text{m})$  (Plate 86a, Table 32 & 34).

**Abaxial surface**

Shape of epidermal cells is irregular, anticlinal wall is smooth, thin-walled. Epidermal cells length is  $(31.5 \pm 2.03 \mu\text{m})$  and width is  $(15.6 \pm 1.4 \mu\text{m})$ . Stomata type is anomocytic. Stomata length is  $(18.5 \pm 1.27 \mu\text{m})$  and width is  $(17.1 \pm 0.95 \mu\text{m})$ . Length of subsidiary cells is  $(31 \pm 1.27 \mu\text{m})$  and width is  $(15 \pm 2.23 \mu\text{m})$ . Length of guard cells is  $(14.6 \pm 1.24 \mu\text{m})$  and width is  $(6.55 \pm 0.43 \mu\text{m})$ . Length of stomatal pore is  $(11.6 \pm 0.96 \mu\text{m})$  and width is  $(2.55 \pm 0.16 \mu\text{m})$ . Stomatal index is 17.9%. Trichomes are Multicellular. Trichomes length is  $(168 \pm 25.1 \mu\text{m})$  and width is  $(32.0 \pm 4.13 \mu\text{m})$  (Plate 86b, Table 32 & 34).

**e) *Dipterygium glaucum* Decne.**

Leaves are amphistomatic.

**Adaxial surface**

Shape of epidermal cells is Polygonal to elongated, rectangular and anticlinal wall is smooth, thick-walled. Epidermal cells length is  $(54 \pm 4.97 \mu\text{m})$  and width is  $(40.8 \pm 2.18 \mu\text{m})$ . Stomata type is Paracytic. Stomata length is  $(14.8 \pm 0.81 \mu\text{m})$  and width is  $(10 \pm 0.79 \mu\text{m})$ . Length of subsidiary cells is  $(26.5 \pm 2.31 \mu\text{m})$  and width is  $(9.05 \pm 1.23 \mu\text{m})$ . Length of guard cells is  $(14.8 \pm 0.81 \mu\text{m})$  and width is  $(4.05 \pm 0.58 \mu\text{m})$ . Length of stomatal pore is  $(11.7 \pm 1.17 \mu\text{m})$  and width is  $(1.45 \pm 0.42 \mu\text{m})$ . Stomatal index is 25.1% (Plate 86c, Table 32 & 34).

**Abaxial surface**

Shape of epidermal cells is polygonal, anticlinal wall is smooth, thick-walled. Epidermal cells length is  $(44.5 \pm 5.66 \mu\text{m})$  and width is  $(32.4 \pm 2.85 \mu\text{m})$ . Stomata type is Paracytic. Stomata length is  $(14.6 \pm 1.23 \mu\text{m})$  and width is  $(8 \pm 0.94 \mu\text{m})$ . Length of subsidiary cells is  $(25 \pm 1.36 \mu\text{m})$  and width is  $(7.95 \pm 0.52 \mu\text{m})$ . Length of guard cells is  $(14.6 \pm 1.23 \mu\text{m})$  and width is  $(4.1 \pm 0.60 \mu\text{m})$ . Length of stomatal pore is  $(10.2 \pm 1.32 \mu\text{m})$  and width is  $(1.6 \pm 0.23 \mu\text{m})$ . Stomatal index is 35.8% (Plate 86d, Table 32 & 34).

### 3.4.11 Identification Keys Based on Foliar Anatomy of Capparaceae taxa

1. + Trichomes present on both surface.....2
- Trichomes absent on both surfaces.....3
2. + Unicellular trichomes present on both surfaces.....*Capparis decidua*
- Multicellular trichomes present on both surfaces.....4
3. + Stomata present on both surfaces; anticlinal cell wall pattern smooth on abaxial surface.....*Dipterygium glaucum*
- 4 + Hydathode and stellate trichomes present; hexagonal epidermal cells present on adaxial surface.....*Capparis spinosa*
- Hydathode and stellate trichomes present; hexagonal epidermal cells absent on adaxial surface.....5
5. + Epidermal cells irregular on both surfaces; anticlinal cell wall thin on adaxial surface.....*Cleome brachycarpa*
- Epidermal cells polygonal on both surfaces; anticlinal cell wall thick on adaxial surface.....6
6. + Anticlinal cell wall thick on abaxial surface, stomatal index on abaxial surface 17.9%.....*Cleome viscosa*

**Table 32.** Qualitative foliar anatomical features of Capparaceae species.

S. No.	Capparaceae species	Ad/Ab	Shape of epidermal cells	Anticlinal Cell wall Pattern	Shape of Stomata	Stomata	Guard cells	Trichome
1.	<i>Capparis decidua</i> (Forssk.) Edgew.	Ad	Irregular	Thin-walled, smooth	Oval to Slightly circular	Paracytic	Bean-shaped	Unicellular with gradually tapering at both ends
		Ab	Irregular	Thin-walled, smooth	Oval	Paracytic	Bean-Shaped	Unicellular with gradually tapering at both ends
2.	<i>Capparis spinosa</i> L.	Ad	Square, triangular	Thin-walled, smooth	Oval	Paracytic	Bean-shaped	Multicellular, hydathode, stellate
		Ab	Irregular to triangular or square	Thick-walled, undulate to slightly smooth	Oval	Paracytic	Bean-shaped	Multicellular, hydathode, stellate
3.	<i>Cleome brachycarpa</i> (Forssk.) Vahl ex DC.	Ad	Polygonal	Thick-walled, smooth	Oval to Slightly circular	Paracytic	Bean-shaped	Multicellular with broad base
		Ab	Polygonal	Slightly Thick-walled, smooth	Oval to Slightly circular	Paracytic	Bean-shaped	Multicellular with broad base
4.	<i>Cleome viscosa</i> L.	Ad	Irregular	Thin-walled, smooth	Circular to slightly oval	Paracytic	Bean-shaped	Multicellular, glandular
		Ab	Irregular	Slightly thick-walled, smooth	Oval	Paracytic	Bean-shaped	Multicellular, glandular hairs
5.	<i>Dipterygium glaucum</i> Decne.	Ad	Polygonal to elongated	Thick-walled, smooth	Circular to slightly oval	Paracytic	Bean-shaped	Absent
		Ab	Polygonal	Thick-walled, smooth	Circular to oval	Paracytic	Bean-shaped	Absent

**Table 33.** Quantitative measurement of epidermal cells and stomata for Stomatal Index determination.

S. No.	Capparaceae species	Ad/Ab	Stomata P/A	Number of Epidermal cell (mm <sup>2</sup> )	Number of Stomata (mm <sup>2</sup> )	Stomatal Index (%)
1.	<i>Capparis decidua</i> (Forssk.) Edgew.	Ad	P	43	23	34.5
		Ab	P	80	38	32.2
2.	<i>Capparis spinosa</i> L.	Ad	P	59	22	27.4
		Ab	P	68	46	40.4
3.	<i>Cleome brachycarpa</i> (Forssk.) Vahl ex DC.	Ad	P	60	22	27.4
		Ab	P	67	34	33.5
4.	<i>Cleome viscosa</i> L.	Ad	P	81	15	15.2
		Ab	P	72	16	17.9
6.	<i>Dipterygium glaucum</i> Decne.	Ad	P	51	17	25.1
		Ab	P	63	36	35.8

**Table 34.** Quantitative characters of foliar epidermal anatomy of Capparaceae species.

Sr. No.	Capparaceae species	Ad/Ab	Epidermal cells (x± S.E)		Stomata (x± S.E)		Subsidiary cells (x± S.E)		Guard cells (x± S.E)		Stomatal pore (x± S.E)		Trichome (x± S.E)	
			L	W	L	W	L	W	L	W	L	W	L	W
1.	<i>Capparis decidua</i> (Forssk.) Edgew.	Ad	42.0±4.7	45.5±6.72	16.6±0.95	7.50±0.79	23.6±1.72	4.9±0.06	16.6±2.13	3.35±1.44	11.5±0.99	2.65±0.39	306±47.9	19±2.03
		Ab	38.5±1.87	33±4.35	12.6±0.79	8.4±0.43	19±1.00	4.15±0.43	12.6±1.78	2.75±0.46	9.50±0.93	1.6±0.39	300±47.7	19±2.31
2.	<i>Capparis spinosa</i> L.	Ad	39±5.09	23±3.74	15.3±0.98	8±0.93	24±0.61	8.3±1.23	13.8±1.22	3.05±0.48	3.45±0.63	3.45±0.63	87.5±2.50	7.35±0.43
		Ab	43.0±4.35	24±2.57	10.6±0.92	5±0.79	23±1.83	9.15±1.43	9.5±0.50	2.50±0.13	4.80±0.12	4.8±0.12	85.0±2.85	7.25±0.27
3.	<i>Cleome brachycarpa</i> (Forssk.) Vahl ex DC.	Ad	30.5±1.22	22.5±2.50	18.5±0.61	14.9±0.71	41±6.10	19.5±0.93	14.1±0.57	5.60±0.65	12.3±0.61	2.35±0.12	151±24.4	24.5±2
		Ab	31.5±2.03	15.6±1.40	18.5±1.27	17.1±0.95	31±1.27	15±2.23	14.6±1.24	6.55±0.43	11.6±0.96	2.55±0.16	168±25.1	32.0±4.13
4.	<i>Cleome viscosa</i> L.	Ad	30.5±1.22	22.5 ±2.50	18.5 ±0.6	14.9 ±0.71	41±6.10	19.5 ±0.93	14.1 ±0.57	5.60 ±0.65	12.3 ±0.61	2.35±0.12	151±24.4	24.5±2.00
		Ab	31.5±2.03	15.6 ±1.40	18.5±1.2	17.1 ±0.95	31±1.27	15.0 ±2.23	14.6 ±1.24	6.55 ±0.43	11.6 ±0.96	2.55±0.16	168 ±25.1	32±4.13
5.	<i>Dipterygium glaucum</i> Decne.	Ad	54±4.97	40.8±2.18	14.8±0.81	10±0.79	26.5±2.31	9.05±1.23	14.8±0.81	4.05±0.58	11.7±1.17	1.45±0.42	Absent	Absent
		Ab	44.5±5.66	32.4±2.85	14.6±1.23	8±0.94	25±1.36	7.95±0.52	14.6±1.23	4.10±0.60	10.2±1.32	1.6±0.23	Absent	Absent

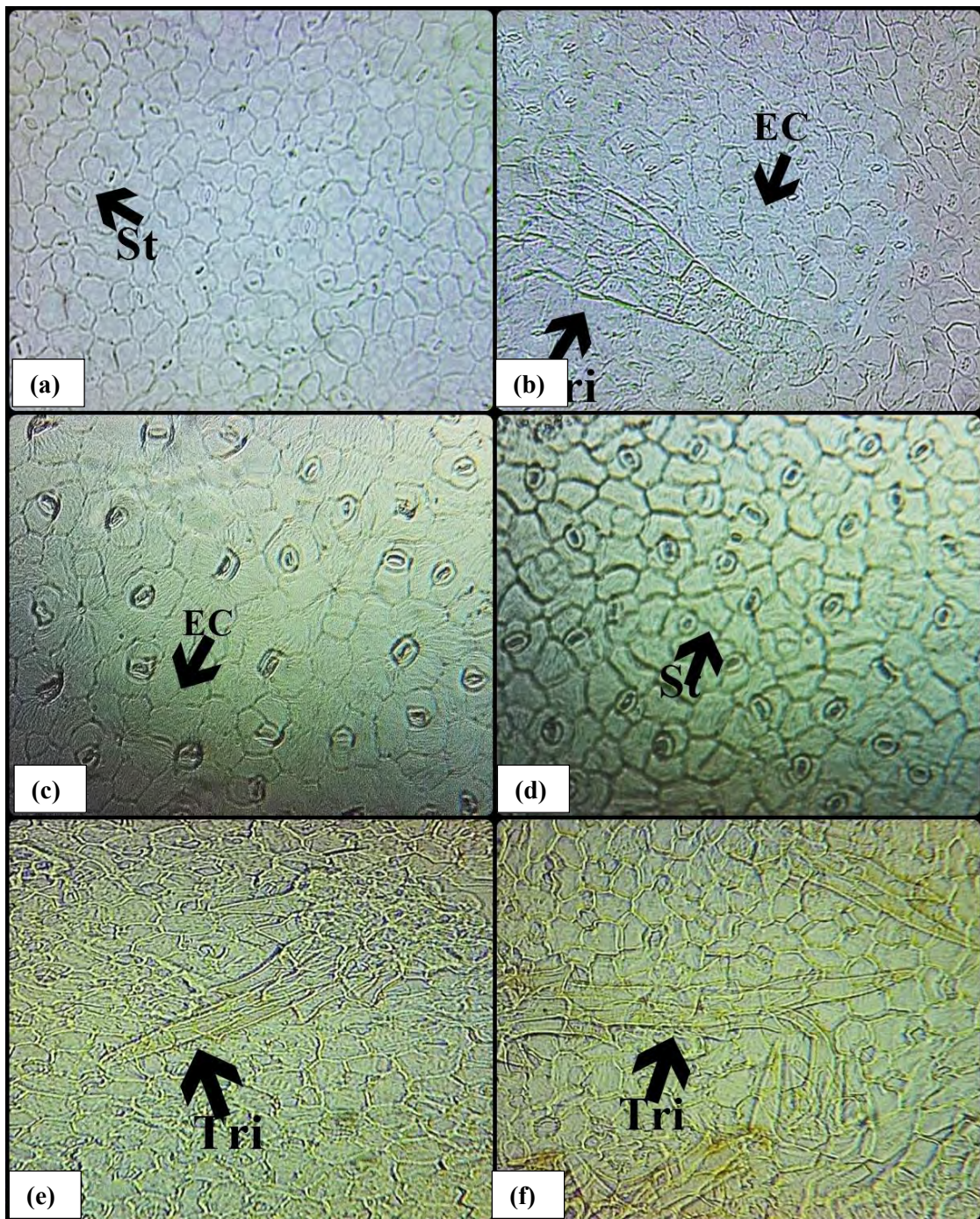


**Plate 85.** Light Micrographs (LM) illustrated stomata, epidermal cells and trichomes of Capparaceae species; *Capparis decidua* (a) Adaxial surface showing stomata (b) Abaxial surface showing epidermis cells, *Capparis spinosa* (c) Adaxial surface showing epidermal cells (d) Abaxial surface showing stomata, *Cleome brachycarpa* (h) Adaxial surface showing trichome (i) Abaxial surface showing trichome and epidermis cells.

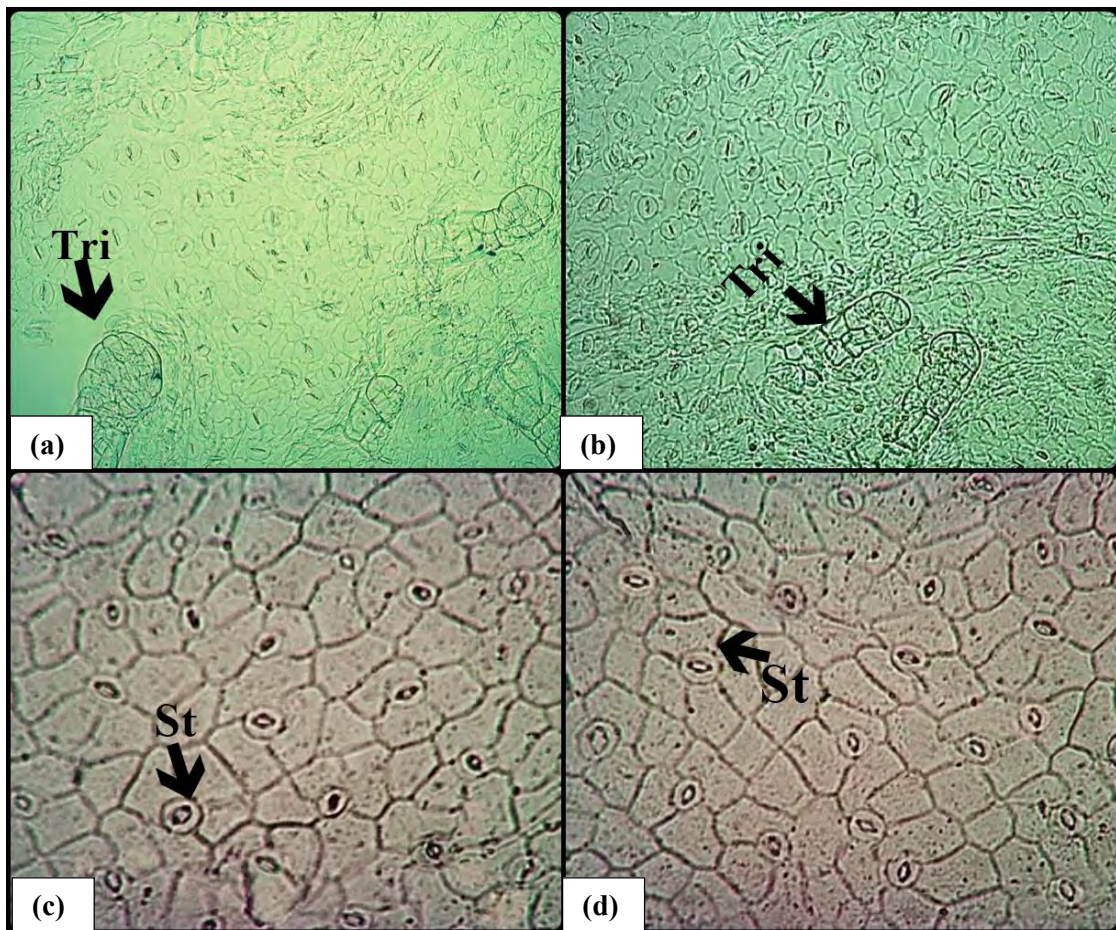


**Plate 86.** Light Micrographs (LM) illustrated stomata, epidermal cells and trichomes of Capparaceae species; *Cleome viscosa* (a) Adaxial surface showing glandular trichome (b) Abaxial surface showing stomata and trichomes, *Dipterygium glaucum* (c) Adaxial surface showing stomata (d) Abaxial surface showing straight anticlinal walls and paracytic stomata.



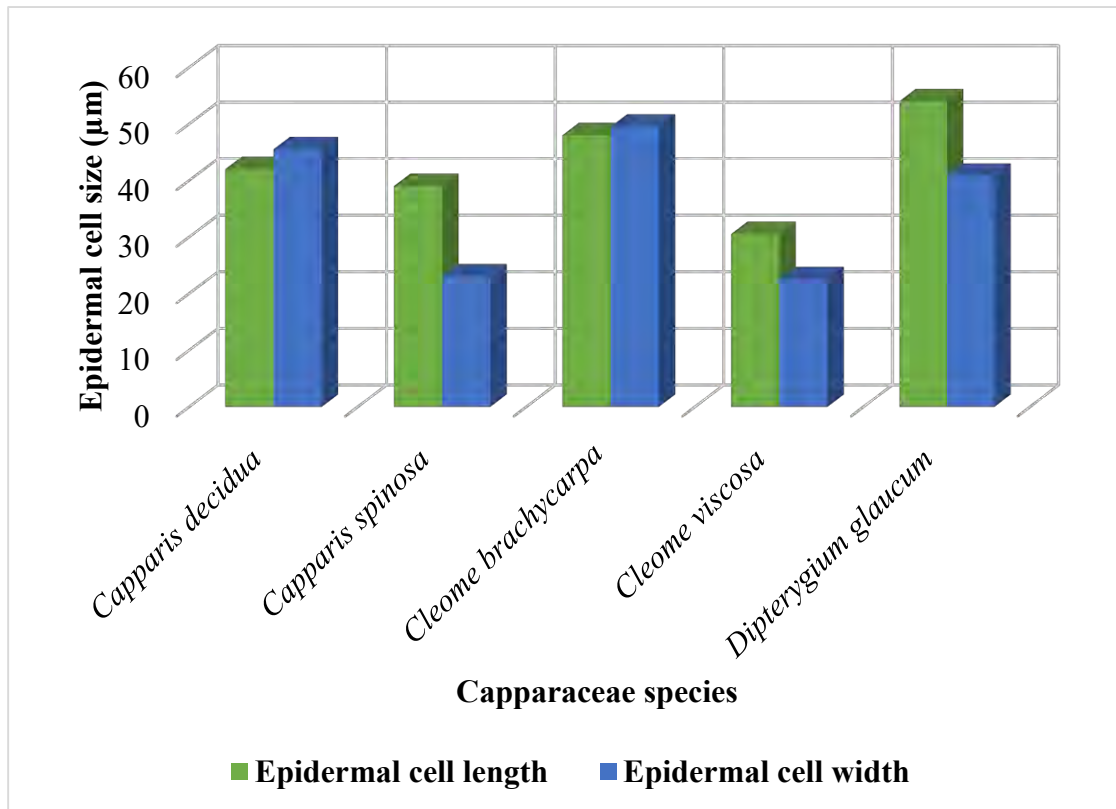


**Figure 55.** Mean epidermal cell size along adaxial surface in Capparaceae species

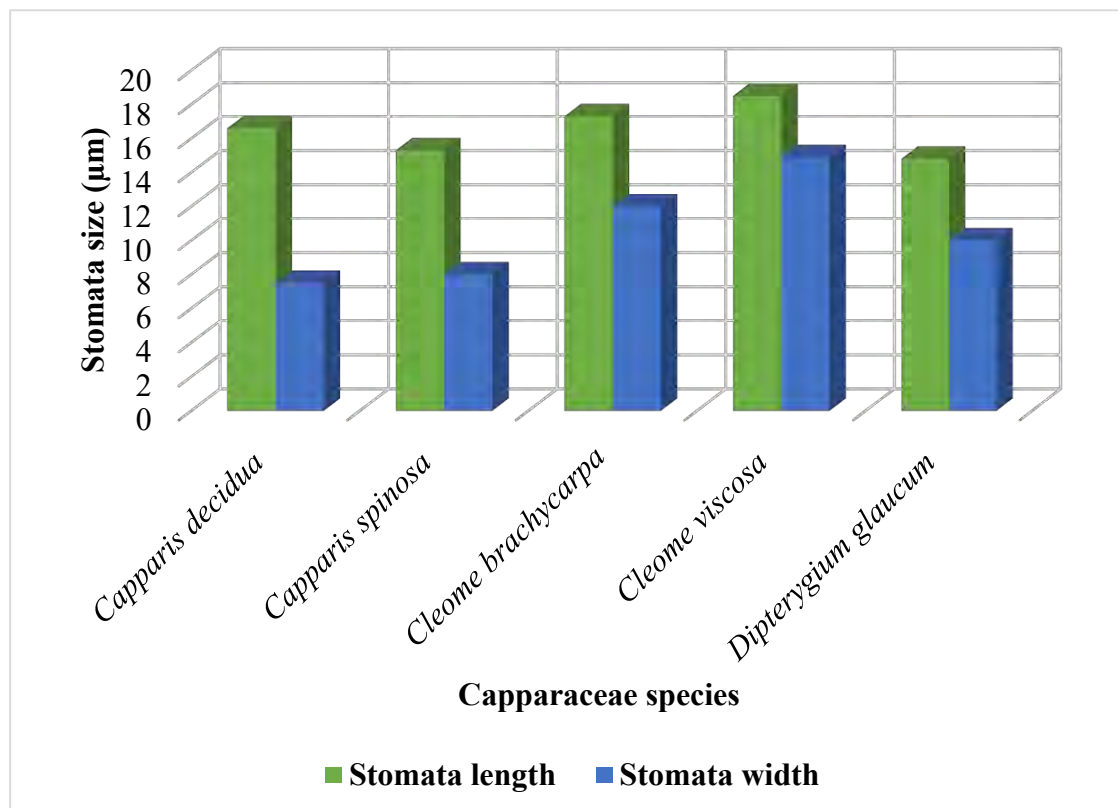


**Figure 56.** Average stomatal size along adaxial surface in Capparaceae species

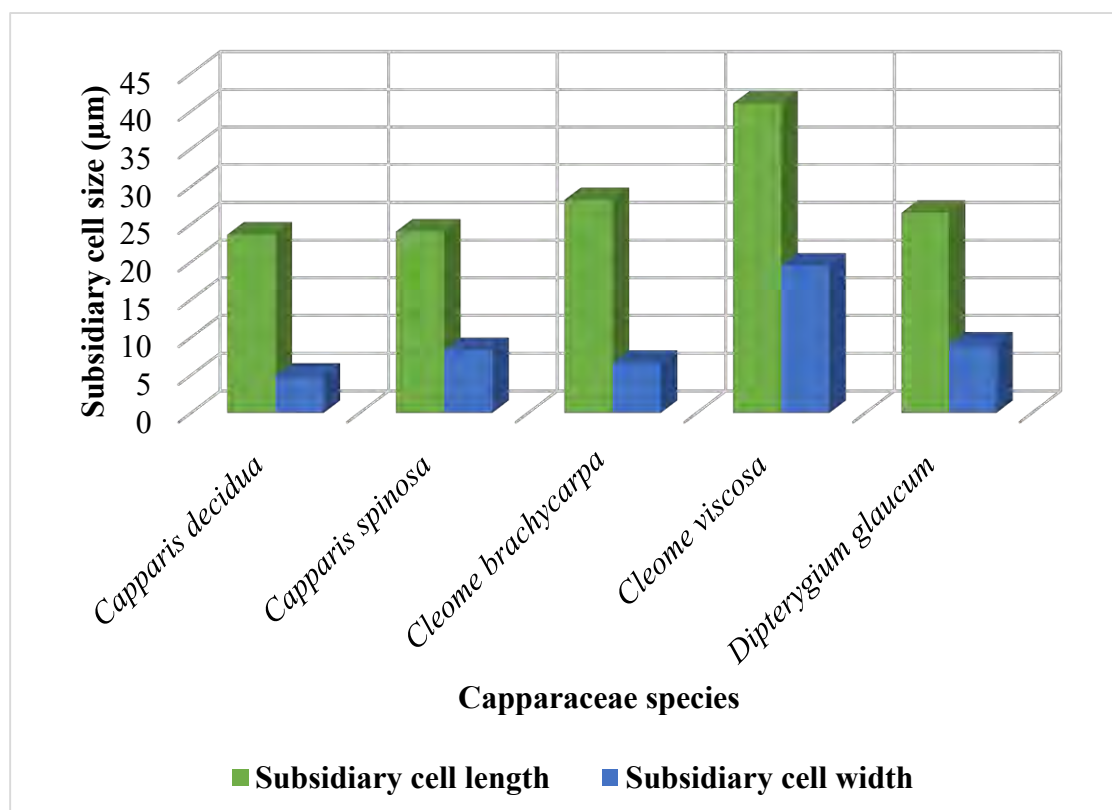


Figure 57. Average subsidiary cell size along adaxial surface in Capparaceae

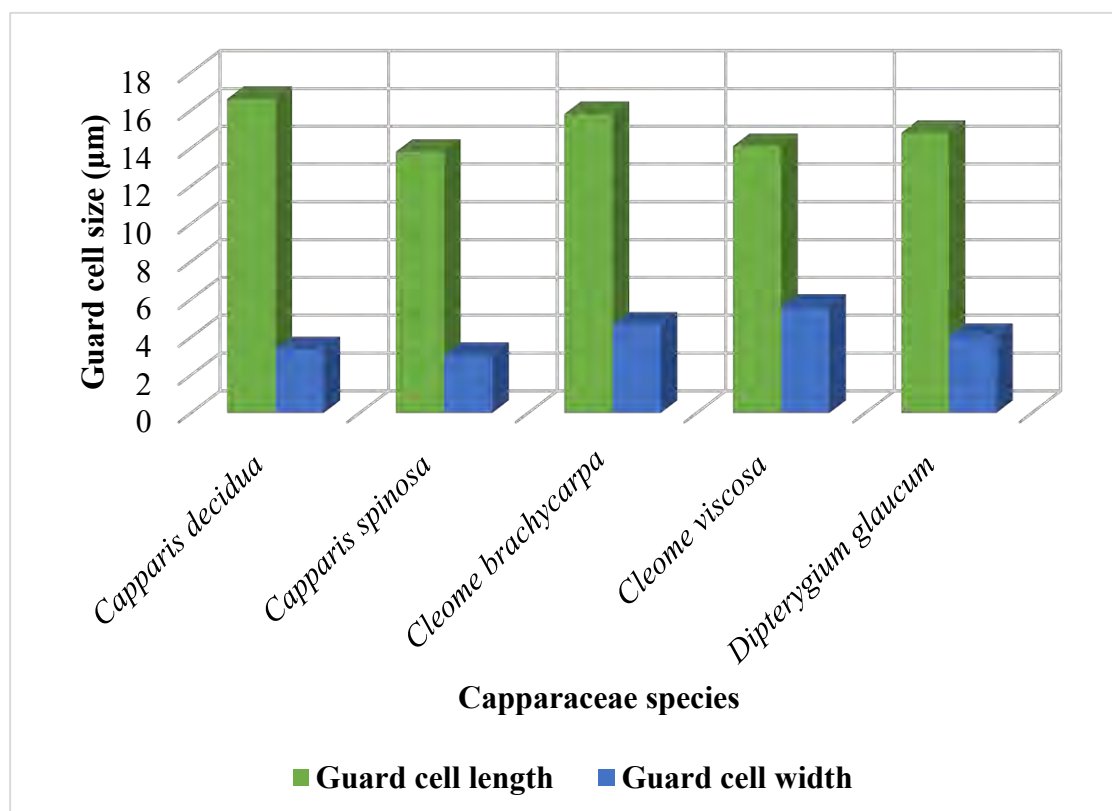
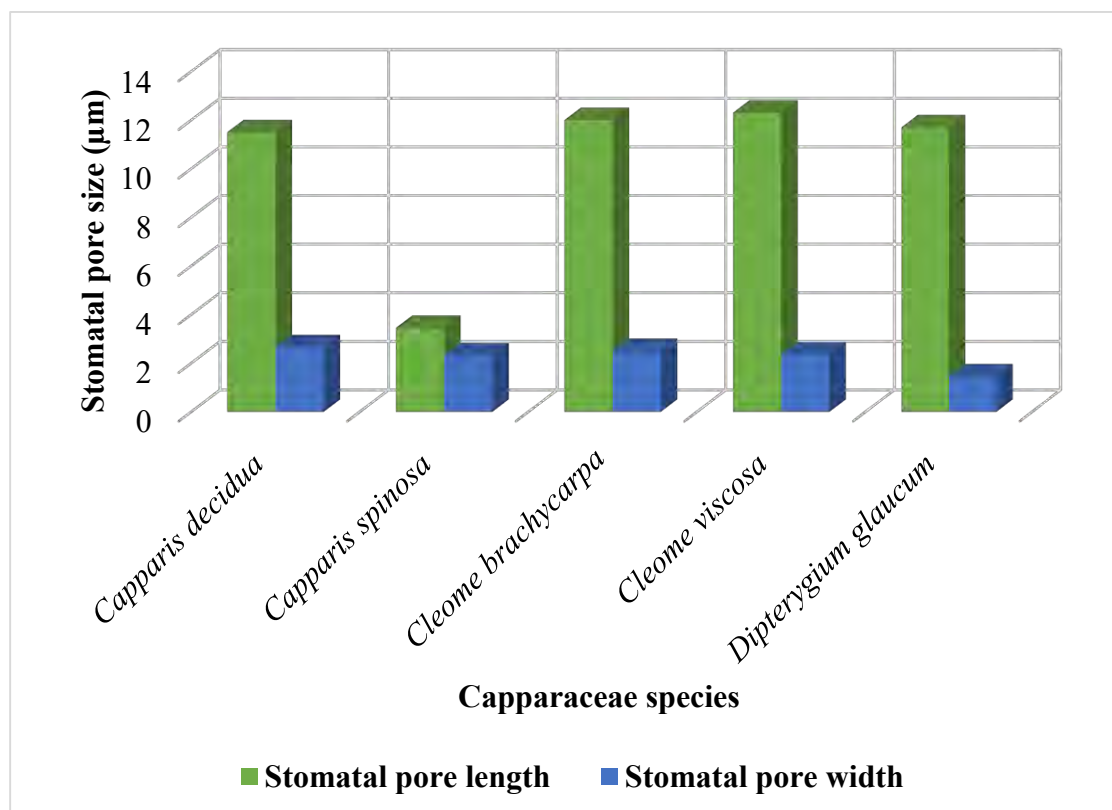
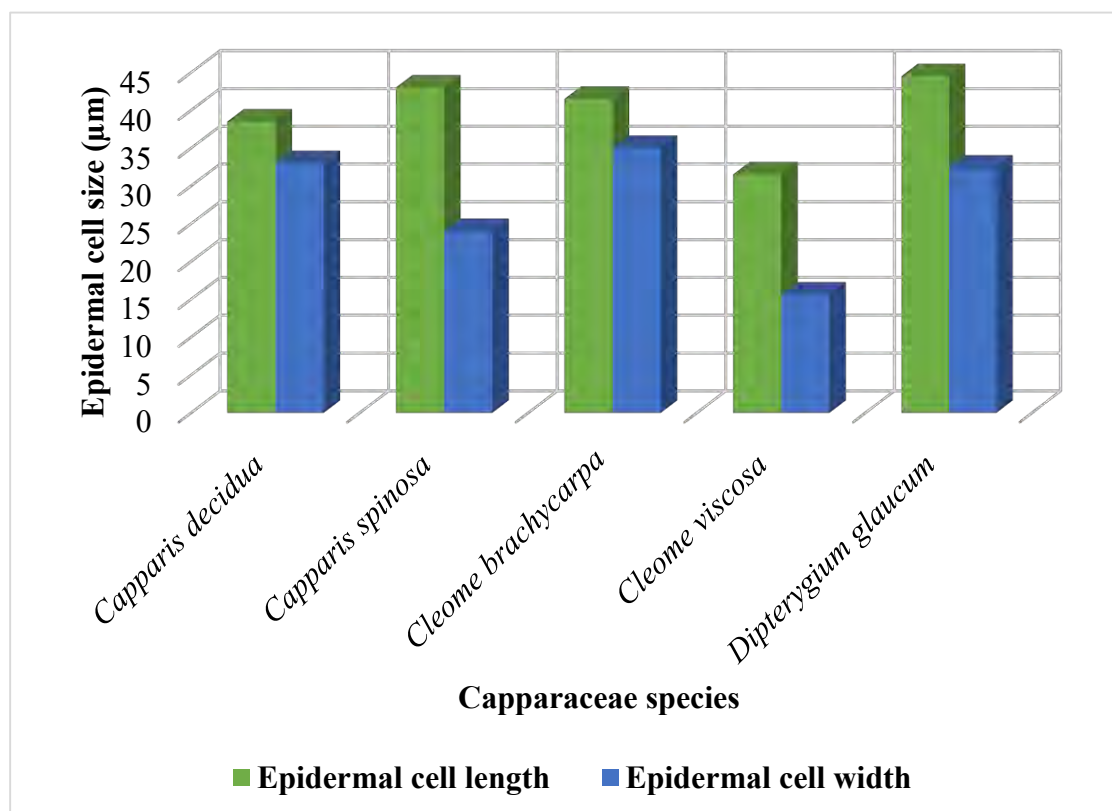


Figure 58. Average guard cells size along adaxial surface in Capparaceae species



**Figure 59.** Mean stomatal pore size along adaxial surface in Capparaceae species



**Figure 60.** Mean epidermal cell size along abaxial surface in Capparaceae species

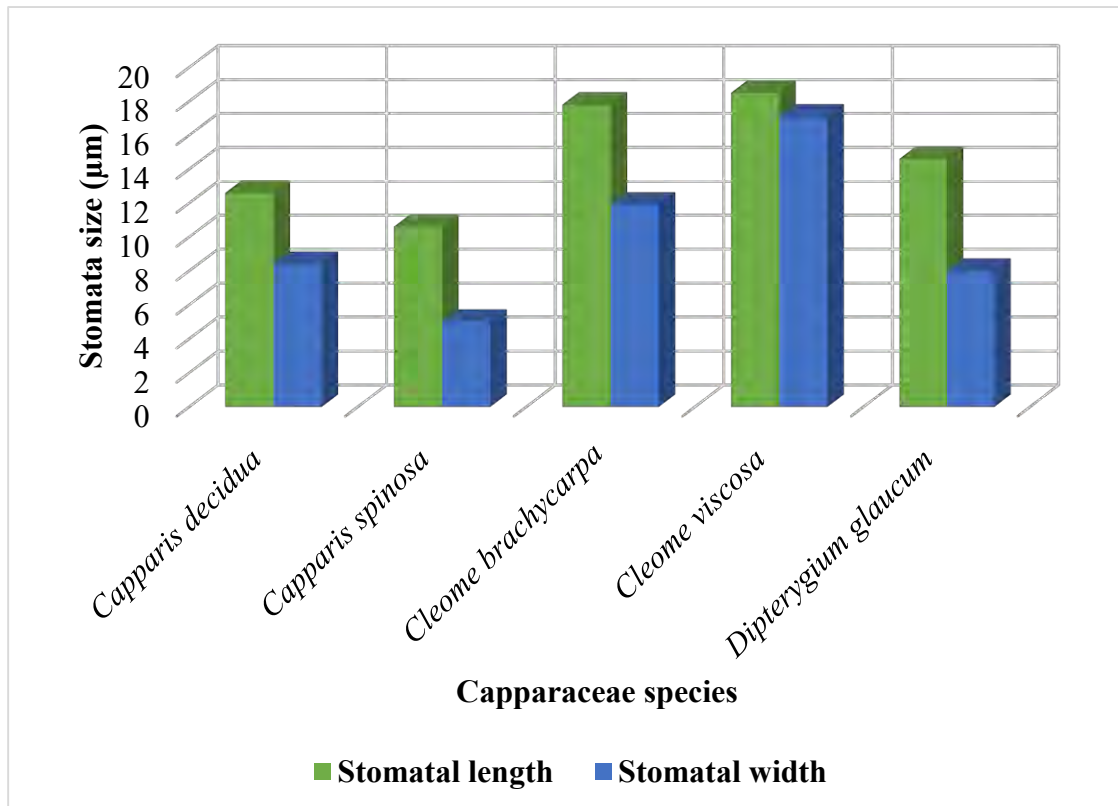


**Figure 61.** Stomata length and width along abaxial surface in Capparaceae species

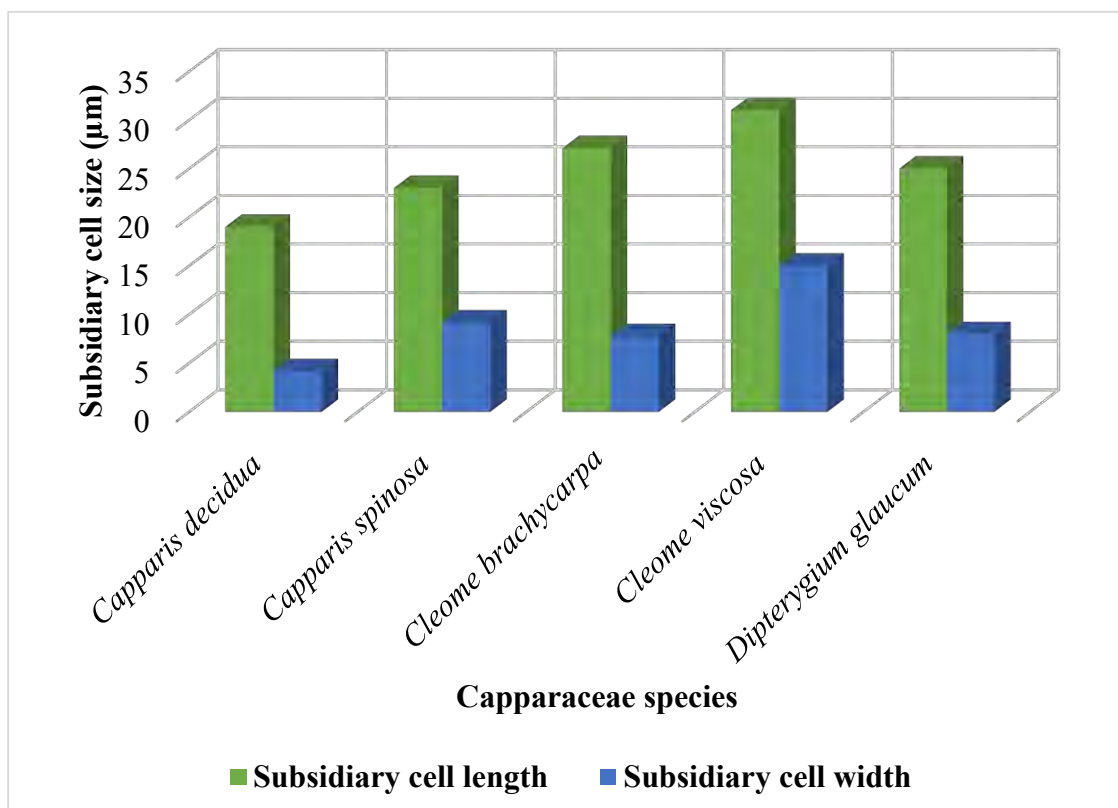


**Figure 62.** Mean subsidiary cell size along abaxial surface in Capparaceae species

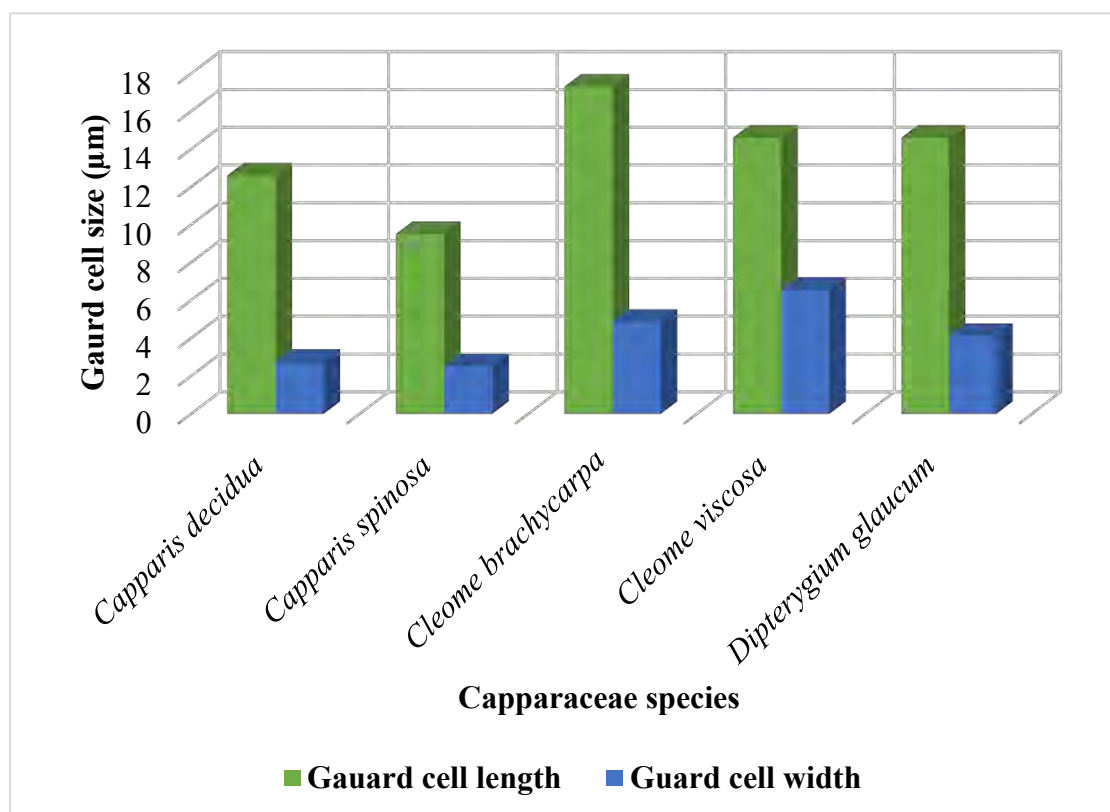


**Figure 63.** Mean guard cell size along abaxial surface in Capparaceae species

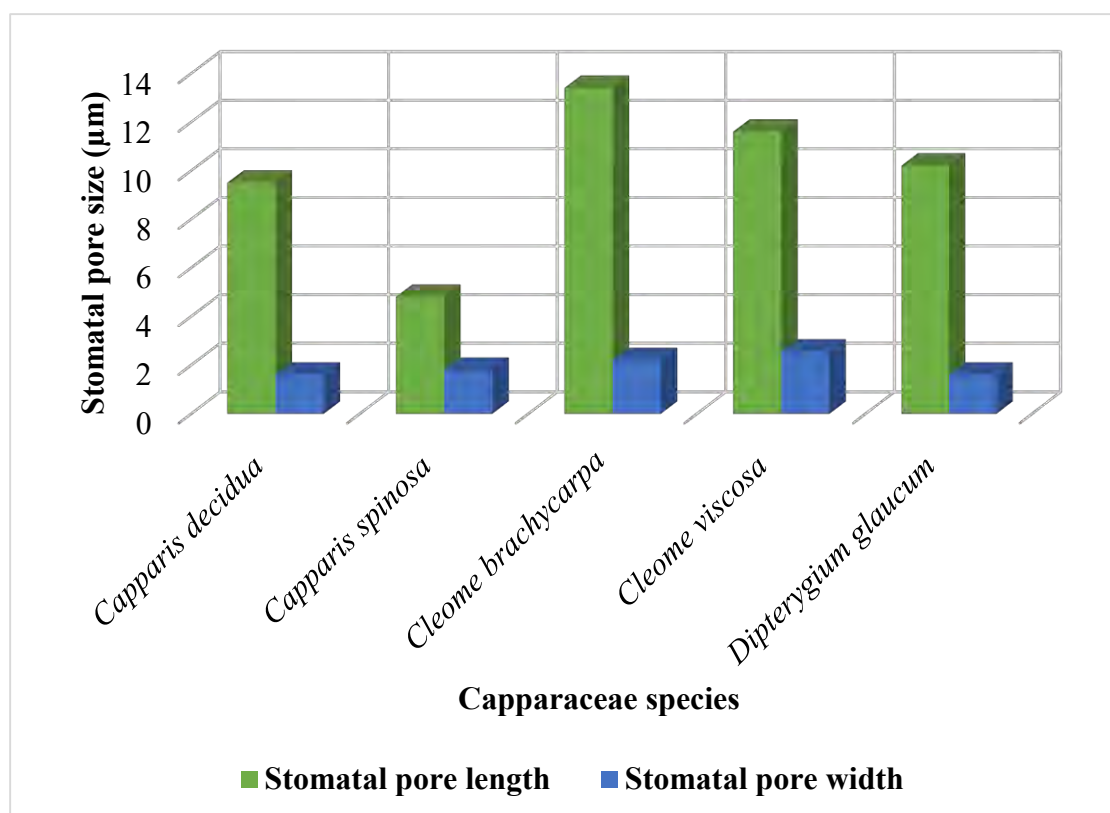


**Figure 64.** Mean stomatal pore size along abaxial surface in Capparaceae species

### 3.4.12 Discussion

Leaf anatomical records on Capparaceae species are very inadequate and available data on the micromorphological features is also very scarce. Anatomical studies comprised of size, shape and number of epidermal cells, size, shape and number of stomata, Length and width of subsidiary cells, length and width of guard cells, length and width of stomatal pore, length and width of trichomes, anticlinal cell wall pattern and type of stomata. There is no variation in type of stomata among all these 5 species. Stomata type is paracytic. Variation in trichomes has been observed. *C. decidua* has unicellular trichomes. However, *C. spinosa* has multicellular, hydathode and stellate trichomes useful at various taxonomic levels. Trichomes are absent in *Dipterygium glaucum*. There is some variation in shape of epidermal cells and anticlinal cell wall pattern. Key to species based on anatomical characters has been constructed to easily understand the diagnostic characters of the species.

Well-developed trichomes and the waxy-like, water-repellent cutin covering the epidermis have also been frequently observed in plants that grow in dry areas (Bosu and Wagner, 2014; Khan et al., 2018). The length, width, and shape of epidermal cells, the indumentum, and epicuticular wax on the leaf surface, and seed surface sculpture are regarded as useful characters in distinguishing different subspecies and varieties of *Capparis* (Fici, 2004; Jiang et al., 2007; Chimona et al., 2012). A single layer of epidermis with rectangular cells of different sizes and thickness in inner and outer walls was observed in all taxa studied, which is in concordance with Keshavarzi and Mosafiri (2022). Although the range of stomata recorded by Zokain (2015) is in accord with our observations, the size of stomata was smaller in our samples.

Fici (2004) studied the micromorphological features of the leaf of *Capparis* and pointed to the presence of simple trichomes, a reticulate to undulate cuticle, anomocytic stomata surrounded by a peristomal rim although the size of stomata shows some variation. Gan et al., (2013) studied the adaptive micromorphological and anatomical features in *C. spinosa*. They compared stem, root, and leaf anatomical structures between seedlings grown in the laboratory (control) and in nature. They stated that some of the leaf blade anatomical features in *Capparis* showed adaption to the drought. They found that evenly distributed stomata on both sides of leaves that open during the day, were of adaptive value for *C. spinosa* life in dry habitats. Chedraoui et al., (2017)

studied the anatomical features of *C. spinosa* and stated that the epicuticular wax and different kinds of trichomes facilitate the life of this species in arid conditions. . Levizou et al., (2004) and Gan et al. (2013) reported in *C. spinosa* that stomata were distributed below the epidermal cells and remained open throughout the day in the growing season were in agreement with current observation. According to Ahmad et al., (2010), in *C. brachycarpa* polygonal and irregular type of leaf epidermal cells were observed. The species with same epidermal cells were also distinguishable on the basis of foliar micromorphology in this study. In another study by Khalid et al., (2009) examined amphianisocytic stomata in *C. brachycarpa* and disagreed with our findings which revealed paracytic type stomata. *C. brachycarpa* has a distinct combination of leaf epidermal features, as well as multicellular broad base trichomes, which were exclusively present according to the previous work of Riaz and Abid (2021).

Onja (2016) performed the microscopic examination, the lower and upper epidermis contains anomocytic stomata and glandular trichomes as the main observable features in *C. viscosa* however our research also visualized similar features. Recently Shahzad et al., (2022) analyzed undulate anticlinal wall in *C. viscosa* while current observation revealed thin smooth wall pattern. *D. glaucum* showed maximum root area in sand dunes and revealed high adaxial epidermis thickness in the saline habitat. Leaf hair density was minimum on the leaf surface (Ameen, 2020). Whereas our observation showed in *D. glaucum* polygonal to rectangular shape cells and bean shape guard cells.

### 3.4.13 Stem Epidermal Micromorphology of Cactaceae Species

In this study, the morpho-anatomical attributes of two *Opuntia* species, which are growing in desert habitat were examined. Through morphological characterization of studied taxa were designated and the descriptions were expanded with support from taxonomic features utilizing microscopic techniques (Butt et al., 2021; Zafar et al., 2021). The morphology of the stem, areoles, glochids and flower are essential to separate the examined taxa. The anatomical features showed that the species had similar anatomical surface architecture; however, their epidermal cell shape, and anticlinal wall pattern were different between the taxa have taxonomic importance.

#### a) *Opuntia dillenii* (Ker-Gawl) Haw

Shape of epidermal cells are irregular, anticlinal wall straight, epidermal cells length is ( $37.40 \pm 6.25 \mu\text{m}$ ) and width of cells is ( $27.85 \pm 4.17 \mu\text{m}$ ). Average epidermal cells number is  $124 \text{ mm}^2$  per unit area. Stomata is paracytic, superficial, mean value of no. of stomata is  $4 \text{ mm}^2$  per unit area. Stomata length and width is ( $37.35 \pm 1.20 \mu\text{m}$ ) and ( $17.60 \pm 1.20 \mu\text{m}$ ) respectively. Kidney shape guard cell observed with noted length is ( $50.95 \pm 1.22 \mu\text{m}$ ) and width is ( $11.80 \pm 0.52 \mu\text{m}$ ). Subsidiary cells length measurement is ( $52.90 \pm 1.19 \mu\text{m}$ ) and width is ( $14.15 \pm 0.63 \mu\text{m}$ ). Length of stomatal pore is ( $28.60 \pm 2.14 \mu\text{m}$ ) and width is ( $11.80 \pm 0.52 \mu\text{m}$ ). Stomatal index value is 3.31% (Plate 87a).

#### b) *Opuntia monacantha* (Willd.) Haw

Shape of epidermal cells are irregular and zigzag, anticlinal wall is sinuate, epidermal cells length is ( $53.25 \pm 2.05 \mu\text{m}$ ) and width is ( $35.10 \pm 5.19 \mu\text{m}$ ). Average epidermal cells number is  $116 \text{ mm}^2$  per unit area. Stomata paracytic, superficial with observed length is ( $52.95 \pm 1.39 \mu\text{m}$ ) and width is ( $33.60 \pm 1.56 \mu\text{m}$ ). Mean value of no. of stomata is  $4 \text{ mm}^2$  per unit area. Length of subsidiary cell is ( $63.65 \pm 2.27 \mu\text{m}$ ) and width is ( $5.35 \pm 0.78 \mu\text{m}$ ). Length and width of guard cells ( $53.85 \pm 1.59 \mu\text{m}$ ) and ( $20.45 \pm 0.80 \mu\text{m}$ ) respectively. Length of stomatal pore is ( $24.30 \pm 1.23 \mu\text{m}$ ) and width is ( $9.60 \pm 0.55 \mu\text{m}$ ). Stomatal index is 3.23% (Plate 87b).



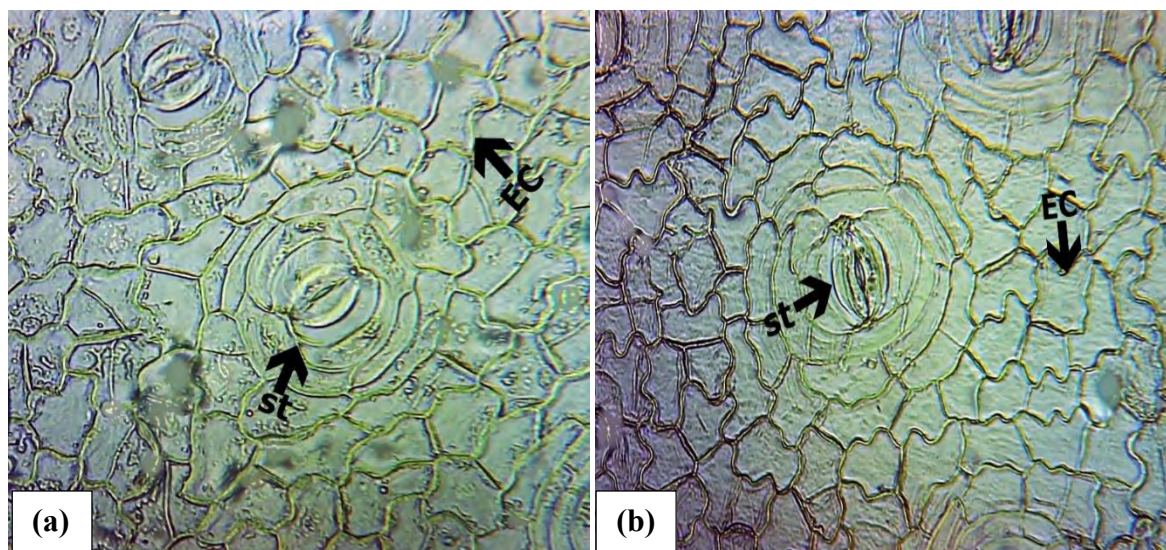


**Plate 87.** Stem anatomical micrographs taken at 10X showing (EC) epidermal cells and (st) stomata of (a) *Opuntia dillenii*, (b) *Opuntia monacantha*

### 3.4.14 Discussion

Previous work on anatomical features of the family Cactaceae shows adaptations important to aridity, where the majority of family representatives are present, and are characterized by high stomatal frequency, presence of palisade cortex, large intercellular spaces, cortical and medullary beams, and wood modifications (Gibson and Nobel 1986; Nobel, 2002). Stem epidermal anatomical findings provides features are significantly and taxonomically important for the genus *Opuntia*. The significance of stem epidermal anatomy previously indicated by some other authors in the delimitation of plant species of Cactaceae (Calvente et al., 2008; Janu and Raghuvanshi, 2011). Epidermal cells in surface view showed variability of anticlinal cell wall patterns. It appears as a Cactaceae features, because it was previously mentioned by Loza-Cornejo and Terrazas (2003) for the Cactoideae subfamily. The waviness of epidermal cell walls had been associated with environmental factors, such as latitude, altitude, and combined temperature and precipitation (Perrotta and Arambarri 2018). In fact, it is not clear in the present research, but we are working with another organ, and we can hypothesize this characteristic may be also influenced by stem grows, flattened and rounded. In a drought-stressed condition the plants show substantial wilting, and the cell walls become to bend if they do not have enough rigidity (Schulze et al., 2005). Therefore, we think that those species with small

epidermal cells, more or less rectilinear walls, and thicker periclinal cell walls plus cuticle and epicuticular waxes. The superficial stomata position agrees with data reported by Arruda and Melo-de-Pina (2015) in their research on Opuntioideae, and it is supposed to the deep stomatal chamber goes through thickened multiseriate hypodermis.

In this research study, epidermal cells of two types irregular in *O. dillenii* and irregular zigzag in *O. monacantha* were observed. The epidermal cells anticlinal wall pattern showed the straight wall in *O. dillenii* and slightly sinuate pattern in *O. monacantha*. The quantitative findings also show differences in average number and size of epidermal cells, stomata, subsidiary cells, guard cells and stomatal pore. Whereas stomatal index values showed that *O. dillenii* has 3.31 while *O. monacantha* has 3.23 on stem surface. de Arruda and Melo-De-Pinna (2016) give the anatomical description of the areolar structure of (*Opuntia microdasy*, *Opuntia monacantha* and *Opuntia rufida*) to observed different patterns of areole morphology from Brazil. Whereas the previous findings of da Silva et al., (2010) describe the anatomical aspects of *Opuntia undulata* from semi-arid region of Brazil with contrasting insect resistance showing the greatest thickness of anatomical structures using morpho-anatomical analysis. The anatomical description of areole structure of four *Opuntia* species provided new characters believed to be important contribution for the understanding of evolutionary aspects.

### 3.4.15 Petiole Micromorphology of Amaranthaceous Species

In this research petiole anatomical traits of Amaranthaceous taxa were examined for the first time in detail as summarized in Table 35 and 36. The findings of Amaranthaceous taxa are given below:

#### a) *Aerva lanata* (L.) Juss.

Petiole had flat shape with blunt tips and its recorded length was 270  $\mu\text{m}$ . Irregular epidermal cells were seen on both sides of epidermis. The mean length of epidermal cells was (5.25  $\mu\text{m}$ ) and 7.5  $\mu\text{m}$  on abaxial and adaxial surfaces respectively while mean width value range from 4.1 to 5.6  $\mu\text{m}$  on both surfaces. Polyhedral parenchyma cells of length range (4.2-7.6  $\mu\text{m}$ ) and width range (4-8.5  $\mu\text{m}$ ) were measured. Ten vascular bundles of almost spherical shape were found at the center. Annular collenchyma was observed beneath epidermal cells. The average mean size range of collenchyma varies from 6.2 to 6.3  $\mu\text{m}$  (Plate 88, Table 35 & 36).

#### b) *Achyranthes aspera* L.

The shape of petiole was cordate type with irregular tips and mean length (360  $\mu\text{m}$ ). Cells of epidermis were ovoid on both adaxial and abaxial sides with mean length range (5.6-7.9)  $\mu\text{m}$  and width range (4.4-5.3  $\mu\text{m}$ ). Polygonal parenchyma cells were observed in which average length range (8-13.5  $\mu\text{m}$ ) and width range (6.5-12  $\mu\text{m}$ ). 6 polygonal shape vascular bundles were found. Lamellar collenchyma was examined with mean length 3.8  $\mu\text{m}$  and width 4.6  $\mu\text{m}$  respectively (Plate 89, Table 35 & 36).

#### c) *Alternanthera ficoidea* (L.) Sm.

Oval type petiole with blunt tips and average length of 445  $\mu\text{m}$  was measured. The cells of epidermis were irregular on both surfaces in which the length range is (2.05-1.8  $\mu\text{m}$ ) and width range is (1.2-1.4  $\mu\text{m}$ ). Isodiametric parenchyma cells were observed with length range (5.6-12.1  $\mu\text{m}$ ) and width range is (3.5-8.2  $\mu\text{m}$ ). 9 large polygonal shape vascular bundle was examined at center with two blunt tips. Angular collenchyma was noted beneath epidermal cells in which cell length range was (4.25-7.6  $\mu\text{m}$ ) and width range was (4-8.5  $\mu\text{m}$ ) as shown in Plate 90 and Table 35 & 36.

**d) *Alternanthera sessilis* (L.) R.Br. ex DC.**

Sulcate shape petiole with circular regions and recorded mean length was (520  $\mu\text{m}$ ). Circular cells were seen on both adaxial and abaxial epidermis with mean length (6.8  $\mu\text{m}$ ) and width range (6.3-6.7  $\mu\text{m}$ ). Irregular parenchyma cells were observed. 11 spherical shape vascular bundles were located at central circular region. Annular collenchyma was observed beneath epidermal cells with measured mean length (8.7  $\mu\text{m}$ ) and width (5.3  $\mu\text{m}$ ) as illustrated in Plate 91 and Table 35 & 36.

**e) *Amaranthus graecizans* L.**

U shaped petiole with three circular regions and of length (430  $\mu\text{m}$ ) was observed. Polygonal epidermal cells were observed on epidermal surface in which the variations in length were (3.5-7.6  $\mu\text{m}$ ) and width range was (3.2-7.9  $\mu\text{m}$ ). Ovoid parenchyma cells were examined. The observed vascular bundles were isodiametric in shape and arranged in such way that 1 was in the larger central circular region and 2 at the other two circular regions. Lamellar collenchyma was observed with the cell's length range (4.3-9.2  $\mu\text{m}$ ) and width range (3.4-8  $\mu\text{m}$ ). Trichomes were present along epidermis margins (Plate 92, Table 35 & 36).

**f) *Amaranthus retroflexus* L.**

Petiole shape was winged type with rounded tips and length (760  $\mu\text{m}$ ). Isodiametric epidermal cells were found on both surfaces. The recorded length and width range in epidermal cells was (3.8-9.3  $\mu\text{m}$ ) and (3.6-7.8  $\mu\text{m}$ ), respectively. The observed parenchyma cells were elongated shape, and the recorded length range was (6-10.7  $\mu\text{m}$ ) and variations were also seen in width (5.2-10.5  $\mu\text{m}$ ). Rounded shape vascular bundles were arranged along the rounded tips. Lamellar collenchyma was observed and trichomes were present (Plate 93, Table 35 & 36).

**g) *Amaranthus viridis* L.**

Petiole was U shaped with small protuberances and acute tips and its recorded length was 170  $\mu\text{m}$ . Elongated epidermal cells were seen on epidermal surface. The length and width mean value in abaxial epidermis cells were (7.8  $\mu\text{m}$ ) and (6.95  $\mu\text{m}$ ) respectively and (L = 4.6  $\mu\text{m}$  and W = 5.16  $\mu\text{m}$ ) along adaxial surface, respectively. Polygonal parenchyma cells were recorded with mean length (12.05  $\mu\text{m}$ ) and width (10.4  $\mu\text{m}$ ). Vascular bundles of polygonal shape were seen in which the central one

was large. Annular collenchyma was observed in which mean length and width was measured (8.24  $\mu\text{m}$ ) and (7.8  $\mu\text{m}$ ) respectively. Trichomes were observed (Plate 94, Table 35 & 36).

**h) *Atriplex stocksii* Boiss.**

Flat type petiole with obtuse angles and length (230  $\mu\text{m}$ ) was observed. Cells of the epidermis were isodiametric on both surfaces measured mean length and width (9.33  $\mu\text{m}$ ) and (6.83  $\mu\text{m}$ ), respectively. Isodiametric parenchyma cells were recorded with average length (11.25  $\mu\text{m}$ ) and width (6.25  $\mu\text{m}$ ). Spherical shape vascular bundles were arranged in a rectangular shape. Angular collenchyma was observed in which length (L = 6.75  $\mu\text{m}$ ) and width (W = 4.1  $\mu\text{m}$ ). Trichomes were observed along the surface of the petiole (Plate 95, Table 35 & 36).

**i) *Bassia indica* (Wight) A.J.Scott**

Petiole shape was flat type with rounded tips and length (345  $\mu\text{m}$ ). The shapes of epidermal cells were circular on both adaxial and abaxial surfaces with average length and width (4.93  $\mu\text{m}$ ) and (6.26  $\mu\text{m}$ ) respectively. Polygonal parenchyma cells were noted with mean length and width range (L = 4.33  $\mu\text{m}$  and W = 3.7  $\mu\text{m}$ ), respectively. Slightly spherical shape vascular bundles were arranged along the epidermal boundaries. Annular collenchyma was observed. Mean value calculated of collenchyma cells were (L = 6.15 $\mu\text{m}$ ) and (W = 6.4 $\mu\text{m}$ ) as illustrated in Plate 96 and Table 35 & 36.

**j) *Chenopodium album* L.**

C shaped petiole type with small protuberances and length (285  $\mu\text{m}$ ) was analyzed. Irregular shape epidermal cells were noticed on both epidermal sides with mean length and width range (3.95-5.9  $\mu\text{m}$ ) and (2.5-4.05  $\mu\text{m}$ ), respectively. The observed parenchymatic cells showed elongated shape and average size (L = 3.45  $\mu\text{m}$  and W = 4.3  $\mu\text{m}$ ). Spherical vascular bundles were arranged in the central part along with margins. Annular collenchyma cells were examined with mean length 6.45  $\mu\text{m}$  and width 4.4  $\mu\text{m}$  (Plate 97, Table 35 & 36).

**k) *Chenopodium ficifolium* Sm.**

C shaped type petiole with obtuse angles and mean length (420  $\mu\text{m}$ ) were observed. Cells of epidermis were isodiametric on both sides, with mean length and width range (4.9-10.25  $\mu\text{m}$ ) and (2.9-6.26)  $\mu\text{m}$ , respectively. Parenchyma cells of isodiametric types were recorded with average  $L = 8.95 \mu\text{m}$  and  $W = 2.8 \mu\text{m}$ , respectively. Elongated shape vascular bundles were arranged in a rectangular shape. Annular collenchyma was observed in which length and width average value was (14.3  $\mu\text{m}$ ) and (10  $\mu\text{m}$ ), respectively (Plate 98, Table 35 & 36).

**l) *Chenopodium murale* L.**

Petiole shape was sulcate with rounded tips and length (301)  $\mu\text{m}$ . The shapes of epidermal cells were polygonal on both surfaces with length and width range (8.66-12.3  $\mu\text{m}$ ) and (6.5-7.05)  $\mu\text{m}$  respectively. Polygonal parenchyma cells were noted with mean length and width (1.8  $\mu\text{m}$ ) and (1.38  $\mu\text{m}$ ), respectively. Isodiametric vascular bundles were arranged along the epidermal boundaries. Lamellar collenchyma cells and average size ( $L = 4.66 \mu\text{m}$  and  $W = 4 \mu\text{m}$ ). Trichomes were observed along petiole surface (Plate 99, Table 35 & 36).

**m) *Digera muricata* (L.) Mart.**

Elliptic type petiole with small protuberances and length (380  $\mu\text{m}$ ) was measured. Elongated shape epidermal cells were noticed on both adaxial and abaxial surfaces with length and width range (4.2-4.6  $\mu\text{m}$ ) and (1.92-5.8  $\mu\text{m}$ ), respectively. The observed parenchymatic cells showed elongated shapes in which length and width range was (13-22  $\mu\text{m}$ ) and (3.2-7  $\mu\text{m}$ ), respectively. Elliptical shape vascular bundles were observed in central part of petiole. Lamellar collenchyma cell was examined (Plate 100, Table 35 & 36).

**n) *Gomphrena celosioides* Mart**

Petiole was flat type with small protuberances and acute tips and its recorded length (350  $\mu\text{m}$ ). isodiametric epidermal cells were seen on the abaxial surface and irregular on the adaxial. The length and width range in abaxial epidermal cells were (3.2-5.4  $\mu\text{m}$ ) and (3.5-7.3  $\mu\text{m}$ ) respectively and (3.3-6.5  $\mu\text{m}$ ) and (1.2-2.6  $\mu\text{m}$ ) in the adaxial surface, respectively. Polyhedral parenchyma cells were recorded with mean  $L = 17.54 \mu\text{m}$  and  $W = 4.5 \mu\text{m}$  were examined. 3 vascular bundles of elongated shape

were seen in which the central one was large and the two smaller at the corners. Annular collenchyma was observed in which length and width range was (13-23)  $\mu\text{m}$  and (6-11)  $\mu\text{m}$  as shown in Plate 101 and Table 35 & 36.

### 3.4.16 Hierarchical Cluster Analysis (UPGMA) Dendrogram

The phenogram analysis based on the characters reveals various levels of phenotypic relationships. The cluster analysis was performed by the Euclidean distance method, based on 14 petiole micromorphological attributes. The presence of sulcate-type petiole in *Chenopodium murale* is explained by dendrogram analysis with single-out group cluster C1. Cluster C1 was composed of two sub clusters, C1a in which *Amaranthus retroflexus* and *Chenopodium ficifolium* share common isodiametric epidermal cell shape. The second C1b consists of two further subgroups: *Alternanthera ficoidea*, *Bassia indica*, and *Chenopodium album*, comprise the first sub-group C1b1. *Bassia indica* and *Chenopodium album* in sub-cluster C1b1 were closely placed due to annular collenchymatous cells type. The second sub-cluster C1b2 comprising *Alternanthera sessilis*, *Gomphrena celosioides*, *Amaranthus graecizans*, *Aerva lanata*, *Amaranthus. viridis*, *Atriplex stocksii*, *Achyranthes aspera* and *Digera muricata*.

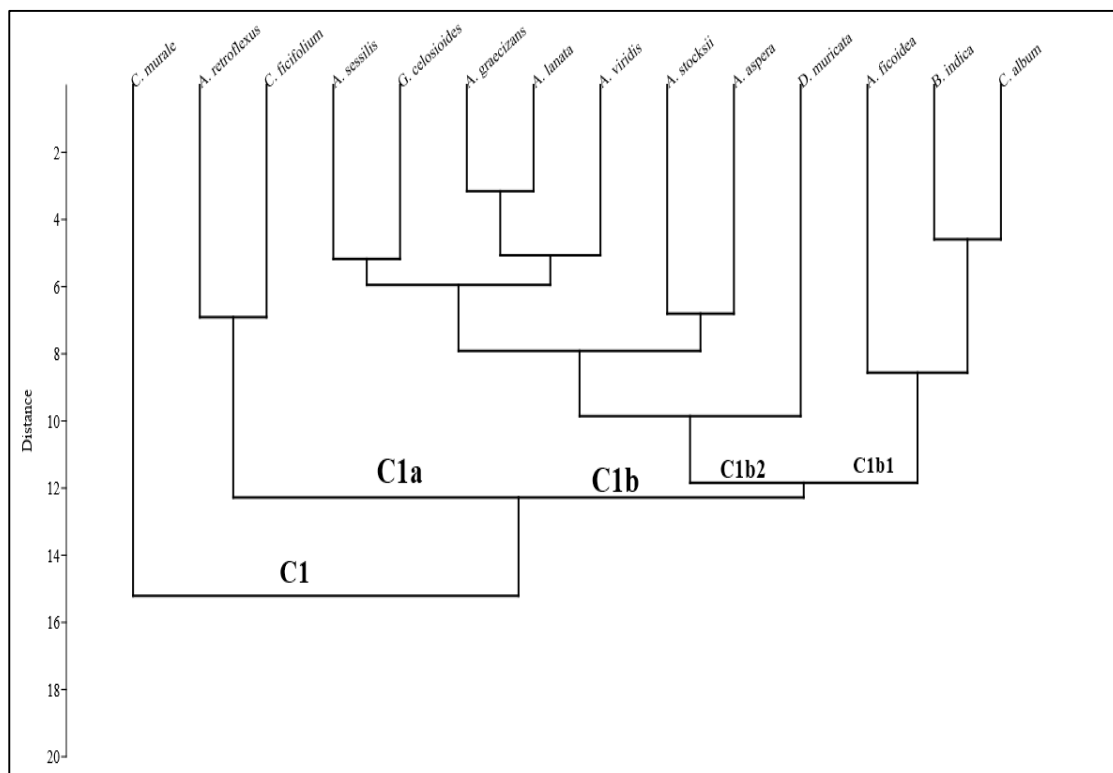


**Figure 65.** Cluster groupings via UPGMA dendrogram of Amaranthaceous species based on petiole morphometric features.

In sub-cluster C1b2, *Amaranthus graecizens* and *Aerva lanata* was closely placed due to less euclidean distance. They have similar lamellar-type collenchyma layers (Figure 65).

### 3.4.17 Identification Keys Based on Amaranthaceous Petiole Features

1 + Trichome absent.....	2
- Trichome present.....	9
2 + Vascular bundle spherical shape, Flat petiole.....	<i>A. aspera</i>
- Polygonal vascular bundle shape.....	3
3 + Cordate petiole outline.....	<i>A. lanata</i>
- Polygonal vascular bundle .....	4
4 + Oval petiole outline, isodiametric parenchyma cells.....	<i>A. ficoidea</i>
- Spherical vascular bundle.....	5
5 + Sulcate petiole outline, annular collenchyma cells.....	<i>A. sessilis</i>
- Slightly spherical vascular bundle .....	6
6 + Flat petiole, annular collenchyma cells.....	<i>B. indica</i>
- Spherical vascular bundle .....	7
7 + C shape petiole.....	<i>C. album</i>
- Elongated vascular bundle.....	8
8 + C shape petiole, Annular collenchyma .....	<i>C. ficifolium</i>
- Elliptical vascular bundle.....	9
9 + Elliptical outline petiole.....	<i>D. muricata</i>
- Trichome present, Isodiametric vascular bundle.....	10
10 + U-shaped petiole.....	<i>A. graecizens</i>
- Rounded vascular bundle.....	11
11 + Winged shape petiole, lamellar collenchyma.....	<i>A. retroflexus</i>
- Polygonal vascular bundle .....	12
12 + U-shaped petiole outline.....	<i>A. viridis</i>
- Spherical vascular bundle .....	13
13 + Flat petiole outline, Angular collenchyma.....	<i>A. stocksii</i>
- Isodiametric vascular bundle shape.....	14
14 + Sulcate petiole, lamellar collenchyma.....	<i>C. murale</i>
- Isodiametric vascular bundle .....	15
15 + Cordate petiole outline.....	<i>G. celosioides</i>



**Table 35.** Petiole micromorphological qualitative attributes of Amaranthaceous species.

<b>Amaranthaceous taxa</b>	<b>Petiole shape</b>	<b>VB Shape</b>	<b>Shape of Epidermal cells</b>	<b>Shape of Parenchyma cells</b>	<b>Shape of Collenchyma cells</b>	<b>Trichomes</b>
<i>Achyranthes aspera</i> L.	Flat	Spherical	Irregular	Polyhedral	Annular	Absent
<i>Aerva lanata</i> (L.) Juss.	Cordate	Polygonal	Ovoid	Polygonal	Lamellar	Absent
<i>Alternanthera ficoidea</i> (L.) Sm.	Oval	Polygonal	Irregular	Isodiametric	Angular	Absent
<i>Alternanthera sessilis</i> (L.) R.Br. ex DC.	Sulcate	Spherical	Circular	Irregular	Annular	Absent
<i>Amaranthus graecizans</i> L.	U Shaped	Isodiametric	Polygonal	Ovoid	Lamellar	Present
<i>Amaranthus retroflexus</i> L.	Winged	Rounded	Isodiametric	Elongated	Lamellar	Present
<i>Amaranthus viridis</i> L.	U Shaped	Polygonal	Elongated	Polygonal	Annular	Present
<i>Atriplex stocksii</i> Boiss.	Flat	Spherical	Isodiametric	Isodiametric	Angular	Present
<i>Bassia indica</i> (Wight) A.J.Scott	Flat	Slightly spherical	Circular	Polygonal	Annular	Absent
<i>Chenopodium album</i> L.	C Shaped	Spherical	Irregular	Elongated	Annular	Absent
<i>Chenopodium ficifolium</i> Sm.	C Shaped	Elongated	Isodiametric	Isodiametric	Annular	Absent
<i>Chenopodium murale</i> L.	Sulcate	Isodiametric	Polygonal	Polygonal	Lamellar	Present
<i>Digera muricata</i> (L.) Mart.	Elliptic	Elliptical	Elongated	Elongated	Lamellar	Absent
<i>Gomphrena celosioides</i> Mart.	Cordate	Isodiametric	Irregular	Polyhedral	Annular	Present

**Table 36.** Quantitative Characters of Petiole anatomical studies of selected Amaranthaceous species.

Amaranthaceous taxa	PL (µm)	No of VB	Collenchyma layers			Abaxial Epidermis		Adaxial Epidermis	
			Ab	Ad	C	L (µm)	W (µm)	L (µm)	W (µm)
<i>Aerva lanata</i> (L.) Juss.	270	10	6	4	3	(4.5-6) = 5.25±0.2	(3.6-4.8) = 4.1±0.32	(6-8.7) = 7.5±0.42	(4.3-6.5) = 5.6±0.52
<i>Achyranthes aspera</i> L.	360	6	4	8	6	(5.5-9) = 7.9±1.05	(4.5-6) = 5.3±0.56	(3-8) = 5.6±1.19	(2.5-6.8) = 4.4±1.03
<i>Alternanthera ficoidea</i> (L.) Sm.	445	9	5	4	8	(1.2-2.5) = 1.8±0.4	(0.8-1.5) = 1.2±0.05	(1.3-2.8) = 2.05±0.2	(0.8-1.9) = 1.42±0.4
<i>Alternanthera sessilis</i> (L.) R.Br. ex DC.	520	11	3	7	5	(5-8) = 6.8±0.24	(4-9.6) = 6.7±0.85	(5.5-8) = 6.8±1.45	(4.2-8.6) = 6.3±1.14
<i>Amaranthus graecizans</i> L.	430	8	2	6	1	(3.5-5.6) = 4.45±0.56	(3.5-7.9) = 5.8±0.39	(5.2-7.6) = 6.4±1.26	(3.2-4.6) = 3.86±0.94
<i>Amaranthus retroflexus</i> L.	760	7	7	2	3	(6.5-8.3) = 7.25±0.37	(4.8-7.3) = 6.28±1.1	(5.3-8.5) = 6.9±1.73	(3.6-7.8) = 6.05±1.45
<i>Amaranthus viridis</i> L.	170	6	4	7	6	(6-9.3) = 7.8±1.21	(5.5-8.3) = 6.95±1.3	(3.8-5.4) = 4.6±0.76	(4.6-5.8) = 5.16±0.43
<i>Atriplex stocksii</i> Boiss.	230	5	2	5	7	(8-10) = 9.33±1.25	(6-7.5) = 6.83±0.67	(4.5-12.8) = 9.3±2.5	(4-9.3) = 6.55±1.62
<i>Bassia indica</i> (Wight) A.J.Scott	345	4	8	3	5	(3.8-6) = 4.93±1.25	(5-7.5) = 6.26±0.67	(4.3-6.5) = 5.4±1.35	(2.3-4.5) = 3.35±1.09
<i>Chenopodium album</i> L.	285	8	2	5	6	(3.2-4.7) = 3.95±1.	(1.6-3.8) = 2.5±1.05	(3.8-7.8) = 5.9±1.1	(2.5-5.7) = 4.05±1.16
<i>Chenopodium ficifolium</i> Sm.	420	7	4	2	7	(5-16) = 10.25±3.5	(4.2-8) = 6.26±2.85	(2.8-7.5) = 4.9±2.7	(1.5-4.3) = 2.9±1.6
<i>Chenopodium murale</i> L.	290	5	5	1	4	(6.5-11) = 8.66±1.12	(4.1-8.7) = 6.5±1.02	(10-14) = 12.3±1.14	(5.2-9.3) = 7.05±1.54

<i>Digera muricata</i> (L.) Mart.	380	4	7	2	4	(3.2-5.4) 4.22±1.07	=	(3.5-7.3) = 5.8±1.3	(3.3-6.5) = 4.6±0.79	(1.2-2.6) = 1.92±0.34
<i>Gomphrena celosioides</i> Mart.	260	9	3	8	6	(4.5-7.9) = 6.2±1.63		(2.8-6.4) = 4.7±1.86	(3-8.5) = 5.78±1.88	(4.1-6.6) = 5.42±1.16

**Keywords:** PL= Petiole length; VB= Vascular bundle; Ad= Adaxial; Ab= Abaxial; C= Central; L= Length; W= Width; μm= micrometer

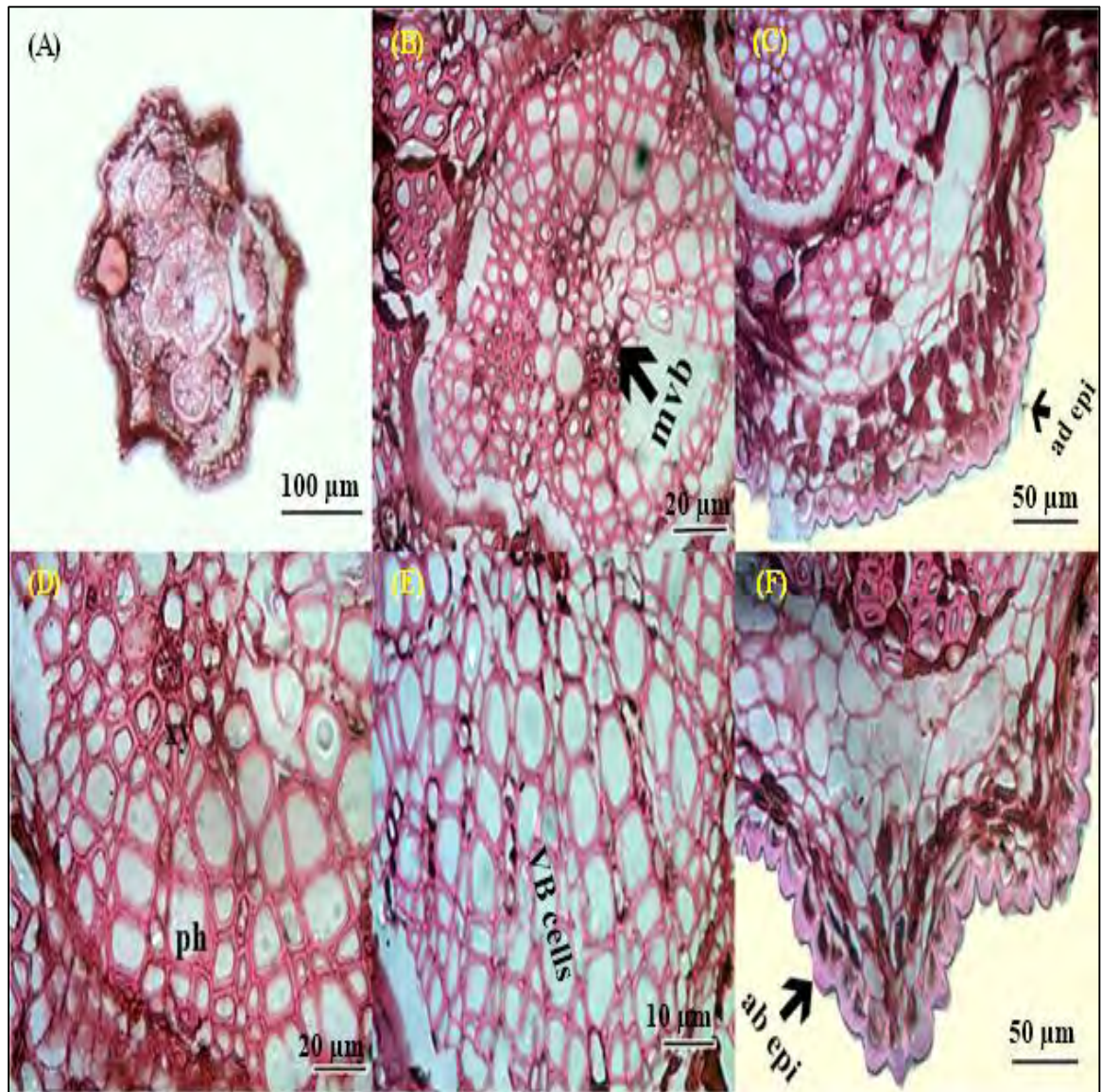


**Plate 88.** Photomicrographs of Petiole Section of *Aerva lanata* (L.) Juss. (A): Transverse Section (100 μm), (B): Section of median vascular bundle (20 μm), (C): Adaxial epidermis Section (50 μm), (D): Section of vascular bundle showing xylem and phloem (20 μm), (E): Sectioning of vascular bundle cells (10 μm), (F) Abaxial epidermal surface (50 μm). TS=Transverse section, mvb= Median Vascular Bundle, ad epi= adaxial epidermis, ab epi= abaxial epidermis, co=Collenchyma, xy= xylem, ph=phloem, VB= vascular bundle

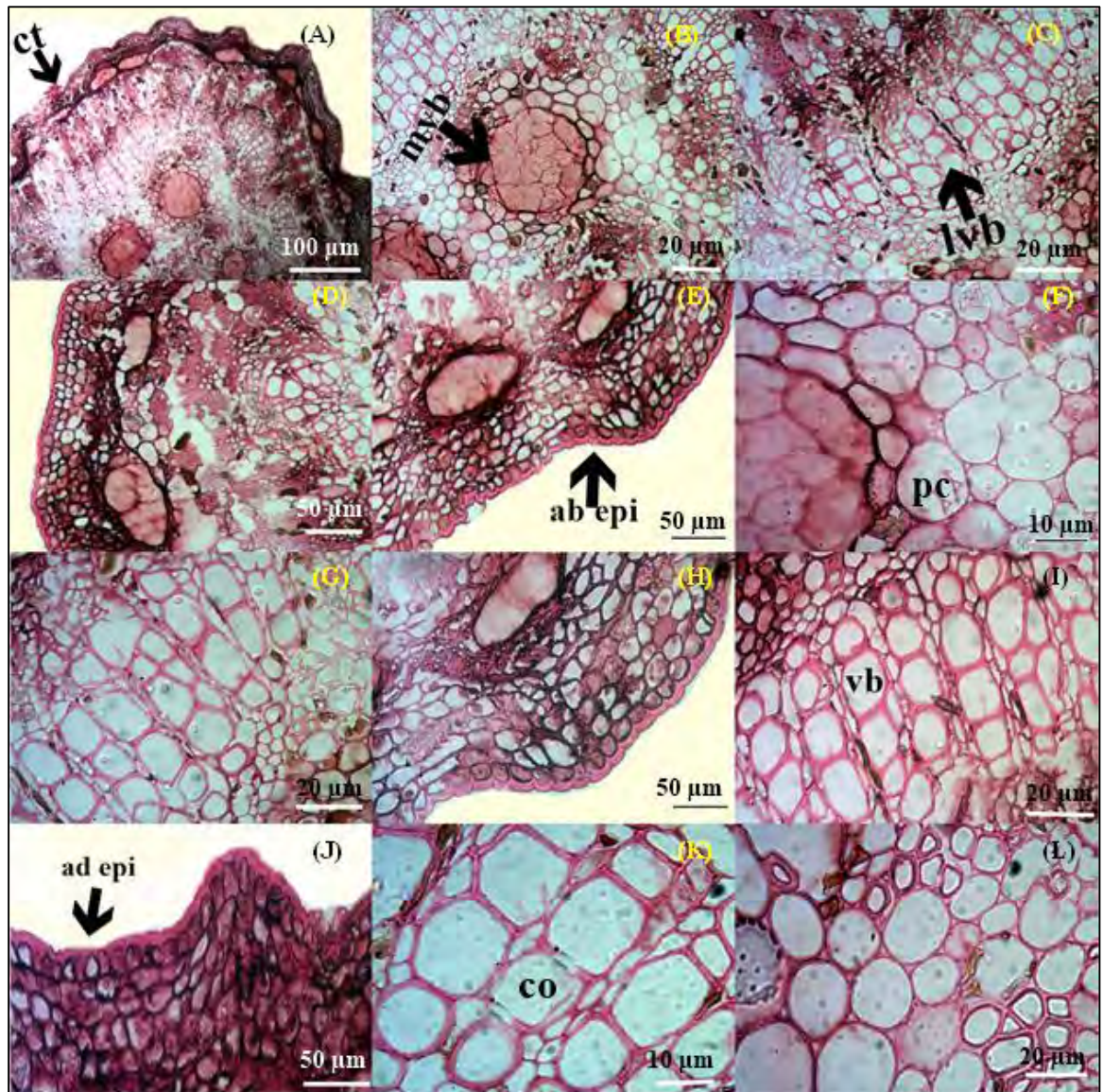


**Plate 89.** Photomicrographs of Petiole Section of *Achyranthes aspera* L. (A) Transverse Section showing cuticle layer (100 µm), (B) Section of median vascular bundle (20 µm), (C) Section of lateral vascular bundle (20 µm), (D) Lateral side view of transverse section (50 µm), (E) Abaxial epidermal surface (50 µm), (F) Sectioning of parenchymatous cell (10 µm), (G) Sectioning of VB (20 µm), (H) cell layering (50 µm) (I) VB (20 µm), (J) Adaxial epidermis section (50 µm), (K) collenchymatous cell (10 µm), (L) parenchyma cell surface (20 µm). TS=Transverse section, mvb= Median Vascular Bundle, lvb=Lateral vascular bundle, ad epi= adaxial epidermis, ab epi= abaxial epidermis, co=Collenchyma, pc=Parenchyma, po epi= Polygonal epidermal cell, VB= vascular bundle

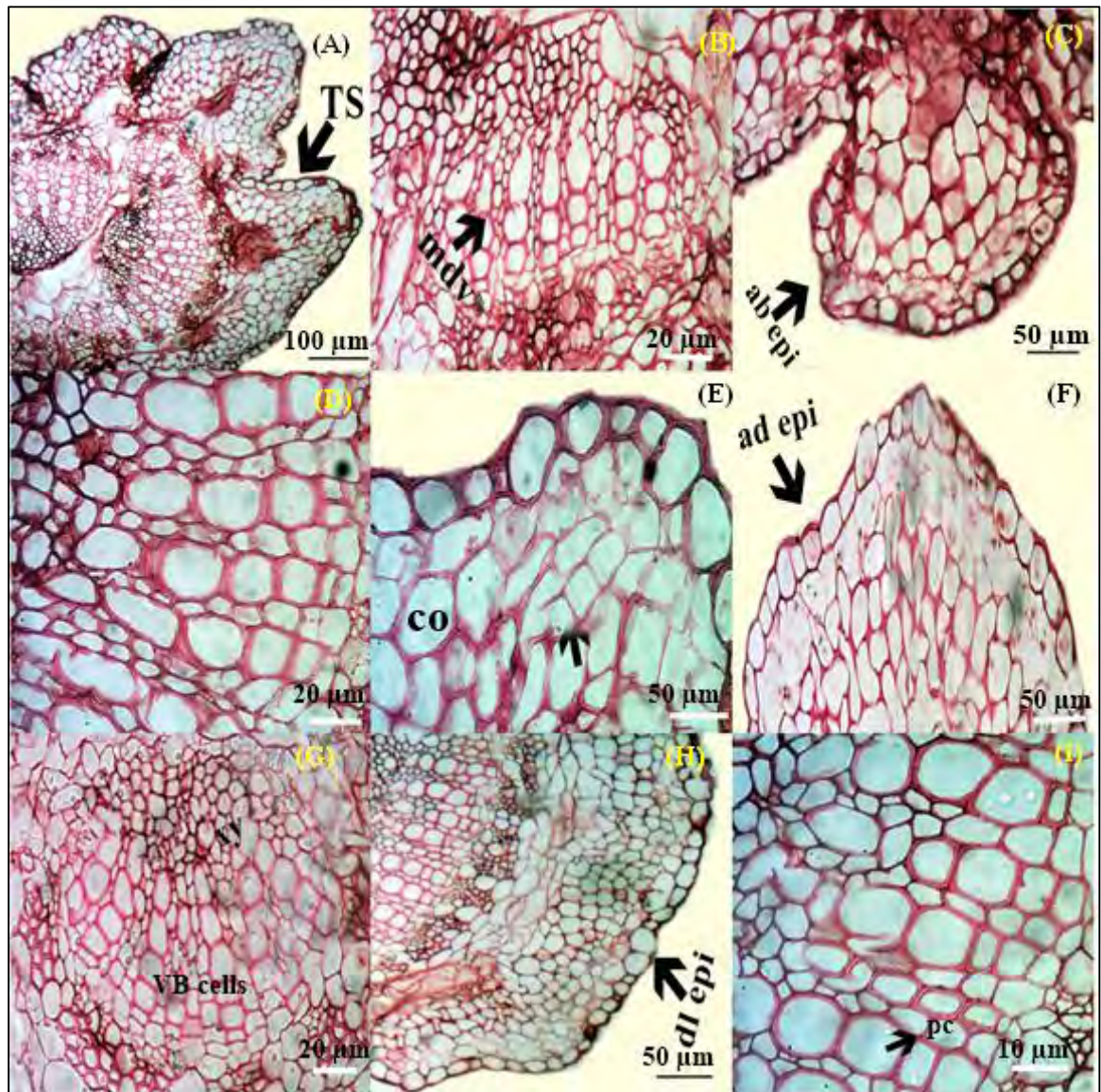


**Plate 90.** Photomicrographs of Petiole Section of *Alternanthera ficoidea* (L.) Sm. (A) Transverse Section (100  $\mu\text{m}$ ), (B) Section of median vascular bundle (20  $\mu\text{m}$ ), (C) Abaxial epidermal surface (50  $\mu\text{m}$ ), (D) Petiole cell layering (20  $\mu\text{m}$ ), (E) Collenchyma cell layering (50  $\mu\text{m}$ ), (F) Adaxial epidermis cell (50  $\mu\text{m}$ ), (G) VB cell layering (20  $\mu\text{m}$ ), (H) Dorsolateral epidermal layer (50  $\mu\text{m}$ ), (I) Parenchyma cells (10  $\mu\text{m}$ ). TS=Transverse section, mrv= Median Vascular Bundle, ad epi= adaxial epidermis, ab epi= abaxial epidermis, co=Collenchyma, pc= Parenchyma, dl epi= Dorsolateral epidermis, VB= vascular bundle, xy= xylem, ph= phloem.

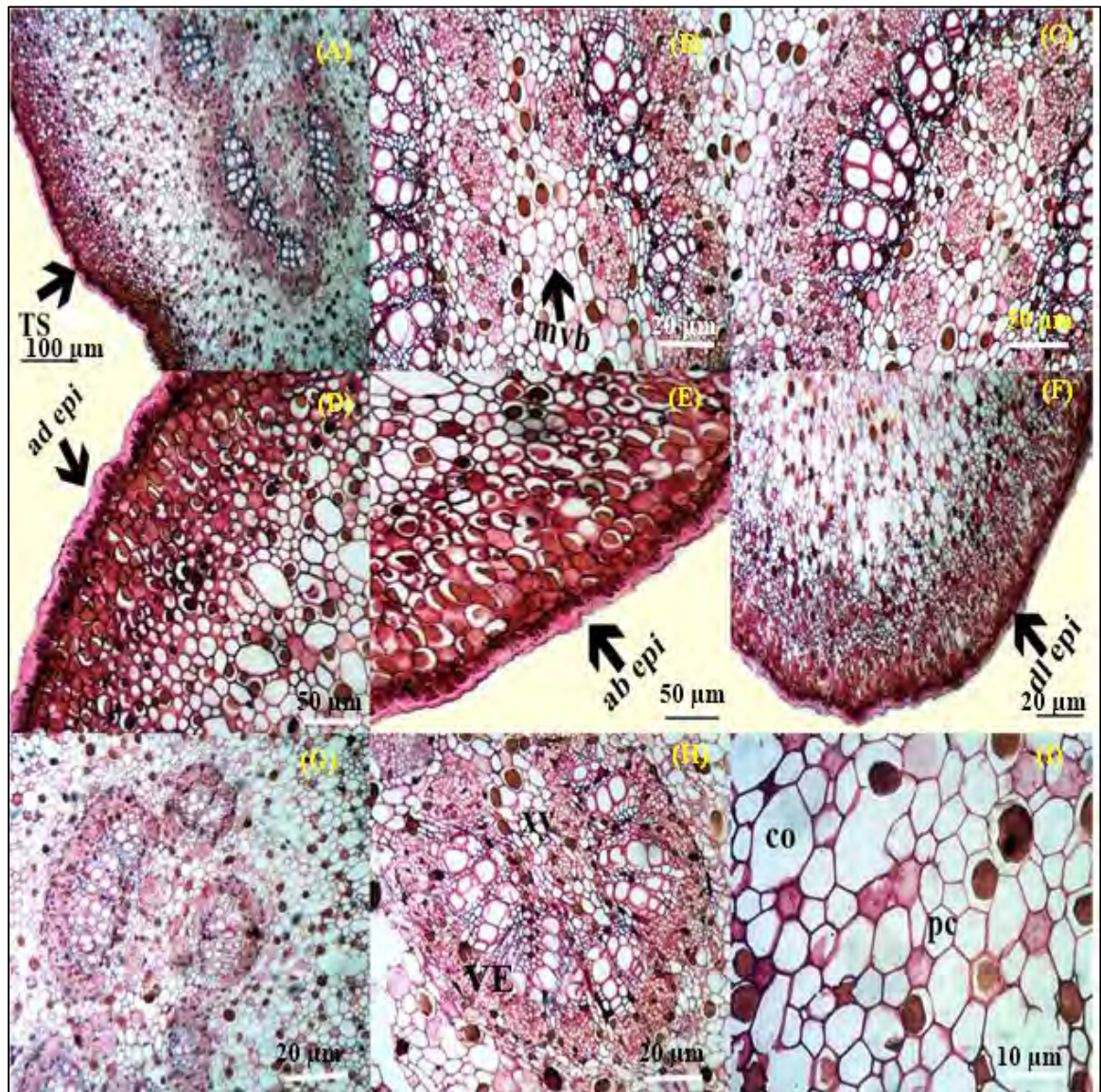


**Plate 91.** Photomicrographs of Petiole Section of *Alternanthera sessilis* (L.) R.Br. ex DC. (A). Transverse Section (100  $\mu\text{m}$ ), (B and C) Section of median vascular bundle (20  $\mu\text{m}$ ), (D) Adaxial epidermis section (50  $\mu\text{m}$ ), (E) Abaxial epidermal layer (50  $\mu\text{m}$ ), (F) Dorsolateral epidermis (50  $\mu\text{m}$ ), (G) VB section (20  $\mu\text{m}$ ), (H) Vessel elements (20  $\mu\text{m}$ ), (I) Collenchyma and Parenchyma cells (10  $\mu\text{m}$ ). TS=Transverse section, mvb= Median Vascular Bundle, ad epi= adaxial epidermis, ab epi= abaxial epidermis, co=Collenchyma, pc= Parenchyma, dl epi= Dorsolateral epidermis, VB= Vascular bundle, VE = Vessel elements, xy= xylem, ph=phloem.

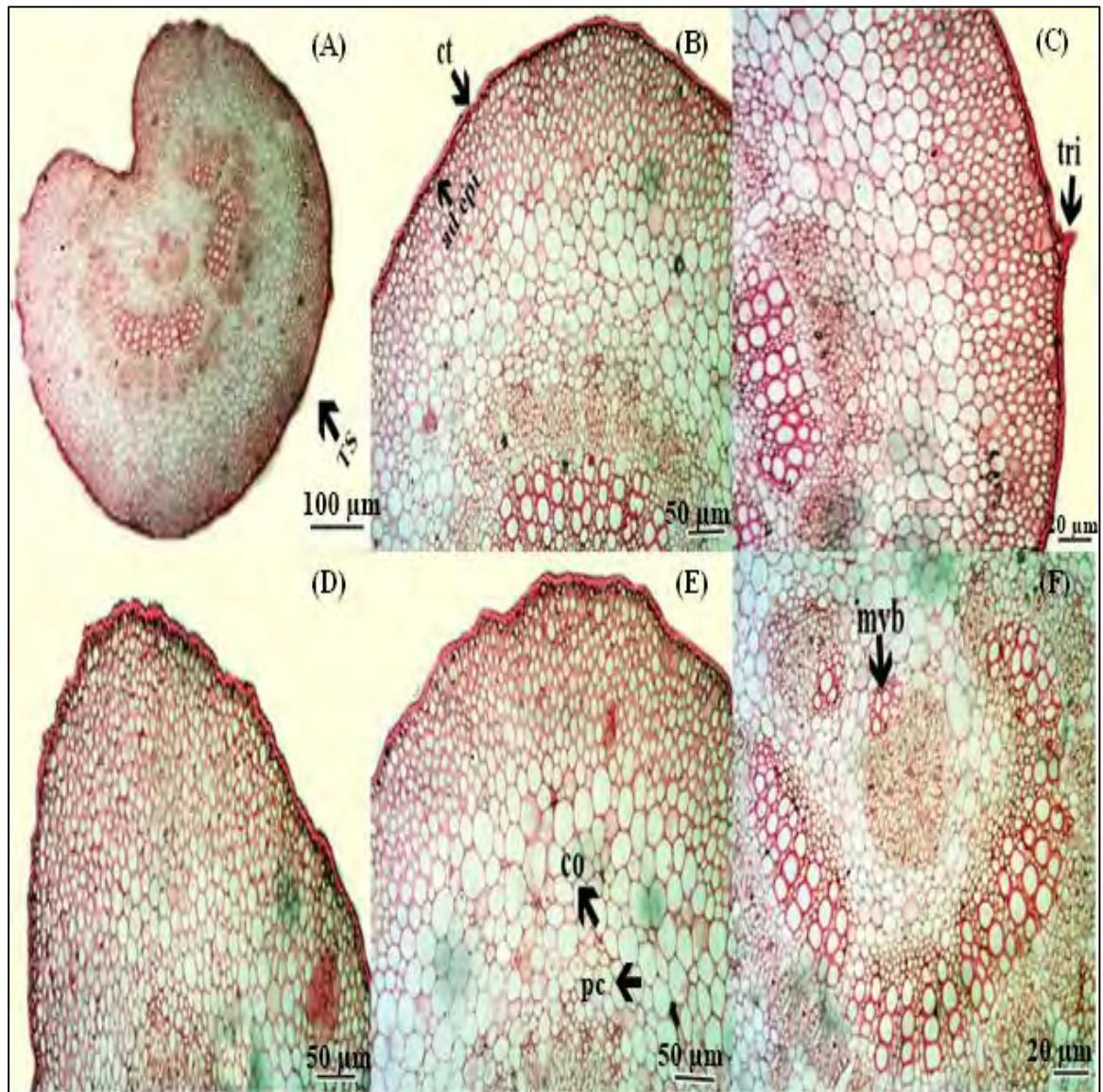


**Plate 92.** Photomicrographs of Petiole Section of *Amaranthus graecizans* L. (A) Transverse Section (100  $\mu\text{m}$ ), (B) Adaxial epidermis and cuticle layer (50  $\mu\text{m}$ ), (C) Trichome (20  $\mu\text{m}$ ), (D) cell layering (50  $\mu\text{m}$ ), (E) Collenchyma and parenchyma cells (50  $\mu\text{m}$ ), (F) Section of median vascular bundle (20  $\mu\text{m}$ ). TS=Transverse section, mvb= Median Vascular Bundle, ad epi= Adaxial epidermis, ab epi= Abaxial epidermis, co=Collenchyma, ct=Cuticle, pc= Parenchyma, dl epi= Dorsolateral epidermis, tri=Trichome, VB= vascular bundle, xy= xylem, ph=ploem.



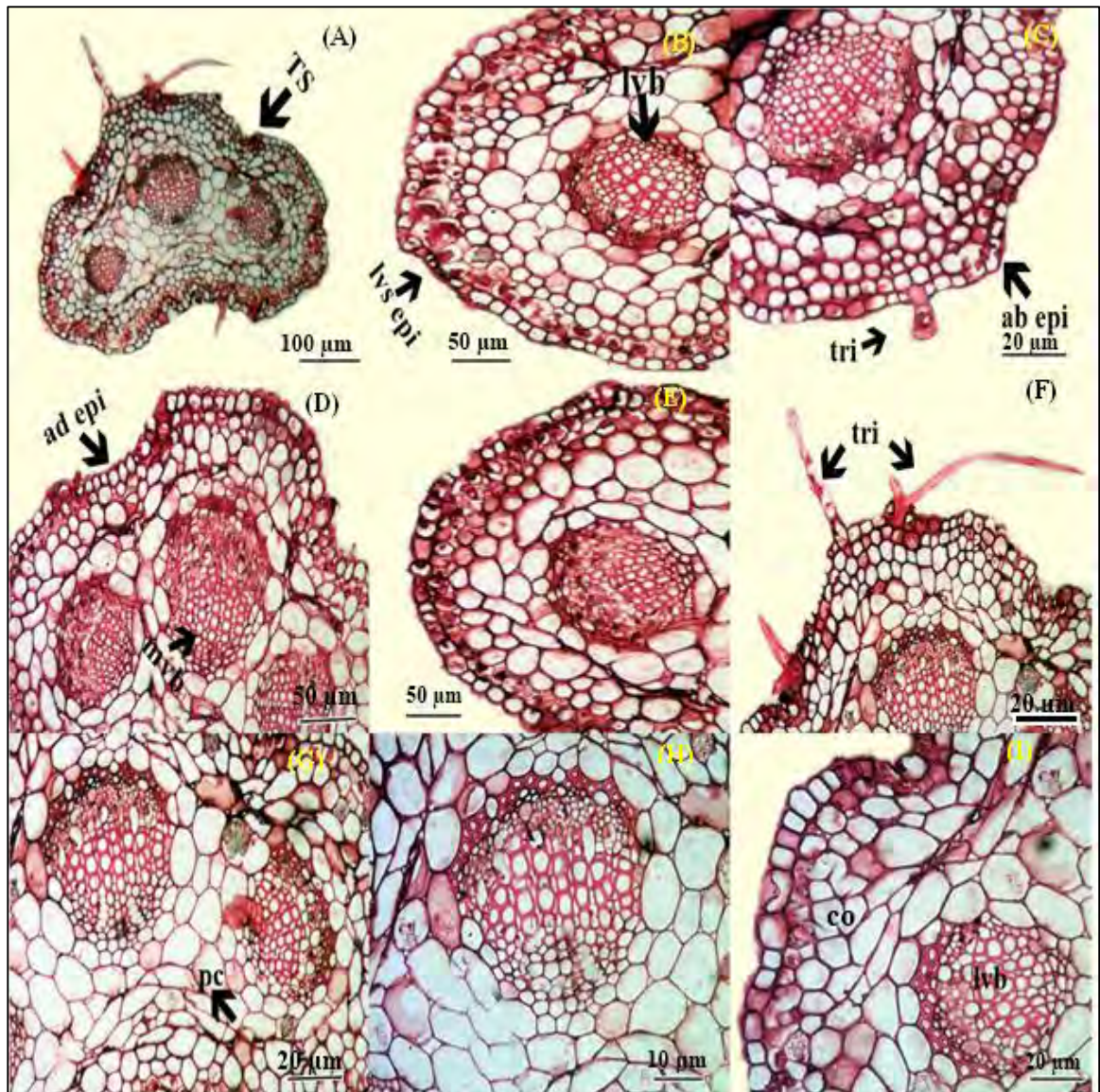


**Plate 93.** Photomicrographs of Petiole Section of *Amaranthus retroflexus* L. (A) Transverse Section (100  $\mu\text{m}$ ), (B) Lateral ventral side epidermis and bundle (50  $\mu\text{m}$ ), (C) Adaxial epidermis and trichome (20  $\mu\text{m}$ ), (D) Adaxial epidermis and median vascular bundle section (50  $\mu\text{m}$ ), (E) Lateral side view of TS (50  $\mu\text{m}$ ), (F) Trichomes (20 $\mu\text{m}$ ), (G) Parenchymatous cell (20  $\mu\text{m}$ ), (H) Cell layering around vascular bundles (10  $\mu\text{m}$ ), (I) Lateral VB and collenchyma cells (20  $\mu\text{m}$ ). TS=Transverse section, mvb= Median Vascular Bundle, lvs epi= Lateral ventral side epidermis, lvb= Lateral vascular bundle, ad epi= Adaxial epidermis, ab epi= Abaxial epidermis, co=Collenchyma, pc= Parenchyma, tri=Trichome, VB= vascular bundle, xy= xylem, ph=phloem.

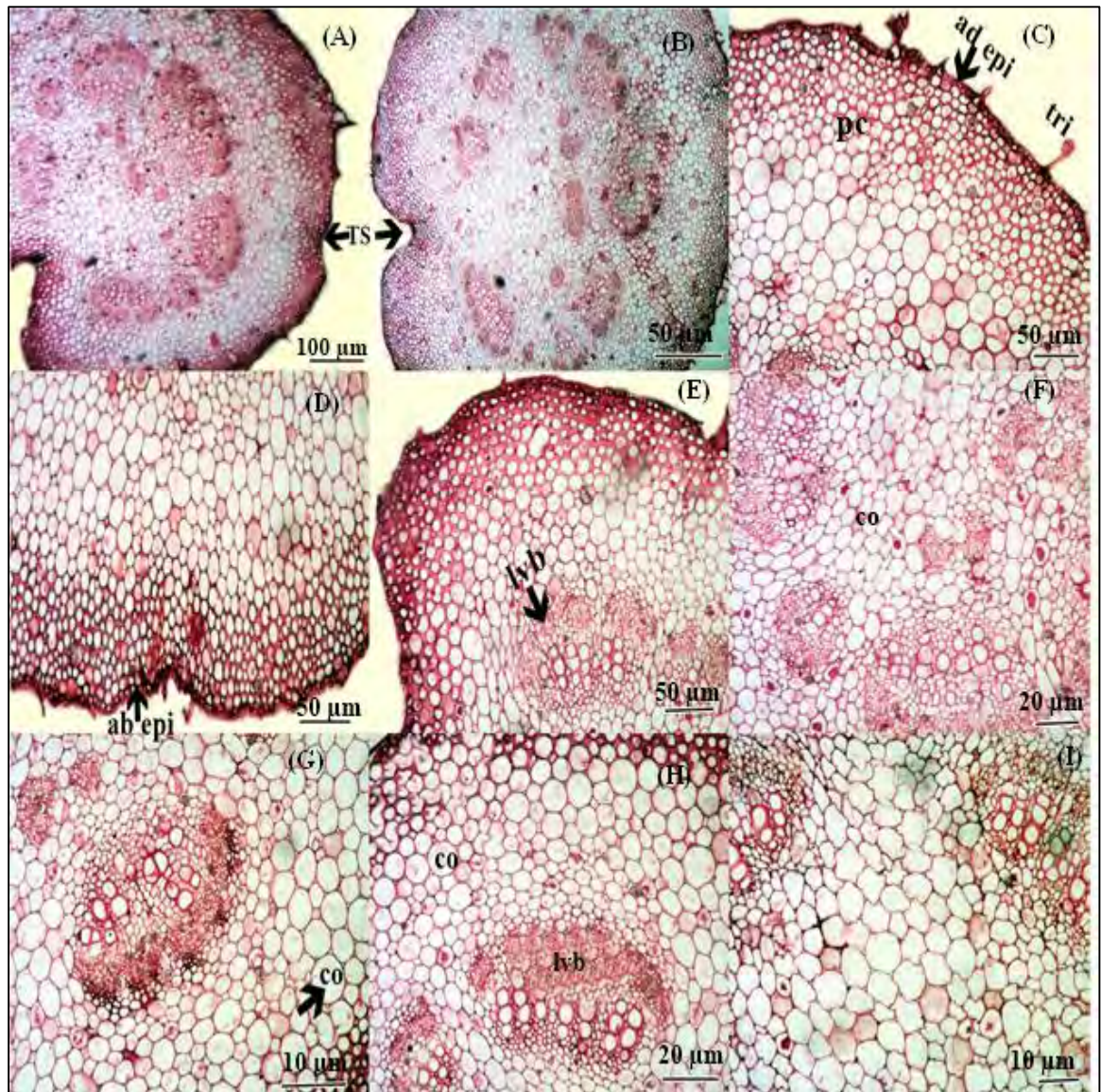


**Plate 94.** Photomicrographs of Petiole Section of *Amaranthus viridis* L. (A and B) Transverse Section (100  $\mu\text{m}$ ), (C) Adaxial epidermal surface along with trichome and parenchymatous cells (50  $\mu\text{m}$ ), (D) Abaxial epidermal surface (50  $\mu\text{m}$ ), (E) Lateral VB (50  $\mu\text{m}$ ), (F) Collenchyma cell layering between vascular bundles (20 $\mu\text{m}$ ), (G) Collenchyma cells (10  $\mu\text{m}$ ), (H) Lateral vascular bundle rings (20  $\mu\text{m}$ ), (I) Cells layering (10  $\mu\text{m}$ ). TS=Transverse section, lvb= Lateral vascular bundle, ad'epi= Adaxial epidermis, ab'epi= Abaxial epidermis, co=Collenchyma, pc= Parenchyma, tri=Trichome, VB= vascular bundle, xy= xylem, ph=phloem.

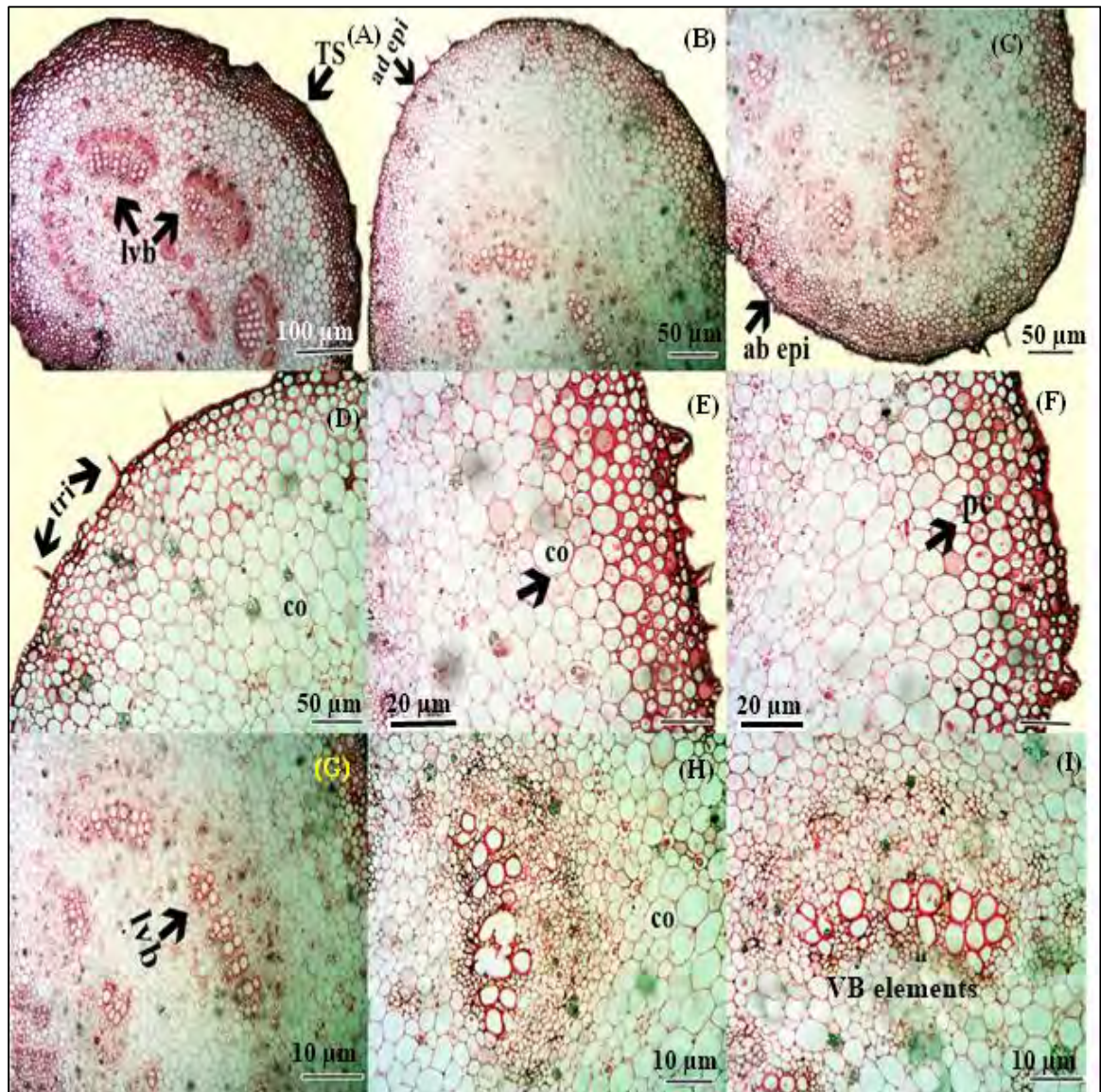


**Plate 95.** Photomicrographs of Petiole Section of *Atriplex stocksii* Boiss. (A) Transverse Section showing lateral vascular bundle (100  $\mu\text{m}$ ), (B) Adaxial epidermal surface (50  $\mu\text{m}$ ), (C) Abaxial epidermis (50  $\mu\text{m}$ ), (D) Trichomes (50  $\mu\text{m}$ ), (E) Collenchyma cells (20  $\mu\text{m}$ ), (F) Parenchyma cells (20  $\mu\text{m}$ ), (G) Lateral VB (10  $\mu\text{m}$ ), (H) Collenchymatous cells between vascular bundles (10 $\mu\text{m}$ ), (I) Vascular bundles elements (10  $\mu\text{m}$ ). TS=Transverse section, lvb= Lateral vascular bundle, ad epi= Adaxial epidermis, ab epi= Abaxial epidermis, co=Collenchyma, pc= Parenchyma, tri=Trichome, VB= vascular bundle, xy= xylem, ph=ploem.

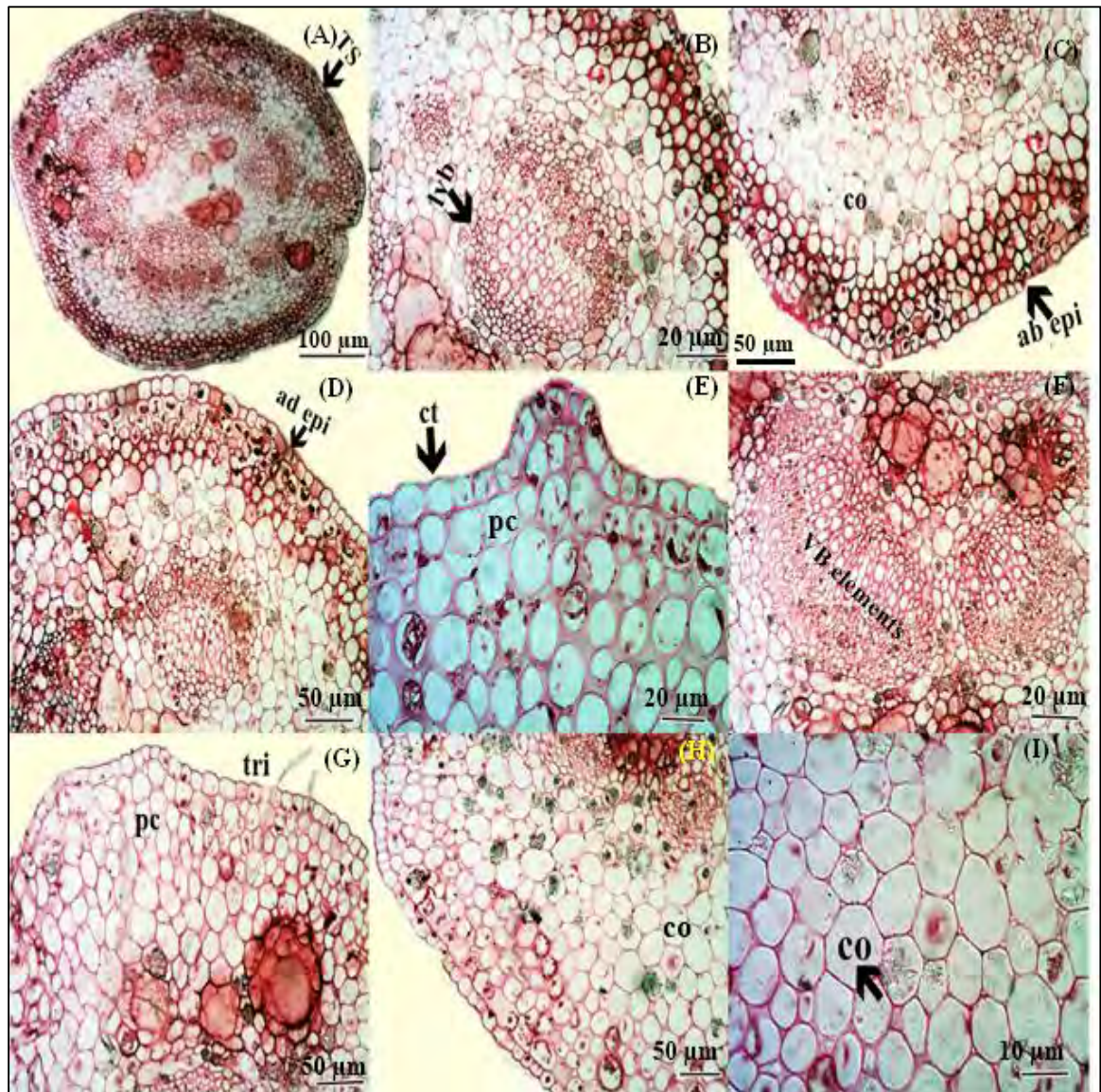


**Plate 96.** Photomicrographs of Petiole Section of *Bassia indica* (Wight) A.J.Scott. (A) Transverse Section (100  $\mu\text{m}$ ), (B) Lateral vascular bundle (20  $\mu\text{m}$ ), (C) Abaxial epidermis and collenchymatous layering (50  $\mu\text{m}$ ), (D) Adaxial epidermis (50  $\mu\text{m}$ ), (E) Cuticle and parenchymatous cell layer (20  $\mu\text{m}$ ), (F) Vascular bundle elements (20  $\mu\text{m}$ ), (G) Trichomes and parenchyma cells (50  $\mu\text{m}$ ), (H) Collenchyma cells along abaxial side (50  $\mu\text{m}$ ), (I) Annular Collenchyma cells (10  $\mu\text{m}$ ). TS=Transverse section, lvb= Lateral vascular bundle, ad epi= Adaxial epidermis, ab epi= Abaxial epidermis, co=Collenchyma, pc= Parenchyma, tri=Trichome, VB= vascular bundle, ct= Cuticle

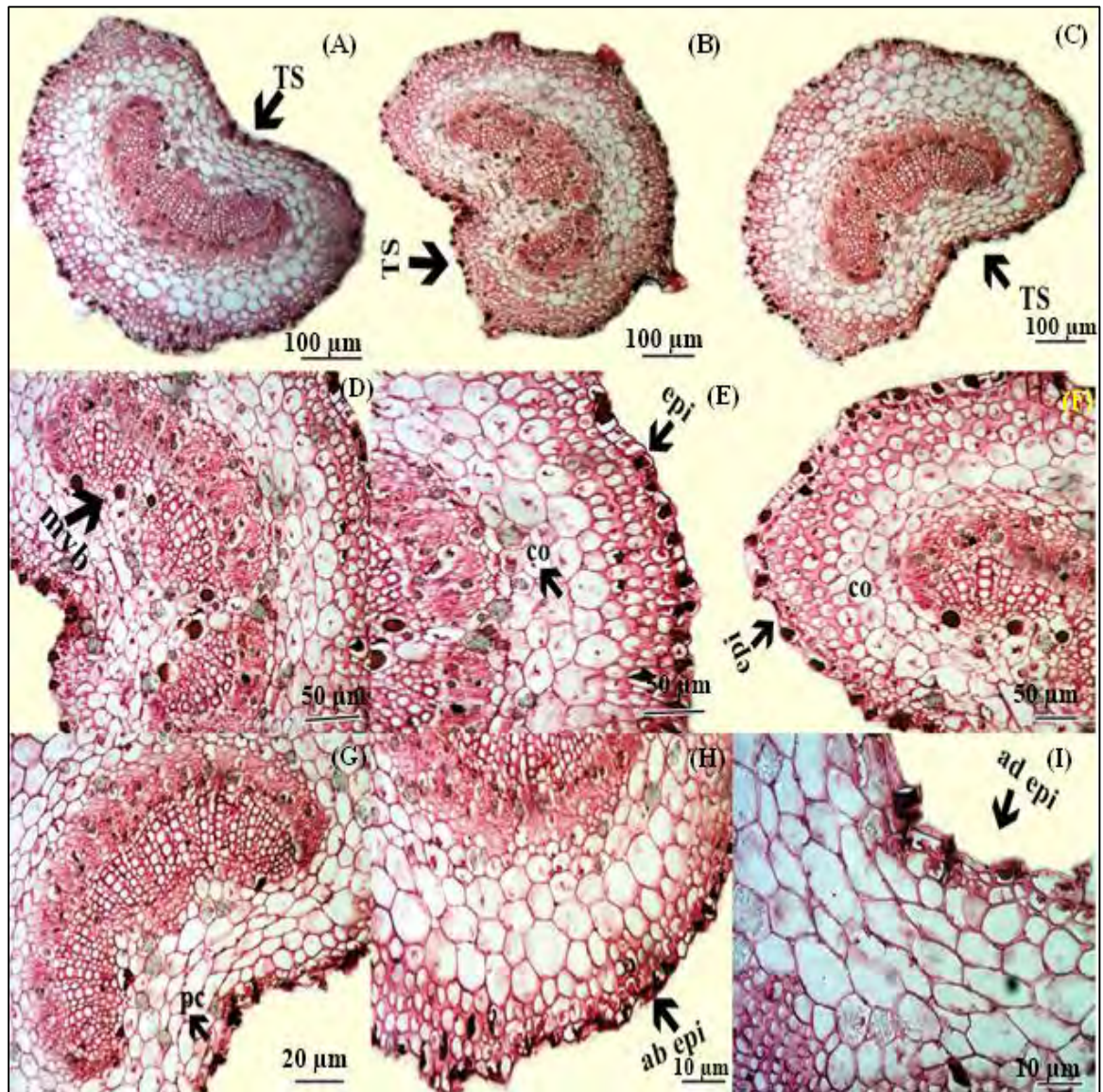


**Plate 97.** Photomicrographs of Petiole Section of *Chenopodium album* L. (A, B and C) Different view of transvers section (100 µm), (D) Median vascular bundle (50 µm), (E and F) Lateral epidermis and collenchyma cell layers (50 µm), (G) Parenchyma cells (20 µm), (H) Abaxial epidermis (10 µm), (I) Adaxial epidermis (10 µm). TS=Transverse section, mvpb= Median vascular bundle, ad epi= Adaxial epidermis, ab epi= Abaxial epidermis, co=Collenchyma, pc= Parenchyma.

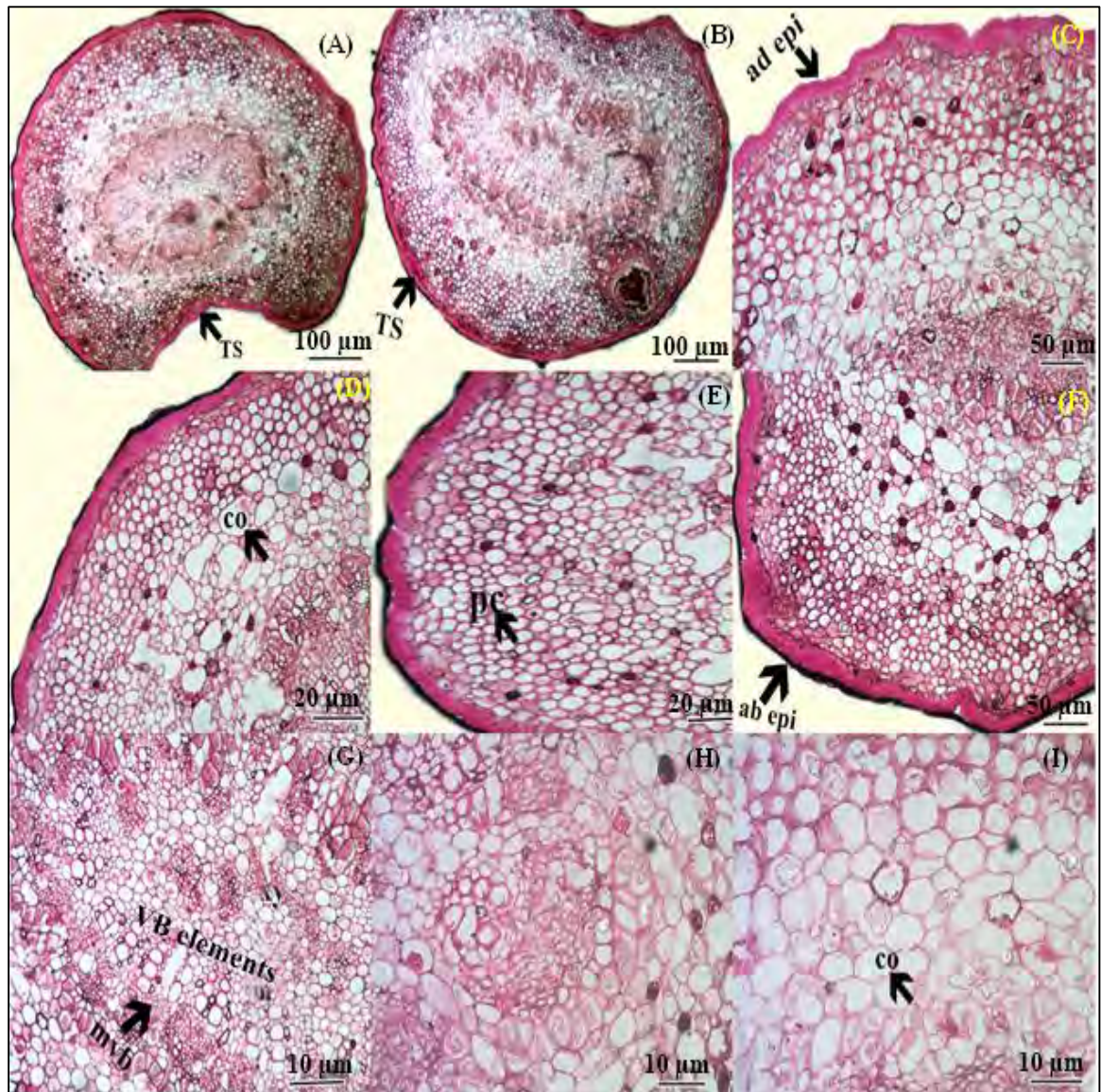


**Plate 98.** Photomicrographs of Petiole Section of *Chenopodium ficifolium* Sm. (A and B) Different view of transvers section (100 μm), (C) Adaxial epidermis (50μm), (D) Collenchyma cells layer (20μm), (E) Parenchyma cell sectioning (20 μm), (F) Abaxial epidermal surface (50 μm), (G and H) Median VB section elements (10 μm), (I) Annular Collenchyma cells (10 μm). TS=Transverse section, mvb= Median vascular bundle, ad epi= Adaxial epidermis, ab epi= Abaxial epidermis, co=Collenchyma, pc= Parenchyma, xy= xylem, ph= phloem.

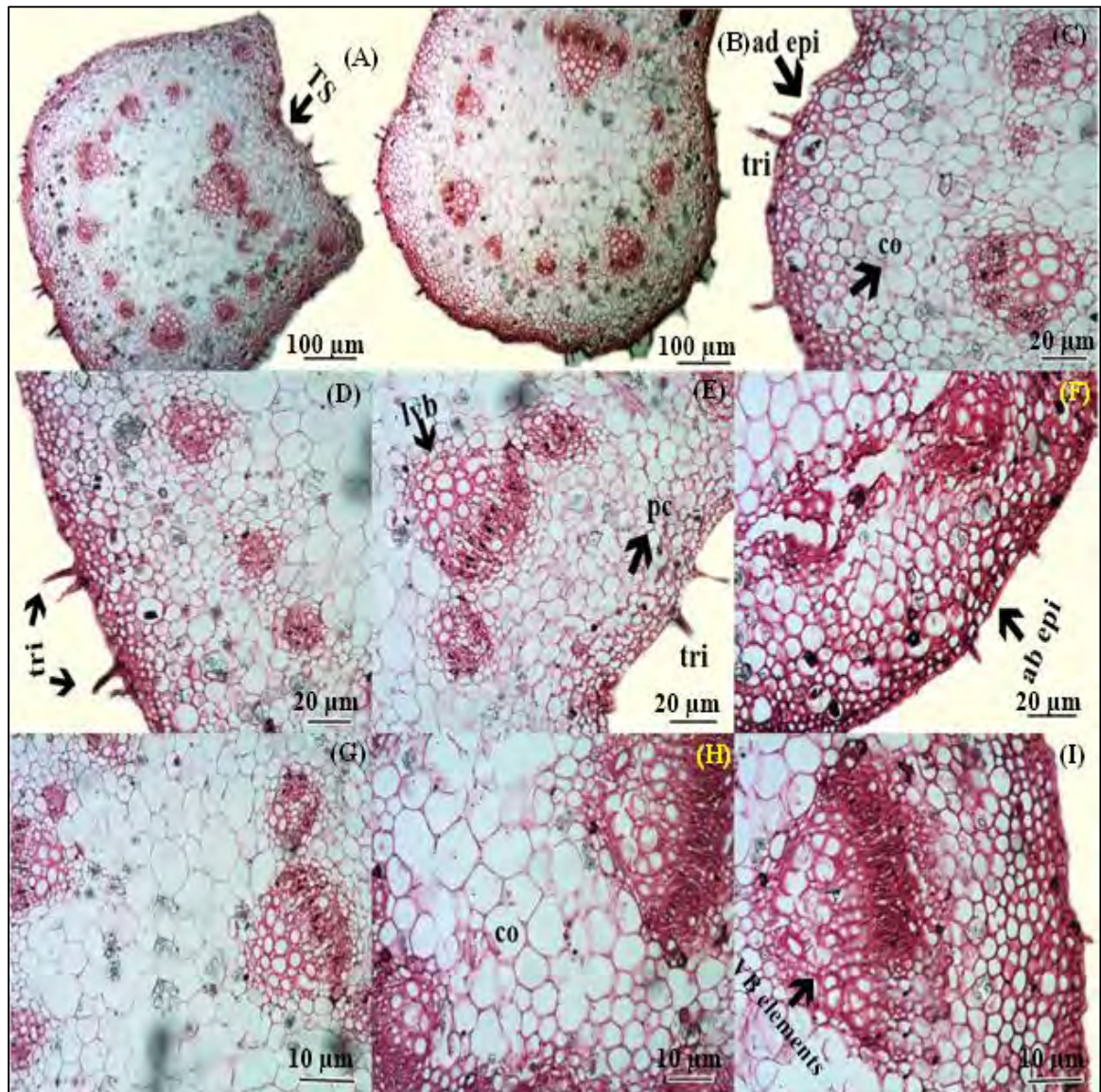


**Plate 99.** Photomicrographs of Petiole Section of *Chenopodium murale* L. (A and B) Transverse Section (100  $\mu\text{m}$ ), (C) Adaxial epidermis layer (20  $\mu\text{m}$ ), (D) Trichomes (20  $\mu\text{m}$ ), (E) Lateral VB and parenchymatous cell (20  $\mu\text{m}$ ), (F) Abaxial layering of epidermis (20  $\mu\text{m}$ ), (G and H) Lamellar collenchyma cells (10  $\mu\text{m}$ ), (I) VB showing vessel elements (10  $\mu\text{m}$ ). TS=Transverse section, lvb= Lateral vascular bundle, ad epi= Adaxial epidermis, ab epi= Abaxial epidermis, co=Collenchyma, pc= tri= Trichomes, Parenchyma, xy= xylem, ph= phloem.

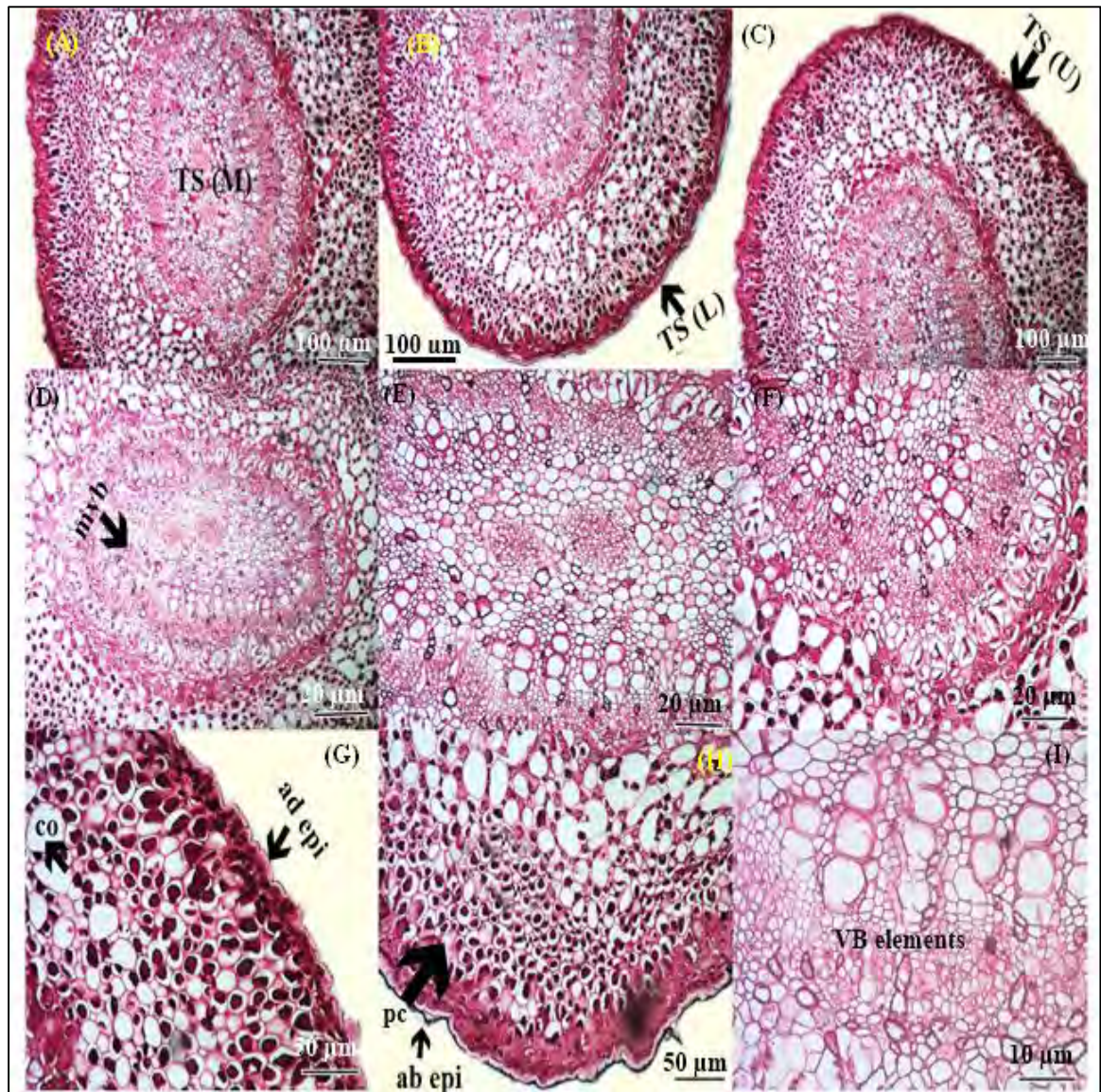


**Plate 100.** Photomicrographs of Petiole Section of *Digera muricata* (L.) Mart. (A) Mid view of Transverse section (100  $\mu$ m), (B) Lower side of TS (100  $\mu$ m), (C) Upper side view of TS (100  $\mu$ m), (D, E and F) Median VB sectioning (20  $\mu$ m) (G) Adaxial epidermal layer with collenchymatous cell (50  $\mu$ m), (H) Abaxial epidermis and parenchyma cells (50  $\mu$ m), (I) Vessel elements in VB (10  $\mu$ m). TS=Transverse section, mvb= Median vascular bundle, ad epi= Adaxial epidermis, ab epi= Abaxial epidermis, co=Collenchyma, pc= Parenchyma, xy= xylem, ph= phloem.



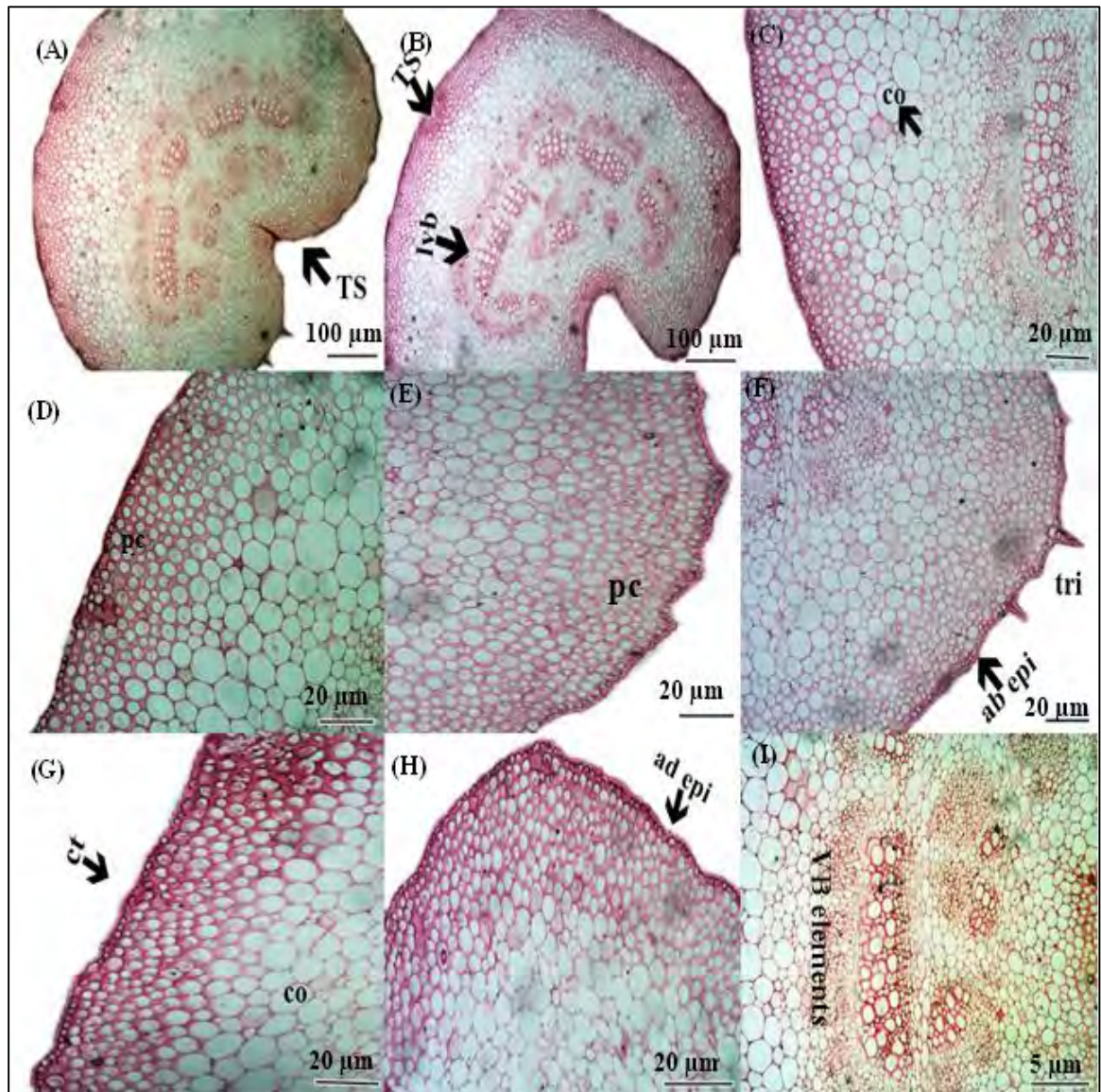


**Plate 101.** Photomicrographs of Petiole Section of *Gomphrena celosioides* Mart. (A and B) TS and lateral vascular bundle (100 μm), (C) Collenchyma layering of cell (20 μm), (D and E) Lateral side views of TS showing parenchymatous cells (20 μm), (F) Abaxial epidermis with trichomes (20 μm), (G) Cuticle layer and collenchymatous cells (20 μm), (H) Adaxial epidermal side (20 μm), (I) VB portioned into xylem and phloem (5 μm). TS=Transverse section, lvb= Lateral vascular bundle, ad epi= Adaxial epidermis, ab epi= Abaxial epidermis, co=Collenchyma, pc= Parenchyma, ct= Cuticle, tri= Trichome, xy= xylem, ph= phloem.

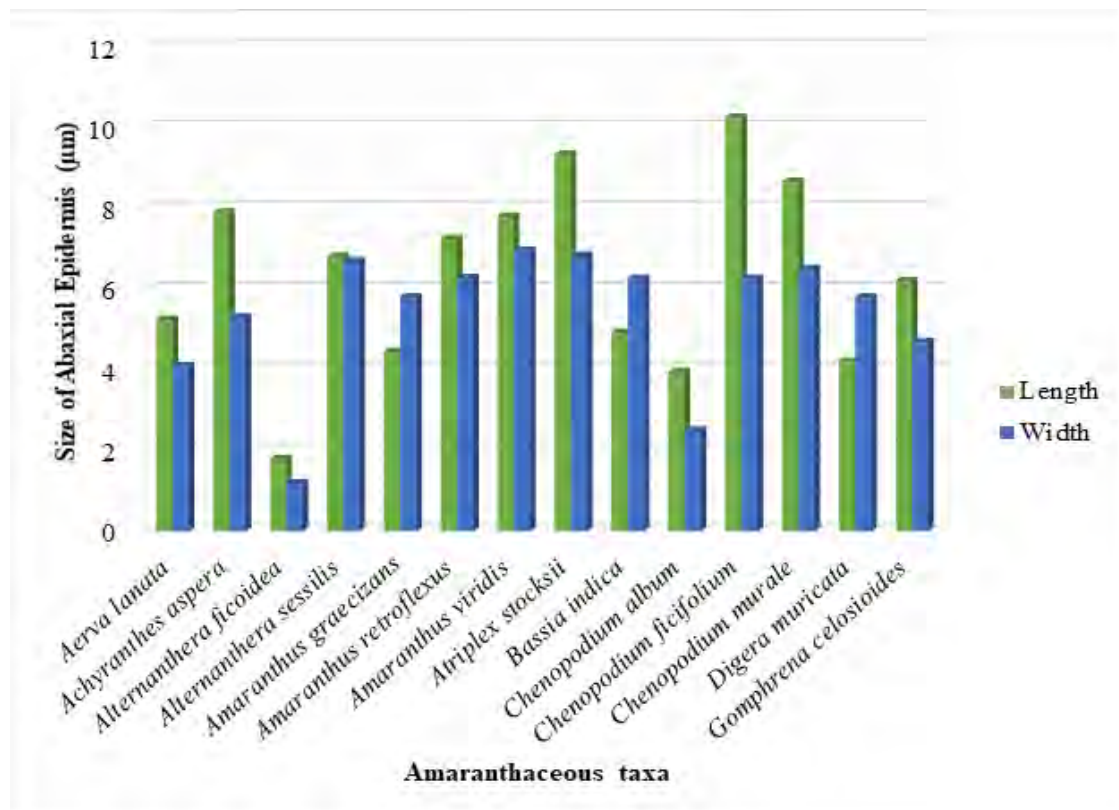


Figure 66. Mean epidermal cells size on abaxial surface in Amaranthaceae taxa

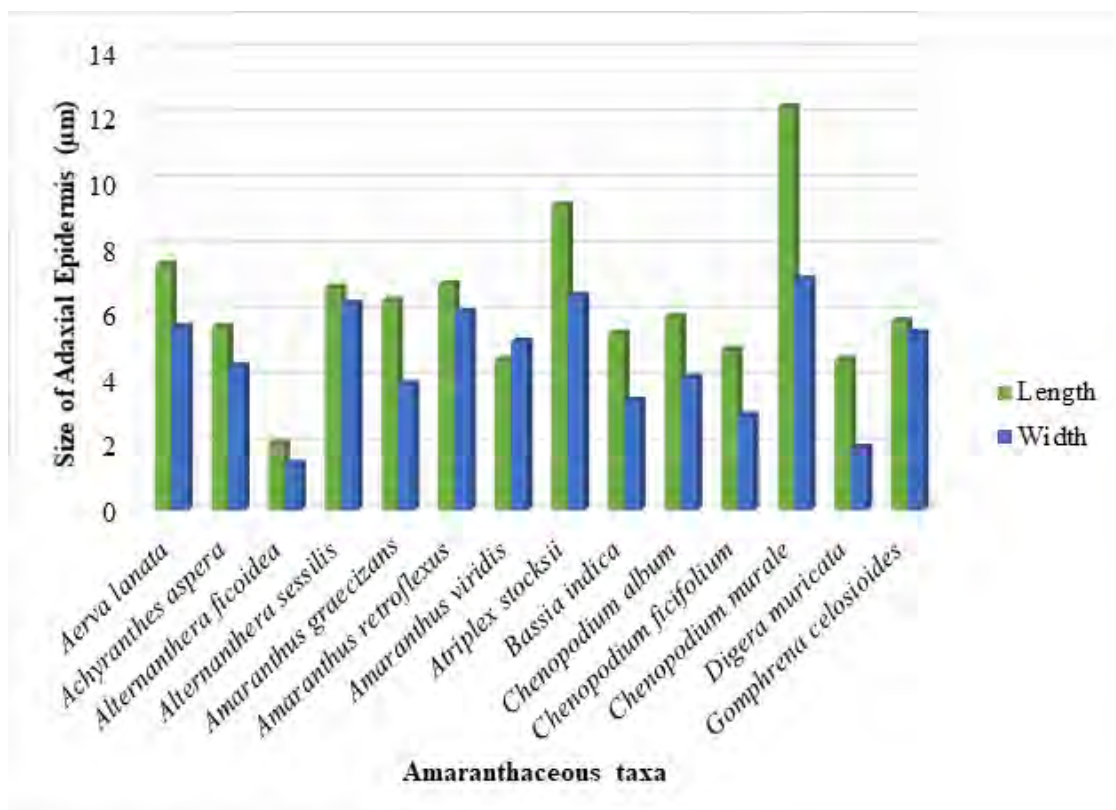


Figure 67. Mean epidermal cells size on adaxial surface in Amaranthaceae taxa.

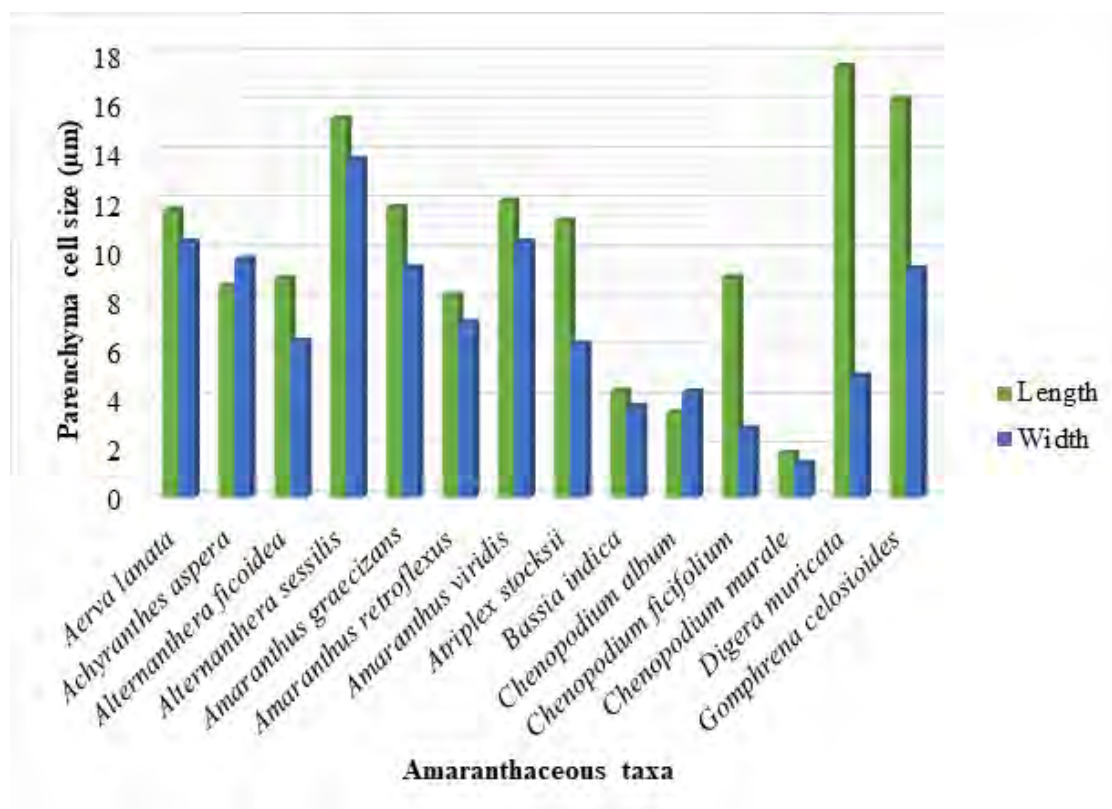


Figure 68. Variations of parenchyma cell size in Amaranthaceous taxa

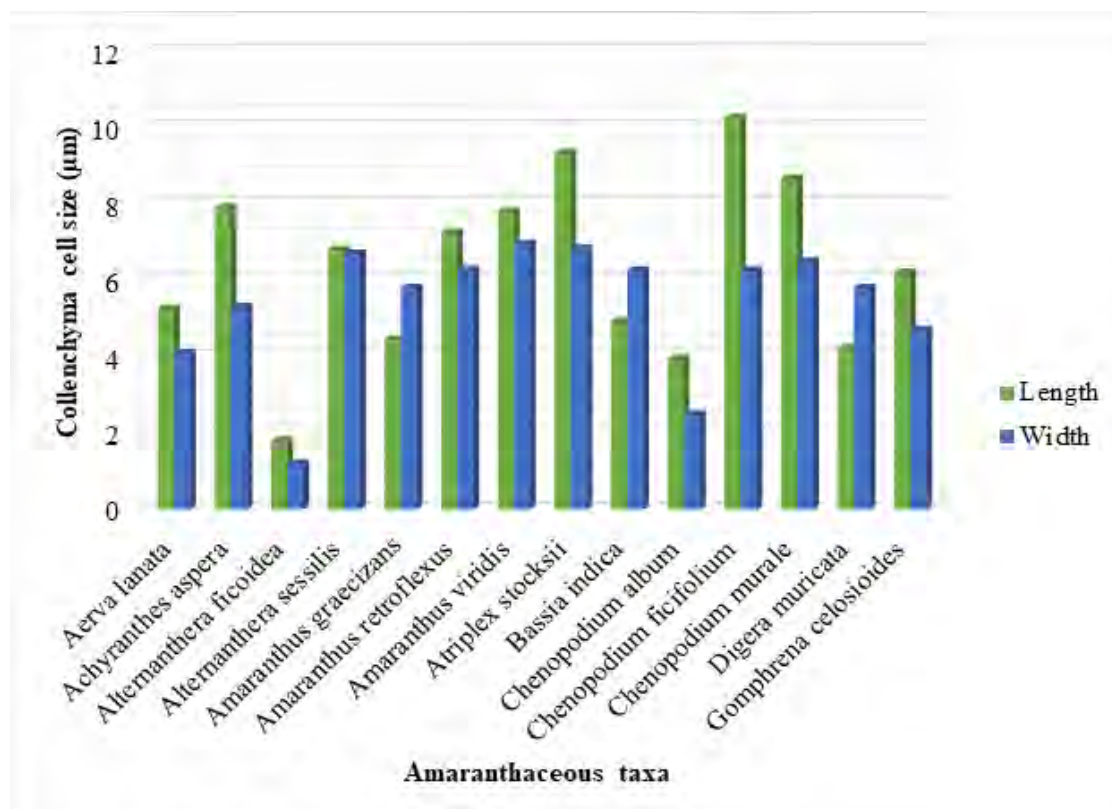


Figure 69. Mean collenchyma cell size variations in Amaranthaceous taxa

### 3.4.18 Discussion

A total of 14 Amaranthaceous species were investigated for petiole vasculature from the Thal desert. Amaranthaceae is considered one of the dominant families in deserted regions. Previously, research on the micromorphological parameters of several Amaranthaceous species was done in Pakistan (Hussain et al., 2018; Nazish et al., 2020). However, no comprehensive study on the petiole vascularization of Amaranthaceae from the desert rangeland has been reported. Therefore, the objective of the current study was to develop a petiole microanatomy-based identification guide for Amaranthaceous taxa.

The histology of the families Amaranthaceae and Chenopodiaceae has been studied by numerous authors globally (El-Ghamery et al., 2017; Zumaya-Mendoza et al., 2019; Safiallah et al., 2017; Viana et al., 2021). Nazish et al., (2020) researched the foliar leaf micromorphology and systematics of halophytic *Amaranthus* taxa from the salt range. Her studies demonstrate that quantitative parameters of the leaf epidermis provide information about the micro-histological organization. Hussain et al., (2018) identified Amaranthaceous taxa based on anatomical peculiarities, including stomata type, trichomes and epidermal cell form, glands, stomatal index, and guard cell. Comparative anatomical structures of leaves and stems from the genus *Amaranthus* reported by El-Ghamery et al., (2017) from Egypt, explored uniseriate epidermis and ground tissue of angular-shaped collenchyma and thin-walled parenchyma. Recently Belmonte et al., (2022) described the foliar structures of three *Tillandsia* species from the arid Atacama Desert. *Tillandsia* species have hypostomatic leaves, anomocytic stomata, and squamiform trichomes. In another study by (Ashfaq et al., 2019) to characterize and identify the Convolvulaceous species, it was hypothesized that the density of glandular trichomes decreased with increasing aridity factor. Asteraceous species inhabited in xeric Mexico ecological zone were shown foliar epidermal traits possess mesomorphic leaf architecture (Rivera et al., 2017). The xeric Asteraceous taxa possessed mesomorphic traits to have multiple layers of palisade parenchyma bundle sheaths, single-layered epidermis, and simple lamina. Morales-Tapia et al., (2019) used scanning microscopy to unveil histological sections of *Argylia radiata* to describe the survival in the driest desert of Chile and Peru. The adaptations

on the leaf surface of *Argylia radiata* enhance gas exchanges with flat spongy parenchyma cells and amphistomatous leaves.

The data analyzed using microscopic tools validated the implications of petiole vasculature as a taxonomic approach in the Amaranthaceous taxa and proved helpful in identifying valuable intergeneric features. Alwadie (2005) showed in *Aerva javanica* the uniseriate, multi-articulate, and stellate base trichomes on the leaf surface, while our findings described no trichome features along the petiole margins. Nameer et al., (2017) analyzed a cross-sectional view to show that *Amaranthus albus* has a crescent-shaped quadric side, while *Amaranthus gracilis* has a crescent-shaped but winged-side petiole. El-Ghamery et al., (2017) studied the root anatomy of *Amaranthus* species with the formation of successive cambia, which has been noticed to be used in the delimitation of microanatomical traits. The most important character state visualized is the type of petiole vascular bundles: closed collateral and concentric types. *Bassia* species have resulted in cambia comprised of three rings of vascular collateral-type bundles separated by parenchymatous cellulose rays (Aurelia et al., 2013). Amaranthaceae are characterized by a predominant successive cambium that is concentric and successive cambium patches are less frequent (Zumaya-Mendoza et al., 2019).

Duarte and Debur (2004) explained that collateral vascular bundles, varying in number and arrangement in the midrib and petiole, are mentioned for the *Alternanthera spp.* Hussain et al., (2018) reported irregular epidermal cells on both leaf surfaces and multicellular capitate trichomes only on the abaxial side of *Alternanthera sessilis*. Our research explains the circular-shaped epidermis cells and the lack of trichome features in the petiole section of *Alternanthera sessilis*. We found irregular-shaped epidermal cells with isodiametric parenchyma cells in *Alternanthera ficoidea*, which is somehow similar to the findings of Patil and Kore (2018). The micromorphology of trichomes along the petiole surface in *Atriplex stocksii* was investigated to characterize unicellular, pointed, e-glandular trichomes. A study by Tahmasebi (2021) on the stem epidermis in Chenopodiaceae revealed trichomes in *Atriplex* species show a great variety in terms of unicellular or multi-cellular and tuberous types.

Gaafar (2019) elaborates that stem morpho-anatomy from Egypt reported that epidermal cells were undulated in *Chenopodium album* and *Chenopodium ficifolium*,

and straight in *Chenopodium murale*. An angular stem shape is observed in *Chenopodium ficifolium* while in our case, *Chenopodium album* has a C-shaped petiole and irregular epidermal cells. It was also noted that *Chenopodium murale* had a sulcate petiole and a polygonal epidermis cell shape, while *Chenopodium ficifolium* had isodiametric epidermis cells with a C-shaped petiole outline. Ishtiaq et al., (2018) performed microscopic transverse sectioning of *Amaranthus graecizans* subsp. *Silvestris* leaves, stem, and root. Periderm was found on both the stem and the leaf. Palisade tissue, spongy mesophyll tissues, and trichomes were also visible in the transverse section of the leaf. However, this study mentioned U-shaped petiole outline and lamellar collenchymatous layers in *Amaranthus graecizans*.

Okeke et al., (2020) recently explained the cup-shaped petiole with a single-layered epidermis, 2-3 layers of collenchyma cells, and 5 crescent-shaped vascular bundles in *Celosia argentea*. A crescent-shaped petiole with a single-layered epidermis, two to three pinkish layers of collenchyma cells, and three vascular bundles near the upper section were reported in *Gomphrena celosioides*. Previously, Shaheen (2007) mentioned secondary vascular bundles in the petioles of legumes vary between leaf trace structures and this is considered as a defining feature in phylogeny. Taia et al., (2020) explained that the petiole concentric amphivasal vascular bundles of *Amaranthus spinosus* and *Amaranthus hybridus* are compatible with earlier findings by El-Ghamery et al., (2017). Variations were also observed in petiole vascular bundles and trichomes observed in *Amaranthus hybridus* (Ozimedede et al., 2019).

This study reveals that the petiolar vascularization of Amaranthaceae is taxonomically fundamental in defining the species. The basic inquiry is to identify petiole features and maximize their significance for character correlations using a statistical approach. Anatomical traits have proven to be quite helpful in determining linkages between genera and species, which become increasingly important in evolutionary relationships.

### 3.4.19 Petiole Micromorphology of Euphorbiaceous Species

Different petiolar characters of eight Euphorbiaceous taxa were studied. Petiole was measured both quantitatively and qualitatively shown in (Table 37, 38 & 39). Euphorbiaceous taxa showed extensive variation in shape and size viewing their recorded taxonomic assessment (Plate 102 to 109).

Data on qualitative and quantitative features of the petiole provided significant characters to be considered in taxonomic studies of the petiole of some Euphorbiaceous species. A combination of petiole anatomical characteristics may be helpful in the identification of taxa. Though the composition and pattern of distribution of tissues are approximately uniform in the studied taxa, there are distinguishing qualitative characteristics such as the shape of petiole and vascular bundle, the shape of collenchyma cells, parenchyma and epidermal cells, presence, and absence of wings and trichomes (Table 37). Significant quantitative characteristics include variation in the number of vascular bundles, vessel element, layers of collenchyma, parenchyma and epidermal cells, length, and width of parenchyma, collenchyma, and epidermal cells (Table 38 & 39). Anatomical observations on the transverse section of the petiole of studied species revealed interspecific variations that are important in the classification and delimitation of taxa.

#### a) Petiole Outline

Results showed great diversity in the shape of the petiole in transverse view. Six different shapes were observed; *C. plicata* and *E. helioscopia* has irregular arc-shaped outlines (Plate 102 & 106). Rounded petiole outline found in the *C. bonplandianus* and *E. hirta* (Plate 104 & 107). Flat with lateral wings shaped petiole was found in *C. tinctoria* (Plate 103). *E. granulata* has a round shape (Plate 105). *E. sarpens* has a flat with a slightly U-shaped petiole (Plate 107). *R. communis* has a Flat closed U-shaped with pointed margins petiole (Plate 108).

#### b) Vascular Bundle

The findings of the present study revealed the presence of vascular bundles in each studied taxa organized around the parenchymatous tissues. The maximum number of vessel elements was found in the *E. helioscopia* (67) while the minimum was noted in *E. granulata* (17 in each). Mostly the species showed indistinguishable vascular

bundles organized with no clear boundary. The highest numbers of vascular bundles were found in *E. sarpens* (9) and lowest were found in *E. hirta* (2). Variations found in vascular bundle shape; rounded vascular bundle found in *C. plicata* and *E. sarpens*, open arc-shaped with incurved ends vascular bundle found in *C. tinctoria* and *E. granulata*, open arc-shaped in *C. bonplandianus* and *R. communis*, *E. helioscopia* has closed rectangular shaped and *E. hirta* has an open round with incurved ends vascular bundles.

### c) Epidermal Cells

Different types of epidermal cells were examined. *C. tinctoria*, *E. hirta*, and *R. communis* cells are irregular in shape. *C. plicata*, *E. granulata*, and *E. sarpens* have rectangular to square shape cells. Polygonal to oval-shaped cells are found in *C. bonplandianus* while rectangular isodiametric cells are found in *E. helioscopia*. Quantitatively along the abaxial surface maximum cell length and width were observed in *C. plicata* (21.4  $\mu\text{m}$ ) and *C. tinctoria* (17.25  $\mu\text{m}$ ) respectively. Whereas epidermis cell minimum length (8.5  $\mu\text{m}$ ) in *E. helioscopia* and width (6.65  $\mu\text{m}$ ) in *E. granulata* were measured (Figure 70). Along the adaxial side highest cell length and width were recorded for *C. tinctoria* (28.9  $\mu\text{m}$ ) and (21.4  $\mu\text{m}$ ) respectively. However, the lowest cell length (6.12  $\mu\text{m}$ ) and width (7.04  $\mu\text{m}$ ) were calculated for *E. granulata* (Figure 71).

### d) Parenchyma Cells

Parenchyma cells cover a large part of the petiole and different shapes of cells were detected such as polygonal cells found in *C. plicata*, and *R. communis*. Irregular cells were found in *C. tinctoria* and *E. hirta*. Polygonal to irregular in *C. bonplandianus*. Rectangular to irregular cells were present in *E. granulata* whereas rounded polygonal was found in *E. hirta*. Polygonal to isodiametric parenchyma cells were examined in *E. sarpens*. Parenchyma was found to be multilayered, and maximum cell length (55.4  $\mu\text{m}$ ) and width (54.6  $\mu\text{m}$ ) were measured for *R. communis*. While the minimum length was calculated for *C. bonplandianus* (26.2  $\mu\text{m}$ ) and width for *E. granulata* (15.3  $\mu\text{m}$ ) as shown in Figure 73.

### e) Collenchyma Cells

Collenchyma cells were generally observed were detected to be of diverse shapes such as angular in *C. plicata*, *E. helioscopia*, and *R. communis*. The lamellar



type was detected in *C. tinctoria*, *E. granulate*, *E. hirta*, and *E. sarpens*. Angular and lamellar both types of cells were observed in *C. bonplandianus*. The highest number of collenchyma layers was 19, found in *E. hirta* and the lowest was nine found in *C. plicata*. Similarly, the maximum length and width were recorded for *C. tinctoria* (35.6  $\mu\text{m}$ ) and (22.45  $\mu\text{m}$ ) respectively. Whereas the lowest length (10.9  $\mu\text{m}$ ) and width (8.6  $\mu\text{m}$ ) were noted for *C. bonplandianus* (Figure 72).

#### **f) Trichomes**

In the present study, only two species showed the trichomes outgrowths such as *E. hirta* and *E. sarpens*. Both species have glandular unicellular capitate trichomes features. According to Gales and Toma (2006) trichomes found in *Euphorbia* were simple, unicellular, and uniseriate. Aldhebiani and Jury (2013) presented the same observations. Sereena and Shahida (2015) reported only uniseriate trichomes in *E. hirta* which was in accordance with the present observation.

### 3.4.20 Identification Keys Based on Euphorbiaceous Petiole Features

1 + Petiole wings absent.....	2
- Petiole wings present.....	7
2 + U shaped petiole, lamellar collenchyma.....	<i>E. granulata</i>
- Closed rectangular vascular bundle.....	3
3 + Irregular arc-shape petiole, angular collenchyma cells.....	<i>E. helioscopia</i>
- Open arc shaped vascular bundle.....	4
4 + Flat closed U shaped petiole.....	<i>R. communis</i>
- Slightly U shaped petiole outline.....	5
5 + Rounded vascular bundle, trichome present.....	<i>E. serpens</i>
- Open Round with incurved ends vascular bundles.....	6
6 + Round shape petiole, trichome present.....	<i>E. hirta</i>
- Irregular arc shaped petiole.....	7
7 + Rounded vascular bundle, petiole wings present.....	<i>C. plicata</i>
- Lateral winged flat petiole.....	8
8 + Open arc-shaped incurved ends petiole, lamellar collenchyma.....	<i>C. tinctoria</i>
- Rounded petiole outline.....	9
9 + Open arc winged vascular bundle, both lamellar and angular collenchyma.....	<i>C. bonplandianus</i>
-	

**Table 37.** Petiole micro-morphological qualitative attributes of Euphorbiaceous species.

Sr. No.	Euphorbiaceous taxa	Petiole shape	Vascular bundle shape	Epidermal cell shape	Collenchyma type	Parenchyma type	Trichomes (+, -)	Petiole wings (+,-)
1.	<i>Chrozophora plicata</i> (Vahl) A.Juss. ex Spreng.	Irregular arc-shaped	Rounded	Rectangular to square	Angular	Polygonal	-	+
2.	<i>Chrozophora tinctoria</i> (L.) A.Juss.	Flat with lateral wings	Open arc-shaped with incurved ends	Irregular	Lamellar	Irregular	-	+
3.	<i>Croton bonplandianus</i> Baill.	Rounded	Open arc-shaped	Polygonal to oval	Angular and Lamellar	Polygonal to irregular	-	+
4.	<i>Euphorbia granulata</i> Forssk.	U-shaped	Open arc-shaped with incurved ends	Rectangular to square	Lamellar	Rectangular to irregular	-	-
5.	<i>Euphorbia helioscopia</i> L.	Irregular arc-shaped	Closed rectangular shaped	Rectangular isodiametric	Angular	Irregular	-	-
6.	<i>Euphorbia hirta</i> L.	Rounded	Open Round with incurved ends	Irregular	Lamellar	Rounded polygonal	+	-
7.	<i>Euphorbia serpens</i> Kunth	Flat with slightly U shaped	Rounded	Rectangular to square	Lamellar	Polygonal to isodiametric	+	-
8.	<i>Ricinus communis</i> L.	Flat closed U-shaped with pointed margins	Open arc-shaped	Irregular	Angular	Polygonal	-	-

**Keywords:** (+) = Present; (-) = Absent

**Table 38.** Quantitative measurements of petiole anatomical traits of selected Euphorbiaceous species.

Sr. No.	Euphorbiaceous taxa	PL (µm)	No of VB	Collenchyma layers			Abaxial Epidermis		Adaxial Epidermis	
				Ab	Ad	C	(Min-Max)= x ± SE (µm)			
							Length	Width	Length	Width
1.	<i>Chrozophora plicata</i> (Vahl) A.Juss. ex Spreng.	210	7	3	5	1	(19.35-22.7)=21.4±1.04	(11.4-14.25)=13.1±1.05	(25-30.3)=27.6±0.76	(14.2-17)=15.7±1.08
2.	<i>Chrozophora tinctoria</i> (L.) A.Juss.	190	3	6	4	3	(15.5-26.2)=20.85±3.4	(13.7-19.5)=17.25±1.09	(27-30.5)=28.9±1.09	(20.1-22.5)=21.4±0.5
3.	<i>Croton bonplandianus</i> Baill.	310	6	3	7	2	(18.3-23.5)=21.15±1.02	(11.2-13.5)=12.2±0.73	(12-14.8)=13.5±1.2	(8.8-13.5)=11.2±1.32
4.	<i>Euphorbia granulata</i> Forssk.	240	5	4	2	4	(13-16)=14.95±1.1	(5.9-7.35)=6.65±0.39	(4.8-7.6)=6.12±0.87	(5.5-8.4)=7.04±0.61
5.	<i>Euphorbia helioscopia</i> L.	330	8	5	8	3	(6.2-10.4)=8.5±1.18	(6.15-8.35)=7.55±0.63	(9.1-13.9)=11.3±1.3	(6.85-10.6)=8.9±1.76
6.	<i>Euphorbia hirta</i> L.	275	2	8	6	5	(14.2-17.5)=16.2±1.05	(9.1-11.45)=10.4±0.91	(13-16.3)=14.8±1.82	(7.45-10.4)=9.3±0.54
7.	<i>Euphorbia serpens</i> Kunth	160	9	2	4	7	(16-18.5)=17.4±0.97	(8.5-10.7)=9.75±0.68	(12-15.2)=13.8±1.33	(7.5-9.3)=8.25±0.62
8.	<i>Ricinus communis</i> L.	295	6	6	2	4	(14.5-18.2)=16.4±1.51	(10.3-14.7)=12.6±1.43	(17-20.9)=19.5±0.7	(18.3-21.6)=20.1±0.5

**Keywords:** PL= Petiole length; VB= Vascular bundle; Ad= Adaxial; Ab= Abaxial; C= Central; Min = Minimum; Max = Maxim; ; x = Mean; SE = Standard Error; µm= micrometer

**Table 39.** Quantitative measurements of petiole anatomical traits of selected Euphorbiaceous species.

Sr. No.	Euphorbiaceous taxa	Vessel Elements	Collenchyma (Min-Max)= $\bar{x} \pm SE$ ( $\mu\text{m}$ )		Parenchyma (Min-Max)= $\bar{x} \pm SE$ ( $\mu\text{m}$ )	
			Length	Width	Length	Width
1.	<i>Chrozophora plicata</i> (Vahl) A.Juss. ex Spreng.	19	(20.3-30.8)=25.3 $\pm$ 3.04	(10.1-21)=15.09 $\pm$ 1.46	(42-58.5)=50.1 $\pm$ 4.57	(27-43.7)=35.8 $\pm$ 3.92
2.	<i>Chrozophora tinctoria</i> (L.) A.Juss.	34	(31-42.5)=35.6 $\pm$ 3.91	(20.3-24)=22.45 $\pm$ 1.32	(44.5-56.5)=51.5 $\pm$ 2.62	(24-37.5)=30.4 $\pm$ 1.28
3.	<i>Croton bonplandianus</i> Baill.	28	(9.5-12.3)=10.9 $\pm$ 0.58	(7.5-9.65)=8.6 $\pm$ 0.88	(22-29.3)=26.2 $\pm$ 1.43	(19.15-23.4)=21.8 $\pm$ 1.04
4.	<i>Euphorbia granulata</i> Forssk.	17	(12-15.5)=13.1 $\pm$ 1.15	(9.5-11.55)=10.51 $\pm$ 0.56	(31-39.2)=34.7 $\pm$ 2.52	(14-16.5)=15.3 $\pm$ 1.19
5.	<i>Euphorbia helioscopia</i> L.	67	(31.5-34.8)=33.45 $\pm$ 1.41	(18-20.9)=19.7 $\pm$ 0.85	(42-49.5)=46.5 $\pm$ 1.86	(41.2-48.6)=45.2 $\pm$ 1.7
6.	<i>Euphorbia hirta</i> L.	29	(11.4-15.5)=13.6 $\pm$ 1.23	(8.5-10.6)=9.63 $\pm$ 0.74	(37.5-44.1)=40.9 $\pm$ 1.95	(25-33.5)=29.2 $\pm$ 1.07
7.	<i>Euphorbia serpens</i> Kunth	34	(31.5-35)=33.4 $\pm$ 0.86	(17-22.2)=19.2 $\pm$ 1.53	(42.5-52.5)=47.8 $\pm$ 2.08	(24-31.3)=27.95 $\pm$ 2.19
8.	<i>Ricinus communis</i> L.	39	(19-31.25)=25.5 $\pm$ 2.88	(16.2-21.7)=19.4 $\pm$ 1.67	(48.2-62.4)=55.4 $\pm$ 3.39	(44.8-59.5)=54.6 $\pm$ 3.91

**Keywords:** Min = Minimum; Max = Maxim;  $\bar{x}$  = Mean; SE = Standard Error;  $\mu\text{m}$ = micrometer

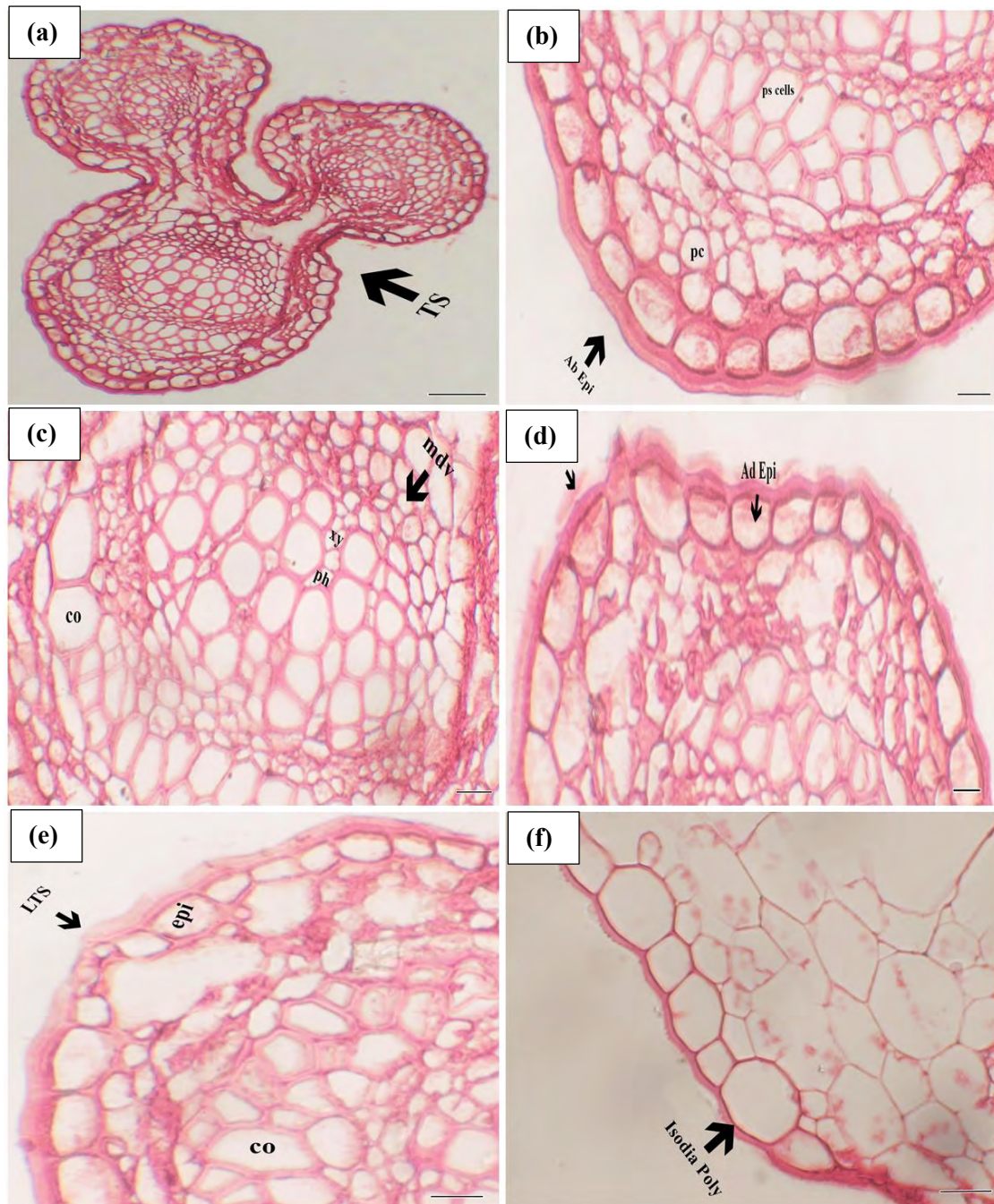


**Plate 102.** Photomicrographs of Petiole Section of *Chrozophora plicata* (Vahl) A.Juss. ex Spreng. (L.) Juss. (a): Transverse Section (100  $\mu\text{m}$ ), (b): Section of abaxial epidermis, palisade cells and parenchyma cells (20  $\mu\text{m}$ ), (c): Median vascular bundle (10  $\mu\text{m}$ ), (d): Section of adaxial epidermis and cuticle (20  $\mu\text{m}$ ), (e): Sectioning of lateral side epidermis and collenchyma cell (10  $\mu\text{m}$ ), (f) Abaxial isodiametric polygonal epidermal cell (10  $\mu\text{m}$ ). TS=Transverse section, mdv= Median Vascular Bundle, ad epi= adaxial epidermis, ab epi= abaxial epidermis, co=Collenchyma, xy= xylem, ph=phloem, VB= vascular bundle, pe = parenchyma

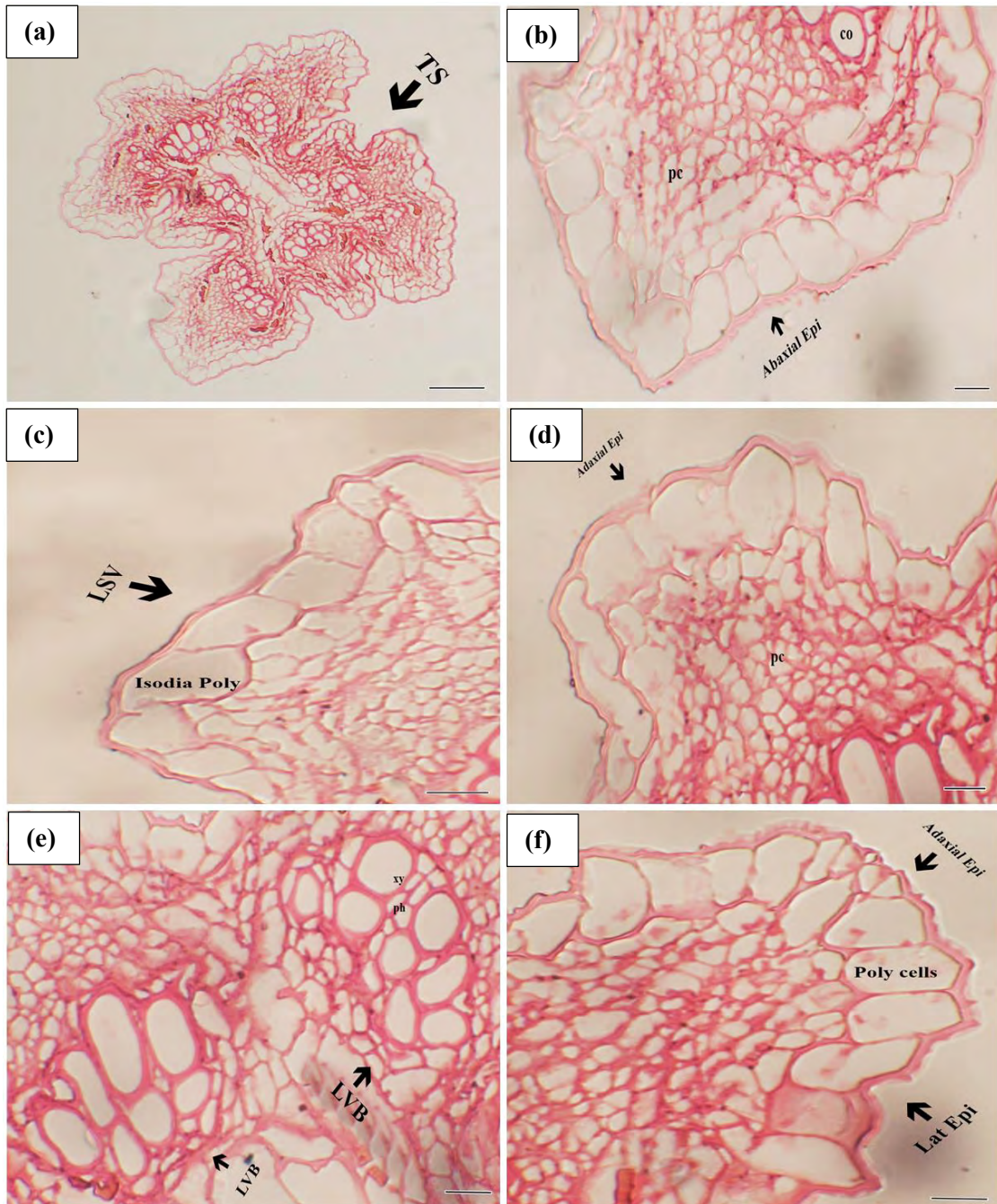
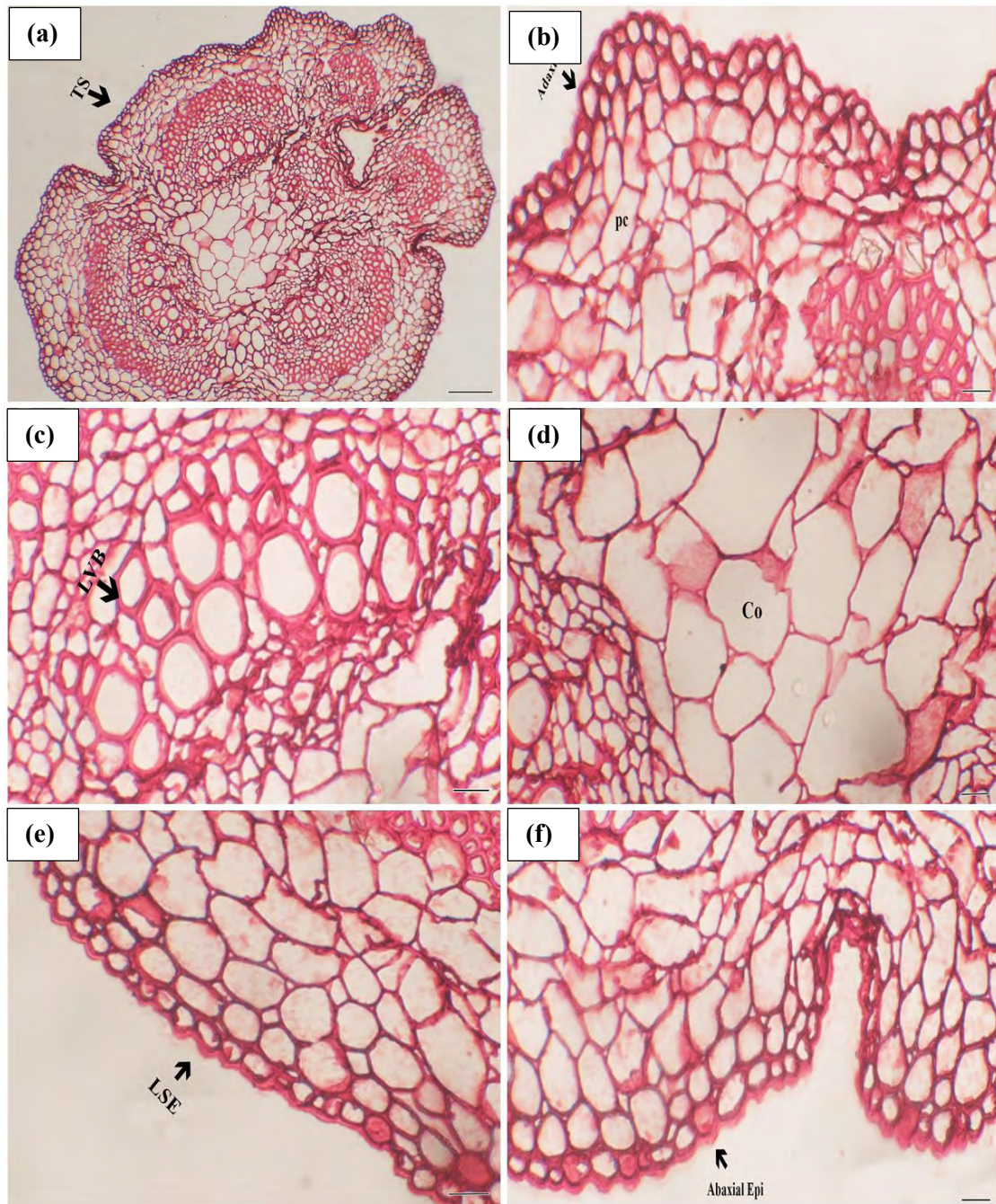
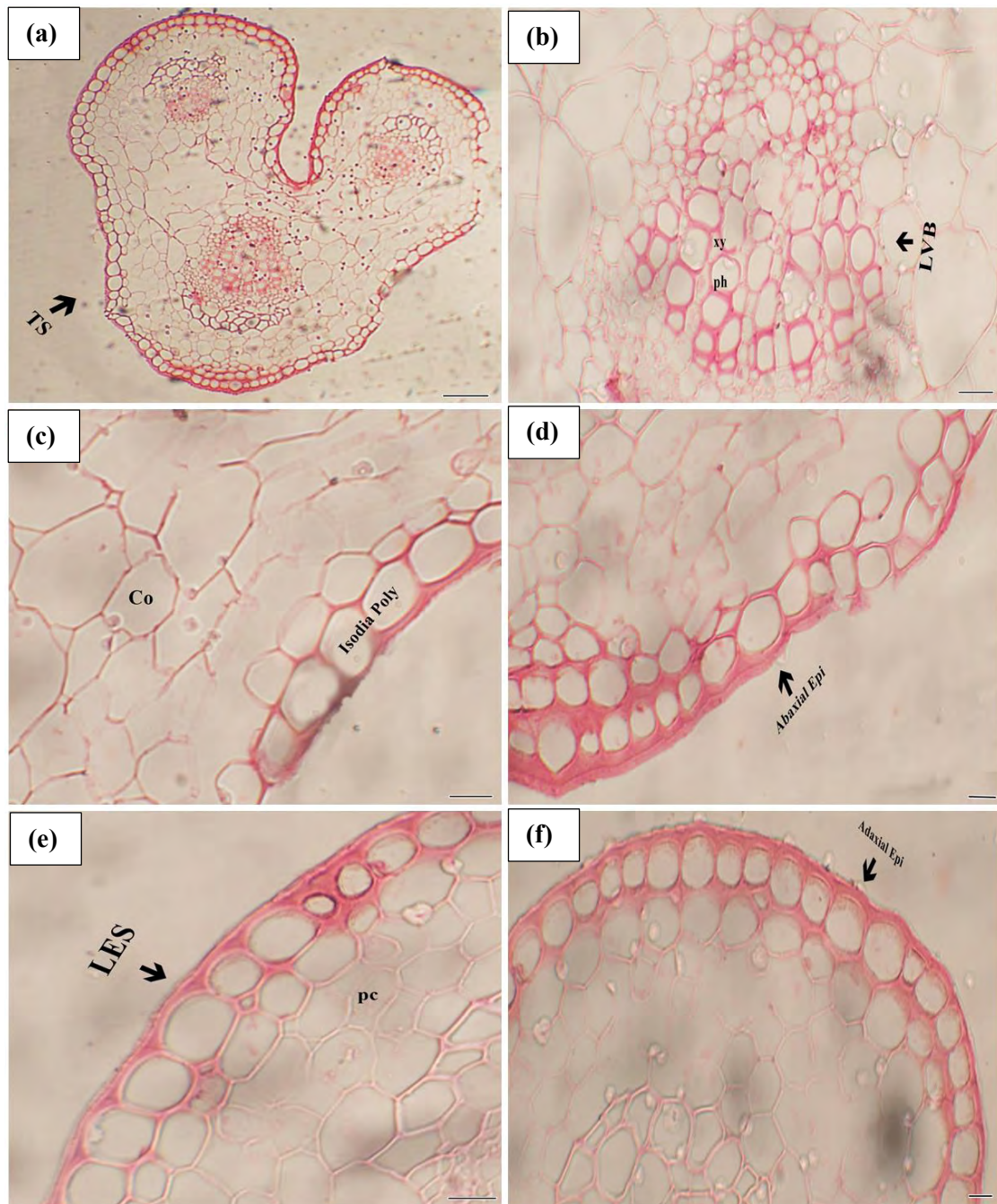


Plate 103. Photomicrographs of Petiole Section of *Chrozophora tinctoria* (L.) A.Juss. (a): Transverse Section (100  $\mu\text{m}$ ), (b): Section of abaxial epidermis, and parenchyma cells (50  $\mu\text{m}$ ), (c): Lateral ventral side isodiametric polygonal cells (20  $\mu\text{m}$ ), (d): Section of adaxial epidermis (20  $\mu\text{m}$ ), (e): Sectioning of lateral vascular bundle (10  $\mu\text{m}$ ), (f) Abaxial isodiametric polygonal epidermal cell and lateral epidermis (10  $\mu\text{m}$ ). TS=Transverse section, LVB= Lateral Vascular Bundle, ad epi= adaxial epidermis, ab epi= abaxial epidermis, VB= vascular bundle, pe = parenchyma, Isodia poly = Isodiametric polygonal.



**Plate 104.** Photomicrographs of Petiole Section of *Croton bonplandianus* Baill. (a): Transverse Section (100  $\mu\text{m}$ ), (b): Section of adaxial epidermis cells and parenchyma cells (50  $\mu\text{m}$ ), (c): Lateral vascular bundle (20  $\mu\text{m}$ ), (d): Section of collenchyma cells (10  $\mu\text{m}$ ), (e): Sectioning of lateral side epidermis (10  $\mu\text{m}$ ), (f) Abaxial isodiametric polygonal epidermal cell (10  $\mu\text{m}$ ). TS=Transverse section, LVB= Lateral Vascular Bundle, ad epi= adaxial epidermis, ab epi= abaxial epidermis, pe = parenchyma, co = collenchyma cells; LSE = Lateral side epidermis.





**Plate 105.** Photomicrographs of Petiole Section of *Euphorbia granulata* Forssk. (a): Transverse Section (100  $\mu\text{m}$ ), (b): Section of lateral vascular bundle showing xylem and phloem vessels (10  $\mu\text{m}$ ), (c): Collenchyma and isodiametric polygonal epidermis cells (10  $\mu\text{m}$ ), (d): Section of abaxial epidermis (20  $\mu\text{m}$ ), (e): Sectioning of lateral side epidermis (10  $\mu\text{m}$ ), (f) Adaxial isodiametric polygonal epidermal cell (20  $\mu\text{m}$ ). TS=Transverse section, LVB= Lateral Vascular Bundle and parenchyma cells, ad epi= adaxial epidermis, ab epi= abaxial epidermis, pc = parenchyma, co = collenchyma cells; LES = Lateral side epidermis.

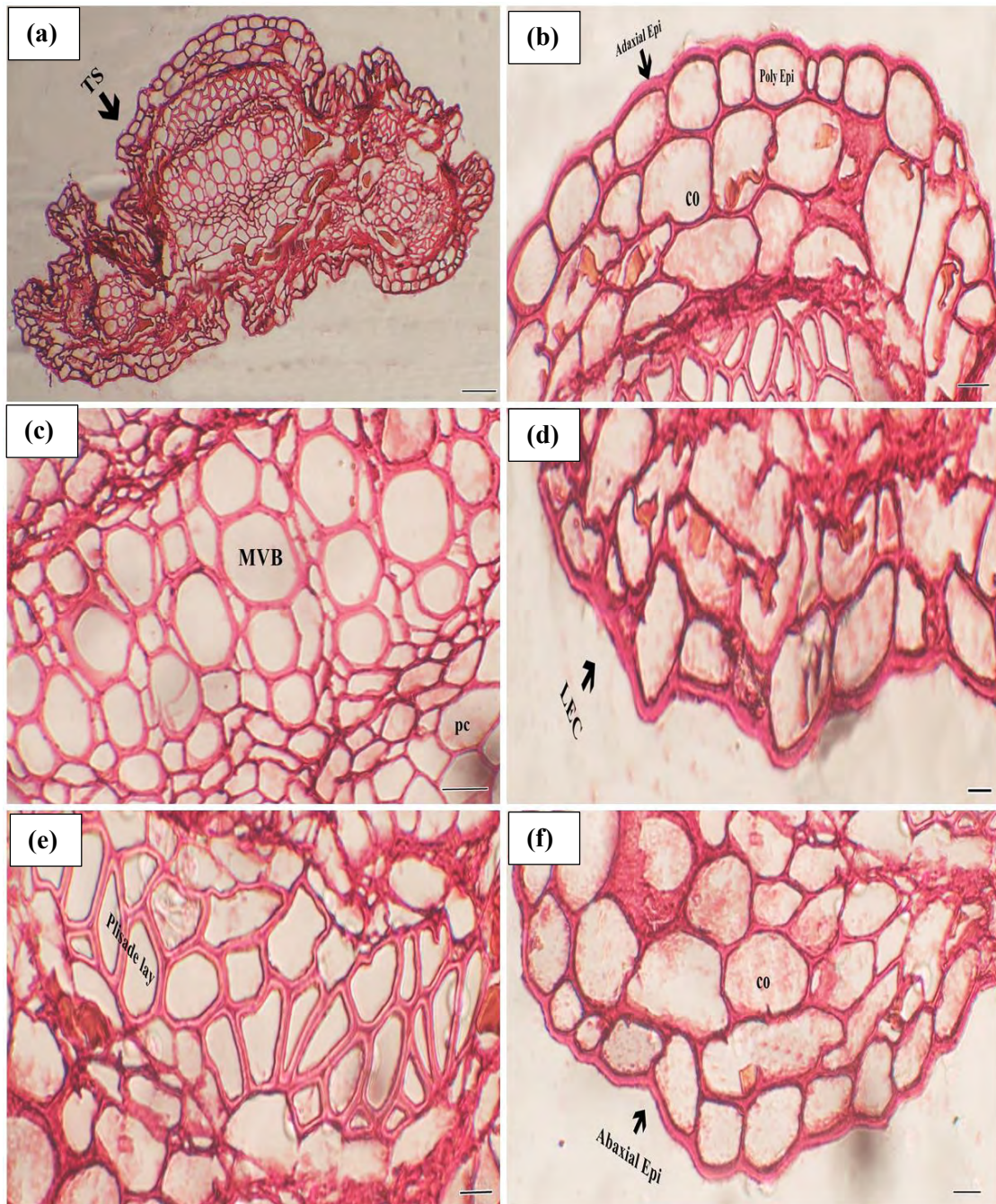


**Plate 106.** Photomicrographs of Petiole Section of *Euphorbia helioscopia* L. (a): Transverse Section (100 μm), (b): Section of adaxial epidermis cells and collenchyma cells (20 μm), (c): Median vascular bundle (10 μm), (d): Section of lateral epidermal cells (20 μm), (e): Sectioning of palisade layer (5 μm), (f) Abaxial epidermis and collenchyma cells (20 μm). TS=Transverse section, MVB= Median Vascular Bundle, ad epi= adaxial epidermis, ab epi= abaxial epidermis, co = collenchyma cells; LEC = Lateral epidermal cells.

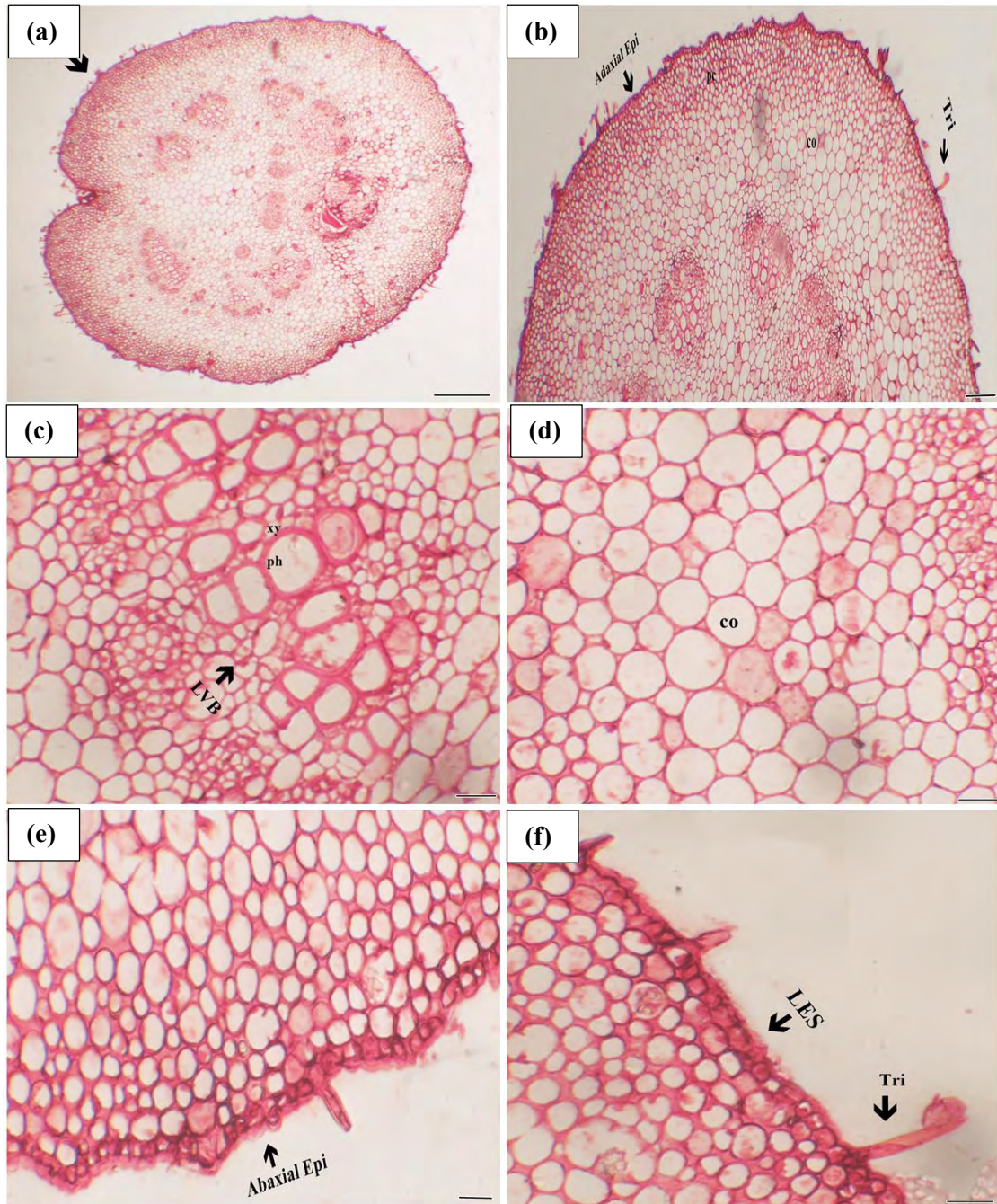


**Plate 107.** Photomicrographs of Petiole Section of *Euphorbia hirta* L. (a): Transverse Section (100  $\mu\text{m}$ ), (b): Section of adaxial epidermis cells and trichome (50  $\mu\text{m}$ ), (c): Lateral vascular bundle (10  $\mu\text{m}$ ), (d): Section of collenchyma cells (5  $\mu\text{m}$ ), (e): Sectioning of abaxial epidermis (20  $\mu\text{m}$ ), (f) Lateral epidermis side and trichome (10  $\mu\text{m}$ ). TS=Transverse section, LVB= Median Vascular Bundle, ad epi= adaxial epidermis, ab epi= abaxial epidermis, co = collenchyma cells; LES = Lateral epidermal surface, tri=Trichome

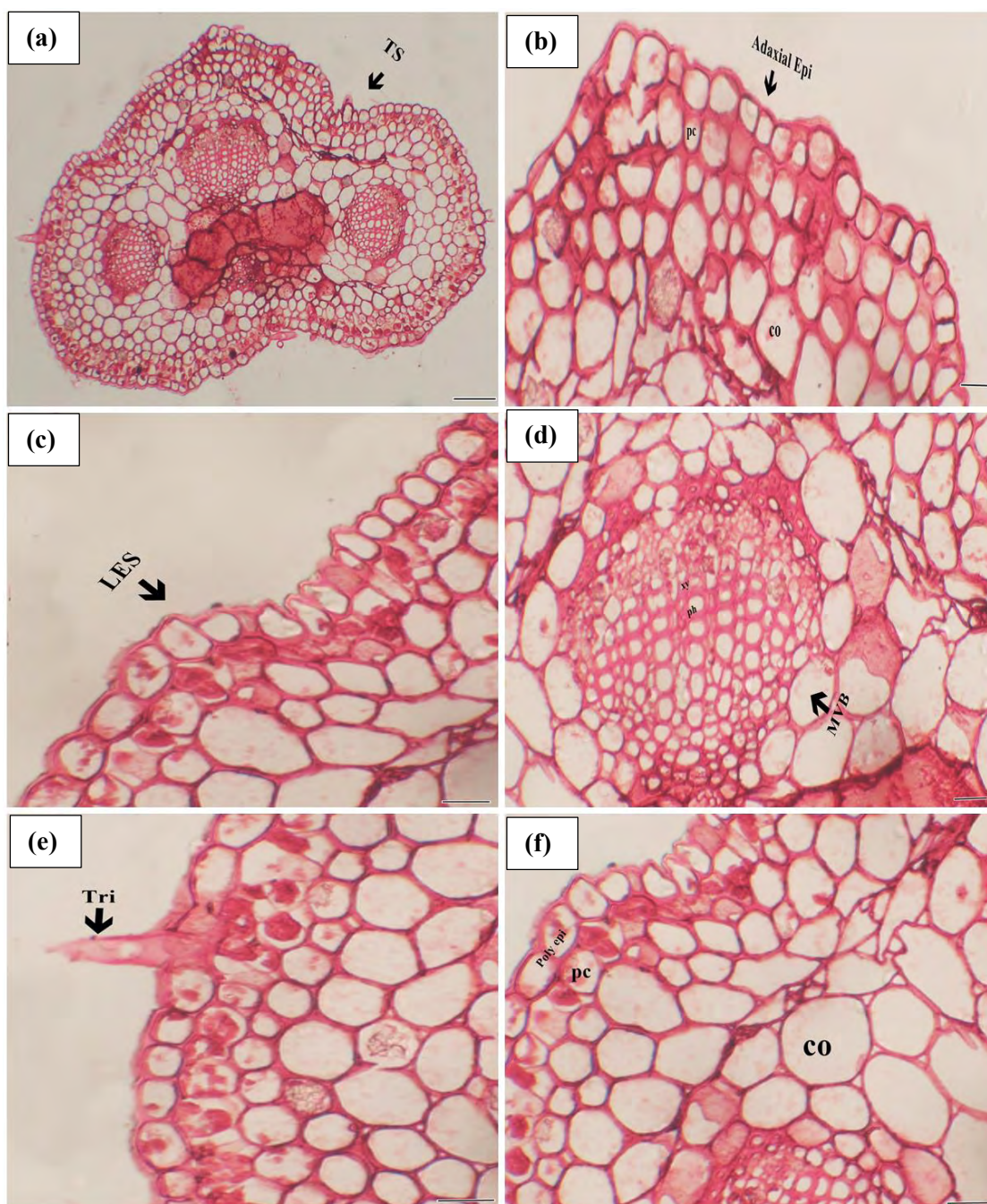


**Plate 107.** Photomicrographs of Petiole Section of *Euphorbia serpens* Kunth (a): Transverse Section (100  $\mu\text{m}$ ), (b): Section of adaxial epidermis (50  $\mu\text{m}$ ), (c): Lateral epidermal side (10  $\mu\text{m}$ ), (d): Section of median vascular bundle showing xylem and pholem (5  $\mu\text{m}$ ), (e): Sectioning of trichome (10  $\mu\text{m}$ ), (f) Polygonal epidermis cells parenchyma and collenchyma cells(10  $\mu\text{m}$ ). TS=Transverse section, MVB= Median Vascular Bundle, ad epi= adaxial epidermis, ab epi= abaxial epidermis, co = collenchyma cells, pc = parenchyma, LES = Lateral epidermal surface, Tri=Trichome, xy = xylem, ph = pholem

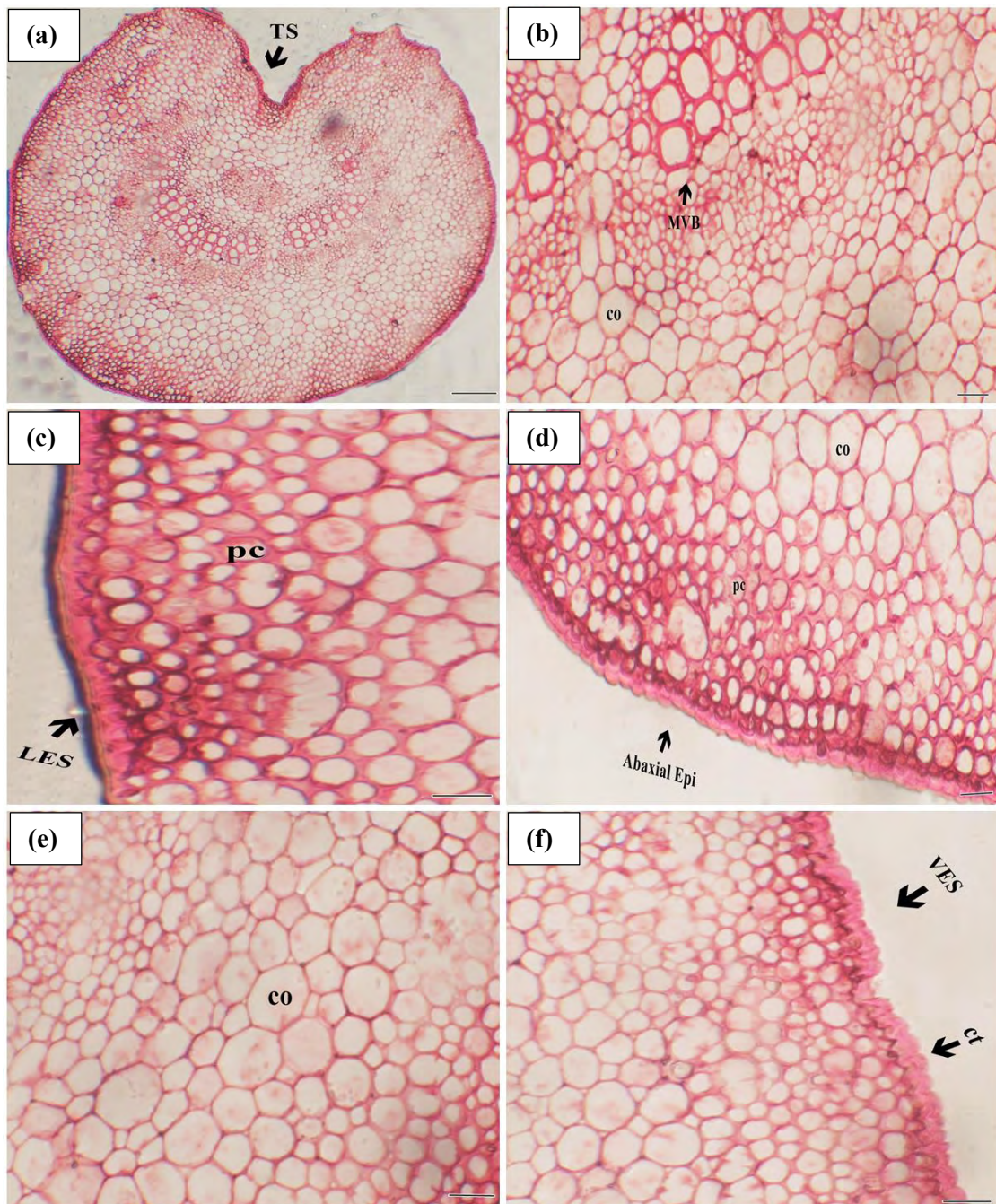


**Plate 109.** Photomicrographs of Petiole Section of *Ricinus communis* L. (a): Transverse Section (100  $\mu\text{m}$ ), (b): Section of median vascular bundle (20  $\mu\text{m}$ ), (c): Lateral epidermis side and parenchyma cells (10  $\mu\text{m}$ ), (d): Section of abaxial epidermis (10  $\mu\text{m}$ ), (e): Collenchyma cells (5  $\mu\text{m}$ ), (f) Ventral epidermis side and cuticle (10  $\mu\text{m}$ ). TS=Transverse section, MVB= Median Vascular Bundle, ad epi= adaxial epidermis, ab epi= abaxial epidermis, co = collenchyma cells; pc = parenchyma cells; VES= Ventral epidermal surface, ct= Cuticle

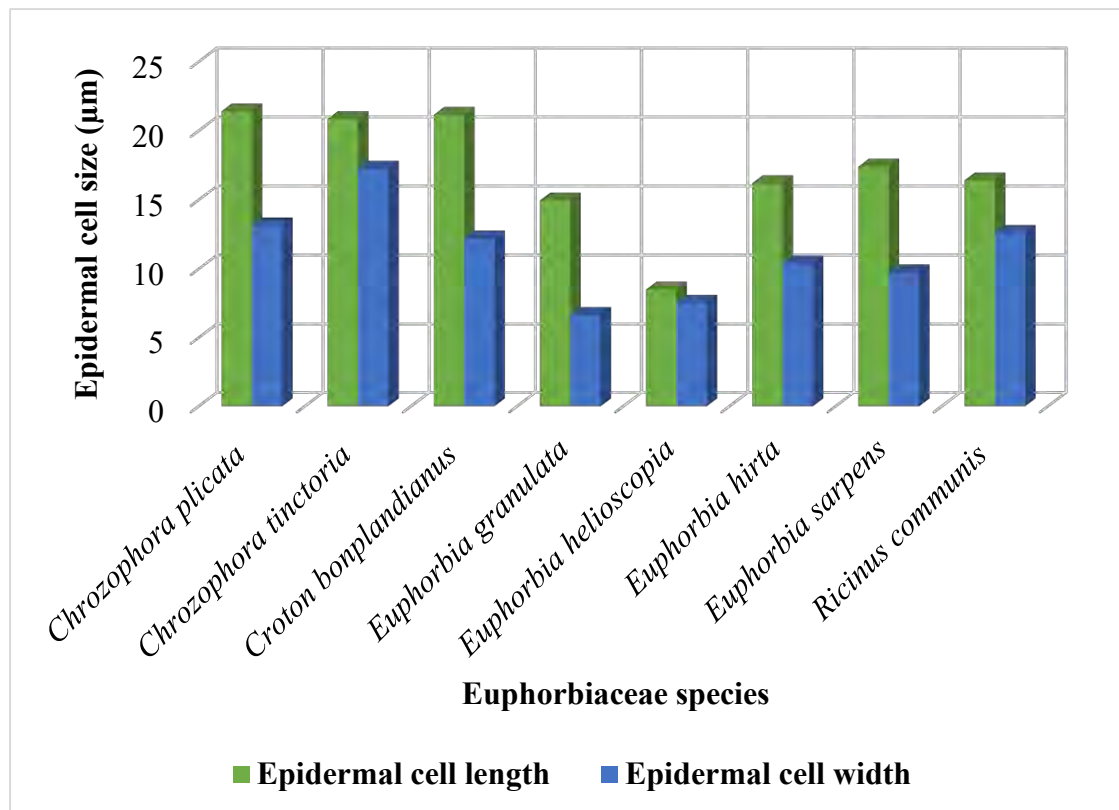


**Figure 67.** Mean epidermal cells size on abaxial surface in Euphorbiaceous taxa

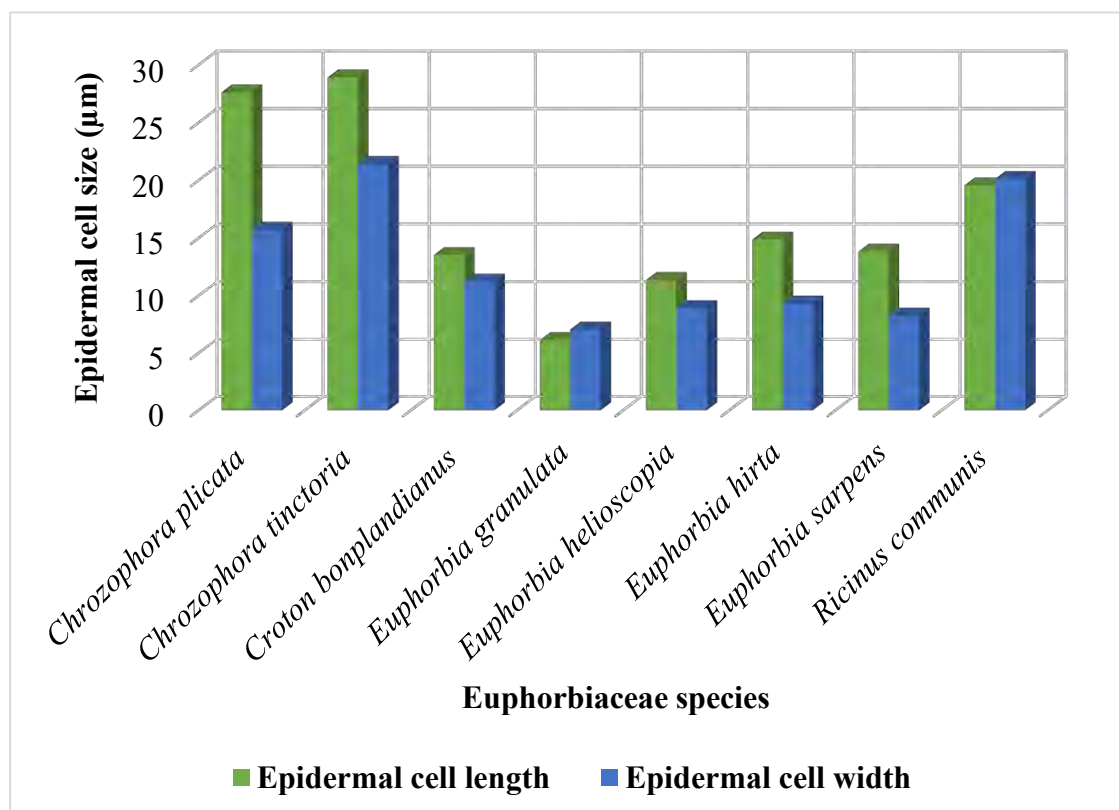


**Figure 68.** Mean epidermal cells size on adaxial surface in Euphorbiaceous taxa

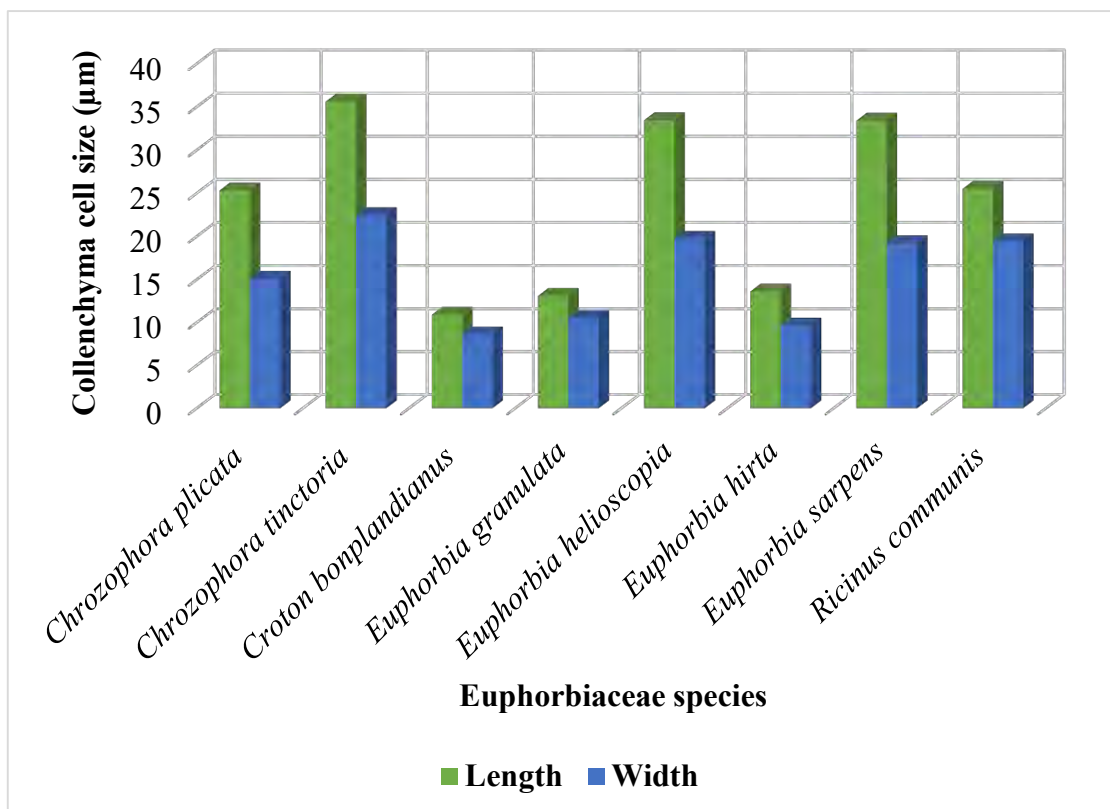


**Figure 69.** Mean collenchyma cell size variations in Euphorbiaceous taxa

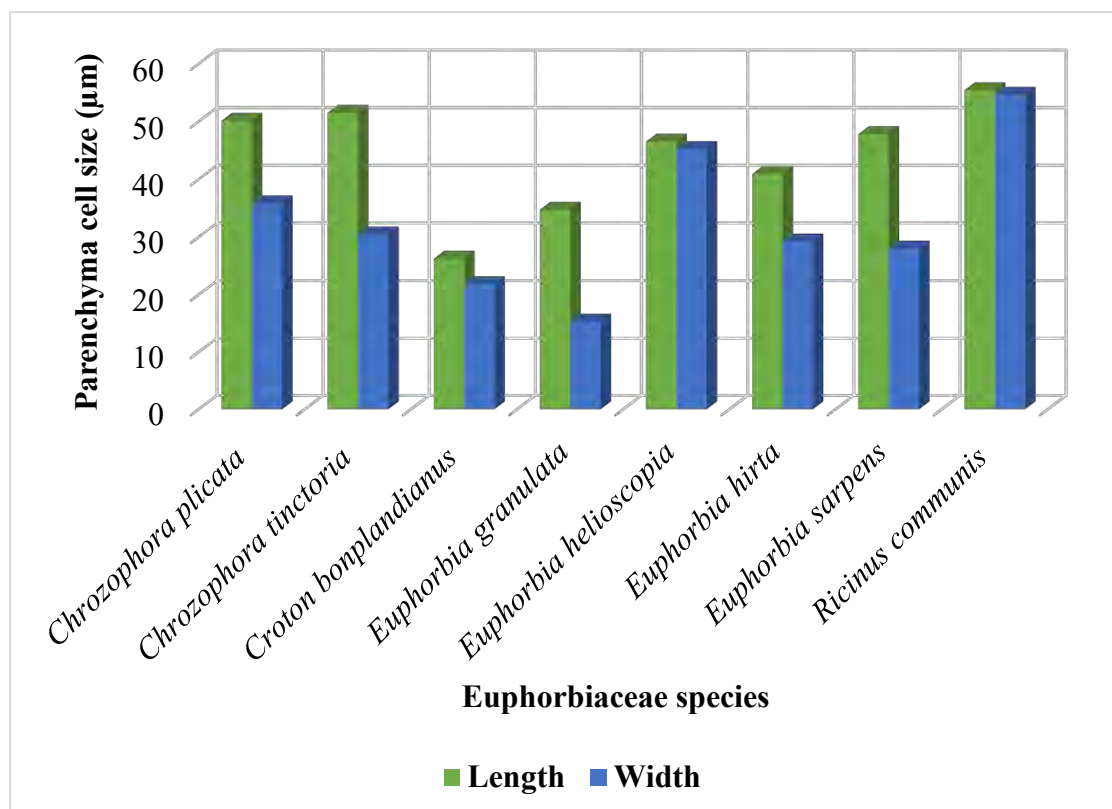


**Figure 70.** Variations of parenchyma cell size in Euphorbiaceous taxa

### 3.4.21 Discussion

Anatomical observations on the transverse section of the petiole of studied species revealed interspecific variations that are important in the classification and delimitation of taxa. The growth adaptations in reaction to the environmental stimuli can modify the petiole structure. The vascular system is an important element for the evolutionary findings, supporting the growth of plants and habituating to a wide range of ecological environmental conditions (Cho et al., 2017).

Most previous anatomical investigations have been carried out on the other species of the family Euphorbiaceae. In many species of this family, it is reported that there are laticiferous cells and vessels. In our anatomical examination, none of these structures were observed in *C. tinctoria*. These results show conformity with findings for other members of the Euphorbiaceae family (Metcalf and Chalk, 1957).

Baslar (2000) reported the root cross-section of *C. tinctoria* revealed the outer layers of the epidermis followed, by the cortex, which consisted of sclerenchyma and parenchyma. In the stem histology of *C. tinctoria*, it was observed that there was one layer of the epidermis. Beneath the epidermis, cortex cells consist of collenchyma and parenchyma cells. In this study, we observed petiole histological vasculature of *C. tinctoria* with flat-shaped winged petiole, open arc-shaped vascular bundle, lamellar collenchyma cells, and irregular epidermal and parenchymatous cells were examined. Keerthana et al., (2020) performed the histological transverse section of the *C. rotleri* petiole shows almost circular in outline and the epidermis is a single layer, small cubical-shaped cells, abundant stellate trichomes, layered collenchymatous cells. A single vascular bundle in the middle is filled with ground tissue of large parenchymatous cells. While our study described the petiole sectioning of *C. plicata* as winged irregular arc-shaped with rounded vascular bundles. Epidermal cells were rectangular to square, collenchyma cells angular, and parenchyma cells polygonal in shape were observed.

In the petiole cross-section of *C. bonplandianus*, the epidermis is a single cell layer covered by a thick cuticle follow by continuous layers of collenchyma and then ground parenchyma tissues (Rosa et al., 2021). We observed for *C. bonplandianus* rounded petiole and open-arc shape vascular bundles. This study in comparison to the previous one described angular and lamellar shape collenchymatous cells, and



polygonal to irregular parenchyma tissue. Bhavan et al., (2020) reported barrel-shaped parenchyma cells and triangular outline of petiole in *C. bonplandianus* were inconsistent with our findings. Aldhebiani and Jury (2013) explained the anatomical parameters of *E. granulata*, and described both leaf surfaces as hairy and glabrous. Nobarinezhad et al., (2018) analyzed the zigzag, papillate ad light wavy type cell walls of the epidermis in *E. granulata*. In this study, we visualized rectangular to square shape epidermal cells of the petiole section of *E. granulata*.

Singh and Isfaq (2017) detailed anatomical studies revealed that the transverse section of root, stem, and a leaf of *E. helioscopia* was encircled by cork cells, phelloderm 6-8 layered, multiseriate medullary rays. The stem showed the presence of parenchymatous cells containing laticiferous canals. The stem section outline appears to be semi-circular in *E. helioscopia* mentioned by Najmaddin in 2020. However, this work shows irregular arc-shaped petiole and closed rectangular shape vascular bundles in *E. helioscopia*. Alyas et al., (2020) explained the foliar epidermal traits of *E. helioscopia* as irregular shape cells on both the abaxial and adaxial sides. While rectangular isodiametric epidermal cells were reported in our study. Vyas et al., (2019) explained petiole vasculature of *E. hirta* parenchymatous ground tissue and three small collateral vascular bundles arranged in a crescent manner while open vascular bundles with incurved ends were examined in our case. Scattered latex cells in the ground tissue. Jafari and Nasseh (2009) described laticifers tissues found in petiole regions dissimilar to our observation.

Aldhebiani and Jury (2013) performed a foliar anatomical structure of *E. serpens* with two different epidermal cells on the leaf surfaces usually having three sheathed veins with closed margins and anomocytic stomata were detected. However, we analyzed the petiole micromorphology of *E. serpens* with rectangular to square shape epidermal cells with a slightly U-shaped petiole outline. Tadavi and Bhadane (2014) have recorded medullary bundles in the petiole of *R. communis*. Recently Wunnrnberg et al., (2021) described vasculature of *R. communis* petiole with one ring of the vascular bundle and central medullary canal. However, our research described angular collenchyma cells and flat closed U-shaped petiole.



**Conclusion & Future  
Recommendations**

## 4. Conclusion

This is the first comprehensive documentation with respect to taxonomic characteristics (LM & SEM) of Dicot flora, 111 species belonging to 26 families and 80 genera along the Thal Desert in Pakistan. It is concluded from this study that palynological, seed micromorphological and anatomical features are very helpful in the identification and delimitation of dicot angiosperms species.

### Palynology

The pollen attributes of the 77 dicot angiosperms were helpful in the comparison among the species, and statistical analysis revealed significant information about the resemblance among the dicot species. Amaranthaceae was the most dominating family representing 14 species revealed different types of exine stratification such as smooth sparsely granulate, scabrate-spinulose, micro-spinulose perforate, meta-reticulate, granulate, nano-spinulate, granulate-spinulose perforate, and granulate-perforate echinate. Exine thickness was highest in *Salsola tragus* 2.15  $\mu\text{m}$  and lowest in *Amaranthus graecizens* 0.78  $\mu\text{m}$ . Taxonomic keys were constructed based on findings that highlight the importance of the micromorphological ultrastructural diversity of pollen.

### Seed Morphology

The taxonomic significance of seed micromorphology in identifying dicot angiosperms has been recognized. This research analyzed the seed ultrastructure of 27 species belonging to 14 families that are most widespread in the Thal desert. Scanning imaging analysis revealed significant taxonomic diversity among various species and gave useful data on seed coat ornamentation in the context of phylogeny. Seeds were mostly minute and small and slightly larger than 1 mm in length except for *Acacia nilotica*, *Astragalus hamosus* and *Prosopis juliflora*. Anticlinal wall seed coat patterns can be categorized into various types: striate foveolate, striate regulate, striate, foveolate rugose, reticulate, foveolate, foveolate striate, papillate, papillate rugose, papillate scabrate, papillate foveolate, rugose, rugose papillate, rugose scabrate, striate reticulate, rugose striate, papillate smooth, undulated granulate and wrinkled spiny. The variability in seed architecture among dicot angiosperms was very helpful for proper identification and classification and indicated that micro-structural attributes have important taxonomic implications.

## Anatomy

The leaf micromorphology of 37 selected dicot species growing in the arid Thal desert rangeland reveals that foliar anatomical features, including the diversity of epidermal cells, trichome morphology, and variation of stoma types, are potentially useful to delimit the taxa at a species level. Amaranthaceous species can easily be differentiated on account of their epidermal cell shape reported as irregular, rectangular, polygonal, undulated, isodiametric, and uniseriate. The largest epidermal cells were examined in *Aerva lanata* (55.5  $\mu\text{m}$ ) on the adaxial and *Alternanthera ficoidea* (38.5  $\mu\text{m}$ ) on the abaxial surface. It is concluded that scanning electron microscopic character identification of xeric inhabited dicot species proved to be significant in classification.

The petiole vasculature in Amaranthaceous and Euphorbiaceous taxa showed variations via microscopic imaging analysis. The shape of petiole, variations in vascular bundles, collenchyma layers, shape of parenchyma and epidermal cells and trichomes features are indeed important for taxonomic evaluation. Maximum 18 collenchyma layers were present in *Achyranthes aspera* and minimum of nine layers in *Amaranthus graecizans*. The observations suggest that a combination of qualitative and quantitative petiole characters through clustering (UPGMA dendrogram) was helpful in the taxonomic identification of species and their evolutionary implications.

## **5. Future Perspectives**

- Phylogenetic analysis using advanced analytical techniques will be needed to better understand the placement of dicot families in the evolutionary tree.
- Advanced molecular, chromatographic, and spectroscopic methodologies will be used for the identification of desert medicinal species to incorporate them into the pharmaceutical industry.
- Exploration of desert floral diversity and their potential in drug development in the herbal industry and their propagation, preservation, and conservation practices will be practiced.
- Efforts are needed to develop a floral catalog of Deserts plants which will be helpful for research communities of allied disciplines and the herbal industry for socio-economic uplift of local community specifically the elimination of diseases.



## **References**

- Abd El-Ghani, M.M., Huerta-Martínez, F.M., Hongyan, L. and Qureshi, R. (2017). *Plant responses to hyperarid desert environments*. Springer International Publishing, XV, 598. <https://doi.org/10.1007/978-3-319-59135-3>
- Abd Elhalim, M.E., Abo-Alatta, O.K., Habib, S.A. and Abd Elbar, O.H. (2016). The anatomical features of the desert halophytes *Zygophyllum album* LF and *Nitraria retusa* (Forssk.) Asch. *Annals of Agricultural Sciences*, 61(1), 97-104. <https://doi.org/10.1016/j.aoas.2015.12.001>
- Abdel Khalik, K. and Hassan, N.M.S. (2012). Seed and trichome morphology of the Egyptian *Fagonia* (Zygophyllaceae) with emphasis on their systematic implications. *Nordic Journal of Botany*, 30(1), 116-126. <https://doi.org/10.1111/j.1756-1051.2011.01112.x>
- Abdel Khalik, K. and Osman, A.K. (2007). Seed morphology of some species of Convolvulaceae from Egypt (Identification of species and systematic significance). *Feddes Repertorium*, 118(1-2), 24-37. <https://doi.org/10.1002/fedr.200711123>
- AbdulRahaman, A.A. and Oladele, F.A. (2004). Types, densities and frequencies of trichomes in some Nigerian vegetable species. *Nigerian Journal of Pure and Applied Science*, 19(2), 1653-1658.
- Abdulrahaman, A.A., Oyedotun, R.A. and Oladele, F.A. (2011). Diagnostic significance of leaf epidermal features in the family Cucurbitaceae. *Insight Botany*, 1(2), 22-27.
- Abeyasinghe, P.D. and Scharaschkin, T. (2019). Taxonomic value of petiole anatomy in the genus *Cinnamomum* (Lauraceae) found in Sri Lanka. *Ruhuna Journal of Science*, 10(1), 1-17. <http://doi.org/10.4038/rjs.v10i1.47>
- Abid, R., Kanwal, D. and Qaiser, M. (2015). The seed atlas of Pakistan-x. Cucurbitaceae. *Pakistan Journal of Botany*, 47(2), 429-436.
- Aboulela, M.A., El-Karemy, Z.A., Hosni, H.A., Saleh, S.M. and Faried, A.M. (2021). Taxonomic implications of seed morphology and storage proteins in three tribes of the subfamily Papilionoideae (Fabaceae) in Egypt. *Phytotaxa*, 484(1), 75-95. <https://doi.org/10.11646/phytotaxa.484.1.3>

- Aftab, R., and Perveen, A. (2006). A palynological study of some cultivated trees from Karachi. *Pakistan Journal of Botany*, 38(1), 15-28.
- Agogbua, J.U. (2020). Comparative Taxonomic study on *Crotalaria* L. from some parts of South-Eastern Nigeria. *Bulletin of Pure & Applied Sciences-Botany*, 39(2), 94-105.
- Aguilar-García, S.A., Figueroa-Castro, D.M. and Castañeda-Posadas, C. (2012). Pollen morphology of *Pachycereus weberi* (Cactaceae): an evaluation of variation in pollen size. *Plant Systematics and Evolution*, 298(10), 1845-1850. <https://doi.org/10.1007/s00606-012-0685-6>
- Ahmad, K., Khan, M.A., Ahmad, M., Shaheen, N., and Nazir, A. (2010). Taxonomic diversity in epidermal cells of some sub-tropical plant species. *International Journal of Agriculture and Biology*, 12(1), 115-118.
- Ahmad, K., Shaheen, N., Ahmad, M. and Khan, M.A. (2010). Pollen fertility estimation of some sub-tropical flora of Pakistan. *African Journal of Biotechnology*, 9(49), 8313-8317. DOI: [10.5897/AJB09.676](https://doi.org/10.5897/AJB09.676)
- Ahmad, K.Z., Sheidai, M. and Attar, F. (2011). Morphometry and palynological study of the genus *Cousinia* sect. *Cousinia* (Asteraceae) in Iran. *Iranian Journal of Botany*, 17(2), 158-166.
- Ahmad, M., Ali, M., Zafar, M., Sultana, S., Majeed, S., Yaseen, G. and Ahmad, S. (2021). Palynological diversity of Melliferous flora around apiaries from district Mardan Khyber Pakhtunkhwa-Pakistan. *The Botanical Review*, 1-34. <https://doi.org/10.1007/s12229-021-09268-w>
- Ahmad, M., Bano, A., Zafar, M., Khan, M.A., Chaudhry, M.J.I. and Sultana, S. (2013). Pollen morphology of some species of the family Asteraceae from the alpine zone, Deosai Plateau, northern Pakistan. *Palynology*, 37(2), 189-195. <https://doi.org/10.1080/01916122.2012.758920>
- Ahmad, M., Zafar, M. and Dawood, S. (2022). Scanning electron microscopic identification of ten novel, non-edible oil seeds for bioenergy production. *Microscopy Research and Technique*, 85(9), 3245-3255. <https://doi.org/10.1002/jemt.24181>



- Ahmad, M., Zafar, M., Bahadur, S., Sultana, S., Taj, S., Celep, F. and Majeed, S. (2022). Palynomorphological diversity among the Asteraceous honeybee flora: An aid to the correct taxonomic identification using multiple microscopic techniques. *Microscopy Research and Technique*, 85(2), 570-590. <https://doi.org/10.1002/jemt.23932>
- Ahmad, S., Zafar, M., Ahmad, M., Ali, M.I., Sultana, S., Rashid, N., Butt, M.A., Shah, S.N., Ozdemir, F.A., Kutlu, M.A. and Afza, R. (2020). Seed morphology using SEM techniques for identification of useful grasses in Dera Ghazi Khan, Pakistan. *Microscopy Research and Technique*, 83(3), 249-258. <https://doi.org/10.1002/jemt.23408>
- Ahmad, S., Zafar, M., Ahmad, M., Ozdemir, F.A., Yaseen, G., Sultana, S. and Kutlu, M.A. (2020). Palynological studies of winter weeds melliferous flora of district Bannu, Khyber Pakhtunkhwa, Pakistan. *Annali di Botanica*, 10, 77-86. <https://doi.org/10.13133/2239-3129/14863>
- Ahmed, N., Mahmood, A., Tahir, S.S., Bano, A., Malik, R.N., Hassan, S. and Ashraf, A. (2014). Ethnomedicinal knowledge and relative importance of indigenous medicinal plants of Cholistan desert, Punjab Province, Pakistan. *Journal of Ethnopharmacology*, 155(2), 1263-1275. <https://doi.org/10.1016/j.jep.2014.07.007>
- Akhani, H., Ghobadnejhad, M. and Hashemi, S.M. (2003). Ecology, biogeography and pollen morphology of *Bienertia cycloptera* Bunge ex Boiss.(Chenopodiaceae), an enigmatic C4 plant without Kranz anatomy. *Plant Biology*, 5(2), 167-178. <https://doi.org/10.1055/s-2003-40724>
- Akhtar, A., Ahmad, M., Mahmood, T., Khan, A.M., Arfan, M., Abbas, Q., Zafar, M., Sultana, S., Batool, R., Fatima, A. and Khan, S. (2022). Microscopic characterization of petiole anatomy of Asteraceous taxa of Western Himalaya-Pakistan. *Microscopy Research and Technique*, 85(2), 591-606. <https://doi.org/10.1002/jemt.23933>
- Akhtar, N., Khan, S.A. and Khattak, U. (2019). Palynological characteristics of some selected species of family Cucurbitaceae (Juss.) using light and scanning

- electron microscopy techniques. *Microscopy Research and Technique*, 82(11), 1852-1861. <https://doi.org/10.1002/jemt.23352>
- Akinsulire, O.P., Oladipo, O.T., Akinkunmi, O.C., Adeleye, O.E. and Adelalu, K.F. (2020). Leaf and Petiole Micro-Anatomical Diversities in Some Selected Nigerian Species of Loe fl.: the Significance in Species Identification at Vegetative State. *Acta Biologica Marisiensis*, 3(1), 15-29.
- Akinsulire, O.P., Oladipo, O.T., Akinloye, A.J. and Illoh, H.C. (2018). Structure, distribution and taxonomic significance of leaf and petiole anatomical characters in five species of *Terminalia* (L.)(Combretaceae: Magnoliopsida). *Brazilian Journal of Biological Sciences*, 5(10), 515-528. <https://doi.org/10.21472/bjbs.051027>
- Akram, N.A., Ashraf, M., Ashraf, M. and Sadiq, M. (2020). Exogenous application of L-methionine mitigates the drought-induced oddities in biochemical and anatomical responses of bitter gourd (*Momordica charantia* L.). *Scientia Horticulturae*, 267, 109333. <https://doi.org/10.1016/j.scienta.2020.109333>
- Al Nawaihi, A.S., Hassan, S.A. and Elwan, Z.A. (2006). Exomorphic seed characters of some species of the Apocynaceae sl in Egypt. *Feddes Repertorium: Zeitschrift für botanische Taxonomie und Geobotanik*, 117(7-8), 437-452. <https://doi.org/10.1002/fedr.200611114>
- Alam, F., Ahmad, M., Zafar, M., Shinwari, M.I., Luqman, M., Novruz, N.E., Sultana, S., Ullah, F. and Ahmad, M. (2019). Intraspecific variation in spermoderm pattern of tribe Acacieae (Mimosoideae) using scanning electron microscopy techniques. *Microscopy Research and Technique*, 82(2), 114-121. <https://doi.org/10.1002/jemt.23116>
- Albert, S. and Sharma, B. (2013). Comparative foliar micromorphological studies of some *Bauhinia* (Leguminosae) species. *Turkish Journal of Botany*, 37(2), 276-281. DOI: [10.3906/bot-1201-37](https://doi.org/10.3906/bot-1201-37)
- Aldhebiani, A. and Jury, S. (2013). Anatomical studies on the genus *Euphorbia* L. Saudi Arabia (Subgenera: *Triucalli*, *Ermophyton*, *Esula* and *Chamaesyce*). *International Research Journal of Plant Science*, 4(6), 168-191.

- Alege, G.O. and Daudu, S.M. (2014). A comparative foliar epidermal and morphological study of five species of the genus *Amaranthus*. *European Journal of Experimental Biology*, 4(4), 1-8.
- Al-Ghamdi, F.A. and Al-Zahrani, R.M. (2010). Seed morphology of some species of *Tephrosia* Pers.(Fabaceae) from Saudi Arabia Identification of species and systematic significance. *Feddes Repertorium*, 121(1-2), 59-65. <https://doi.org/10.1002/fedr.201011128>
- Ali, M.A. and Al-Hemaid, F.M. (2011). Taxonomic significance of trichomes micromorphology in Cucurbits. *Saudi journal of Biological Sciences*, 18(1), 87-92. <https://doi.org/10.1016/j.sjbs.2010.10.003>
- Ali, M.A., Al-Hemaid, F.M., Pandey, A.K. and Lee, J. (2013). Taxonomic significance of spermoderm pattern in Cucurbitaceae. *Bangladesh Journal of Plant Taxonomy*, 20(1), 61-65. <https://doi.org/10.3329/bjpt.v20i1.15465>
- Ali, M.E.S. and Amar, M.H. (2020). A systematic revision of Capparaceae and Cleomaceae in Egypt: an evaluation of the generic delimitations of *Capparis* and *Cleome* using ecological and genetic diversity. *Journal of Genetic Engineering and Biotechnology*, 18(1), 1-15. <https://doi.org/10.1186/s43141-020-00069-z>
- Ali, N., Akhtar, N., Khan, S.A. and Ul Uza, N. (2021). Palynological investigation of selected species of family Asteraceae using light and scanning electron microscopic techniques. *Microscopy Research and Technique*, 84(2), 261-270. <https://doi.org/10.1002/jemt.23583>
- Ali, S.I. (1983). Asclepiadaceae. In: Flora of Pakistan, Nasir, E. and S.I. Ali (Eds.). Pakistan Agricultural Research Council, Islamabad, Pakistan, 150-165.
- Almousawi, U.M.N. and Alwan, A.A. (2011). Pollen Grains Characters and Their Evolutionary Significance in the family Papaveraceae in Iraq and some Iranian species. *8th National Conference on Environment and Natural Resources*, 142-165.
- Al-Quran, S. (2004). Pollen morphology of Solanaceae in Jordan. *Pakistan Journal of Biological Sciences*, 7(9), 1586-1593.

- Al-Saadi, S.A.A. and Al-Mayah, A.R.A. (2012). Pollen morphological study of the dicots wetland plants of Southern Marshes of Iraq. *Marsh Bulletin*, 7(2), 169-188.
- Aluri, J.S.R. and Chappidi, P.R. (2018). Reproductive ecology of *Allmania nodiflora*, *Celosia argentea* var. *margaritacea*, and *Digera muricata* (Amaranthaceae). *Botanica Serbica*, 42(2), 185-198.
- Al-Wadi, H.M. and Lashin, G.M. (2007). Palynological and cytological characters of three species of genus *Solanum* (Family: Solanaceae) from Saudi Arabia. *Journal of Biological sciences*, 7(4), 626-631. <https://dx.doi.org/10.3923/jbs.2007.626.631>
- Alwadie, H.M. (2002). Ultrastructure of *Withania somnifera* (L.) Dunal pollen grains. *Arab Gulf Journal of Scientific Research (1989)*, 20(2), 92-95.
- Alwadie, H.M. (2005). Morphology and distribution of three genera of Amaranthaceae in the south western area of Saudi Arabia. *Journal of King Saud University–Science*, 18, 51-62.
- Alyas, T., Shaheen, S., Amber, U., Harun, N., Khalid, S., Hussain, K., Hanif, U. and Khan, F. (2020). Applications of scanning electron microscopy in taxonomy with special reference to family Euphorbiaceae. *Microscopy Research and Technique*, 83(9), 1066-1078. <https://doi.org/10.1002/jemt.23497>
- Ameen, S. (2021). *Diversity and Morpho-Anatomical variations of some Desert shrub populations growing under different Microhabitats* (Doctoral dissertation).
- Amina, H., Ahmad, M., Bhatti, G.R., Zafar, M., Sultana, S., Butt, M.A., Bahadur, S., Haq, I.U., Ghufraan, M.A., Ahmad, S. and Ashfaq, S. (2020). Microscopic investigation of pollen morphology of Brassicaceae from Central Punjab-Pakistan. *Microscopy Research and Technique*, 83(4), 446-454. <https://doi.org/10.1002/jemt.23432>
- Angelini, P., Bricchi, E., Gigante, D., Poponessi, S., Spina, A. and Venanzoni, R. (2014). Pollen morphology of some species of Amaranthaceae s. lat. common in Italy. *Flora Mediterranea*, 24, 247-272. doi: [10.7320/FlMedit24.247](https://doi.org/10.7320/FlMedit24.247)

- Anil Kumar, V.S., Maya Nair, C. and Murugan, K. (2015). Pollen morphology of selected taxa of the genus *Solanum* from Southern Western Ghats, Kerala, India. *Rheedea*, 25(2), 128-145.
- Aoyama, J.T., Maier, P., Servaes, S., Serai, S.D., Ganley, T.J., Potter, H.G. and Nguyen, J.C. (2019). MR imaging of the shoulder in youth baseball players: anatomy, pathophysiology, and treatment. *Clinical Imaging*, 57, 99-109. <https://doi.org/10.1016/j.clinimag.2019.05.005>
- Araii, F.E., Keshavarzi, M., Sheidaii, M. and Ghadam, P. (2011). Fruit and seed morphology of the *Fumaria* L. species (Papaveraceae) of Iran. *Turkish Journal of Botany*, 35(2), 167-173. DOI: [10.3906/bot-0909-160](https://doi.org/10.3906/bot-0909-160)
- Arora, A. and Modi, A. (2011). Pollen morphology of some desertic Crucifers. *Indian Journal of Fundamental and Applied Life Sciences*, 1(1), 11-15. <http://www.cibtech.org/jls.htm>
- Arruda, E.C.P.D. and Melo-de-Pinna, G.F.D.A. (2015). Anatomical characters of stem segments in species of Opuntioideae (Cactaceae) subfamily. *Hoehnea*, 42, 195-205. <https://doi.org/10.1590/2236-8906-12/2014>
- Arshad, M. and Rao, A.U.R. (1994). Flora of Cholistan Desert (Systematic list of trees, shrubs and herbs). *Journal of Economic and Taxonomic Botany*, 18, 615-625.
- Arshad, M., Ashraf, M. and Arif, N. (2006). Morphological variability of *Prosopis cineraria* (L.) Druce, from the Cholistan desert, Pakistan. *Genetic Resources and Crop Evolution*, 53(8), 1589-1596. <https://doi.org/10.1007/s10722-005-8563-5>
- Arshad, S., Ahmad, M., Saboor, A., Ibrahim, F.H., Mustafa, M.R.U., Zafar, M. and Ashfaq, S. (2019). Role of trees in climate change and their authentication through scanning electron microscopy. *Microscopy Research and Technique*, 82(2), 92-100. <https://doi.org/10.1002/jemt.23106>
- Ashfaq, S., Ahmad, M., Zafar, M., Sultana, S., Bahadur, S., Ahmed, S.N., Gul, S. and Nazish, M. (2020). Pollen morphology of family Solanaceae and its taxonomic significance. *Anais da Academia Brasileira de Ciências*, 92(3), 1-16. <https://doi.org/10.1590/0001-3765202020181221>

- Ashfaq, S., Ahmad, M., Zafar, M., Sultana, S., Bahadur, S., Ullah, F., Zaman, W., Ahmed, S.N. and Nazish, M. (2019). Foliar micromorphology of Convolvulaceous species with special emphasis on trichome diversity from the arid zone of Pakistan. *Flora*, 255, 110-124. <https://doi.org/10.1016/j.flora.2019.04.007>
- Atar, M. (2006). *Centaurea Kilaea Boiss. Ve Centaurea Cunneifolia Sm. üzerinde Morfolojik Ve Palinolojik arařtırmalar* (Doctoral dissertation, Marmara Universitesi (Turkey).
- Attar, F., Esfandani-Bozchaloyi, S., Mirtadzadini, M., Ullah, F. and Zaman, W. (2019). Foliar and stem epidermal anatomy of the tribe Cynoglosseae (Boraginaceae) and their taxonomic significance. *Microscopy Research and Technique*, 82(6), 786-802. <https://doi.org/10.1002/jemt.23223>
- Attique, R., Zafar, M., Ahmad, M., Zafar, S., Ghufran, M.A., Mustafa, M.R.U., Yaseen, G., Ahmad, L., Sultana, S., Zafar, A. and Majeed, S. (2022). Pollen morphology of selected melliferous plants and its taxonomic implications using microscopy. *Microscopy Research and Technique*, 85(7), 2361-2380. <https://doi.org/10.1002/jemt.24091>
- Aurelia, I. M., Grigore M.N., Magdalena, Z.M., Toma C. (2013). Histo-Anatomical Aspects Referring To the Vegetative Organs on Some Halophytes from Romania. *University of Agricultural Sciences and Veterinary Medicine "Ion Ionescu De La Brad" Iasi, Horticulture Series*, 56(1), 25-30.
- Awachat, S.V. (2015). Pollen Diversity Studies in Some Taxa of Bicarpellatae from Nagpur. *International Journal of Researches In Biosciences, Agriculture & Technology, Special Issue (I)*, 96-100.
- Ayaz, S., Ahmad, M., Zafar, M., Ali, M.I., Sultana, S., Mustafa, M.R.U., Kilic, O., Çobanođlu, D.N., Demirpolat, A., Ghani, A. and Afza, R. (2020). Taxonomic significance of cypsela morphology in tribe Cichoreae (Asteraceae) using light microscopy and scanning electron microscopy. *Microscopy research and technique*, 83(3), 239-248. <https://doi.org/10.1002/jemt.23407>
- Azeez, S.O., Faluyi, J.O. and Oziegbe, M. (2019). Cytological, foliar epidermal and pollen grain studies in relation to ploidy levels in four species of *Physalis* L.

- (Solanaceae) from Nigeria. *International Journal of Biological and Chemical Sciences*, 13(4), 1960-1968. <https://doi.org/10.4314/ijbcs.v13i4.4>
- Aziz, A., Ahmad, M., Ullah, R., Bari, A., Khan, M.Y., Zafar, M., Sultana, S., Ameen, M. and Anar, M. (2022). Microscopic techniques for characterization and authentication of oil-yielding seeds. *Microscopy Research and Technique*, 85(3), 900-916. <https://doi.org/10.1002/jemt.23959>
- Azizi, H., Sheidai, M., Mozaffarian, V. and Noormohammadi, Z. (2022). Molecular (ISSR, cp DNA, ITS) and morphological study of the genus *Tragopogon* L. (Asteraceae). *Genetic Resources and Crop Evolution*, 1-20. <https://doi.org/10.1007/s10722-022-01443-1>
- Azizi, H., Sheidai, M., Mozaffarian, V. and Noormohammadi, Z. (2021). Pollen Morphology of the Genus *Tragopogon* (Asteraceae). *Acta Botanica Hungarica*, 63(1-2), 31-43. <https://doi.org/10.1556/034.63.2021.1-2.2>
- Azzazy, M. (2016). Environmental impacts of industrial pollution on pollen morphology of *Eucalyptus globulus* Labill. (Myrtaceae). *Journal of Applied Biology and Biotechnology*, 4(5), 0-6. [DOI: 10.7324/JABB.2016.40509](https://doi.org/10.7324/JABB.2016.40509)
- Azzazy, M.F. (2011). Morphological studies of the pollen grains of wadi el-Natron plants, West Nile delta, Egypt. *Plant Systematics and Evolution*, 294(3), 239-251. <https://doi.org/10.1007/s00606-011-0460-0>
- Bahadur, S., Ahmad, M., Zafar, M., Sultana, S., Begum, N., Ashfaq, S., Gul, S., Khan, M.S., Shah, S.N., Ullah, F. and Saqib, S. (2019). Palyno-anatomical studies of monocot taxa and its taxonomic implications using light and scanning electron microscopy. *Microscopy Research and Technique*, 82(4), 373-393. <https://doi.org/10.1002/jemt.23179>
- Bahadur, S., Taj, S., Long, W. and Hanif, U. (2022). Pollen Morphological Peculiarities of Selected Mimosoideae Taxa of Hainan Island and Their Taxonomic Relevance. *Agronomy*, 12(5), 1122. <https://doi.org/10.3390/agronomy12051122>

- Bahar Gürdal, M. and Özhatay, E. (2019). Pollen Morphology of 5 *Centaurea* L. and 3 *Psephellus* Cass. Taxa in Turkey, *Yuzuncu Yil University Journal of Agricultural Science*, 29(4), 738-744. <https://doi.org/10.29133/yyutbd.631954>
- Bancheva, S., Kaya, Z. and Binzet, R. (2014). *Centaurea aytugiana* (Asteraceae), a new species from North Anatolia, Turkey. *Novon: A Journal for Botanical Nomenclature*, 23(2), 133-138. <https://doi.org/10.3417/2011026>
- Bano, A., Ahmad, M., Rashid, S., Zafar, M., Ashfaq, S., Rehman, S.U., Ali, M.I., Sultana, S., Shaheen, S. and Ahmad, S. (2019). Microscopic investigations of some selected species of Papilionaceae through SEM and LM from Skardu valley, northern Pakistan. *Microscopy Research and Technique*, 82(4), 452-458. <https://doi.org/10.1002/jemt.23188>
- Baretta-Kuipers, T. (1981). Wood anatomy of Leguminosae: its relevance to taxonomy. *Advances in legume systematics*. 677-705.
- Basarkar, U.G. (2017). Light microscopic studies of pollen grains by acetolysis method. *International Journal of Researches in Biosciences, Agriculture and Technology*, 3, 1-10. <https://doi.org/10.29369/ijrbat.2017.05.iii.0010>
- Bashir, S. and Khan, M.A. (2003). Pollen morphology as an aid to the identification of medicinal plants: *Trianthema portulacastrum* L., *Boerhaavia procumbens* banks ex Roxb., and *Alternanthera pungens* Kunth. *Hamdard Medicus (Pakistan)*, 46(1), 7-9.
- Başlar, S. (2000). An Investigation on *Chrozophora tinctoria* (L.) Rafin. Distributed in WestAnatolia. *Turkish Journal of Botany*, 24(2), 103-112.
- Batista-Franklin, C.P.R. and Gonçalves-Esteves, V. (2008). Palynology of species of *Solanum* L. (Solanaceae A. Juss.) from the restingas of Rio de Janeiro State, Brazil. *Acta Botanica Brasílica*, 22, 782-793. <https://doi.org/10.1590/S0102-33062008000300015>
- Bayoumy, A.T., Mohamed, A.H., Hussein, M.I., Tantawy, M.E. and Salim, M.A. (2020). Pollen criteria as a taxonomic tool to clarify the relationships between some taxa of Chenopodiaceae and Amaranthaceae. *The Egyptian Journal of*



- Experimental Biology (Botany)*, 16(1), 49-49. DOI: [10.5455/egyjebb.20200322081510](https://doi.org/10.5455/egyjebb.20200322081510)
- Begum, N. and Mandal, S. (2016). Diversity and Identification of the Pollen Flora of Birbhum District, West Bengal, India. *Phytomorphology: An International Journal of Plant Morphology*, 66(3), 112-132.
- Beier, B.A., Nylander, J.A.A., Chase, M.W. and Thulin, M. (2004). Phylogenetic relationships and biogeography of the desert plant genus *Fagonia* (Zygophyllaceae), inferred by parsimony and Bayesian model averaging. *Molecular phylogenetics and evolution*, 33(1), 91-108. <https://doi.org/10.1016/j.ympev.2004.05.010>
- Beilstein, M.A., Al-Shehbaz, I.A. and Kellogg, E.A. (2006). Brassicaceae phylogeny and trichome evolution. *American journal of Botany*, 93(4), 607-619. <https://doi.org/10.3732/ajb.93.4.607>
- Belmonte, E., Arriaza, B., Arismendi, M. and Sepúlveda, G. (2022). Foliar Anatomy of Three Native Species of *Tillandsia* L. from the Atacama Desert, Chile. *Plants*, 11(7), 870. <https://doi.org/10.3390/plants11070870>
- Bhat, N.A., Jeri, L., Mipun, P. and Kumar, Y. (2018). Systematic Studies (Micro-Morphological, Leaf Architectural, Anatomical and Palynological) of Genus *Physalis* (Solanaceae) in Northeast India. *Plant Archives*, 18(2), 2229-2238.
- Bhavana, R., Ramya, R. and Binu, T. (2020). Comparative studies on morphology, anatomy and phytochemistry of selected species of *Croton* L. (Euphorbiaceae). *Plant Archives*, 20(1), 639-656.
- Bianchimano, A.S., Murray, M.G., Aztiria, M.E., Montes, B., Calfuán, M.L. and Prat, M.I. (2014). Morphological and immunochemical characterization of the pollen grains of *Chenopodium album* L. (Chenopodiaceae) in a temperate urban area in Argentina. *Phyton, International Journal of Experimental Botany*, 83(1), 9-15. <http://dx.doi.org/10.32604/phyton.2014.83.009>
- Bibi, N., Akhtar, N., Hussain, M. and Khan, A.M. (2010). Systematic implications of pollen morphology in the family Malvaceae from North West frontier province, Pakistan. *Pakistan Journal of Botany*, 42(4), 2205-2214.

- Bidak, L.M., Kamal, S.A., Halmy, M.W.A. and Heneidy, S.Z. (2015). Goods and services provided by native plants in desert ecosystems: Examples from the northwestern coastal desert of Egypt. *Global Ecology and Conservation*, 3, 433-447. <https://doi.org/10.1016/j.gecco.2015.02.001>
- Bigazzi, M. and Selvi, F. (1998). Pollen morphology in the Boragineae (Boraginaceae) in relation to the taxonomy of the tribe. *Plant Systematics and Evolution*, 213(1), 121-151. <https://doi.org/10.1007/BF00988912>
- Bijauliya, R.K., Jain, S.K., Alok, S., Dixit, V. and Singh, V.K. (2017). Macroscopical, microscopical and physico-chemical studies on leaves of *Dalbergia sissoo* Linn. (Fabaceae). *International Journal of Pharmaceutical Sciences and Research*, 8(4), 1865-1873. DOI: [10.13040/IJPSR.0975-8232.8\(4\).1865-73](https://doi.org/10.13040/IJPSR.0975-8232.8(4).1865-73)
- Birjees, M., Ahmad, M., Zafar, M., Khan, A.S. and Ullah, I. (2022). Palyno-anatomical characters and their systematic significance in the family Apiaceae from Chitral, eastern Hindu Kush, Pakistan. *Microscopy Research and Technique*, 85(3), 980-995. <https://doi.org/10.1002/jemt.23967>
- Biyiklioğlu, O., Çeter, T. and Barış, B. (2018). Pollen and achene morphology of Some *Centaurea* L. taxa (Asteraceae), Turkey. *Mellifera*, 18(2), 26-36.
- Blackmore, S. (1982). A functional interpretation of Lactuceae (Compositae) pollen. *Plant systematics and evolution*, 141(2), 153-168. <https://doi.org/10.1007/BF00986415>
- Blackmore, S., Van Helvoort, H.A.M. and Punt, W. (1984). On the terminology, origins and functions of caveate pollen in Compositae. *Review of Palaeobotany and Palynology*, 43(4), 293-301. [https://doi.org/10.1016/0034-6667\(84\)90001-0](https://doi.org/10.1016/0034-6667(84)90001-0)
- Blair, W.F. and Turner, B.L. (1972). The integrative approach to biological classification. *Challenging biological problems*, 193-217.
- Bona, C. (1993). Comparative morpho-anatomical study of the vegetative organs of *Alternanthera philoxeroides* (Mart.) Griseb. and *A. aquatica* (Parode) Chodat (Amaranthaceae). Curitiba, 1993. 196p. [Dissertation of Master in Botany. Biological Sciences Sector, Federal University of Paraná].

- Borsch, T. (1998). Pollen types in the Amaranthaceae. Morphology and evolutionary significance. *Grana*, 37(3), 129-142. <https://doi.org/10.1080/00173139809362658>
- Borsch, T. and Barthlott, W. (1998). Structure and evolution of metareticulate pollen. *Grana*, 37(2), 68-78. <https://doi.org/10.1080/00173139809362646>
- Borsch, T., Flores-Olvera, H., Zumaya, S. and Müller, K. (2018). Pollen characters and DNA sequence data converge on a monophyletic genus *Iresine* (Amaranthaceae, Caryophyllales) and help to elucidate its species diversity. *Taxon*, 67(5), 944-976. <https://doi.org/10.12705/675.7>
- Bose, A., Roy, B. and Paria, N.D. (2012). Study of pollen morphology of some dicotyledonous plants occurring in Ballygunge Science College Campus. *Journal of Botanical Society of Bengal*, 66, 111-117.
- Bosu, P.P. and Wagner, M.R. (2014). Effects of induced water stress on leaf trichome density and foliar nutrients of three elm (*Ulmus*) species: implications for resistance to the elm leaf beetle. *Environmental entomology*, 36(3), 595-601. [https://doi.org/10.1603/0046-225X\(2007\)36\[595:EOIWSO\]2.0.CO;2](https://doi.org/10.1603/0046-225X(2007)36[595:EOIWSO]2.0.CO;2)
- Bowles, V.G., Mayerhofer, R., Davis, C., Good, A.G. and Hall, J.C. (2010). A phylogenetic investigation of *Carthamus* combining sequence and microsatellite data. *Plant systematics and evolution*, 287(1), 85-97. <https://doi.org/10.1007/s00606-010-0292-3>
- Bülbül, A.S., Tarıkahya-Hacıoğlu, B., Arslan, Y. and Subaşı, İ. (2013). Pollen morphology of *Carthamus* L. species in Anatolian flora. *Plant systematics and evolution*, 299(3), 683-689. <https://doi.org/10.1007/s00606-012-0753-y>
- Butt, M.A., Zafar, M., Ahmad, M., Kayani, S., Bahadur, S., Ullah, F. and Khatoon, S. (2021). The use of taxonomic studies to the identification of wetlands weeds. *Advances in Weed Science*, 39. <https://doi.org/10.51694/AdvWeedSci/2021;39:000013>
- Butt, M.A., Zafar, M., Ahmad, M., Sultana, S., Ullah, F., Jan, G., Irfan, A. and Naqvi, S.A.Z. (2018). Morpho-palynological study of Cyperaceae from wetlands of

- Azad Jammu and Kashmir using SEM and LM. *Microscopy Research and Technique*, 81(5), 458-468. <https://doi.org/10.1002/jemt.22999>
- Calvente, A.M., Andreato, R.H. and Vieira, R.C. (2008). Stem anatomy of *Rhipsalis* (Cactaceae) and its relevance for taxonomy. *Plant Systematics and Evolution*, 276(1), 1-7. <https://doi.org/10.1007/s00606-008-0052-9>
- Carlquist, S. (2003). Wood and stem anatomy of woody Amaranthaceae ss: ecology, systematics and the problems of defining rays in Dicotyledons. *Botanical Journal of the Linnean Society*, 143(1), 1-19. <https://doi.org/10.1046/j.1095-8339.2003.00197.x>
- Center, D. (2013). Comparative morphological and anatomical studies on *Cucurbita maxima* Duchesne and *Lagenaria siceraria* (Molina) Standl. *Research Journal of Agriculture and Biological Sciences*, 9(6), 296-307.
- Chaturvedi, M., Datta, K. and Pal, M. (1999). Pollen anomaly—a clue to natural hybridity in *Argemone* (Papaveraceae). *Grana*, 38(6), 339-342. <https://doi.org/10.1080/00173130050136127>
- Chaturvedi, M., Prasad, R.N., Sharma, M., Sharma, A.K. and Chaturvedi, H.C. (1999). Pollen morphology in *Solanum surattense* Burm. f. (Solanaceae)—diploid, colchitetraploid and a stable androgenic somaclonal variant. *Feddes Repertorium*, 110(5-6), 413-418. <https://doi.org/10.1002/fedr.19991100511>
- Chaudhari, S.K., Arshad, M., Ahmed, E., Mustafa, G., Fatima, S., Akhtar, S. and Amjad, M.S. (2013). Ethnobotanical evaluation of grasses from Thal Desert, Pakistan. *Archive Sciences*, 66(5), 248-255.
- Chaudhary, N., Husain, S.S. and Ali, M. (2014). Chemical composition and antimicrobial activity of volatile oil of the seeds of *Cuminum cyminum* L. *World Journal of Pharmaceutical and Pharmacological Sciences*, 3(7), 1428-1441.
- Chedraoui, S., Abi-Rizk, A., El-Beyrouthy, M., Chalak, L., Ouaini, N. and Rajjou, L. (2017). *Capparis spinosa* L. in a systematic review: A xerophilous species of multi values and promising potentialities for agrosystems under the threat of global warming. *Frontiers in Plant Science*, 8, 1-18. <https://doi.org/10.3389/fpls.2017.01845>

- Cheema, S.I., Ahmad, M., Ullah, R., Mothana, R.A., Noman, O.M., Zafar, M., Sultana, S., Hameed, A., Naz, S. and Akhtar, M.T. (2021). Implication, visualization, and characterization through scanning electron microscopy as a tool to identify nonedible oil seeds. *Microscopy Research and Technique*, 84(3), 379-393. <https://doi.org/10.1002/jemt.23595>
- Chimona, C., Stamellou, A., Stamellou, A. and Rhizopoulou, S. (2012). Study of variegated and white flower petals of *Capparis spinosa* expanded at dusk in arid landscapes. *Journal of Arid Land*, 4(2), 171-179. <https://doi.org/10.3724/SP.J.1227.2012.00171>
- Cho, B.K., Kim, Y.M., Choi, S.M., Park, H.W. and SooHoo, N.F. (2017). Revision anatomical reconstruction of the lateral ligaments of the ankle augmented with suture tape for patients with a failed Broström procedure. *The Bone & Joint Journal*, 99(9), 1183-1189.
- Çildir, H., Kahraman, A., Doğan, M. And Büyükkartal, H.N. (2017). Comparative Anatomical and Micromorphological studies on some species of *Lathyrus* L. section *Lathyrus* (Papilionoideae, Fabaceae). *Commagene Journal of Biology*, 1(1), 42-50. <https://doi.org/10.31594/commagene.392133>
- Commander, L.E., Golos, P.J., Miller, B.P. and Merritt, D.J. (2017). Seed germination traits of desert perennials. *Plant Ecology*, 218(9), 1077-1091. <https://doi.org/10.1007/s11258-017-0753-7>
- Corner, E.J.H. and Corner, E.J.H. (1976). *The Seeds of Dicotyledons: Volume 1* (Vol. 1). Cambridge University Press.
- Costea, M., Sanders, A. and Waines, G. (2001). Preliminary results toward a revision of the *Amaranthus hybridus* species complex (Amaranthaceae). *SIDA, Contributions to Botany*, 931-974.
- Coutinho, A.P., Aguiar, C.F., Bandeira, D.S.D. and Dinis, A.M. (2011). Comparative pollen morphology of the Iberian species of *Pulicaria* (Asteraceae, Inuleae, Inulinae) and its taxonomic significance. *Plant systematics and evolution*, 297(3), 171-183. <https://doi.org/10.1007/s00606-011-0505-4>

- Coutinho, A.P., Silveira, P., Pita, C., Santos, M.J., Saraiva, C. and Perpétuo, N.C. (2021). Pollen morphology of *Xanthium* L.(sl)(Asteraceae, Asteroideae, Heliantheae, Ambrosiinae) in the Iberian Peninsula-a palynotaxonomic approach to a poisonous, allergenic and invasive genus. *Grana*, 60(1), 35-56. <https://doi.org/10.1080/00173134.2020.1737729>
- Cuadrado, GA and Garralla, SS (2009). Palynology of the Cactaceae genera *Maihuenia* (Maihuenioideae) and *Pereskia* (Pereskioideae) from Argentina. *Bonplandia*, 5-12.
- Cutler, D.F. and Brandham, P.E. (1977). Experimental evidence for the genetic control of leaf surface characters in hybrid *Aloineae* (Liliaceae). *Kew Bulletin*, 23-32. <https://doi.org/10.2307/4117256>
- da Silva, M.G.S., Dubeux Jr, J.C.B., Cortes, L.C.D.S.L., Mota, D.L., da Silva, L.L.S., dos Santos, M.V.F. and dos Santos, D.C. (2010). Anatomy of different forage cacti with contrasting insect resistance. *Journal of Arid Environments*, 74(6), 718-722. <https://doi.org/10.1016/j.jaridenv.2009.11.003>
- Dane, F., Aksoy, Ö.D. and Yılmaz, G. (2007). Karyological and palynological studies on *Astragalus hamosus* and *A. glycyphyllos* in Turkey. *Phytologia Balcanica*, 13(3), 387-391.
- Das, S. and Iamónico, D. (2014). *Amaranthus bengalense* (Amaranthaceae) a new species from India, with taxonomical notes on *A. blitum* aggregate. *Phytotaxa*, 181(5), 293-300. <http://dx.doi.org/10.11646/phytotaxa.181.5.4>
- Davis, P.H. and Heywood, V.H. (1963). Principles of angiosperm taxonomy. *Principles of angiosperm taxonomy*. Oliver & Boyd, Edinburgh and London, xx-556 pp.
- Davitashvili, N. and Karrer, G. (2010). Taxonomic importance of seed morphology in *Gentiana* (Gentianaceae). *Botanical Journal of the Linnean Society*, 162(1), 101-115. <https://doi.org/10.1111/j.1095-8339.2009.01020.x>
- Dawood, S., Ahmad, M., Zafar, M., Ali, M.I., Ahmad, K., Sultana, S., Usma, A., Nazish, M., Butt, M.A., Ozdemir, F.A. and Kilic, O. (2020). Identification of novel nonedible oil seeds via scanning electron microscopy for biodiesel

- production. *Microscopy Research and Technique*, 83(2), 165-175.  
<https://doi.org/10.1002/jemt.23399>
- de Arruda, E.C.P. and Melo-De-Pinna, G.F. (2016). Areolar structure in some Opuntioideae: occurrence of mucilage cells in the leaf-glochid transition forms in *Opuntia microdasys* (Lhem.) Pfeiff. *Adansonia*, 38(2), 267-274.  
<https://doi.org/10.5252/a2016n2a10>
- De Craene, L.P.R., Yang, T.A., Schols, P. and Smets, E.F. (2002). Floral anatomy and systematics of *Bretschneidera* (Bretschneideraceae). *Botanical Journal of the Linnean Society*, 139(1), 29-45. <https://doi.org/10.1046/j.1095-8339.2002.00045.x>
- de Queiroz, R.T., Goulart de Azevedo Tozzi, A.M. and Lewis, G.P. (2013). Seed morphology: an addition to the taxonomy of *Tephrosia* (Leguminosae, Papilionoideae, Millettieae) from South America. *Plant Systematics and Evolution*, 299(2), 459-470. <https://doi.org/10.1007/s00606-012-0735-0>
- De Vogel, E.F. (1987). Guidelines for the preparation of revisions. Manual of herbarium taxonomy theory and practice, UNESCO, Jakarta.
- Dehghani, M. and Akhiani, H. (2009). Pollen morphological studies in subfamily Suaedoideae (Chenopodiaceae). *Grana*, 48(2), 79-101.  
<https://doi.org/10.1080/00173130902842968>
- Dehghani, M., Djamali, M. and Akhiani, H. (2021). Pollen morphology of the subfamily Salicornioideae (Chenopodiaceae) in Eurasia and North Africa. *Palynology*, 45(2), 245-258.  
<https://doi.org/10.1080/01916122.2020.1784304>
- Devarkar, V.D. (2011). Baseline inventory for angiospermic pollen diversity in Osmanabad District (Ms), India. *Bioscience Discovery*, 2(3), 288-293.
- Dias, G.B., Gomes, V.M., Moraes, T.M., Zottich, U.P., Rabelo, G.R., Carvalho, A.O., Moulin, M., Gonçalves, L.S.A., Rodrigues, R. and Da Cunha, M. (2013). Characterization of *Capsicum* species using anatomical and molecular data. *Genetics and Molecular Research*, 12(4), 6488-6501.

- Dickison, W.C. (2000). *Integrative plant anatomy*. Academic press 1st edition, 1-560 pp.
- Diez, M.J., Mejías, J.A. and Moreno-Socías, E. (1999). Pollen morphology of *Sonchus* and related genera, and a general discussion. *Plant Systematics and Evolution*, 214(1), 91-102. <https://doi.org/10.1007/BF00985733>
- dos Santos, F.D.A.R., Watanabe, H.M. and de Hamburgo Alves, J.L. (1997). Pollen morphology of some Cactaceae of north-eastern Brazil. *Bradleya*, 1997(15), 84-97. <https://doi.org/10.25223/brad.n15.1997.a11>
- Du, T., Zhao, C. and Liu, J. (2018). The pollen of *Solanum* L. and its systematic significance. *Palynology*, 42(3), 291-310. <https://doi.org/10.1080/01916122.2017.1346527>
- Duarte, M.R. and Wolf, S. (2005). Anatomical characters of the phyllode and stem of *Acacia podalyriifolia* A. Cunn. ex G. Don (Fabaceae). *Revista Brasileira de Farmacognosia*, 15, 71-76. <https://doi.org/10.1590/S0102-695X2005000100015>
- Dural, H. and Yilmaz Çitak, B. (2015). Morphology and anatomy of *Hedysarum pannosum* (Boiss.) Boiss. (Fabaceae). *Acta Botanica Croatica*, 74(1), 19-29. <https://doi.org/10.1515/botcro-2015-0009>
- Durdana, K. and Rubina, A. (2017). Taxonomic assessment of the family Amaranthaceae with special emphasis on seed morphology. *Pakistan Journal of Botany*, 49(S1), 43-68.
- Ekeke, C. and Agogbua, J.U. (2020). Comparative Taxonomic study on *Crotalaria* L. from some parts of South-Eastern Nigeria. *Bulletin of Pure and Applied Sciences*, 39(2), 94-105. [DOI: 10.5958/2320-3196.2020.00015.4](https://doi.org/10.5958/2320-3196.2020.00015.4)
- Ekeke, C. and Mensah, S.I. (2015). Comparative anatomy of midrib and its significance in the taxonomy of the family Asteraceae from Nigeria. *Journal of Plant Sciences*, 10(5), 200-205.
- Ekici, M., Yüzbaşıoğlu, D. and Aytaç, Z. (2005). Morphology, pollen, seed structure and karyological study on *Astragalus ovalis* Boiss. and *Balansa* (sect. *Ammodendron*) in Turkey. *International Journal of Botany*, 1(1), 74-78.



- El Ghazali, G.E. (1993). A study on the pollen flora of Sudan. *Review of palaeobotany and palynology*, 76(2-4), 99-345. [https://doi.org/10.1016/0034-6667\(93\)90077-8](https://doi.org/10.1016/0034-6667(93)90077-8)
- El Ghazali, G.E. (2022). Pollen morphological studies in Amaranthaceae s. lat.(incl. Chenopodiaceae) and their taxonomic significance: A review. *Grana*, 61(1), 1-7. <https://doi.org/10.1080/00173134.2021.1950829>
- El Ghazaly. (1995). Pollen morphology of the family Boraginaceae in Qatar. *Qatar University Science Journal*, 15(1), 65-75.
- El-Ghamery, A.A., Hosni, H. and Sadek, A. (2018). Pollen and seed morphology of some endemic taxa in Saint Catherine, Sinai, Egypt. *Taeckholmia*, 38(1), 40-60. <https://dx.doi.org/10.21608/taec.2018.11916>
- El-Ghamery, A.A., Khafagi, A.F. and Ragab, O.G. (2018). Taxonomic implication of pollen morphology and seed protein electrophoresis of some species of solanaceae in Egypt. *Al-Azhar Bulletin of Science*, 29(1-C), 43-56. <https://dx.doi.org/10.21608/absb.2018.33757>
- El-Ghamery, A.A., Sadek, A.M. and Abdelbar, O.H. (2017). Comparative anatomical studies on some species of the genus *Amaranthus* (Family: Amaranthaceae) for the development of an identification guide. *Annals of Agricultural Sciences*, 62(1), 1-9. <https://doi.org/10.1016/j.aogas.2016.11.001>
- Eliseu, S.A. and Dinis, A.M. (2008). Ultrastructure and cytochemistry of *Eucalyptus globulus* (Myrtaceae) pollen grain. *Grana*, 47(1), 39-51. <https://doi.org/10.1080/00173130801923364>
- Elkordy, A. and Faried, A. (2017). Pollen morphology and numerical analysis of *Tamarix* L. (Tamaricaceae) in Egypt and its systematic implication. *Bangladesh Journal of Plant Taxonomy*, 24(1), 91-105. <https://doi.org/10.3329/bjpt.v24i1.33036>
- El-Naga, A.A., Rabei, S., Khedr, A.A. and Al-Shibany, F., Pollen morphology of Aizoaceae in Egypt. *Scientific Journal for Damietta Faculty of Science*, 3(2), 133-139.

- Endress, P.K., Baas, P. and Gregory, M. (2000). Systematic plant morphology and anatomy-50 years of progress. *Taxon*, 49(3), 401-434. <https://doi.org/10.2307/1224342>
- Erdtman, G. (1971). On the Affinities of Aquilapollenites Rouse: Addendum: On the taxonomic position of *Gnetum*. *Grana*, 11(1), 15-17. <https://doi.org/10.1080/00173137109427405>
- Erdtman, G. (1972). *Pollen morphology and plant taxonomyangiosperms (an introduction to palynology. I)* (No. 561.13 E7).
- Erdtman, G. (1986). *Pollen morphology and plant taxonomy: Angiosperms* (Vol. 1). Brill Archive.
- Esfandani-Bozchaloyi, S. and Zaman, W. (2018). Taxonomic significance of macro and micro-morphology of *Geranium* L. species using scanning electron microscopy. *Microscopy Research and Technique*, 81(12), 1520-1532. <https://doi.org/10.1002/jemt.23159>
- Faghir, M., Ashori, F. and Mehrmanesh, A. (2017). Comparative leaf and petiole anatomy and micro morphology of the genus *Geum* (Rosaceae) from Iran. *Iranian Journal of Plant Biology*, 9(1), 45-58. <https://dx.doi.org/10.22108/ijpb.2017.21555>
- Fajuke, A.A., Makinde, A.M., Oloyede, F.A. and Akinloye, J.A. (2018). Comparative epidermal anatomical studies in six taxa of genus *Nephrolepis* Swart in Nigeria. *Tropical Plant Researh*, 5(1), 19-26.
- Fakhireh, A., Ajourlo, M., Shahryari, A., Mansouri, S., Nouri, S. and Pahlavanravi, A. (2012). The autecological characteristics of *Desmostachya bipinnata* in hyper-arid regions. *Turkish Journal of Botany*, 36(6), 690-696. [DOI: 10.3906/bot-1108-1](https://doi.org/10.3906/bot-1108-1)
- Farzana, K., Ali, S.A., Tahir, S.S., Rajput, M.T. and Akhter, M.T. (2010). Comparative morphological and biochemical studies of *Salvadora* species found in Sindh, Pakistan. *Pakistan Journal of Botany*, 42(3), 1451-1463.
- Fatima, A., Zafar, M., Ahmad, M., Yaseen, G., Sultana, S., Gulfraz, M. and Khan, A.M. (2018). Scanning electron microscopy as a tool for authentication of oil yielding

- seed. *Microscopy research and technique*, 81(6), 624-629.  
<https://doi.org/10.1002/jemt.23017>
- Fawzi, N.M., Hanan, S.A. and Mohamed, A.A. (2015). Numerical taxonomy of the tribe Cassieae (Leguminosae: Caesalpinioideae) in Egypt. *International Journal of Environment*, 4(4), 262-270.
- Fici, S. (2004). Micromorphological observations on leaf and pollen of *Capparis* L. sect. *Capparis* (Capparaceae). *Plant biosystems*, 138(2), 125-134.  
<https://doi.org/10.1080/11263500412331283753>
- Fici, S., 2004. Micromorphological observations on leaf and pollen of *Capparis* L. sect. *Capparis* (Capparaceae). *Plant biosystems*, 138(2), pp.125-134.
- Finot, V.L., Marticorena, C. and Marticorena, A. (2018). Pollen grain morphology of *Nolana* L. (Solanaceae: Nolanoideae: Nolaneae) and related genera of southern South American Solanaceae. *Grana*, 57(6), 415-455.  
<https://doi.org/10.1080/00173134.2018.1458897>
- Flores-Olvera, H., Czaja, A., Estrada-Rodríguez, J.L. and Méndez, U.R. (2016). Floristic diversity of halophytic plants of Mexico. In *Sabkha Ecosystems* (pp. 299-327). Springer, Cham.
- Franceschini, M.C. and Tressens, S.G. (2004). Morphology of fruits, seeds and embryos of Argentinian *Capparis* L. (Capparaceae). *Botanical Journal of the Linnean Society*, 145(2), 209-218. <https://doi.org/10.1111/j.1095-8339.2003.00279.x>
- Freitag, H., Brandt, R., Chatrenoor, T. and Akhani, H. (2013). *Suaeda iranshahrii*, a new species of *Suaeda* subgenus *Brezia* (Chenopodiaceae) from the Persian Gulf coasts. *Rostaniha*, 14(1), 68-80.  
<https://dx.doi.org/10.22092/botany.2013.101318>
- G. Erdtman. (1966). A propos de la stratification de l'exine. *Pollen Spores*, 8, 5-7
- Gaafar, A. (2019). Morphology and Stem Anatomy of *Chenopodium* Species from Egyptian Flora. *Egyptian Journal of Botany*, 59(1), 53-58.  
<https://dx.doi.org/10.21608/ejbo.2018.4699.1193>

- Gaafar, A., Kasem, W.T., Marei, H. and El-Fadaly, H.G. (2015). Morphological and stem anatomical description of 6 *Amaranthus* species L. from Jazan, Saudi Arabia. *International Journal of Current Research*, 7(2), 12277-12281.
- Gabr, D.G. (2014). Seed morphology and seed coat anatomy of some species of Apocynaceae and Asclepiadaceae. *Annals of Agricultural Sciences*, 59(2), 229-238. <https://doi.org/10.1016/j.aogas.2014.11.010>
- Gabr, D.G.I. (2018). Taxonomic importance of pollen morphology for some species of Brassicaceae. *Pakistan Journal of Biological Sciences*, 21(5), 215-223.
- Gamoun, M. (2014). Grazing intensity effects on the vegetation in desert rangelands of Southern Tunisia. *Journal of Arid Land*, 6(3), 324-333. <https://doi.org/10.1007/s40333-013-0202-y>
- Gamoun, M., Belgacem, A.O. and Louhaichi, M. (2018). Diversity of desert rangelands of Tunisia. *Plant diversity*, 40(5), 217-225. <https://doi.org/10.1016/j.pld.2018.06.004>
- Gan, L., Zhang, C., Yin, Y., Lin, Z., Huang, Y., Xiang, J., Fu, C. and Li, M. (2013). Anatomical adaptations of the xerophilous medicinal plant, *Capparis spinosa*, to drought conditions. *Horticulture, Environment, and Biotechnology*, 54(2), 156-161. <https://doi.org/10.1007/s13580-013-0162-3>
- Garralla, S. and Cuadrado, G.A., 2007. Pollen morphology of *Austrocylindropuntia* Backeb., *Maihueniopsis* Speg., *Opuntia* Mill. and *Tephrocactus* Lem.(Cactaceae, Opuntioideae) of Argentina. *Review of Palaeobotany and Palynology*, 146(1-4), 1-17. <https://doi.org/10.1016/j.revpalbo.2007.01.002>
- Garralla, S.S., Cuadrado, G.A., Lattar, E.C. and Salgado, C.R. (2013). Cactaceae. Cactoideae-Opuntioideae-Pereskioideae. *Polynic Flora of Northeast Argentina IV. Corrientes: University Publishing House of the National University of the Northeast*, 37-46.
- Gaskin, J.F., Ghahremani-nejad, F., Zhang, D.Y. and Londo, J.P. (2004). A systematic overview of Frankeniaceae and Tamaricaceae from nuclear rDNA and plastid sequence data. *Annals of the Missouri Botanical Garden*, 401-409.

- Gasma, M.M., Yeok, F.S., Lu, D., Lye, G.T. and Nasrollahzadeh, S.H. (2020). Morphological study of pollen from three Ecozones in Nigeria. *Journal of Critical Reviews*, 7(6), 1083-92.
- Gazer, H., Bous, E. and Mona, M. (2017). Palynotaxonomic studies on Boraginaceae in Saudi Arabia and its taxonomic significance. *Life Science Journal*, 14(4), 36-51.
- Ghimire, B., Ghimire, B.K. and Heo, K. (2011). Seed characteristics of *Withania somnifera* (Solanaceae). *Korean Journal of Plant Taxonomy*, 41(2), 103-107.
- Ghimire, B., Jeong, M.J., Choi, G.E., Lee, H., Suh, G.U., Heo, K. and Ku, J.J. (2015). Seed morphology of the subfamily Helleboroideae (Ranunculaceae) and its systematic implication. *Flora-Morphology, Distribution, Functional Ecology of Plants*, 216, 6-25. <https://doi.org/10.1016/j.flora.2015.07.004>
- Ghimire, B., Jeong, M.J., Suh, G.U., Heo, K. and Lee, C.H. (2018). Seed morphology and seed coat anatomy of *Fraxinus*, *Ligustrum* and *Syringa* (Oleaceae: Oleaceae) and its systematic implications. *Nordic Journal of Botany*, 36(10), p.e01866. <https://doi.org/10.1111/njb.01866>
- Ghosh, S. and Mandal, S. (2016). Pollen atlas of Santiniketan, West Bengal, with reference to Aeropalynology. *International Journal of Current Microbiology and Applied Sciences*, 5(5), 983-1000. <http://dx.doi.org/10.20546/ijcmas.2016.505.104>
- Gibson, A.C. and Nobel, P.S. (1986). *The cactus primer*. Harvard University Press. (1-286 pp).
- Gill, L.S., Olabanji, G.O. and Husaini, S.W.H. (1982). Studies on the structural variation and distribution of stomata in some Nigerian legumes. *Willdenowia*, 87-94.
- Glimn-Lacy, J. and Kaufman, P.B. (2006). Flowering Plant Classification. *Botany Illustrated: Introduction to Plants, Major Groups, Flowering Plant Families*, 75-75. <https://doi.org/10.1007/0-387-28875-9>

- Green, B.O., and Horsefall, U. (2008). Taxonomic and Biosystematic studies in certain members of family Cucurbitaceae in niger delta. *Ewopean Journal of scientific Research*, 20(1), 6-13.
- Grozeva, N., Terzieva, S., Gerdzhikova, M. and Pavlov, D. (2018). Chromosome and pollen morphology of *Salsola Soda* L. and *Salsola Tragus* L. in Bulgaria. *Bulgarian Journal of Agricultural Science*, 24(1), 59-67.
- Gul, F., Malik, K., Qureshi, R., Ahmad, M., Ansari, L., Zafar, M., Hussain, S., Khalid, S., Imran, M. and Rashid, N. (2022). Palyno-morphological attributes of some selected plant species of family Asteraceae from district Dera Ismail Khan, KPK, Pakistan. *Microscopy Research and Technique*, 85(4), 1392-1409. <https://doi.org/10.1002/jemt.24003>
- Gul, S., Ahmad, M., Zafar, M., Bahadur, S., Sultana, S., Ashfaq, S., Ullah, F., Kilic, O., Hassan, F.U. and Siddiq, Z. (2019). Foliar epidermal anatomy of Lamiaceae with special emphasis on their trichomes diversity using scanning electron microscopy. *Microscopy Research and Technique*, 82(3), 206-223. <https://doi.org/10.1002/jemt.23157>
- Gültepe, M., Coşkunçelebi, K., Makbul, S. and Terzioğlu, S. (2016). Taxonomic notes on *Tragopogon*, and two newly described taxa from Anatolia. *Nordic Journal of Botany*, 34(5), 529-537. <https://doi.org/10.1111/njb.01133>
- Gültepe, M., Makbul, S., Okur, S. and Coşkunçelebi, K. (2018). Contribution to the pollen morphology of *Tragopogon* (Asteraceae) in Turkey. *Phytotaxa*, 361(2), 168-182. <https://doi.org/10.11646/phytotaxa.361.2.3>
- Gune, F. and Ali, C. (2011). Seed characteristics and testa textures some taxa of genus *Lathyrus* L. (Fabaceae) from Turkey. *International Journal of Agriculture and Biology*, 13(6), 888-894.
- Hacioglu, B.T., Arslan, Y., Subasi, I., Katar, D., Bulbul, A.S. and Ceter, T. (2012). Achene morphology of Turkish' *Carthamus*' species. *Australian Journal of Crop Science*, 6(8), 1260-1264.

- Halbritter, H., Ulrich, S., Grímsson, F., Weber, M., Zetter, R., Hesse, M., Buchner, R., Svojtka, M. and Frosch-Radivo, A. (2018). *Illustrated pollen terminology*. Springer. [https://doi.org/10.1007/978-3-319-71365-6\\_3](https://doi.org/10.1007/978-3-319-71365-6_3)
- Hamdi, S.M.M., Malekloo, M., Assadi, M. and Nejadstari, T. (2009). Pollen micromorphological studies of the genus *Chenopodium* (Chenopodiaceae) in Iran. *Asian Journal of Plant Sciences*, 8(2), 129-137. <http://dx.doi.org/10.3923/ajps.2009.129.137>
- Hameed, A., Zafar, M., Ullah, R., Shahat, A.A., Ahmad, M., Cheema, S.I., Haq, I.U., Sultana, S., Usma, A. and Majeed, S. (2020). Systematic significance of pollen morphology and foliar epidermal anatomy of medicinal plants using SEM and LM techniques. *Microscopy Research and Technique*, 83(8), 1007-1022. <https://doi.org/10.1002/jemt.23493>
- Harker, M. and Jiménez-Reyes, N. (2002). *Verbesina barrancae* (Compositae, Heliantheae), a new species from Jalisco, Mexico. *Brittonia*, 54(3), 181-189. [https://doi.org/10.1663/0007-196X\(2002\)054\[0181:VBCHAN\]2.0.CO;2](https://doi.org/10.1663/0007-196X(2002)054[0181:VBCHAN]2.0.CO;2)
- Hassan, N.M., Meve, U. and Liede-Schumann, S. (2005). Seed coat morphology of Aizoaceae–Sesuvioideae, Gisekiaceae and Molluginaceae and its systematic significance. *Botanical Journal of the Linnean Society*, 148(2), 189-206. <https://doi.org/10.1111/j.1095-8339.2005.00407.x>
- Hassan, R.A. and Amer, W.M. (2019). Biosystematic study of the Egyptian *Datura stramonium* (Solanaceae). *Phytotaxa*, 408(3), 178-194. <https://doi.org/10.11646/phytotaxa.408.3.3>
- Hasson, S.M., AL-Qaraawi, H.A.H. and Abu-Serag, N.A. (2019). Study of some taxonomic aspects for some species of Cucurbitaceae in Iraq. *Plant Archives*, 19(2), 1966-1973.
- Hayat, M.Q., Ashraf, M., Jabeen, S., Shaheen, N., Yasmin, G. and Khan, M.A. (2010). Taxonomic implications of foliar epidermal characteristics with special reference to stomatal variations in the genus *Artemisia* (Asteraceae). *International Journal of Agriculture Biology*, 12, 221-226.

- Hayrapetyan, A.M. and Gabrielian, E.T. (2008). Features of the exine ornamentation of pollen grains in the family Solanaceae Juss. I. the simple types of ornamentation. *Electronic Journal of Natural Sciences*, 11(2), 46-50.
- Hong, J., Jiang, D.A., Weng, X.Y., Wang, W.B. and Hu, D.W. (2005). Leaf anatomy, chloroplast ultrastructure, and cellular localisation of ribulose-1, 5-bisphosphate carboxylase/oxygenase (RuBPCO) and RuBPCO activase in *Amaranthus tricolor* L. *Photosynthetica*, 43(4), 519-528. <https://doi.org/10.1007/s11099-005-0084-0>
- Hussain, A.N., Zafar, M., Ahmad, M., Khan, R., Yaseen, G., Khan, M.S., Nazir, A., Khan, A.M. and Shaheen, S. (2018). Comparative SEM and LM foliar epidermal and palyno-morphological studies of Amaranthaceae and its taxonomic implications. *Microscopy Research and Technique*, 81(5), 474-485. <https://doi.org/10.1002/jemt.23001>
- Iamónico, D. (2012). *Amaranthus powellii* subsp. *cacciatoi* comb. et stat. nov. (Amaranthaceae). *Nordic Journal of Botany*, 30(1), 12-16. <https://doi.org/10.1111/j.1756-1051.2011.01080.x>
- Ibrahim, H.M., Al-Dhawi, N.M., Al-Kherbi, G.M. and Al-Gifri, A.N.A. (2021). Palynological Characters of *Solanum* L. Species grown in Sana'a University (New Campus), Yemen. *Biological Research*, 6(2), 25-33.
- Ingole, S.N. and Kaikade, R.S. (2015). Study of petiolar anatomy of some medicinal plants mentioned in the Atharvaveda. *International Journal of Research Studies in Biosciences (IJRSB)*, 3(3), 103-106.
- Ismail, R.Y. and Shahbaz, S.E. (2020). Use of Pollen Morphology Traits for Identifying Species of *Centaurea* L. Asteraceae in Kurdistan-Iraq. *Science Journal of University of Zakho*, 8(4), 131-138. <https://doi.org/10.25271/sjuoz.2020.8.4.754>
- Ishtiaq, S., Hanif, U., Ajaib, M., Shaheen, S., Afridi, M.S.K. and Siddiqui, M.F. (2018). Pharamcognostical and physicochemical characterization of *Amaranthus graecizans* subsp. *silvestris*: An anatomical perspective. *Pakistan Journal of Botany*, 50(1), 307-312.



- Jafari, A. and Nasseh, Y. (2009). An internal structure investigation on *Euphorbia* L. species in North-East of Iran. *Asian Journal of Plant Sciences*, 8(1), 86-88.
- Jafari, E. and Ghanbarian, G.H. (2007). Pollen morphological studies on selected taxa of Asteraceae. *Journal of Plant Sciences*, 2(2), 195-201. <https://dx.doi.org/10.3923/jps.2007.195.201>
- Jalilzadeh, A., Hamdi, S.M.M., Asri, Y., Assadi, M. and Iranbakhsh, A. (2021). Pollen micromorphological study of some Chenopodiaceae species and their taxonomical relationships in Iran. *Rostaniha*, 22(2), 209-222. <https://dx.doi.org/10.22092/botany.2021.355379.1261>
- James, O.E., Green, B.O., Ajuru, M.G. and Wilson, V. (2021). Foliar epidermal anatomy and its taxonomic implications within the family Euphorbiaceae in the Niger Delta Region of Nigeria. *International Journal of Frontier Research in Science*, 1(1), 048-055. <https://doi.org/10.53294/ijflsr.2021.1.1.0036>
- Jamwal, R. (2021). Pollen Morphology of Some Selected Bee Floral Resources of *Apis cerana* F. And *Apis mellifera* L. using Scanning Electron Microscopy from Himachal Pradesh, India. *Uttar Pradesh Journal of Zoology*, 42(17), 8-16.
- Janu, V. and Raghuvanshi, R.K. (2011). Microscopic Studies on Epidermal Cells and Stomatal Behavior of Some Globular Cacti (*Mammillaria* spp.). *Insight Botany*, 1(1), 1-4. <http://dx.doi.org/10.5567/BOTANY-IK.2011.1.4>
- Jehanzeb, S., Zafar, M., Ahmad, M., Sultana, S., Zaman, W. and Ullah, F. (2020). Comparative petioler anatomy of tribe Mentheae subfamily Nepetoideae, Lamiaceae from Pakistan. *Feddes Repertorium*, 131(3), 163-174. <https://doi.org/10.1002/fedr.202000009>
- Jiang, H.E., Li, X., Ferguson, D.K., Wang, Y.F., Liu, C.J. and Li, C.S. (2007). The discovery of *Capparis spinosa* L.(Capparidaceae) in the Yanghai Tombs (2800 years bp), NW China, and its medicinal implications. *Journal of Ethnopharmacology*, 113(3), 409-420. <https://doi.org/10.1016/j.jep.2007.06.020>

- Jibril, S.M. and Bello, H.J. (2016). Leaf epidermal structures and stomata ontogeny in some members of the family Cucurbitaceae. *International Journal of Plant Soil Science*, 9(2), 1-9. [DOI: 10.9734/IJPSS/2016/20615](https://doi.org/10.9734/IJPSS/2016/20615)
- Joujeh, R., Zaid, S. and Mona, S. (2019). Pollen morphology of some selected species of the genus *Centaurea* L. (Asteraceae) from Syria. *South African Journal of Botany*, 125, 196-201. <https://doi.org/10.1016/j.sajb.2019.07.040>
- Kadiri, A.B., Utubor, D., and Ogundipe, O.T. (2013). Taxonomic relationships in *Lagenaria Seringe* (Cucurbitaceae) based on foliar epidermal morphology, *Thaiszia Journal of Botany*, 23(1), 47-59.
- Kahraman, A., Çildir, H. and Doğan, M. (2014). Anatomy, macro-and micromorphology of *Lathyrus* sect. *Nissolia* (Fabaceae) and their taxonomic significance. *Proceedings of the National Academy of Sciences, India Section B: Biological Sciences*, 84(2), 407-417. <https://doi.org/10.1007/s40011-013-0222-6>
- Kamel, M.A., El Hadidy, A.M., Hamed, S.T. and Hussein, N.R. (2018). A Palynological review for some species of family Boraginaceae Juss. From the Egyptian Flora. *Annual Research & Review in Biology*, 1-16. <https://doi.org/10.9734/ARRB/2018/46408>
- Kandemir, N., Çelik, A., Ullah, F., Shah, S.N. and Zaman, W. (2019). Foliar epidermal anatomical characteristics of taxa of *Iris* subg. *Scorpiris* Spach (Iridaceae) from Turkey. *Microscopy Research and Technique*, 82(6), 764-774. <https://doi.org/10.1002/jemt.23221>
- Kanwal, K., Zafar, M., Khan, A.M., Mahmood, T., Abbas, Q., Ozdemir, F.A., Ahmad, M., Sultana, S., Fatima, A., Aziz, A. and Niazi, A. (2022). Implication of scanning electron microscopy and light microscopy for oil content determination and seed morphology of Verbenaceae. *Microscopy research and technique*, 85(2), 789-798. <https://doi.org/10.1002/jemt.23950>
- Karaismailoğlu, M.C. (2018). Comparison of the karyotype analyses of two *Aethionema speciosum* subspecies from Turkey. *Caryologia*, 71(2), 128-132. <https://doi.org/10.1080/00087114.2018.1447629>

- Karakish, E.A., Moawed, M.M. and Tantawy, M.E. (2013). Seed morphology and protein patterns (SDS-PAGE) as a mean in classification of some taxa of the subfamily Mimosoideae (Fabaceae). *Annual Research & Review in Biology*, 367-388.
- Kasem, W.T. (2015). Macro and micromorphological studies on seven species of *Heliotropium* L. (Boraginaceae Juss.) in south west of Saudi Arabia. *American Journal of Plant Sciences*, 6(09), 1370. <http://www.scirp.org/journal/PaperInformation.aspx?PaperID=57000&#abstract>
- Kasem, W.T., Ghareeb, A. and Marwa, E. (2011). Seed morphology and seed coat sculpturing of 32 taxa of family Brassicaceae. *Journal of American Science*, 7(2), 166-178.
- Kaya, A., Ünal, M., Özgökce, F., Doğan, B. and Martin, E. (2011). Fruit and seed morphology of six species previously placed in *Malcolmia* (Brassicaceae) in Turkey and their taxonomic value. *Turkish Journal of Botany*, 35(6), 653-662. [DOI: 10.3906/bot-1010-99](https://doi.org/10.3906/bot-1010-99)
- Kayani, S., Hussain, M., Ahmad, M., Zafar, M., Sultana, S., Butt, M.A., Ali, S., Shah, G.M. and Mir, S. (2019). Scanning electron microscopy (SEM) and light microscopy (LM)-based Palyno-morphological views of Solanaceae in Western Himalaya. *Microscopy Research and Technique*, 82(2), 63-74. <https://doi.org/10.1002/jemt.23097>
- Keerthana, P. (2020). Pharmacognostic and phytochemical evaluation of *Chrozophora rottleri* (Geiseler) A. Juss. ex Spreng. *Journal of Pharmacognosy and Phytochemistry*, 9(3), 2066-2072.
- Keshavarzi, M. and Mosaferi, S. (2022). Leaf anatomy and micromorphology of the *Capparis spinosa* (Capparaceae) group in Iran. *Plant Biosystems-An International Journal Dealing with all Aspects of Plant Biology*, 1-14. <https://doi.org/10.1080/11263504.2022.2100501>
- Khalid, A., Mir, A.K., Mushtaq, A., Muhammad, Z., Muhammad, A. and Farooq, A. (2009). Taxonomic diversity of stomata in dicot flora of a district tank (NWFP) in Pakistan. *African journal of Biotechnology*, 8(6), 1052-1055.

- Khan, A., Ahmad, M., Zafar, S., Abbas, Q., Arfan, M., Zafar, M., Sultana, S., Ullah, S.A., Khan, S., Akhtar, A. and Kilic, O. (2022). Light and scanning electron microscopic observation of palynological characteristics in spineless *Astragalus* L. (Fabaceae) and its taxonomic significance. *Microscopy Research and Technique*. <https://doi.org/10.1002/jemt.24097>
- Khan, D. (2020). Seedling morphology of parrot tree [*Albizia lebbbeck* (L.) Benth. (Family Mimosaceae)] from Oud Metha Park, Dubai, UAE. *International Journal of Biology and Biotechnology*, 17(1), 137-158.
- Khan, D., Shaukat, S.S., Zaki, M.J. and Ali, S.V. (2018). Surface Microstructure of Leaf of *Capparis Cartilaginea* Decaisne (Family Capparaceae). *International Journal of Biology and Biotechnology*, 15(1), 85-97.
- Khan, F.M. (2009). Ethno-veterinary medicinal usage of flora of Greater Cholistan desert (Pakistan). *Pakistan Veterinary Journal*, 29(2), 75-80.
- Khan, K., Ahmad, M., Zafar, M., Malik, K., Sultana, S., Ahmad, S., Khan, F. and Ullah, K. (2021). Palyno-Morphological Study of Weedy Melliferous (Bee Visited) Plants Using Light Microscopic Techniques From Southern Khyber Pakhtunkhwa, Pakistan. *Pakistan Journal of Weed Science Research*, 27(2), 163-172. <https://doi.org/10.28941/pjwsr.v27i2.925>
- Khan, M.A. (2004). Variation in Pollen-Morphology of Selected Genera Belonging to Amaranthaceae from Pakistan. *Science*, 23(3), 53-60.
- Khan, R. (2005). Studies on the pollen morphology of the genus *Sisymbrium* and monotypic genera *Atelanthera* and *Arcyosperma* (Brassicaceae) from Pakistan. *Pakistan Journal of Botany*, 37(1), 15-22.
- Khan, R., Abidin, S.Z.U., Ahmad, M., Zafar, M., Liu, J., Jamshed, S. and Kiliç, Ö. (2019). Taxonomic importance of SEM and LM foliar epidermal micro-morphology: A tool for robust identification of gymnosperms. *Flora*, 255, 42-68. <https://doi.org/10.1016/j.flora.2019.03.016>
- Khan, S., Jan, G., Ahmad, M., Gul, F., Zafar, M., Mangi, J.U.D., Bibi, H., Sultana, S., Usma, A. and Majeed, S. (2021). Morpho-palynological assessment of some species of family Asteraceae and Lamiaceae of District Bannu, Pakistan on the

- bases of light microscope & scanning electron microscopy. *Microscopy Research and Technique*, 84(6), 1220-1232. <https://doi.org/10.1002/jemt.23681>
- Khan, S.U., Khan, R.U., Mehmood, S., Subhan, M. and Ullah, I. (2013). Anatomical study of selected weeds in high stress area of Bannu, Khyber Pakhtunkhwa, Pakistan. *Pakistan Journal of Weed Science Research*, 19(3), 327-340.
- Khan, S.U., Zafar, M., Ahmad, M., Anjum, F., Sultana, S., Kilic, O., Ozdemir, F.A., Nazir, A., Yaseen, G., Aabidin, S.Z. and Abbas, Q. (2019). Pollen micromorphological analysis of tribe Acacieae (Mimosaceae) with LM and SEM techniques. *Microscopy Research and Technique*, 82(9), 1610-1620. <https://doi.org/10.1002/jemt.23327>
- Khan, S.U., Zafar, M., Ullah, R., Shahat, A.A., Ahmad, M., Sultana, S. and Malik, K., 2021. Pollen diversity and its implications to the systematics of Mimosaceous species by LM and SEM. *Microscopy Research and Technique*, 84(1), 42-55. <https://doi.org/10.1002/jemt.23563>
- Khatamsaz, M. (2001). Pollen morphology of Iranian Boraginaceae family and its taxonomic significance. *Iranian Journal of Botany*, 9(1), 27-40.
- Khirade, P. and Dudhe, S. (2022). Morphological, Micromorphological and Eds Studies of Some Leguminous Seeds of Chandrapur District (M.S.), India. *International Journal of Researches in Biosciences, Agriculture and Technology*, 2(10), 132-138.
- Kiesling, R. (1984). Studies in Argentine Cactaceae: *Maihueniopsis*, *Tephrocactus* and related genera (Opuntioideae). *Darwiniana*, 25(4), 171-215.
- Kilian, N. (1997). Revision of *Launaea* Cass. (Compositae, Lactuceae, Sonchinae). Botanischer Garten und Botanisches Museum Berlin-Dahlem. *Englera*, 17, 1-478.
- Kirkbride J.H., Gunn C.R., Weitzman A.L. (2003). Fruits and seeds of genera in the subfamily Faboideae (Fabaceae), Vol 1. United States Department of Agriculture, Agricultural Research Service, Technical Bulletin Number 1890, Washington.

- Koul, K.K., Nagpal, R. and Raina, S.N. (2000). Seed coat microsculpturing in *Brassica* and allied genera (subtribes Brassicinae, Raphaninae, Moricandiinae). *Annals of Botany*, 86(2), 385-397. <https://doi.org/10.1006/anbo.2000.1197>
- Kraehmer, H. and Baur, P. (2013). *Weed anatomy*. John Wiley & Sons, (1-504 pp).
- Krishnamurthy, K.H. and Kannabiran, B. (1970). Histomorphology of foliar epidermis and pharmacognosy in Asclepiadaceae. *Journal of Indian Botanical Society*, 49 105–113.
- Krishnan, V. and Gopi, M. (2018). Botanical standardization of some Solanaceae members. *Indian Journal of Economics and Development*, 6(6), 1-9.
- Kumar, A., Sharma, S.S. and Kumar, B. (2020). Palynological studies on some plants of Boraginaceae. *Journal of Biotechnology and Biochemistry*, 6(5), 4-12. DOI: [10.9790/264X-0605020412](https://doi.org/10.9790/264X-0605020412)
- Kusumawardani, W., Muzzazinah and Ramli, M. (2019). Plant taxonomy learning and research: A systematics review. In *AIP Conference Proceedings* (Vol. 2194, No. 1, p. 020051). AIP Publishing LLC.
- Levi, A., Harris, K.R., Wechter, W.P., Kousik, C.S. and Thies, J.A. (2010). DNA markers and pollen morphology reveal that *Praecitrullus fistulosus* is more closely related to *Benincasa hispida* than to *Citrullus* spp. *Genetic resources and crop evolution*, 57(8), 1191-1205. <https://doi.org/10.1007/s10722-010-9559-3>
- Levizou, E., Drilias, P. and Kyparissis, A. (2004). Exceptional photosynthetic performance of *Capparis spinosa* L. under adverse conditions of Mediterranean summer. *Photosynthetica*, 42(2), 229-235. <https://doi.org/10.1023/B:PHOT.0000040594.85407.f4>
- Linn, S.S. (2020). Pollen Morphology of Ten Species Found in Nyaung Myint Village, Meiktila Township (Doctoral dissertation, MERAL Portal).
- Lippi, M.M., Gonnelli, T. and Raffaelli, M. (2007). Pollen morphology of trees, shrubs and woody herbs of the coastal plain and the monsoon slopes of Dhofar (Sultanate of Oman). *Webbia*, 62(2), 245-260. <https://doi.org/10.1080/00837792.2007.10670826>

- Liu, J., Hua, W., Yang, H.L., Zhan, G.M., Li, R.J., Deng, L.B., Wang, X.F., Liu, G.H. and Wang, H.Z. (2012). The BnGRF2 gene (GRF2-like gene from *Brassica napus*) enhances seed oil production through regulating cell number and plant photosynthesis. *Journal of experimental botany*, 63(10), 3727-3740. <https://doi.org/10.1093/jxb/ers066>
- Loza-Cornejo, S. and Terrazas, T. (2003). Epidermal and hypodermal characteristics in North American cactoideae (Cactaceae). *Journal of Plant Research*, 116(1), 27-35. <https://doi.org/10.1007/s10265-002-0066-2>
- Lu, K.Q., Xie, G., Li, M., Li, J.F., Trivedi, A., Ferguson, D.K., Yao, Y.F. and Wang, Y.F. (2018). Dataset of pollen morphological traits of 56 dominant species among desert vegetation in the eastern arid central Asia. *Data in brief*, 18, 1022-1046. <https://doi.org/10.1016/j.dib.2018.03.122>
- Luqman, M., Zafar, M., Ahmad, M., Ozturk, M., Sultana, S., Alam, F. and Ullah, F. (2019). Micromorphological observation of seed coat of *Eucalyptus* species (Myrtaceae) using scanning electron microscopy technique. *Microscopy Research and Technique*, 82(2), 75-84. <https://doi.org/10.1002/jemt.23099>
- Mabel, A.F., Johnson, A.A. and Temitope, O.O. (2014). Pollen grain morphology of some selected species of Asteraceae in South Western Nigeria. *Research in Plant Biology*, 4(6), 17-23.
- Mabel, A.F., Johnson, A.A., Olufemi, O.O. and Ayomipo, A.A.T. (2014). Foliar anatomy of some species of Asteraceae in South Western Nigeria. *African Journal of Plant Science*, 8(9), 426-440. <https://doi.org/10.5897/AJPS2014.1196>
- Majeed, S., Ahmad, M., Ozdemir, F.A., Demirpolat, A., Şahan, Z., Makhkamov, T.K., Nasirov, M., Zafar, M., Sultana, S., Yaseen, G. and Nabila (2023). Micromorphological Characterization of Seeds of Dicot Angiosperms from the Thal Desert (Pakistan). *Plant Biosystems-An International Journal Dealing with all Aspects of Plant Biology*, 1-27. <https://doi.org/10.1080/11263504.2023.2165553>
- Majeed, S., Zafar, M., Ahmad, M., Zafar, S., Ghufran, A., Ayoub, M., Sultana, S., Yaseen, G. and Raza, J., Nabila. (2022). Morpho-palynological and anatomical

- studies in desert cacti (*Opuntia dillenii* and *Opuntia monacantha*) using light and scanning electron microscopy. *Microscopy Research and Technique*, 85(8), 2801-2812. <https://doi.org/10.1002/jemt.24129>
- Maleklou, M., Hamdi, S.M.M., Asadi, M. And Nezhadsatari, T. (2010). Morphological, micromorphological and anatomical studies of *Chenopodium album* complex in Iran. *The Iranian Journal of Botany*, 16(1), 69-75.
- Malik, S., Ahmad, S., Sadiq, A., Alam, K., Wariss, H.M., Ahmad, I., Hayat, M.Q., Anjum, S. and Mukhtar, M. (2015). A comparative ethno-botanical study of Cholistan (an arid area) and Pothwar (a semi-arid area) of Pakistan for traditional medicines. *Journal of Ethnobiology and Ethnomedicine*, 11(1), 1-20. <https://doi.org/10.1186/s13002-015-0018-2>
- Mallick, P.K. (2017). Palynological studies on ten species of angiosperms from Nepal. *International Journal of Applied Sciences and Biotechnology*, 5(3), 361-365. <https://doi.org/10.3126/ijasbt.v5i3.18294>
- Malyshkina, T.P. and Ward, D.J. (2016). The Turanian Basin in the Eocene: The new data on the fossil sharks and rays from the Kyzylkum Desert (Uzbekistan). *Proceedings of the Zoological Institute PAH*, 320(1), 50-65.
- Mamoona, M., Mir, A.K., Mushtaq, A., Arshad, M.A., Muhammad, Z., Kiran, Y.K., Kanwal, T., Saira, T., Sidra, N.A., Ume, H. and Abida, B. (2011). Taxonomic potential of foliar epidermal anatomy among the wild culinary vegetables of Pakistan. *Journal of Medicinal Plants Research*, 5(13), 2857-2862.
- Mamoona, M., Mir, A.K., Mushtaq, A., Nighat, S., Sidra, N.A., Kanwal, T., Saira, T., Tehmeena, M., Madhia, A. and Shazia, B. (2011). Foliar epidermal anatomy of some ethnobotanically important species of wild edible fruits of northern Pakistan. *Journal of Medicinal Plants Research*, 5(24), 5873-5880.
- Mao, R., Xia, P., Liu, J., Li, X., Han, R., Liu, F., Zhao, H. and Liang, Z. (2018). Genetic diversity and population structure assessment of Chinese *Senna obtusifolia* L. by molecular markers and morphological traits of seed. *Acta physiologiae plantarum*, 40(1), 1-14. <https://doi.org/10.1007/s11738-017-2586-3>



- Martins da Costa Rodrigues, I., Fernandes Falcão, B., Stehmann, J.R. and Girardi Bauermann, S. (2016). Pollen morphology in *Athenaea* sendtn. and *Aureliana* sendtn.(Solanaceae). *Palynology*, 40(2), 202-215. <https://doi.org/10.1080/01916122.2015.1022908>
- Martins, C., Oliveira, R., Mendonca Filho, C.V., Lopes, L.T., Silveira, R.A., de Silva, J.A.P., Aguiar, L.M. and Antonini, Y. (2016). Reproductive biology of *Cipocereus minensis* (Cactaceae)—A columnar cactus endemic to rupestrian fields of a Neotropical savannah. *Flora-Morphology, Distribution, Functional Ecology of Plants*, 218, 62-67. <https://doi.org/10.1016/j.flora.2015.11.010>
- Marzouk, R.I., El-Darier, S.M., Kamal, S.A. and Nour, I.H. (2021). Comparative Taxonomic Study of *Launaea* Cass. (Asteraceae, Cichorioideae) in Egypt. *Taxonomy*, 1(3), 192-209. <https://doi.org/10.3390/taxonomy1030014>
- Maskour, L., Alami, A., Agorram, B. and Zaki, M. (2016). Study of some learning difficulties in plant classification among university students. *The Eurasia Proceedings of Educational and Social Sciences*, 5, 294-297.
- Maw, K.H., Than, K.N. and Yee, N.N. (2020). Pollen morphology of some ornamental plants in Yadanabon university campus, Mandalay. In *Third Myanmar Korea Conference Research Journal*, 3(1), 203-210.
- Mazari, P., Khan, M.A., Ahmad, M., Khan, K.Y., Zafar, M., Ali, B. and Niamat, R. (2012). Pollen fertility estimation of selected taxa of Kaghan valley, Pakistan. *Research in Plant Biology*, 2(4), 16-21.
- Mehrabian, A.R., Zare, S., Azizian, D. and Podlech, D. (2007). Petiole anatomy in *Astragalus* sect. *Incarni* DC. (Fabaceae) in Iran (A Phylogenetical approach). *The Iranian Journal of Botany*, 13(2), 138-145.
- Memon, R.A., Bhatti, G.R., Khalid, S., Arshad, M., Mirbahar, A.A. and Qureshi, R. (2010). Microstructural features of seeds of *Spergularia marina* (L.) Griseb., (Caryophyllaceae). *Pakistan Journal of Botany*, 42(3), 1423-1427.
- Meo, A.A. and Khan, M.A. (2003). Pollen morphology of some medicinal plants of family Compositae (Asteraceae) from Pakistan. In *International Workshop on*

*Conservation and Sustainable uses of Medicinal of Aromatic Plants in Pakistan, Islamabad. Proceeding of the international Workshop, 130-135.*

- Metcalf, C.R. and Chalk, L. (1979). Anatomy of the dicotyledons. Systematic anatomy of the leaf and stem with a Brief History of the Subject. 2nd Edition, Vol. 1, Clarendon Press, Oxford, 40-41.
- Metcalf, C.R. (1968). Current developments in systematic plant anatomy. In Modern methods in plant taxonomy, 45-57.
- Metcalf, C.R. and Chalk, L. (1957). Anatomy of the Dicotyledons–Leaves, stem, and wood in relation to taxonomy with notes on economic uses. 2nd Edition, Clarendon Press, Oxford.
- Miesen, F., De Porras, M.E. and Maldonado, A. (2015). Pollen morphology of Cactaceae in Northern Chile. *Gayana Botánica*, 72(2), 258-271.  
<http://dx.doi.org/10.4067/S0717-66432015000200010>
- Mir, S., Ahmad, M., Khan, M.A., Zafar, M., Jahan, S., Sultana, S., Jabeen, M. and Majeed, S. (2019). Palyno-morphological investigations of subtropical endangered flora of Capparidaceae through light and scanning electron microscopy. *Microscopy Research and Technique*, 82(9), 1401-1409.  
<https://doi.org/10.1002/jemt.23292>
- Mohamed, M.B., Keerthikaw, A., Gupta, D.K., Shukla, A.K. and Jangid, B.L. (2018). Effect of seed morphometric variability on germination and seedling characteristics of *Prosopis cineraria* (L.) Druce under arid condition of Rajasthan. *Range Management and Agroforestry*, 39(1), 126-129.
- Mohsen, L. and Badr, A. (2019). Description of seed and pollen micromorphology and their taxonomic impact in some *Solanum* L. species. *Taekholmia*, 39(1), 1-17.  
<https://dx.doi.org/10.21608/taec.2019.11353.1003>
- Morales-Tapia, P., Gambardella, M., Gómez, M. and Montenegro, G 2019. Morpho-anatomical adaptations of *Argylia radiata* (L.) D. Don to an arid environment. *Flora*, 258, p.151440.  
<https://doi.org/10.1016/j.flora.2019.151440>

- Moreira, G.L., Cavalcanti, T.B., Mendonça, C.B.F. and Gonçalves-Esteves, V. (2019). Pollen morphology of Brazilian species of *Verbesina* L. (Heliantheae-Asteraceae). *Acta Botanica Brasilica*, 33, 128-134. <https://doi.org/10.1590/0102-33062018abb0395>
- Müller, K. and Borsch, T. (2005). Multiple origins of a unique pollen feature: stellate pore ornamentation in Amaranthaceae. *Grana*, 44(4), 266-282. <https://doi.org/10.1080/00173130500477787>
- Munir, M., Ahmad, M., Waseem, A., Zafar, M., Saeed, M., Wakeel, A., Nazish, M. and Sultana, S. (2019). Scanning electron microscopy leads to identification of novel nonedible oil seeds as energy crops. *Microscopy Research and Technique*, 82(7), 1165-1173. <https://doi.org/10.1002/jemt.23265>
- Munir, U., Perveen, A. and Qamarunnisa, S. (2014). Comparative Pharmacognostic evaluation of some species of the genera *Suaeda* and *Salsola* leaf (Chenopodiaceae). *Pakistan journal of pharmaceutical sciences*, 27(5), 1309-1315.
- Mustafa, E.M.A., Alkamali, H.H. and Eltahir, A.S. (2017). Comparative anatomical study of some *Acacia* taxa seeds grown in central Sudan. *European Journal of Advanced Research in Biological and Life Sciences*, 5(1), 36-44.
- Myers, J.A., Chase, J.M., Jiménez, I., Jørgensen, P.M., Araujo-Murakami, A., Paniagua-Zambrana, N. and Seidel, R. (2013). Beta-diversity in temperate and tropical forests reflects dissimilar mechanisms of community assembly. *Ecology letters*, 16(2), 151-157. <https://doi.org/10.1111/ele.12021>
- Naggar, S.M. (2004). Pollen morphology of Egyptian Malvaceae: An assessment of taxonomic value. *Turkish Journal of Botany*, 28(1), 227-240.
- Naimat, R., Khan, M.A., Khan, K.Y., Ali, B. and Mazari, P. (2012). Palynomorphological characterization of some species of selected genera of family Rhamnaceae. *Research in Plant Biology*, 2(3), 4-9.
- Nalawade, A.S., Bose, A. and Gurav, R.V. (2020). Comparative seed morphology in the genus *Chlorophytum* Ker Gawl. (Agavoideae, Asparagaceae) in India. *Flora*, 273, 151723. <https://doi.org/10.1016/j.flora.2020.151723>

- Nameer, S., Aliwy, S.A., Al-Azerg, L.K.A. and Redah, H. (2017). Anatomical Comparative for Two Species *Amaranthus Albus* L. And *Amaranthus Gracilis* Defs Amaranthaceae) in Iraq. *The Iraqi Journal of Agricultural Science*, 48(6), 1563-1572.
- Nazish, M., Ahmad, M., Ullah, R., Shahat, A.A., Potter, D., Zafar, M. and Sultana, S. (2022). Taxonomic implications of leaf epidermis in halophytes of Amaranthaceae from Salt Range of Punjab, Pakistan. *Plant Biosystems-An International Journal Dealing with all Aspects of Plant Biology*, 156(1), 79-90. <https://doi.org/10.1080/11263504.2020.1837277>
- Nazish, M., Zafar, M., Ahmad, M., Sultana, S., Ullah, R., Alqahtani, A.S., Ullah, F., Ahmad, S., Ashfaq, S. and Ullah, F. (2019). Palyno-morphological investigations of halophytic taxa of Amaranthaceae through SEM from Salt range of Northern Punjab, Pakistan. *Microscopy research and technique*, 82(3), 304-316. <https://doi.org/10.1002/jemt.23173>
- Nicholson, S.E. (2011). Dryland climatology. Cambridge University Press. <https://doi.org/10.1017/CBO9780511973840>
- Nilsson S., and Praglowski, J. (1992). Erdtman's Handbook of Palynology, 2nd edn. Copenhagen: Munksgaard.
- Nilsson, S. (1990). Taxonomic and evolutionary significance of pollen morphology in the Apocynaceae. In *Morphology, development, and systematic relevance of pollen and spores*, 91-102, Springer, Vienna. [https://doi.org/10.1007/978-3-7091-9079-1\\_8](https://doi.org/10.1007/978-3-7091-9079-1_8)
- Ninkaew, S., Pornponggrueng, P., Balslev, H. and Chantaranonthai, P. (2017). Seed morphology of nineteen *Crotalaria* L. (Fabaceae) species in Thailand. *Thai Forest Bulletin (Botany)*, 45(1), 47-57. <https://doi.org/10.20531/tfb.2017.45.1.09>
- Nobarinezhad, M.H., Pakravan, M. and Pahlevani, A. (2018). A biosystematic study of *Euphorbia* subgenus *Chamaesyce* (Euphorbiaceae) in Iran. *Phytotaxa*, 360(3), 179-200. <https://doi.org/10.11646/phytotaxa.360.3.1>

- Nobel, P.S. (2002). *Cacti: biology and uses*. University of California Press; Berkeley, CA, USA: Los Angeles, CA, USA.
- Noedoost, F., Vaezi, J. and Siahkolaee, S.N. (2021). Taxonomic investigation of the *Xanthium strumarium* L. complex (Asteraceae) distributed in Iran inferred from morphological, palynological and molecular data. *Biodiversitas Journal of Biological Diversity*, 22(4), 1961-1974. <https://doi.org/10.13057/biodiv/d220444>
- Nowicke, J.W. (1975). Pollen morphology in the order Centrospermae. *Grana*, 15(1-3), 51-77. <https://doi.org/10.1080/00173134.1975.11864622>
- Nowicke, J.W. (1994). Pollen morphology and exine ultrastructure. In *Caryophyllales* (pp. 167-221). Springer, Berlin, Heidelberg. [https://doi.org/10.1007/978-3-642-78220-6\\_8](https://doi.org/10.1007/978-3-642-78220-6_8)
- Nowicke, J.W. and Skvarla, J.J. (1979). Pollen morphology: The potential influence in higher order systematics. *Annals of the Missouri Botanical Garden*, 66(4), 633-700. <https://doi.org/10.2307/2398914>
- Nowicke, J.W., Takahashi, M. and Webster, G.L. (1999). Pollen morphology, exine structure and systematics of Acalyphoideae (Euphorbiaceae): Part 2. Tribes Agrostistachydeae (*Agrostistachys*, *Pseudagrostistachys*, *Cyttaranthus*, *Chondrostylis*), Chrozophoreae (*Speranskia*, *Caperonia*, *Philyra*, *Ditaxis*, *Argythamnia*, *Chiropetalum*, *Doryxylon*, *Sumbaviopsis*, *Thyrsanthera*, *Melanolepis*, *Chrozophora*), Caryodendreae (*Caryodendron*, *Discoglyprena*, *Alchorneopsis*), *Bernardieae* (*Bernardia*, *Necepsia*, *Paranecepsia*, *Discocleidion*, *Adenophaedra*) and Pycnosomeae (*Pycnoma*, *Drocelonia*, *Argomuellera*, *Blumeodendron*, *Podadenia*, *Ptychopyxis*, *Botryophora*). *Review of Palaeobotany and Palynology*, 105(1-2), 1-62. [https://doi.org/10.1016/S0034-6667\(98\)00069-4](https://doi.org/10.1016/S0034-6667(98)00069-4)
- Oezler, H., Kaya, Z. and Pehlivan, S. (2009). Pollen morphology of some *Centaurea* L., *Psephellus* Cass. and *Cyanus* Miller taxa. *Acta Biologica Cracoviensia Series Botanica* 51(2), 53–66.
- Okeke, N.F., Ilodibia, C.V. and Okoli, B.E. (2020). A Comparative Morphological Study on *Amaranthus spinosus* L., *Celosia argentea* L. and *Gomphrena*

- celosioides* Mart (Amaranthaceae). *Universal Journal of Plant Science*, 8(1), 1-10. [DOI: 10.13189/ujps.2020.080101](https://doi.org/10.13189/ujps.2020.080101)
- Okwuchukwu, A.B. and Uwabukeonye, O.C. (2017). Taxonomic significance of stem and petiole anatomy of three white varieties of *Vigna unguiculata* (L.) Walp. *Archives of Agriculture and Environmental Science*, 2(2), 109-112.
- Onoja, O.J. (2016). Morpho-anatomical study on *Cleome viscosa* L. (Cleomaceae). *Journal of Pharmacognosy and Phytochemistry*, 5(4), 13-16.
- Osman, A.K. (2009). Contributions to the pollen morphology of Tribe Cardueae (Cichorioideae-Compositae). *Feddes Repertorium*, 120(3-4), 145-157. <https://doi.org/10.1002/fedr.200811103>
- Ozbek, F., Ozbek, M.U. and Ekici, M. (2014). Morphological, anatomical, pollen and seed morphological properties of *Melilotus bicolor* Boiss. and *Balansa* (Fabaceae) endemic to Turkey. *Australian Journal of Crop Science*, 8(4), 543-549.
- Ozimele, C.O., Obute, G.C. and Nyananyo, B.L. (2019). Morphological and Anatomical Diversity Study on three Species of *Amaranthus* namely; *A. hybridus* L., *A. viridis* L. and *A. spinosus* L. from Rivers State, Nigeria. *Journal of Applied Sciences and Environmental Management*, 23(10), 1875-1880. <https://doi.org/10.4314/jasem.v23i10.17>
- Padrón-Mederos, M.A. and La Serna-Ramos, I.E. (2011). Pollen morphology of genus *Allagopappus* Cass.(Asteraceae: Inuleae), endemic to the Canary Islands, Spain. *Plant Biosystems-an International Journal Dealing with all Aspects of Plant Biology*, 145(4), 809-817. <https://doi.org/10.1080/11263504.2011.578787>
- Pahlevani, A.H., Liede-Schumann, S. and Akhiani, H. (2015). Seed and capsule morphology of Iranian perennial species of *Euphorbia* (Euphorbiaceae) and its phylogenetic application. *Botanical journal of the Linnean Society*, 177(3), 335-377. <https://doi.org/10.1111/boj.12245>

- Pal, V.C., Singh, O.V., Singh, B. and Ahamad, A. (2013). Pharmacognostical studies of *Amaranthus spinosus* Linn. *Pharmaceutical and Biosciences Journal*, 1(1), 32-37. <https://doi.org/10.20510/ukjpb/1/i1/91112>
- Pan, A.D. (1993). Studies on the pollen morphology of Chenopodiaceae from Xinjiang. *Arid Land Geography*, 16, 22-27.
- Patil, R.B., Kore B.A. (2018). Morphoanatomy, phenology and palynology of an invasive weed *Alternanthera ficoidea* (L.) P. Beauv. *IOSR Journal of Pharmacy and Biological Sciences*, 13(5), 18-23. DOI: [10.9790/3008-1305041823](https://doi.org/10.9790/3008-1305041823)
- Paul, E., Essien, B.C., Idachaba, S.O., Edegbo, E. and Tamenku, M.M. (2014). Comparative Study of Pollen Morphology of some members of Euphorbiaceae family. *Standard Research Journal of Agricultural Sciences*, 2(4), 054-058.
- Pereira Coutinho, A. and Dinis, A.M. (2007). A contribution to the ultrastructural knowledge of the pollen exine in subtribe *Inulinae* (Inuleae, Asteraceae). *Plant Systematics and Evolution*, 269(3), 159-170. <https://doi.org/10.1007/s00606-007-0585-3>
- Perrotta, V.G. and Arambarri, A.M. (2018). Cladodes anatomy of *Opuntia* (Cactaceae) from the province of Buenos Aires (Argentina). *Bulletin of the Argentine Society of Botany*, 53(3), 1-20.
- Perveen, A. (1999). Contributions to the Pollen morphology of the family Compositae. *Turkish Journal of Biology*, 23(4), 523-536.
- Perveen, A. and Qaiser, M. (1995). Pollen flora of Pakistan-IV. Boraginaceae. *Pakistan Journal of Botany*, 27, 327-360.
- Perveen, A. and Qaiser, M. (2000). Pollen Flora of Pakistan-XIX. Aizoaceae. *Turkish Journal of Botany*, 24(1), 29-33.
- Perveen, A. and Qaiser, M. (2001). Pollen flora of Pakistan-XXVII Nyctaginaceae. *Turkish Journal of Botany*, 25(6), 385-388.
- Perveen, A. and Qaiser, M. (2005). Pollen flora of Pakistan-xlvii. Euphorbiaceae. *Pakistan Journal of Botany*, 37(4), 785-796.

- Perveen, A. and Qaiser, M. (2006). Pollen Flora of Pakistan-XLVIII. Umbelliferae. *Pakistan Journal of Botany*, 38(1), 1-14.
- Perveen, A. and Qaiser, M. (2006). Pollen flora of Pakistan-XLVIX. Zygophyllaceae. *Pakistan Journal of Botany*, 38(2), 225-232.
- Perveen, A. and Qaiser, M. (2008). Pollen flora of Pakistan-LVI. Cucurbitaceae. *Pakistan Journal of Botany*, 40(1), 9-16.
- Perveen, A. and Qaiser, M. (2012). Pollen flora of Pakistan-LXX: Chenopodiaceae. *Pakistan Journal of Botany*, 44(4), 1325-1333.
- Perveen, A. and Qaiser, M., 2007. Pollen morphology of family Solanaceae from Pakistan. *Pakistan journal of botany*, 39(7), 2243-2256.
- Perveen, A., and Qaiser, M. (2002). Pollen Flora of Pakistan-XVIII. Amaranthaceae. *Pakistan Journal of Botany*, 34(4), 375-383.
- Perveen, A., Noori, M.Y., Khan, M. and Qureshi, M.A. (2015). Spectrum of allergenic pollen in Karachi and their characterization using conventional and electron microscopy: Potential candidates for allergy vaccines. *Rawal Medical Journal*, 40(1), 7-13.
- Perveen, A., Qaiser, M. and Khan, R. (2004). Pollen Flora of Pakistan–XLII. Brassicaceae. *Pakistan Journal of Botany*, 36(4), 683-700.
- Perveen, N. (1999). Palynological study of selected medicinal plant of family Asteraceae. *Department of Botany of Arid Agriculture. Rawalpindi Palmstan*. 1-38.
- Pinar, A. (2007). Endemic for Turkey *Centaurea cariensis* Boiss. Morphological and Palynological Studies on Subspecies. High Engineering Thesis, Zonguldak Karaelmas University, Institute of Science and Technology.
- Poulsen, A.D. and Nordal, I. (2005). A phenetic analysis and revision of Guineo-Congolese rain forest taxa of *Chlorophytum* (Anthericaceae). *Botanical Journal of the Linnean Society*, 148(1), 1-20. <https://doi.org/10.1111/j.1095-8339.2005.00386.x>



- Prabhakar, R. and Ramakrishna, H. (2014). Pollen diversity of ethnomedicinal plants of nirmal forest division in Adilabad District, Telangana State, India. *World journal of pharmaceutical research*, 3(8), 220-237.
- Praglowski, J. (1987). Pollen morphology of Tribulaceae. *Grana*, 26(3), 193-211. <https://doi.org/10.1080/00173138709428915>
- Pratami, M.P., Chikmawati, T. And Rugayah, R. (2019). Further morphological evidence for separating Mukia Arn. from *Cucumis* L. *Biodiversitas Journal of Biological Diversity*, 20(1), 211-217. <https://doi.org/10.13057/biodiv/d200124>
- Priya, C. and Hari, N. (2018). A study on leaf and petiole anatomy of endemic and vulnerable species of *Garcinia*. *Journal of Emerging Technology and Innovative Research*, 5(12), 509-512.
- Punsalpaamuu, G., Schluetz, F., Gegeensuvd, T. and Saindovdon, D. (2012). On the importance of pollen morphology in classification of Chenopodiaceae in Mongolia. *Erforsch Biological Research, Mongolei*, (12), 429-436.
- Punt, W. and Hoen, P.P. (2009). The Northwest European Pollen Flora, 70: Asteraceae—Asteroideae. *Review of Palaeobotany and Palynology*, 157(1-2), 22-183. <https://doi.org/10.1016/j.revpalbo.2008.12.003>
- Punt, W., Hoen, P.P., Blackmore, S., Nilsson, S. and Le Thomas, A. (2007). Glossary of pollen and spore terminology. *Review of Palaeobotany and Palynology*, 143(1-2), 1-81. <https://doi.org/10.1016/j.revpalbo.2006.06.008>
- Qaiser, M., and Perveen, A. (2004). Pollen Flora of Pakistan-XXXVII. Tamaricaceae. *Pakistan Journal of Botany*, 36(1), 1-18.
- Quamar, M.F., Ali, S.N., Morthekai, P. and Singh, V.K. (2017). Confocal (CLSM) and light (LM) photomicrographs of different plant pollen taxa from Lucknow, India: implications of pollen morphology for systematics, phylogeny and preservation. *Review of Palaeobotany and Palynology*, 247, 105-119. <https://doi.org/10.1016/j.revpalbo.2017.09.005>
- Quesada, E.M. (1997). Taxonomic significance of foliar dermotypes and floral trichomes in some Cuban taxa of *Indigofera* L. (Fabaceae-Faboideae). *Polibotánica*, (6), 1-18.

- Qureshi, M.N., Talha, N., Ahmad, M., Zafar, M. and Ashfaq, S. (2019). Morpho-palynological investigations of natural resources: A case study of Surghar mountain district Mianwali Punjab, Pakistan. *Microscopy research and technique*, 82(7), 1047-1056. <https://doi.org/10.1002/jemt.23252>
- Qureshi, S.J., Awan, A.G., Khan, M.A. and Bano, S. (2002). Palynological study of the genus *Sonchus* from Pakistan. *Journal of Biological Sciences*, 2(2), 98-105.
- Qureshi, S.J., Khan, M.A. and Subhan, K. (2008). Comparative morphology, palynology and anatomy of two Asteraceae species. *Trakia Journal of Sciences*, 6(4), 52-61.
- Radaeski, J.N., Evaldt, A.C.P. and Bauermann, S.G. (2016). Pollen morphology of species of the family Asteraceae Martinov in the hills of Campanha in Rio Grande do Sul, Brazil. *Iheringia, Série Botânica.*, 71(3), 357-366.
- Ragho, K.S. (2020). Role of pollen morphology in taxonomy and detection of adulterations in crud drugs. *Journal of Plant Science and Phytopathology*, 4, 24-27. <https://dx.doi.org/10.29328/journal.jpssp.1001046>
- Raj, P.R. and Reddy, A. (2019). Pollen morphology study of Leguminosae family from Manchippa Reserve Forest, Nizamabad district, Telangana. *Journal of Tree Sciences*, 38(2), 70-84. <http://dx.doi.org/10.5958/2455-7129.2019.00019.0>
- Rajurkar, A.V., Tidke, J.A. and Jadhav, S.S. (2013). Palynomorphological studies on family Mimosaceae. *International Journal of Pharma and Bio Sciences*, 4(3), 273-279.
- Rashid, N., Zafar, M., Ahmad, M., Khan, M.A., Malik, K., Sultana, S. and Shah, S.N. (2019). Taxonomic significance of leaf epidermis in tribe Trifolieae L.(Leguminosae; Papilionoideae) in Pakistan. *Plant Biosystems-an international journal dealing with all aspects of Plant Biology*, 153(3), 406-416. <https://doi.org/10.1080/11263504.2018.1492995>
- Rashid, N., Zafar, M., Ahmad, M., Malik, K., Haq, I.U., Shah, S.N., Mateen, A. and Ahmed, T. (2018). Intraspecific variation in seed morphology of tribe vicieae

- (Papilionoidae) using scanning electron microscopy techniques. *Microscopy research and technique*, 81(3), 298-307. <https://doi.org/10.1002/jemt.22979>
- Rashid, N., Zafar, M., Ahmad, M., Malik, K., Shah, S.N., Sultana, S., Zahid, N., Noshad, Q. and Siddiq, Z. (2022). Use of scanning electron microscopy to analyze sculpturing pattern and internal features of pollen grain wall in some members of Astragaleae (subfamily: Papilionoidae). *Microscopy Research and Technique*, 85(5), 1631-1642. <https://doi.org/10.1002/jemt.24023>
- Rashid, N., Zafar, M., Ahmad, M., Memon, R.A., Akhter, M.S., Malik, K., Malik, N.Z., Sultana, S. and Shah, S.N. (2021). Seed morphology: An addition to the taxonomy of Astragaleae and Trifolieae (Leguminosae: Papilionoidae) from Pakistan. *Microscopy research and technique*, 84(5), 1053-1062. <https://doi.org/10.1002/jemt.23666>
- Rasool, F., Murtaza, G., Zeshan, M., Habib, R., Yousaf, M.M., Ayub, M.M., Ayub, M.A., Sardar, K. and Irshad, H.A. (2016). Comprehensive review on ecology and ethnobotany of *Acacias* and *Acacia jacquemontii* Benth in dry environment. *International Journal of Applied Research*, 2(12), 103-109.
- Raza, J., Ahmad, M., Zafar, M., Athar, M., Sultana, S., Majeed, S., Yaseen, G., Imran, M., Nazish, M. and Hussain, A. (2020). Comparative foliar anatomical and pollen morphological studies of Acanthaceae using light microscope and scanning electron microscope for effective microteaching in community. *Microscopy Research and Technique*, 83(9), 1103-1117. <https://doi.org/10.1002/jemt.23502>
- Raza, J., Ahmad, M., Zafar, M., Yaseen, G., Sultana, S. and Majeed, S. (2022). Systematic significance of seed morphology and foliar anatomy among Acanthaceous taxa. *Biologia*, 1-18. <https://doi.org/10.1007/s11756-022-01137-0>
- Reshmi, G.R. and Rajalakshmi, R. (2019). Systematic significance of pollen morphology of the genus *Acmella* rich. (Heliantheae: Asteraceae). *Iranian Journal of Science and Technology, Transactions A: Science*, 43(4), 1469-1478. <https://doi.org/10.1007/s40995-018-0660-3>

- Rewicz, A., Myśliwy, M., Adamowski, W., Podlasiński, M. and Bomanowska, A. (2020). Seed morphology and sculpture of invasive *Impatiens capensis* Meerb. from different habitats. *PeerJ*, 8, p.e10156. <https://doi.org/10.7717/peerj.10156>
- Rezanejad, F. and Ganjalikhani Hakemi, F. (2017). Studies of Pollen Characteristics in Plants of Fruitless *Tecomella undulata* (Sm.) Seem. (Bignoniaceae) in Golparaki Region of Jiroft City, Iran. *Iranian Journal of Science and Technology, Transactions A: Science*, 41(4), 979-988. <https://doi.org/10.1007/s40995-017-0338-2>
- Riaz, S. and Abid, R. (2018). Significance of seed micromorphological characters and seed coat elements for the taxonomic delimitation of the genus *Cleome* L. (Cleomaceae) from Pakistan. *Pakistan Journal of Botany*, 50(1), 271-277.
- Riaz, S., Abid, R. and Ali, A. (2021). Phenolic Compounds and Elements of Leaves As An Aid For The Taxonomic Delimitation of the Genus *Cleome* L. (Cleomaceae) from Pakistan. *International Journal of Biology and Biotechnology*, 18(2), 307-313.
- Rivera, P., Villaseñor, J.L. and Terrazas, T. (2017). Meso-or xeromorphic? Foliar characters of Asteraceae in a xeric scrub of Mexico. *Botanical Studies*, 58(1), 1-16. <https://doi.org/10.1186/s40529-017-0166-x>
- Robertson, S., Narayanan, N., Deattu, N. and Nargis, N.R. (2010). Comparative anatomical features of *Prosopis cineraria* (L.) Druce and *Prosopis juliflora* (Sw.) DC (Mimosaceae). *International Journal of Green Pharmacy (IJGP)*, 4(4). <https://doi.org/10.22377/IJGP.V4I4.160>
- Rodríguez-Estrella, R., Estrada, C.G., Alvarez-Castañeda, S.T. and Ferrer-Sánchez, Y. (2019). Comparing individual raptor species and coarse taxonomic groups as biodiversity surrogates in desert ecosystems. *Biodiversity and Conservation*, 28(5), 1225-1244. <https://doi.org/10.1007/s10531-019-01721-y>
- Roohi, A. and Muhammad, Q. (2015). Cypsela morphology of *Lactuca* L. and its allied genera (Cichoreae-Asteraceae) from Pakistan and Kashmir. *Pakistan Journal of Botany*, 47(5), 1937-1955.

- Rosa, A.C., Ferraro, A., da Silva, R.H., Pott, V.J., Victório, C.P. and Arruda, R.D.C.D.O. (2021). Leaf anatomy of two medicinal *Croton* species: Contribution to plant recognition. *Microscopy Research and Technique*, 84(8), 1685-1695. <https://doi.org/10.1002/jemt.23727>
- Rozina., Ahmad, M., Zafar, M., Yousaf, Z., Ullah, S.A., Sultana, S. and Bibi, F. (2022). Identification of novel, non-edible oil seeds via scanning electron microscopy as potential feedstock for green synthesis of biodiesel. *Microscopy Research and Technique*, 85(2), 708-720. <https://doi.org/10.1002/jemt.23942>
- Sá, R.D., Cadena, M.B., Padilha, R.J.R., Alves, L.C. and Randau, K.P. (2018). Anatomical Study and Characterization of Metabolites in Leaves of *Momordica charantia* L. *Pharmacognosy Journal*, 10(5), 823-826. <http://dx.doi.org/10.5530/pj.2018.5.140>
- Saadaoui, E., Gómez, J.J.M. and Cervantes, E. (2013). Intraspecific variability of seed morphology in *Capparis spinosa* L. *Acta Biologica Cracoviensia Series Botanica*, 55(2), 99-106. DOI: [10.2478/abcsb-2013-0027](https://doi.org/10.2478/abcsb-2013-0027)
- Saad-Limam, S.B., Nabli, M.A. and Rowley, J.R. (2005). Pollen wall ultrastructure and ontogeny in *Heliotropium europaeum* L. (Boraginaceae). *Review of Palaeobotany and Palynology*, 133(1-2), 135-149. <https://doi.org/10.1016/j.revpalbo.2004.09.005>
- Saber, A., Atar, F. And Javadi, S.B. (2009). Studies of pollen grains in the sect. Stenocephalae (*Cousinia* Cass.-Asteraceae) in Iran. *The Iranian Journal of Botany*, 15(1), 114-128.
- Sadeq, Z.G. and Aliwy, S.A. (2019). Micro-morphology study of pollen grains and cypsela of seven selected species, belong to Asteraceae Family in Al-Jadriya campus. *The Iraqi Journal of Agricultural Science*, 50(3), 1138-1152. <https://doi.org/10.36103/ijas.v50i4.758>
- Sadia, H., Zafar, M., Ahmad, M., Khan, M.P., Yaseen, G., Ali, M.I., Sultana, S., Kilic, O., Şahan, Z., Alam, N. and Abbas, Q. (2020). Foliar epidermal anatomy of some selected wild edible fruits of Pakistan using light microscopy and scanning electron microscopy. *Microscopy Research and Technique*, 83(3), 259-267. <https://doi.org/10.1002/jemt.23409>

- Saensouk, S. And Saensouk, P. (2022). Pollen morphology of some species in family Amaranthaceae from Thailand. *Biodiversitas Journal of Biological Diversity*, 23(1), 601-611. [DOI: 10.13057/biodiv/d230165](https://doi.org/10.13057/biodiv/d230165)
- Saha, S. and Begum, K.N. (2020). A comparative analysis on pollen morphology of the genus *Brassica* L. (Brassicaceae) in Bangladesh. *International Journal of Botany Studies*, 5(5), 191-194.
- Safiallah, S., Hamdi, S.M.M., Grigore, M.N. and Jalili, S., 2017. Micromorphology and leaf ecological anatomy of *Bassia* halophyte species (Amaranthaceae) from Iran. *Acta Biologica Szegediensis*, 61(1), pp.85-93.
- Sahreen, S., Khan, M.A., Khan, M.R. And Khan, R.A. (2010). Leaf epidermal anatomy of the genus *Silene* Caryophyllaceae from Pakistan. *Biological Diversity and Conservation*, 3(1), 93-102.
- Saini, M.L., Saini, R., Roy, S. and Kumar, A. (2008). Comparative pharmacognostical and antimicrobial studies of *Acacia* species (Mimosaceae). *Journal of Medicinal Plants Research*, 2(12), 378-386.
- Salamah, A., Luthfikasari, R. and Dwiranti, A. (2019). Pollen morphology of eight tribes of Asteraceae from Universitas Indonesia Campus, Depok, Indonesia. *Biodiversitas Journal of Biological Diversity*, 20(1), 152-159. <https://doi.org/10.13057/biodiv/d200118>
- Samina, B. and Mir Ajab, K. (2003). Pollen morphology as an aid to the identification of medicinal plants: *Trianthema portulacastrum* L., *Boerhaavia procumbens* banks ex Roxb., and *Alternanthera pungens* Kunth. *Hamdard Medicus (Pakistan)*, 46(1), 7-9.
- Sánchez, D., Terrazas, T., Grego-Valencia, D. and Arias, S. (2018). Phylogeny in *Echinocereus* (Cactaceae) based on combined morphological and molecular evidence: taxonomic implications. *Systematics and Biodiversity*, 16(1), 28-44. <https://doi.org/10.1080/14772000.2017.1343260>
- Sánchez-del Pino, I., Fuentes-Soriano, S., Solis-Fernández, K.Z., Pool, R. and Alfaro, R. (2016). The metareticulate pollen morphology of *Alternanthera* Forssk. (Gomphrenoideae, Amaranthaceae) and its taxonomic

- implications. *Grana*, 55(4), 253-277.  
<https://doi.org/10.1080/00173134.2015.1120774>
- Sardar, A.A., Perveen, A., and Khan, Z. (2013). A palynological survey of wetland plants of Punjab, Pakistan. *Pakistan Journal of Botany*, 45(6), 2131-2140.
- Schulze, E.D., Beck, E. and Müller-Hohenstein, K. (2005). *Plant ecology*. Springer Science & Business Media. 702pp. <http://dx.doi.org/10.1093/aob/mcj018>
- Scott, K.A. (2006). Seed coat morphology of *Parkinsonia aculeata* L. & pattern of heat-induced fractures. In *Proceedings of the 15th Australian Weeds Conference (Adelaide, SA, Australia, 24–28 September 2006)*. Weed Management Society of South Australia, Adelaide, SA, 268-271.
- Sehgal, D., Rajpal, V.R., Raina, S.N., Sasanuma, T. and Sasakuma, T. (2009). Assaying polymorphism at DNA level for genetic diversity diagnostics of the safflower (*Carthamus tinctorius* L.) world germplasm resources. *Genetica*, 135(3), 457-470. <https://doi.org/10.1007/s10709-008-9292-4>
- Semerdjieva IB, Yankova-Tsvetkova EP. (2017). Pollen and seed morphology of *Zygophyllum fabago* and *Peganum harmala* (Zygophyllaceae) from Bulgaria. *Phyton*, 86, 318-324.
- Semerdjieva, I., Yankova-Tsvetkova, E., Baldjiev, G. and Yurukova-Grancharova, P. (2011). Pollen and seed morphology of *Tribulus terrestris* L. (Zygophyllaceae). *Biotechnology & Biotechnological Equipment*, 25(2), 2379-2382. <https://doi.org/10.5504/BBEQ.2011.0031>
- Semerdjieva, I.B., and Yankova-Tsvetkova, E.P. (2017). Pollen and seed morphology of *Zygophyllum fabago* and *Peganum harmala* (Zygophyllaceae) from Bulgaria. *Phyton*, 86, 318-324.
- Shabestari, E.S.B., Attar, F., Riahi, H. and Sheidai, M. (2013). Pollen morphology of *Centaurea* L. (Asteraceae) in Iran. *Acta Botanica Brasilica*, 27, 669-679. <https://doi.org/10.1590/S0102-33062013000400004>
- Shah, S.N., Ahmad, M., Zafar, M., Malik, K., Rashid, N., Ullah, F., Zaman, W. and Ali, M. (2018). A light and scanning electron microscopic diagnosis of leaf epidermal morphology and its systematic implications in Dryopteridaceae:

- Investigating 12 Pakistani taxa. *Micron*, 111, 36-49.  
<https://doi.org/10.1016/j.micron.2018.05.008>
- Shah, S.N., Ahmad, M., Zafar, M., Ullah, F., Zaman, W., Mazumdar, J., Khuram, I. and Khan, S.M. (2019). Leaf micromorphological adaptations of resurrection ferns in Northern Pakistan. *Flora*, 255, 1-10.  
<https://doi.org/10.1016/j.flora.2019.03.018>
- Shaheen, A.S.M. (2007). Characteristics of the stem-leaf transitional zone in some species of Caesalpinoideae (Leguminosae). *Turkish Journal of Botany*, 31(4), 297-310.
- Shaheen, H., Qureshi, R., Akram, A. and Gulfraz, M. (2014). Inventory of medicinal flora from Thal desert, Punjab, Pakistan. *African Journal of Traditional, Complementary and Alternative Medicines*, 11(3), 282-290.  
<https://doi.org/10.4314/ajtcam.v11i3.39>
- Shaheen, N., Khan, M.A., Yasmin, G., Ahmad, M., Mahmood, T., Hayat, M.Q. and Zafar, M. (2009). Foliar epidermal anatomy and its systematic implication within the genus *Sida* L. (Malvaceae). *African Journal of Biotechnology*, 8(20), 5328-5336.
- Shaheen, N., Khan, M.A., Yasmin, G., Hayat, M.Q., Munsif, S., and Ahmad, K. (2010). Foliar epidermal anatomy and pollen morphology of the genera *Alcea* and *Althaea* (Malvaceae) from Pakistan. *International Journal of Agriculture and Biology*, 12(3), 329-334.
- Shaheen, S., Fateh, R., Younis, S., Harun, N., Jaffer, M., Hussain, K., Ashfaq, M., Siddique, R., Mukhtar, H. and Khan, F. (2020). Light and scanning electron microscopic characterization of thirty endemic Fabaceae species of district Lahore, Pakistan. *Microscopy research and technique*, 83(12), 1507-1529.  
<https://doi.org/10.1002/jemt.23545>
- Shahzad, K., Zafar, M., Khan, A.M., Mahmood, T., Abbas, Q., Ozdemir, F.A., Ahmad, M. and Sultana, S. (2022). Characterization of anatomical foliar epidermal features of herbaceous flora of Tilla Jogian, Pakistan by using light microscopy techniques. *Microscopy Research and Technique*, 85(1), 135-148.  
<https://doi.org/10.1002/jemt.23890>



- Shakeel, M., Ali, H., Ahmad, S., Said, F., Khan, K.A., Bashir, M.A., Anjum, S.I., Islam, W., Ghramh, H.A., Ansari, M.J. and Ali, H. (2019). Insect pollinators diversity and abundance in *Eruca sativa* Mill. (Arugula) and *Brassica rapa* L.(Field mustard) crops. *Saudi journal of biological sciences*, 26(7), 1704-1709. <https://doi.org/10.1016/j.sjbs.2018.08.012>
- Sheikh, N. and Kumar, Y. (2017). Foliar epidermal, stem and petiole anatomy of *Meghalayan Dioscorea* L. (Dioscoreaceae) and its systematic implication. *Bangladesh Journal of Plant Taxonomy*, 24(1), 53-63. <https://doi.org/10.3329/bjpt.v24i1.33033>
- Shemetova, T., Erst, A., Wang, W., Xiang, K., Vural, C. and Aytac, Z. (2018). Seed morphology of the genus *Astragalus* L. from North Asia. *Turkish Journal of Botany*, 42(6), 710-721. DOI: [10.3906/bot-1802-25](https://doi.org/10.3906/bot-1802-25)
- Singh, M. And Isfaq, M. (2017). Study on Morpho-Anatomical and Phytochemical Characterization of *Euphorbia Helioscopia* L. In Doon Valley, Uttarakhand. *International Journal of Pharmacology of Biological Science*, 8(2), 849-855. DOI: [10.5958/2320-3196.2018.00002.2](https://doi.org/10.5958/2320-3196.2018.00002.2)
- Singh, M.K., Kumari, K. and Kumar, A. (2020). Effect of plant growth regulators on growth and seed yield of bottle gourd [*Lagenaria siceraria* (Mol.) Standl.]. *Journal of Pharmacognosy and Phytochemistry*, 9(2), 794-797.
- Singh, S. and Chaturvedi, S.K. (2016). Morpho-taxonomical studies of some Polyporate pollen grains. *Journal of Advanced Plant Sciences*, 8(1), 22-29.
- Singh, S. and Dixit, A.K., Pollen diversity of some ethnomedicinal plants of Chhattisgarh, India. *International Journal of Creative Research Thoughts*, 6(2), 61-67.
- Soliman, M.S.A., El-Tarras, A.S. and El-Awady, M.A. (2010). Seed exomorphic characters of some taxa from Saudi Arabia. *Journal of American Science*, 6(11), 906-910.
- Song, J.H. and Hong, S.P. (2018). Comparative petiole anatomy of the tribe Sorbarieae (Rosaceae) provide new taxonomically informative characters. *Nordic Journal of Botany*, 36(5), 1-14. <https://doi.org/10.1111/njb.01702>

- Song, J.H. and Hong, S.P. (2020). Fruit and seed micromorphology and its systematic significance in tribe Sorbarieae (Rosaceae). *Plant Systematics and Evolution*, 306(1), 1-14. <https://doi.org/10.1007/s00606-020-01640-4>
- Song, U. (2007). Pollen morphology of the woody Fabaceae in Korea. *Korean Journal of Plant Taxonomy*, 37(2), 87-108.
- Song, Y., Gu, L. and Liu, J. (2019). Pollen morphology of selected species from the family Solanaceae. *Palynology*, 43(3), 355-372. <https://doi.org/10.1080/01916122.2018.1458663>
- Sonia, R., Shaheen, S., Khalid, S., Sharifi-Rad, J., Shahid, M.N., Mukhtar, H., Khalid, Z., Harun, N., Hussain, R.A. and Khan, F. (2022). Light and scanning electron microscopic comparative studies of geminivirus infected and healthy *Eclipta alba* (L.). *Microscopy Research and Technique*. 85(8), 2848-2856. <https://doi.org/10.1002/jemt.24133>
- Sonyan, H.H. and Hayrapetyan, A.M. (2021). Statistical Analysis of the Basic Morphological Characteristics of Pollen within the Limits Of Genus *Salsola* L. Sensu Lato In South Transcaucasia. *Electronic Journal of Natural Sciences*, 36(1), 4-8.
- Sopaladawan, P.N., Namwong, L. and Wongnaikod, S. (2019). Food plant species from pollen load of honey bee (*Apis mellifera*) in Nong Khai Province, Thailand. *NU International Journal of Science*, 16(1), 36-45.
- Srivastava, G., Mehrotra, R.C. and Dilcher, D.L. (2018). Paleocene *Ipomoea* (Convolvulaceae) from India with implications for an East Gondwana origin of Convolvulaceae. *Proceedings of the National Academy of Sciences*, 115(23), 6028-6033. <https://doi.org/10.1073/pnas.1800626115>
- Stenglein, S.A., Colares, M.N., Arambarri, A.M., Novoa, M.C., Vizcaíno, C.E. and Katinas, L. (2003). Leaf epidermal microcharacters of the Old World species of Lotus (Leguminosae: Loteae) and their systematic significance. *Australian Journal of Botany*, 51(4), 459-469. <https://doi.org/10.1071/BT02102>
- Subramaniam, S., Pandey, A.K. and Rather, S.A. (2015). A revised circumscription of the species in Bracteatae complex (section Calycinae) in the genus *Crotalaria*

- L.: evidence from nuclear and chloroplast markers. *Plant Systematics and Evolution*, 301(9), 2261-2290. <https://doi.org/10.1007/s00606-015-1228-8>
- Sukhorukov, A.P. and Kushunina, M. (2017). Taxonomic significance of seed morphology in the genus *Mollugo* sl (Molluginaceae). *Israel Journal of Plant Sciences*, 64(1-2), 31-47. <https://doi.org/10.1080/07929978.2016.1249137>
- Sukhorukov, A.P. and Zhang, M. (2013). Fruit and seed anatomy of *Chenopodium* and related genera (Chenopodioideae, Chenopodiaceae/Amaranthaceae): implications for evolution and taxonomy. *Plos one*, 8(4), p.e61906. <https://doi.org/10.1371/journal.pone.0061906>
- Sukhorukov, A.P., Zhang, M.L., Kushunina, M., Nilova, M.V., Krinitsina, A., Zaika, M.A. and Mazei, Y. (2018). Seed characters in Molluginaceae (Caryophyllales): implications for taxonomy and evolution. *Botanical Journal of the Linnean Society*, 187(2), 167-208. <https://doi.org/10.1093/botlinnean/boy021>
- Swamy, R.K., Singh, A., Surveswaran, S. and Rao, K.S. (2015). *Heliotropium amplexicaule* (Boraginaceae-Heliotropioideae): A new record for Indian sub-continent. *Rheedea*, 25(2), 148-152.
- Tadavi, S.C. and Bhadane, V.V. (2014). Taxonomic significance of the rachis, petiole and Petiolule anatomy in some Euphorbiaceae. *Biolife*, 2(3), 850-857.
- Tahmasebi, A. and Nasrollahi, F. (2021). Morphologic and Genetic study of *Halocnemum strobilaceum* (Amaranthaceae) in rangeland ecosystems of Golestan province. *Rostaniha*, 22(1), 134-146. <https://dx.doi.org/10.22092/botany.2021.355344.1260>
- Taia, W.K., Shehata, A.A., El Shamy, I.M. and Ibrahim, M.M. (2020). Anatomical Variations within Some Egyptian *Amaranthus* L. Species and its taxonomic significance. *The Egyptian Journal of Experimental Biology (Botany)*, 16(2), 115-115.
- Taia, W.K., Shehata, A.A., Elshamy, E.M. and Ibrahim, M.M. (2020). Biosystematic studies for some Egyptian *Amaranthus* L. taxa and their significance in their identification. *Taeckholmia*, 40(1), 85-99. <https://dx.doi.org/10.21608/taec.2020.26080.1018>

- Taiaa, W.K., Ibrahima, M.M., Hassanb, S.A. and Askerc, A.M. (2021). Palynological study of the genus *Fagonia* L. (Zygophyllaceae, Zygophylloideae) in Libya. *Libyan Journal of Science & Technology* 13(1), 29-37.
- Takhtajan, A. ed., 2009. *Flowering plants*. Dordrecht: Springer Netherlands. <https://doi.org/10.1007/978-1-4020-9609-9>
- Talebi, S.M., Noori, M. and Nasiri, Z. (2016). Palynological study of some Iranian *Amaranthus* taxa. *Environmental and Experimental Biology*, 14(1), 1-7. DOI: [10.22364/eeb.14.01](https://doi.org/10.22364/eeb.14.01)
- Talip, N., Cutler, D.F., Puad, A.A., Ismail, B.S., Ruzi, A.R. and Juhari, A.A. (2017). Diagnostic and systematic significance of petiole anatomy in the identification of *Hopea* species (Dipterocarpaceae). *South African Journal of Botany*, 111, 111-125. <https://doi.org/10.1016/j.sajb.2017.03.008>
- Tao, S., Khanizadeh, S., Zhang, H. and Zhang, S. (2009). Anatomy, ultrastructure and lignin distribution of stone cells in two *Pyrus* species. *Plant Science*, 176(3), 413-419. <https://doi.org/10.1016/j.plantsci.2008.12.011>
- Tarhouni, M. and Nedjraoui, D. (2018). The Maghreb (North Africa) Rangelands. Evolution Over Forty Years: Regreening or Degradation? In *Desertification*, 73-106.
- Teena, A. and Yadav, A.S. (2007). Micromorphology of the leaf epidermis of *Achyranthes aspera* L. *Journal of Phytological Research*, 20(1), 61-66.
- Tellería, M.C. (2017). Spines vs. microspines: an overview of the sculpture exine in selected basal and derived Asteraceae with focus on Asteroideae. *Journal of plant research*, 130(6), 1023-1033. <https://doi.org/10.1007/s10265-017-0956-y>
- Terzieva, S., Grozeva, N. and Velichkova, K. (2019). Morphological studies on three *Amaranthus* species. *Bulgarian Journal of Agricultural Science*, 25(3), 136-140.
- Terzieva, S.R. and Grozeva, N.H. (2021). Chromosome and Pollen Morphology of *Amaranthus hybridus* L. and *Amaranthus retroflexus* L. in Bulgaria. *Ecologia Balkanica, Special Issue*, 181-189.

- Tlili, N., Saadaoui, E., Sakouhi, F., Elfalleh, W., Gazzah, M.E., Triki, S. and Khaldi, A.I. (2011). Morphology and chemical composition of Tunisian caper seeds: variability and population profiling. *African Journal of Biotechnology*, 10(11), 2112-2118.
- Toderich, K.N., Idzikowska, K., Wozny, A. and Takabe, K. (2000). Pollen morphology of Asiatic and European species of genus *Salsola* (Chenopodiaceae). In *Proc. of the 12-th European Congress of Electron Microscopy*, 4, 33-34.
- Toderich, K.N., Shuyskaya, E.V., Ozturk, M., Juylova, A. and Gismatulina, L.I.L.Y.A. (2010). Pollen morphology of some Asiatic species of genus *Salsola* (Chenopodiaceae) and its taxonomic relationships. *Pakistan Journal of Botany*, 42(SI), 155-174.
- Tomlinson, P.B. (2012). Rescuing Robert Brown—the origins of angio-ovuly in seed cones of conifers. *The Botanical Review*, 78(4), 310-334. <https://doi.org/10.1007/s12229-012-9104-5>
- Torres, C. (2000). Pollen size evolution: correlation between pollen volume and pistil length in Asteraceae. *Sexual Plant Reproduction*, 12(6), 365-370. <https://doi.org/10.1007/s004970000030>
- Turki, Z., El-Shayeb, F. and Shehata, F. (2006). Taxonomic studies in the Camphorosmeae (Chenopodiaceae) in Egypt. 1. Subtribe Kochiinae (*Bassia*, *Kochia* and *Chenolea*). *Flora Mediterranean*, 16, 275-294.
- Turki, Z., El-Shayeb, F. and Shehata, F. (2008). Taxonomic studies in the Camphorosmeae (Chenopodiaceae) 1. Subtribe: Kochiinae (Genera: *Bassia* All., *Kochia* Roth and *Chenolea* Thunb.). *Acta Botanica Hungarica*, 50(1-2), 181-201. DOI: [10.1556/abot.50.2008.1-2.14](https://doi.org/10.1556/abot.50.2008.1-2.14)
- Ullah, F., Ahmad, M., Zafar, M., Parveen, B., Ashfaq, S., Bahadur, S., Safdar, Q.T.A., Safdar, L.B., Alam, F. and Luqman, M. (2022). Pollen morphology and its taxonomic potential in some selected taxa of Caesalpiniaceae observed under light microscopy and scanning electron microscopy. *Microscopy Research and Technique*, 85(4), 1410-1420. <https://doi.org/10.1002/jemt.24004>

- Ullah, F., Papini, A., Shah, S.N., Zaman, W., Sohail, A. and Iqbal, M. (2019). Seed micromorphology and its taxonomic evidence in subfamily Alsinoideae (Caryophyllaceae). *Microscopy Research and Technique*, 82(3), 250-259. <https://doi.org/10.1002/jemt.23167>
- Ullah, F., Zafar, M., Ahmad, M., Shah, S.N., Razzaq, A., Sohail, A., Zaman, W., Çelik, A., Ayaz, A. and Sultana, S. (2018). A systematic approach to the investigation of foliar epidermal anatomy of subfamily Caryophylloideae (Caryophyllaceae). *Flora*, 246, 61-70. <https://doi.org/10.1016/j.flora.2018.07.006>
- Ullah, F., Zaman, W., Papini, A., Zafar, M., Shah, S.N., Ahmad, M., Saqib, S., Gul, S. and Sohail, A. (2019). Using multiple microscopic techniques for the comparative systematic of *Spergula fallax* and *Spergula arvensis* (Caryophyllaceae). *Microscopy Research and Technique*, 82(4), 352-360. <https://doi.org/10.1002/jemt.23176>
- Ullah, S.A., Zafar, M., Ahmad, M., Ghufuran, M.A., Bursal, E., Kilic, O., Sultana, S., Yaseen, G., Khan, S. and Majeed, S. (2021). Microscopic implication and evaluation of herbaceous melliferous plants of southern Khyber Pakhtunkhwa-Pakistan using light and scanning electron microscope. *Microscopy Research and Technique*, 84(8), 1750-1764. <https://doi.org/10.1002/jemt.23732>
- Ulukus, D. and Tugay, O. (2020). Morphology, anatomy and palynology of two endemic *Cousinia* cass. Species (sect. *Cousinia*, Asteraceae) and their taxonomic implications. *Pakistan Journal of Botany*, 52(1), 297-304.
- Umber, F., Zafar, M., Ullah, R., Bari, A., Khan, M.Y., Ahmad, M. and Sultana, S. (2022). Implication of light and scanning electron microscopy for pollen morphology of selected taxa of family Asteraceae and Brassicaceae. *Microscopy Research and Technique*, 85(1), 373-384. <https://doi.org/10.1002/jemt.23912>
- Umdale, S.D., Patil, P.D., Malik, S.K., Latha, M., Rao, S.R., Yadav, S.R., Gaikwad, N.B. and Bhat, K.V. (2017). Seed coat sculpture of subgenus *Ceratotropis* (Piper) verdc., genus *Vigna Savi* in India and its taxonomic implications. *Botany Letters*, 164(1), 63-78. <https://doi.org/10.1080/23818107.2016.1273795>

- Upadhyay, N., Verma, S., Pratap Singh, A., Devi, S., Vishwakarma, K., Kumar, N., Pandey, A., Dubey, K., Mishra, R., Kumar Tripathi, D. and Rani, R. (2016). Soil ecophysiological and microbiological indices of soil health: a study of coal mining site in Sonbhadra, Uttar Pradesh. *Journal of soil science and plant nutrition*, 16(3), 778-800. <http://dx.doi.org/10.4067/S0718-95162016005000056>
- Usma, A., Ahmad, M., Zafar, M., Ali, M.I., Kilic, O., Ozdemir, F.A., Sultana, S., Nazir, A., Anjum, F. and Kalsoom, N. (2019). Taxonomic significance of caryopsis in subfamily Panicoideae (Poaceae) using scanning electron microscopy and light microscopy. *Microscopy Research and Technique*, 82(10), 1649-1659. <https://doi.org/10.1002/jemt.23331>
- Usma, A., Ahmad, M., Zafar, M., Sultana, S., Lubna, Kalsoom, N., Zaman, W. and Ullah, F. (2020). Micromorphological variations and taxonomic implications of caryopses of some grasses from Pakistan. *Wulfenia*, 27, 86-96.
- Varela, O., Ordano, M., Toledo, G., Lizardo, G., Rotger, S., Montero, A. and Cisneros, M.C. (2021). Diversity and density of the desert seed bank: Interplays between cacti and nurse shrub species. *Journal of Arid Environments*, 191, p.104536. <https://doi.org/10.1016/j.jaridenv.2021.104536>
- Venier, P., Funes, G. and García, C.C. (2012). Physical dormancy and histological features of seeds of five *Acacia* species (Fabaceae) from xerophytic forests in central Argentina. *Flora-Morphology, Distribution, Functional Ecology of Plants*, 207(1), 39-46. <https://doi.org/10.1016/j.flora.2011.07.017>
- Viana, A., de Freitas, E.M. and Silva, S.M., 2021. Morphology, anatomy and leaf ultrastructure of *Froelichia tomentosa* (Mart.) Moq.(Amaranthaceae)-a critically endangered species in Brazil. *Ciência e Natura*, 43, e26-e26. <https://doi.org/10.5902/2179460X40503>
- Vilatersana, R., Garnatje, T., Susanna, A. and Garcia-Jacas, N. (2005). Taxonomic problems in *Carthamus* (Asteraceae): RAPD markers and sectional classification. *Botanical Journal of the Linnean Society*, 147(3), 375-383. <https://doi.org/10.1111/j.1095-8339.2005.00375.x>

- Vilatersana, R., Villodre, J.M., Susanna, A., Garcia-Jacas, N. and Garnatje, T. (2001). Pollen studies in subtribe Centaureinae (Asteraceae): the *Carthamus* complex and the genus *Aegialophila* analyzed with electron microscopy. *Plant Biology*, 3(06), 607-615. [DOI: 10.1055/s-2001-19368](https://doi.org/10.1055/s-2001-19368)
- Vovides, A.P., Clugston, J.A., Gutiérrez-Ortega, J.S., Pérez-Farrera, M.A., Sánchez-Tinoco, M.Y. and Galicia, S. (2018). Epidermal morphology and leaflet anatomy of *Dioon* (Zamiaceae) with comments on climate and environment. *Flora*, 239, 20-44. <https://doi.org/10.1016/j.flora.2017.11.002>
- Vural, C., Ekici, M., Akan, H. and Aytaç, Z. (2008). Seed morphology and its systematic implications for genus *Astragalus* L. sections *Onobrychoidei* DC., *Uliginosi* Gray and *Ornithopodium* Bunge (Fabaceae). *Plant Systematics and Evolution*, 274(3), 255-263. <https://doi.org/10.1007/s00606-008-0025-z>
- Vyas, M.K. (2019). Distinguishing Micro-characters of Medicinal Plant: *Euphorbia hirta* L. and their Significance. *Journal of Pharmacognosy and Phytochemistry*, 8(1), 464-467.
- Wagenitz, G. (1976). Systematics and phylogeny of the Compositae (Asteraceae). *Plant systematics and evolution*, 125(1), 29-46. <https://doi.org/10.1007/BF00986129>
- Waheed, A., Ahmad, M., Ghufuran, M.A., Jabeen, A., Ozdemir, F.A., Zafar, M., Sultana, S., Shah, M.A., Majeed, S. and Khan, A.S. (2021). Implication of scanning electron microscopy in the seed morphology with special reference to three subfamilies of Fabaceae. *Microscopy research and technique*, 84(9), 2176-2185. <https://doi.org/10.1002/jemt.23772>
- Waly, N.M., Al-Zahrani, H.S. and Felemban, W.F. (2012). Taxonomical studies of some *Acacia* seeds growing in Saudi Arabia. *The Journal of American Science*, 8(3), 264-275.
- Wan, Q., Zhang, Y., Huang, K., Sun, Q., Zhang, X., Gaillard, M.J., Xu, Q., Li, F. and Zheng, Z. (2020). Evaluating quantitative pollen representation of vegetation in the tropics: A case study on the Hainan Island, tropical China. *Ecological Indicators*, 114, p.106297. <https://doi.org/10.1016/j.ecolind.2020.106297>



- Wang, K.F. and Wang, X.Z. (1983). Introduction to palynology. *Beijing University Press, Beijing*, 21-29
- Wariss, H.M., Ahmad, S., Anjum, S. and Alam, K. (2014). Ethnobotanical studies of dicotyledonous plants of Lal Suhanra national park, Bahawalpur, Pakistan. *International Journal of Science Research*, 3(6), 2452-2560.
- Wimalasiri, D., Piva, T., Urban, S. and Huynh, T. (2016). Morphological and genetic diversity of *Momordica cochinchinensis* (Cucurbitaceae) in Vietnam and Thailand. *Genetic resources and crop evolution*, 63(1), 19-33. <https://doi.org/10.1007/s10722-015-0232-8>
- Wortley, A.H., Blackmore, S., Chissoe, W.F. and Skvarla, J.J. (2012). Recent advances in Compositae (Asteraceae) palynology, with emphasis on previously unstudied and unplaced taxa. *Grana*, 51(2), 158-179. <https://doi.org/10.1080/00173134.2012.668219>
- Wunnenberg, J., Rjosk, A., Neinhuis, C. and Lautenschläger, T. (2021). Strengthening structures in the petiole–lamina junction of peltate leaves. *Biomimetics*, 6(2), 1-25. <https://doi.org/10.3390/biomimetics6020025>
- Yousaf, Z., Zafar, M., Ahmad, M., Sultana, S., Ozdemir, F.A. and Abidin, S.Z.U. (2022). Palyno-anatomical microscopic characterization of selected species of Boraginaceae and Fabaceae. *Microscopy Research and Technique*, 85(4), 1332-1354. <https://doi.org/10.1002/jemt.23999>
- Zafar, M., Ahmad, M., Shah, G.M., Khan, A.M., Kilic, O., Yilmaz, E., Ozdemir, F.A., Ali, M.I., Shah, M.A., Sultana, S. and Ahmad, S. (2021). Application and implication of scanning electron microscopy for evaluation of palyno-morphological features of Vitaceae from Pakistan. *Microscopy Research and Technique*, 84(4), 608-617. <https://doi.org/10.1002/jemt.23619>
- Zafar, M., Ahmad, M., Shaheen, S., Sultana, S., Rehman, S.U. and Amina, H. (2019). Micromorphological investigation of leaf epidermis and seeds of Vitaceae from Pakistan using light microscopy and scanning electron microscopy. *Microscopy Research and Technique*, 82(4), 335-344. <https://doi.org/10.1002/jemt.23102>

- Zafar, M., Ahmad, M., Sultana, S., Anjum, F., Ozdemir, F.A., Tariq, A., Nazir, A., Yaseen, G., Aabidin, S.Z.U., Gul, H. and Rehman, S.U. (2019). Light microscopy and scanning electron microscopy: Implications for authentication of misidentified herbal drugs. *Microscopy Research and Technique*, 82(10), 1779-1786. <https://doi.org/10.1002/jemt.23344>
- Zarinkamar, F. (2006). Foliar Anatomy of Chenopodiaceae family and xerophytes adaptation. *The Iranian Journal of Botany*, 11(2), 175-183.
- Zhao, X.L., Gao, X.F. and Xu, B. (2016). Pollen morphology of *Indigofera* (Fabaceae) in China and its taxonomic implications. *Plant systematics and evolution*, 302(4), 469-479. <https://doi.org/10.1007/s00606-015-1275-1>
- Zokian, S.A. (2015). Morphological, Anatomical Study and Geographical Distribution in Iraq of *Capparis spinosa* L. *Iraqi Journal of Science*, 56(1A), 100-104.
- Zorić, L., Merkulov, L., Luković, J. And Boža, P. (2010). Comparative seed morphology of *Trifolium* L. species (Fabaceae). *Periodicum biologorum*, 112(3), 263-272.
- Zumaya, S., Flores-Olvera, H. and Borsch, T. (2013). Two new Mexican endemic species of *Iresine* (Amaranthaceae). *Systematic Botany*, 38(2), 434-443. <https://doi.org/10.1600/036364413X666633>
- Zumaya-Mendoza, S., Aguilar-Rodríguez, S., Yáñez-Espinosa, L. and Terrazas, T. (2019). Stem anatomy diversity in *Iresine* (Amaranthaceae s.l): an ecological interpretation. *Brazilian Journal of Botany*, 42, 329-344. <https://doi.org/10.1007/s40415-019-00530-5>





**Thesis Outcome**

## List of Publications

S. No.	Paper title	Year	Impact Factor
1.	Majeed, S., Ahmad, M., Ozdemir, F.A., Demirpolat, A., Şahan, Z., Makhkamov, T.K., Nasirov, M., Zafar, M., Sultana, S., Yaseen, G. and Nabila, 2023. Micromorphological Characterization of Seeds of Dicot Angiosperms from the Thal Desert (Pakistan). <i>Plant Biosystems-An International Journal Dealing with all Aspects of Plant Biology</i> , 1-27.	2023	2.4
2.	Majeed, S., Ahmad, M., Ali, A., Althobaiti, A.T., Ramadan, M.F., Kilic, O., Demirpolat, A., Çobanoğlu, D.N., Zafar, S., Afza, R. and Makhkamov, T., 2023. Pollen Micromorphology among Amaranthaceous Species from Desert Rangeland: Exine Stratification and their Taxonomic Significance. <i>BioMed Research International</i> , 2023.	2023	3.4
3.	Majeed, S., Zafar, M., Althobaiti, A.T., Ramadan, M.F., Ahmad, M., Makhkamov, T., Gafforov, Y., Sultana, S. and Yaseen, G., 2022. Comparative petiole histology using microscopic imaging visualization among Amaranthaceous taxa. <i>Flora</i> , 297, p.152178.	2022	2.2
4.	Majeed, S., Zafar, M., Ahmad, M., Zafar, S., Ghufuran, A., Ayoub, M., Sultana, S., Yaseen, G. and Raza, J., 2022. Morpho-palynological and anatomical studies in desert cacti ( <i>Opuntia dillenii</i> and <i>Opuntia monacantha</i> ) using light and scanning electron microscopy. <i>Microscopy Research and Technique</i> , 85(8), 2801-2812.	2022	2.89



## Micromorphological characterization of seeds of dicot angiosperms from the Thal desert (Pakistan)

Salman Majeed<sup>a</sup>, Mushtaq Ahmad<sup>a,b</sup>, Fethi Ahmet Ozdemir<sup>c</sup>, Azize Demirpolat<sup>d</sup>, Zeynep Şahan<sup>e</sup> , Trobjon Makhkamov<sup>f</sup> , Muhtor Nasirov<sup>g</sup>, Muhammad Zafar<sup>a</sup>, Shazia Sultana<sup>a</sup>, Ghulam Yaseen<sup>h</sup> and Nabila<sup>a</sup>

<sup>a</sup>Department of Plant Sciences, Quaid-i-Azam University, Islamabad, Pakistan; <sup>b</sup>Pakistan Academy of Sciences, Islamabad, Pakistan; <sup>c</sup>Faculty of Science and Literature, Department of Molecular Biology and Genetics, Bingöl University, Bingöl, Turkey; <sup>d</sup>Bingöl University, Vocational School of Food, Agriculture and Livestock, Bingöl, Turkey; <sup>e</sup>Department of Veterinary, Kahta Vocational School, Adiyaman University, Adiyaman, Turkey; <sup>f</sup>Department of Forestry and Landscape Design, Tashkent State Agrarian University, Tashkent region, Uzbekistan; <sup>g</sup>International Relations Office Samarkand State University, Samarkand, Uzbekistan; <sup>h</sup>Department of Botany, Science and Technology Division, Township Campus, University of Education, Lahore, Pakistan

### ABSTRACT

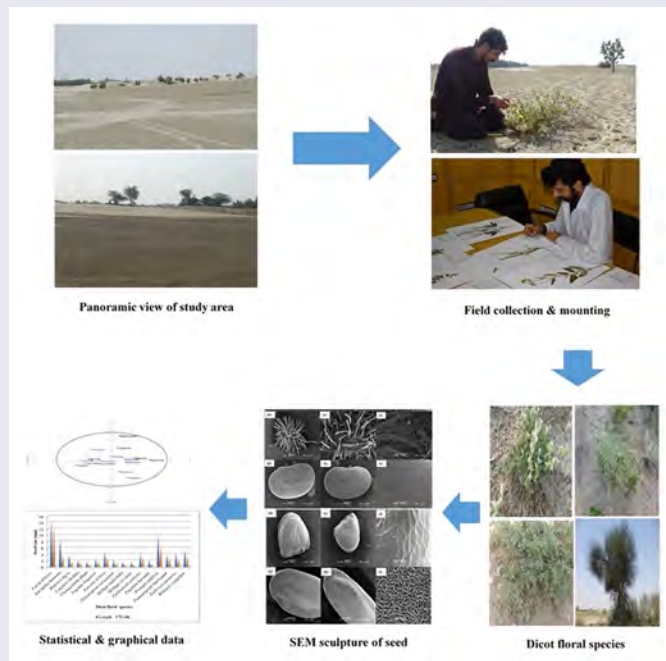
Micromorphological and ultrastructural data have been helpful in determining the evolution, classification, ecology and phylogeny of seed plants. Taxonomic utility of seed characters has been explored, although the value of micro-structure in selected dicot angiosperms from desert areas has not been adequately addressed. We conducted a comparative morphometric analysis of internal and external seed features in the 16 dicot species representing 10 families from the Thal desert (Pakistan) using scanning electron microscopy. Seeds were mostly minute and small and slightly larger than 1 mm in length except for *Acacia nilotica*, *Astragalus hamosus* and *Prosopis juliflora*. Seeds varied in shape from elliptical to obovate, D-shaped, reniform, rhomboid and ellipsoidal. The cell outline, periclinal boundaries and sculpture pattern of the anticlinal wall were generally rugulate, reticulate and striate, papillate and rugose or rarely undulating granulate. The seed coat also comprises diverse forms of epicuticular projections and texture. The phenetics of 84 character-states using principal component and dendrogram statistics supported the affinities among desert species. Here, we identified micromorphological similarities and differences among dicot angiosperms to determine their systematic relationships.

### ARTICLE HISTORY

Received 4 January 2022  
Accepted 2 September 2022




### KEYWORDS

Desert; dicot; sculpturing; seed micromorphology; SEM



## Research Article

# Pollen Micromorphology among Amaranthaceous Species from Desert Rangeland: Exine Stratification and their Taxonomic Significance

Salman Majeed <sup>1,2</sup> Mushtaq Ahmad <sup>1,3</sup> Alamdar Ali,<sup>4</sup> Ashwaq T. Althobaiti,<sup>5</sup> Mohamed Fawzy Ramadan,<sup>6</sup> Omer Kilic,<sup>7</sup> Azize Demirpolat,<sup>8</sup> Duygu Nur Çobanoğlu,<sup>8</sup> Sadia Zafar,<sup>9</sup> Rabia Afza,<sup>10</sup> Trobjon Makhkamov,<sup>11</sup> Akramjon Yuldashev,<sup>12</sup> Yusufjon Gafforov <sup>13,14</sup> Khislat Khaydarov,<sup>15</sup> Muhammad Zafar <sup>1</sup> and Shazia Sultana<sup>1</sup>

<sup>1</sup>Department of Plant Systematics and Biodiversity Lab, Quaid-i-Azam University, 45320 Islamabad, Pakistan

<sup>2</sup>Department of Botany, University of Mianwali, Mianwali 42200, Pakistan

<sup>3</sup>Pakistan Academy of Sciences Islamabad, Pakistan

<sup>4</sup>Nishtar Medical College Multan University of Health Sciences Lahore, Pakistan

<sup>5</sup>Department of Biology, College of Science, Taif University, P.O. Box 11099, Taif 21944, Saudi Arabia

<sup>6</sup>Department of Clinical Nutrition, Faculty of Applied Medical Sciences, Umm Al-Qura University, Makkah, Saudi Arabia

<sup>7</sup>Department of Pharmacy, Adiyaman University, Adiyaman, Turkey

<sup>8</sup>Department of Crop and Animal Production, Vocational School of Food, Agriculture and Livestock, Bingol University, 12000 Bingol, Turkey

<sup>9</sup>Department of Botany, Division of Science and Technology, University of Education Faisalabad, 54770 Punjab, Pakistan

<sup>10</sup>Department of Botany, Hazara University Mansehra, Pakistan

<sup>11</sup>Department of Forestry and Landscape Design, Tashkent State Agrarian University, 2 A., Universitet Str., Kibray District, 100700 Tashkent Region, Uzbekistan

<sup>12</sup>Department of Ecology and Botany, Andijan State University, 129 Universitet Str., 170100 Andijan, Uzbekistan

<sup>13</sup>Mycology Laboratory, Institute of Botany, Academy of Sciences of the Republic of Uzbekistan, 32 Durmon Yuli, Tashkent 100125, Uzbekistan

<sup>14</sup>AKFA University, 264 Milliy Bog Street, 111221 Tashkent, Uzbekistan

<sup>15</sup>Samarkand State University Faculty of Biology, Universitetsty Bulvar Street-15, Smarkand 140104, Uzbekistan

Correspondence should be addressed to Salman Majeed; [salmansunny61@gmail.com](mailto:salmansunny61@gmail.com), Mushtaq Ahmad; [mushtaqflora@hotmail.com](mailto:mushtaqflora@hotmail.com), and Muhammad Zafar; [zafar@qau.edu.pk](mailto:zafar@qau.edu.pk)

Received 27 October 2022; Revised 6 December 2022; Accepted 12 December 2022; Published 20 January 2023

Academic Editor: Amjad Bashir

Copyright © 2023 Salman Majeed et al. This is an open access article distributed under the Creative Commons Attribution License, which permits unrestricted use, distribution, and reproduction in any medium, provided the original work is properly cited.

The aim of the study was to visualize the micromorphology of Amaranthaceous pollen using scanning electron microscopy collected from the Thal Desert. Field collection was conducted from July to September 2021. A total of 14 taxa of the family Amaranthaceae were collected which belong to nine genera. *Achyranthes aspera*, *Aerva javanica*, *Aerva lanata*, *Amaranthus graecizans*, *Amaranthus retroflexus*, *Amaranthus viridis*, *Bassia indica*, *Chenopodium album*, *Chenopodium ficifolium*, *Chenopodium murale*, *Digera muricata*, *Haloxylon stocksii*, *Salsola tragus*, and *Suaeda fruticosa* were studied in terms of pollen morphotypes. Pollen were acetolyzed and observed under optical and scanning microscopy. Qualitative and quantitative characters were measured to analyze the pollen to uncover its taxonomic significance. Qualitative characters observed were the shape of pollen in polar and equatorial views; the most frequent shape observed was spheroidal in the polar view, whereas in the equatorial view, prolate spheroidal was the dominant shape. Exine ornamentation is the key characteristic of pollen which is very helpful, and eight different types of ornamentations were observed in collected taxa: smooth sparsely granulate,



## Comparative petiole histology using microscopic imaging visualization among Amaranthaceous taxa

Salman Majeed<sup>a,b,\*</sup>, Muhammad Zafar<sup>a,\*</sup>, Ashwaq T. Althobaiti<sup>c</sup>, Mohamed Fawzy Ramadan<sup>d</sup>, Mushtaq Ahmad<sup>a,e,\*</sup>, Trobjon Makhkamov<sup>f</sup>, Yusufjon Gafforov<sup>g,h</sup>, Shazia Sultana<sup>a</sup>, Ghulam Yaseen<sup>i</sup>, Nabila<sup>a</sup>

<sup>a</sup> Department of Plant Sciences, Quaid-i-Azam University Islamabad, 45320, Pakistan

<sup>b</sup> Department of Botany, University of Mianwali, Mianwali 42200, Pakistan

<sup>c</sup> Department of Biology, College of Science, Taif University, P.O. Box 11099, Taif 21944, Saudi Arabia

<sup>d</sup> Department of Clinical Nutrition, Faculty of Applied Medical Sciences, Umm Al-Qura University, Makkah, Saudi Arabia

<sup>e</sup> Pakistan Academy of Sciences Islamabad Pakistan, Pakistan

<sup>f</sup> Department of Forestry and Landscape Design, Tashkent State Agrarian University, 2 A., Universitet Str., Kibray District, Tashkent 100700, Uzbekistan

<sup>g</sup> Mycology Laboratory, Institute of Botany, Academy of Sciences of the Republic of Uzbekistan, 32 Durmon Yuli Street, Tashkent 100125, Uzbekistan

<sup>h</sup> AKFA University, 264 Milliy Bog Street, Tashkent 111221, Uzbekistan

<sup>i</sup> Department of Botany, Science and Technology Division, Township Campus, University of Education, Lahore, Pakistan

### ARTICLE INFO

Edited by: Alessio Papini

#### Keywords:

Amaranthaceae  
Cluster analysis  
Histology  
Micromorphology  
Taxonomy

### ABSTRACT

This paper described the microstructural features of the histological vasculature of family Amaranthaceae. The petiole anatomy of 14 Amaranthaceous species categorized into nine genera, including *Amaranthus* and *Chenopodium* (3 species each), *Alternanthera* (2 species), and *Aerva*, *Achyranthes*, *Atriplex*, *Bassia*, *Digera*, and *Gomphrena* (one species each). Amaranthaceous species were collected from different localities of the Thal desert were examined using a microscopic imaging technique. Petiole transverse segments were cut with a Shandon Microtome to prepare slides. The distinguishing features of taxonomic significance include petiole outline, vascular bundle shape, variation in the number of vascular bundles, petiole length and width, trichomes, layers of collenchyma, and the shape of parenchyma. Petiole shapes were observed as cordate, slender, spherical, and ovoid. Quantitative measurements were taken to analyze the data statistically through SPSS software. *Amaranthus retroflexus* had a petiole of a maximum length of 760  $\mu\text{m}$  and a minimum in *Amaranthus viridis* 170  $\mu\text{m}$ . The highest number of vascular bundles, 11 were observed in *Alternanthera sessilis*. The polygonal-shaped parenchyma and the annular type of collenchymatous cells were prominent. A maximum of 18 collenchyma layers were present in *Achyranthes aspera* and a minimum of 9 layers in *Amaranthus graecizans*. Trichomes were examined in six species with bulged pointed ends, and broad glandular bases. Epidermis cells also show great variation, with an irregular shape being dominant. Statistic UPGMA dendrogram and PCA clustering of petiole traits show that histological sections can be utilized to botanical identify Amaranthaceous species and play an important role in future taxonomic and phylogenetic relationships.

### 1. Introduction

For a long time, the families Amaranthaceae and Chenopodiaceae were thought to be closely related. Previous morphological and phylogenetic evidence suggested that both families shared a single evolutionary lineage with closely related species. The [Angiosperm Phylogeny Group \(AGP\) IV system unified the two families in 2016](#) under the name Amaranthaceae, placing them in the order Caryophyllales. The majority

of them are perennial and annual herbs. In the Flora of Pakistan, 32 Amaranthaceae species have been identified, which are dominated by herbaceous and shrubby plants and are primarily found in arid environments ([Nazish et al., 2019](#)). This family is particularly significant in both ecological and economic terms. It flourishes in harsh conditions such as deserts, semi-deserts, and salt marshes. These plants are frequently dominant in plant communities and provide valuable fodder for livestock ([Safiallah et al., 2017](#)).

\* Corresponding authors at: Department of Plant Sciences, Quaid-i-Azam University Islamabad, 45320, Pakistan.

E-mail addresses: [salmansunny61@gmail.com](mailto:salmansunny61@gmail.com) (S. Majeed), [zafar@qau.edu.pk](mailto:zafar@qau.edu.pk) (M. Zafar), [mushtaqflora@hotmail.com](mailto:mushtaqflora@hotmail.com) (M. Ahmad).




<https://doi.org/10.1016/j.flora.2022.152178>

Received 9 July 2022; Received in revised form 28 October 2022; Accepted 30 October 2022

Available online 2 November 2022

0367-2530/© 2022 Elsevier GmbH. All rights reserved.

# Morpho-palynological and anatomical studies in desert cacti (*Opuntia dillenii* and *Opuntia monacantha*) using light and scanning electron microscopy

Salman Majeed<sup>1</sup>  | Muhammad Zafar<sup>1</sup>  | Mushtaq Ahmad<sup>1,2</sup>  | Sadia Zafar<sup>3</sup> | Asad Ghufuran<sup>4</sup> | Muhammad Ayoub<sup>5</sup> | Shazia Sultana<sup>1</sup> | Ghulam Yaseen<sup>6</sup> | Jamil Raza<sup>1</sup> | Nabila<sup>1</sup>

<sup>1</sup>Department of Plant Sciences, Quaid-i-Azam University Islamabad, Islamabad, Pakistan

<sup>2</sup>Pakistan Academy of Sciences, Islamabad, Pakistan

<sup>3</sup>Department of Botany, Division of Science and Technology, University of Education, Faisalabad, Pakistan

<sup>4</sup>Department of Environmental Science, International Islamic University, Islamabad, Pakistan

<sup>5</sup>HICoE-Centre for Biofuel and Biochemical Research (CBBR), Department of Chemical Engineering, Institute of Self-Sustainable Buildin, University Teknologi PETRONAS, Bandar Seri Iskandar, Malaysia

<sup>6</sup>Department of Botany, Division of Science and Technology, Township Campus, University of Education Lahore, Lahore, Pakistan

## Correspondence

Salman Majeed, Department of Plant Sciences, Quaid-i-Azam University Islamabad, Islamabad 45320, Pakistan.

Email: [salmansunny61@gmail.com](mailto:salmansunny61@gmail.com), [zafar@qau.edu.pk](mailto:zafar@qau.edu.pk), [mushtaqflora@hotmail.com](mailto:mushtaqflora@hotmail.com)

## Funding information

Higher Education Commission, Pakistan, Grant/Award Number: NRPU-7837

Review Editor: Paul Verkade

## Abstract

*Opuntia* is the most diverse and widely distributed drought resistant promising genus of family Cactaceae. The cladodes were utilized to quantify the chemical composition of these plants helpful in lignocellulose conversion and their application towards biofuel production. The present study was aimed to evaluate and compare the taxonomic relationship based on morphology, stem anatomy and palynology of important desert cacti including *Opuntia dillenii* and *Opuntia monacantha*. This study also evaluates the potential usefulness of morphological, anatomical and pollen traits using light and scanning electron microscopy. The obtained microcharacters of stem and flowers are considered diagnostic at the generic and specific levels. Some distinguishing morphological features observed were elliptical to obovate cladodes, 1–7 spines per areole and presence of glochidia in *O. dillenii*. Pollen and stem anatomical characters of the studied taxa are considered highly diagnostic at the generic and species levels. The epidermis has irregular and wavy cells, with straight to sinuate wall pattern and paracytic stomata. Pollen grains appear as pantoporate and prolate spheroidal having reticulate to perforate-reticulate sculpturing while exine semi-tectate to tectate. The taxonomic features studied could be valuable to elaborate and helpful in correctly identification of *Opuntia* species. The methods of diverse microscopic examination also providing sufficient evidence about the taxonomy of the *Opuntia* species.

## Research Highlights

- Description and illustration of desert cacti *Opuntia*.
- Morpho-anatomy and palynology were studied with LM and SEM.
- Highly variation in taxonomic qualitative and quantitative features.
- Systematic significance based on taxonomic characters was presented.

## KEYWORDS

cactus, desert, palyno-anatomy, pantoporate pollen, paracytic stomata, SEM